ASPECTS OF THE DESIGN AND BEHAVIOUR OF ROAD STRUCTURES INCORPORATING LIGHTLY CEMENTITIOUS LAYERS

MORRIS DE BEER

ASPECTS OF THE DESIGN AND BEHAVIOUR OF ROAD STRUCTURES INCORPORATING LIGHTLY CEMENTITIOUS LAYERS

by MORRIS DE BEER

A DISSERTATION SUBMITTED AS PART FULFILMENT
for the DEGREE
DOCTOR OF PHILOSOPHY
in the
DEPARTMENT of CIVIL ENGINEERING
FACULTY OF ENGINEERING
UNIVERSITY OF PRETORIA

PRETORIA

FEBRUARY 1990

STATEMENT OF THE AUTHOR

The author hereby states that all the research work reported in this dissertation was initiated by him, and that he was solely responsible for the experimental planning and control of the various tests discussed, as well as the interpretation and reporting of all the results.

The execution of the tests (both laboratory and Heavy Vehicle Simulator (HVS)) was delegated by the author to the available technical assistants, under his direct supervision. The final copy-ready graphical illustrations were done by the drawing office.

..... *February 1990*

Morris De Beer

SUMMARY

Currently very sophisticated pavement design and evaluation methods exist. These methods include for example advanced computer programs and full scale pavement test facilities. However, there appears to be a lack in knowledge regarding actual structural behaviour of a wide variety of pavements and that the gap between theory and practice is not fully bridged yet.

Virtually no information on the behaviour of pavements with relatively lightly cementitious layers was available before this study. This study discusses various structural behavioural characteristics of these pavements, including objective classification based on the strength - balance of these pavements. Design and evaluation guidelines followed from this study are also given as an aid, and also to improve the understanding of basic pavement behaviour.

Chapter 1 discusses the introduction and background to this study, while Chapter 2 the scope and objectives are summarised.

In Chapter 3 the development of an objective in situ pavement classification system based on the results of the Dynamic Cone Penetrometer (DCP) is discussed. This classification is based on two unique parameters calculated from the DCP data, and these parameters describes the in situ strength - balance of the pavement. Deviations in the strength - balance is normally indicative of regions (layers) of relatively higher shear strength overlaying that of relatively lower strengths, or vice versa. This system has the potential to be applied to other flexible pavement types as well as sub - structures for rigid pavements.

In Chapter 4 the permanent deformation behaviour of pavements with cementitious layers is discussed. Most of this behaviour resulted from extensive studies conducted with the Heavy Vehicle Simulator (HVS) by the author. Specific attention is given to two basic types of pave—ments, viz a relatively deep and a relatively shallow pavement struc—ture. Two basic types of failure mechanisms associated with these pavements were identified and are discussed in detail. Investigation

into the rate of deformation indicated that this rate is linear and may assist largely in describing the structural capacities of these pave—ments. Relative damage was also investigated and is amongst others, strongly dependent on the basic pavement composition, loading, materials and environmental conditions.

Compression (crushing) failure of lightly cementitious layers was relatively unknown until this study, and Chapter 5 discusses in a somewhat original approach this behaviour. It is pointed out that compression failure of this materials occurs at very low levels of vertical compressive strains in these layers, and is strongly influenced by the in situ material strength and repetitive contact stress applica—tions. The concept of **life to initiate compression failure** in these layers is introduced and may assist in more effective design and mainte—nance planning of these pavements.

In Chapter 6 the behaviour of the two types of pavement is described with the aid of the DCP, and indicates that this instrument aids largely in the correct identification of the actual failure mechanisms associat—ed with these pavements. The concept of **pavement strength - balance paths** is introduced and provides a simple methodology to illustrate the structural changes in the pavement as a result of traffic loading, based on the classification system outlined in Chapter 1.

Resilient behaviour of pavements is always considered to be very important, especially when the pavement system and behaviour are described mechanistically with the aid of linear elastic theories or those which includes stress dependent parameters. Chapter 7 discusses the resilient responses of the two pavements investigated, and indicates the importance of factors such as surface and depth deflections, effective elastic moduli, induced stresses and strains. The concept of **effective fatigue life** for cementitious base layers is introduced and appears to describe the fatigue behaviour of these layers better than methods currently used in South Africa. Limiting vertical subgrade strain criteria were also verified for the pavements investigated here.

This dissertation also contains six appendices (Appendix A to F). In Appendices A, B and F supplementary results in the form of tables, figures and text are given to assist discussions in Chapters 4, 5, and 7. Appendix C outlines aspects of the various DCP computer programs which was developed during this study to assist in the formal preparation, evaluation and classification of the DCP data and graphical outputs, as discussed in Chapter 3. A photographic record of most of the HVS tests conducted during this study is given in Appendix D. Appendix E summarises the graphical computer output generated by the mentioned computer programs, for most of the HVS tests conducted in this study, and are self explanatory. The DCP data in this appendix is used in Chapter 6.

SAMEVATTING

Huidiglik bestaan daar heelwat gesofistikeerde plaveiselontwerp- en evaluerings metodes. Hoogsgevorderde rekenaarprogrammatuur asook onder andere volskaalse-toetsfasiliteite vir plaveisels is 'n geruime tyd al beskikbaar. Daar is egter nog 'n tekort aan inligting en kennis rakende die werklike strukturelegedrag van 'n verskeidenheid van plaveisels en die gaping tussen die teorie en praktyk is nog nie heeltemaal oorbrug nie. Feitelik geen inligting van die gedrag van plaveisels met relatiewe lig gesementeerdelae was bekend voor hierdie studie nie. In hierdie studie word 'n verskeidenheid van gedragskarakteristieke van hierdie plaveisels bespreek, en sluit onder andere 'n objektiewe plaveisel-klassifikasiesisteem in, gebaseer op die sterktebalans van plaveisels. Riglyne ten opsigte van die ontwerp en evaluering vloei uit die studie voort en word as 'n hulpmiddel gegee om basiese plaveiselgedrag beter te verstaan.

Hoofstuk 1 bespreek die inleiding asook die breë agtergrond tot hierdie studie, terwyl in Hoofstuk 2 die omvang en doelwitte saamgevat word.

In Hoofstuk 3 word die ontwikkeling van 'n objektiewe in situ plaveisel-klassifikasiesisteem, gebaseer op die resultate van die Dinamiese Keëlpenetrometer (DKP) bespreek. Hierdie klassifikasie is gebaseer op twee unieke parameters wat vanuit die DKP-data bereken word. Hierdie parameters beskryf die in situ sterktebalans van die plaveisel. Afwykings in die sterktebalans is normaalweg 'n aanduiding van gebiede of gelaagheid van relatiewe hoë skuifsterkte bo-op gebiede met relatiewe lae skuifsterkte, of omgekeerd. Hierdie sisteem het die potentiaal om ook gebruik te kan word op ander buigbareplaveisels tipes, asook die onderlaagstrukture van starplaveisels.

In Hoofstuk 4 word die permanentedeformasiegedrag van plaveisels met gesementeerdelae bespreek. Die meerderheid van hierdie gedrag is bestudeer tydens uitgebreide studies met die Swaar Voertuignabootser (SVN), deur die skrywer. Spesiale aandag is geskenk aan twee basiese tipes plaveisels, nl 'n diep en 'n vlak plaveiselstruktuur. Twee basiese tipes swigmeganismes eie aan hierdie plaveisels is geïdentifiseer, en

word in detail bespreek. Ondersoek na die tempo van deformasie het aangedui dat hierdie tempo lineêr is en grootliks gebruik kan word om die strukturele kapasiteit van die plaveisels te beskryf. Die relatiewe skade asgevolg van verskillende wielbelastings is ook ondersoek en hang sterk van heelwat faktore af, soos byvoorbeeld basiese plaveiselsamestelling, belasting, materiale en omgewings toestande.

Drukswigting (vergruising) van lig gesementeerde plaveisellae was redelik onbekend tot en met hierdie studie, en word in Hoofstuk 5 word op 'n ietwat oorspronklike wyse benader. Dit word uitgewys dat drukswigting van hierdie materiale by baie lae vlakke van vertikale-drukvervorming voorkom, en word beheer deur die in situ materiaalsterkte en herhalende bandkontakspanning. Die konsep van **lewe tot die inisiering van drukswigting** in hierdie lae word voorgestel en mag meer effektiewe ontwerp - en onderhoudsbeplanning tot gevolg hê.

In Hoofstuk 6 word dir gedrag van hierdie twee tipes plaveisels na aanleiding van die DKP-resultate bespreek en dit word aangedui dat hierdie instrument baie handig is in die identifisering van die korrekte swigmeganisme wat met hierdie plaveisels geassosieer is. Die konsep van **plaveiselsterktebalansroetes** word voorgestel en voorsien 'n eenvoudige metode om die strukturele veranderings as gevolg van verkeersbelasting van die plaveisel te illustreer. Hierdie konsep is gebaseer op die klassifikasiesisteem, soos beskryf in Hoofstuk 1.

Die veerkragtigheidsgedrag van plaveisels word nog altyd as baie belangrik beskou, veral met die beskrywing van die meganistiesegedrag van die plaveiselsisteem met behulp van die lineêr elastiese teorie asook teorië wat spanningsafhanklike parameters gebruik. Hoofstuk 7 bespreek die veerkragtigheids-responsie van die twee plaveisels wat ondersoek is, en toon die belangrikheid aan van faktore soos die oppervlak- en dieptedefleksies, effektiewe-elastisitietsmoduli, gegenereerde spannings en vervormings. Die konsep van **effektiewe-vermoëingslewe** vir gesementeerdekroonlae word voorgestel, en beskryf blykbaar die vermoëingsgedrag van hierdie lae beter as huidige metodes in Suid Afrika. Vertikale-grondlaag-vervormingskriteria is ook ondersoek vir hierdie plaveisels, en word ook bespreek in hierdie hoofstuk.

Hierdie proefskrif bevat ook ses aanhangsels (Aanhangsel A tot F). In Aanhangsels A, B en F word verdere verklarende resultate vir Hoofstukke 4, 5, en 7 in die vorm van tabelle, figure en teks gegee. Aanhangsel C toon sekere aspekte van die rekenaarprogrammatuur aan, wat tydens hierdie studie ontwikkel is om die formele aanbieding, evaluasie en klassifisering van die DKP-data asook grafiese-uitdrukke moontlik te maak, soos beskryf in Hoofstuk 3. ń Fotografiese samevatting van die meeste van die SVN-toetse wat tydens hierdie studie gedoen is word in Aanhangsel D gegee. Aanhangsel E bevat in opsommende vorm, die grafiese-uitdrukke van die DKP-resultate van die meeste van die SVN-toetse. Hierdie uitdrukke bevat die basiese DKP-inligting wat in Hoofstuk 6 gebruik is.

AAN : MARION, MORRIS (jnr) en FREDERIK

ACKNOWLEDGEMENTS

I would like to express my honest and sincere thanks to the following persons and organisations:

Dr S H Kuhn, former Chief Director and Dr C R Freeme, Director of the Division for Transport and Road Research (DRTT) of the CSIR, for the opportunity to do this study and to complete a dissertation on this subject.

My former Group Head of the former Pavement Engineering Group at NITRR, Dr C R Freeme, for his interest, advice and many valuable discussions during the period of accelerated testing of the pavements studied.

My co - superviser Professor P F Savage, for his interest, advice and valuable discussions on the contents of this dissertation.

Mr L J Terblanche, Executive Director of the Roads Branch of the Transvaal Provincial Administration (TPA), for the opportunity to use their Heavy Vehicle Simulator (HVS) and results during this study.

Mr E G Kleyn, Chief Materials Engineer, Roads Branch of the TPA, for his keen interest, advice and many valuable and often exciting discussions during this period of study.

Dr E Horak, Programme Manager of the Pavement Engineering Technology Programme at DRTT, for his continuous support, interest and valuable discussions.

Messers N Kuhn, J M Collett, L Marks, N Ras, S Lacante and their technical teams for their assistance with the substantial amount of HVS data collection and reporting. Without their help it would have been impossible to complete this study.

Mrs Y E Diering and B E Saler of the Drawing office for their help in the preparation of all the drawings.

All my other colleagues in the Division for their help and support during this study.

Ook ń spesiale woord van dank aan my vrou - Marion, baie dankie vir die geduld, ondersteuning en liefde wat ek van jou gekry het tydens hierdie periode van intensiewe studie.

En dan my grootste dankbaarheid aan GOD wat my ook hierin gelei het.

SOLI DEO GLORIA !

CONTENTS

CHAPTER 1

INTRODUCTION AND BACKGROUND

1.1 INTRODUCTION AND BACKGROUND

Pavement design dates back to the early years of the twentieth century and, since then major advancements in the design methods have resulted in the development of an independent mechanistic pavement science. This science is advancing rapidly with the aid of computers and the introduction of full scale testing facilities worldwide today.

Major advancements in the layered theory of pavements have been made since its introduction in the early 1940s, and recently very sophisticated analytical or mechanistic methods exist for the design of new pavements, reconstruction of existing ones and strengthening overlays. Although these methods are theoretically sound, a gap still exists between actual pavement behaviour (practice) and theory.

During the late 1970s, the fleet of newer generation Heavy Vehicle Simulators (HVSs) was introduced in South Africa (Walker, 1985). These machines were developed to subject roads and airfields to accelerated trafficking in order to study their actual behaviour. One of these HVSs commissioned in 1977 belongs to the Tranvaal Provincial Administration (TPA) and has been operated by the Division of Roads and Transport Technology (RTT) on behalf of the TPA.

The initial test programme for the TPA HVS concentrated on the behaviour of light unbound gravel base pavements. Thereafter a major study on the behaviour of high quality crushed stone base pavements was undertaken and completed during 1982. From 1982/83 to 1988 a study on relatively light pavements with cementitious layers was done. A total of approximately 710 million equivalent standard (8200 kg or 80 kN) axle repetitions (E80s) has been applied to the pavements in the Transvaal to date, at a 1988/89 cost of approximately 1,26 cent per E80. Although this cost is relatively high, large savings has already resulted from this work (See last paragraph in this section, as well as Paragraph 4.5 in Chapter 4).

This dissertation reports on the study during the latter period of research (1985/88), and concentrate on the basic behavioural characteristics of pavements with lightly cementitious layers. More than 80 per cent of the pavements in the 46 000 km road network in

the Transvaal consists of cementitious base or subbase layers. If these are to be maintained effectively, or new improved pavement structures designed, it is essential that information regarding their general behaviour characteristics be obtained.

It is believed that this information will not only assist in bridging the gap between practice and theory, but will ensure the construction of better and more cost-effective pavements in the future. It is currently estimated by the TPA that implementation of the HVS research findings for the period 1978 to 1982, entailed an estimated annual saving of approximately R13 million in the Transvaal. The present annual pavement funding requirement for Transvaal is approximately R1000 million and, if the research discussed in this dissertation results in better use of normally underrated materials, further millions of rand may be saved.

1.2 REFERENCES

Walker, R N (1985). The South African Heavy Vehicle Simulator. Proceedings of the Annual Transportation Convention, (ATC 1985), Session S.350, Accelerated Testing of Pavements, 29 July - 2 August, CSIR, Pretoria, 1985.

CHAPTER 2

SCOPE AND OBJECTIVES OF STUDY

2.1 SCOPE AND OBJECTIVES OF THIS STUDY

2.1. Scope

During the early 1980s, it was established that urgent research was needed on the general structural behaviour of pavements with lightly cementitious layers. These layers consist of C3 and C4 (TRH 13, DRTT, 1986) materials, and the term "cementitious" is used, inter alia, with the term "cemented". (The term "cemented" may be misunderstood in that it reflects only materials stabilised with portland cement; "cementitious" is preferred because some of the aspects discussed here may be valid for materials stabilised with stabilisers other than cement, including lime, fly - ash, milled granulated blast furnace slag, bitumen emulsion etc).

This study follows an earlier study completed during 1985 (De Beer, 1985) on the same type of materials, but used as subbases under bituminous base pavement structures. This study, however, concentrates primarily on pavements with cementitious bases, designed to carry relatively light traffic, viz 0,4 to 1,0 million standard repetitions (E80s) over a design period of 20 years.

Major uncertainties existed regarding the real behaviour of these pavements, and included aspects such as definition of the actual pavement system, viz layer thickness and quality, distress modes and failure mechanisms, both long and short term durability, erodibility and design considerations. The scope of this study is to evaluate these factors with the aid of the HVS and other relevant tools such as the Dynamic Cone Penetrometer (DCP), Multi - Depth Deflectometer (MDD), Road Surface Deflectometer (RSD) and the linear elastic theory.

2.2 OBJECTIVES AND MOTIVATION

The layout of this study is illustrated in Figure 2.1, and each chapter including the appendixes, is indicated separately in the flow diagram. Each chapter is representative of a major area and conveys the most important findings following from the research. The detailed objectives and motivation for each chapter are discussed in its introduction and only the overall objectives are discussed here.

The overall objective of this study is to investigate and report on the structural behavioural characteristics of pavements with lightly cementitious layers in order to identify the most important factors controlling their behaviour and hence structural capacity.

To achieve the abovementioned overall objective this study consists of a number of sub - objectives, which are listed and discussed below.

These include:

(a) **The development of an in situ pavement classification system (Chapter 3).**

Experience with the HVS testing over the years indicated that it is of crucial importance to define the actual in situ pavement system correctly. Numerous examples exist where these conditions differ completely from that originally proposed during the design phase, and that the ultimate structural behaviour of these pavements, ie rutting, cracking, pumping etc. is controlled mainly by factors associated with these differences in pavement/material quality. For pavements with cementitious layers this is even more important and often critical because inefficient mixing of the stabiliser, detrimental carbonation, inadequate layer thickness, interlayers, horizontal cracking etc., contribute largely to and often control the structural capacity of these pavements. The actual failure mechanism is a function of the pavement structure, and therefore it is necessary to establish an objective method to describe and classify in situ pavements in addition to normal

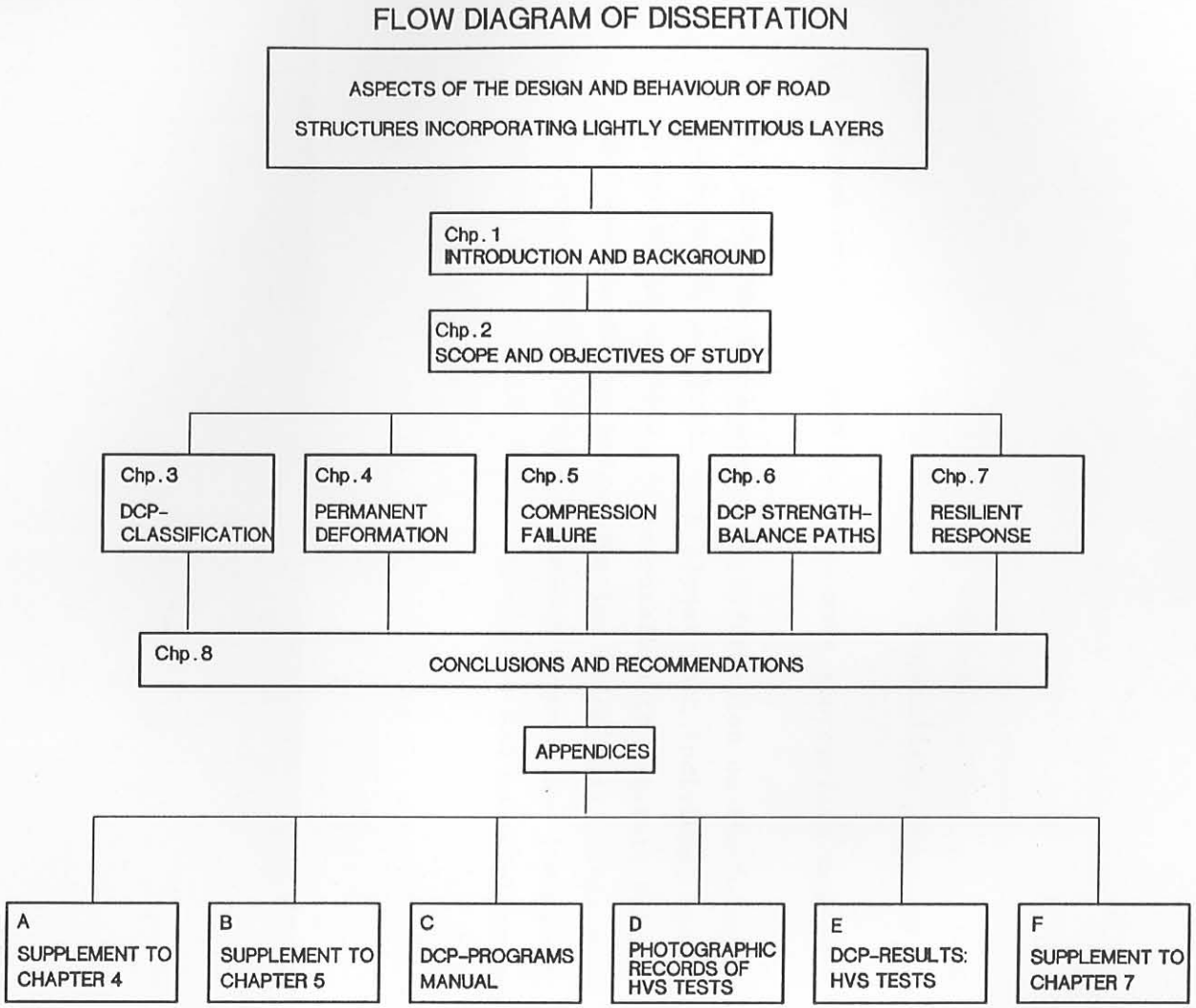

FIGURE 2.1

LAYOUT OF THIS DISSERTATION

design classification and grouping of pavements as is illustrated, for example in current design documents such as TRH 4 (TRH 4, DRTT, 1985). Furthermore this classification system may also assist in an improved understanding of pavement behaviour.

(b) **Evaluation of permanent deformation development (Chapter 4)**

Permanent deformation development as a result of traffic loading is one of the most fundamental characteristics of pavements which is studied to indicate and quantify its structural capacity.

(c) **Evaluation and description of actual failure mechanisms (Chapters 4, 5, 6, and 7).**

It is all very well to measure the deformation development and the effects of cracking on the surface of the pavement, but in order to understand the reasons for this behaviour fully it is necessary to investigate its origin and the state of layers/materials within the pavement system. Normally there is a "weakest link/layer" in the pavement which controls its behaviour and which has to be identified so that it can be isolated or be taken into account during the design phase for similar pavements in the future. Aspects addressed here are:

- Fatigue failure of cementitious layers
- Compression failure of cementitious layers
- Methods to describe pavement behaviour
- Resilient responses of the pavements
- Reference to erodibility (durability)

(d) **Development of additional and more appropriate design guidelines**

By using the HVS a wealth of information on the behaviour of a pavement is generated with almost each individual test. With this large amount of data, it is possible to generate better and more appropriate design and evaluation guidelines. This will lead to the improvement of current design methods and increased confidence in the use of local design, pavements and material systems.

2.2 REFERENCES

De Beer, M (1985). Behaviour of Cementitious Subbase Layers in Bitumen Base Road Structures. M(Eng), Faculty of Engineering, University of Pretoria, Pretoria, 1985.

Division of Roads and Transport Technology, (DRTT) (1985). Structural Design of Interurban and Rural Road Pavements. Technical Recommendations for Highways, TRH4: 1985, CSIR, Pretoria, 1985.

Division of Roads and Transport Technology, (DRTT) (1986). Cementitious Stabilisers in Road Construction. Technical Recommendations for Highways, Draft TRH13: 1986, CSIR, Pretoria, 1986.

CHAPTER 3

IN SITU PAVEMENT CLASSIFICATION SYSTEM BASED ON THE RESULTS OF THE DYNAMIC CONE PENETROMETER (DCP)

CONTENTS PAGE

3.1 INTRODUCTION

The Transvaal Provincial Administration (TPA) initiated the application of the Dynamic Cone Penetrometer (DCP) to evaluate in situ structural conditions of their pavements during the early 1970s. Over the past few years, the DCP has established itself as a valuable pavement design and evaluation tool in South Africa and elsewhere (Kleyn, 1984, Kleyn et al, 1982a; 1982b; 1982c; 1987; Livneh et al, 1987; Chua, 1988).

The DCP is mainly used on pavements with unbound granular and lightly cemented layers (7-day soaked Unconfined Compressive Strength (UCS) $\leq$ 4 MPa). The majority of roads in the developing countries in Southern Africa fall into this category. Bituminous surfaced roads comprise approximately 25 per cent of the total road network in these developing countries. In the province of the Transvaal, more than 80 per cent of the pavements incorporate lightly cementitious layers. For these countries, including South Africa, to continue to develop towards their full potential, improvements to their road networks are necessary. This is normally done by upgrading existing pavements, constructing new ones and rehabilitating bituminous - surfaced pavements which have reached the end of their design life. Experience to date indicates that the potential use of the DCP is very high on both unbound gravels and lightly cementitious materials and that very useful information regarding the behaviour of pavements and pavement definition is obtained with the DCP. In a recent study Chua (1988) indicated that the determination of the in situ elastic moduli (effective elastic moduli) is also possible using the DCP. However, it is my opinion that there is a need for objective methods for analysing DCP results in general, and furthermore, to explain basic pavement behaviour, also under accelerated testing. A standardised output format is also needed.

During the inititation of this study, the above mentioned problem was identified as one of the most important aspects to be adressed before proper use could be made of the DCP results, especially in association with the research with the Heavy Vehicle Simulator (HVS) regarding pavement behaviour. It was considered that a standard method could be developed against which all DCP results should be evaluated. It is my opinion that such a system should form the corner stone of the analysis of DCP results in future, even on pavements without lightly cementitious layers.

In this chapter the development of a universal pavement strength - balance classification system based on DCP results, is discussed. As mentioned, until this study, no generally accepted method for classifying DCP data existed and such a classification system, similar to some well - known soil classification systems (Lambe et al, 1969; Scott, 1974), is much needed to enhance the interpretation of DCP results. Such a classification system will also increase objectivity in the classification, interpretation and comparison of DCP results. This will not only enhance the use of the DCP instrument, but also the understanding of in situ pavement definition and basic pavement behaviour, especially amongst inexperienced users of the DCP.

Most of the DCP results discussed in this chapter originated from tests on pavements with lightly cementitious layers, but the principles discussed here are also generally applicable to unbound granular pavement types. At this stage, however, bituminous and concrete base pavements are excluded from this analysis. After a discussion of the pavement strength - balance concept, the classification system is presented. Various examples are given to illustrate the different DCP categories in which pavements can be classified in according to this system.

In Chapter 6, a detailed analysis, based on this classification system, of the DCP results measured on pavements with cementitious layers evaluated during this study, is discussed.

3.2 THE CONCEPT OF PAVEMENT STRENGTH - BALANCE

3.2.1 Background

Fundamentally, the strength - balance of a pavement structure is defined as the change in the strength of the pavement layers with depth (Kleyn et al, 1982a, 1982b, 1982c, Kleyn, 1984). Normally, the strength of the pavement decreases with depth and, in principle, if this decrease is smooth and without any severe discontinuities, the pavement is regarded as balanced or in a state of balance.

The development of the strength - balance concept of pavements, including the Standard Pavement Balance Curves (SPBCs), however, originated from numerous DCP results obtained on unbound granular type pavements (Kleyn et al, 1987). The

name Standard Pavement Balance Curves (SPBCs) in this dissertation is used instead of the name Pavement Strength - Balance Curves, which is used in most the references indicated above. This was necessary to distinguish between a balance curve described by the BN, and the balance curve described by the B parameter (For definition of parameters B and BN see following paragraphs, and Paragraph 3.2.2, as well as the above mentioned references in this paragraph).

With respect to the DCP, the average rate of penetration (DN, in mm per blow) through the various pavement layers, is proportional to the in situ shear strength of the material and is correlated to the California Bearing Ratio (CBR) or UCS of the material. It is therefore considered that layers of relatively high and relatively low strength, respectively, will be distinguished from each other. Not only will the rates of penetration of the individual layers be known, but also the strength relations between the different layers within the total pavement structure. From this knowledge, the balance of the pavement can be evaluated.

During the development of the pavement strength - balance equations (Kleyn et al, 1987), a simple formula, describing the relation between the pavement structure number, DSN in %, the pavement depth, D in % and a parameter, B, describing the SPBCs, was obtained. According to Kleyn et al (1987), it was found that the equation for a rectangular hyperbola describes remarkably well the strength balance of the pavements tested. According to this equation, there are, in theory, an infinite number of SPBCs for flexible pavement structures with relatively thin surfacings (< 50 mm), and is used as a basis for the pavement strength - balance classification system, described in this chapter. The formula is given below :

$$DSN\ (\%) = \frac{D*[400*B + (100 - B)^2]}{4*B*D + (100 - B)^2} \quad \text{.....3.1}$$

where : DSN = pavement structure number, as percentage (%)
B = parameter, defining the standard pavement balance curve (SPBC)
D = pavement depth, as percentage (%)

In Figure 3.1, a graphic illustration of this formula is given and show two curves from a family of balance curves. These curves indicates that the pavement strength decreases with pavement depth. If B = 0, the balance curve (SPBC) is a straight line from DSN = 0 per cent to D = 100 per cent.

Normally, the **total number of blows** needed to penetrate the total pavement depth, say 800 mm, is indicated as DSN_{800}, in **blows**. As indicated earlier, there are an infinite number of balance curves (SPBCs), and balance curves other than those discussed above can be obtained graphically by interpolation or by calculation using Equation 3.1.

In Figures 3.2(a), 3.2(b), 3.2(c) and 3.2(d), typical examples of various DCP results, plotted in the format discussed above, are indicated. In Figure 3.2(a) an example of a **balanced pavement structure** is illustrated, while in Figures 3.2(b) and 3.2(d) examples of **unbalanced pavements** are shown. The **imbalance** is indicated by the deviation of the **DCP data** (DSN data, as a percentage) from the **SPBCs**, which will be discussed in Paragraph 3.2.4 in more detail. Although the **normal case** is that pavements **decrease in strength with depth** ($B \geq 0$), as is illustrated in Figure 3.2(a),(b) and (d), pavements can also **increase in strength** with **depth** ($B < 0$) as is illustrated in Figure 3.2(c) and are normally refered to as "upside down" or inverted pavement structures.

3.2.2 Parameter B versus BN

The parameter B varies, in theory, from - 100 to + 100, which ultimately defines **comprehensive SPBCs** in this dissertation. The SPBCs with $B < 0$ is a mirror image of the SPBCs where $B > 0$, as is illustrated in Figure 3.3, for a pavement depth (PD) of 800 mm. In this figure, parameter B varies between -90 and +90, with intervals of 10 units between individual curves. In this approach **the parameter B is used to define the various SPBCs**, and is different from that used by Kleyn et al (1988), where the **Balance Number, BN, (BN = DSN in per cent at D = 12,5 per cent)** is used. The selection of B in this dissertation instead of BN to define the balance curves, however, was necessary to develop the classification system, firstly, because of its simplicity, as expressed in previous Equation 3.1, and secondly, that BN defines only a single point on the full balance curve of the pavement while B defines the curve for the full pavement depth. The BN only defines the balance curve accurately <u>if the pavement is perfectly balanced</u>, which, however, is not the normal case for most pavements and another more relevant parameter is needed.

THE FORMULA FOR STANDARD PAVEMENT BALANCE CURVES*

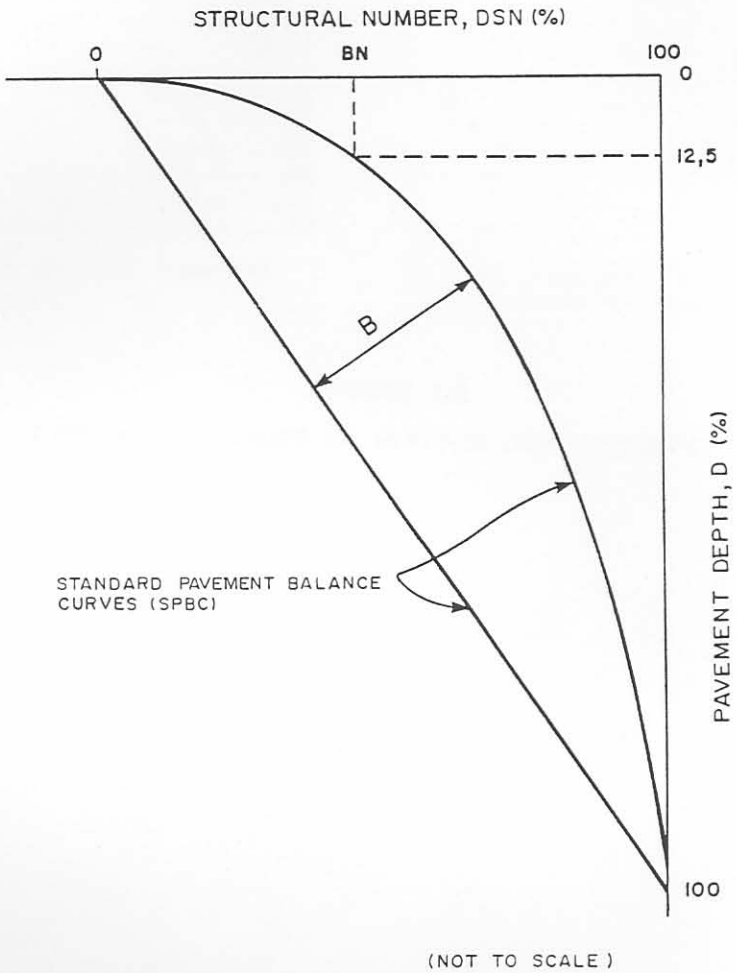

$$^{*}DSN\ (\%) = \frac{D\,[\,400B + (100 - B)^2\,]}{4DB + (100 - B)^2}$$

FIGURE 3.1

GRAPHIC REPRESENTATION OF THE FORMULA FOR STANDARD PAVEMENT BALANCE CURVES (SPBC)

940-4-5729/1

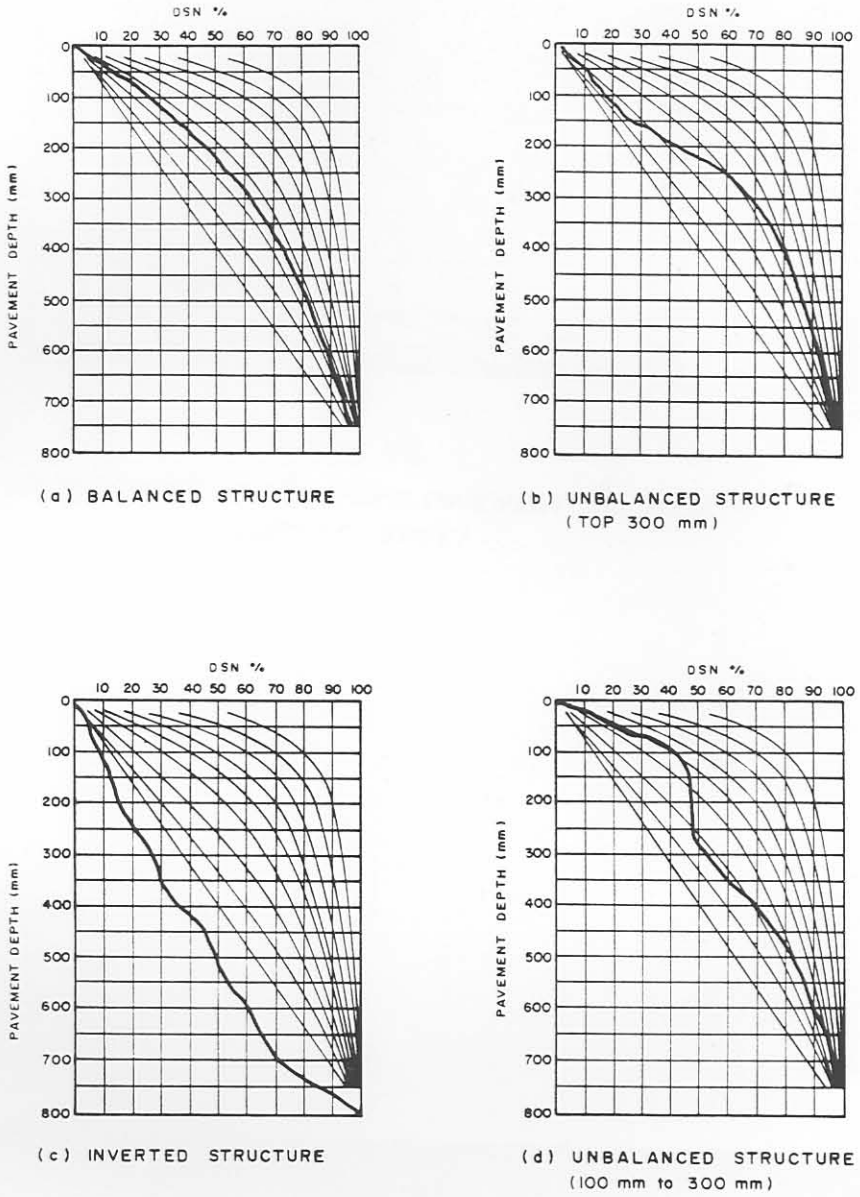

FIGURE 3.2

TYPICAL EXAMPLES OF VARIOUS DCP-RESULTS

940-4-5729/2 BD

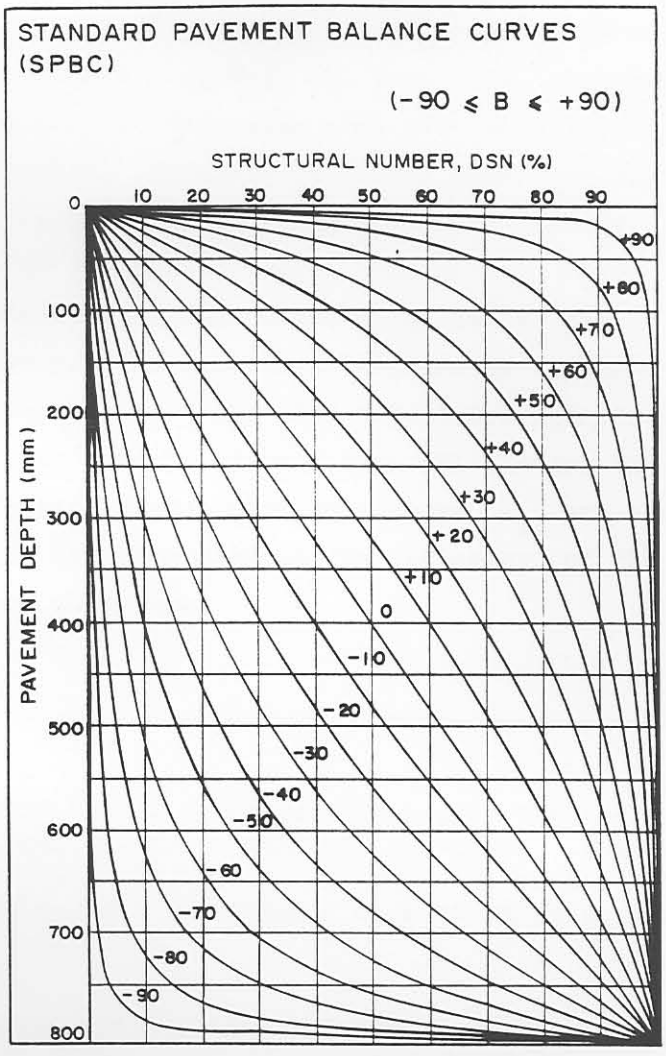

FIGURE 3.3

COMPREHENSIVE STANDARD PAVEMENT BALANCE CURVES (SPBC)

940-4-5729/3 BD

Inspection of the given formulation (Equation 3.1) then revealed the use of B, instead of BN, because B describes the total balance curve, which may then be assigned to a pavement, and is used in this dissertation to characterise the "deepness" or "shallowness" of the pavement.

3.2.3 Deviation from SPBCs

It must, however, be remembered that both B and BN fail to indicate or quantify deviations in the strength balance of the pavement from the idealised balance curve (SPBCs). This leads to the additional requirement for the classification system that the state of the balance (deviation from SPBC) of the pavement has to be quantified, because most of real pavements are not perfectly strength - balanced. The original method only provides for strength - balanced pavements (Kleyn et al, 1988). In order to quantify the deviation in the strength - balance of real pavements from the SPBCs, the deviation (area) between the best fit SPBC for the data, and the actual data (DSN data), is used. In Figure 3.4, the method for calculating this deviation in terms of area A_i, is illustrated.

3.2.4 Best fit SPBC

The total area (A) between the DCP data and a series of SPBCs is calculated, and the SPBC resulting in the minimum area is then assigned to the pavement. This "best fit" SPBC* is then regarded as unique to that data (pavement) under consideration. Figure 3.4 indicates that the best fit SPBC for the DCP data indicated in the figure, is where B = 38. The absolute (mod) area (A) is calculated in a discrete order by calculating the difference between the DSN of the SPBC and the DSN of the DCP data (DSN data). This is done at different depths in the pavement, using increments of 8 mm in this case. These differences are then used to calculate the area of a trapezoid with a width of 8 mm, and at both sides of the SPBC. Per definition, the areas to the left of the SPBC are negative, but this is ignored when calculating the total area, A (see Equation 3.2). Finally, these individual areas, A_i, are added together and the sum of the areas (A) is then used as the indicator of the state of balance of the in situ pavement structure.

---

* The "best fit" SPBC is not always the "average" SPBC of the data, and differs slightly on well and averagely balanced pavements. This difference, however, increase markedly with an increase in imbalance or A. The advantage of the "best fit" method is that deviations from the SPBC is more accentuated.

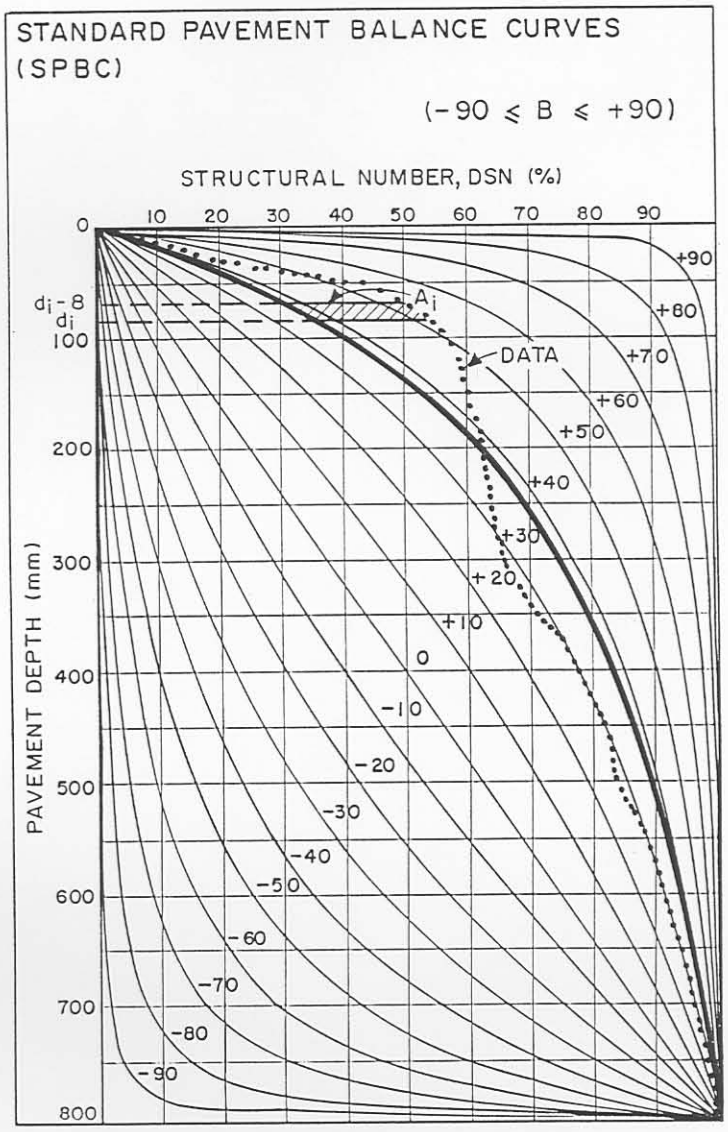

FIGURE 3.4

CALCULATION OF THE DEVIATION (AREA) OF THE DCP-DATA FROM THE STANDARD PAVEMENT BALANCE CURVES (SPBC)

For a pavement depth of 800 mm, the sum total of the absolute areas is as follows:

$$\text{AREA (A)} = \sum_{i=1}^{100} |A_i| \quad \ldots\ldots\ldots\ldots\ldots\ldots\ldots\ldots\ldots\ldots 3.2$$

where A is %.mm

For a perfect strength - balanced pavement, the area A = 0. This means that the deviation (area) between the DCP data balance curve and the "best fit" SPBC of the data, is equal to zero.

From the discussion above it is evident that the two distinct parameters, B and A, are used to define the DCP data. These two parameters, therefore, form the basis for the proposed pavement strength - balance classification system, which will be described in the next section.

3.3 PAVEMENT STRENGTH - BALANCE CLASSIFICATION SYSTEM

3.3.1 Analysis of some DCP data

Following the definition and description of the two unique parameters, B and A, an analysis of approximately 275 DCP measurements was carried out on both lightly cemented and granular base pavement structures. Figure 3.5 gives the various DCP data, indicating the spread in terms of balance (B) and deviation from balance (A). These DCPs were measured mainly on three different pavements: on Road 1932 and Road 2212, north of Pretoria, where extensive Heavy Vehicle Simulator (HVS) tests were recently done, and on granular pavements in the Benoni area.

The figure indicates that parameter B varies between approximately -20 and +60, and parameter A between 600 and 8000 %.mm. The figure also indicates that the centre of gravity of the two sets of data for the cemented roads (1932 and 2212) is at different locations in terms of parameter B, but with approximately the same deviation from the balance, parameter A. This is an indication that the relative strength distribution in the layers of these two pavements is different.

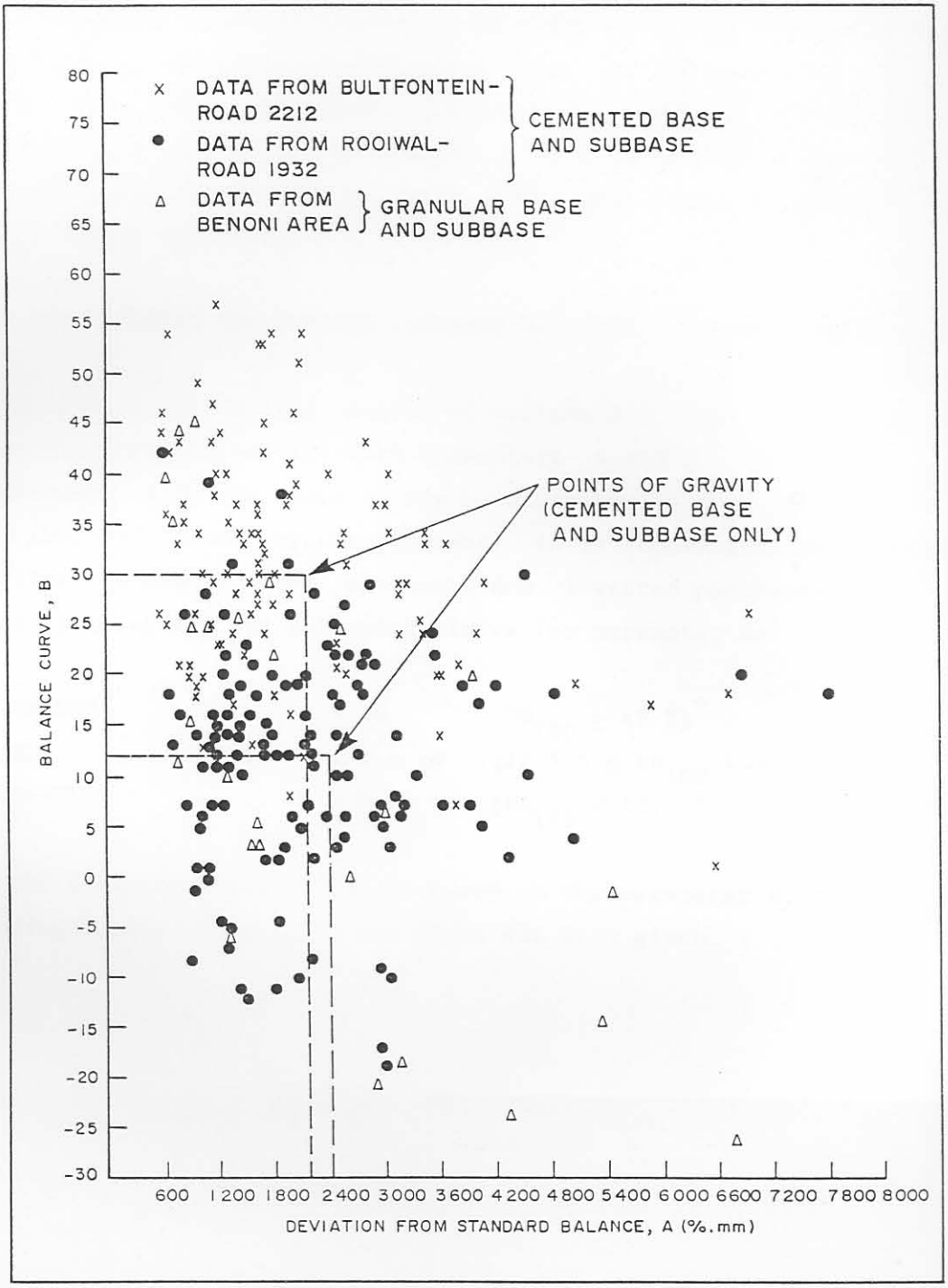

FIGURE 3.5

VARIOUS DCP-DATA INDICATING THE SPREAD IN THE RESULTS IN TERMS OF BALANCE AND DEVIATION FROM THE STANDARD PAVEMENT BALANCE CURVES

940-4-5729/5 BD

For Road 2212, with an average B value of 30, the upper pavement layers (base and subbase), contribute relatively more to the total pavement strength, in terms of total number of blows to penetrate the full pavement depth, than the lower layers. For Road 1932, however, with an average B value of 12, there is a relatively greater contribution by the lower layers to the total pavement strength. Thus the higher the value of B parameter, the greater the contribution to the total strength from the upper layers, and vice versa. From this example it is clear that the higher the B parameter the "shallower" the pavement structure and the lower the B parameter the "deeper" the pavement structure. This is analogous to BN used by Kleyn et al (1988), for the same purpose. Although most of the above data originated from pavements incorporating lightly cemented layers, parameters B and A of unbound granular pavement types also fall between the following limits:

$$-90 \leq B \leq +90 \quad \text{and}$$

$$0 \leq A \leq 10\,000$$

As indicated earlier, positive B values (or BN $\geq$ 12,5 %) are indicative of pavements decreasing in strength with depth, as is the case for most of the DCP data. On the other hand, negative B values (or BN < 12,5 %) are indicative of pavements increasing in strength with depth. This is generally the case where relatively weak upper layers and/ or rocky underlying layers are present within the defined pavement structure.

3.4 LIMITS FOR DEFINING THE VARIOUS PAVEMENT STRENGTH - BALANCE CATEGORIES

From experience with the balance curves of various DCP data it was decided to define three distinct ranges for both parameters A and B. In order to group together pavements with the same strength distribution from the top of the pavement to the full depth of the pavement, it is convenient to distinguish between shallow pavements, deep pavements and inverted pavements. This was accomplished by selecting the following limits for parameter B:

SHALLOW PAVEMENTS	:	$B \geq 40$	;$(BN_{100} \geq 42\ \%)^*$
DEEP PAVEMENTS	:	$0 \leq B < 40$	;$(12{,}5\ \% \leq BN_{100} < 42\ \%)$
INVERTED PAVEMENTS	:	$B < 0$	;$(BN_{100} < 12{,}5\ \%)$

* Although the classification system is based on the parameter B, the corresponding limits in BN_{100} of the SPBCs are also given.

In order to group pavements with the same state of "balance" together, it is convenient to distinguish between well - balanced, averagely balanced and poorly balanced pavement structures by selecting the following limits for parameter A:

WELL - BALANCED : $0 \leq A \leq 1200$
AVERAGELY BALANCED : $1200 < A \leq 3000$
POORLY BALANCED : $A > 3000$

These limits are illustrated in Figure 3.6, where they have been superimposed on the previous DCP data from Figure 3.5. Figure 3.6, with these limits, but without the DCP data, represents the pavement strength - balance or DCP classification sheet. By means of this approach, nine distinct pavement strength - balance or DCP categories are defined. These categories are summarised in Table 3.1.

TABLE 3.1 DEFINITION OF THE NINE DIFFERENT PAVEMENT STRENGTH - BALANCE CATEGORIES

LIMITS FOR PARAMETERS B AND A		DESCRIPTION OF CATEGORY
$B \geq 40$; $0 \leq A \leq 1200$;	(I)	WELL - BALANCED SHALLOW STRUCTURE (WBS)
$B \geq 40$; $1200 < A \leq 3000$;	(II)	AVERAGELY BALANCED SHALLOW STRUCTURE (ABS)
$B \geq 40$; $A > 3000$;	(III)	POORLY BALANCED SHALLOW STRUCTURE (PBS)
$0 \leq B < 40$; $0 \leq A \leq 1200$;	(IV)	WELL - BALANCED DEEP STRUCTURE (WBD)
$0 \leq B < 40$; $1200 < A \leq 3000$;	(V)	AVERAGELY BALANCED DEEP STRUCTURE (ABD)
$0 \leq B < 40$; $A > 3000$;	(VI)	POORLY BALANCED DEEP STRUCTURE (PBD)
$B < 0$; $0 \leq A \leq 1200$;	(VII)	WELL - BALANCED INVERTED STRUCTURE (WBI)
$B < 0$; $1200 < A \leq 3000$;	(VIII)	AVERAGELY BALANCED INVERTED STRUCTURE (ABI)
$B < 0$; $A > 3000$;	(IX)	POORLY BALANCED INVERTED STRUCTURE (PBI)

In Figures 3.7(a) and 3.7(b), various examples of the different categories are shown. These figures should be read together with Table 3.1. In Figure 3.8, the examples illustrated in Figures 3.7(a) and 3.7(b) are indicated on the DCP classification sheet.

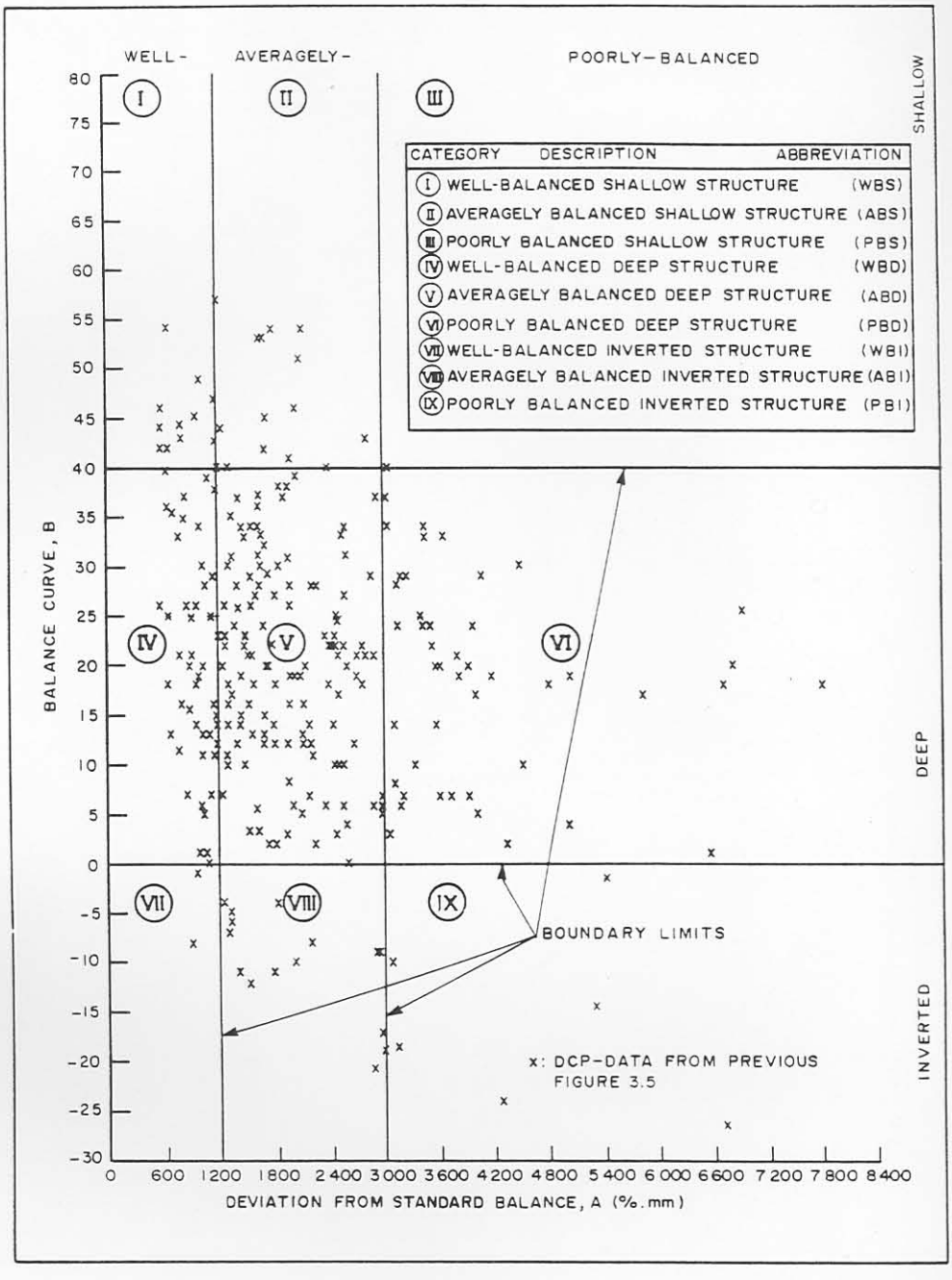

FIGURE 3.6

CLASSIFICATION LIMITS IN THE A AND B-PARAMETERS DEFINING THE NINE DIFFERENT CATEGORIES FOR THE DCP-DATA

940-4-5729/6 BD

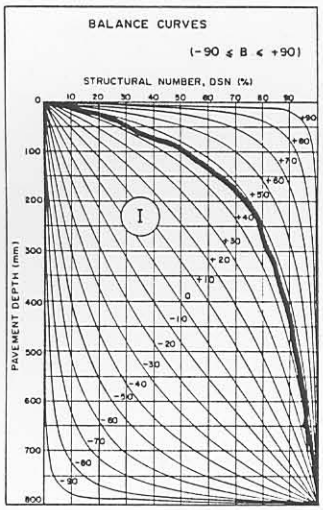

(a) WELL - BALANCED SHALLOW (WBS)

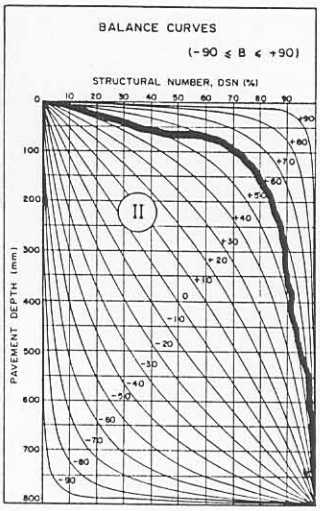

(b) AVERAGELY-BALANCED SHALLOW (ABS)

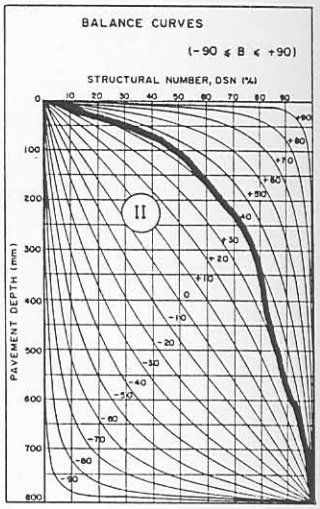

(c) AVERAGELY - BALANCED SHALLOW (ABS)

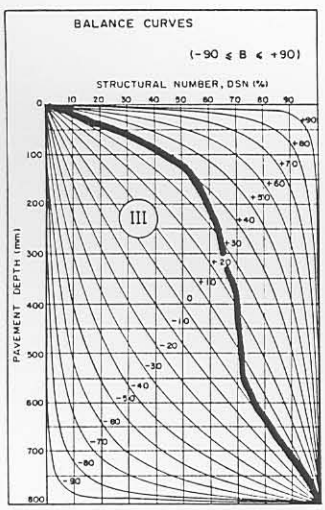

(d) POORLY - BALANCED SHALLOW (PBS)

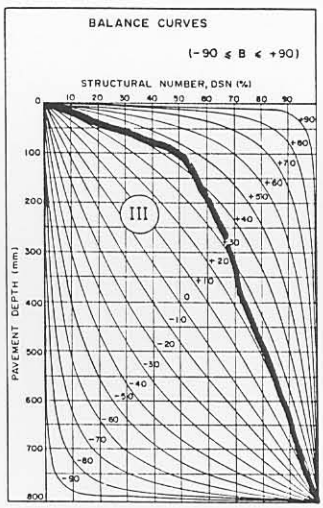

(e) POORLY - BALANCED SHALLOW (PBS)

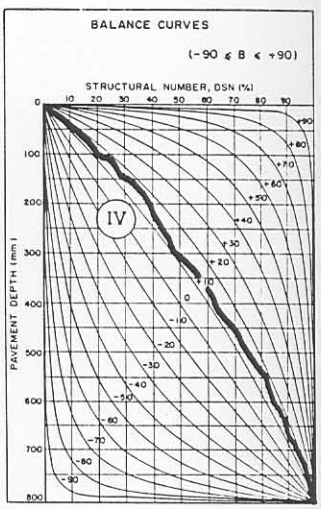

(f) WELL - BALANCED DEEP (WBD)

① : DCP CATEGORY

FIGURE 3.7(a)

EXAMPLES OF DIFFERENT DCP CATEGORIES

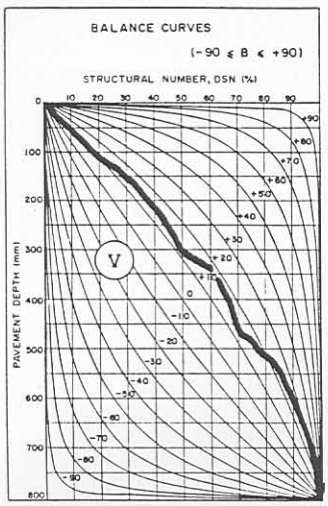

(a) AVERAGELY - BALANCED DEEP (ABD)

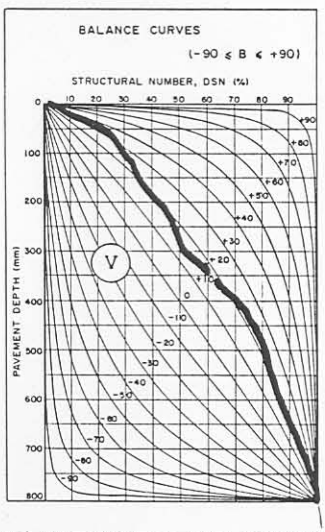

(b) AVERAGELY- BALANCED DEEP (ABD)

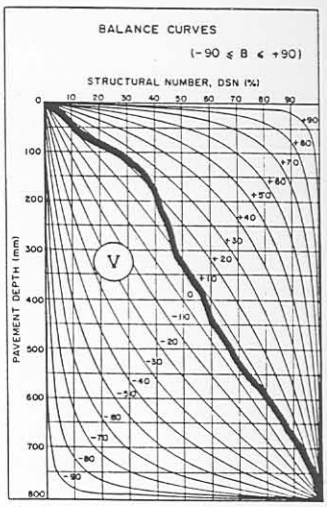

(c) AVERAGELY- BALANCED DEEP (ABD)

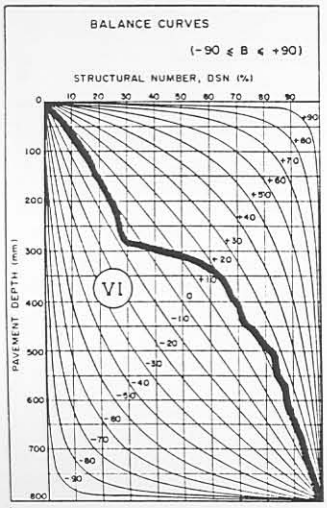

(d) POORLY - BALANCED DEEP (PBD)

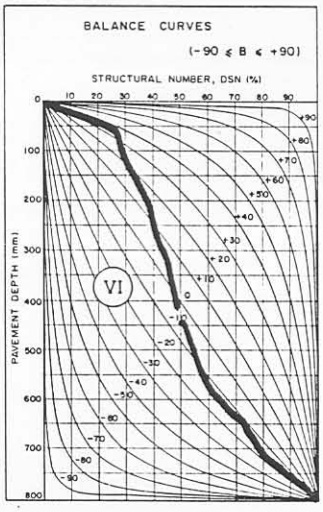

(e) POORLY - BALANCED DEEP (PBD)

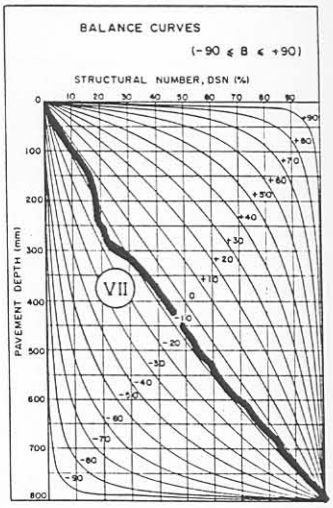

(f) WELL- BALANCED INVERTED (WBI)

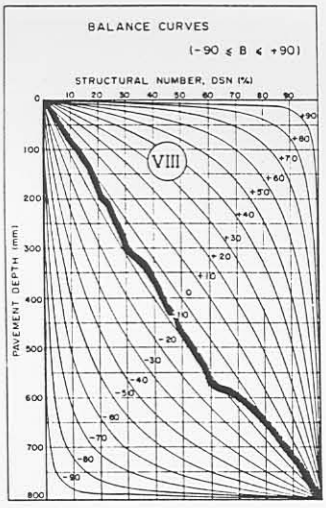

(g) AVERAGELY-BALANCED INVERTED (ABI)

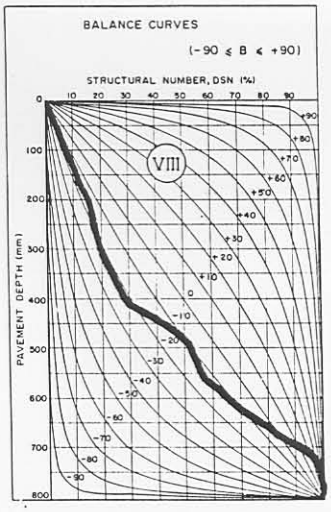

(h) AVERAGELY - BALANCED INVERTED (ABI)

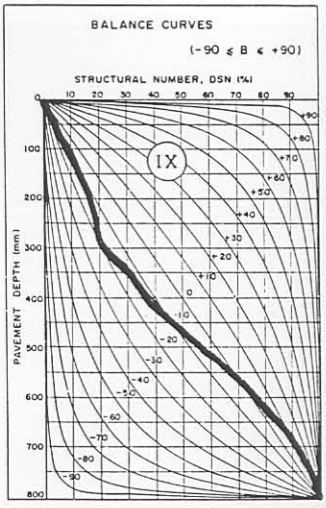

(i) POORLY - BALANCED INVERTED (PBI)

Ⓥ : DCP CATEGORY

FIGURE 3.7(b)

EXAMPLES OF DIFFERENT DCP CATEGORIES

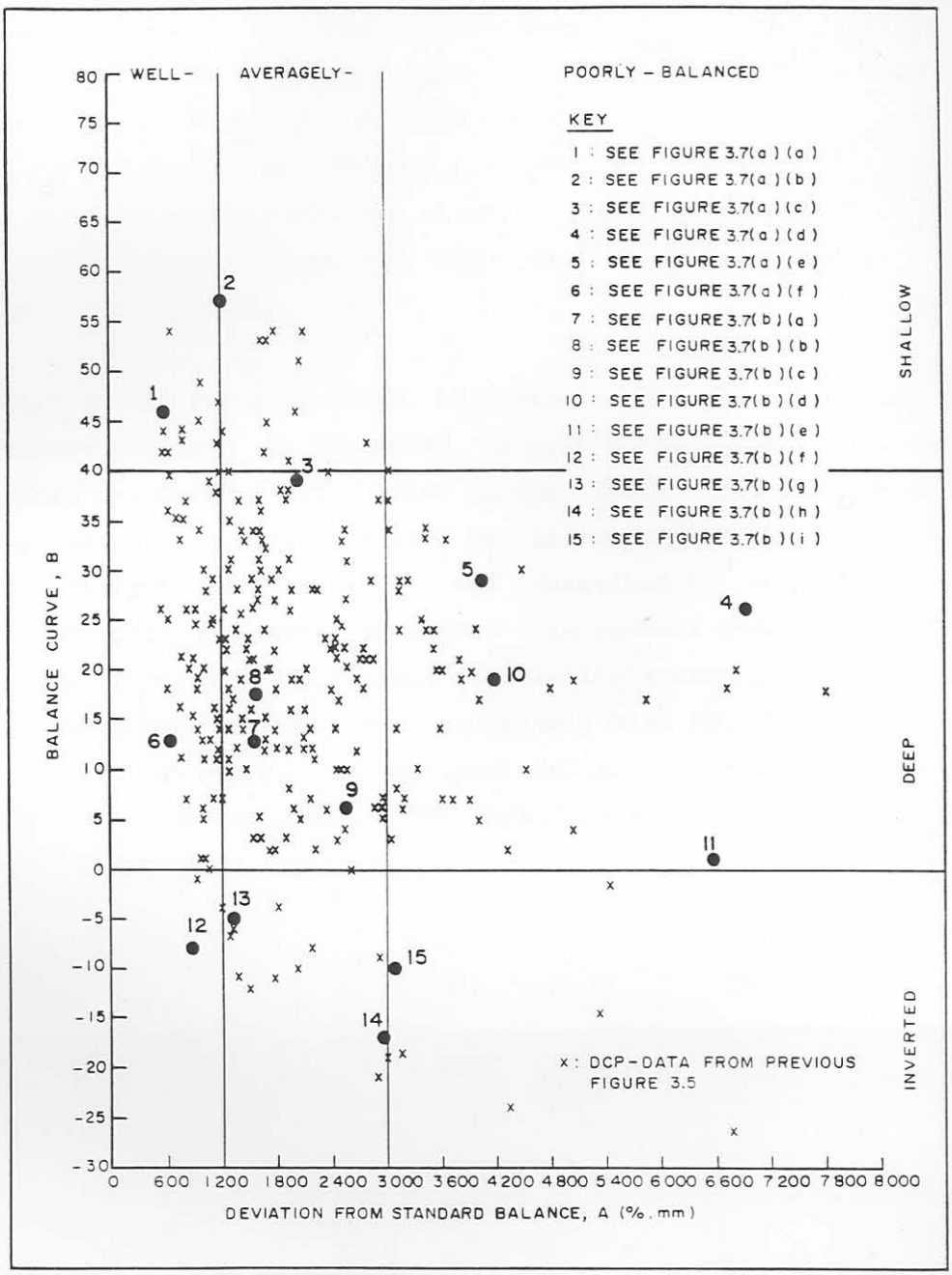

FIGURE 3.8

EXAMPLES OF THE DIFFERENT DCP-CATEGORIES ON THE DCP-CLASSIFICATION SHEET

940-4-5729/9 BD

3.5 INFERENCES FROM THE DCP DATA IN TERMS OF BALANCE

With the pavement strength - balance classification system defined, it is also possible to locate deviations in the balance of the pavement structure. This is accomplished by studying the balance curve of the data in relation to the "best fit" SPBC for the same data. In Figure 3.9 an example of DCP data and the related SPBC, B = 43, is illustrated. The figure shows relatively large deviations of (parameter A) the data from the related SPBC at depths of approximately 80 mm and 210 mm. There are discontinuities in the pavement structure at these depths. Normally this occurs when a relatively strong layer overlies a relatively weak layer, or vice versa. When parameter A_i increase towards the right of the SPBC, this is indicative of a relatively strong layer over a relatively weak layer, and vice versa if A_i decrease towards the left of the SPBC. These relative changes in A_i may occur on the positive side, both positve and negative, or the negative side of the SPBC (See Figures 3.10 and 3.11, later).

To distinguish more accurately between the layer interfaces, i.e. where these discontinuities occur within the pavement structure, a normalized curve of the deviations, A_i, at different depths in the pavement is compiled. The normalized curve for the DCP data of Figure 3.9, is illustrated in Figure 3.10. The figure shows that the deviations, A_i, vary with pavement depth, and can be either positive, zero or negative. Further, maximum and minimum values for parameter A_i reflect discontinuities within the pavement structure. The interfaces of the different in situ layers in the pavement structure are therefore defined by the depths where these maximum and minimum values for parameter A_i occur. By means of this approach, new layer thicknesses are defined on the basis of the relative strength of the in situ layers.

This is very useful in the evaluation of pavement structures, as the in situ pavement structure (layers) in the field is seldom the structure (layers) as designed, or what one assumes will exist in the field. Also indicated in the figure are the average penetration rates, DN, in mm per blow, for the different layers. The "strength" of the layers are described by their DN - values. Inspection of the normalized curve in Figure 3.10 reveals that an increasing and then decreasing A, with depth, reflects a relatively strong layer (relatively low DN) upon a relatively weaker layer (relatively high DN), and vice versa. In Figure 3.11, various examples of normalized deviation curves on Road 2212 at Bultfontein (Tvl), are illustrated. From this figure the variations in

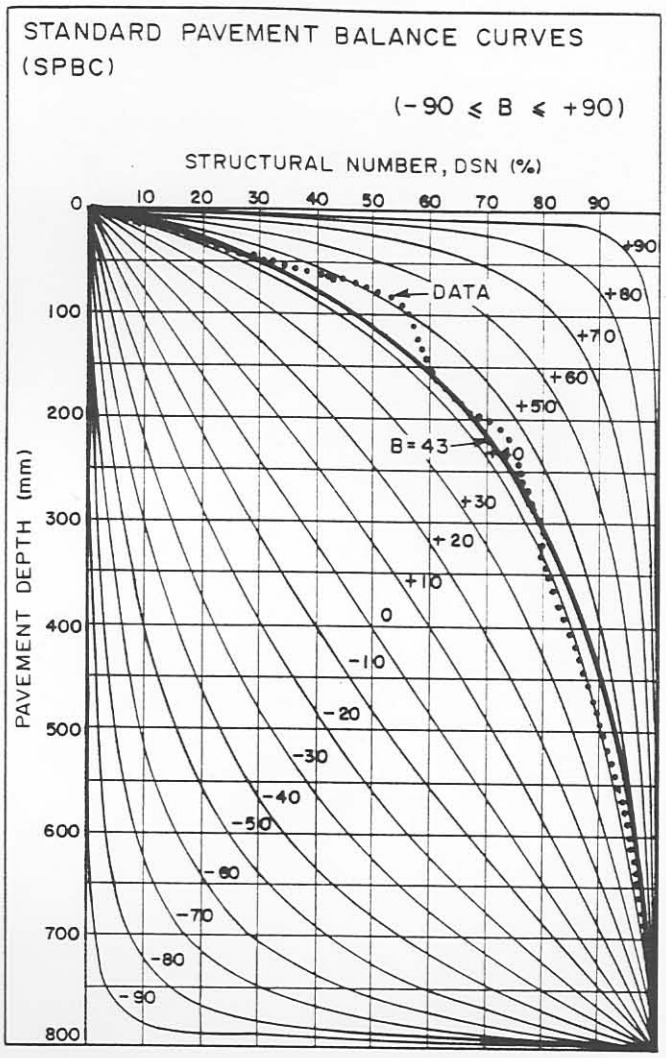

FIGURE 3.9

EXAMPLE OF DCP-DATA AROUND THE STANDARD PAVEMENT BALANCE CURVE, B = 43, FROM WHICH NORMALIZED CURVES OF THE DEVIATION ARE DRAWN

940-4-5729/10 BD

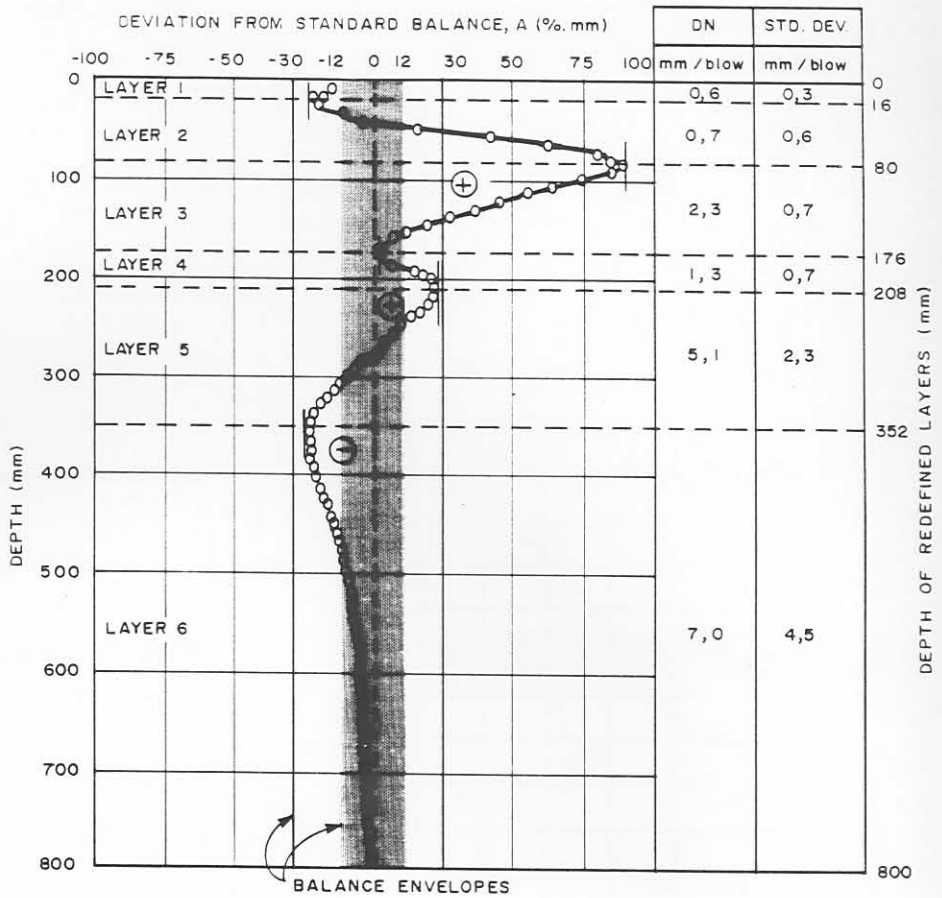

FIGURE 3.10

NORMALIZED CURVE OF THE DEVIATION (A) VS PAVEMENT DEPTH OF DCP-DATA FROM THE STANDARD PAVEMENT BALANCE CURVE, B=43

940-4-5729/11 BD

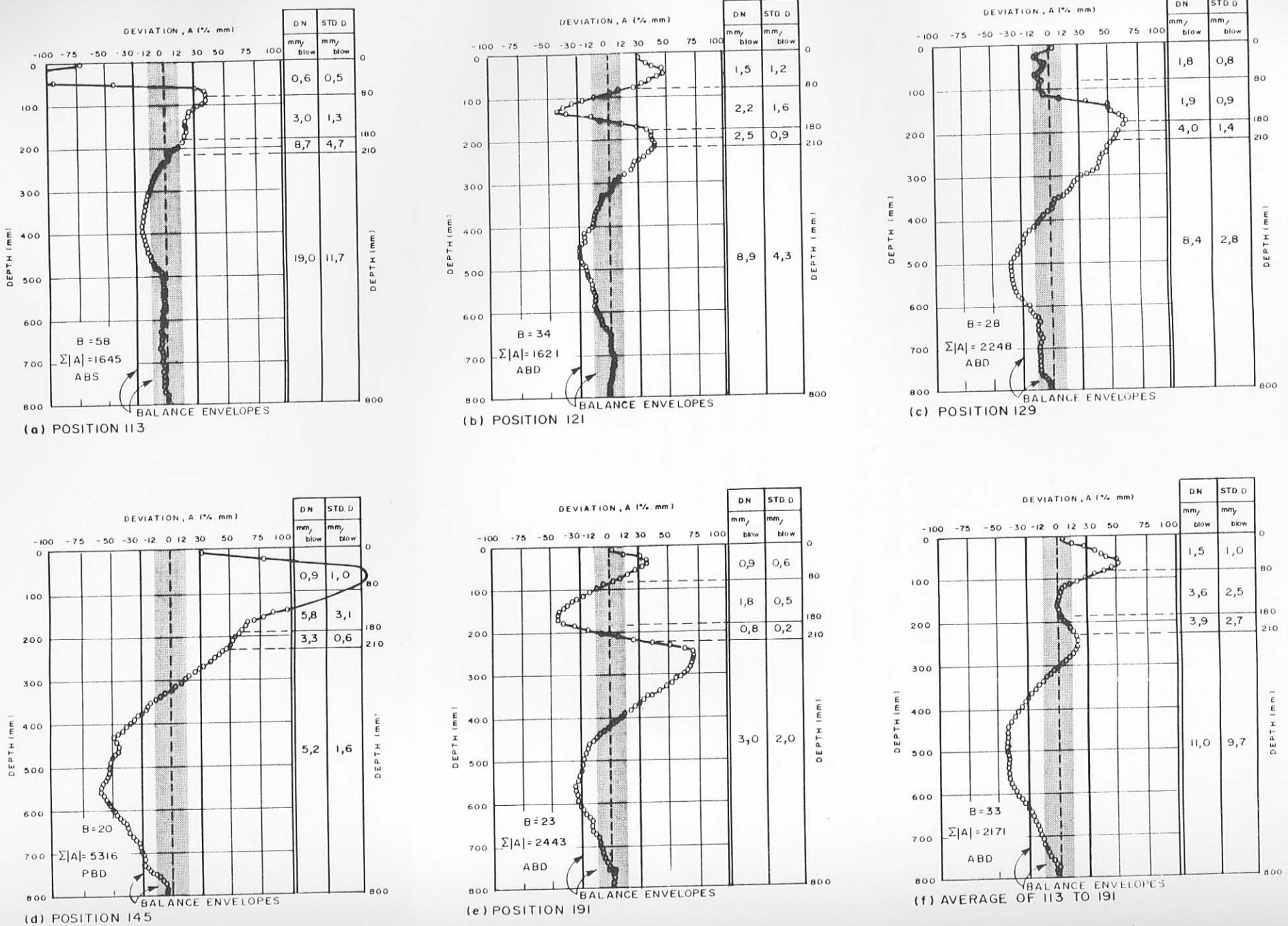

FIGURE 3.11 *VARIOUS EXAMPLES OF NORMALIZED DEVIATION CURVES ON ROAD 2212 AT km 12,65 (BULTFONTEIN, TVL)*

composition of the "same" pavement, as measured with the DCP, are obvious. This is very important information, not only for the analysis of basic pavement behaviour, but also for pavement rehabilitation design.

3.6 DCP COMPUTER PROGRAMS

Two **DCP computer programs** to evaluate the DCP data have been developed at the Division for Roads and Transport Technology. The names of these programs are **DCPB** and **AVEB** and they can be run on IBM compatible personal computers.
The program **DCPB** is used to evaluate DCP data measured at a **single** position, while program **AVEB** is used to evaluate the average of up to **50 individual DCP measuring positions**. Both programs calculate average penetration rates through the pavement for the different layers, including certain percentile values, depending on the category of the road under consideration.

The **pavement strength - balance classification** is done automatically, as is an evaluation of the **state of balance** including the **redefinition** of the thicknesses of the layers based on in situ measured strength.

In Appendix C the users manual, the data input as well as the output format of the various DCP programs are given. In Chapter 6 as well as in Appendix E, examples of the graphical output of the pavements studied in this dissertation using these programs, are also given.

3.7 SUMMARY AND CONCLUSIONS

In this chapter a **universal pavement classification system**, based on the **concept of strength - balance of pavements**, is described. The **strength - balance** of the pavement is calculated by means of the data obtained with the **Dynamic Cone Penetrometer (DCP).**

This **classification** is based on two unique parameters, B and A. **Parameter B** defines the **Standard Pavement Balance Curve (SPBC)** of the data, and **parameter A** describes the **state of balance** of the same data. The DCP data are classified into one of **nine possible pavement strength - balance categories.**
With this data the pavement can be classified as either a **shallow, deep or inverted pavement** structure, which can be either **well - balanced, averagely balanced or poorly balanced.**

Furthermore, the pavement can be divided into different layers, based upon the in situ measured strength, by using the variation in the deviation (parameter A) of the Standard Pavement Balance Curve (SPBC), with depth. These newly defined layer interfaces correspond to discontinuities within the in situ pavement structure and are **essential** in defining the pavement structure with regard to the **analysis and understanding** of **basic pavement behaviour**.

Two **DCP computer programs** have been developed to **analyse** and **classify** the DCP data in terms of the concept of **pavement balance**. Based on the relative DCP strength of the individual pavement layers, the failure mechanisms such as **permanent deformation** and **fatigue cracking** of pavements may also be explained.

It is my opinion that this method of classification, will be of great assistance in particular to inexperienced users of the DCP instrument as a pavement design and evaluation tool. It is further envisage that this universal method of classifying DCP data and hence flexible pavements, will contribute largely towards a sound **basis of comparison** between different pavements and different failure mechanisms of pavements in general.

The implementation of the pavement strength - balance classification system will improve current methods for designing new pavements and rehabilitating existing pavements, particularly in the developing countries in southern Africa where the existing road network needs to be extended or rehabilitated.

As mentioned earlier, this system was used to analyse all the DCP results in this study and it was found very helpful in the definition of the in situ pavements structure as well as changes in the pavement owing to traffic loading and certain moisture conditions.

Finally, it is recommended to apply this classification system (and the associated concepts) to other flexible pavement types, as well as the supporting structure of rigid pavements in order to verify and possibly adjust some the concepts indicated in this chapter for wider application.

3.8 REFERENCES

Chua, K M (1988). Determination of CBR and elastic modulus of soils using a portable pavement dynamic cone penetrometer. Proceedings of the First International Symposium on Penetration testing, ISOPT-1, Orlando, 20-24 March 1988.

KLEYN, E G, MAREE, J H and SAVAGE, P F (1982a). Application of a Portable Pavement Dynamic Cone Penetrometer to determine in situ Bearing Properties of Road Pavement Layers and Subgrades in South Africa. Proceedings of the Second European Symposium on Penetration Testing, 24-27 May 1982, Amsterdam, 1982.

KLEYN, E G and SAVAGE, P F (1982b). The application of the Pavement DCP to determine the Bearing Properties and Performance of Road Pavements. International Symposium on Bearing Capacity of Roads and Airfields, 23-25 June 1982, Trondheim, Norway, 1982.

KLEYN, E G, VAN HEERDEN, M J J and ROSSOUW, A J (1982c). An Investigation to determine the Structural Capacity and Rehabilitation Utilization of a Road Pavement using the Pavement Dynamic Cone Penetrometer. International Symposium on Bearing Capacity of Roads and Airfields, 23-25 June 1982, Trondheim, Norway, 1982.

KLEYN, E G, (1984). Aspects of Pavement Evaluation and Design as determined with the Dynamic Cone Penetrometer. M Eng thesis (in Afrikaans), Faculty of Engineering, University of Pretoria, Pretoria, 1984.

KLEYN, E G, FREEME, C R and TERBLANCHE, L J (1985). The Impact of Heavy Vehicle Simulator Testing in Transvaal. Proceedings of the Annual Transportation Convention, Session on Accelerated Testing of Pavements, S.350, Pretoria, CSIR, 1985.

KLEYN, E G, DE WET, L F and SAVAGE, P F (1987). The Development of an Equation for the Strength- Balance of Road Pavement Structures. Transvaal Provincial Administration, Roads Branch, Report L7/87, Pretoria, 1987.

LAMBE, T W and WHITMAN, R V (1969). Soil Mechanics. Massachusetts Institute of Technology, John Wily and Sons, Inc., New York, 1969.

LIVNEH, M and ISHAI, I (1987). Pavement and Material Evaluation by a Dynamic Cone Penetrometer. Proceedings of the Sixth International Conference on Structural Design of Asphalt Pavements. Ann Arbor, Michigan, 13-17 July 1987, Vol 1, 1987.

SCOTT, C R (1974). Soil Mechanics and Foundations. Applied Science Publishers Ltd, London, 1974.

CHAPTER 4

PERMANENT DEFORMATION BEHAVIOUR OF PAVEMENTS WITH LIGHTLY CEMENTITIOUS LAYERS

CONTENTS

4.1 INTRODUCTION

More than 80 percent of the pavement structures in the Province of the Transvaal incorporate lightly cementitious gravel base and/or subbase layers. This type of material is also often used by the other Provinces, as well as some of the independent and self governing states in southern Africa, because this material provides a relatively economical way of improving the structural strength (bearing capacity) of marginal granular materials. This type of material is also used on a large scale as subbase layers for bituminous base and granular base pavements in South Africa today (De Beer, 1985; Freeme et al, 1982; Freeme et al, 1984; Van Zyl et al, 1983; Otte, 1972, 1978).

Following a major study, undertaken by the Division for Roads and Transport Technology (DRTT) and the Directorate Roads Branch of the Transvaal Provincial Administration (TPA), on the behavioural characteristics of pavements with granular layers, the TPA requested the DRTT to investigate the structural characteristics of pavements with lightly cementitious gravel layers. The previous study on the granular materials was completed during the period 1978 to 1981, and is reported elsewhere (Maree, 1982; Kleyn et al, 1985).

This chapter discusses the permanent deformation characteristics of the series of Heavy Vehicle Simulator (HVS) tests on relatively deep - and relatively shallow pavements. The terms "deep" and "shallow" refers to the DCP-classification system described in Chapter 3. The Provincial numbers of these pavements are 1932 and 2212, respectively, and are situated north of Pretoria near the Rooiwal Power Station. Hereafter, they shall be referred to as Road 1932 (Rooiwal) for the relatively deep pavement and Road 2212 (Bultfontein) for the relatively shallow pavement.

In the discussion of the behaviour of these pavements, the following characteristics are addressed:

- Total permanent deformation on the surface (rutting) of the HVS test sections;

- permanent deformation at different depths in the pavement;
- rate of deformation in both relatively dry and relatively wet conditions and
- failure mechanisms occurring under accelerated testing.

4.2 BEHAVIOUR OA A DEEP PAVEMENT: ROAD 1932 (ROOIWAL)

In this section the emphasis will be on the permanent deformation characteristics of the deep pavement, as quantified under accelerated testing by the TPA - HVS.

4.2.1 Pavement structure and location of HVS - test sections

The layout of the various HVS test sections on this road is illustrated in Figure 4.1(a). The pavement sections were selected with the aid of the DCP, and according to these results a relatively deep pavement section was identified. (See Chapters 3 and 6 for detail DCP-classification and DCP-analysis of this pavement). The test wheel load as well as the tyre pressure used during HVS testing are also indicated on the figure and will be discussed in more detail in Paragraph 4.2.3.

In Figure 4.1(b), the general in situ pavement structure is illustrated. The figure indicates that the base and subbase were of C3-quality (TRH4, DRTT, 1985), stabilised with 3 percent Portland blastfurnace cement (PBFC). The parent material for both base and subbase layers, including the selected (G4) and in situ (G5) layers, is of a relatively good quality ferricrete. Stabilisation of the base and subbase however was necessary to reduce the plasticity and to improve the bearing capacity of these layers. According to the as-built records of TPA (Pienaar, 1979), the in situ material was non - plastic, with a grading modulus of approximately 2, and a CBR of approximately 45 percent at 100 percent modified AASHTO density.

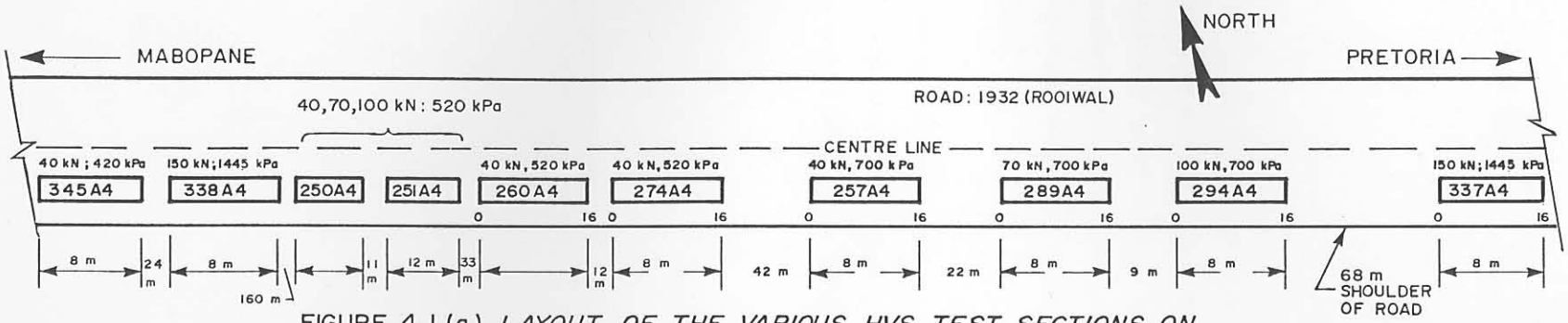

FIGURE 4.1 (a) *LAYOUT OF THE VARIOUS HVS TEST SECTIONS ON ROAD 1932 (ROOIWAL)*

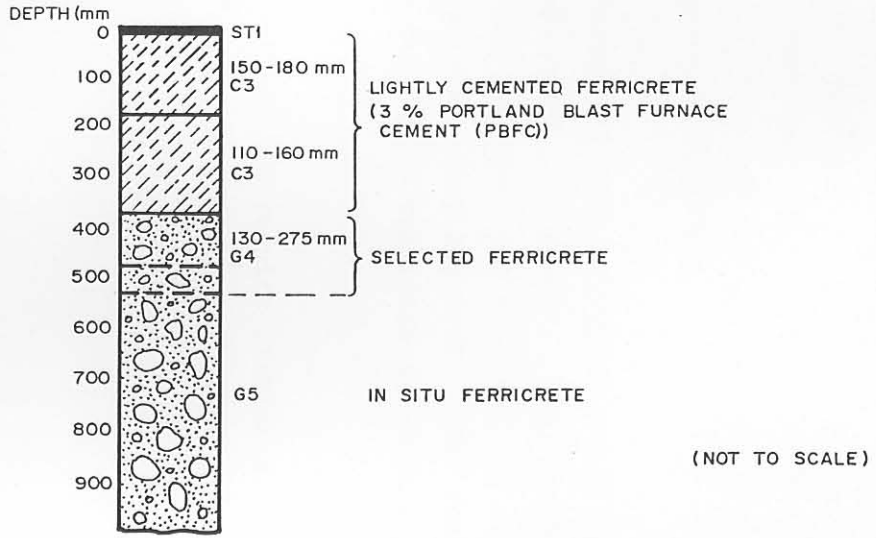

FIGURE 4.1 (b) *DETAIL OF THE RELATIVELY DEEP PAVEMENT STRUCTURE AT THE HVS SITE (km 2,9) ON ROAD 1932, NEAR ROOIWAL*

4.2.2 Original design considerations

The design was a typical TPA Class III pavement, designed to carry 0,4 to 1 million E80s (Transvaal Roads Department, 1978, Kleyn, 1988). Owing to the relatively good in situ material as well as the use of an above - average quality of material for the selected layers, a relatively deep pavement resulted (Kleyn et al., 1985).

According to the DCP structural capacity model, originally developed by Kleyn (1984) for relatively light gravel base and subbase pavements (Model 3 in Chapter 6), the structural capacity of this road is in excess of 10 million E80s. However, it must be noted that this model is not calibrated for pavements incorporating cementitious layers, and therefore the prediction of the structural capacity of such pavements is overestimated, and must be viewed critically especially if DCP-defined poorly-balanced or inverted pavements (Chapter 3, De Beer et al., 1988) are analysed. The reason for this is that the current DCP model for structural capacity is strictly a function of the DSN_{800}, which is the total number of blows taken to penetrate 800 mm of the pavement structure. It is my opinion that the model must be further calibrated and improved to compensate for structural imbalance as well as for inverted pavement structures, as a high DSN_{800} is not necessary an indication of a high structural capacity. A correction factor, however, is already introduced to compensate for in situ moisture content. Detailed analysis, however, of this model as well as the development of alternative models are discussed in Chapter 6.

In Appendix A, Table A.1, a summary of the design data for the base and subbase material of this pavement is given. The table indicates relatively good parent material for both the base and the subbase, but in order to achieve a relatively deep pavement with less erodible (pumpable) materials, it was decided to stabilise the materials for both layers.

According to the initial laboratory UCS-results (Tables A.1 and A.2, in Appendix A), a minimum of 3 per cent PBFC was necessary to provide a C3-quality material (TRH13, DRTT, 1986).

The pavement was constructed during 1978 and was approximately 7 years old at the start of HVS testing in 1985.

4.2.3 HVS test programmes on Road 1932 (Rooiwal)

A summary of the HVS test programmes followed on Road 1932 (Rooiwal) is given in Appendix A, Table A.3. On this pavement a total of 12 different HVS tests were done over a test period of approximately three years. During this period a total of 150 million E80s (r=4 in $(P/40)^r$) were applied to this road. The dual wheel load (P) varied between 40 kN and 100 kN, and tyre pressures between 420 kPa and 700 kPa. Two tests, however, were done at excessively high single wheel loadings, using an aircraft wheel (Boeing 747). The single wheel load for the two tests was 150 kN, with tyre pressures varying between 960 kPa and 1445 kPa (see Table A.3, HVS-Sections 337A4 and 338A4, in Appendix A). During most of the test periods, in situ moisture (relatively dry and natural rain) temperature conditions prevailed. Moisture was also introduced artificially on the surface as well as in depth of the pavement at selected intervals.

4.2.4 Permanent deformation behaviour and failure mechanism

The permanent deformation (plastic deformation, rutting), as a direct result of traffic loading, measured on the surface of the pavement is normally used to describe the state and behaviour of the pavement. This is also one of the primary indicators of the behaviour of HVS test sections under accelerated testing.

Detailed analysis into the prime reasons for the development and origin of the permanent deformation, facilitates the accurate identification of the failure mechanism of the pavement, and is therefore of utmost importance to be done effectively.

4.2.4.1 Permanent deformation on the surface (rutting)

Typical permanent deformation behaviour, as measured under a 3 m straight edge is illustrated in Figure 4.2(a) and (b). The figures indicate the average maximum permanent deformation development on the

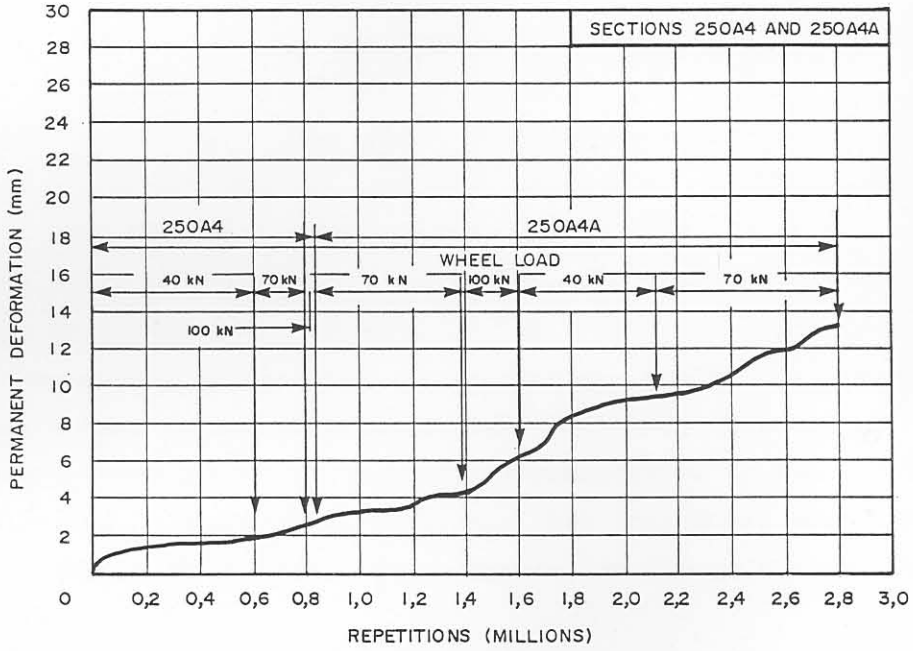

(a) HVS SECTIONS 250A4 AND 250A4A

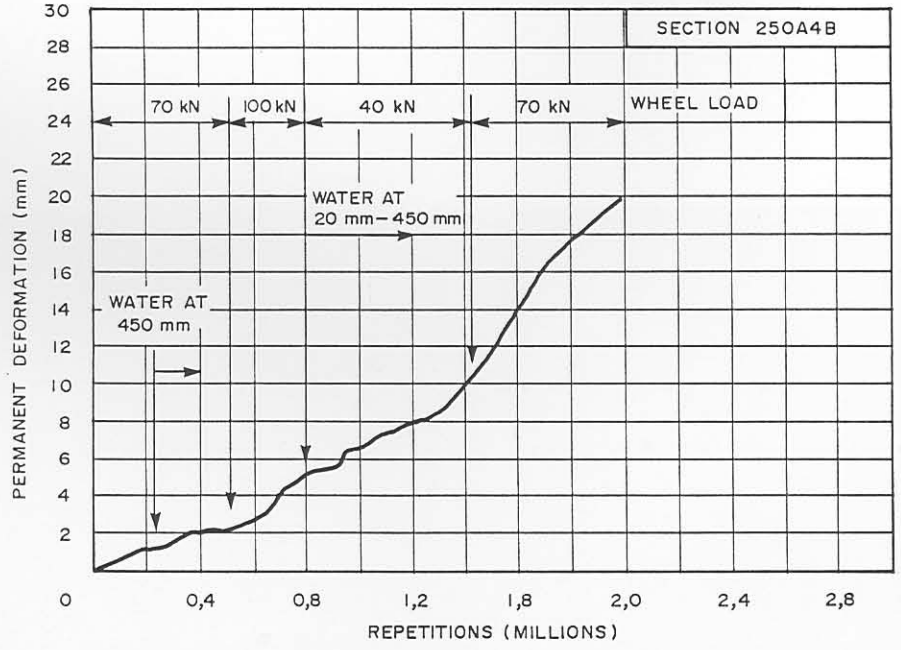

(b) HVS SECTION 250A4B

FIGURE 4.2

AVERAGE PERMANENT DEFORMATION AS MEASURED IN HVS TESTS 250A4, 250A4A AND 250A4B UNDER INDICATED DUAL WHEEL LOADS ON ROAD 1932 (ROOIWAL)

surface of the test sections after various stages of trafficking, loading and under certain moisture conditions. In general, the figures indicate that the rate of deformation (per wheel load) is linear for all practical purposes, and increase with the introduction of surface water especially (mostly rain) on the sections. The permanent deformation results of the rest of the HVS test sections are illustrated in Appendix A, Figures A.1, A.2 and A.3.

Excessive potholing, however, resulted on Sections 251A4, 275A4 and 294A4 (See Figures A.1(a)), A.2(b)) and A.3(b), in Appendix A). On the two latter sections, it was found that the top 50 mm to 75 mm of the cemented gravel base was pumped out, resulting in potholes, while the rest of the base and the subbase, although fatigued, was structurally sound. According to the DCP-results, before and after HVS testing, the top 50 mm to 75 mm of the base material had decreased in strength, indicating an effective weakening in the cemented material. This crushing was primarily responsible for the loss of support to the asphalt surfacing layer (13 mm/6 mm double seal in this case). These HVS tests, again, demonstrate the destructive effect of water under pressure (excessive porewater pressure state, EPWP) in this weak upper layer, which caused the ultimate failure (potholing) of this pavement.

4.2.4.2 Permanent deformation at different depths

On four of the HVS test sections, viz Sections 260A4, 274A4, 275A4 and 294A4, permanent deformation at different depths in the pavement were measured using the Multi-depth deflectometer (MDD). The MDD is normally used to measure the depth deflections in accelerated testing of pavements in South Africa (De Beer et al., 1988), but are also used to measure permanent deformation at different depths by studying the permanent change in the vertical position of these instruments (LVDTs). In Figure 4.3 the layout of the MDD instrumentation in the test sections is illustrated. The figure indicates that the MDDs were located at different depths in the pavement structure, mostly at the various layer interfaces.

In Figures 4.4 (a), (b) and (c), typical permanent deformations at different depths and at various stages of trafficking are illustrated.

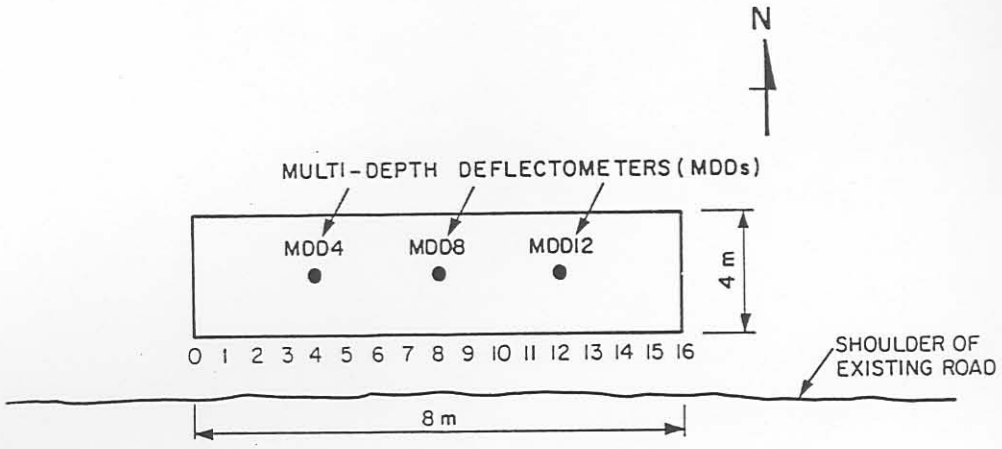

(a) Typical layout of an HVS test section

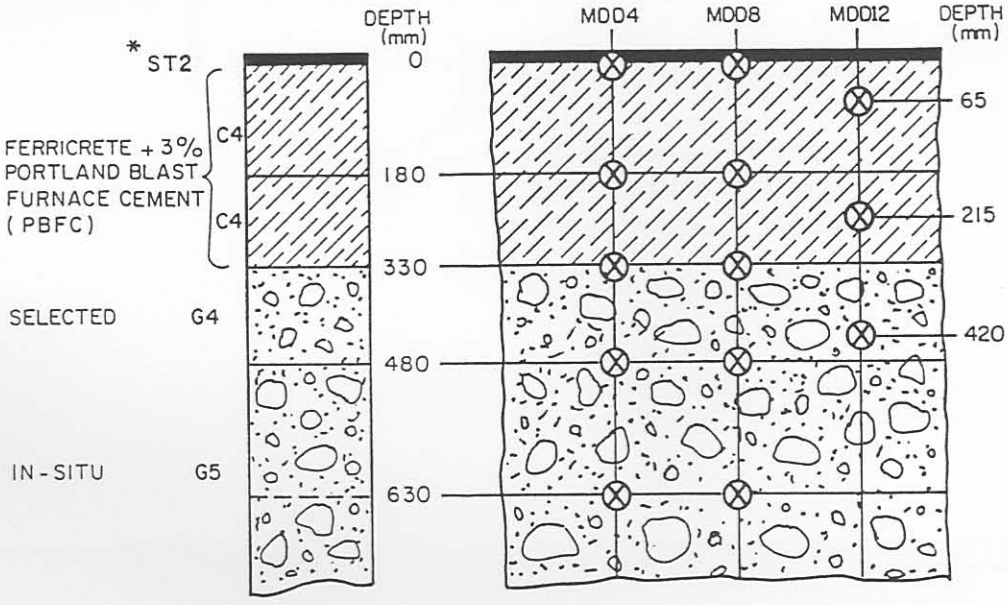

*MATERIAL CODES IN ACCORDANCE WITH TRH14 (NITRR, 1985)

⊗ MDD MODULES

(b) Pavement structure and MDD layout

FIGURE 4.3

LAYOUT OF HVS TEST SECTIONS FOR PERMANENT DEFORMATION MEASUREMENTS ON ROAD 1932 (ROOIWAL)

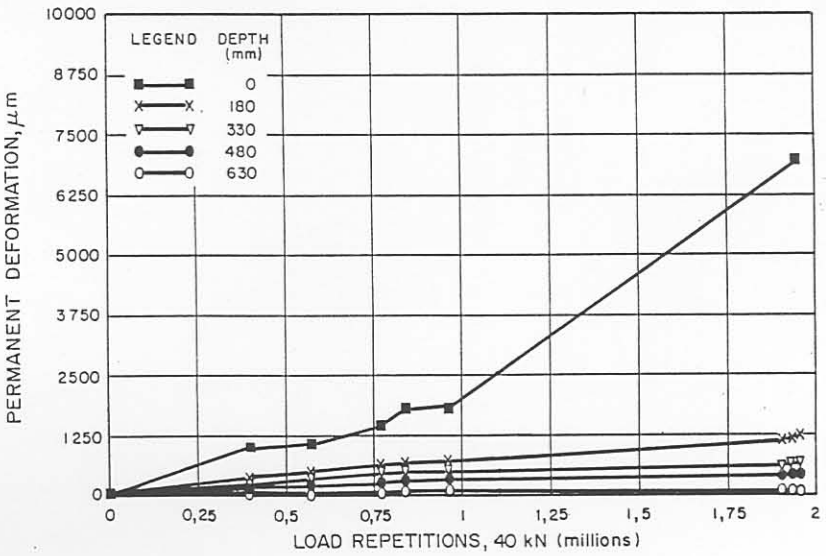

(a) MDD4

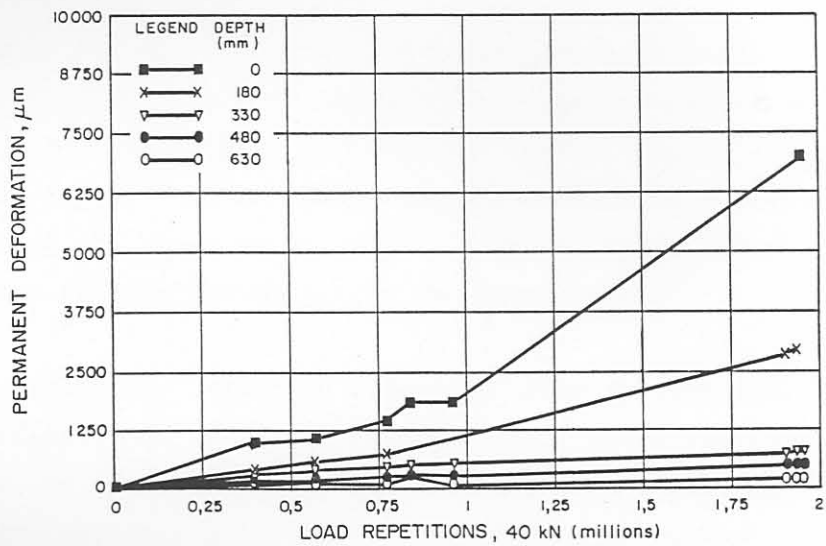

(b) MDD8

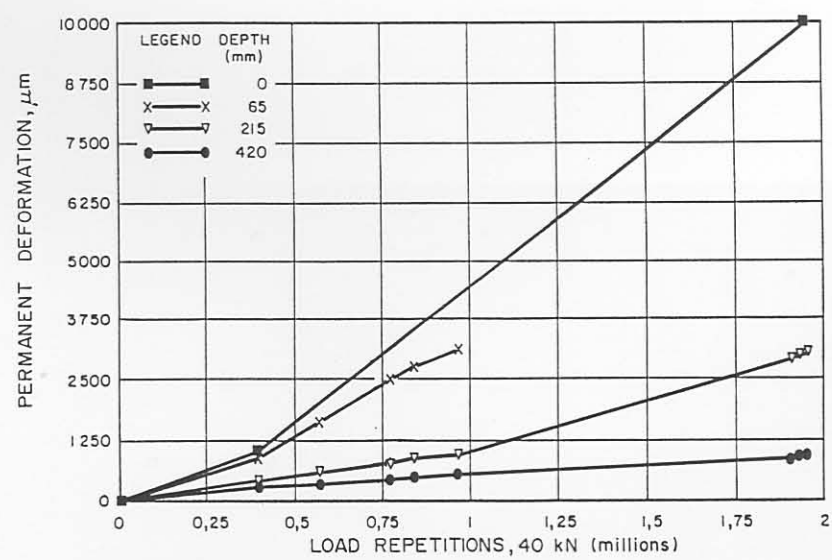

(c) MDD12

FIGURE 4.4

PERMANENT DEFORMATION AT DIFFERENT DEPTHS AT VARIOUS STAGES OF TRAFFICKING ON HVS TEST SECTION 260A4 (ROAD 1932,ROOIWAL)

For the rest of the test section these permanent deformations are illustrated in Appendix A, Figures A.4, A.5, A.6. The figures indicate that most of the deformation occurred between 0 mm and 180 mm, that is, in the cemented gravel base layer, and increase towards the end of the tests.

In Table 4.1, a summary of the average percentage permanent deformations in the different layers, at the end of the various tests, are given. The table indicates that approximately 67 per cent of the permanent deformation in the relatively dry state and approximately 75 per cent of the permanent deformation in the relatively wet state, occurred in the base layer only. This is indicative of the crushing failure mechanism in the base layer, discussed in the following section.

4.2.4.3 Crushing failure mechanism

Test pits made after HVS testing on all these test sections confirmed that a crushed zone of approximately 50 mm to 75 mm developed directly under the seal in the top of the base layer, as a result of trafficking.

Back - analysis of the effective elastic moduli of the base layer, using linear elastic analysis (based on measured depth deflections, (MDD)), indicates a marked reduction in effective elastic moduli of the base layer, thereby indicating a weakening, ie crushing in this case, of the layer (see Chapter 6, as well as De Beer, 1986a, 1986b, 1986c, 1986d).

It must, however, be emphasised that this failure mechanism is strictly associated with relatively deep pavements because the deeper strength of the pavement structure provides relatively strong support to the upper layers in the system, thereby increasing the repetitive stresses in the upper section of the base layer. These higher stresses then initiate the compression failure (crushing) in the base layer.

This failure mechanism, which is different from the classical fatigue failure associated with cemented road building materials (Otte, 1972, 1978), led to the development of the "**crushing life**" concept for lightly cemented gravel pavement materials. According to published research on the compression failure of lightly cemented materials, compression

failure (crushing) of the materials occurs at low compressive strains, ie at approximately one (1) per cent axial strain (see Chapter 5 for detailed analysis of these strains). Using this definition of crushing failure, together with permanent deformation measurements at the different depths in the above mentioned test sections, the **crushing life span, Nc**, for the different test sections could be determined. It was shown that Nc was more a function of the tyre contact pressure on the roads surface, than the load. Detailed description and analysis of this crushing failure is given in Chapter 5.

TABLE 4.1 AVERAGE PERCENTAGE PERMANENT DEFORMATION MEASURED AT THE END OF THE HVS TESTS ON THE VARIOUS TEST SECTIONS (%)

DEPTHS (mm)	RELATIVELY DRY STATE	RELATIVELY WET STATE
0-180	67 (17)	75 (7)
180-330	9 (4)	11 (7)
330-480	10 (7)	7 (3)
480- ∞	14 (9)	7 (2)

( ) Standard deviation

4.2.4.4 Rate of permanent deformation, R_L, and relative damage

The structural life (capacity) of a pavement may be defined in many different ways. One method is to determine the number of equivalent standard 80 kN axles (E80s) which will cause a specific level of permanent deformation on the pavement. Normally, a terminal level of 20 mm deformation over a certain length of the road (depending on the road category (TRH4, DRTT, 1985a), at the end of the structural design period, is selected. With this definition of structural life of the pavement, no identification is given to the actual failure mechanism nor the effective rate of failure (deformation).

It is, however, my opinion that the permanent behaviour of pavements, and hence structural capacity, may be better described by using the **rate of deformation**, rather than the total number of E80s carried during the structural life of the pavement. Kleyn et al (1985) indicates that this

rate of failure may be seen as representing the "absolute damage rate" of a particular load on a particular pavement. The rate of permanent deformation, R_L, of a pavement in terms of mm per million load repetitions at a particular load, L, affords a very useful means of describing the structural life of pavements, and may assist in better defining the failure mechanism associated with that pavement.

Furthermore, the deformation rate for a standard (P=40 kN) wheel load may then be seen as indicating the basic bearing capacity for that pavement. Comparing the deformation rate of a wheel load with the standard wheel load would give the relevant equivalency factor, D_L. By applying the relative damage formula $D_{80} = (P/40)^r$, the relative damage coefficient, r, relating the rate of damage, may then be calculated (Kleyn et al., 1985).

The different R_L and D_L-factors for the various test sections on Road 1932 (Rooiwal) is summarised in Table 4.2. The table indicates that the rate of deformation increases with increased wheel load and moisture conditions. In this case then "dry" refers to the in situ moisture condition of the base layer, which was approximately optimum (before stabilisation) plus 2,5 per cent. "Wet" refers to the moisture condition of the base layer after rain or the artificial introduction of water on the test section, and was approximately optimum plus approximately 3,5 per cent. On average the rate of deformation, R_L, during the "wet" conditions is approximately 2,7 to 3,8 times higher then during the "dry" conditions on this pavement.

In Figure 4.5 the rate of permanent deformation for various wheel loads and moisture contents on this pavement is illustrated. The effect of wheel load and moisture content of the base layer is well illustrated on the figure.

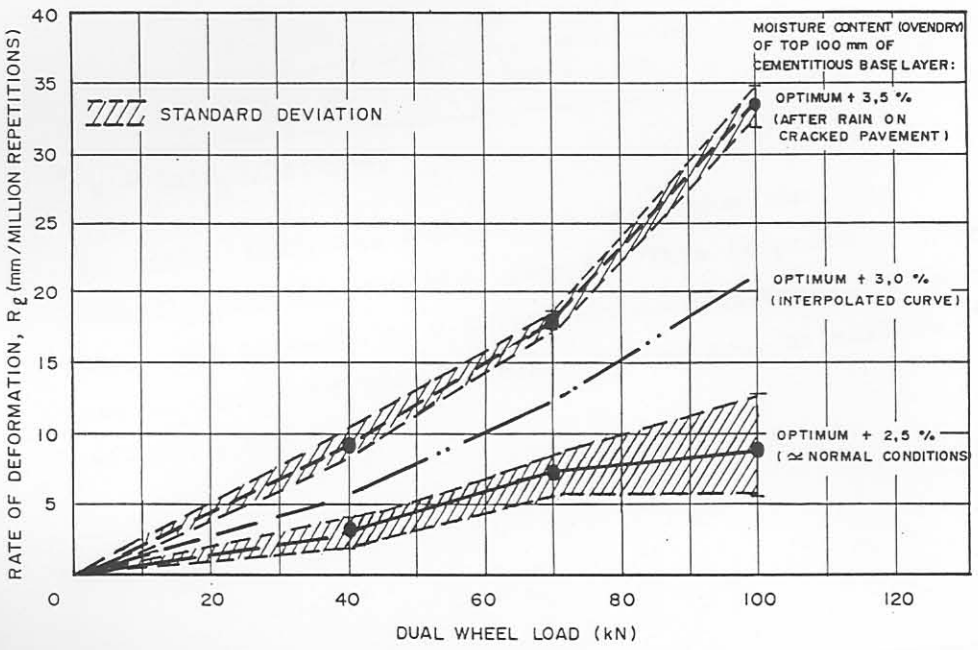

FIGURE 4.5

RATE OF PERMANENT DEFORMATION (R_ℓ) FOR VARIOUS DUAL WHEEL LOADS AND MOISTURE CONDITIONS ON A RELATIVELY DEEP PAVEMENT WITH LIGHTLY CEMENTITIOUS BASE LAYERS (SITE: ROAD 1932, ROOIWAL)

940-4-5900/26 BD

TABLE 4.2 PAVEMENT PARAMETERS OF ROAD 1932 (ROOIWAL)

HVS-SECTION	R_L-FACTOR, mm/million reps					D_L*			
	P=40 kN		P=70 kN		P= 100 kN		P=70 kN		P=100 kN	
	DRY	WET	DRY	WET	DRY	WET	DRY	WET	DRY	WET
250A4	3,33	-	6,36	-	8,75	-				
250A4B	-	8,33	5,00	18,18	12,50	-				
251A4	-	-	7,50	-	-	35,00				
260A4	2,50	9,48	-	-	-	-				
274A4	3,33	8,33	-	-	-	-				
275A4	2,50	11,33	-	-	-	-				
289A4	-	-	8,75	17,50	-	-				
294A4	-	-	-	-	5,56	32,35				
AVERAGE	2,92	9,37	6,90	17,84	8,94	33,68	2,36	1,90	3,06	3,59
STD. DEV.	0,48	1,41	1,60	0,48	3,47	1,87				

* $D_L = R_L(P)/R_L(40) = (P/40)^r$, with P=trafficking wheel load and
r= relative damage coefficient

In Table 4.3 the average relative damage coefficients, r, for this road are summarised. It must, however, be emphasised that although r is the coefficient equating the **rate in deformation** in this case, it is the same as the relative damage coefficient normally used for the **absolute deformation** after a specified number of repetitions because the rate of deformation is taken as approximately linear, in the cases discussed in this dissertation.

TABLE 4.3 AVERAGE RELATIVE DAMAGE COEFFICIENT, r^* (ROAD, 1932)

70 kN		100 kN	
DRY	WET	DRY	WET
1,53	1,15	1,22	1,39

* $r = \ln(D_L)/\ln(P/40)$

The table indicates that r is less than the value of 4, which is normally used for relative damage. This is probably related to the fact that this pavement is a relatively deep pavement, which is normally not as load sensitive in terms of fatigue, as shallow pavements (Kleyn et al., 1985).

4.2.4.5 In situ densities and moisture contents

In situ nuclear dry density (drilled through the cemented layers) and oven dried moisture contents were measured on all the test sections concerned to investigate the effect of traffic loading on these parameters. These measurements were taken on the section as well as outside the tested area (positions A,B,C and D), using test pits (see Figure 4.6), in all the pavement layers.

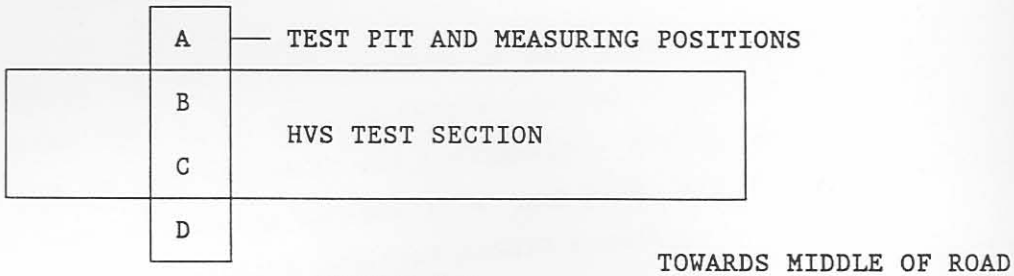

FIGURE 4.6

TYPICAL LAYOUT OF A TEST PIT ON THE HVS TEST SECTION AFTER HVS TESTING

The actual measurements are summarised in Table A.5, in Appendix A. The results indicate that some densification on Sections 250A4A and 250A4B, occurred inside the trafficked area (positions B and C). On the rest of the sections some de-densification was measured, with the highest on Section 294A4. The de-densification on this section (top 50 mm of the base layer) varied between 0,74 per cent and 4,84 per cent, if the inside density (B and C) is compared to that outside (A and D) the test area. This is an indication of the crushing effect in the base, which was mentioned in Paragraphs 4.2.4.2 and 4.2.4.3. It must be noted, however, that it appears that the nuclear apparatus did not always indicate the crushing as a de-densified zone, as most of the density measurements were taken in a drilled hole through the upper 100 mm of the cemented base, while close observation in the test pits confirmed that the thickness of the crushed zone was approximately 50 mm to 75 mm. In most cases large areas of this crushed zone were pumped out as a result of an excessive porewater pressure state, and it was not possible to measure the densities very effectively. In general, the in situ moisture contents of the upper layers (> 400 mm) appears to be higher than those of the deeper layers, and is believed to be related to rain and surface water ingression.

4.3 BEHAVIOUR OF A SHALLOW PAVEMENT: ROAD 2212 (BULTFONTEIN)

As for the deep pavement, the emphasis will be on the permanent deformation behaviour of this pavement, as was quantified under accelerated testing with the TPA - HVS.

4.3.1 Pavement structure and location of HVS - test sections

In Figure 4.7 (a), the layout of the various HVS test sections on this road at km 12,6 is illustrated. These pavement sections were selected by using the DCP, and according to these results a relatively shallow pavement section was identified (see also Chapter 6, for detail DCP-classification and analysis of this pavement). The test wheel load as well as the tyre pressure used during testing are also indicated in the figure, and will be discussed later in more detail in Paragraph 4.3.3.

In Figure 4.7 (b), the general in situ pavement structure is illustrated. The figure indicates that the base and subbase were of C3 and C4-quality (TRH4, DRTT, 1985a), stabilised with 3 and 2 per cent Portland blastfurnace cement (PBFC), respectively. The parent material for both base and subbase layers, including the selected (G4) and in situ (G5) layers, is of a relatively good quality mix granophyre and ferricrete (see Marais, 1981). Stabilisation of the base and subbase however was necessary in order to reduce the plasticity and to improve the bearing capacity of these layers.

According to the as - built records of TPA (Marais, 1981), the selected layers were 110 mm to 120 mm ferricrete and a 140 mm layer of river sand. The in situ material was a slightly - plastic ferricrete, with a grading modulus varying between 1,74 and 2,34, and a CBR approximately 30 percent at 97 percent modified AASHTO density.

At the time of selecting the test sections, DCP measurments as well as observations in an open test pit, indicated that there was a relatively

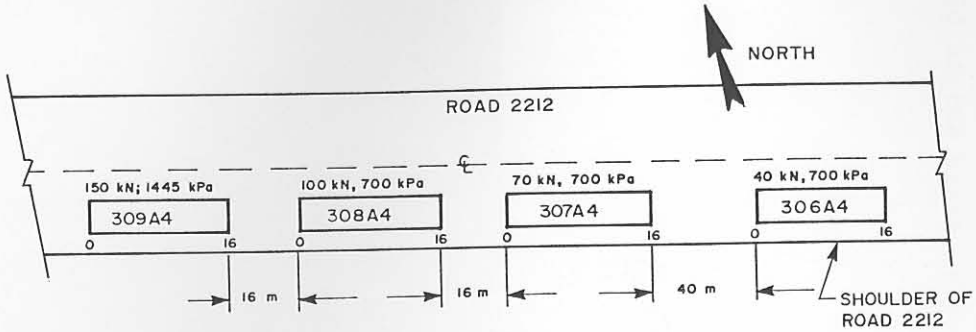

FIGURE 4.7 (a) *LAYOUT OF THE VARIOUS HVS TEST SECTIONS ON ROAD 2212, BULTFONTEIN*

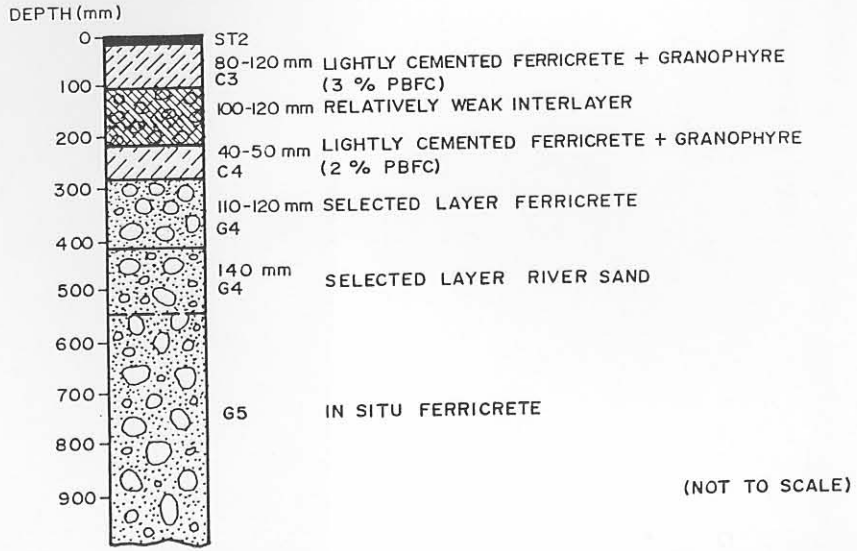

FIGURE 4.7 (b) *DETAIL OF THE RELATIVELY SHALLOW PAVEMENT STRUCTURE AT THE HVS SITE AT km 12,6, ON ROAD 2212 NEAR BULTFONTEIN*

weak zone of approximately 100 mm to 120 mm between the base and subbase layer (see Figure 4.7 (b)). According to the theory of the strength balance (DCP-defined) of pavements (see Chapters 3 and 6), it was suspected that this weak zone would have a marked effect on the permanent deformation behaviour of this pavement. The test pit detail and the DCP, showed the base layer (80 mm to 120 mm) to be relatively well-cemented with in situ UCS of approximately 3 MPa. The relatively weak support underneath the base made the pavement load sensitive and therefore fatigue failure of the base should dominate the behaviour. This, however, will be discussed later in more detail in Chapter 7.

4.3.2 Original design considerations

This typical TPA Class II pavement was designed to carry 0,2 to 0,4 million E80s (Transvaal Roads Department (TPA), 1978; Marais, 1981). Owing to the relatively weak in situ material as well as the use of average quality material for the selected layers, a shallower pavement than the previously discussed deep pavement resulted. Detailed analysis of the DCP-results, however, is discussed in Chapter 6.

In Appendix A, Tables A.6 and A.7, a summary of some of the original design data for this pavement is given, and indicate characteristics of the parent material for both the base and the subbase. As this was a TPA-Class II pavement, and the fact that the material was plastic, stabilisation was necessary to achieve less erodible (pumpable) materials for both the base and subbase of this pavement. According to the initial laboratory UCS-results (Appendix A, Table A.7, a minimum of 3 per cent PBFC was necessary in order to provide a C3 - quality base material and 2 per cent PBFC to provide a C4 - quality subbase material (TRH13, DRTT, 1986).

This pavement was constructed during 1981 and was approximately 6 years old at the start of HVS testing during 1987.

4.3.3 HVS test programmes on Road 2212 (Bultfontein)

A summary of the HVS test programme followed on Road 2212 (Bultfontein, Transvaal) is given in Appendix A, Table A.8.

On this road a total of 4 different HVS tests was done over a test period of 19 months. During this period a total of almost 129 million E80s (r=4 in $(P/40)^r$) was applied to this road. The dual wheel loading (P) varied between 40 kN and 100 kN, with a tyre pressure of 700 kPa. One test on this pavement, however, was done at an excessively high single wheel loading, using an aircraft wheel (Boeing 747), similar to two additional tests on the deep pavement (Road 1932 at Rooiwal), (see later in Paragraph 4.4). The single wheel load for these latter tests was 150 kN, with a tyre pressure varying between 960 kPa and 1445 kPa (see Appendix A, Table A.8, HVS-Section 309A4). Detailed discussions of these tests are given in Paragraph 4.4.

HVS testing was done during in situ moisture and natural temperature conditions up to approximately one million load repetitions. Water was introduced artificially on the surface as well as into the pavement after approximately one million repetitions on Sections 306A4, 307A4 and 308A4.

4.3.4 Permanent deformation behaviour and failure mechanism

Permanent deformation as a direct result of trafficking as measured on the the surface of the pavement (as mentioned for the deep pavements), is used to describe the state and behaviour of the pavement. It is also one of the primary indicators of the behaviour of the HVS test sections on this relatively shallow pavement under accelerated testing.

4.3.4.1 Permanent deformation on the surface (rutting)

The permanent deformation behaviour, as measured under a 3 m straight edge, of the various test sections is illustrated in Figure 4.8 (a), and (b) and Figure 4.9. The figures indicate the average maximum permanent

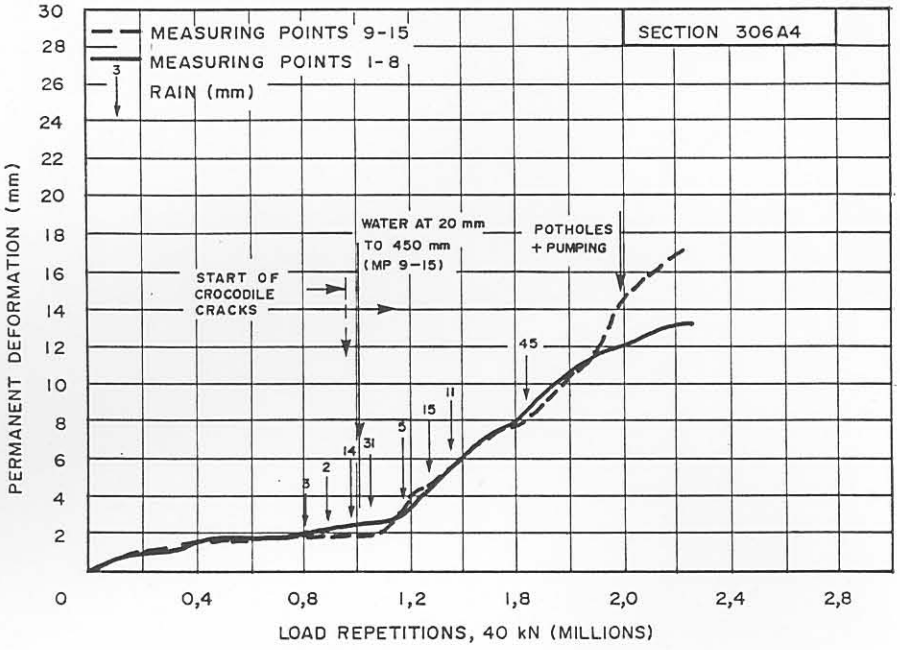

(a) HVS SECTION 306A4

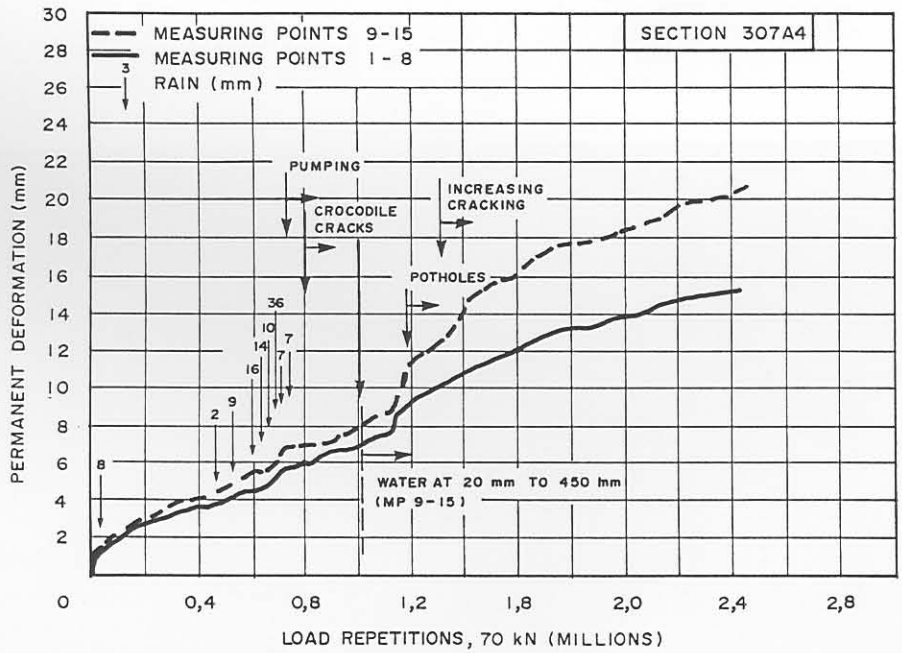

(b) HVS SECTION 307A4

FIGURE 4.8

AVERAGE PERMANENT DEFORMATION AT VARIOUS STAGES OF TRAFFICKING ON HVS TESTS 306A4 AND 307A4 UNDER THE INDICATED DUAL WHEEL LOADS ON ROAD 2212 (BULTFONTEIN)

940-4-5900/16 BD

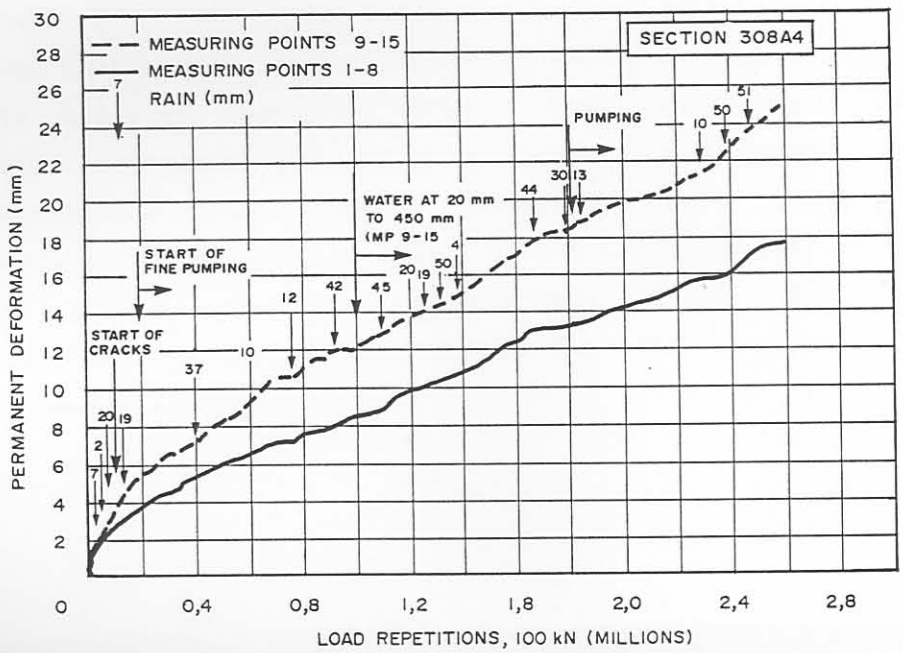

FIGURE 4.9

AVERAGE PERMANENT DEFORMATION AT VARIOUS STAGES OF TRAFFICKING ON HVS TEST 308A4 UNDER A 100 kN DUAL WHEEL LOAD ON ROAD 2212 (BULTFONTEIN)

deformation development on the surface of the test sections after various stages of trafficking, loading and under certain moisture conditions. In general, the figures indicate that the rate of deformation per wheel load is approximately linear (similar to that of the previous deeper pavement) and increases with the introduction of surface water (mostly rain) and the artificial introduction of depth water into the pavement structure.

Figure 4.8 (a) illustrates the permanent deformation development on Section 306A4, and indicates that after approximately 1,1 million repetitions, the rate of deformation, R_L, increased from 2,27 mm per million repetitions to 10 mm per million repetitions. At this turning point in the deformation development, crocodile cracks were observed on the surface of the test section and approximately 50 mm of rain had fallen on the test section during this period.

At this stage water was also introduced into one part of the section (measuring points 9 to 15), using perforated metal pipes, which were placed at a depth of 20 mm to 450 mm. These pipes were installed about 600 mm to the side of the test section.

With the introduction of water into the depth of the pavement the increase in the rate of deformation was minimal, as the measured increase was not exclusive to this wetter part of the test section, (ie measuring positions 9 to 15, see Figure 4.8 (a)). Almost the same increase in rate of deformation occurred on the drier part of the section where no water was introduced (ie measuring positions 1 to 8).

Although it rained on the entire section, no HVS trafficking was allowed during that period. HVS trafficking commenced after the rain. However, it is believed that rain water entered the fatigue cracks on the section, increasing the moisture content on the sides of the cracks, weakening the load transfer (cohesion) at the cracks, as well as increasing the moisture content of the weak zone at the bottom of the base layer at a depth of approximately 110 mm. This weaker zone is believed to be the primary reason for the increase in the rate of deformation on this section.

The number of repetitions (E80s in this case) at this turning point (increase in rate of deformation) may be described as the **"effective fatigue life"** of the cemented gravel base layer, and is approximately one million E80s. A more detailed discussion of this aspect based on linear elastic analysis may be found in Chapter 7.

Towards the end of the HVS test, excessive potholing and pumping resulted on this section at measuring points 9 to 15. This was a result of the introduction of surface water and rain. Test pits after the HVS test on this section confirmed that compression failure (crushing) had also occurred in the upper 50 mm to 75 mm of the cemented gravel base layer of this pavement, similar to those found on the deep pavement discussed in Paragraph 4.2.4.3.

4.3.4.2 Failure mechanisms: "deep" versus "shallow" pavements

Although similar crushing behaviour was noted on both the deeper and shallower pavements towards the end of the HVS tests, there is an important difference: for the deeper pavement, crushing failure dominates from the beginning of the test (traffic loading), while for the shallower pavement, classical fatigue failure initially dominates (effective fatigue life), after which crushing failure occurs in the upper section of the base, similar to that of a deeper pavement. This is probably so because of the <u>initial</u> imbalance in the base and subbase of the shallow pavement. It is important to note that this failure mechanism is what was observed during the tests and must not be construed as applicable to all similar pavements without further evidence.

Owing to this imbalance, "traffic moulding" occurs during traffic loading of the pavement, "punching" the relatively well-cemented cracked base material into the softer underlying weak layer. This process continues until the weaker layer is more densely compacted than in its initial state, thereby increasing its load-bearing capacity, and hence its support to the already-cracked base. Eventually, the repetitive stresses in the base increase and caused the crushing failure in the upper section of the cemented base.

4.3.4.3 Permanent deformation at different depths and discussion

The typical permanent deformation development as measured with the MDD equipment at different depths in the HVS test Section 306A4, on the shallow pavement (Road 2212 at Bultfontein) is illustrated in Figure 4.10. The figure indicates that almost the same deformation develops at the top and bottom of the cemented gravel base layer (0 mm and 110 mm) up to approximately one million load repetitions (E80s). This complies almost exactly with the average permanent deformation measured on the surface of the test section (see also previous Figure 4.8 (a)). From one million repetitions onwards, deformation in the base was also recorded and is similar to that of the deep pavement, indicating the crushing failure in the upper section of the base. For the other test sections the permanent deformation results are illustrated in Appendix A, Figures A.7 and A.8. Less crushing was found on HVS Section 307A4, as is indicated in Figure A.7, but compaction of the weaker layer, however, is well defined.

On Section 308A4, permanent deformation behaviour similar to that of Section 306A4 was recorded, but without a well-defined fatigue failure (turning point). This is probably so because tests 307A4 and 308A4 were done with higher wheel loads, ie 70 kN and 100 kN, respectively (40 kN used on Section 306A4). Close inspection of the test results and linear elastic analysis (see Chapter 7), however, indicated that fatigue failure of the cemented gravel base occurred almost immediately after the start of the higher wheel load tests (see Figures A.7 and A.8 in Appendix A).

The preceding results indicate the load-sensitivity in terms of fatigue of the shallower pavement, and also that a 40 kN wheel load is critical in terms of fatigue failure of this pavement. Therefore overloaded vehicles on this road should be avoided.

In Table 4.4, the percentage permanent deformation at various stages of trafficking on the three sections of the shallow pavement is given. The table indicates that up to a million repetitions on the three sections, approximately 34 to 53 percent of the total permanent deformation measured on the surface of the pavement originated from the relatively weak interlayer and the subbase layer (110 mm to 310 mm). The

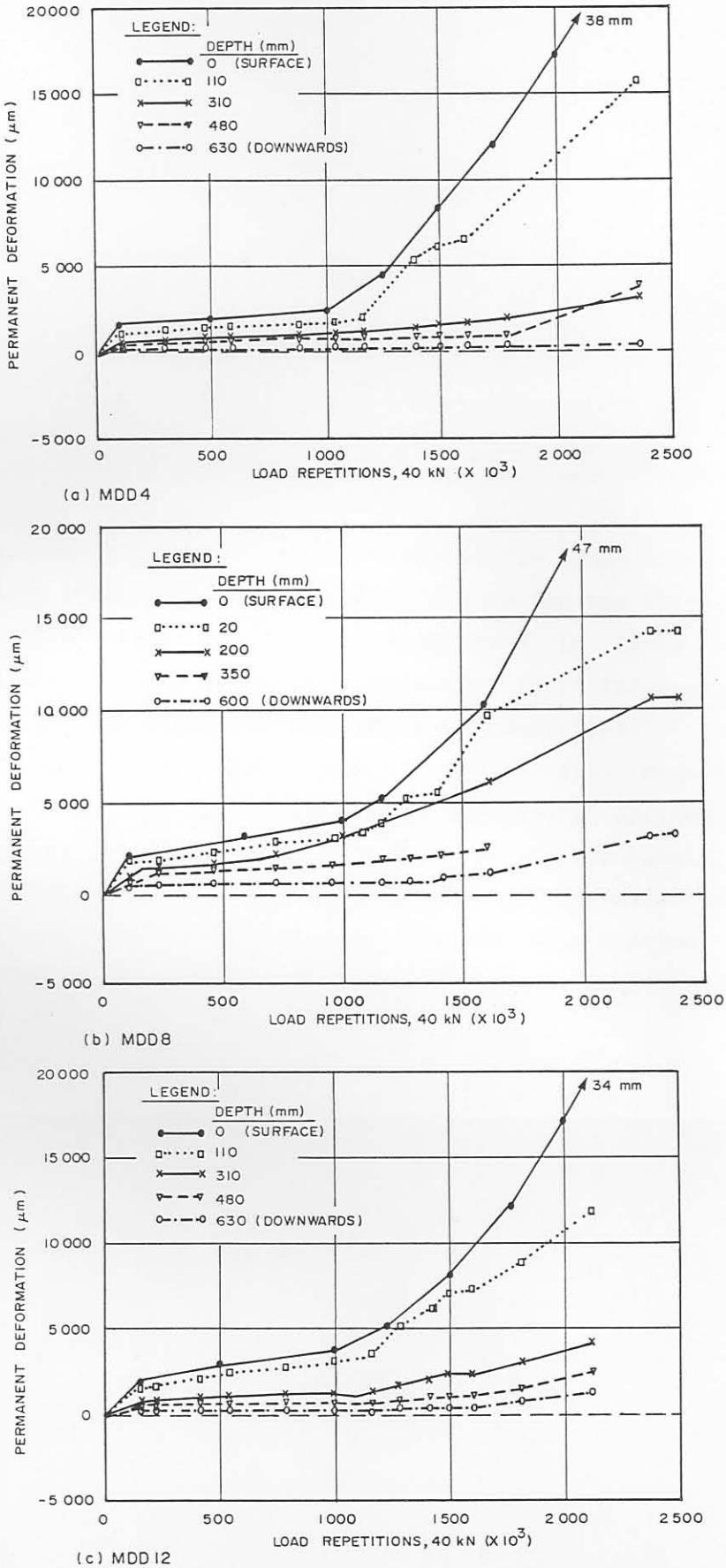

FIGURE 4.10

PERMANENT DEFORMATION AT DIFFERENT DEPTHS AT VARIOUS STAGES OF TRAFFICKING OF A 40 kN DUAL WHEEL LOAD ON HVS TEST SECTION 306A4 (ROAD 2212, BULTFONTEIN)

deformation percentage from the base (0 mm to 110 mm) varied between 5 and 35 per cent during this period. At the end of these tests, the percentages were 20 to 36 for the weak interlayer and the subbasse, and 15 to 65 for the base, respectively. This illustrates, in terms of permanent deformation, the initial compaction (densification) in the weak layer, and towards the end of the tests, the subsequent crushing of the base layer.

TABLE 4.4 PERCENTAGE PERMANENT DEFORMATION MEASURED AT THE END OF THE HVS TESTS ON THE VARIOUS TEST SECTIONS ON ROAD 2212 (BULTFONTEIN) (%)

HVS-SECTION	DEPTH (mm)	AT 10^6 REPS.		AT END OF TEST	
		MDD4	MDD12	MDD4	MDD12
306A4	0-110	32	25	58	65
	110-310	34	45	28	24
	310-480	9	10	0	4
	480-630	34	10	8	3
	630- ∞	1	10	6	4
307A4	0-110	35	11	29	15
	110-310	37	49	36	35
	310-480	10	12	15	20
	480-630	15	28	11	21
	630- ∞	3	0	9	9
308A4	0-110	5	17	32	46
	110-310	53	40	32	20
	310-480	13	16	8	10
	480-630	12	13	12	7
	630- ∞	17	14	16	17

4.3.4.4 Rate of permanent deformation, R_L, and relative damage

The different R_L and D_L factors, similar to those calculated earlier for the deep pavement (see Paragraph 4.2.4.4) for the three test sections on Road 2212 (Bultfontein), is summarised in Table 4.5. The table indicates that the rate of deformation (R_L) increases with increased wheel load and higher in situ moisture conditions.

In this case "dry" also refers to the in situ (eqiulibrium) moisture condition of the base, which was laboratory optimum at mod. AASHTO compaction (before stabilisation) plus approximately 2,5 per cent. "Wet" refers to the moisture condition of the base after rain or the introduction of artificial water into the test section, and was optimum (defined as above) plus approximately 3,5 per cent.

On average the rate of deformation, R_L, during the "wet" conditions is approximately 5,5 to 6,5 times higher than during the "dry" conditions on this shallow pavement, and is almost 1,4 times that found for the deep pavement under 40 kN wheel loading (see previous Table 4.2). This indicates a greater load sensitivity in terms of fatigue, of the shallow pavement, compared to that of the deep pavement.

TABLE 4.5 PAVEMENT PARAMETERS OF ROAD 2212 (BULTFONTEIN)

HVS-SECTION	R_L-FACTOR, mm/million reps					D_L*					
	40 kN		70 kN		100 kN		70 kN		100 kN		
	DRY	WET	DRY	WET	DRY	WET	DRY	WET	DRY	WET	
306A4	2,00	13,08	-	-	-	-					
307A4	-	-	5,45	13,57	-	-	2,72	1,03			
308A4	-	-	-	-	8,46				4,23		

* $D_L = (P/40)^r$ (see also Table 4.2)

In Table 4.6 the average relative damage coefficients, r, for this road are summarised.

TABLE 4.6 AVERAGE RELATIVE DAMAGE COEFFICIENT, r * (ROAD 2212)

70 kN		100 kN	
DRY	WET	DRY	WET
1,79	0,05	1,57	-

* See Table 4.3.

The table indicates that r (dry conditions) is almost similar for the 70 kN and the 100 kN, on this road. These values are 16 to 28 per cent higher than those obtained for the deeper pavement (see previous Table 4.3), and indicates a slightly higher load sensitivity of this pavement. Limited deformation results, however, exits for the wet conditions, inhibiting proper calculation of r for the 100 kN test, but indications are that r is very low and indicates damage almost independent of load during wet (excessive porewater pressure) conditions.

It is interesting to note, however, that the relative damage coefficients (r) of Road 2212, are much lower than those obtained from an HVS test on a "very shallow" pavement, ie Road P95/1, near Bronkhorstspruit (Kleyn et al., 1985). On this latter road, which was constructed with a 70 mm lightly-cemented base on an untreated natural gravel subbase, much higher deformation rates and r-coefficients than those found on Road 2212 were obtained.

The corresponding R_L, D_L and r parameters for this pavement (Road P95/1) are summarised in Table 4.7.

TABLE 4.7 PAVEMENT PARAMETERS FOR ROAD P95/1 (BRONKHORSTSPRUIT) (AFTER KLEYN ET AL., 1985)

HVS-WHEEL LOAD	RL- FACTOR (mm/million reps)		D_L - FACTOR		r - coefficient	
(kN)	INITIAL*	FINAL*	INITIAL	FINAL	INITIAL	FINAL
40	13	6	1,0	1,0	-	-
70	82	22	6,3	3,7	3,3	2,3
100	780		32,3		4,5	-

* In Table 4.7, "initial" denotes the condition before fatigue cracking of the cemented gravel base and "final" the state thereafter (equivalent granular state). The initial R_{70} is much higher than R_{40} but decreases markedly in the final state. This is also reflected in the relative damage factor (D_L) as well as the relative damage coefficient, r.

The table indicates that much higher deformation rates (R_L) were obtained for this pavement than for both the two pavements discussed above, indicating that this pavement is much more load sensitive and hence the "weakest" pavement of the three.

4.3.4.5 In situ densities and moisture contents

The in situ nuclear dry densities and oven dry moisture contents on the various test sections after HVS testing were also measured, similar to that of the deep pavement (see Figure 4.6). The results are summarised in Appendix A, Table A.9, and indicate that slight densification was measured in most of the layers within the trafficked areas of the three test sections (positions B and C). For Section 306A4, densification was measured to a depth of approximately 320 mm, and for Sections 307A4 and 308A4, to approximately 450 mm and 600 mm, respectively.

This is in accordance with the permanent deformation results summarised in Table 4.4, which indicates that, at the end of the HVS tests, higher deformations were measured deeper down in the pavement Sections 307A4 and 308A4 than those on Section 306A4, because of the relatively higher HVS test wheel load usedon these sections.

Although crushing failure (similar to that observed on the deep pavement) was noted in the upper section of the cemented gravel base on all the test sections, it was impossible to measure any significant de-densification with the nuclear apparatus, because the crushed layer was not well-defined and relatively thin. The thickness of the crushed layer varied between 10 mm and 30 mm and, in isolated cases, up to 50 mm to 75 mm. The effect of crushing, however, is well illustrated by the permanent deformation results measured on Section 308A4 (see Figure A.8 in Appendix A).

In general, relatively higher final moisture contents were measured in the upper 100 mm of the bases on Sections 306A4 and 308A4, than on Section 307A4, because of the higher rainfall on these sections towards the end of the tests.

The moisture contents measured in the shallow pavement are lower than those found in the deep pavement. These higher moisture contents in the deep pavement are believed to be caused by rain as well as the artificial introduction of water into the deep pavement. Another contributing factor may be the greater extent of the crushing failure in the surfacing and base layer of the deep pavement.

4.4 EXCESSIVELY HIGH SINGLE WHEEL LOAD TESTS

Included in the HVS test programmes on the deep and shallow pavements, excessive high single wheel load tests were planned to verify the failure mechanisms indicated by the relatively lower dual wheel load tests, ie 40 kN, 70 kN and 100 kN.

An aircraft wheel (Boeing 747) at 150 kN with tyre pressure of approximately 960 kPa to 1445 kPa was used for the testing on both the deep and shallow pavements. Two sections (337A4 and 338A4) were tested on the deep pavement (Road 1932 at Rooiwal), and one section (309A4) on Road 2212 at Bultfontein.

4.4.1 Permanent deformation on the road surface

The average permanent deformation development (rut) at various stages of trafficking on the three sections is illustrated in Figure 4.11 (a), (b) and (c). The figure indicates that relatively higher deformation occurred on the shallow pavement (HVS Section 309A4), compared to that of the deep pavement (HVS Sections 337A4 and 338A4).

The higher deformation on the shallow pavement was expected, and again demonstrates the load sensitivity of this pavement in terms of fatigue failure of the cemented gravel base layer. The deep pavement is less load sensitive and hence the lower deformation under the same loading and moisture conditions.

It is, however, interesting to note that higher deformation occurred on Section 337A4 of the deep pavement, than on Section 338A4. On the latter section a lower tyre pressure was used, ie 960 kPa, and it is believed that this is mainly responsible for the difference in deformation behaviour on these two tests. In Chapter 5 it is indicated that the rate of crushing (compression failure) in the cemented base and hence the development of permanent deformation, is directly related to the tyre pressure.

Figure 4.11 also indicates that the rate of deformation on all three sections is not constant, but decreases towards the end of the tests.

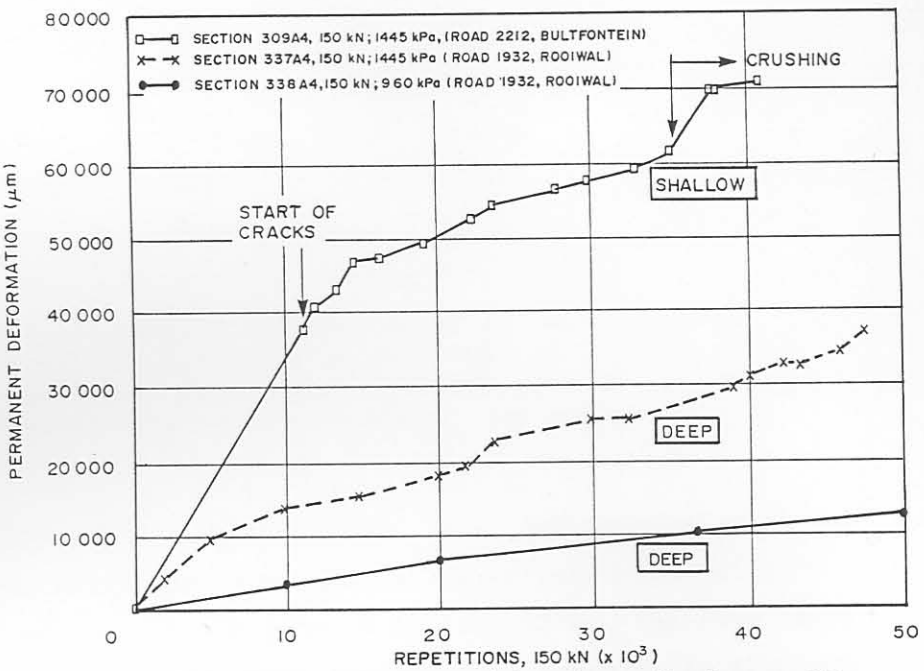

(a) Comparison of the permanent deformation on the three sections

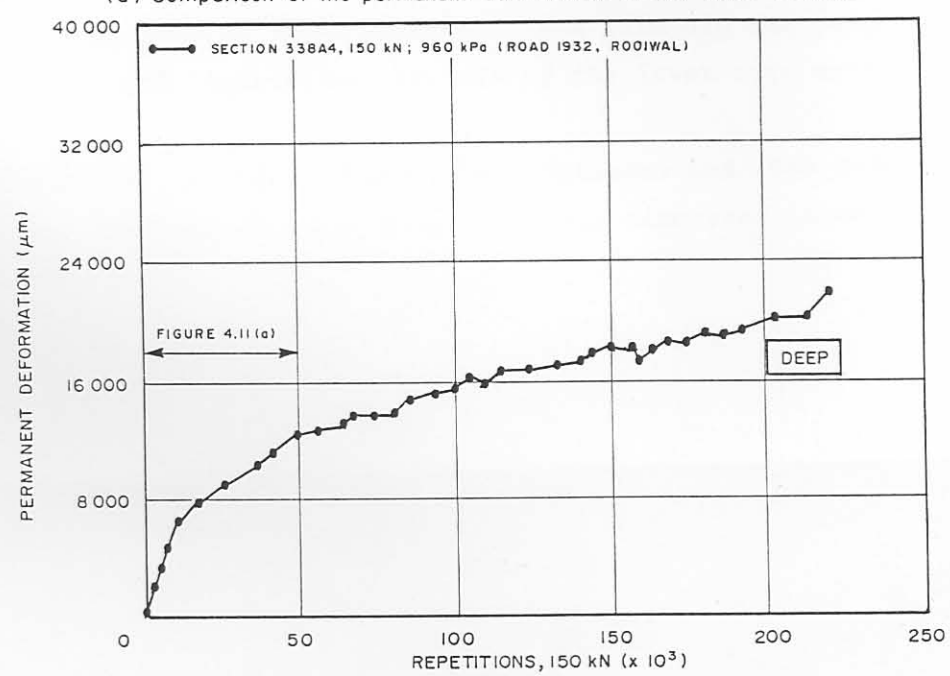

(b) Section 338A4 (Road 1932, Rooiwal)

FIGURE 4.11

AVERAGE PERMANENT DEFORMATION (RUT) AT VARIOUS STAGES OF TRAFFICKING OF A 150 kN SINGLE WHEEL LOAD ON THREE DIFFERENT SECTIONS

940-4-5920/1 BD

In the case of the shallow pavement (Section 309A4) this is probably related to the fatigue failure of the base, and subsequent densification of the lower layers, tending to produce a deeper pavement (see Chapter 6).

Excessive cracking of the base was observed at approximately 11 000 repetitions on this section, after which the rate of deformation decreased up to approximately 36 000 repetitions. Hereafter, crushing failure occurred in the base and an increase in the rate of deformation occurred again.

The rates of deformation of the three sections is summarised in Table 4.8.

TABLE 4.8 RATE OF DEFORMATION, R_L^*, OF THE THREE SECTIONS IN mm PER 10^4 REPETITIONS

ROAD	HVS-SECTION	PAVEMENT TYPE	TYRE PRESSURE (kPa)	INITIAL	INTERMEDIATE	FINAL (CRUSHING)
2212	309A4	SHALLOW	1445	33,0	7,5	≈ 33
1932	337A4	DEEP	1445	13,0	5,0	≈ 13
1932	338A4	DEEP	960	4,0	1,3	-

* R_L in this case is measured in mm per ten thousand repetitions, and not million repetitions as indicated in previous Tables 4.2 and 4.8. This is done because of the relatively high deformation rates associated with the single wheel load tests.

The table also indicates that the deformation rates on the deeper pavement decreased from initial relatively high values to intermediate lower values. In the case of Section 337A4, the rate increased towards the end of the test owing to excessive crushing in the upper section of the base. On Section 338A4, however, the rate did not increase during the first 50 000 repetitions, because of the lower tyre pressure.

The effects of crushing (compression failure) and the development of "crushing life" curves from these tests are discussed in more detail in Chapter 5.

4.4.2 Permanent deformation at different depths

In Figure 4.12 (a) and (b), the permanent deformation development at different depths in HVS Section 309A4 is illustrated. The figure indicates the initial fatigue failure of the base, with subsequent compaction in the lower layers, especially the weaker layer and the subbase (depths 110 mm to 310 mm) in the pavement. Towards the end of the test, crushing failure in the base occurred as is indicated by the deformation in the base (depths 0 mm to 110 mm), especially at MDD 10 (see Figure 4.12 (b)).

Figure 4.13 indicates that relatively high deformation occurred in the base from the beginning of the test on HVS Section 337A4, indicating the crushing failure. Relatively low deformations occurred in the lower layers, when compared to those of the shallow pavement (Figure 4.12).

Figure 4.14 illustrates the deformation on Section 338A4, and shows that it is approximately 50 per cent of those measured on Section 337A4 at approximately 50 000 repetitions, and is believed to be directly related to the lower tyre pressure.

Although the variation in strength (bearing capacity) between the two test sections of the deep pavement may have attributed to the difference in deformation development, the effect of crushing in the cemented gravel base was well demonstrated by these tests. So too is the marked difference in failure mechanisms between the deep and shallow pavements.

In Figure 4.15, the various stages in the failure of the shallow pavement is illustrated. The figure indicates that the failure mechanism consists of various stages, starting with fatigue failure of the cementitious gravel bases, followed by "punch in" into the relative soft underlying subbase layer, crushing and then complete fracturing.

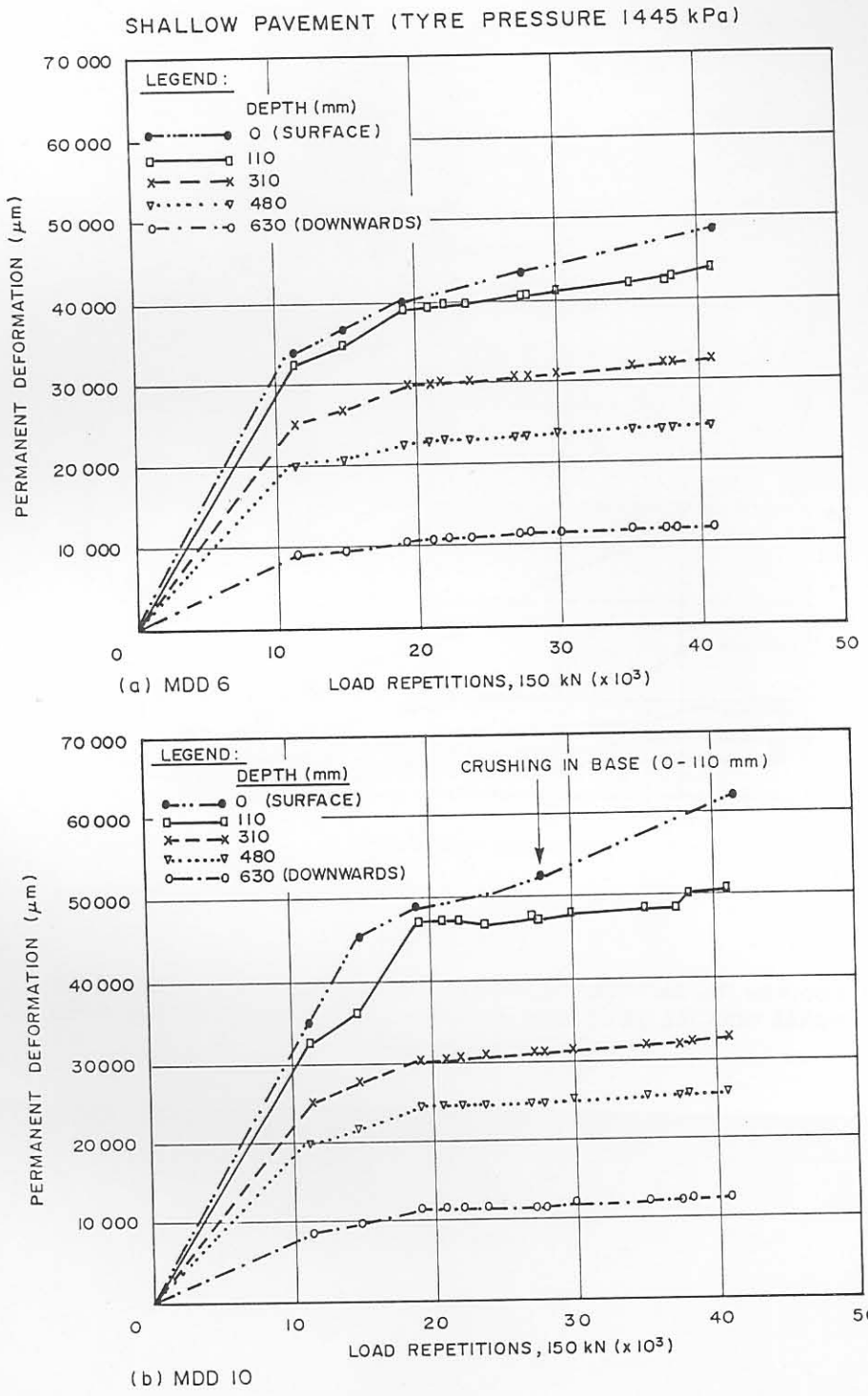

FIGURE 4.12

PERMANENT DEFORMATION AT DIFFERENT DEPTHS AT VARIOUS STAGES OF TRAFFICKING OF A 150 kN SINGLE WHEEL LOAD ON HVS TEST SECTION 309A4 (ROAD 2212 (BULTFONTEIN)

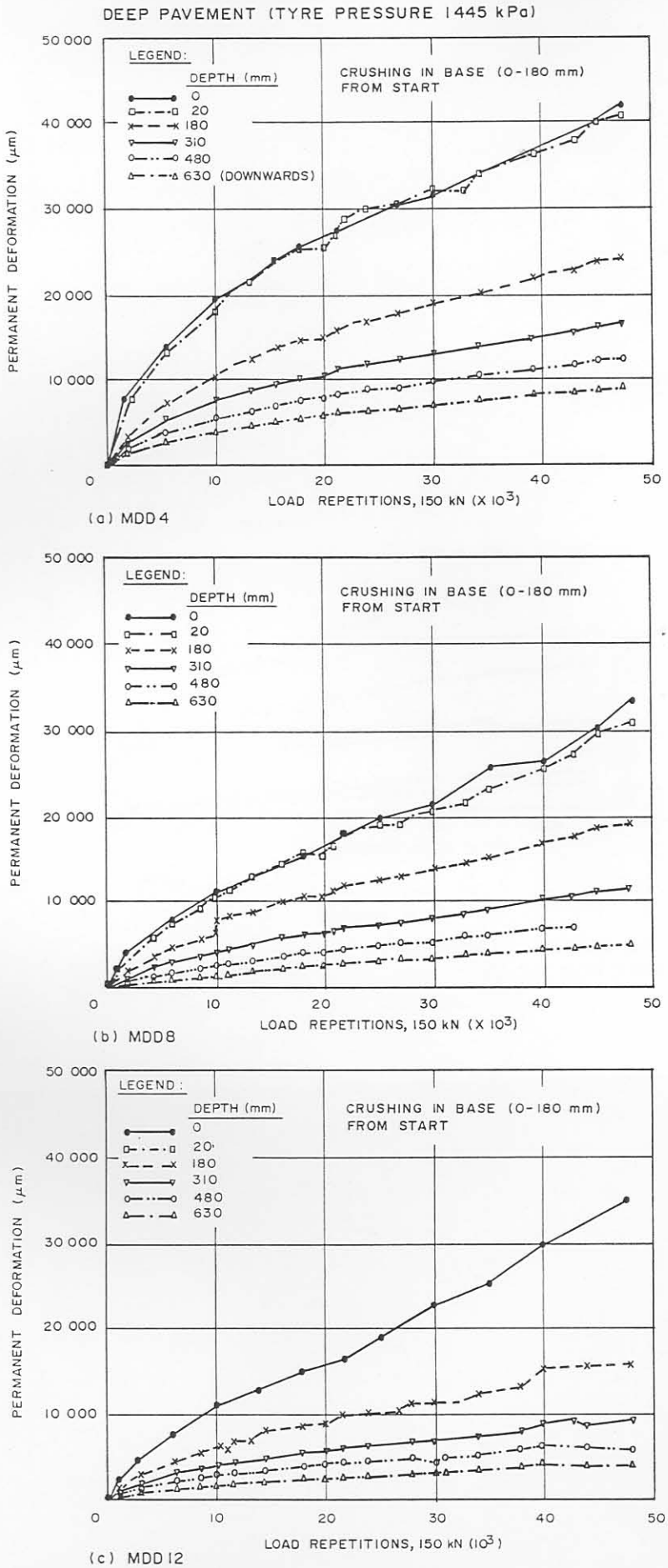

FIGURE 4.13

PERMANENT DEFORMATION AT DIFFERENT DEPTHS AT VARIOUS STAGES OF A 150 kN SINGLE WHEEL LOAD ON HVS TEST SECTION 337A4 (ROAD 1932, ROOIWAL)

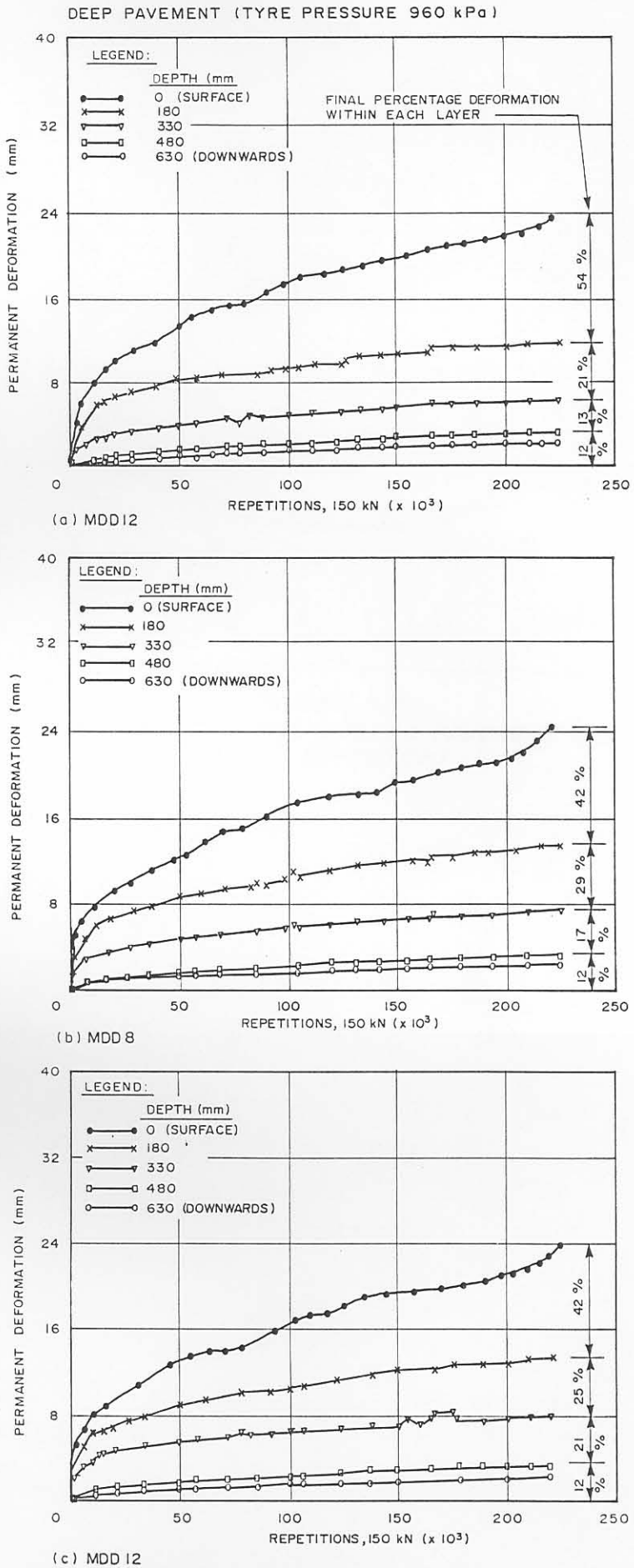

FIGURE 4.14

PERMANENT DEFORMATION AT DIFFERENT DEPTHS AT VARIOUS STAGES OF TRAFFICKING ON HVS TEST SECTION 338A4 (ROAD 1932, ROOIWAL)

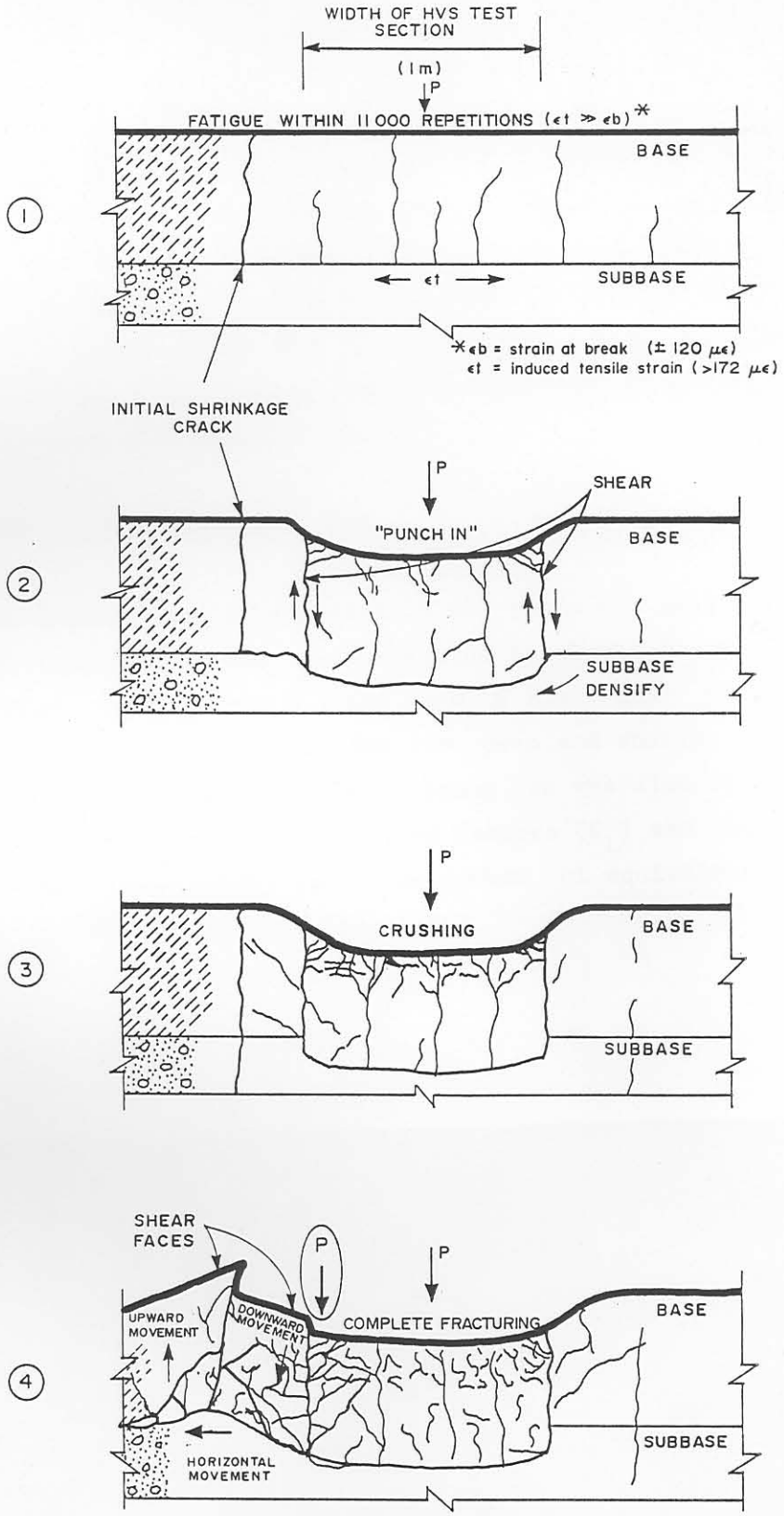

FIGURE 4.15

STAGES OF FAILURE IN THE SHALLOW PAVEMENT 2212, SECTION 309A4 (BULTFONTEIN)

940-4-5900/22 BD

For the deep pavement the stages of failure consist only of the last two phases depicted in Figure 4.15, viz crushing and complete fracturing, without excessive deformation and densification in the lower layers.

4.4.3 In situ densities and moisture contents

In situ nuclear dry density (Appendix A, Table A.9) and oven dry moisture contents on the previous discussed sections (309A4 and 337A4), indicate that the density in the upper 100 mm of the cemented gravel base of the shallow Section 309A4 at measuring point 4 (MP 4), is relatively low, especially at position C when compared to that at a depth of 200 mm to 300 mm. This is a reflection of the excessive crushing of the base that occurred during HVS testing on this section. At position D, excessive fracturing of the base layer outside the test section inhibited accurate measurement of density.

Marked densification, however, occurred from a depth of 200 mm to approximately 875 mm on this section. This was also indicated by the permanent deformation measurements illustrated in Figure 4.12.

De-densification (crushing) was measured in the upper 100 mm, in the base of Section 337A4 (at positions A and B). Crushing and fracturing occurred well outside the test area (position A) as was also found on Section 309A4. This was largely due to the excessively high single wheel loading, which approached a point load situation on these sections, resulting in these excessive failures, both inside and outside the trafficked area (See Figure 4.15).

4.5 PERMANENT DEFORMATION VERSUS E80s

The permanent deformations of the various HVS tests can only be compared if the actual load repetitions are normalised in terms of equivalent 80 kN axles (E80s). Paragraphs 4.2.4.4 and 4.3.4.4 give the relative damage factors and r-coefficients for the deep and shallow pavements. These parameters do not appear to be constant, as was also indicated by Maree (1982). By applying the calculated factors (D_L) and coefficients (r) to the actual load repetitions, the number of equivalent E80s for each loading other than 40 kN is calculated.

Figure 4.16 illustrates the permanent deformation of the deep pavement, at different stages of equivalent E80s, and is a summary of the previous results similar to Figure 4.2. The figure indicates that the rate of deformation is largely influenced by the moisture content of the base. Similar rates of deformation were obtained on the different sections under the same moisture conditions. The figure also indicates that the time of increase in the moisture content is of critical importance to the **effective structural capacity** of the pavement. Taking a failure criterion of 20 mm rut (limit for deformation), relatively early wetting of the base may result in an effective structural capacity of approximately 1 to 2 million E80s, while the capacity during relatively dry conditions is in excess of 4 to 5 million E80s for this pavement.

Although there is a large difference in capacity mainly related to the moisture conditions in the base of this pavement, a capacity of **more than twice** the original capacity for which this pavement was designed, was measured. It appears that this type of design may be used for higher traffic classes than currently used by the TPA (TPA, 1978). According to the TPA-classification of pavements, this pavement was originally designed as a TPA-Class III pavement (0,4 to 1 million E80s) and according to the results above, this pavement design may easily be used for a **Class IV or even Class V category**, under relatively dry conditions. On this type of pavement, however, the **tyre pressure** should be strictly controlled in order to further extend the life of these pavements by avoiding premature crushing failure of the base.

Figure 4.17 illustrates the permanent deformation of the different HVS test sections on the shallow pavement at various stages of equivalent traffic (E80s). Although this type of pavement is load sensitive in terms of fatigue, the rate of deformation is also largely influenced by the moisture content and the state of the base and subbase layers. This pavement was designed as a relatively shallow pavement to carry 0,2 to 0,4 million E80s, ie TPA-Class II. HVS results show that the effective structural capacity of this pavement appears also to be much higher than originally anticipated. This pavement can also be used for **Class IV**, and even **Class V**, under relatively dry conditions.

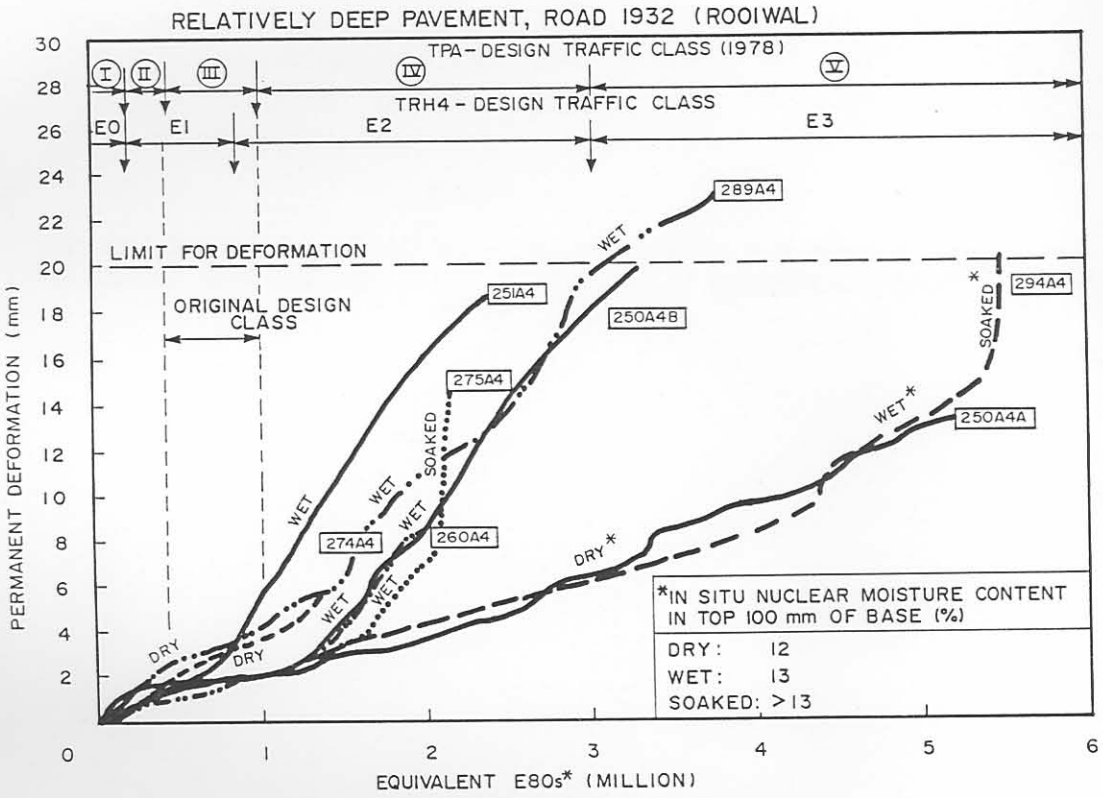

* $D_L = \left(\frac{P_L}{40}\right)^r$ = VARIABLE, AS INDICATED IN TABLE 4.3

FIGURE 4.16

THE PERMANENT DEFORMATION OF THE DIFFERENT HVS TEST SECTIONS ON THE RELATIVELY DEEP PAVEMENT (ROAD 1932), AT DIFFERENT STAGES OF EQUIVALENT (E80s) TRAFFIC

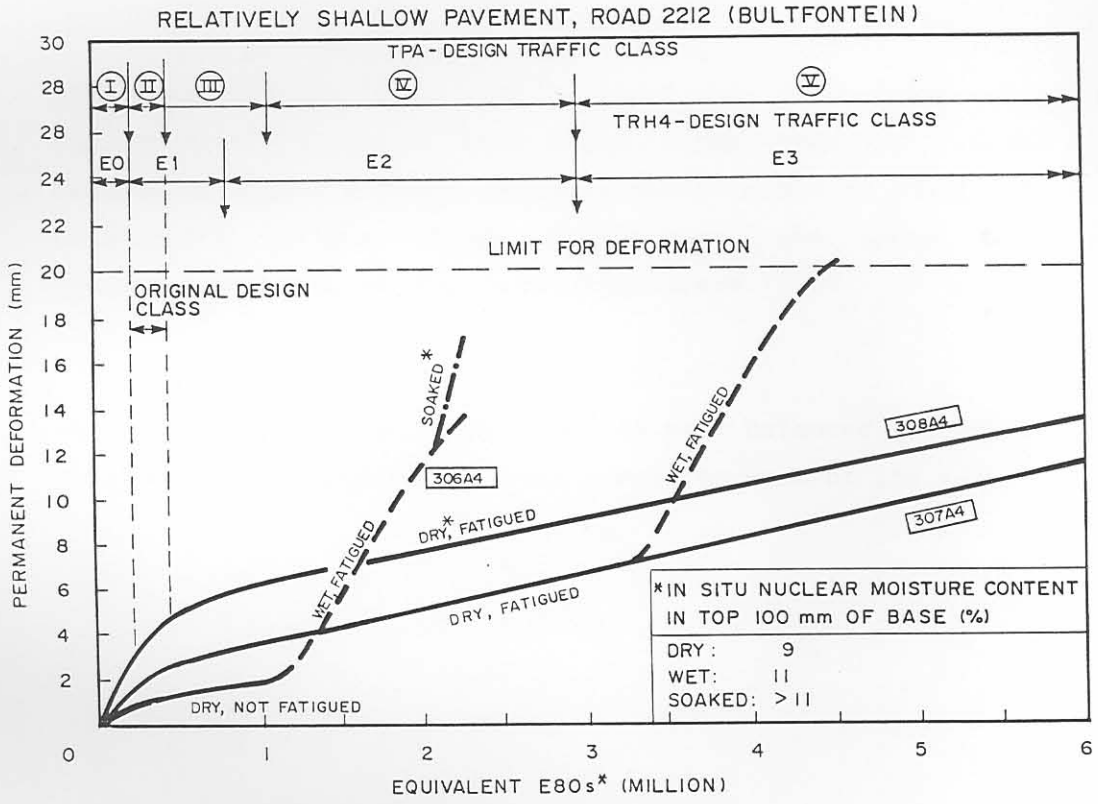

* $D_L = \left(P_L/40\right)^r$ = VARIABLE, AS INDICATED IN TABLE 4.6

FIGURE 4.17

THE PERMANENT DEFORMATION OF THE DIFFERENT HVS TEST SECTIONS ON THE RELATIVELY SHALLOW PAVEMENT (ROAD 2212), AT DIFFERENT STAGES OF EQUIVALENT (E80s) TRAFFIC

Overloading of this type of pavement however must be avoided in order to extent the life of the base further without premature fatigue failure.

The above are some of the most important findings from these HVS tests and also indicate large potential savings for the TPA, and the costs of pavements in general (Without the savings calculated during this current study, estimations by the TPA are that the HVS-program in Transvaal is currently saving approximately R13 million per year, directly as a result of HVS and HVS-related research in that Province, Kleyn, 1989).

4.6 SUMMARY OF THE PERMANENT DEFORMATION BEHAVIOUR OF PAVEMENTS WITH CEMENTITIOUS BASE LAYERS

The permanent deformation behaviour of pavements where cemented bases and subbases are the main controlling layers, is illustrated in Figures 4.18 and 4.19. Figure 4.18 indicates that the strength - balance of these pavement largely controls the rate of deformation. This rate, which is a prime indicator of the behaviour of the pavement, is basically linear for shallow pavements, but may increase markedly at a point of fatigue of the base layer, which is primarily controlled by the trafficking wheel load and to a lesser extend by the in situ moisture content of the lower layers. If the wheel load is higher than the critical load for fatigue of the base, fatigue failure occurs almost immediately, after which the rate may decreases owing to better balance of the pavement system (compaction of lower layers, etc).

Conversely, if the wheel load is lower than the critical load, fatigue failure occurs at a much later stage, after which the rate may increase because of higher moisture contents which result in lower load transfer between the fatigue cracks in the base, and lower shear strength (bearing capacity) of the supporting layers.

If the pavement (deep or shallow) is well balanced and maintained, the rate should approximate a linear curve for most of its life.

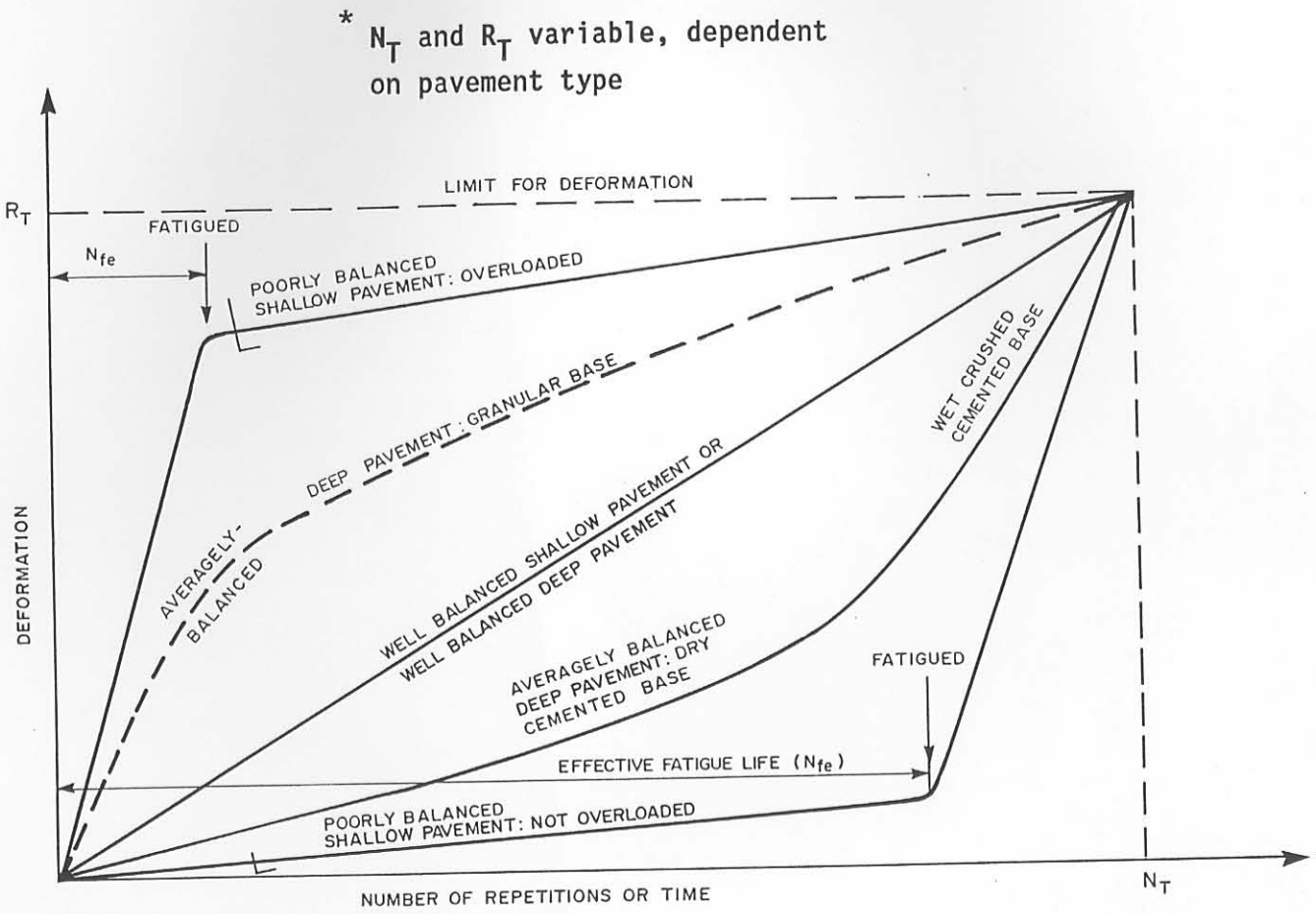

FIGURE 4.18

GRAPHICAL REPRESENTATION OF THE PERMANENT DEFORMATION OF LIGHTLY CEMENTED GRAVEL BASE AND GRANULAR BASE PAVEMENTS

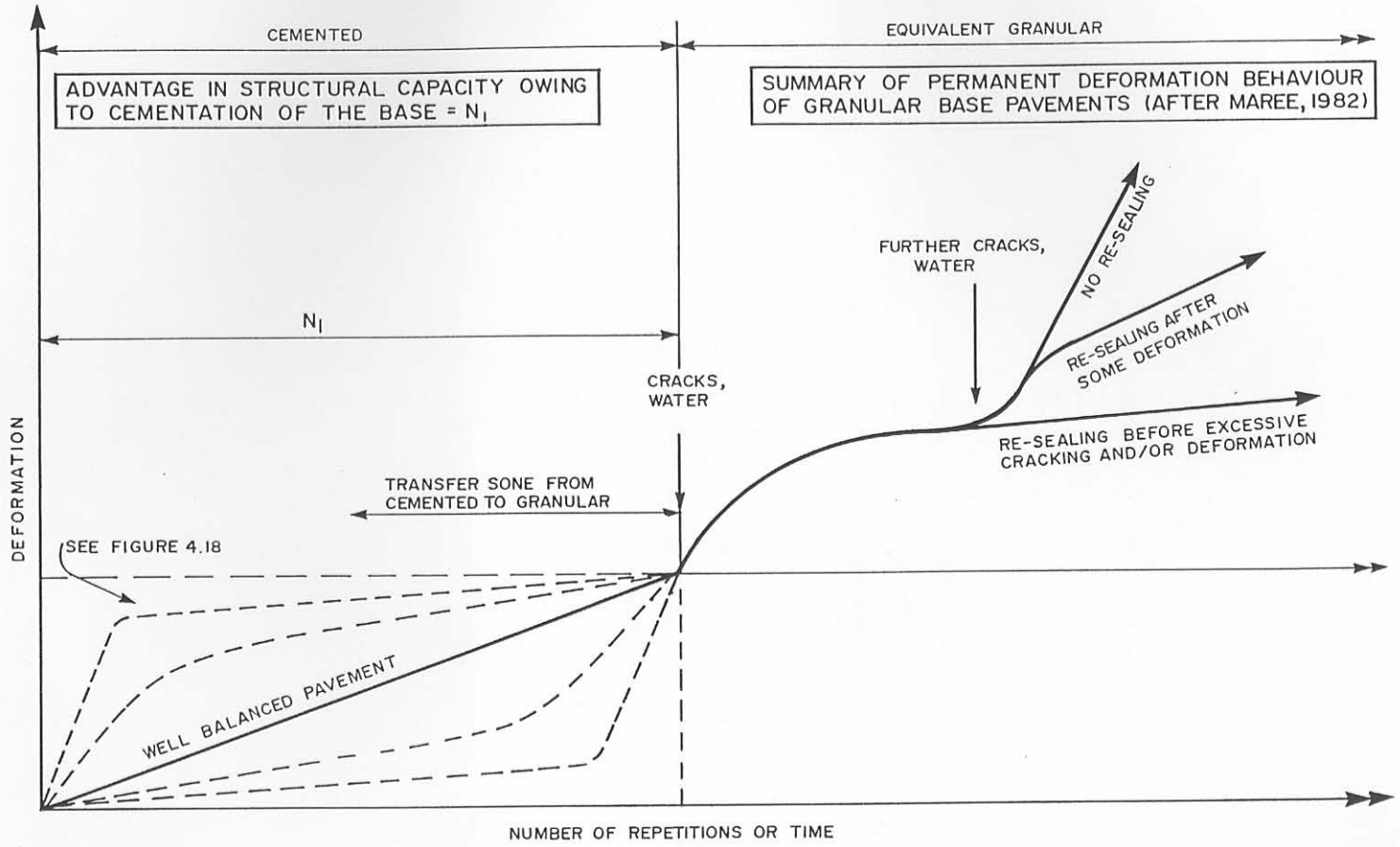

FIGURE 4.19

GRAPHICAL SUMMARY OF THE PERMANENT DEFORMATION OF LIGHTLY CEMENTED GRAVEL BASE PAVEMENTS, IN BOTH THE CEMENTED AND EQUIVALENT GRANULAR STATES

For relatively deep cemented base pavements, the rate appears to be non - linear, owing to crushing failure, which reverts the cemented base to an equivalent granular base. If the moisture content of the crushed material increases, the rate of deformation also increases.

For deep granular base pavements, the rate is also non - linear, mainly owing to slight densification of the granular material (if material is of good quality). During densification the rate decreases, but may increase owing to an increase in moisture content of the base.

In Figure 4.19 a summary of the behaviour of pavements with initial cemented base and subbase layers is given. The figure indicates that the behaviour of a cemented pavement may change to that of a granular pavement (see Maree, 1982). Changes in the rate of deformation, however, are strictly a function of the pavement balance, the moisture contents of the various pavement layers, quality of materials, maintenance, etc.

The potential advantage in structural capacity, owing to the initial cementation (or cohesion) of the base, is well illustrated in the figure.

4.7 CONCLUSIONS

(a) Extensive HVS testing on two basic type of pavements with lightly cemented layers indicated that these pavements can carry more than double the design traffic than was originally anticipated. The effective structural capacity of these pavements may be in excess of 5 million E80s if tyre pressure and overloading is controlled.

(b) The moisture content of the base layer is of critical importance, and is one of the major parameters influencing the rate of deformation in both shallow and deep pavements.

(c) The basic failure mechanism of relatively deep pavements with lightly cemented base layers is crushing (compression) failure in the upper portion (0 mm to 75 mm) of the base layer, changing the pavement from a deep to an inverted pavement.

This may be termed a "shallow" failure owing to the relatively good support from the lower layers and subsequent deformation from the top of the base layer.

(e) The basic failure mechanism of relatively shallow pavements with cemented bases, is a quite sudden fatigue failure of the base layer ("sudden death"). This failure may be termed a "deep" failure, owing to the initial lack of support and subsequent deformation in the lower layers.

(f) The rate of deformation of pavements with lightly cementitious layers is approximately linear but may change as a result of fatigue failure of the base and increase in moisture content of the lower layers.

(g) The relative damage coefficient based on the rate of deformation of pavements with cemented layers is relatively low, and varies between 1,2 to 1,5 for deep, and between 1,6 and 1,8 for relatively shallow, and up to 4,5 for very shallow pavements in the relatively dry conditions. For relatively deep granular materials a value of 3,0 is recommended (Maree, 1982).

(h) Surface deflection is not a good indicator of the effective rate of deformation on these pavements. The combination, however, of several DCP parameters viz DN, DNR, DSN, for the upper layers as well as surface deflection may provide a better prediction of behaviour (See Appendix A for discussion on this aspect).

(i) The current DCP model for structural capacity, based on the DSN_{800} only (Kleyn, 1984) totally overestimates the effective structural capacity of these pavements. The model should be improved to compensate for the important effect of strength - balance of pavements also (See also Chapter 6).

(k) In the deep pavements tested, more than 67 per cent of the permanent deformation during the relatively dry state, and 75 per cent during the relatively wet state, originates from the base layer owing to crushing and subsequent deformation in the upper section of the layer.

(l) Relatively low deformations (5 to 35 per cent) resulted initially from the base of the shallower pavements tested. Owing to fatigue failure and subsequent crushing, this percentage increased to a final range of 15 to 65 per cent.

(m) The permanent deformation measured on the surface of the pavement is an accumulation of the deformation at different depths in the pavement and may not correctly explain the complete failure mechanism.

(n) Permanent deformation at different depths in the pavement (measured with the MDD) appears to be very useful in assisting with the description of the failure mechanism associated with the pavements tested.

(o) In situ nuclear dry density and moisture content measurements in and outside the test area assisted in explaining the failure mechanisms of the pavements.

(p) As was found for granular base pavements, the state of the surfacing can have a major influence on the behaviour of the pavement, because the surfacing controls the penetration of water into the cemented gravel base and large pothloles may develop in the deeper pavements especially, due to the crushed state in the top of the base.

4.8 REFERENCES

De Beer, M (1985) Behaviour of Cementitious Subbase Layers in Bitumen Base Road Structures. M(Eng), Faculty of Engineering, University of Pretoria, Pretoria, 1985.

De Beer, M, Kleyn, E G and Savage, P F (1988). Towards a Classification System for the Strength-Balance of Thin Surfaced Flexible Pavements. Proceedings of the Eighth Quinquennial Convention of SAICE in co-operation with the 1988 Annual Transportation Convention (SAICE-ATC 1988), University of Pretoria, Pretoria, 1988.

De Beer, M (1986a). Mechanistic analysis: HVS-section 260A4 (Rooiwal). Unpublished Technical note TP/146/86 (in Afrikaans), Division of Roads and Transport Technology, CSIR, Pretoria, 1986.

De Beer, M (1986b). Mechanistic analysis: HVS-section 275A4 (Rooiwal). Unpublished Technical note TP/14/86 (in Afrikaans), Division of Roads and Transport Technology, CSIR, Pretoria, 1986.

De Beer, M (1986c). Mechanistic analysis: HVS-section 289A4 (Rooiwal). Unpublished Technical note TP/91/86 (in Afrikaans), Division of Roads and Transport Technology, CSIR, Pretoria, 1986.

De Beer, M (1986d). Mechanistic analysis: HVS-section 294A4 (Rooiwal). Unpublished Technical note TP/43/86 (in Afrikaans), Division of Roads and Transport Technology, CSIR, Pretoria, 1986.

De Beer M, Horak E and Visser A T (1988). The Multi-Depth Deflectometer(MDD) System for determining the Effective Elastic Moduli of Pavement Layers. Unpublished paper accepted for publication in a ASTM Special Technical Publication (STP) of the first International Symposium on Nondestructive Testing of Pavements and Backcalculation of Moduli, Baltimore, USA, 1988.

Division of Roads and Transport Technology, (DRTT) (1985a). Structural Design of Interurban and Rural Road Pavements. Technical Recommendations for Highways, TRH4: 1985, CSIR, Pretoria, 1985.

Division of Roads and Transport Technology, (DRTT) (1985b). Guidelines for Road Construction Materials. Technical Recommendations for Highways, TRH14: 1985, CSIR, Pretoria, 1985.

Division of Roads and Transport Technology, (DRTT) (1986). Cementitious Stabilisers in Road Construction. Technical Recommendations for Highways, Draft TRH13: 1986, CSIR, Pretoria, 1986.

Freeme, C R, Maree, J H and Viljoen A W (1982). Mechanistic Design of Asphalt Pavements and Verification Using the Heavy Vehicle Simulator. Proceedings of the Fifth International Conference on the Structural Design of Asphalt Pavements, Delft, August 1982, Vol 1, 1982.

Freeme, C R and Walker, R N (1984). Economic Design of Bituminous Pavements. Proceedings of the Fourth Conference on Asphalt Pavements for Southern Africa, CAPSA 84, Cape Town, Vol 1, 1984.

Horak, E (1988). Aspects of Deflection Basin Parameters used in a Mechanistic Rehabilitation Design Procedure for Flexible Pavements in South Africa. Ph.D Dissertation, Faculty of Engineering, University of Pretoria, Pretoria, South Africa, 1988.

Kleyn, E G (1988). Personal Communication.

Kleyn, E G (1989). Personal Communication.

Kleyn, E G (1984). Aspects of Pavement Evaluation and Design as determined with the aid of the Dynamic Cone Penetrometer (DCP). M Eng. thesis (In Afrikaans, Faculty of Engineering, University of Pretoria, Pretoria, 1984.

Kleyn, E G, Freeme C R and Terblanche L J (1985). The Impact of Heavy Vehicle Simulator Testing in the Transvaal. Paper delivered at the Annual Transportation Convention during 29 July - 2 August 1985 (ATC 1985), Session S.350, Accelerated testing of pavements, CSIR, Pretoria, 1985.

Marais, F J (1981). Strength Gain of Stabilised Layers. Internal Report S2/81, (In Afrikaans), Transvaal Roads Department, Roads Branch, Pretoria, June 1981.

Maree, J H (1982). Aspects of the Design and Behaviour of Pavements incorporating Granular Bases. DSc Dissertation (In Afrikaans), Faculty of Engineering, University of Pretoria, Pretoria, 1982.

Otte, E (1972). The Stress-Strain Properties of Cement-Stabilised Materials. MSc Thesis (In Afrikaans), Faculty of Engineering, University of Pretoria, Pretoria, 1972.

Otte, E (1978). A Structural Design Procedure for Cement-Treated Layers in Pavements. DSc Dissertation, Faculty of Engineering, University of Pretoria, Pretoria, 1978.

Pienaar, S (1979). DCP - Evaluation of the Hardening of Stabilised Pavement Layers. Internal Report S4/79, (In Afrikaans), Transvaal Roads Department, Roads Branch, Pretoria, July 1979.

TRANSVAAL ROADS DEPARTMENT (1978). Pavement and Materials Design Manual. Report L1/78, Transvaal Roads Department, Materials Branch, January 1978.

CHAPTER 5

COMPRESSION FAILURE OF LIGHTLY CEMENTITIOUS MATERIALS

CONTENTS PAGE

5.1 INTRODUCTION

5.1.1 Background

The investigation described in Chapter 4, indicated that the actual failure mechanisms of deep and shallow pavements differ, in that the origin of permanent deformation differs. It was concluded that deep pavements fail predominantly in compression (crushing) in the upper portion of the cementitious base layer, while the shallow pavements fail predominantly in fatigue of the cementitous base layer.

This chapter concentrates on compression (crushing) failure of lightly cementitious pavement layers. It is believed that there is a need to establish a correct understanding of this failure mechanism, as till now this was relatively unknown and unquantified for pavements. This includes the development of applicable failure criteria for this particular failure, so that for example, effective rehabilitation may be implemented on these types of pavements (Maree et al., 1987).

5.1.2 The Problem

Evidence exists in South Africa that relatively thin surface seals on pavements with lightly cementitious base layers show fatigue failure and become loose relatively early in the roads life, resulting in potholes during the wet periods. This problem is accentuated on roads carrying heavy traffic loads and under high contact stresses near commercial sand- and gravel quarries and coalmines, for example, in the Eastern Transvaal. Inspection of failures on these pavements revealed the presence of loose (crushed) base material at the interface between the seal and the base.

Laboratory investigations of these base materials indicated that the inherent quality of the material was adequate and within current specifications for cementitious materials (TRH4, DRTT, 1985). Curing and construction practices were adequately controlled (Kleyn, 1988).

When designing a new road, the Transvaal Roads Department (TRD) considers it sound policy to invest in the supporting pavement layers by providing a relatively deep structure which reduces the structural demand on the upper layers including the wearing course (Kleyn et al., 1986, 1987).

5.1.3 Extent

Evidence of loose seals and surfacings also exists in the Orange Free State (Du Pisani, 1988) and the Cape area (De Villiers, 1988). In a study by Jordaan (1988) compression failure (crushing) was also noted near the top of a cementitious base pavement (MR 27) in the Cape area. This is a clear indication that compression failure of lightly cementitious pavement materials must also be evaluated in addition to the rather well - known fatigue failure analysis of these layers (Otte, 1972, 1978).

In these cases, however, it is not clear if the problem is material, construction and/or traffic associated as with many other pavements in South Africa (Netterberg et al.,1987), as well as with pavements containing weathered igneous aggregates in Botswana (Pinhard, 1987).

5.1.4 Research

Most of the research on lightly cementitious road building materials (C3 and C4) to date concentrates primarily on its fatigue characteristics when the material is used as structural pavement layers. This is probably because of the similarity between the fatigue behaviour of relatively strongly cementitious materials (C1, C2 and lean concrete) and portland cement concrete (PCC) pavement materials. In this chapter, however, an investigation into the behavioural characteristics of relatively lightly cementitious materials (C3 and C4) is described.

Extensive full scale testing with the Heavy Vehicle Simulator (HVS) was done on a relatively deep pavement structure, as defined with the Dynamic Cone Penetrometer (DCP) survey (De Beer et al., 1988). The testing was on Road 1932 near Rooiwal, north of Pretoria (De Beer, 1986a, 1986b, 1986c, 1986d). The base and subbase are of C3/C4 quality. In Chapter 4 the permanent deformation characteristics of this pavement are discussed.

The results indicated that compression failure near the top of the base layer predominantly governed the rate of permanent deformation ("plastic deformation") as measured on the surface of the pavement. In the case of this pavement, and to a lesser extent, on a relatively shallow Road 2212 (Bultfontein), compression failure of the base layer contributed largely towards the total permanent deformation (rutting) on the surface of the pavement after extensive HVS testing. It is therefore important to study this type of failure to quantify its effect and also to provide guidelines accounting for this occurrence during initial design stages.

In this chapter these guidelines are given as tentative design and analysis curves from which the number of load repetitions needed to initiate compression failure (Nc) in lightly cementitious layers is obtained for a given tyre contact stress (pressure) on the pavement and a given in situ Unconfined Compressive Strength (UCS) of the material. It is proposed that these curves be used in conjunction with the mechanistic design method and maintenance planning for these types of pavements.

5.2 COMPRESSION STRENGTH PARAMETERS OF CEMENTITIOUS MATERIALS

5.2.1 Cohesion c and angle of internal friction ϕ

Several investigators presented the strength properties of cementitious materials according to the Mohr - Coulomb theory (Wissa et al., 1965; Balmer, 1958; Rocha, et al., 1961; Nash et al., 1965; Ferguson et al., 1968; Christensen, 1969; Mitchell, 1976; Clough et al., 1981; Akinmusuru, 1987; and Dupas et al., 1979).

According to the Mohr - Coulomb theory, the cohesion intercept c and the angle of internal friction ϕ are the most important strength parameters of untreated (natural) soil. It was, however, found by the above - mentioned investigators that c and ϕ adequately describe the compression strength of relatively lightly cementitious materials. In Figure 5.1 two methods for determining the c and ϕ are illustrated, based on the Mohr-Coulomb theory. In Figure 5.1(a) the direct method is illustrated whereby c and ϕ are determined directly from the

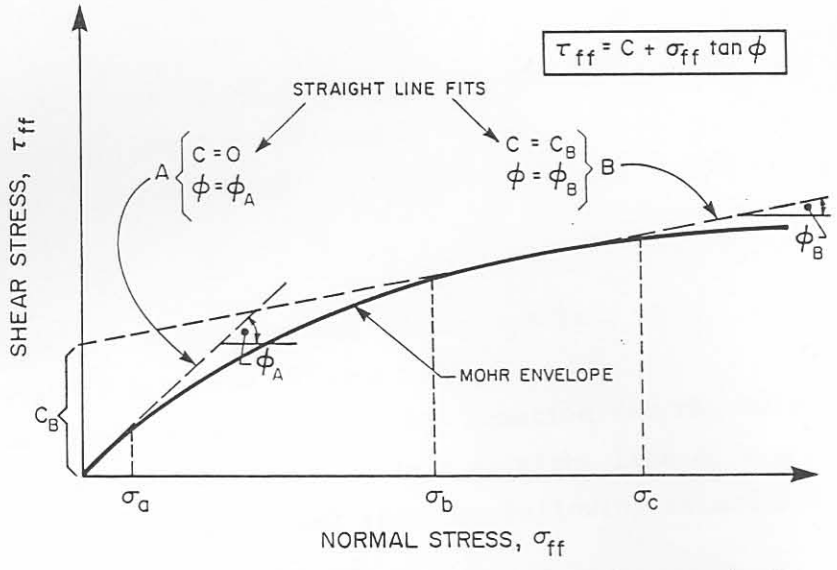

(a) Mohr envelope from Mohr circles (direct method)

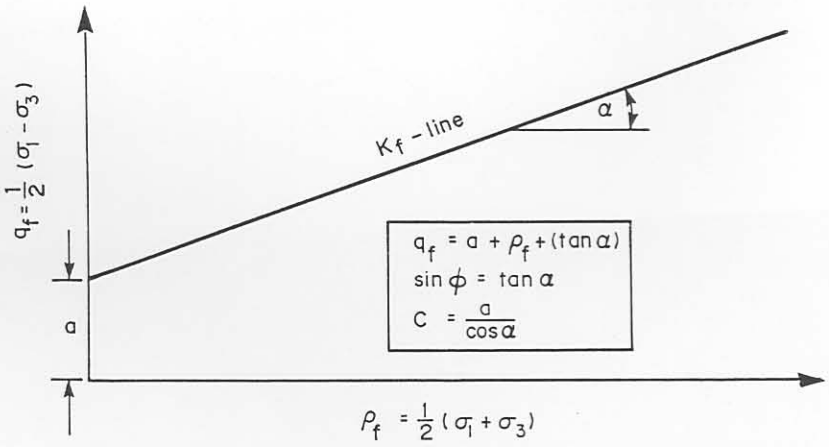

(b) K_f-line from ρ - q diagram (indirect method)

FIGURE 5.1

THE METHODS OF DETERMINING C AND ϕ FROM A SERIES OF TRIAXIAL TESTS USING THE MOHR-COULOMB THEORY

940-4-5810/21 BS

Mohr-Coulomb circles, utilising the shear strength at failure, τ_{ff}, and the normal stress at failure, σ_{ff}. From straight line approximations, c and ϕ are determined for the relevant normal stress range. In Figure 5.1(b), the indirect method is illustrated whereby c and ϕ are indirectly calculated from the K_f-line parameters, a and α, derived from a p_f-q_f diagram. The relationships for c and ϕ are as follows:

$$q_f = a + p_f \tan \alpha \quad \ldots\ldots 5.1$$

$$\sin \phi = \tan \alpha \quad \ldots\ldots 5.2$$

$$\text{and } c = a/\cos \phi \quad \ldots\ldots 5.3$$

where q_f = shear stress
p_f = normal stress
c = cohesion

The p_f-q_f diagram is obtained from the results of normal triaxial tests and a straight line regression may be performed on the results from the maximum τ-values at each stress state, to obtain the relevant parameters a and α from which c and ϕ are computed (Lambe et al., 1969), using equations 5.1, 5.2 and 5.3.

In one of his studies, Thompson (1966) used a statistical method proposed by Herrin (1954) to determine c and ϕ of cementitious materials. This method is illustrated in Figure 5.2 and includes the following procedure:

1. A plot of σ_1, maximum normal stress applied, vs σ_3, confining pressure, is prepared (Figure 5.2).
2. The best least-squares regression equation for the data is determined. If the equation is a straight line $\sigma_1 = a + b\sigma_3$, the c and ϕ are calculated from the following relationships:

$$c = a/(2\sqrt{b}) \quad \ldots\ldots 5.4$$

$$\text{and } \sin \phi = (b-1)/(b+1) \quad \ldots\ldots 5.5$$

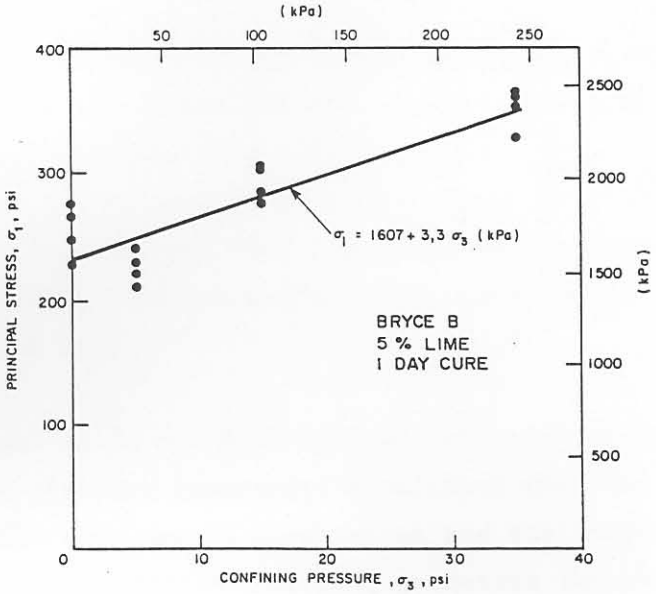

FIGURE 5.2
INFLUENCE OF CONFINING PRESSURE ON MAXIMUM PRINCIPAL STRESS (Thompson, 1966)

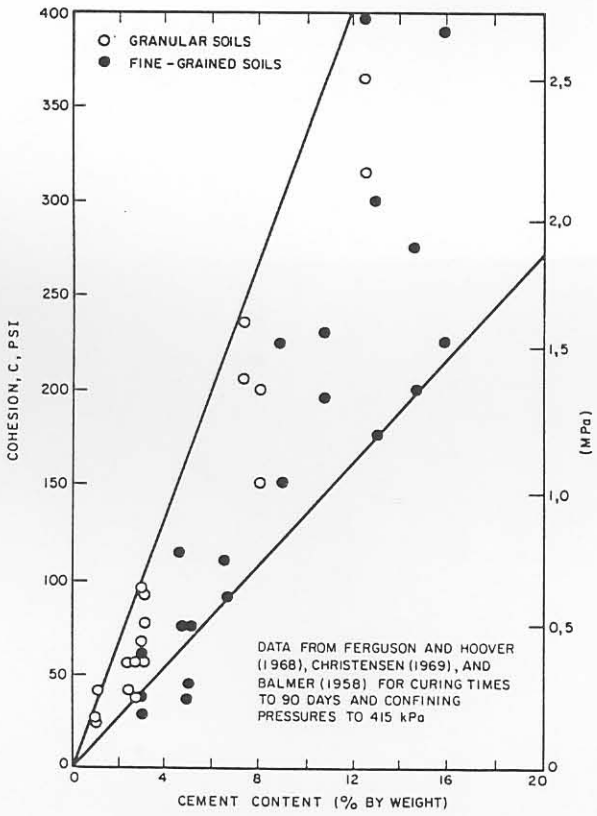

FIGURE 5.3
THE EFFECT OF CEMENT CONTENT ON THE COHESION INTERCEPT FOR SEVERAL SOIL AND CEMENT MIXTURES (MITCHELL, 1976)

5.2.2 Major findings of previous research

Some of the most important findings on the effects of c and ϕ of cementitious materials reported by Wissa et al. (1965) are listed below:

(1) The effective stress principle applies to the strength behaviour of saturated stabilised soils, ie, the Mohr-Coulomb envelope in terms of effective stresses is essentially independent of drainage conditions whereas the total stress envelope is dependent on the drainage conditions during shear.

(2) The addition of a cementing material such as hydrated lime or portland cement can substantially increase the Mohr-Coulomb effective cohesion c, of both coarse-grained and fine-grained soils. The c increases with increasing cement content and increasing curing time (strength of the cement). The development of shrinkage cracks owing to volume changes which occur during curing or weathering (cycles of wet-dry) will cause a decrease in c, and may induce premature fracture at low consolidation pressures (while the cracks remain open) which exhibits itself as an apparent further decrease in c and an apparent increase in ϕ.

(3) Cementation has essentially no effect on the angle of internal friction ϕ of a coarse-grained soil provided the density of the soil excluding the cement is kept constant. Cementation can increase ϕ of a fine-grained soil by as much as 10 degrees. The more plastic the soil and more cement added the larger is the increase. Curing time (strength of the cementation) and weathering have no effect on ϕ.

(4) For stabilised soils the Mohr-Coulomb criterion of failure in terms of effective stresses represents conditions when the sum of the cohesive resistance due to cementation and the frictional resistance due to particle contact, geometric interference (interlocking of particles), and dilatancy in the case of drained shear, is a maximum.

(5) At any given axial strain the total shearing resistance of a soil cemented with hydrated lime or portland cement can be considered to have two components: a cohesive resistance, independent of effective stress and a frictional resistance, dependent on effective stress and therefore a function of the pore pressures developed during shear.

(6) The maximum cohesive resistance of a soil cemented with a nonductile material, such as lime or cement, occurs at smaller strains than the effective Mohr-Coulomb envelope. The c is lower than the maximum cohesive resistance because partial breakdown of the cementation has occurred by the time the envelope is reached and it can be as little as 30 per cent of the maximum value. By the time ultimate conditions are reached the cohesive resistance in the zone of shearing is completely destroyed and the shearing resistance is purely frictional (crushed state).

(7) The maximum frictional resistance occurs at larger strains than the Mohr-Coulomb envelope and it is fully mobilised at ultimate conditions when the effective stress and shear stress remain constant with further straining. It can be 5 to 10 degrees higher than the Mohr-Coulomb ϕ.

(8) The larger increase in the frictional resistance of a fine-grained soil when a stabiliser such as lime or cement is added is believed to be due to the formation of strongly cemented large aggregates of fine-grained particles which are held together by a weaker continuous cementation. The aggregation forms during mixing and compaction and remains essentially constant during curing which accounts for ϕ being independent of length of cure. In the case of sands, aggregation does not occur during mixing because of the relatively large size of the grains and therefore ϕ is independent of the cementation per se.

(9) The addition of lime or cement to a fine-grained soil causes its undrained shear strength to increase because of increase in c and in some cases ϕ. The excess pore pressures which develop during undrained shear are not significantly influenced by the cementation.

(10) The shear strength of a stabilised soil increases with increasing consolidation pressure. The rate of increase in strength with increase in consolidation pressure is greater in drained shear than in undrained shear.

(11) The addition of lime or cement to a soil causes an increase in its initial tangent modulus of elasticity and reduces the strain required to reach the maximum principle stress difference.

5.2.3 Parameters influencing c

In Figures 5.3, 5.4 (a), (b), (c) and (d) the effects of stabiliser content, age of curing and compaction density on cohesion, c, as was found by several investigators, are illustrated. Figure 5.3 illustrates the linear relationships between cohesion c and cement content of both granular and fine-grained soils as was summarised by Mitchell (1976), and indicates a general increase in c and cement content.

Figure 5.4(a) illustrates nonlinear relationships between cohesion and cement content, as found by Dupas et al. (1979), and the figure indicates that c increases with the increase in both compaction density and curing age. Figure 5.4(b) indicates a very marked increase in c with increase in curing age and cement content of a uniformly - graded beach sand, stabilised with cement (Akinmusuru, 1987). Thompson (1966) also found that c increases with curing age, but the rate of increase may differ and may even decrease with increase in curing age, depending on the soil and stabiliser type, see Figure 5.4(c). In Figure 5.4(d), Mitchell (1976) shows that the rate of increase in c related to curing age of a cement - stabilised silty soil, is markedly higher than that of a cement - stabilised A-1 sand.

Generally, c increases with an increase in cement content, curing age and compaction density, mainly because of the formation of stronger cementitious bonds between the aggregates. With an increase in compressive strain, these bonds are destroyed and the cohesion strength c decreases to zero as a result of increasing strain, while the frictional strength ϕ increases to a maximum value, when fully mobilised. This effect is illustrated in Figure 5.5. The initial increase in c is

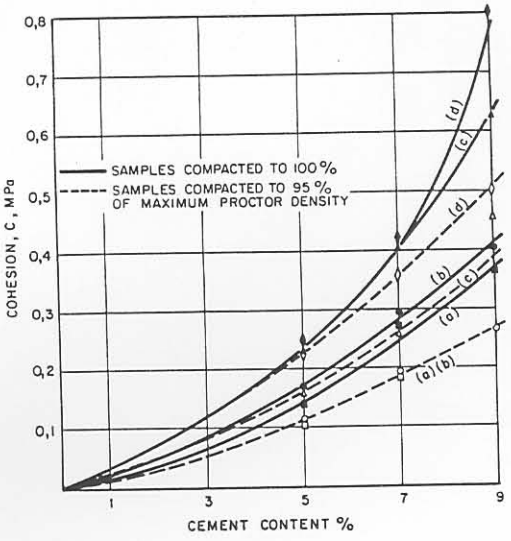

FIGURE 5.4(a)
COHENSION OF UPPER SAND-CEMENT SAMPLES: (a) 14 DAYS; (b) 28 DAYS - 90 DAYS; (d) 180 DAYS (DUPAS et al., 1979)

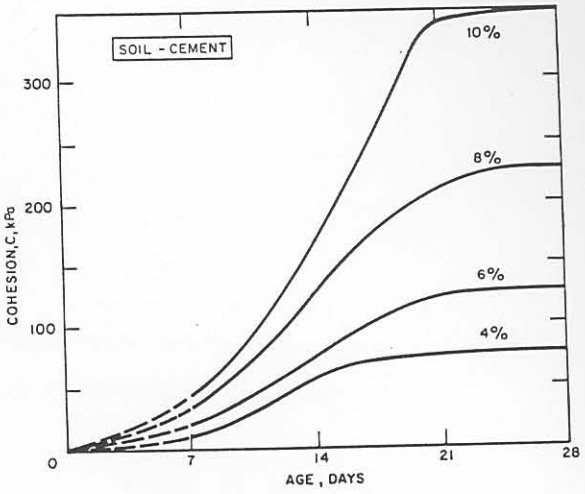

FIGURE 5.4(b)
EFFECT OF CURING AGE ON THE COHESION FOR DIFFERENT CEMENT CONTENTS (AKINMUSURU, 1987)

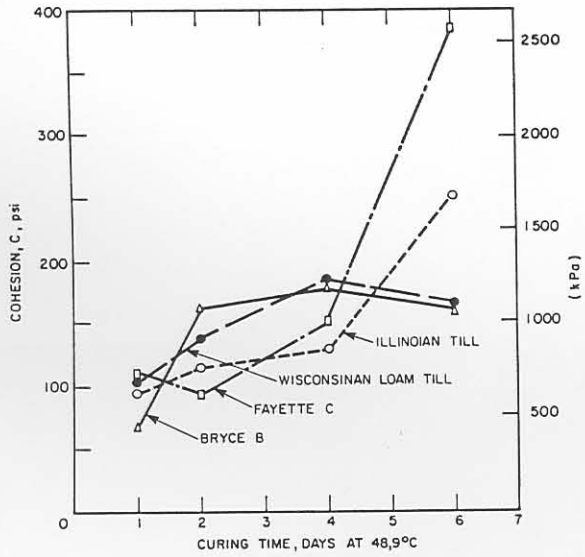

FIGURE 5.4(c)
INFLUENCE OF CURING TIME ON COHESION OF LIME-SOIL MIXTURES (THOMPSON, 1966)

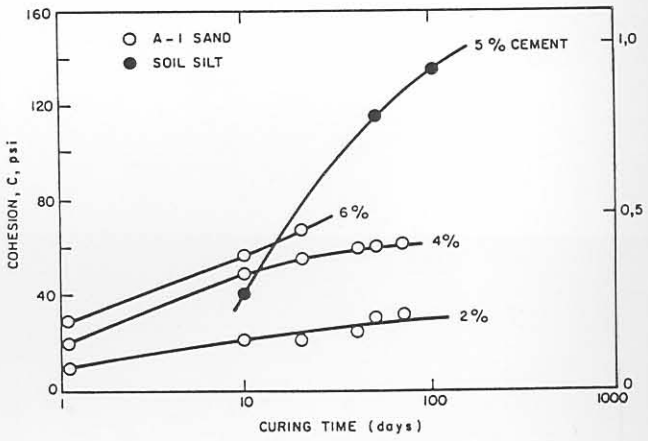

FIGURE 5.4(d)
THE EFFECT OF CURING TIME ON THE COHESION INTERCEPT FOR DIFFERERNT CEMENT TREATMENT LEVELS (Mitchell, 197

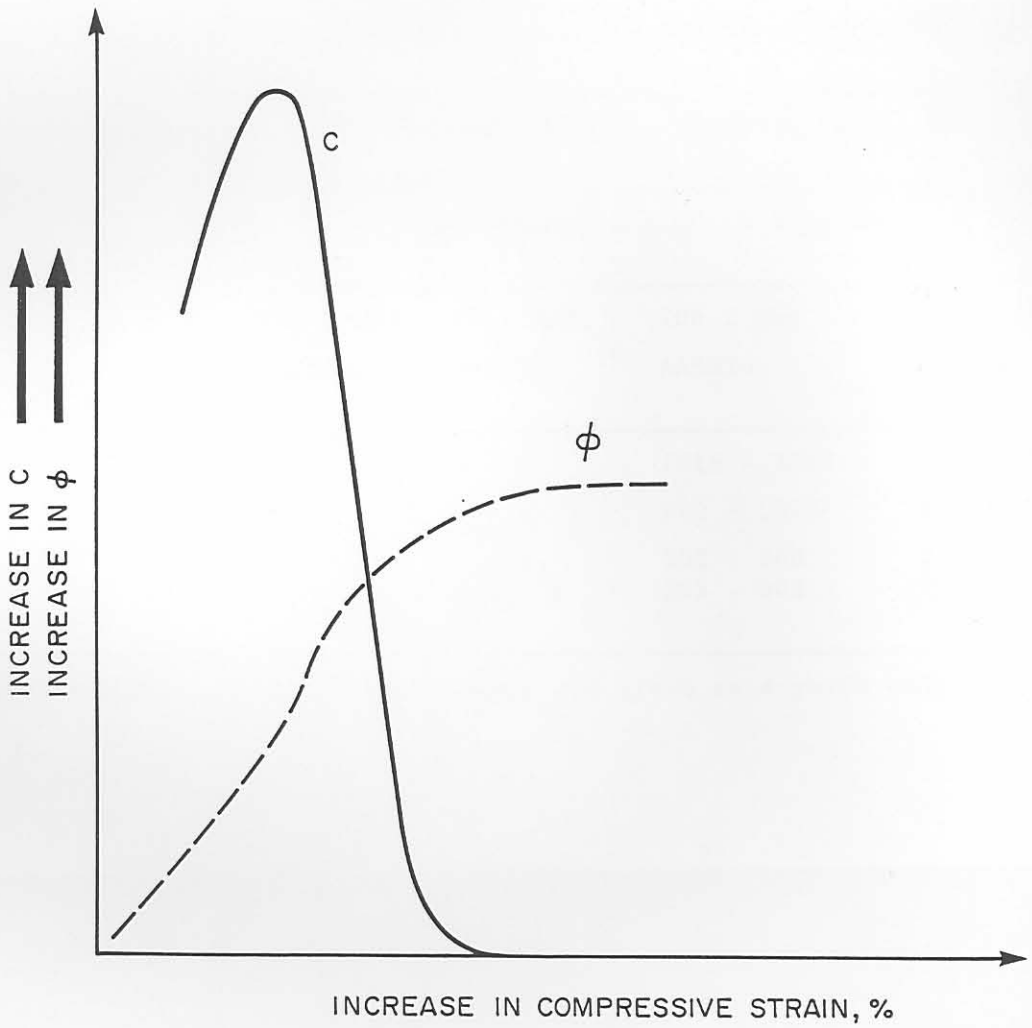

FIGURE 5.5

EFFECTIVE COHESION AND EFFECTIVE ANGLE OF INTERNAL FRICTION VERSUS COMPRESSIVE STRAIN FOR UNIFORMLY CEMENTED SAND, AS A PERCENTAGE (SAXENA et al, 1978)

most probably related to micro fractures within the cementitious material. These fractures close as a result of increasing compressive strain, before the breakdown of the cementitious bonds (decrease in c) is initiated.

5.2.4 Relationships between c and Unconfined Compressive Strength (UCS)

In Figures 5.6 and 5.7, linear relationships between c and UCS are illustrated. The relationships are :

$$c = 64 + 0{,}292UCS \quad \ldots\ldots\ldots\ldots\ldots\ldots\ldots\ldots 5.6$$

with c and UCS in kPa,

as was found by Thompson (1966) for lime stabilised materials, and

$$c = 48 + 0{,}225UCS \quad \ldots\ldots\ldots\ldots\ldots\ldots\ldots\ldots 5.7$$

with c and UCS in kPa,

as was found by Mitchell (1976) for fine-grained cement stabilised soils. Applying Equation 5.6 to the current UCS limits for the cementitious categories indicated in TRH14 (NITRR, 1985), the estimated cohesion values for the different cementitious materials are indicated in Table 5.1.

TABLE 5.1 ESTIMATED COHESION (C) VALUES FOR CEMENTITIOUS MATERIALS

Cemented material	UCS-range (MPa)		Cohesion-range, c (kPa)	
	Laboratory design, 7-days at:			
	100 % Mod. AASHTO	97 % Mod. AASHTO	100 % Mod. AASHTO	97 % Mod. AASHTO
C1	6 - 12	4 - 8	1816 - 3568	1232 - 2400
C2	3 - 6	2 - 4	940 - 1816	648 - 1232
C3*	1,5 - 3,0	1 - 2	502 - 940	356 - 648
C4*	0,75 - 1,5	0,5 - 1	283 - 502	210 - 356

* These maximum strength requirements are given as a guide only.

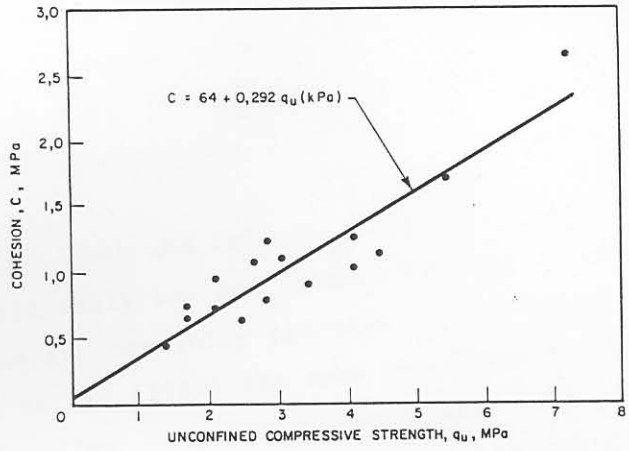

FIGURE 5.6
COHESION vs UNCONFINED COMPRESSIVE STRENGTH OF LIME-SOIL MIXTURES. (Thompson, 1966)

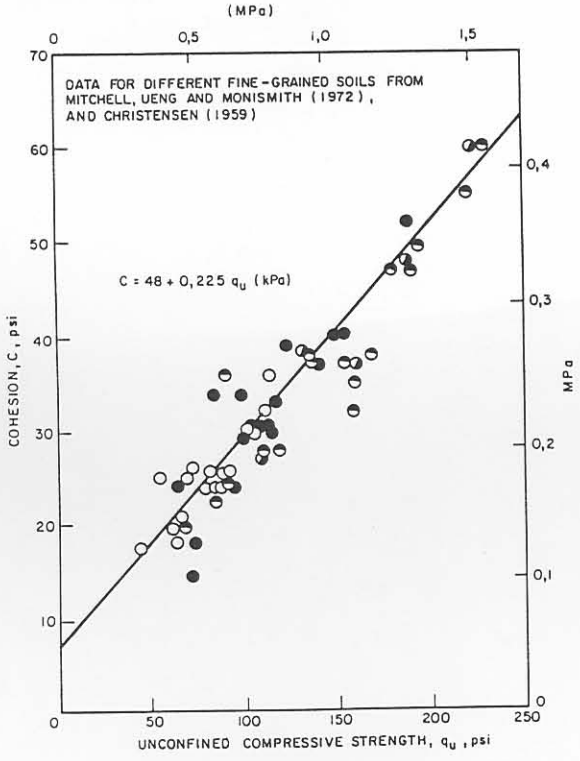

FIGURE 5.7
THE RELATION BETWEEN THE UNCONFINED COMPRESSIVE STRENGTH AND THE COHESION INTERCEPT OF FINE GRAINED SOIL AND CEMENT MIXTURES (Mitchell, 1976)

The cohesion values indicated in the table are 10 to 40 times higher than those obtained for relatively high quality crushed - stone materials (G1/G2/G3) and even more for the lower quality granular materials indicated by Maree, (1982). This is a clear indication of the beneficial effect of cementation in order to withstand shear failure in cementitious layers.

The friction angle ϕ appears to be constant and not affected by cementation, therefore the friction angle values proposed by Maree (1982) for the different crushed - stone materials should be used to calculate the safety factor against shear failure, if cementation of the material is considered.

5.3 ELASTIC PROPERTIES OF CEMENTITIOUS MATERIALS

According to Thompson (1966) the elastic properties in compression of cementitious materials may be determined using a composite or average stress - strain relationship at a given confining pressure, σ_3. See Figure 5.8.

In Figure 5.9 typical stress - strain curves for natural and lime-treated soil are illustrated. The effect of cementation is well illustrated in the figure. The figure also indicates that the percentage compressive strain at failure of the cementitious material is markedly lower than that of natural (untreated) soil, and is approximately at 1 per cent strain.

Alfi (1978) also found that the failure strain of relatively strongly cemented sand was relatively low and varied between 1 and 1,5 per cent strain with increase in confining pressure. See Figure 5.10. In a study by Robbertson et al. (1987) the same was found for cement treated materials, but for lime - treated materials, the failure strain increased with increase in lime content, approaching that of raw (natural) soil. This is an illustration of the greater flexibility of a soil - lime mixture above that of a soil - cement mixture, produced from the same raw material. See Figure 5.11.

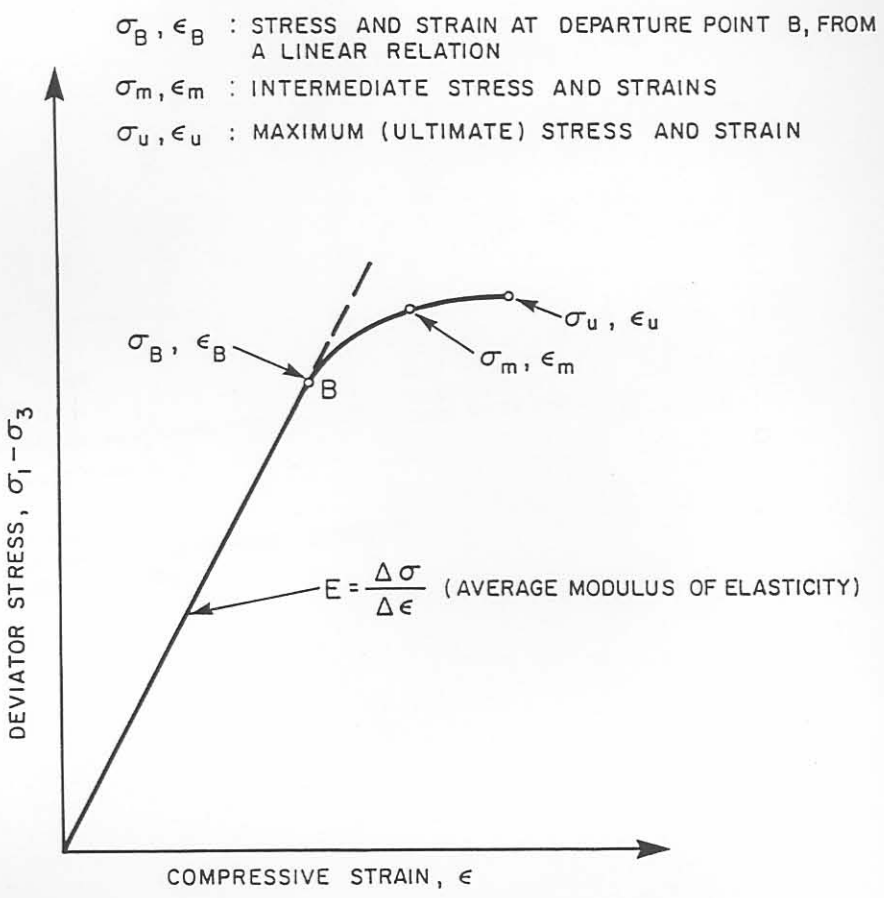

FIGURE 5.8

COMPOSITE STRESS-STRAIN CURVE OF CEMENTITIOUS MATERIALS (Thompson, 1966)

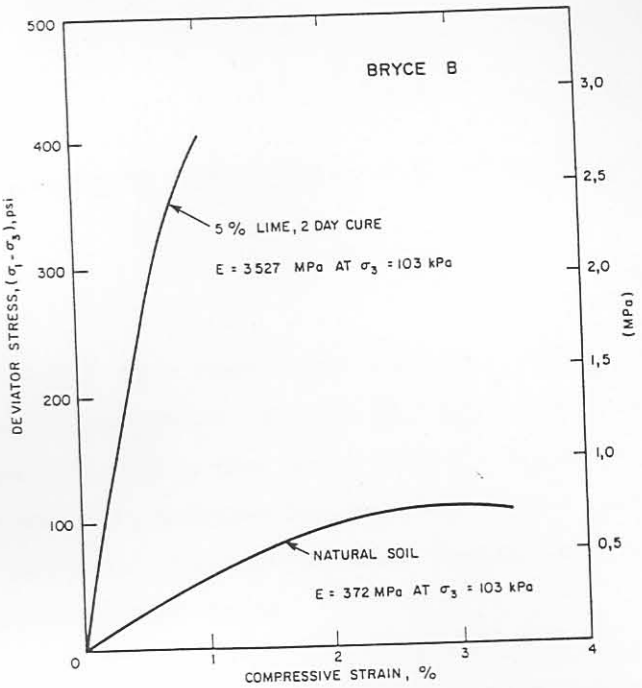

FIGURE 5.9
TYPICAL STRESS-STRAIN CURVES FOR NATURAL AND LIME TREATED SOIL (Thompson, 1966)

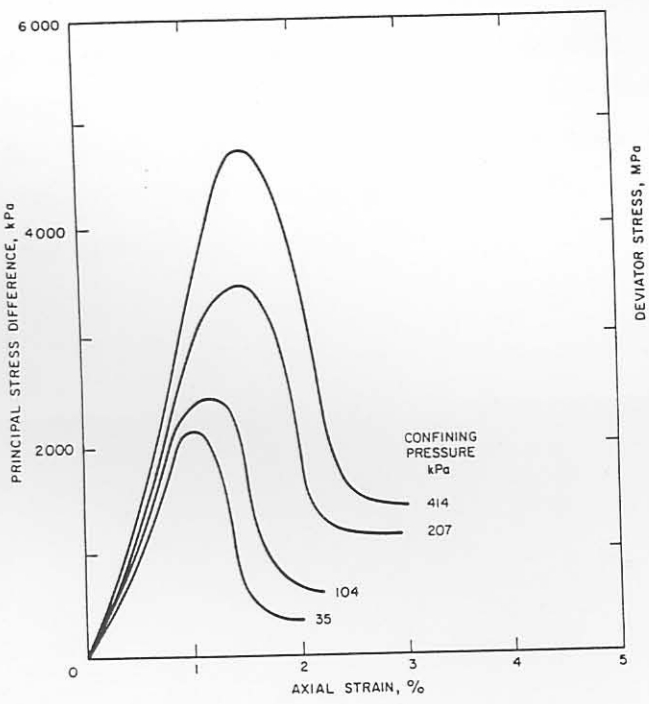

FIGURE 5.10
TYPICAL STRESS-STRAIN CURVES, OF A STRONGLY CEMENTED SAND (Alfi, 1978)

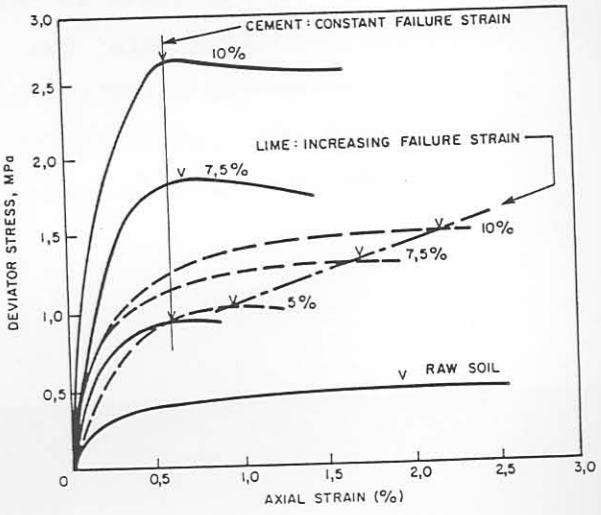

FIGURE 5.11
STRESS-STRAIN CHARACTERISTICS OF SOIL-CEMENT AND SOIL-LIME PRODUCED WITH THE SAME SOIL, ILLUSTRATING THE GREATER FLEXIBILITY OF SOIL-LIME WITH INCREASING STABILIZER CONTENT. (Robbertson, et al 1987)

A summary of the percentage failure strains obtained by several investigators for naturally uncemented, naturally cemented and artificially cemented materials is given in Appendix B, Table B.1. The table indicates that the highest percentage strains occurred for the naturally uncemented materials (1 to 12 per cent), and for naturally cemented materials 1 to 9 per cent. For artificially cementitous materials, the failure strain is approximately 1 to 2 per cent, depending on the age and the curing conditions. From the literature it is evident that the compressive failure strain of cementitious materials decreases in relation to that of untreated (unstabilised) materials. According to Thompson (1966) the average ultimate (failure) strain at confining pressure of 103 kPa for cementitious materials is approximately 1 per cent.

It is therefore my opinion that if the vertical permanent deformation (as a result of load repetitions) within a cementitious pavement layer exceeds approximately 1 per cent of the layer thickness, it may be regarded as the **initiation of compression failure** within the layer itself.

5.4 PERMANENT DEFORMATION MEASUREMENTS WITH DEPTH ON A DEEP PAVEMENT

5.4.1 General

In order to establish the number of in situ stress repetitions (Nc) needed to initiate compression failure in these pavements, the vertical permanent deformation within the layer must be measured. Nc is obtained at the point where the deformation exceeds the 1 per cent criterion stated in the previous paragraph, and indicates the **initiation of compression failure** in that layer.

With the accelerated testing (HVS) programme in South Africa, the Multi - Depth Deflectometer (MDD) was developed to measure the resilient deflection profiles at different stages of trafficking in pavements primarily. However, these instruments are also perfectly suited to measure the permanent deformation in the different pavements layers at different stages of stress repetitions (trafficking) (De Beer et al., 1988). In the following section the results of several of these tests and results are discussed.

5.4.2 MDD results

The results of twenty two (22) different multi-depth deflection (MDD) measuring positions on eight (8) test sections (Sections 260A4, 274A4, 275A4, 289A4, 294A4, 309A4, 337A4 and 338A4) were used to investigate the in situ permanent deformation characteristics of a relatively deep (DCP- defined) pavement structure, viz Road 1932, near Pretoria. The structure of the pavement, HVS test layout and the different depths of the MDD modules are illustrated in Figure 5.12. The MDD modules of MDD4 and MDD8 (all sections) were placed at depths of 0, 180, 330, 480 mm , and for Sections 260A4 and 274A4 also at a depth of 630 mm in the pavement. For MDD 12, the depths were 65, 215, and 420 mm respectively.

The permanent deformation on the surface of the pavement was measured with the electronic profilometer and also with a straight edge. The thicknesses of the cementitious base and subbase layer were approximately 180 mm and 150 mm respectively.

Based on the **compressive failure criterion of 1 per cent compressive failure strain**, the number of load repetitions (Nc) needed to initiate compressive failure within the cementitious layer is obtained by studying the MDD measured permanent deformation results. The principle of this method is illustrated in Figure 5.13. For the base layer, initiation of compression failure was assumed to occur when the permanent deformation exceeded 1,8 mm (1 per cent of 180 mm), and for the subbase 1,5 mm (1 per cent of 150 mm). It is also important to note that fatigue failure of the 13 mm double seal (surface treatment) on top of the cementitious base layer was observed soon after Nc was reached during HVS testing. This was found on all the sections tested and is possibly related to the loss of support because of compression failure in the upper section of the the cementitious base. After extensive fatigue failure, the seal came loose from the base and was also crushed and granulated, even during the dry state of HVS testing.

Figure 5.14 shows the typical manifestation of compression failure in the base of this road. Typical permanent deformation results at different depths measured with the MDDs on HVS test Sections 274A4, are illustrated in Figure 5.15 (a) and (b). Also indicated on the figures are the different Nc - values. Deformation results at different depths

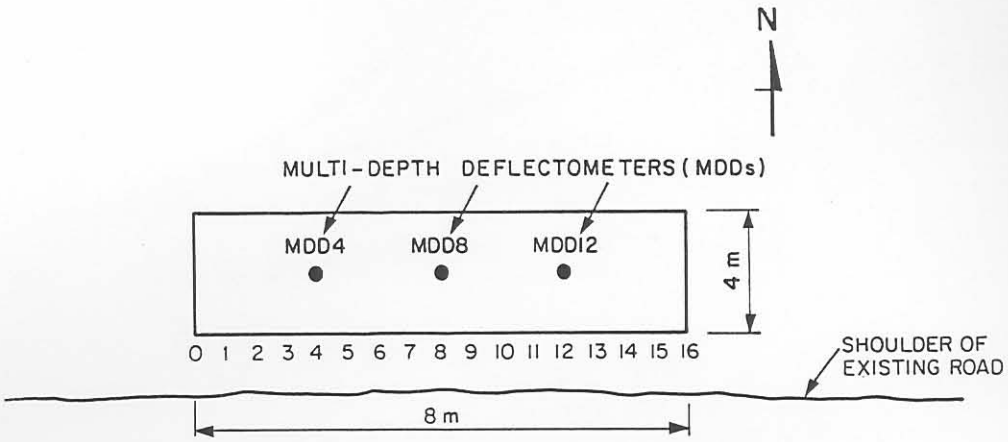

(a) Typical layout of an HVS test section

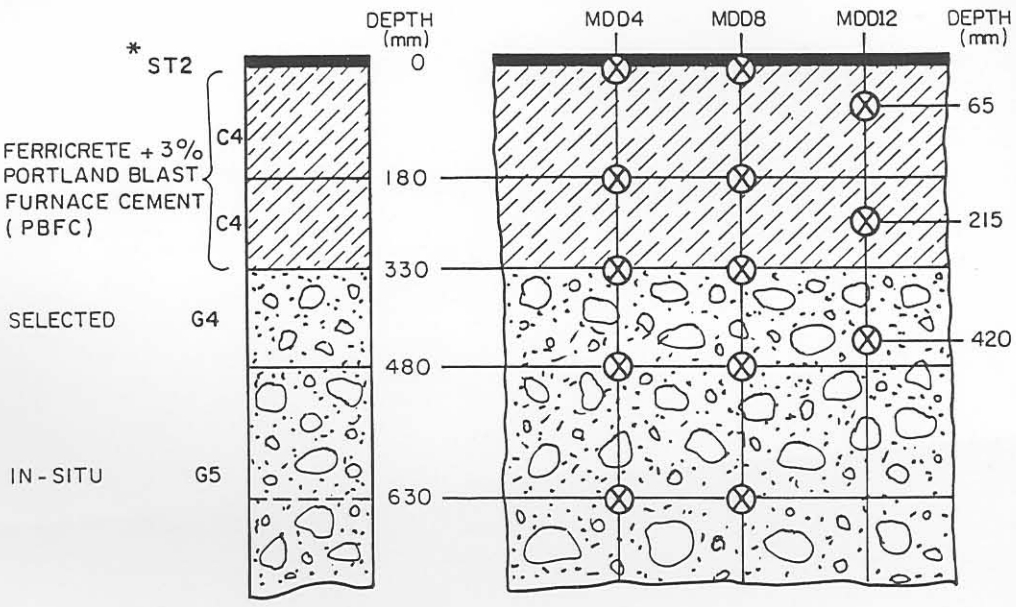

*MATERIAL CODES IN ACCORDANCE WITH TRH14 (DRTT, 1985b)

⊗ MDD MODULES

(b) Pavement structure and MDD layout

FIGURE 5.12

LAYOUT OF HVS TEST SECTIONS FOR PERMANENT DEFORMATION MEASUREMENTS ON ROAD 1932 (ROOIWAL)

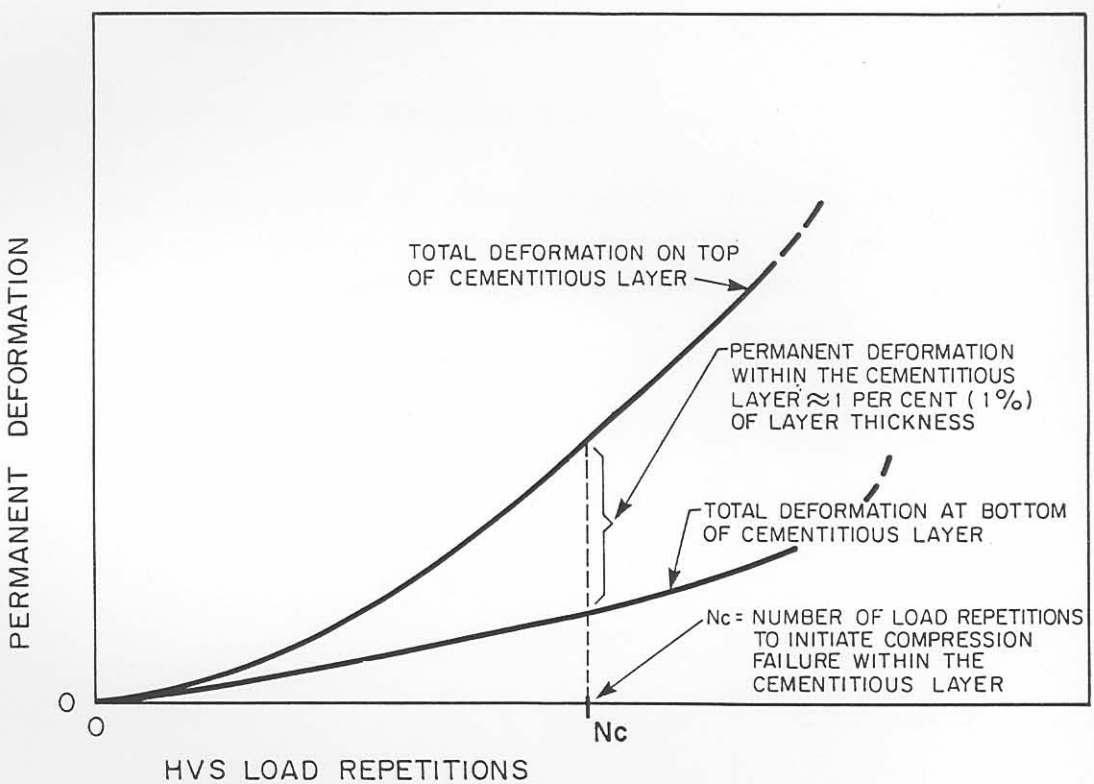

FIGURE 5.13

DETERMINATION OF THE NUMBER OF HVS LOAD REPETITIONS TO INITIATE COMPRESSION FAILURE WITHIN LIGHTLY CEMENTITIOUS LAYERS

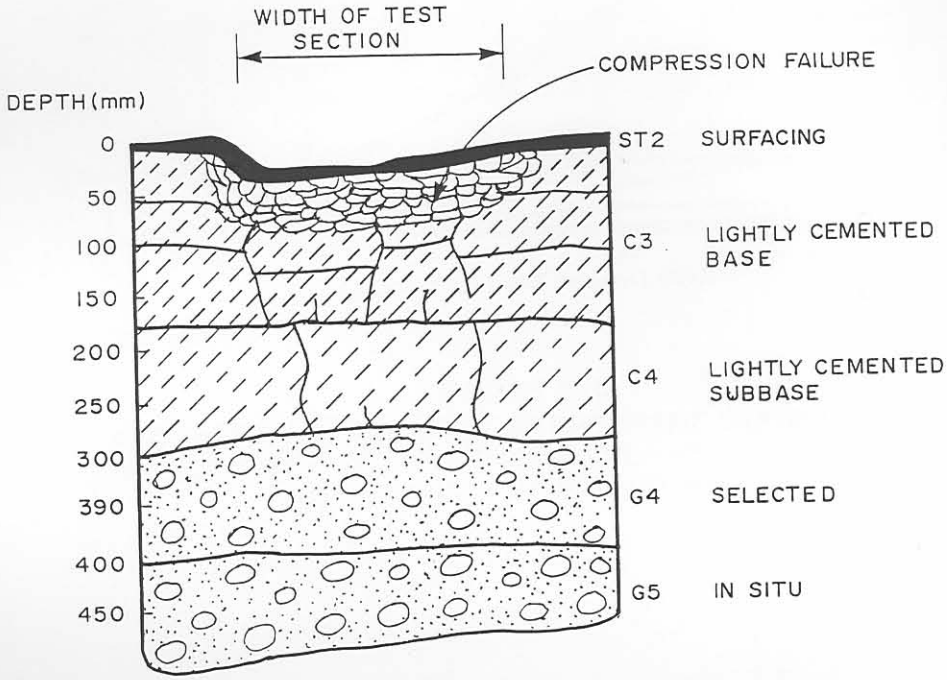

FIGURE 5.14

MANIFESTATION OF COMPRESSION FAILURE IN THE LIGHTLY CEMENTITIOUS BASE LAYER OF A DEEP PAVEMENT (ROAD 1932, ROOIWAL)

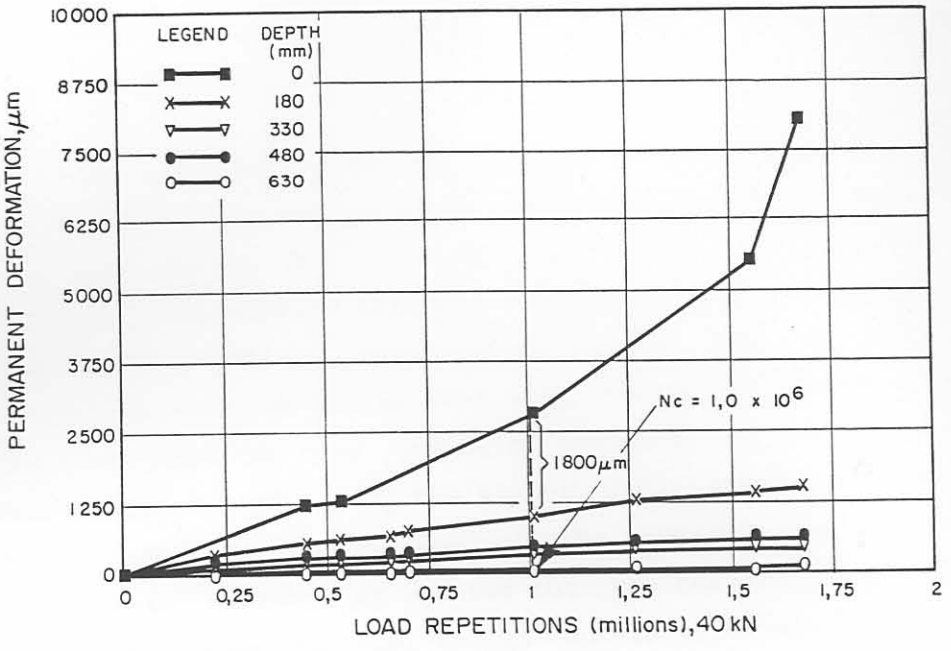

(a) MDD4

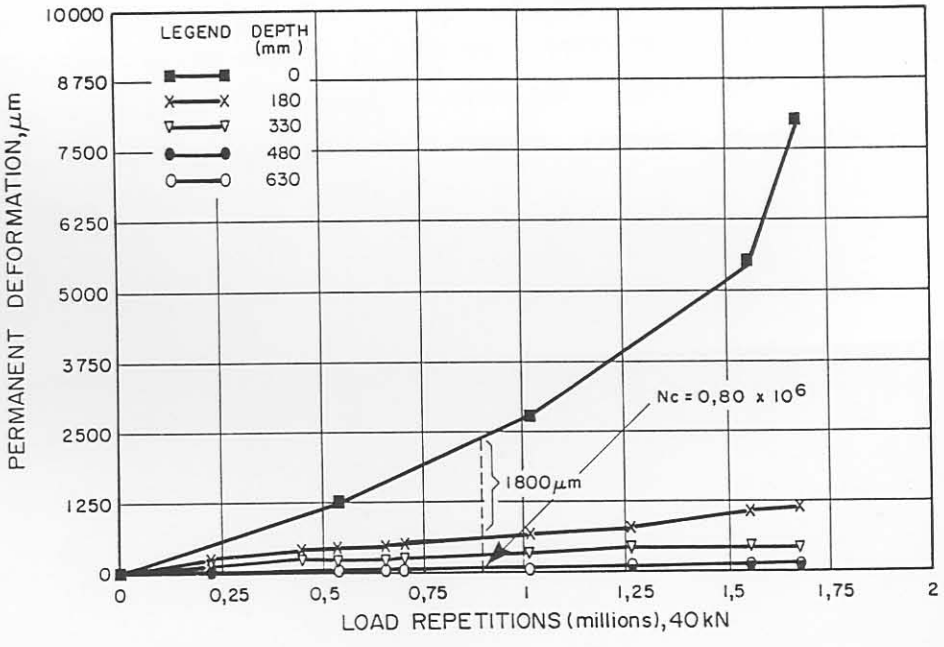

(b) MDD8

FIGURE 5.15

PERMANENT DEFORMATION AT DIFFERENT DEPTHS AT VARIOUS STAGES OF TRAFFICKING ON HVS TEST SECTION 274A4 (ROAD 1932, ROOIWAL)

940 - 4 - 5810/ 18 BS

for other test sections are given in Appendix B, Figures B.1, B.2 and B.3. These figures clearly indicate that most of the permanent deformation occurred within the cementitious base and subbase layers. Close inspection of the top 65 mm of the cementitious base layer and in some cases, the cementitious subbase, revealed that visible compression failure (crushing) did indeed occur, and contributed largely (more than 80 per cent) towards the total permanent deformation (rutting) on the pavement towards the end of the HVS tests. The crushing process, however, is an ongoing failure of the cementitious layers, ie: when Nc for 180 mm is reached, crushing occurs thus reduces the effective layer thickness. A new Nc for the layer with reduced thickness causes a further crushing so that eventually the top of the layer is cracked (crushed) far more than the bottom of the layer as shown in Figure 5.14. As a result of complete crushing and subsequent pumping (moisture accelerated distress, MAD) in the top of the base, the crushed material was completely removed from the test section resulting in extensive potholing. This is an indication of the importance of establishing Nc, for both initial design and maintenance planning on these type of pavements.

5.4.3 Nc - values

Table 5.2 gives a summary of the Nc - values and associated data for the different test sections and measuring positions together with the tyre contact stress during HVS testing. The table indicates that Nc (initiation of compression failure) varies from 500 repetitions to approximately 2,14 million repetitions, whilst the vertical cyclic stress varies between 420 kPa to 1445 kPa. (Normally, the tyre contact stress is lower than the tyre inflation pressure, but in this case the conservative approach of using the higher inflation pressure equal to the contact stress on the surface of the pavement was used in the analysis). It is, however, my opinion that the results in the table may assist in establishing practical design curves to obtain the number of load (stress) repetitions needed to initiate compression failure (Nc) in lightly cementitious layers. To accomplish this, the following assumption has to be made: if the tyre contact stress σ_t approaches the in situ Unconfined Compressive Strength (UCS) of the cementitious material, compression failure starts almost immediately in the cementitious layer, i.e. at Nc = 1.

TABLE 5.2 NUMBER OF HVS REPETITIONS NEEDED TO INITIATE COMPRESSION FAILURE (Nc) ON THE DIFFERENT SECTIONS TESTED

Test-Section	MDD-position	Contact stress,* σ_t (kPa)	UCS** (kPa)	Repetitions, Nc,(million)		Stress Ratio σ_t/UCS
				At MDDs	AVERAGE	
260A4	4	700	1720	1,123		0,407
	8	700	1720	1,270		0,407
	12	700	1720	0,725	1,04	0,407
274A4	4	520	1454	1,000		0,358
	8	520	1454	0,800	0,90	0,358
275A4	4	700	2007	1,580		0,349
	8	700	2007	1,650		0,349
	12	700	2007	1,500	1,58	0,349
289A4	4	700	1433	0,280		0,488
	8	700	1433	0,080		0,488
	12	700	1433	0,300	0,22	0,488
294A4	4	700	2671	1,990		0,262
	8	700	2671	1,380		0,262
	12	700	2671	2,140	1,84	0,262
309A4	6	1445	2115	0,001		0,683
	10	1445	2115	0,001	0,001	0,683
337A4	4	1445	1706	0,0005		0,847
	8	1445	1706	0,0015		0,847
	12	1445	1706	0,001	0,001	0,847
338A4	4	960	1803	0,022		0,532
	8	960	1803	0,021		0,532
	12	960	1803	0,017	0,02	0,532
345A4	4,8,12	420	1445	1,100	1,10	0,291

* Tyre Contact stress assumed = tyre inflation pressure
** UCS: DCP-derived (Kleyn, 1984), in situ Unconfined Compressive Strength of the upper 50 mm of the cementitious gravel base

From this assumption, "additional" data is obtained at Nc = 1, which can be used with the data in Table 5.2, to aid in the development of the design curves. The in situ UCS of the upper 50 mm of the cementitious base was determined with the DCP (Kleyn, 1984) at start of testing on each section, and is also indicated in Table 5.2. The results from Table 5.2 are illustrated in Figure 5.16.

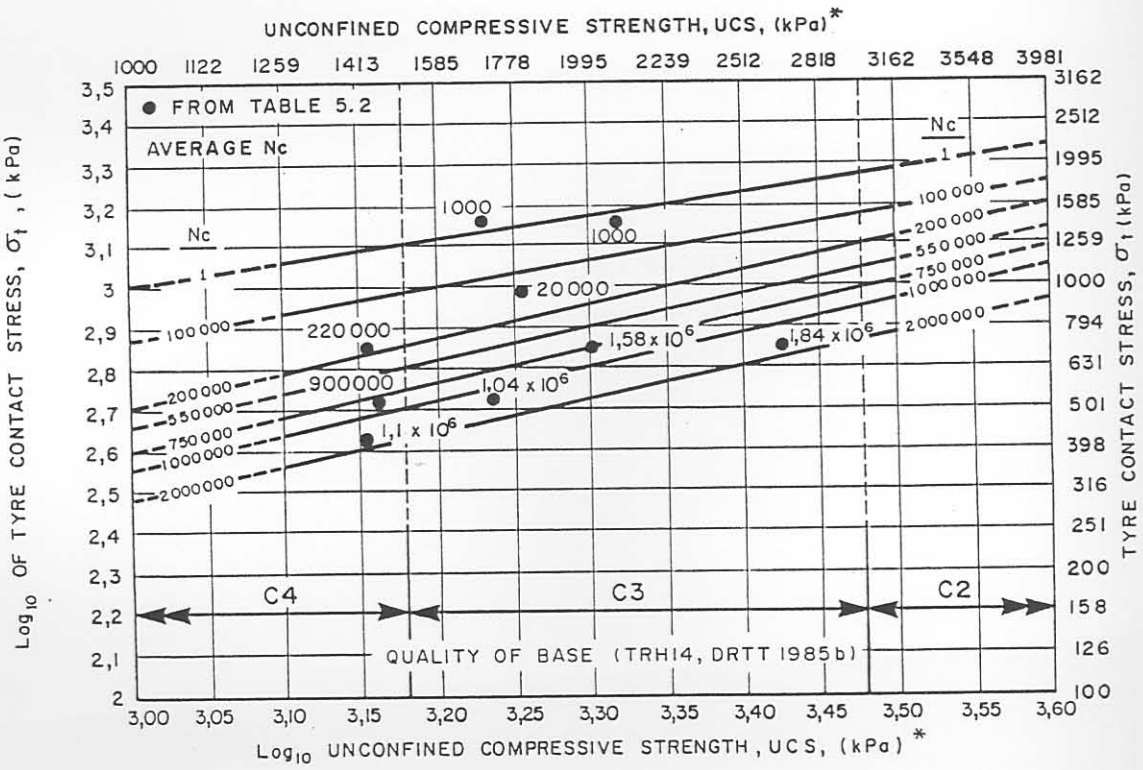

* DCP – DERIVED IN SITU UCS (KLEYN, 1984)

FIGURE 5.16

SUGGESTED RELATIONSHIPS BETWEEN TYRE CONTACT STRESS (σ_t), IN SITU DCP-DERIVED UNCONFINED COMPRESSIVE STRENGTH (UCS) AND NUMBER OF STRESS REPETITIONS (Nc) TO INITIATE COMPRESSION FAILURE (CRUSHING) IN THE TOP 50 mm OF LIGHTLY CEMENTITIOUS BASES. THE HVS RESULTS ARE ALSO INDICATED

Too little data, however, exist to perform any regression analysis between these two variables in Figure 5.16, therefore the curves in are hand-drawn to indicate only possible relationships.

The figure also demarcates the strength boundaries for the different quality of cementitious gravel materials (DRTT,1985a, 1985b) as summarised in Table 5.1. The curves are only valid for C3-materials and to a lesser extent for C2- and C4- materials. The suggested curves, without the HVS data, are illustrated in Figure 5.17 and are proposed for use in determining the Nc of pavements with lightly cementitious gravel bases, if the in situ UCS (upper 50 mm of the cementitious gravel base) and the tyre contact stress, σ_t, are known.

Generally, the higher the tyre contact stress on a specific pavement, the lower Nc, and vice versa. For example, if the UCS is 1995 kPa and σ_t is 630 kPa, Nc is approximately one (1) million (See Figure 5.17).

The information in Figure 5.17 may be presented using a single compression failure curve by normalising, as depicted in Figure 5.18. This curve is similar to the better known fatigue curves of cementitious materials (De Beer, 1989) and concrete. In Figure 5.18, the ratio between tyre contact stress, σ_t, and in situ UCS (σ_t/UCS), is plotted against the measured number of stress repetitions (N_c).

The compression failure curve is also described below:

$$N_c = 10^{8,21(1 - \sigma t/(1,2UCS))} \quad \ldots\ldots\ldots\ldots\ldots\ldots 5.8$$

with N_c = stress repetitions to initiate compression failure in weakly cemented materials (UCS: 0,75 MPa to 3 MPa)

σ_t = tyre contact stress in kPa (σ_t assumed = tyre inflation pressure)

UCS = in situ unconfined compressive strength derived from DCP measurements (Kleyn, 1984).

R^2 = 0,89 and n= 22

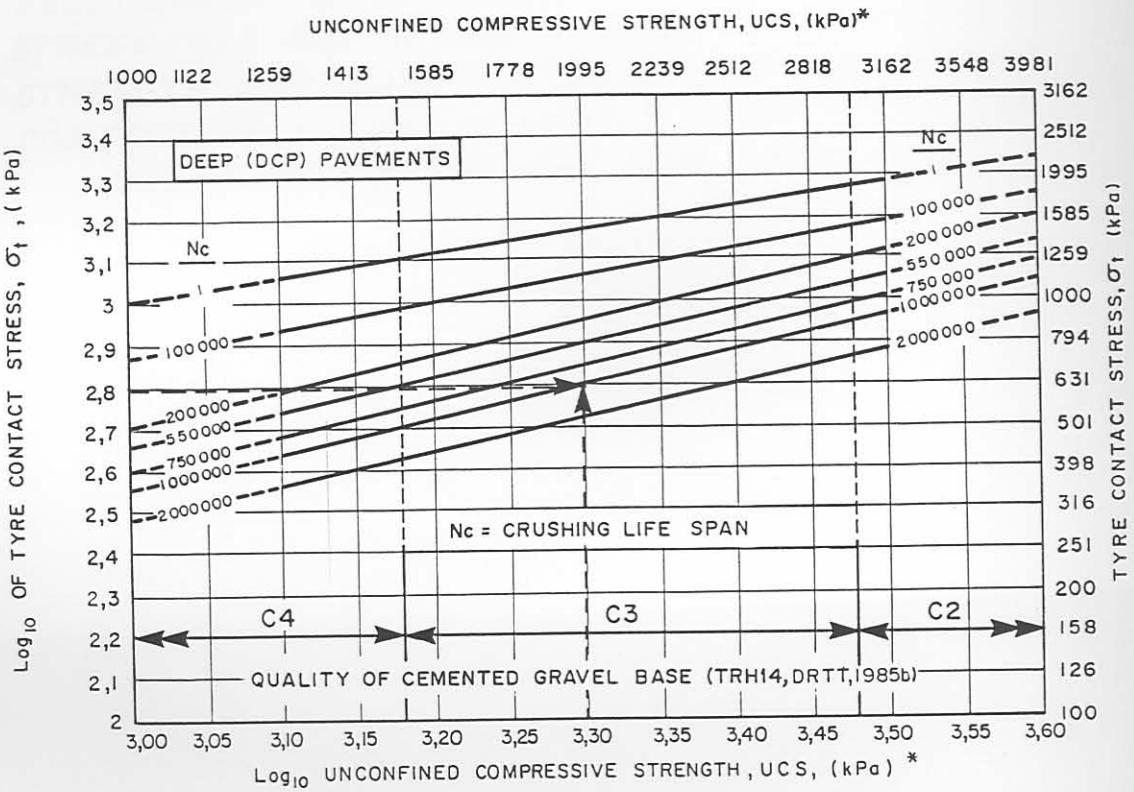

* DCP – DERIVED IN SITU UCS OF TOP 50 mm OF CEMENTITIOUS GRAVEL BASE

FIGURE 5.17

SUGGESTED RELATIONSHIPS BETWEEN TYRE CONTACT STRESS (σ_t) AND UNCONFINED COMPRESSIVE STRENGTH (UCS) TO DETERMINE THE STRESS REPETITIONS (Nc) TO INITIATE COMPRESSION FAILURE IN LIGHTLY CEMENTITIOUS BASE

PROPOSED CRUSHING CURVE

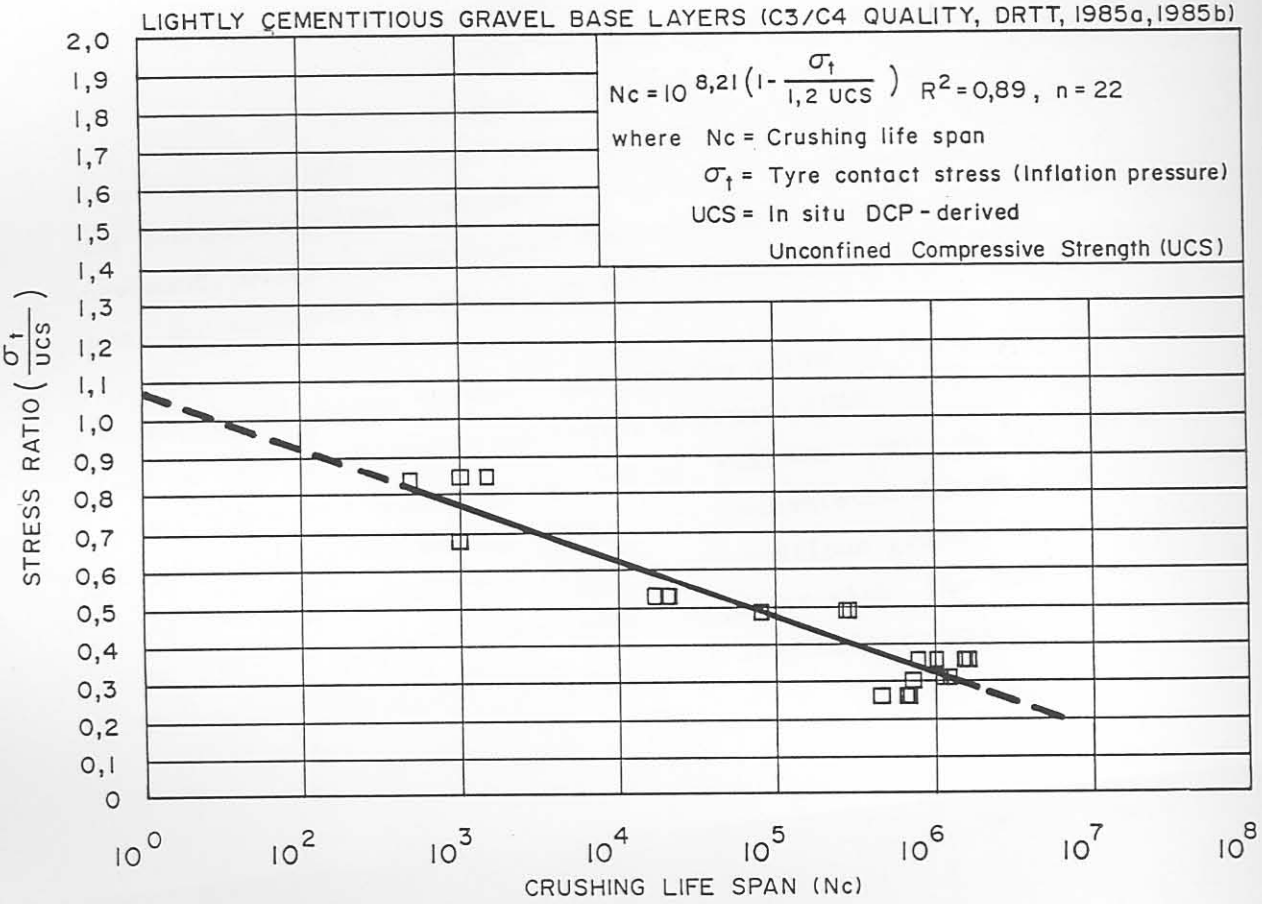

FIGURE 5.18

RELATIONSHIP BETWEEN THE RATIO OF TYRE CONTACT STRESS (σ_t) AND IN SITU UNCONFINED COMPRESSIVE STRENGTH AND NUMBER OF REPETITIONS TO INITIATE COMPRESSION FAILURE IN LIGHTLY CEMENTITIOUS BASE LAYERS WITH RELATIVELY THIN SURFACINGS

This compression failure relationship is proposed as a tentative design curve to obtain estimates (50 % probability) be used in new designs, rehabilitation and/or during maintenance planning on pavements with lightly cementitious gravel base and/or subbase layers. Future research, however, should be done to establish an improved curve with more data on a wider range of cementitious materials.

5.5 SUMMARY AND CONCLUSIONS

In this chapter, a summary of the strength parameters of lightly cementitious materials, namely, cohesion c, and angle of internal friction ϕ is given. A description is also given of compression failure of lightly cementitious layers under repetitive loading (stress) conditions. The strength of cementitious materials is described mainly by the cohesion, which increases as a result of the type of raw material, stabiliser content, curing time and compaction density. The c and ϕ can be determined using the Mohr-Coulomb theory, or using p_f-q_f diagrams.

Compression failure (crushing) of lightly cementitious layers is a reality and must be taken into account during design and maintenance planning of these types of pavements. During compression failure, the cohesion (cemented strength) of the material decreases as a result of compressive axial strains in excess of 1 per cent. These compression failures are measured as permanent deformation in the cementitious layers with the MDD equipment (De Beer et al., 1988b). If the vertical permanent deformation exceeds 1 per cent of the layer thickness, compression failure is considered to have started (initiation of crushing) within the cementitious layer. Soon after compression failure, fatigue failure of the asphalt surface treatment occurs. If moisture enters the cracked pavement, moisture-accelerated distress (MAD) occurs, resulting in loss of seal and excessive potholing on this type of pavement.

An empirical design curve, relating the ratio of tyre contact stress σ_t and in situ unconfined compressive strength (UCS) to the number of stress repetitions to initiate compression failure (Nc), is proposed (Figure 5.18). This curve can be used in the mechanistic design, and maintenance planning of pavements with lightly cementitious gravel layers, to estimate the life of surface treatments, together with the number of expected stress repetitions needed to initiate compression failure.

Preventive maintenance by timeous sealing, as well as by controlling the tyre contact pressure of heavy vehicles or provision of a stress distribution layer, for example, G1/G2, may largely increase the life of pavements with lightly cementitious gravel layers.

It is also important to note that this information indicates that lightly cementitious gravel base materials must be of adequate strength (UCS) to increase the crushing life span (Nc), especially if relatively high tyre contact stresses are expected.

Although the compression failure results discussed here were strictly derived from the cementitious base layers, it is my opinion that cementitious sub-layers in the pavement system may also be evaluated for this failure, using Equation 5.8, substituting the tyre contact stress (σt) by the calculated vertical stress on top of the cementitious layer under consideration. Further research, however, is necessary to verify this assumption.

5.6 REFERENCES

Abboud, M M (1973). Mechanical Properties of Cement-Treated Soils in Relation to their Use in Embankment Construction. PhD Dissertation University of California, Berkely, USA, 1973.

Alfi, A A S (1978). Experimental Study of a Strongly Cemented Sand. Thesis presented to Stanford University, at Stanford, California, in partial fulfilment of the requirements for the degree of Bachelor of Engineering, California, USA, 1978.

Akinmusuru, J O (1987). The effects of cementation on the stress - strain behavior of a sand. Proceedings of the 9th Regional Conference for Africa on Soil Mechanics and Foundation Engineering, Lagos, September, 1987.

Balmer, G G (1958). Shear Strength and Elastic Properties of Soil-Cement Mixtures Under Triaxial Loading. ASTM Proceedings Volume 58, USA, 1958.

Christensen, A P (1969). Cement Modification of Clay Soils. (RD002.-015), Portland Cement Association, USA, 1969.

Clough, G W, Sitar, N, Bachus, R C and Rad, N S (1981). Cemented Sands Under Static Loading. Journal of the Geotechnical Engineering Division, ASCE, USA, 1981.

De Beer, M, Kleyn, E G and Savage, P F (1988). Towards a Classification System for the Strength-Balance of Thin Surfaced Flexible Pavements. Proceedings of the Eighth Quinquennial Convention of SAICE in co-operation with the 1988 Annual Transportation Convention (SAICE-ATC 1988), University of Pretoria, Pretoria, 1988.

De Beer, M (1986a). Mechanistic analysis: HVS-section 260A4 (Rooiwal). Unpublished Technical note TP/146/86 (in Afrikaans), Division of Roads and Transport Technology, CSIR, Pretoria, 1986.

De Beer, M (1986b). Mechanistic analysis: HVS-section 275A4 (Rooiwal). Unpublished Technical note TP/14/86 (in Afrikaans), Division of Roads and Transport Technology, CSIR, Pretoria, 1986.

De Beer, M (1986c). Mechanistic analysis: HVS-section 289A4 (Rooiwal). Unpublished Technical note TP/91/86 (in Afrikaans), Division of Roads and Transport Technology, CSIR, Pretoria, 1986.

De Beer, M (1986d). Mechanistic analysis: HVS-section 294A4 (Rooiwal). Unpublished Technical note TP/43/86 (in Afrikaans), Division of Roads and Transport Technology, CSIR, Pretoria, 1986.

De Beer M, Horak E and Visser A T (1988). The Multi-Depth Deflectometer(MDD) System for determining the Effective Elastic Moduli of Pavement Layers. Unpublished paper accepted for publication in a ASTM Special Technical Publication (STP) of the first International Symposium on Nondestructive Testing of Pavements and Backcalculation of Moduli, Baltimore, USA, 1988.

De Villiers, E M (1988). Personal Communication, 1988.

Division of Roads and Transport Technology, (DRTT) (1985). Structural Design of Interurban and Rural Road Pavements. Technical Recommendations for Highways, TRH4: 1985, CSIR, Pretoria, 1985.

Division of Roads and Transport Technology, (DRTT) (1985). Guidelines for Road Construction Materials. Technical Recommendations for Highways, TRH14: 1985, CSIR, Pretoria, 1985.

Dupas, J M and Pecker, A (1979). Static and Dynamic Properties of Sand-Cement. Journal of the Geotechnical Engineering Division, ASCE, Vol. 107, 1979.

Du Pisani, K (1988). Personal Communication, 1988.

Ferguson, E G and Hoover, J M (1968). Effect of Portland Cement Treatment of Crushed Stone Base Materials as observed from Triaxial shear tests. Highway Research Record No. 255, Highway Research Board, 1968.

Hammond, A A (1981). Measurement of Autogenous Healing in Stabilized Soils. 10th International Conference on Soil Mechanics and Foundation Engineering, Stockholm, Sweden, 1981.

Herrin, M (1954). Effects of Aggregate Shape on the Stability of Bituminous Mixes. PhD thesis, Purdue University, 1954.

Jordaan, G J, Rust, F W and Viljoen, A W (1985). Rehabilitation Investigation on a Strongly Cemented Base Pavement. Technical Note PC/1/85, (Unpublished), Division for Roads and Transport Technology, CSIR, Pretoria, 1985.

Kleyn, E G (1984). Aspects of Pavement Evaluation and Design as determined with the aid of the Dynamic Cone Penetrometer (DCP). M Eng. thesis (In Afrikaans, Faculty of Engineering, University of Pretoria, Pretoria, 1984.

Kleyn, E G and Strauss, P J (1986). The Selection of Asphalt Wearing Courses in the Management of Pavements. Proceedings of the Annual Transportation Convention, 4-7 August 1986, Volume 3B, Session S.396, CSIR, Pretoria, 1986.

Kleyn, E G, Renshaw, R H and Strauss, P J (1987). Evaluation of a Holding Operation: A Transvaal Case Study. Proceedings of the Annual Transportation Convention, 3-7 August 1987, Volume 3A, Session S.425, CSIR, Pretoria, 1987.

Kleyn, E G (1988). Personal Communication (1988).

Lambe, T W and Whitman, R V (1969). Soil Mechanics. Massachusetts Institute of Technology, John Wiley and Sons, Inc., New York, 1969.

Maree, J H (1982). Aspects of the Design and Behaviour of Pavements incorporating Granular Bases. DSc Dissertation (In Afrikaans), Faculty of Engineering, University of Pretoria, Pretoria, 1982.

Maree, J H, Kleyn, E G and Van Zyl, G D (1987). A Multiple Analysis Approach to Pavement Rehabilitation Design. Proceedings of the Annual Transportation Convention, 3-7 August 1987, Volume 3A, Session S.425, CSIR, Pretoria, 1987.

Mitchell, J K (1976). The Properties of Cement-Stabilized Soils. Paper prepared for Residential Workshop on Materials and Methods for Low Cost Road, Rail and Reclamation Works, Leura, Australia, September 6-10, 1976.

Nash, J K T L, Jardine, F M and Humphrey, J D (1965). The Economic and Physical Feasibility of Soil-Cement Dams. Sixth International Conference on Soil Mechanics and Foundation Engineering, Montreal, Canada, 1965.

Netterberg, F, Paige-Green, P, Meiring, K and Von Solms, C L (1987). Prevention of Surface Carbonation of Lime and Cement Stabilised Pavement Layers by Appropriate Curing Techniques. Proceedings of the Annual Transportation Convention, 3-7 August 1987, Volume 4A, Session S.425, CSIR, Pretoria, 1987.

Otte, E (1972). The Stress-Strain Properties of Cement-Stabilised Materials. MSc Thesis (In Afrikaans), Faculty of Engineering, University of Pretoria, Pretoria, 1972.

Otte, E (1978). A Structural Design Procedure for Cement-Treated Layers in Pavements. DSc Dissertation, Faculty of Engineering, University of Pretoria, Pretoria, 1978.

Pinard, M I (1987). Durability Aspects of lime-stabilised weathered basalt road bases- a case study from Botswana. Proceedings of the Annual Transportation Convention, 3-7 August 1987, Volume 4A, Session S.425, CSIR, Pretoria, 1987.

Rocha, M, Folque, J and Esteves, V P (1961). The Application of Cement Stabilized Soils in the Construction of Earth Dams. Fifth International Conference on Soil Mechanics and Foundation Engineering, Paris, 1961.

Robbertson, J A, Bental, G M and Blight, G E (1987). Stabilized soil as a material for dam construction in Africa. Proceedings of the 9th Regional Conference for Africa on Soil Mechanics and Foundation Engineering, Lagos, September, 1987.

Saxena, S K and Lastrico, R M (1978). Static Properties of Lightly Cemented Sand. Journal of the Geotechnical Engineering Division, ASCE, Vol. 104,No. GT12, Proc. Paper 14259, December 1978.

Thompson, M R (1966). Shear Strength and Elastic Properties of Lime-Soil Mixtures. Highway Research Record No. 139, Highway Research Board, USA, 1966.

Wissa, A E Z and Ladd, C C (1965). Shear Strength Generation in Stabilized Soils. MIT, Department of Civil Engineering, Research Report No. R65-17, Soils Publication No. 173, June 1965.

CHAPTER 6

DYNAMIC CONE PENETROMETER (DCP)- AIDED EVALUATION OF THE BEHAVIOUR OF PAVEMENTS WITH CEMENTITIOUS LAYERS

CONTENTS PAGE

6.1 INTRODUCTION AND BACKGROUND

Permanent deformation measurements (Chapter 4) as well as the in situ resilient properties (Chapter 7) of pavement systems are normally used to describe the behaviour of the pavement. As was indicated in Chapter 3, the Dynamic Cone Penetrometer (DCP) is also used to measure in situ strength conditions of pavements, and hence may be used to aid the understanding of specific behavioural patterns observed during traffic loading of pavements. Marais et al (1982) confirmed the use of the DCP in the evaluation of pavement strength and pavement composition, in association with the HVS. They concluded that the internal strength of the various pavement layers could be evaluated before HVS tests started and changes occurring as a result of traffic loading could be monitored with the DCP. This assisted in quantifying the concepts of traffic moulding, pavement strength - balance and load sensitivity, which confirmed that a pavement behaves as a system.

In this chapter, a description of the behaviour of pavements with lightly cementitious layers according to the DCP is given. A new concept, viz **"Pavement Strength - Balance Paths"** is introduced which assists in describing the behaviour of pavements on a more quantitative basis than in the past.

6.2 CONCEPT OF PAVEMENT STRENGTH - BALANCE PATHS

In Chapter 3, the DCP- classification system for pavements is described in detail. This classification system is based on the two unique DCP - parameters, viz A and B. Parameter B describes the **Standard Pavement Strength Balance Curve (SPBCs)**, while parameter A describes the **Degree of Balance** in terms of the total deviation (area) of the DCP data from the best fit SPBC.

According to this classification system, each DCP measurement (and therefore the pavement) is classified according to its in situ strength - balance at the time of measurement, which is sufficiently defined by the parameters A and B. If the pavement is monitored during HVS testing, ie at various stages of trafficking, changes in A and/or B, may reflects changes in the pavement owing to traffic loading.

According to the findings of Marais et al (1982), lightly unbound gravel base pavement systems showed a tendency to be "moulded" as a result of traffic into states of strength which differ from the original values before HVS testing.

They further stated that:

"The discrete strength values in successive layers become modified so that there is a more gradual reduction in strength with depth. The relatively abrupt interlayer strength variations are smoothed out, and the extent to which this phenomenon manifests itself is determined by the load sensitivity of the pavement, ie the strength and composition of the various pavement layers relative to the traffic load. Thus it may be observed that a particular pavement exhibits no traffic - associated deformation for many years, whilst another may show early signs of traffic moulding, manifested as deformation."

Traffic moulding of overstressed pavement layers occurs as a result of trafficking. This concept is illustrated in Figure 6.1. As shown, this moulding usually results in the densification of one or more of these unbound layers, thereby increasing their strength (mainly shear) sufficiently to withstand the traffic loading. Alternatively, depending on the quality of material, a layer may not attain sufficient strength and may fail in shear. Also, the moulding deformation in a layer may be such that the layer above it cannot accommodate the strain and becomes overstressed and fails.

This phenomenon may cause either an increase or a decrease in the bearing capacity of the pavement, but always results in a loss of riding quality. A decrease in riding quality does not therefore necessarily constitute a reduction in pavement bearing capacity, but a continuing or accelerating decrease in riding quality is likely to do so.

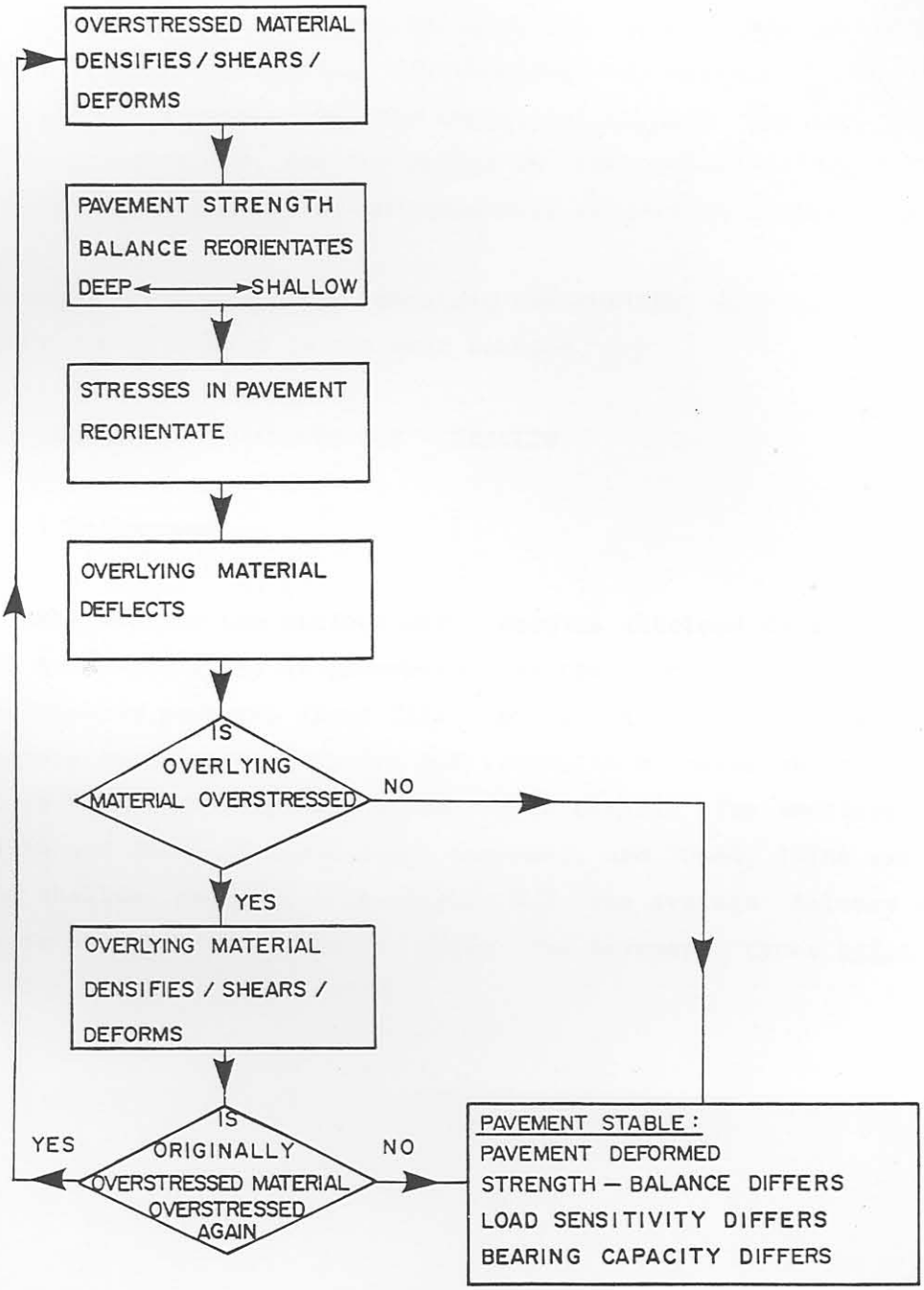

FIGURE 6.1

TRAFFIC MOULDING OF OVERSTRESSED PAVEMENT LAYERS

(Marais et al, 1982)

In addition, pavement mouldability and load sensitivity show seasonal variations since the strength of materials can strongly be affected by environmental conditions, especially the moisture content.

Marais et al (1982) concluded that for lightly unbound pavements it appears that the ultimate effect of the moulding phenomenon is the achievement of a better strength-balanced pavement system, because of a smoother relationship of strength versus depth. It is, however, my opinion that this is not always true for pavements with lightly cementitious layers, as fatigue failure and crushing in the top of the cemented base under traffic may result in an even more unbalanced pavement. This concept, however, is useful and contributes to the understanding of pavement behaviour.

The concept of Pavement Strength - Balance Paths, however, may assist in a better quantitative description of traffic moulding of a pavement.

The **Pavement Strength - Balance Path** is defined as the **change in the pavement strength - balance relationship as a direct result of traffic loading under prevailing environmental conditions. The strength - balance is described by the degree of balance (A) and the pavement balance number (B), and any change in one or both of these values as a result of traffic and/or environmental conditions defines the path.**

Strength - balance paths obtained for the HVS sections tested in this study are discussed in the next section.

6.3 ANALYSIS OF VARIOUS DCP - RESULTS

6.3.1 Background

In this section the various DCP - results obtained during HVS testing on the two basic types of pavements, ie the deep (Road 1932, Rooiwal) and the shallow pavement (Road 2212, Bultfontein) are considered. For the purpose of this chapter, the DCP - results of three of the HVS sections of each pavement type are discussed in detail. The sections are 275A4, 289A4 and 294A4, for the deep pavement, and 306A4, 307A4 and 308A4 for the shallow pavement. In Figure 6.2 the **average Balance Curves** and **Layer Strength Diagrams** of these two pavement types before any HVS trafficking are illustrated.

The figure indicates that the average balance curves of the pavements are different, with that of the deep pavement at a lower balance number (B = 19) and that of the shallow pavement at a higher balance number (B = 41). The shaded areas on Figures 6.2 and 6.3 refer to the 20th and 80th percentile of all the results used to calculate the average values. (In Appendix E, a detailed summary of the various DCP results on these two pavements are given according to the computerised graphical layout, described in Appendix C. The average results in Figures 6.2 and 6.3, were calculated from the results in Figures E.11, E.19, and E.27, for the deep pavement, and from the results in Figures E.38, E.48 and E.56, for the shallow pavement).

Figure 6.2 also indicates the two sets of Layer Strength Diagrams for these pavements with important differences in DCP penetration rates of the various layers notable. For the balance curves and the layer strength diagrams, both the 20th and 80th percentile values are also indicated. (The DCP results discussed here are limited to only six measurements per type of pavement (two per test section), because of the relative destructive nature of the DCP test on cemented pavement layers on an HVS test section. Therefore the average and percentile values of these results are given only as estimates of the pavement definition, and are mainly used to compare the two pavement types, rather than to be representative of very accurate "statistical" descriptions of these pavements. In the latter event, at least 30 different DCP measurements per pavement type is necessary to define the pavement structure properly, using the normal distribution theory).

In Figure 6.3 the Normalised Curves and the Layer Strength Diagrams of the re - defined layers (in terms of layer thickness) of the two pavements are illustrated. The normalised curves show the deviation (A_i) from the Standard Pavement Balance Curve (SPBC) with depth (see Chapter 3). For the shallow pavement, a maximum positive deviation occurs at approximately 75 mm, which is indicative of the average in situ (effective) thickness of the cemented base layer of this pavement. For the deep pavement, the maximum deviation occurs at approximately 160 mm, indicating a thicker cemented base. The layer strength diagrams also indicate large differences in the penetration rates for both the upper and lower layers of both pavements. Detailed DCP analysis of the two pavements are given in Appendix E, see Figures E1 to E10.

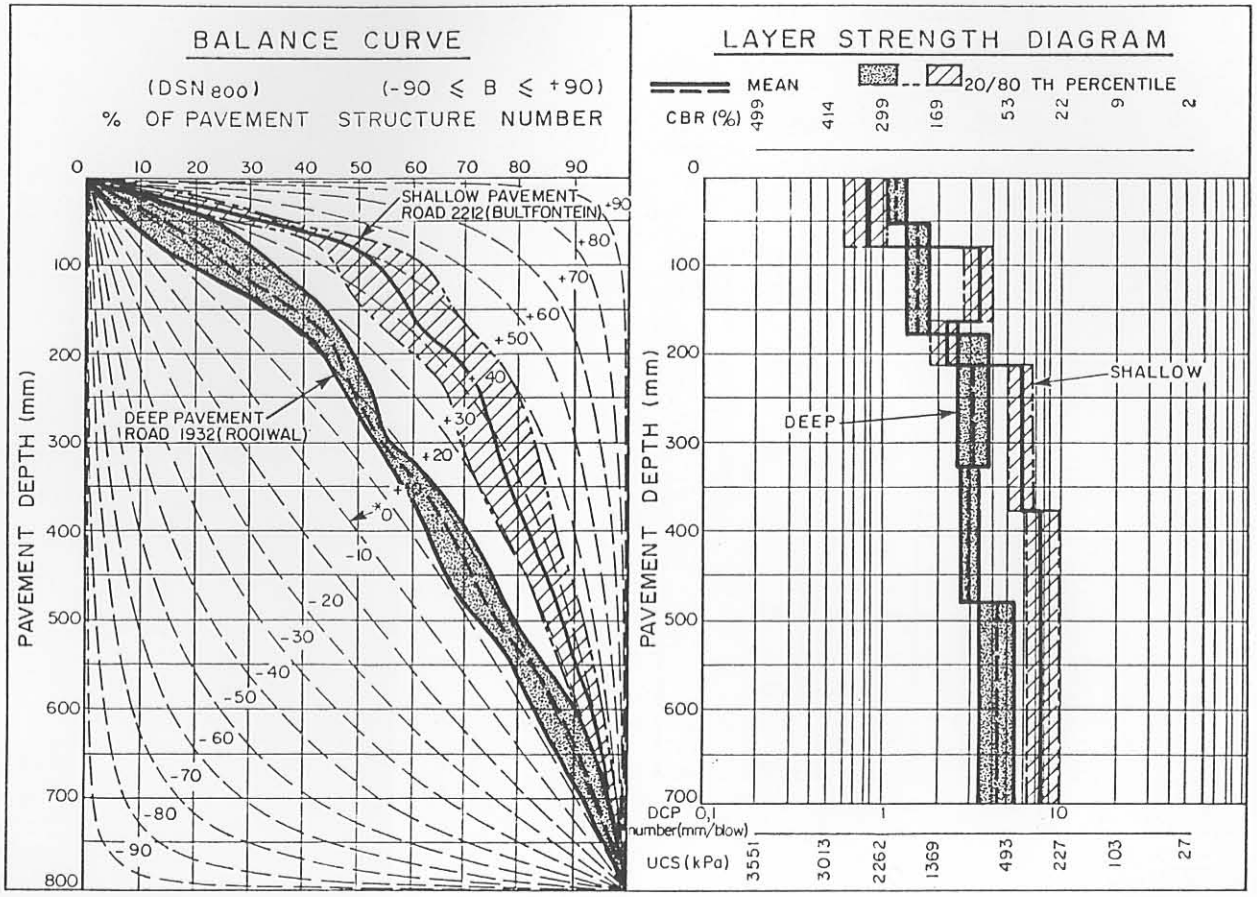

* Numerical (B-value) refers every time to the curve below.

FIGURE 6.2
DCP – BALANCE CURVES AND LAYER STRENGTH DIAGRAMS OF THE TWO TYPES OF PAVEMENTS STUDIED

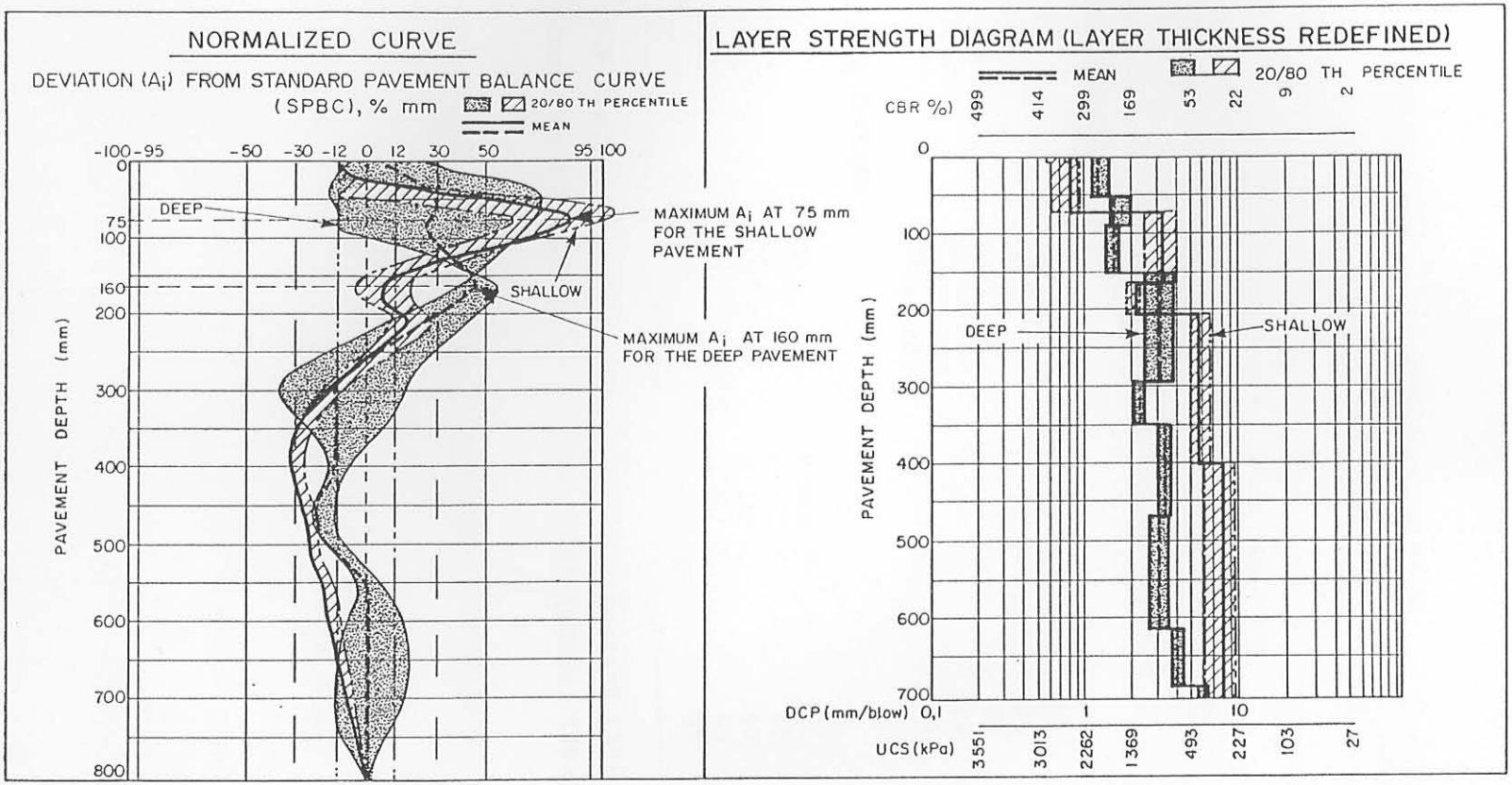

FIGURE 6.3

NORMALIZED CURVES AND LAYER STRENGTH DIAGRAMS OF THE REDEFINED LAYERS (IN SITU THICKNESS) OF THE DEEP AND SHALLOW PAVEMENTS STUDIED

A summary of the average measured basic DCP-parameters for these two pavement types before HVS trafficking (N = 0) are given in Tables 6.1 and 6.2. Table 6.1 indicates that the balance number B of the shallow pavement is almost twice that of the deep pavement, and, together with BN_{100}, is the strongest indicator of the basic difference between these two types of pavements. Table 6.2 indicates the DCP numbers (average penetration rates) at various depths in these pavements, together with the DCP - derived California Bearing Ratio (CBR) and Unconfined Compression Strength (UCS). Note the relatively smooth decrease in these values with increasing depth of the deep pavement, while irregularities at a depth of approximately 81 to 160 mm are evident in the shallower pavement, causing a higher imbalance of the pavement (see Table 6.1).

TABLE 6.1 AVERAGE BASIC DCP-PARAMETERS FOR THE TWO PAVEMENTS (HVS SECTIONS 275A4, 289A4 AND 294A4)

DCP-PARAMETER	DEEP (ROAD 1932)	SHALLOW (ROAD 2212)
DSN_{800}	397	352
B	19	41
A	1398	2089
BN_{100}	27	56
DCP-CLASSIFICATION	AVERAGELY BALANCED DEEP (ABD)	AVERAGELY BALANCED SHALLOW (ABS)

TABLE 6.2 AVERAGE DCP - PENETRATION RATES, CBR AND UCS (HVS SECTIONS 306A4, 307A4 AND 308A4)

DEPTH (mm)	PARAMETER	DCP NUMBER (mm/blow)	CBR*	UCS*
DEEP PAVEMENT:				
0-50	DN_{50}	1,3(0,2)	251	1940
51-180	DN_{51-180}	1,7(0,3)	198	1574
181-330	$DN_{181-330}$	3,2(0,7)	93	809
331-480	$DN_{331-480}$	3,1(0,4)	96	832
481-800	$DN_{481-800}$	4,2(1,2)	66	598
SHALLOW PAVEMENT:				
0-80	DN_{80}	0,8(0,3)	331	2474
81-160	DN_{81-160}	3,5(0,7)	85	746
161-210	$DN_{161-210}$	2,3(0,4)	145	1197
211-375	$DN_{211-375}$	5,9(1,0)	43	410
376-800	$DN_{376-800}$	7,7(2,0)	30	299

* DCP derived parameters for California bearing ratio (CBR) and Unconfined Compressive Strength (UCS) (Kleyn, 1984).

6.3.2 Deep pavement (Road 1932 at Rooiwal): Results and discussion

In the following paragraphs the emphasis is on the changes in the pavement system as a result of traffic loading rather than the actual differences between the two pavements as discussed in Paragraph 6.3.1. The HVS trafficking was done with the normal dual wheel load configuration.

In Table 6.3 the average DCP-numbers (DN in mm per blow) at different depths and at different number of load repetitions on the three sections of the deep pavement are given.

TABLE 6.3 AVERAGE DCP-NUMBERS OF THE THREE TEST SECTIONS ON THE DEEP PAVEMENT AT ROOIWAL

HVS-SECTION (HVS Test Load)	REPETITIONS	DCP NUMBER (mm/blow)		IN SITU MOISTURE
		DN_{50} *	DN_{50-180} **	
275A4 (40 kN)	0	1,2 (0,3)	1,8 (0,4)	DRY
	10^6	1,3 (0,3)	1,8 (0,5)	DRY
	$2,1 \times 10^6$	2,2 (0,5)	1,8 (0,4)	DRY
	$2,1 \times 10^6$	3,2 (0,3)	2,9 (0,4)	WET
289A4 (70 kN)	0	1,9 (0,4)	1,1 (0,3)	DRY
	10^6	2,7 (0,5)	1,7 (0,4)	DRY
	$1,9 \times 10^6$	2,6 (0,3)	2,2 (0,5)	DRY
	$1,9 \times 10^6$	2,2 (0,3)	2,0 (0,6)	WET
294A4 (100 kN)	0	0,7 (0,3)	2,1 (0,6)	DRY
	10^6	1,2 (0,2)	2,6 (1,0)	DRY
	$1,8 \times 10^6$	1,8 (0,6)	2,5 (0,5)	DRY
	$1,8 \times 10^6$	2,2 (0,8)	3,3 (1,4)	WET

* DN_{50} = the average rate of penetration in the top 50 mm of the cemented base layer.

** DN_{50-180} = the average rate of penetration from a depth of 50 mm to a depth of 180 mm in the cemented base layer.

() Standard deviation in the rate of penetration.

The table indicates that the DN_{50} increases at a higher rate than DN_{50-180}, especially for Sections 275A4 and 294A4. Furthermore, the DN_{50} at the end of the various tests is two to three times higher for all sections than the initial DN_{50}, indicating a weakening in the upper 50 mm of the base layer. In Chapters 4 and 5, this weakening was described as a compression failure (crushing) at the top of the cemented base layer.

In Section 289A4, evidence of a decrease in DN_{50} after approximately 1,9 x 10^6 repetitions in the wet state indicates compaction (densification) in the top of the layer, which was directly responsible for a relatively high rate of deformation in this section (see also Paragraph A.2, in Appendix A). The table indicates that traffic moulding of the deep pavement is caused by crushing failure as well as compaction (Section 289A4) in the top of the pavement, depending on the initial state of the base layer. Detailed DCP analyses of the various HVS test sections are also summarised in Appendix E. The information summarised in Appendix E (Figures E11 to E34) in respect of the deep pavement, indicates that more drastic changes in the rate of penetration occurred in the upper layers (0-180 mm) than in the lower layers, and illustrates the type of "shallow" failure expected for deep pavements.

In Figures 6.4, 6.5 and 6.6 balance curves and layer strength diagrams of these three sections of the deep pavement at various stages of HVS trafficking are illustrated. The figures indicate that there is a reduction in the B-value as a result of trafficking, which is also reflected in changes in the layer strength diagrams owing to fatigue and crushing failure of the base. In Table 6.4 the average calculated A and B parameters at various stages of trafficking and moisture conditions are given.

TABLE 6.4 AVERAGE A AND B PARAMETERS FOR THE THREE SECTIONS ON THE DEEP PAVEMENT.

HVS-SECTION	TEST LOAD* (kN)	REPETITIONS (ACTUAL)	A	B
275A4	40	0	956	20
		10^6	1109	9
		2,1 X 10^6 (DRY)	1413	11
		2,1 X 10^6 (WET)	956	5
289A4	70	0	2285	18
		10^6	1772	8
		1,9 X 10^6 (DRY)	1226	-3
		1,9 X 10^6 (WET)	1224	1
294A4	100	0	3134	18
		10^6	2790	9
		1,9 X 10^6 (DRY)	2077	-3
		1,9 X 10^6 (WET)	1637	1

* Dual wheel load

940-4-5910/ BS

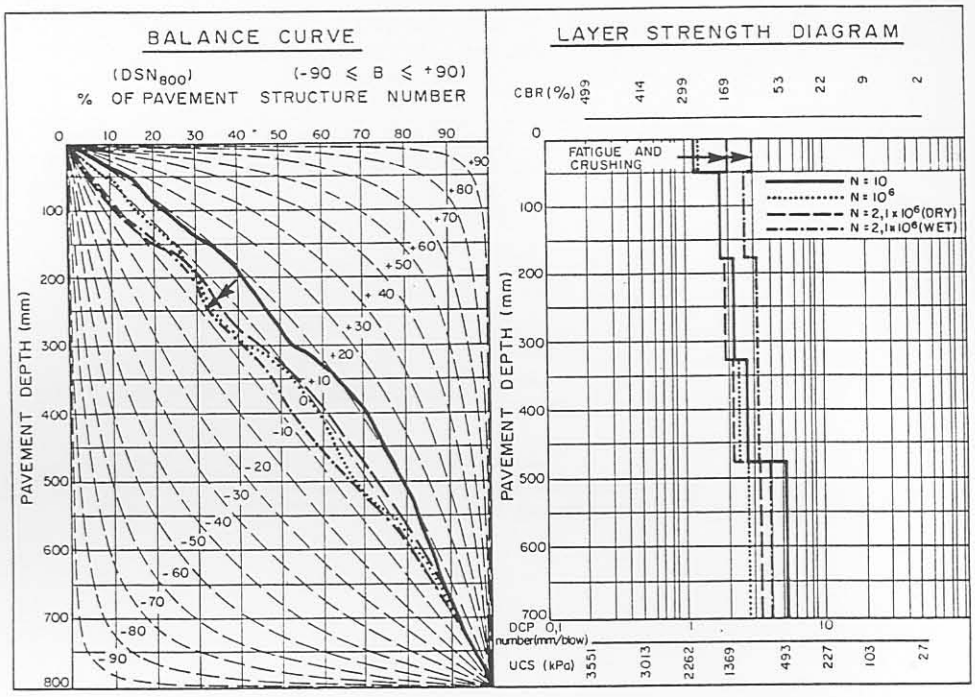

FIGURE 6.4

DCP BALANCE CURVES AND LAYER STRENGTH DIAGRAMS OF HVS TEST SECTION 275A4
(INITIAL DCP-CATEGORY IV : WELL BALANCED DEEP STRUCTURE (WBD))

940-4-5910/ BS

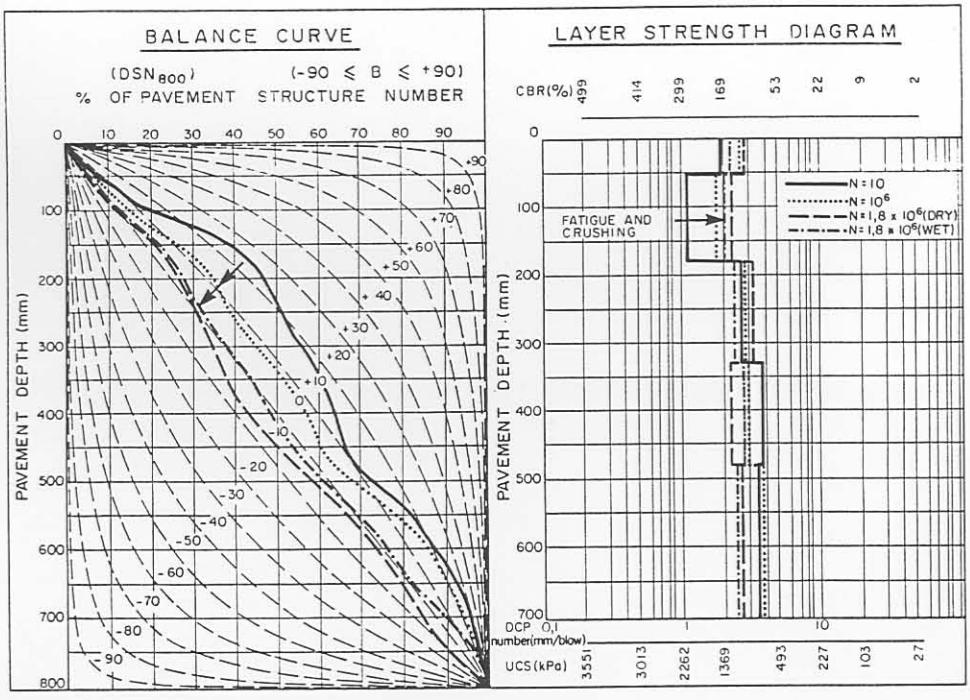

FIGURE 6.5

DCP BALANCE CURVES AND LAYER STRENGTH DIAGRAMS OF HVS TEST SECTION 289A4
(INITIAL DCP-CATEGORY V: AVERAGELY BALANCED DEEP STRUCTURE(ABD))

940-4-5910/ BS

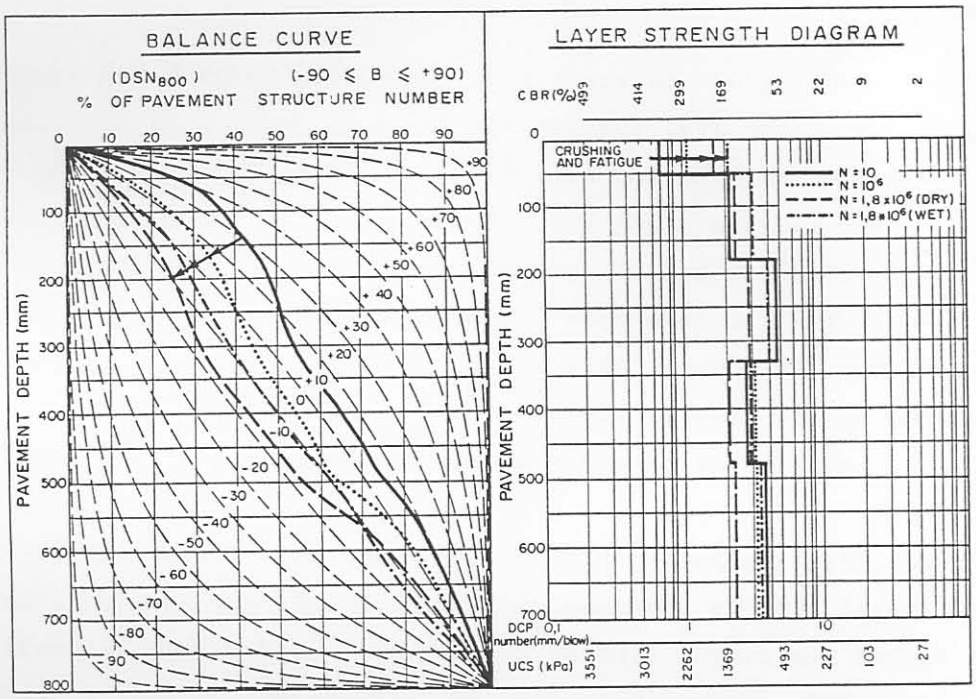

FIGURE 6.6

DCP BALANCE CURVES AND LAYER STRENGTH DIAGRAMS OF HVS TEST SECTION 294A4 (INITIAL DCP - CATEGORY VI : POORLY BALANCED DEEP STRUCTURE (ABD))

The table indicates that the Balance Number (B) changes more rapidly than the deviation from standard balance (A). Figure 6.7 shows the change in A at various stages of trafficking on the three sections of the deep pavement, and appears to improve (A_i decrease to zero) as the traffic moulding process progresses, especially in the upper layers of the pavement.

To aid the illustration of the changes caused by to traffic loading in the pavement, the **concept of balance - paths** has been introduced. In Figure 6.8 typical balance - paths (changes in A and B) for the deep pavement as a result of trafficking are illustrated. The figure indicates that the deep pavement becomes deeper (decrease in B-parameter) as a result of traffic loading, and slightly better balanced (decrease in A-parameter). With further increase in trafficking B becomes negative, indicating an **inverted pavement**, according to the classification system described in Chapter 3. This is a further quantification of the crushing failure effect in the top of the cemented base layer of deep pavements. A higher penetration rate (DCP number) in the top of the pavement as a result of crushing failure, in this case, implies a lower balance number, B.

Figure 6.8 further indicates that there was a greater initial (N = 0) variation in A, than in B, of the various test sections. Parameter A is sensitive to variations in the in situ pavement structure, because A is the area (deviation) between the DCP data and the best fit standard pavement balance curve, B. Variation in the different layer strengths in a pavement system is therefore reflected more by the A parameter, than the B parameter. The figure also shows the combined effect of trafficking and an increase in moisture content of the pavement layers on A and B, depicted by the broken lines in the figure.

It is also postulated that a pavement's balance - path may change as a result of <u>changes</u> in the moisture content of the layers <u>without</u> the effect of trafficking. Wetting of certain layers may reduce the in situ shear strength, which will be reflected by the DCP penetration rate (DCP-Number), and hence the A and B-parameters. Close inspection of these balance - paths may, however, assist in discovering the underlying reasons for these changes by identifying moisture sensitive layers,

DEVIATION FROM STANDARD PAVEMENT BALANCE CURVES (SPBCs),(DEVIATION, A_i)

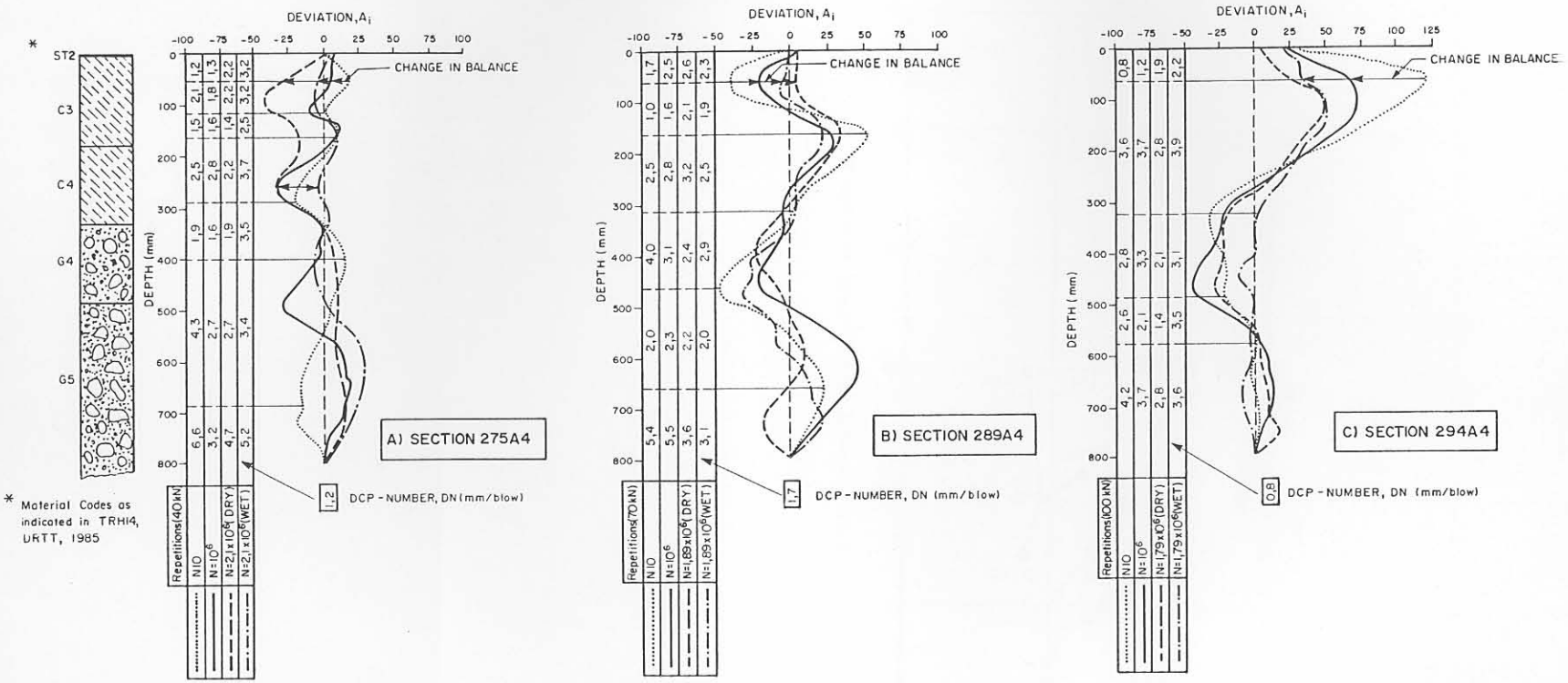

FIGURE 6.7

CHANGE IN DEVIATION FROM STANDARD BALANCE (A_i) AT VARIOUS STAGES OF TRAFFICKING ON THREE OF THE HVS TEST SECTIONS ON THE DEEP PAVEMENT (ROAD 1932, ROOIWAL)

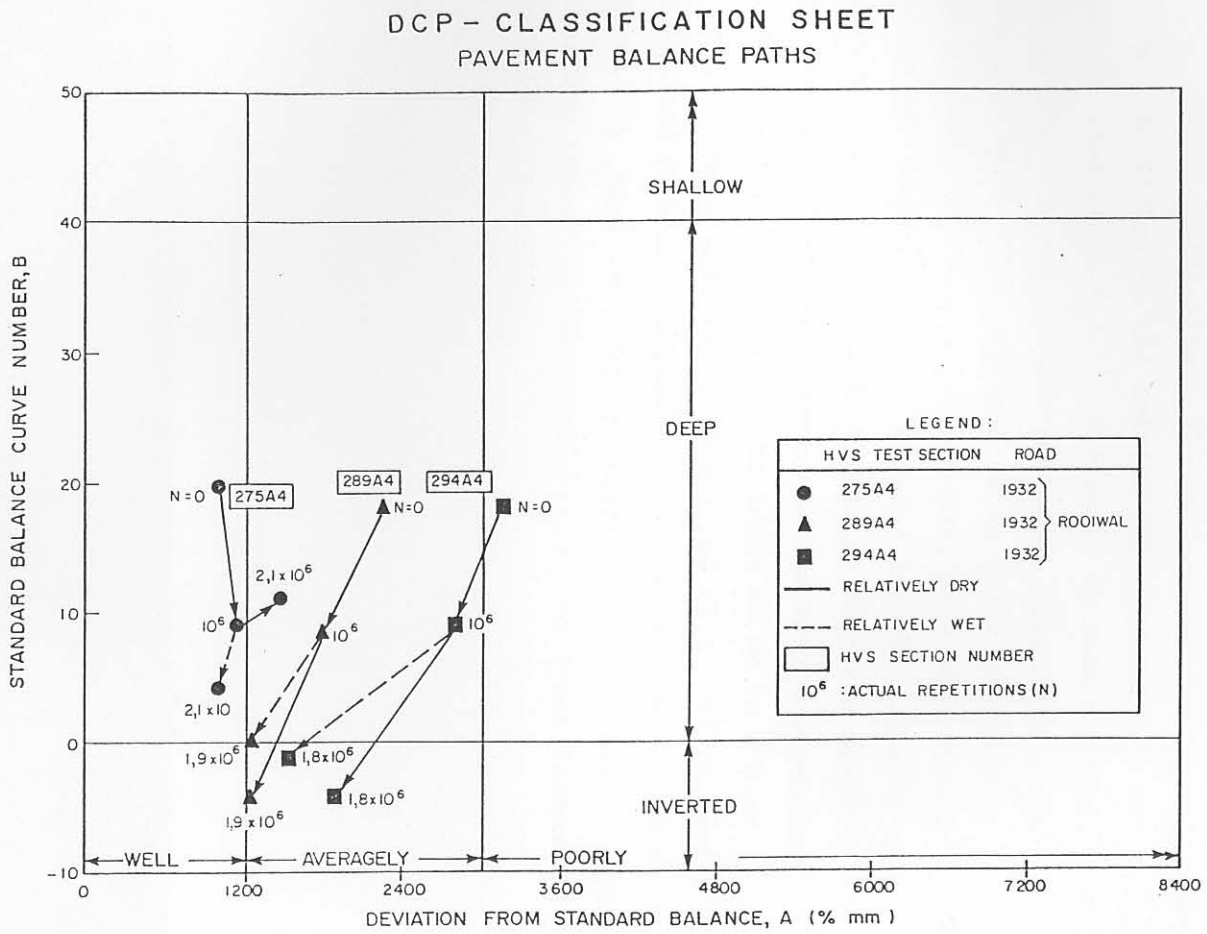

FIGURE 6.8

ILLUSTRATION OF THE BALANCE PATHS FOUND DURING ACCELERATED (HVS) TESTING FOR THE VARIOUS SECTIONS TESTED ON THE DEEP PAVEMENT (ROOIWAL)

which in itself may assist in the description of the general pavement behaviour.

In summary, the balance - paths of the deep pavements evaluated here, show that both the balance number (B) and the degree of balance or deviation from standard balance (A), decrease as a result of traffic loading, and/or the effect of an increase in moisture content of the layers.

6.3.3 Shallow pavement (Road 2212 at Bultfontein): Results and discussion.

In this paragraph the shallow pavement structure is analysed. These sections were also trafficked with the normal dual wheel load configuration. The test sections are described by the various DCP parameters and are discussed as for deep pavements. In Table 6.5 the average DCP-numbers of the four test sections on the shallow pavement are given.

The table shows the DCP numbers (DN_i) at different depths and at various stages of HVS trafficking. The main reason for the variations in depth is that, according to the initial DCP measurements and degree of balance analysis (Paragraph 6.3.1), different in situ pavement layer thicknesses were obtained in the shallow pavement structure from those in the deep pavement (Table 6.3). Variations in layer thickness between the various test sections on the shallow pavement were also measured, and therefore average DCP numbers were calculated for the in situ layer thicknesses for each section. The table indicates that the upper 64 mm to 90 mm on this pavement is strongly cemented, as very low penetration rates were obtained compared to that of the lower 64 mm to 184 mm. The DCP numbers for the stronger base layer <u>increased</u> with traffic loading, indicating fatigue and crushing failure in this layer. On the other hand, the DCP numbers in most of the sections for the lower layers <u>decreased</u> indicating compaction or densification in these layers as a result of trafficking (moulding).

TABLE 6.5 AVERAGE DCP-NUMBERS OF THE THREE SECTIONS ON THE SHALLOW PAVEMENT AT BULTFONTEIN

HVS-SECTION (HVS Wheel Load)	REPETITIONS	DCP NUMBER (mm/blow)		IN SITU MOISTURE
		DN_{90} *	DN_{90-170} **	
306A4 (40 kN)	0	0,7 (0,4)	2,5 (0,4)	DRY
	10^6	0,7 (0,3)	1,4 (0,3)	DRY
	$1,4 \times 10^6$	1,2 (0,3)	1,8 (0,7)	DRY
	$2,45 \times 10^6$	2,0 (0,7)	2,8 (0,8)	DRY
	$2,45 \times 10^6$	2,0 (0,5)	1,9 (0,4)	WET
		DN_{64} *	DN_{64-152} **	
307A4 (70 kN)	0	0,9 (0,3)	4,3 (1,6)	DRY
	10^6	1,7 (0,5)	2,6 (1,0)	DRY
	$2,45 \times 10^6$	1,2 (0,4)	0,7 (0,2)	DRY
	$2,45 \times 10^6$	1,7 (0,3)	1,0 (0,2)	WET
		DN_{80} *	DN_{80-184} **	
308A4 (100 kN)	0	0,8 (0,4)	3,4 (1,0)	DRY
	10^6	1,7 (0,4)	3,1 (1,4)	DRY
	$2,46 \times 10^6$	1,3 (0,4)	3,2 (0,6)	DRY
	$2,46 \times 10^6$	0,7 (0,2)	2,0 (0,9)	WET

* DN_i = the average rate of penetration in the top i mm of the cemented base layer.

** DN_{i-r} = the average rate of penetration from a depth of i mm to a depth of r mm in the cemented base layer.

() = Standard deviation in the rate of penetration.

The table also shows that the DN of the top 64 mm to 90 mm (DN_{64}, DN_{80}, and DN_{90}) increased during dry conditions, while that of the weaker subbase layer (DN_{90-170}, DN_{64-152} and DN_{80-184}) decreased. This is a direct result of the densification in the subbase, as also shown by the MDDs (see Paragraph 4.3.4.3, Chapter 4). According to the MDD results, approximately 34 to 53 percent of the permanent deformation measured on the surface of the pavement occurred within the subbase.

In Figures E38 to E63 in Appendix E, detailed DCP analyses of the sections on the shallow pavement are summarised and illustrated. A summary of the most important DCP analysis on these test sections is given in Figures 6.9, 6.10 and 6.11. These figures indicate the balance curves and layer strength diagrams at various stages of

940-4-5910/ BS

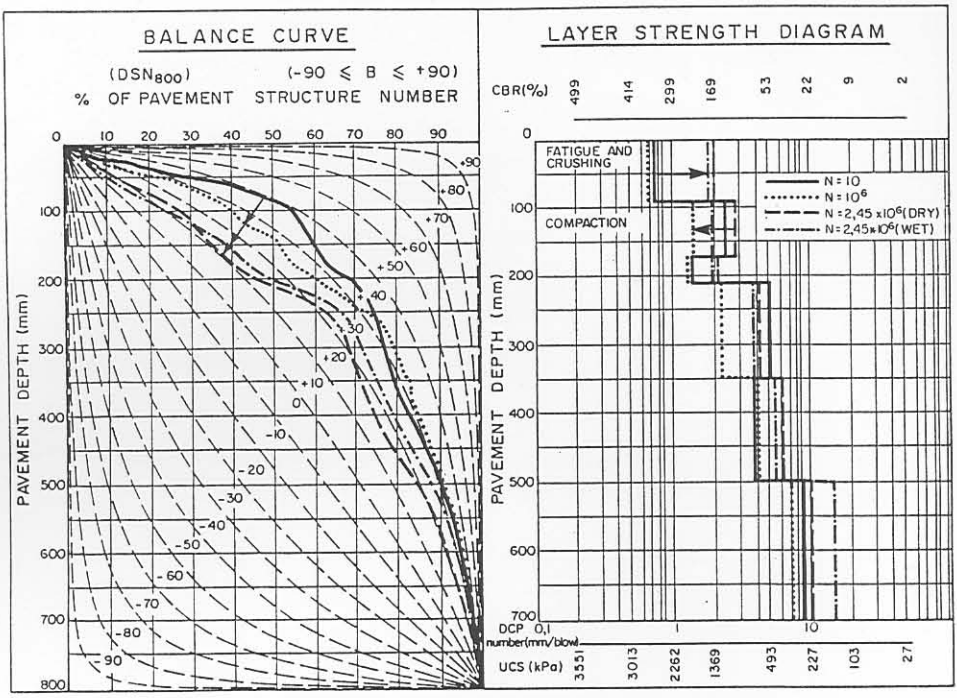

940-4-5910/

FIGURE 6.9

DCP BALANCE CURVES AND LAYER STRENGTH DIAGRAMS OF HVS TEST SECTION 306A4 (INITIAL DCP - CATEGORY II : AVERAGELY BALANCED SHALLOW STRUCTURE (ABS))

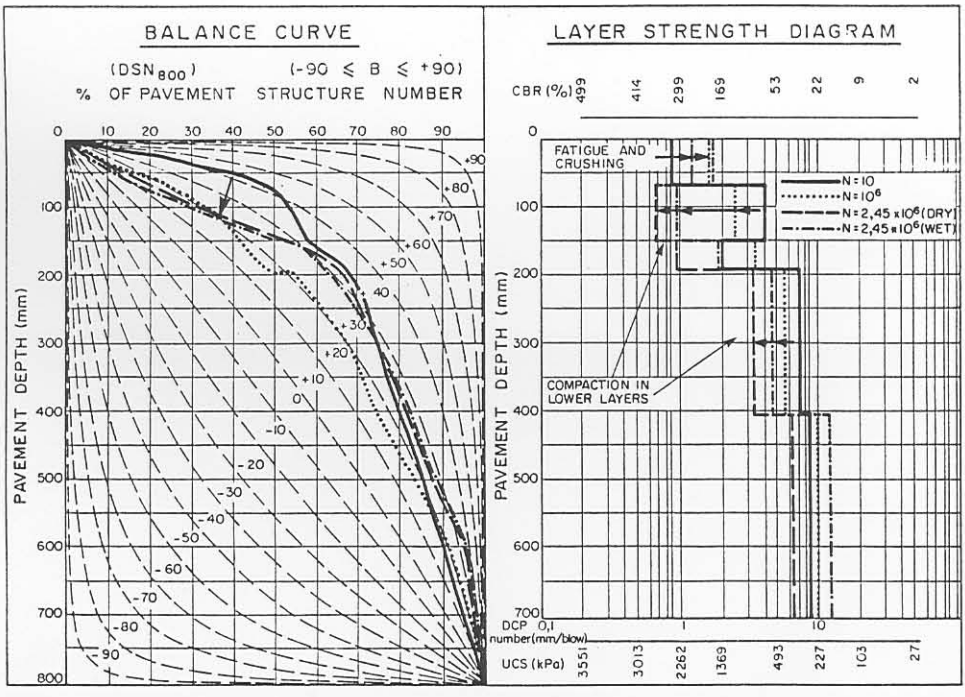

FIGURE 6.10

DCP BALANCE CURVES AND LAYER STRENGTH DIAGRAMS OF HVS TEST SECTION 307A4 (INITIAL DCP - CATEGORY II : AVERAGELY BALANCED SHALLOW STRUCTURE (ABS))

540-4-5910/ BS

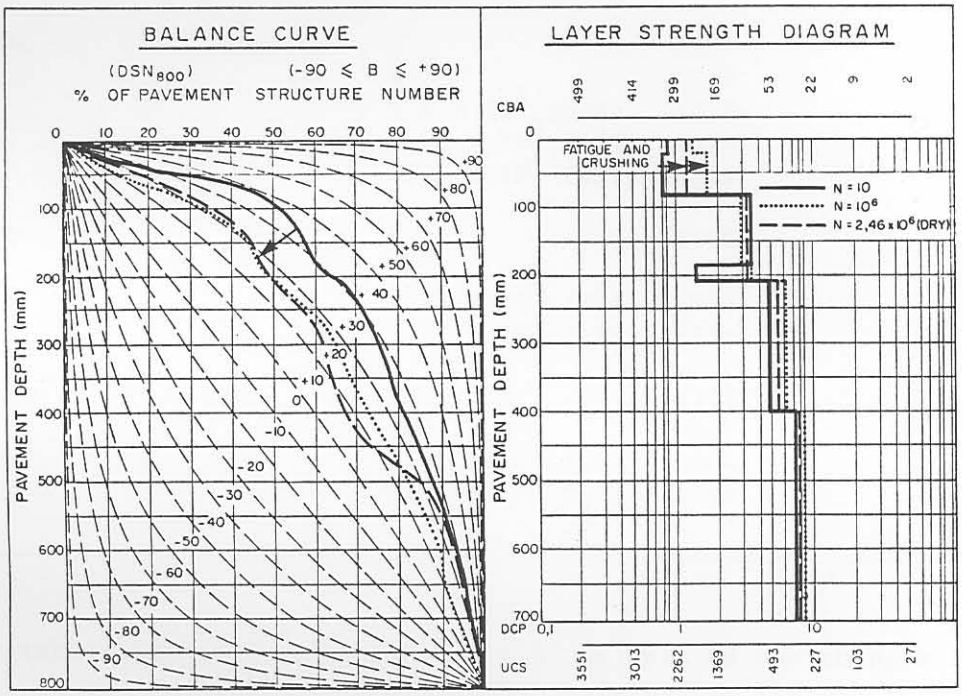

FIGURE 6.11

DCP BALANCE CURVES AND LAYER STRENGTH DIAGRAMS OF HVS TEST SECTION 308A4 (INITIAL DCP-CATEGORY V : AVERAGELY BALANCED DEEP STRUCTURE (ABD))

trafficking of three of the sections tested on this pavement, viz 306A4, 307A4 and 308A4. Decreases in the balance curves (B) are also evident here, with accompanying changes in the layer strength diagrams, as a result of trafficking. Note the densification in the lower layers of Sections 306A4 and 307A4 (Figures 6.9 and 6.10).

In Figure 6.12, changes in the deviation from standard balance (A) with HVS - trafficking are illustrated. The figure indicates that most of the changes occurred in the upper 200 mm of the pavement. Unlike that of the deep pavement (Figure 6.7), the A parameter decreased towards zero and increased numerically again towards relatively high negative values. This is indicative of the pavement becoming better balanced initially (lower A) and then becoming poorly balanced again (higher negative A), but with improved strength in the initial weaker subbase. During this process the strength of the initial well-cemented base decreased owing to fatigue failure and crushing.

In Table 6.6 the average calculated A and B parameters associated with the DCP measurements at various stages of trafficking and environmental conditions on the shallow pavement are given.

TABLE 6.6 AVERAGE A AND B PARAMETERS FOR THE THREE SECTIONS ON THE SHALLOW PAVEMENT.

HVS-SECTION	TEST LOAD (kN)	REPETITIONS (ACTUAL)	A	B
306A4	40	0	1711	42
		10^6	1057	39
		$1,4 \times 10^6$ (DRY)	1235	33
		$2,45 \times 10^6$ (DRY)	1629	28
		$2,45 \times 10^6$ (WET)	2717	33
307A4	70	0	2986	42
		10^6	836	29
		$2,45 \times 10^6$ (DRY)	1984	37
		$2,45 \times 10^6$ (WET)	1724	38
308A4	100	0	1709	39
		10^6	1311	27
		$2,46 \times 10^6$ (DRY)	2304	27
		$2,46 \times 10^6$ (WET)	1218	36

The table indicates the decrease in B, as well as the changes in A. The balance paths for these pavement sections are illustrated in Figure 6.13.

DEVIATION FROM STANDARD PAVEMENT BALANCE CURVES (SPBCs), (DEVIATION, A_i)

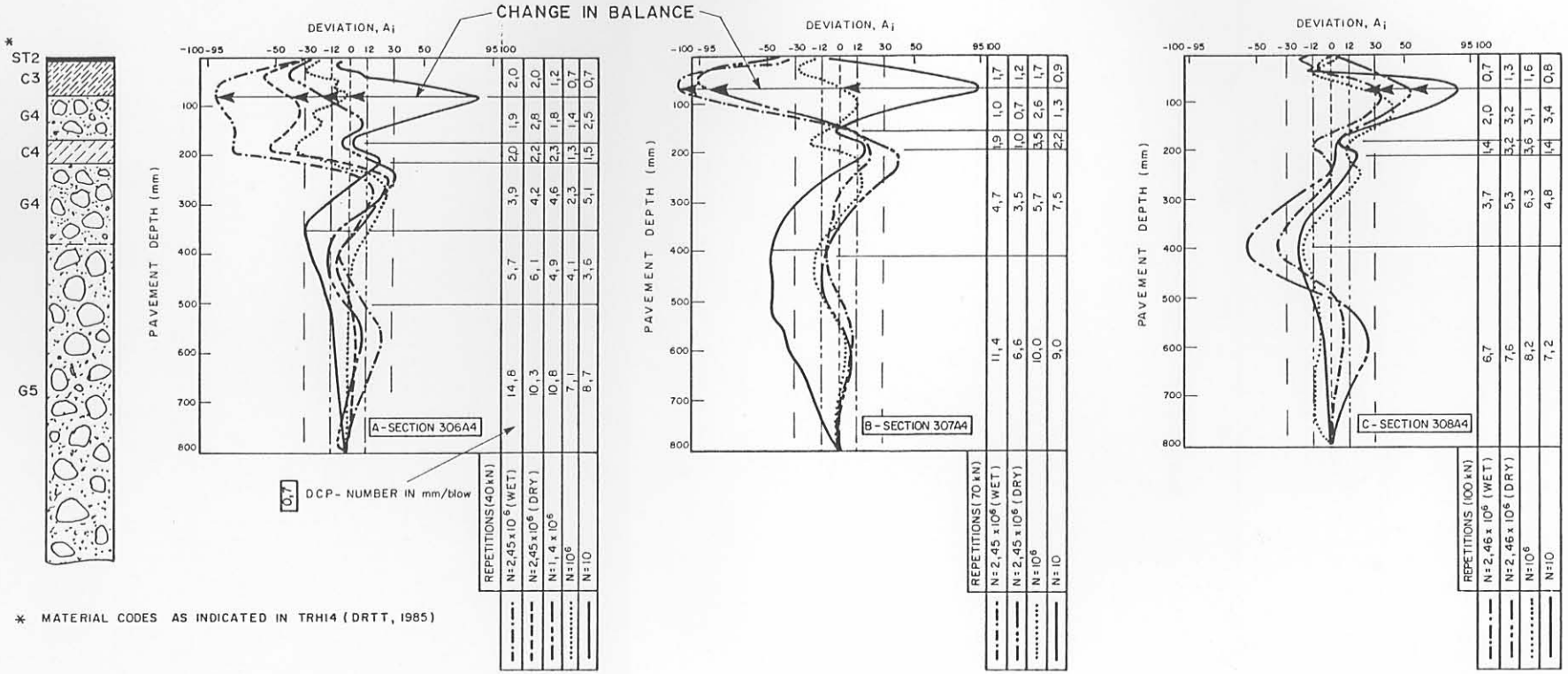

* MATERIAL CODES AS INDICATED IN TRH14 (DRTT, 1985)

FIGURE 6.12

CHANGE IN DEVIATION FROM STANDARD BALANCE (A_i) AT VARIOUS STAGES OF HVS-TRAFFICKING ON THREE OF THE SECTIONS ON THE SHALLOW PAVEMENT (ROAD 2212, BULTFONTEIN)

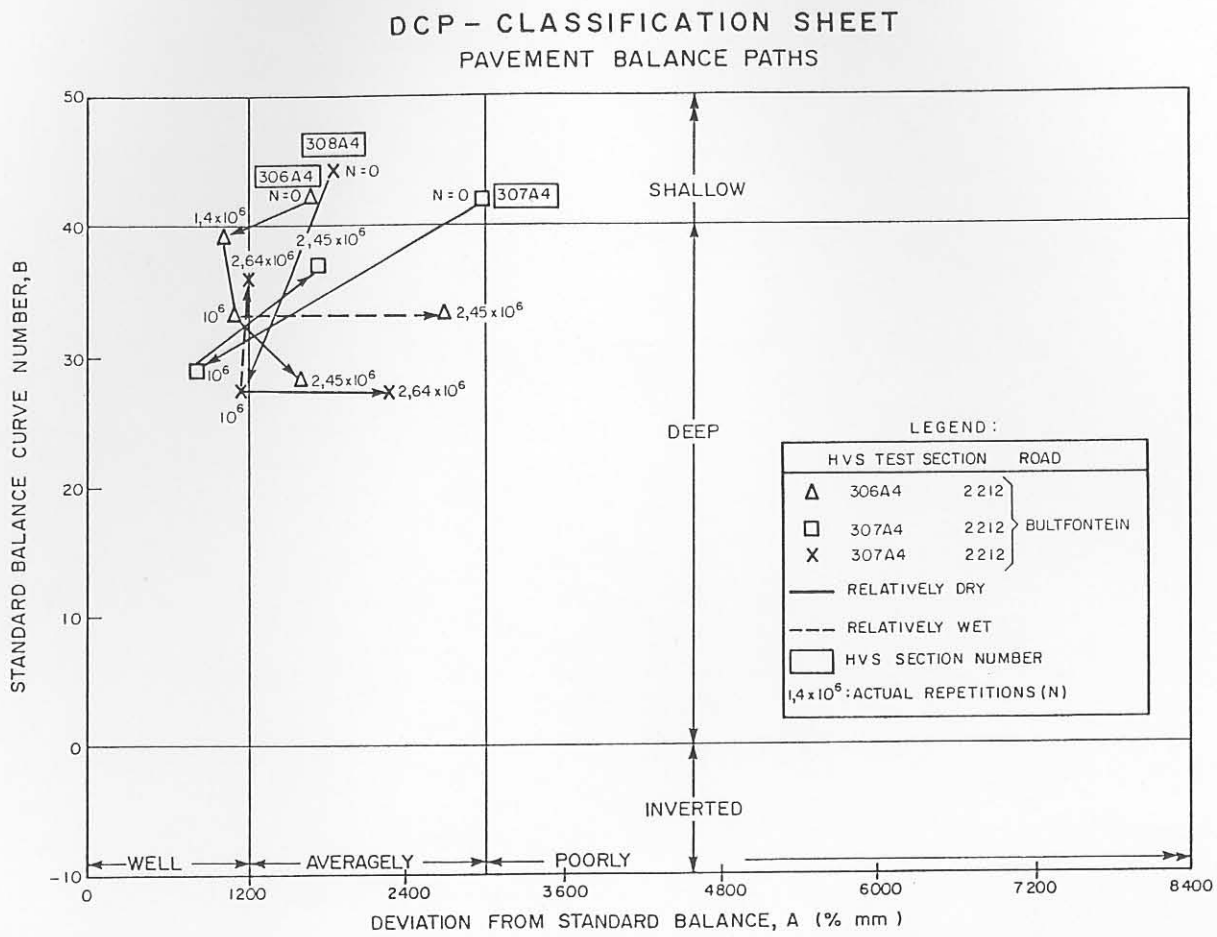

FIGURE 6.13

ILLUSTRATION OF THE BALANCE PATHS FOUND DURING ACCELERATED (HVS) TESTING FOR THE VARIOUS SECTIONS TESTED ON THE SHALLOW PAVEMENT (BULTFONTEIN)

The figure shows that, as for deep pavements, B decreases with increased traffic, but that the degree of balance A does not improve significantly (decrease in A).

It must, however, be remembered that the balance paths shown here are based on relatively few DCP results, and that variations in A and B are also possible owing to both vertical and horizontal variations in natural pavement layer strengths. To incorporate these variations for better definition of the the balance paths, additional DCP measurements are necessary.

The concept of balance paths, nevertheless, appears to be a useful method for quantifying pavement moulding as a result of trafficking, and although this may be improved in the future, it already quantifies traffic moulding better than methods used previously.

6.3.4 Balance paths for excessively high single wheel load tests

In addition to the previously discussed test sections, two relatively high single wheel load tests (150 kN single wheel load, aircraft wheel, see Paragraph 4.4 in Chapter 4) were performed; one on each type of pavement (deep and shallow, HVS test Sections 337A4 and 309A4, respectively). In Table 6.7 the average DCP penetration rates at different stages of trafficking on both sections are given, and indicates that the penetration rate for the upper 64 mm to 112 mm of both pavements increased as a result of trafficking. This increase is directly related to the fatigue and crushing failure of the upper section of the base layer. Note the relatively few load (stress) repetitions needed to initiate these failures compared to that of the normal dual wheel load tests (40 kN to 100 kN) discussed in Paragraphs 6.3.2 and 6.3.3. This is a clear indication of the damaging effect of higher contact stresses on the cementitious base layer.

The DCP penetration rate of the lower layers, however, decreased which is indicative of densification (compaction) as a result of trafficking. Therefore the lower layers became relatively stronger, whereas the upper layers became weaker, converting the shallow pavement to a deep pavement.

TABLE 6.7 AVERAGE DCP-NUMBERS OF THE TWO EXCESSIVELY LOADED TEST SECTIONS.

HVS-SECTION (HVS Wheel Load)	REPETITIONS	DCP NUMBER (mm/blow)		IN SITU MOISTURE
		DN_{112} *	$DN_{112-272}$ **	
337A4	0	1,5 (0,5)	2,9 (0,9)	DRY
(150 kN)	48 000	2,4 (0,4)	1,8 (0,1)	DRY
		DN_{64} *	DN_{64-120} **	
309A4	0	1,1 (0,2)	2,1 (0,4)	DRY
(150 kN)	19 000	1,1 (0,7)	1,8 (0,7)	DRY
	46 000	2,0 (0,1)	2,0 (0,1)	DRY
		$DN_{193-456}$ *	$DN_{456-800}$ **	
309A4 (cont.)	0	9,6 (2,2)	20,6 (3,9)	DRY
(150 kN)	19 000	3,3 (0,8)	6,2 (3,6)	DRY
	46 000	2,3 (0,2)	5,6 (2,6)	DRY

* DN_i = the average rate of penetration in the top i mm of the cemented base layer.

** DN_{i-r} = the average rate of penetration from a depth of i mm to a depth of r mm in the cemented base layer.

() = Standard deviation in the rate of penetration.

In Figures 6.14 and 6.15, the balance curves and layer strength diagrams at various stages of trafficking on the two sections are illustrated. Both these figures indicate a decrease in B, as a result of compaction of the lower layers, while fatigue and crushing failure occurred in the cemented base layers. In Table 6.8 the A and B parameters at various stages of trafficking on these section are given.

TABLE 6.8 AVERAGE A AND B PARAMETERS FOR THE TWO EXCESSIVELY LOADED TEST SECTIONS.

HVS-SECTION	TEST LOAD (kN)	REPETITIONS (ACTUAL)	A	B
337A4	150	0	1108	38
		48 000	3463	20
309A4	150	0	946	46
		19 000	2484	25
		46 000	2327	12

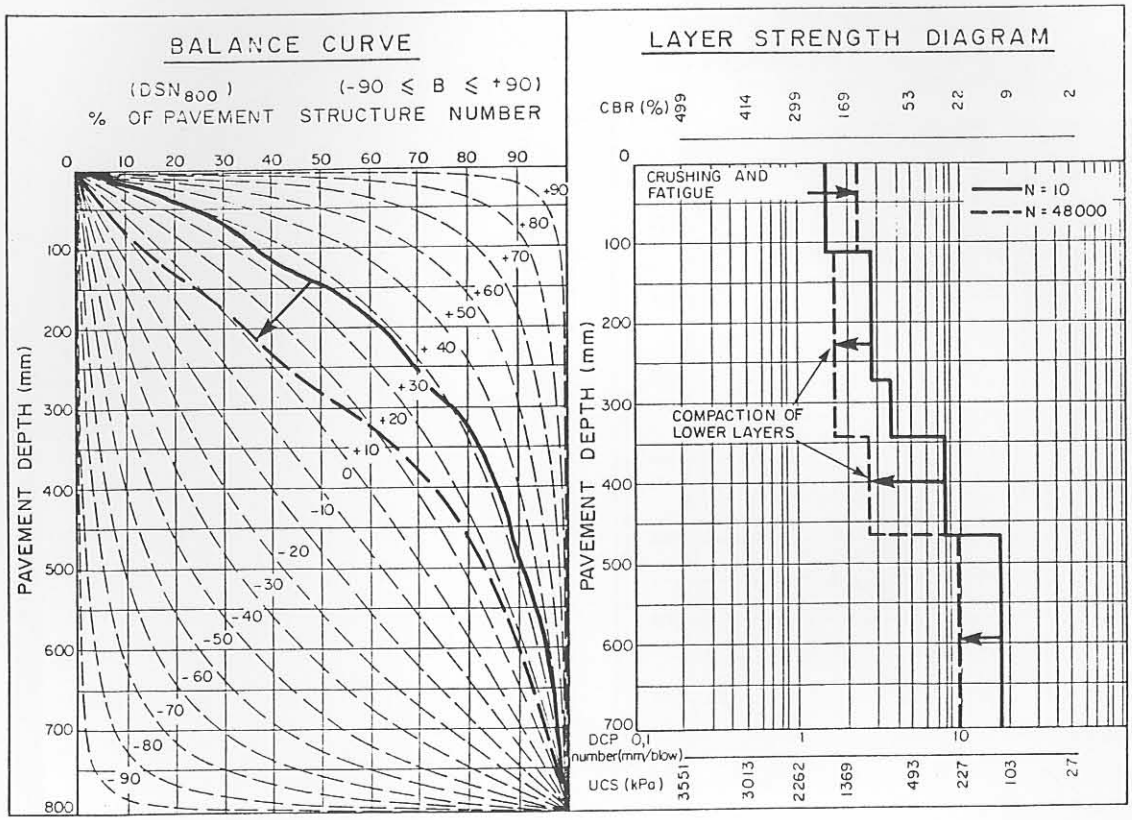

FIGURE 6.14

DCP BALANCE CURVES AND LAYER STRENGTH DIAGRAMS OF HVS SECTION 337A4 (INITIAL DCP-CATEGORY IV : WELL-BALANCED DEEP STRUCTURE - WBD)

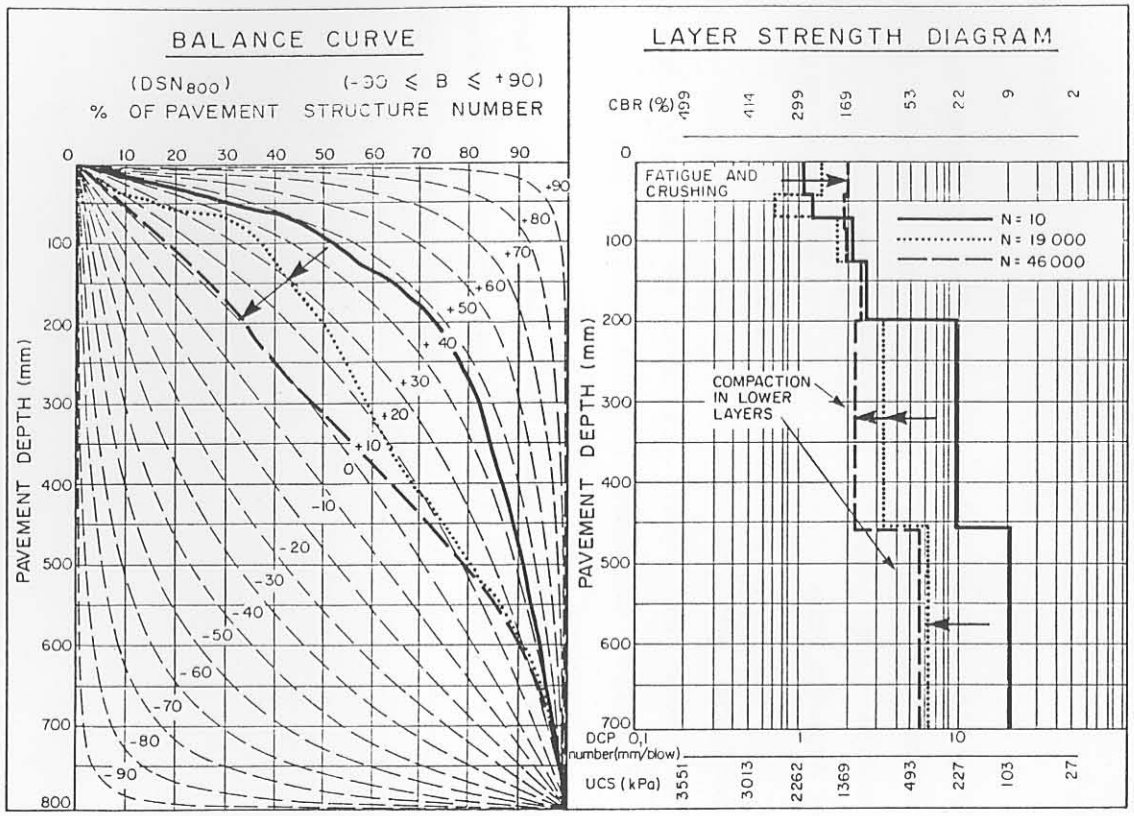

FIGURE 6.15

DCP BALANCE CURVES AND LAYER STRENGTH DIAGRAMS OF HVS TEST SECTION 309A4 (INITIAL DCP - CATEGORY I : WELL-BALANCED SHALLOW STRUCTURE (WBS))

The changes in A are also illustrated in Figure 6.16, indicating that these changes also occurred deeper in the pavement than those for the normal load tests (Figures 6.7 and 6.12). In Figure 6.17 the balance paths for these sections are plotted, and indicate a marked decrease in B, with an increase in A.

Section 337A4, although classified as a deep pavement (Chapter 3) before HVS trafficking, was shallower than the deep sections discussed previously (Paragraph 6.3.2). The initial B of this test section was much higher (B = 38), than those of the previously discussed test sections (B = 19) on the deep pavement. The main reason for this is possibly that this HVS section was situated in a valley area of this route, where relatively softer in situ layers may exist, thus causing it to be relatively shallower than the other sections on the deep pavement.

These two sections (337A4 and 309A4) are thus both relatively shallow and therefore the two balance paths are also similar (see Figure 6.17).

6.4 DCP - AIDED PREDICTION OF STRUCTURAL CAPACITY

6.4.1 Background

The first empirical DCP - based model for the prediction of structural capacity was developed by Kleyn (1984). This model is based on the DSN_{800} in blows and a moisture factor, Cm. Jordaan (1988) recently summarised this work and also suggested some changes to this model.

In this paragraph, an evaluation of the original model with the suggested changes by Jordaan (1988) is made to investigate its suitability and accuracy for the pavements studied in this dissertation.

Alternative models for the prediction of structural capacity for pavements with lightly cemented layers are also proposed and discussed in the following paragraphs.

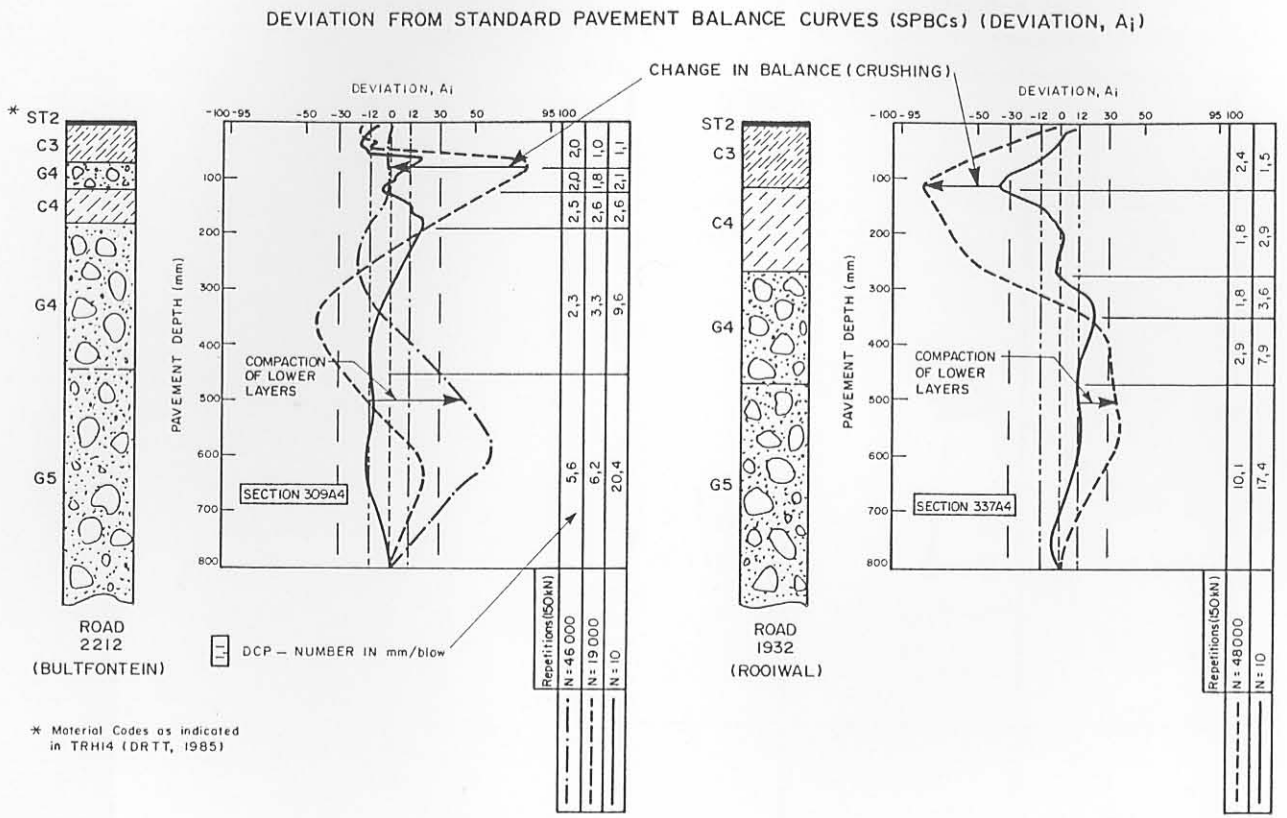

FIGURE 6.16

CHANGE IN DEVIATION FROM STANDARD BALANCE (Ai) AT VARIOUS STAGES OF HVS-TRAFFICKING (150 kN SINGLE WHEEL LOAD) ON SECTIONS 309A4 (SHALLOW) AND 337A4 (DEEP) PAVEMENT SECTIONS

940-3-5910/16 BS

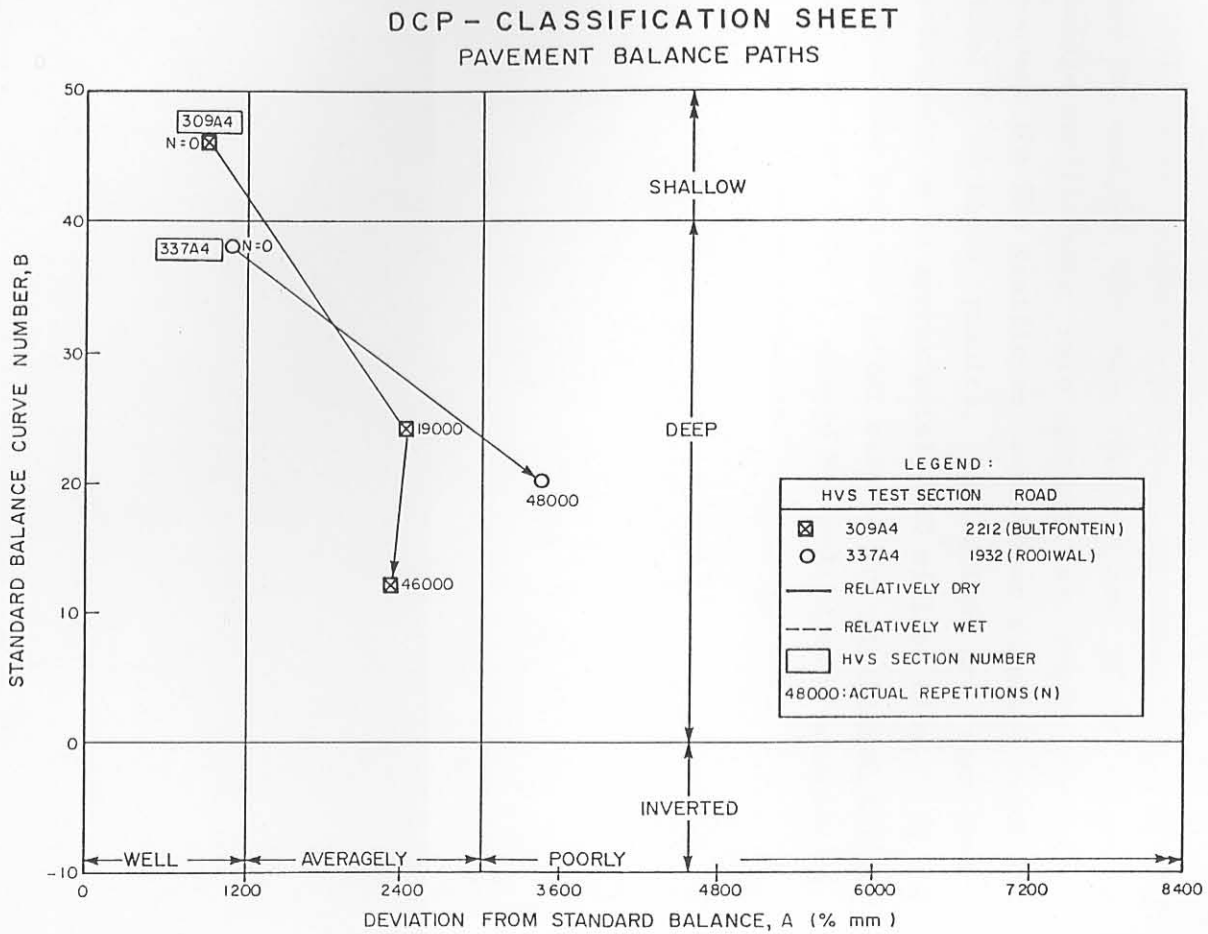

FIGURE 6.17

ILLUSTRATION OF THE BALANCE PATHS FOUND DURING ACCELERATED (HVS) TESTING FOR THE VARIOUS PAVEMENT SECTIONS TESTED

6.4.2 Original models

The original model (Kleyn, 1984), hereafter Model 1, is given below:

$$LIFE = Cm \times 10^{-9} (DSN_{800})^{3,5} \quad \ldots\ldots\ldots\ldots\ldots 6.1$$

with LIFE = Number of standard 80 kN axles to produce 20 mm rutting on the surface of the pavement.

Cm = 6,5 for soaked
= 14 for wet
= 30 for optimum (average)
= 64 for dry conditions

DSN_{800} = Total number of blows to penetrate to a depth of 800 mm in the pavement.

Model 1 originated from the initial research work with the Transvaal HVS on light unbound pavements with gravel bases (Kleyn, 1984, Marais et al, 1982), and appears to predict the effective structural capacity to achieve 20 mm rutting on these pavements very accurately. In Figure 6.18, the correlation between predicted and measured repetitions on one of these pavements (Road P123/1) is illustrated. The figure indicates that a very accurate prediction resulted from the HVS tests on this pavement, irrespective of the test wheel load. The maximum structural capacity (only those tested at 40 kN dual wheel load), however, is relatively low, and is approximately 1×10^6 standard axles. Most of the work reported by Kleyn (1984) was also done at relatively low standard (40 kN) axle repetitions, and it is my opinion that Model 1 is accurate for the lower class pavements only, ie up to 1 million standard axles (E80s). Although pavements were also tested at higher wheel loads (60 kN and 100 kN) than the standard 40 kN (Figure 6.18), relative damage coefficients were assumed or, where possible, calculated to convert the HVS traffic to equivalent standard axles (E80s). Applying Model 1 to these results, indications are that this model predicts accurately up to approximately 10 million E80s. It must, however, be remembered that the latter case is for equivalent traffic, and it is my opinion that Model 1 should be applied with caution on the relatively stronger granular pavements.

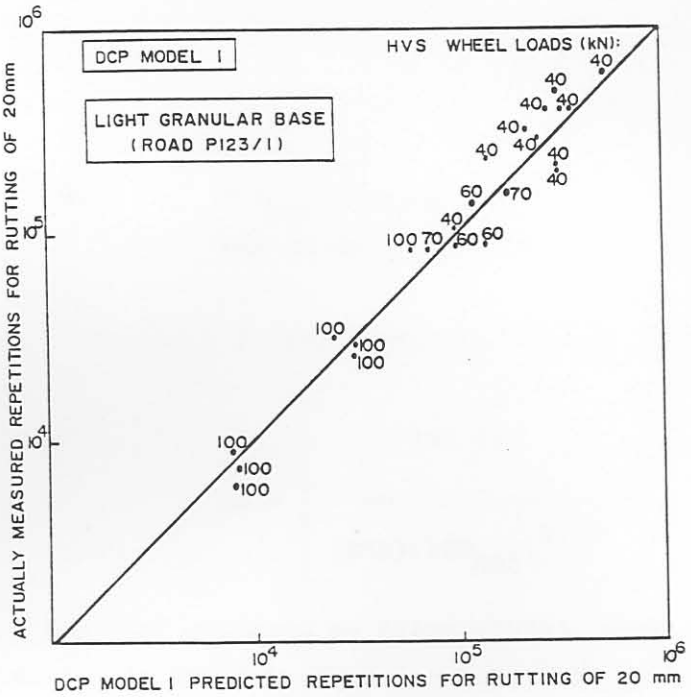

FIGURE 6.18

CORRELATION BETWEEN PREDICTED AND MEASURED REPETITIONS TO ACHIEVE A CHANGE OF 20mm IN THE RUTTING (MARAIS et al., 1982)

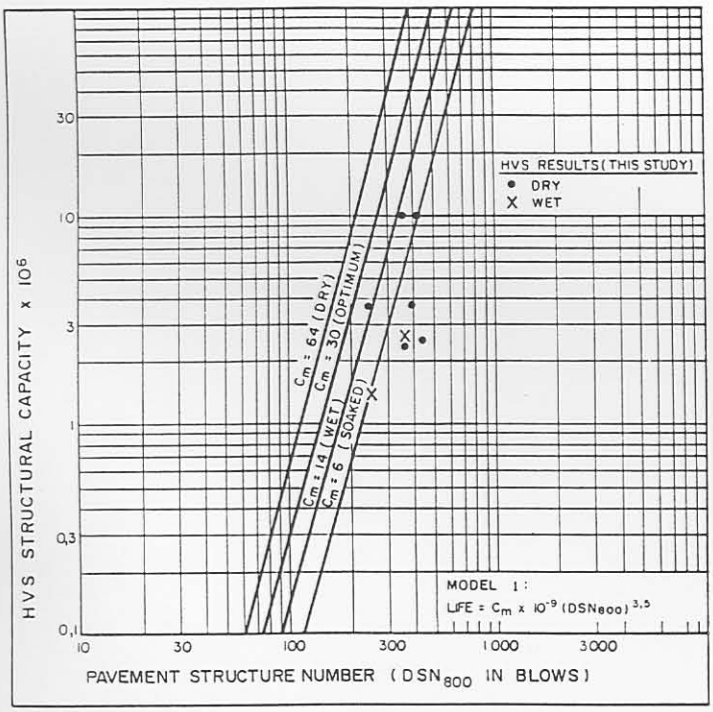

FIGURE 6.19

DCP MODEL 1 SUPERIMPOSED ON ACTUAL HVS MEASURED STRUCTURAL CAPACITY IN RELATION TO THE PAVEMENT STRUCTURAL NUMBER DSN_{800}

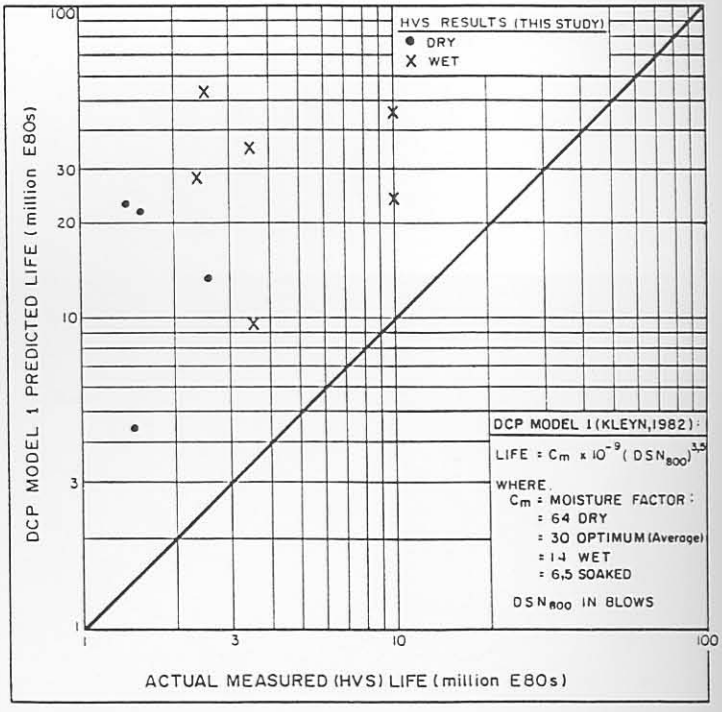

FIGURE 6.20

DCP MODEL 1 PREDICTION OF STRUCTURAL CAPACITY (LIFE) VERSUS ACTUAL MEASURED (HVS) LIFE TO ACHIEVE A CHANGE OF 20 mm IN THE PERMANENT DEFORMATION (RUTTING)

Applying Model 1, however, to the pavement sections tested in this chapter, the structural capacity is overestimated by a factor between 2 and 29, indicating that this model is <u>not</u> suitable for these pavements. See Figures 6.19 and 6.20 for the accuracy of Model 1, applied to the pavement sections investigated in this study.

Jordaan (1988) suggested the use of a combination of DSN_{800} and standard surface deflection (RSD, 40 kN) in order to calculate structural capacity. Following from this work of Jordaan (1988), the structural capacity may be calculated using Model 1, but with a "moisture" factor, Km, different from that of Cm proposed by Kleyn (1984). In Figure 6.21 the relations between deflection (RSD) and DSN_{800} are illustrated.

The relationships between DSN_{800} and deflection (RSD) are also given below (after Jordaan, 1988):

$$DSN_{800} = 339{,}8Km^{-0{,}28}(RSD)^{-1{,}17} \quad \text{.....6.2}$$

$$RSD = 141{,}74Km^{-0{,}24}(DSN_{800})^{-0{,}85} \quad \text{.....6.3}$$

with DSN_{800} in blows
RSD in mm.

From Equations 6.2 and 6.3, the "moisture factor" is calculated:

$$Km = \left[\frac{141{,}74}{(RSD)(DSN_{800})^{0{,}85}} \right]^{4{,}1667} \quad \text{.....6.4}$$

By replacing the "Cm" proposed by Kleyn (1984), with the "Km" calculated with Equation 6.4 in Model 1 (Equation 6.1), the structural capacity is then calculated. For the purpose of this dissertation the latter model is called Model 2. Model 2 overestimates the structural capacity even more than Model 1, by a factor between 1 and 950. This is unacceptable for the pavements in this study, and the need for an alternative model is evident.

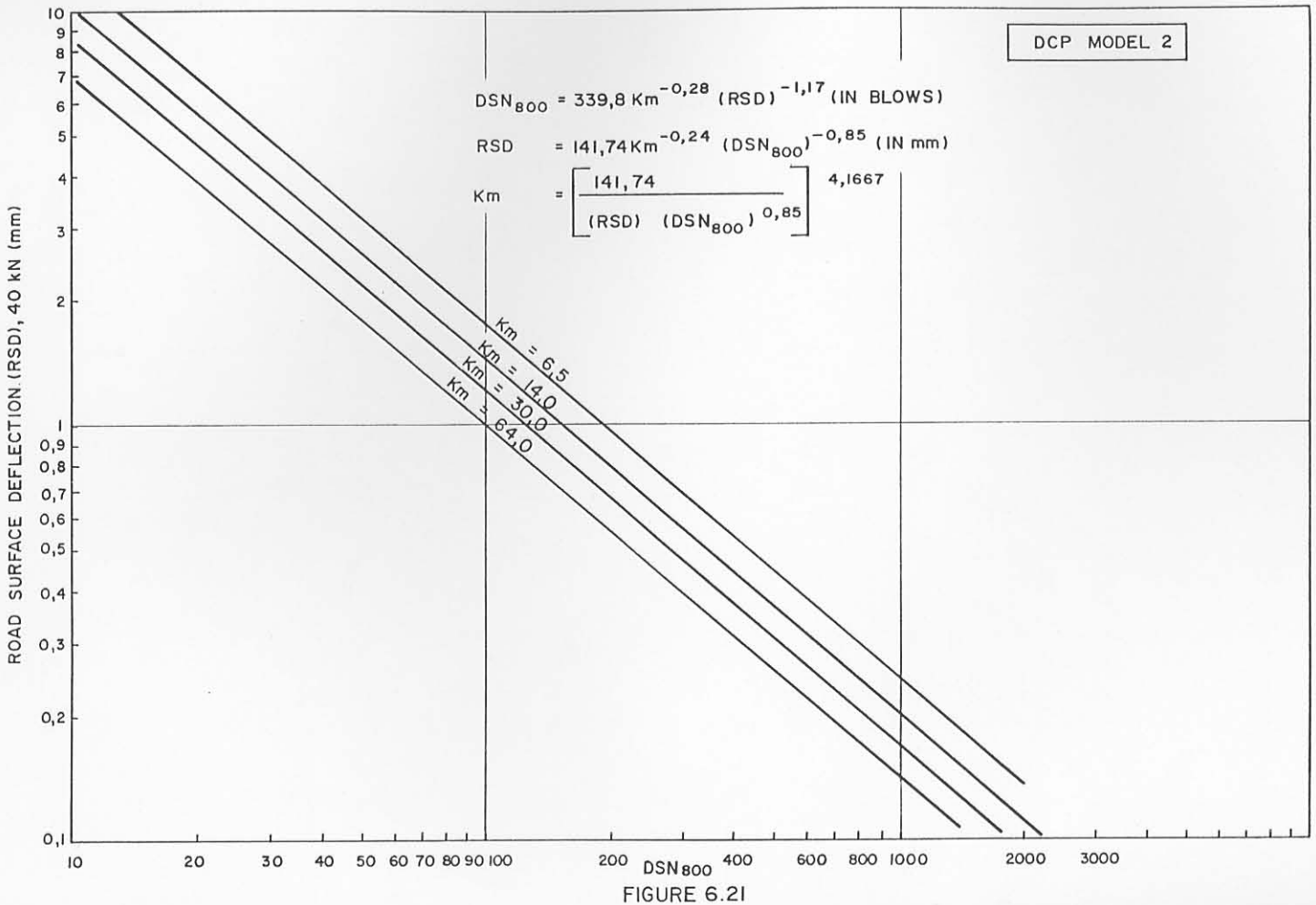

FIGURE 6.21

RELATION BETWEEN DEFLECTION (ASPHALT INSTITUTE) AND DCP STRUCTURE NUMBER DSN_{800} (JORDAAN, 1988)

It is believed that the underlying reasons for the overestimations of structural capacity by both Models 1 and 2 is strongly related to the fact that the basic DCP parameter, DSN_{800}, as well as the RSD, used in these models, is more representative of the total pavement depth (0 to 800 mm), especially the subgrade. If the majority of the permanent deformation originates from the subgrade layers or deeper down in the pavement, as is the case of the light unbound gravel pavements, Models 1 and 2 appear to be more accurate.

In Figure 6.22, the standard surface deflection (RSD) versus the DSN_{800} of the pavement sections studied here is illustrated. The figure illustrates that there is no correlation between the RSD and DSN_{800} for these sections. This is directly related to the fact that the majority of the RSD measured on the surface of these sections originates from the upper layers in the pavement, and not from the lower subgrade layers, and illustrates why Model 2 is incorrect for these pavements.

Both Models 1 and 2 are not recommended for use on pavements other than well- to averagely - balanced light unbound gravel bases, with structural capacity up to a maximum of 10 million E80s. These models appear to be fairly accurate for pavements with structural capacities less than one million E80s.

In Figure 6.23 various relationships between RSD and structural life for different type of bases, suggested by Kennedy et al (1978), are superimposed on the results found in this study. The figure indicates that although a similar trend appears, the results are scattered and do not conform to those published by Kennedy et al (1978), most probably for the reasons discussed above.

It is therefore necessary to investigate alternative parameters (in this case, DCP parameters) to be used in these pavements where the failures (usually deformation) originate in the upper layers of the pavement.

Figure 6.24 illustrates the relation between surface deflection (RSD) and DSN_{200} for the pavements studied here. DSN_{200} was selected because most of the deformation originated within the upper 200 mm of these pavements (both deep and shallow).

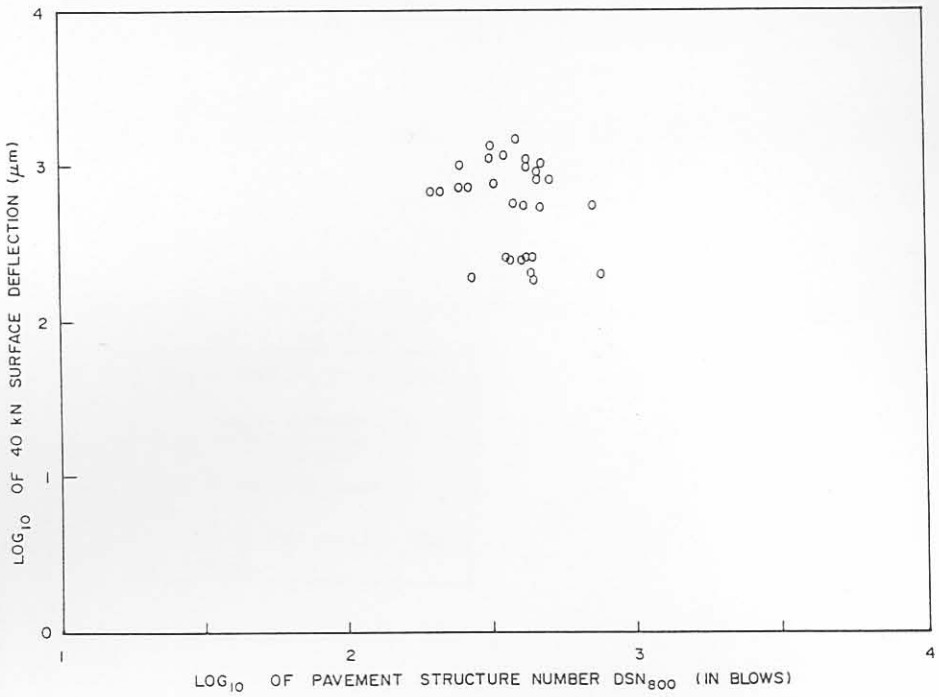

940-4-5915/5 BD

FIGURE 6.22

SURFACE DEFLECTION VERSUS THE PAVEMENT STRUCTURE NUMBER DSN_{800} AT VARIOUS STAGES OF HVS TRAFFICKING (THIS STUDY)

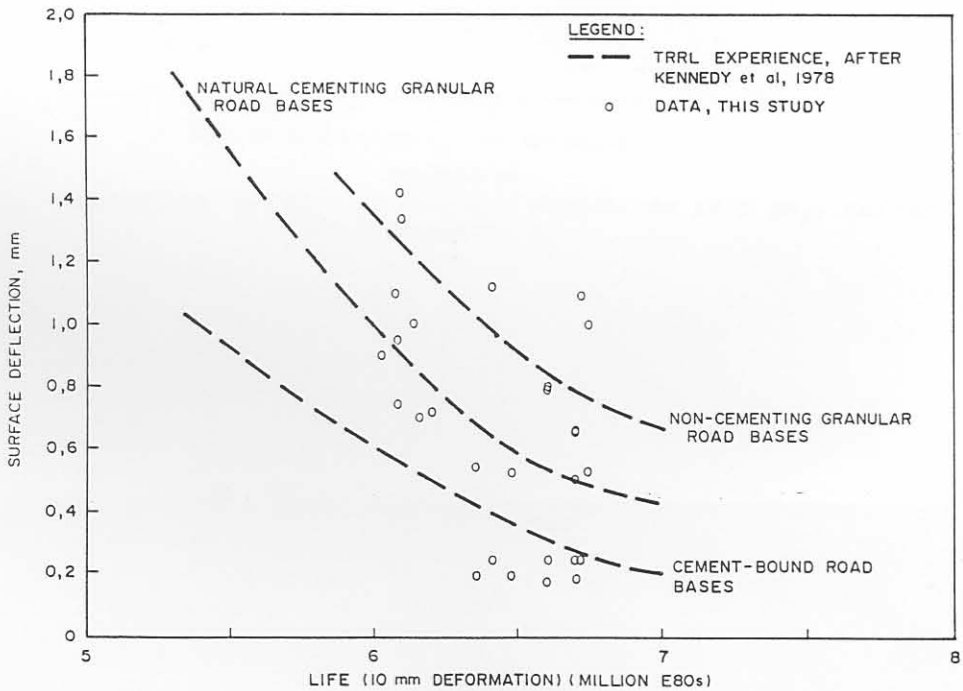

FIGURE 6.23

RELATIONS BETWEEN STANDARD (40 kN DUAL WHEEL) SURFACE DEFLECTION AND LIFE TO ACHIEVE A CHANGE OF 10 mm PERMANENT DEFORMATION ON VARIOUS TYPES OF ROAD BASES IN COMPARISON TO THE FINDINGS OF THIS STUDY

Although the accuracy of the relation is not very high (R^2=54 percent), a similar (promising) trend between deflection and a DCP parameter, suggested by Kleyn (1984) and Jordaan (1988) was found.

The relation is also given below:

$$RSD = 252041(DSN_{200})^{-1,22938} \quad \ldots\ldots\ldots 6.5$$

where RSD in μm

DSN_{200} = Total number of blows needed to penetrate the upper 200 mm of the pavement.

The origin of the permanent deformations (and most of the deflection) in the pavements studied, was found to be in the upper layers owing to fatigue and crushing. Therefore an alternative model is needed for this situation, in which DCP parameters other than the DSN_{800}, are used.

6.4.3 Development of alternative models

In view of abovementioned limitations of the current DCP prediction models, alternative models were investigated based on the results of this study. It must, however, be remembered that these models are strictly applicable to the pavement situations as defined in this study, namely: averagely balanced deep and shallow lightly cemented base and subbase pavements.

As indicated in Chapter 4, the development of permanent deformation on pavements with lightly cementitious layers appears to be linear with HVS trafficking. The rate of deformation (R_L) with trafficking appears to be a reliable indicator of pavement behaviour. It is therefore my opinion that the DCP model for these pavements should be developed on the basis of the prediction of R_L. Because of the relatively "shallow" failures associated with these pavements, DCP parameters in these upper regions of the pavement should be used instead of DSN_{800}.

Various models were evaluated using different DCP parameters. The most significant models and their evaluations are summarised in Table 6.9.

940-4-5915/1 BD

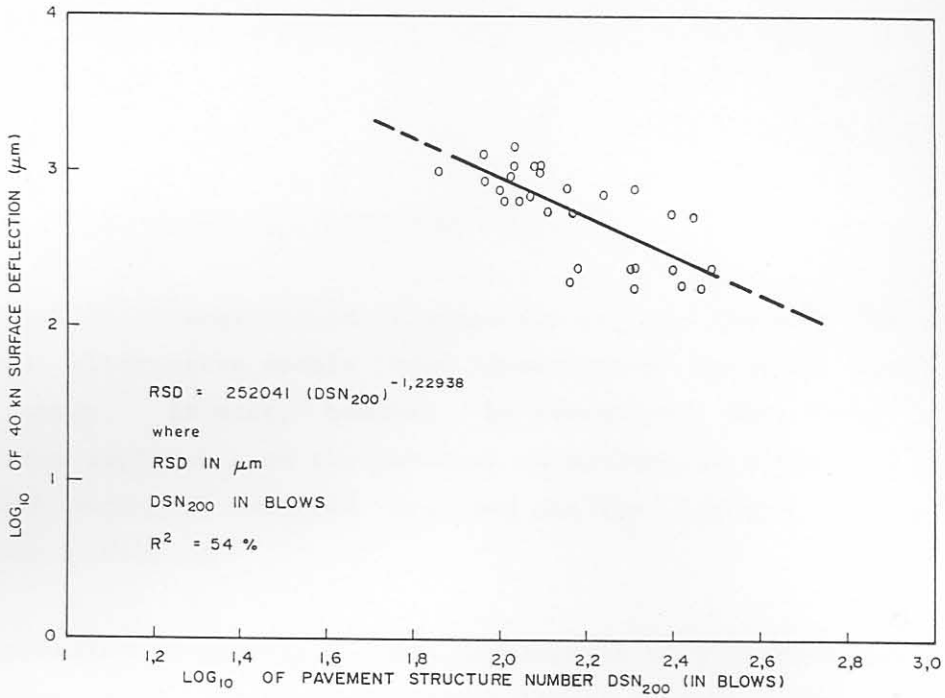

FIGURE 6.24

RELATION BETWEEN STANDARD (40 kN DUAL WHEEL) SURFACE DEFLECTION AND THE PAVEMENT STRUCTURE NUMBER DSN_{200} AT VARIOUS STAGES OF HVS TRAFFICKING

940-4-5914/3 BD

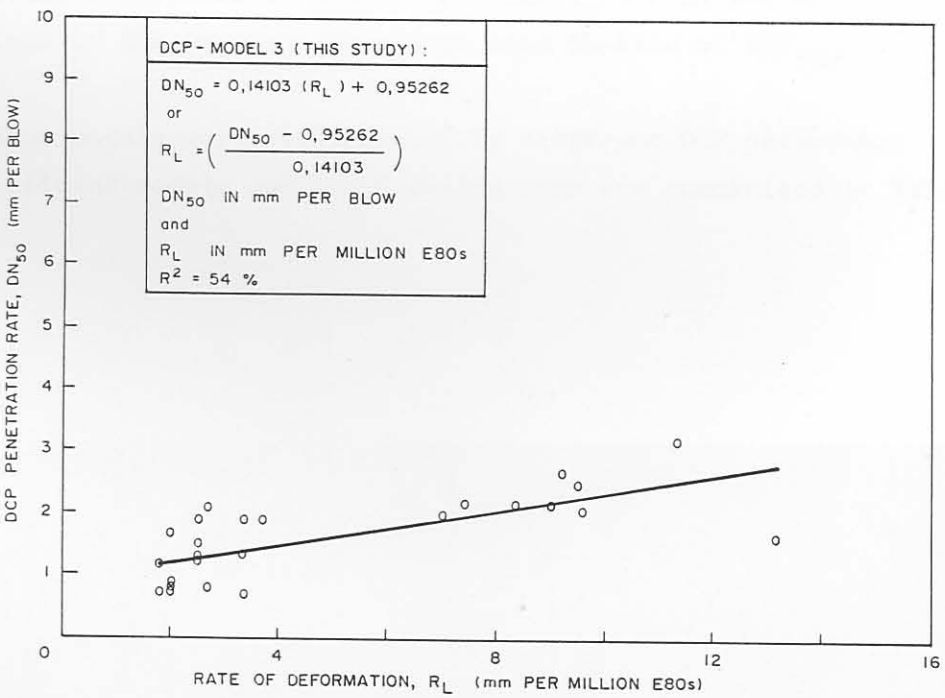

FIGURE 6.25

RELATIONSHIP BETWEEN AVERAGE DCP PENETRATION RATE DN_{50} AND RATE OF DEFORMATION, R_L

TABLE 6.9 EVALUATION OF THE VARIOUS DCP MODELS

REFERENCE	DCP PARAMETERS (VARIABLES)	R^2 (%)	REMARKS
Model 3	$R_L = f(DN_{50})$	54	Linear-linear
Model 4	$R_L = f(DN_{50}, DSN_{200})$	76	Linear-log
Model 5	$R_L = f(DSN_{200})$	36	Linear-log
Model 6	$LIFE_{10mm\ rut} = f(DSN_{200})$	38	Log-log
Model 7	$R_{Ldry} = f(DSN_{100}, DSN_{100-800})$	20	Linear-log
Model 8	$R_{Lwet} = f(DSN_{100}, DSN_{100-800})$	0,4	Linear-log

The table lists 6 models, of which only two appear promising, ie Models 3 and 4.

Model 3 is given below:

$$R_L = 7{,}091DN_{50} - 6{,}755 \quad \text{.....6.5}$$

with R_L in mm per million E80s

DN_{50} = Average penetration rate of the upper 50 mm in the pavement base, in mm per blow.

Figure 6.25 shows Model 3, which is based on DN_{50}, which is the average penetration rate for the upper 50 mm of the pavement (base). Figure 6.26 shows the accuracy of Model 3 relative to HVS rate of deformation (R_L). In Figure 6.27 the random scatter of the residuals is illustrated. (The residuals are defined as the difference between the measured values and the predicted values, and residual plots are used to examine the assumptions made about the error terms and to check for model fit, Galpin, 1981).

940-4-5915/9 BD

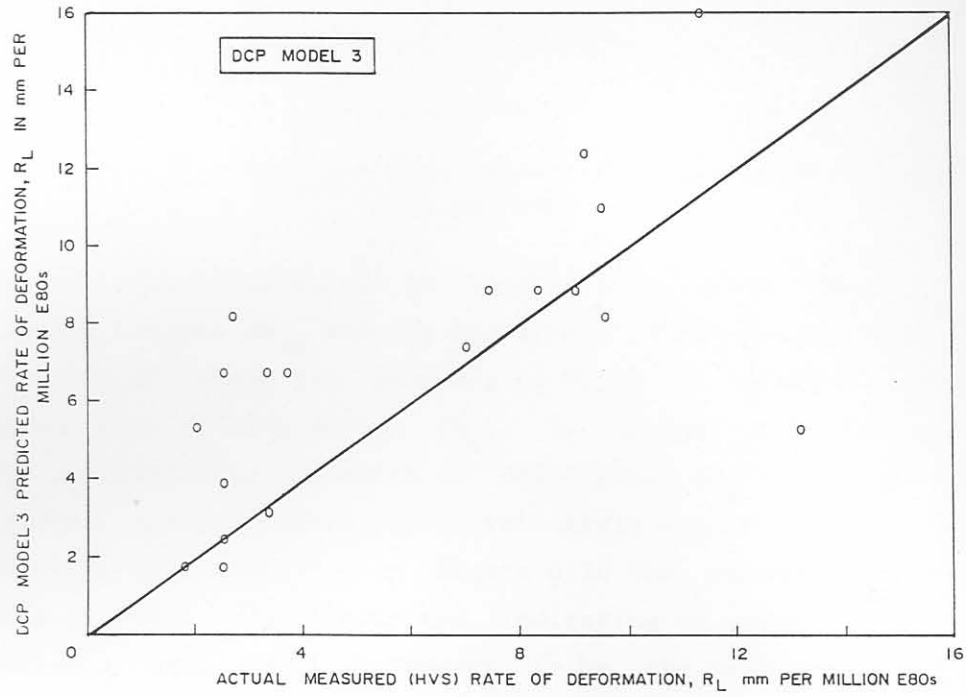

FIGURE 6.26

940-4-5915/7 BD

DCP MODEL 3 PREDICTION OF RATE OF DEFORMATION VERSUS ACTUAL MEASURED (HVS) RATE OF DEFORMATION

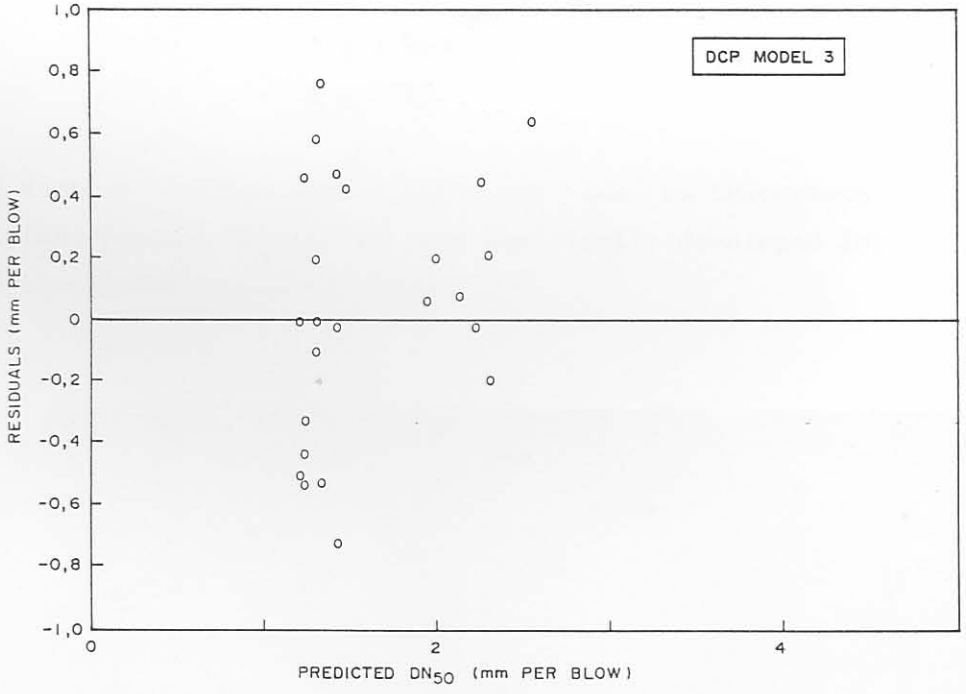

FIGURE 6.27

RANDOM SCATTER OF THE RESIDUALS OF DCP MODEL 3

Although the previous Figures 6.25 and 6.26 show a promising trend, it the accuracy of Model3 may be improved if additional DCP parameters (independent variables) are added. However, the models were kept as simple as possible.

Because the failures associated with the pavements in this study were limited to to the upper 200 mm, it was decided to incorporate the DSN_{200} (DSN_{200} = Total number of blows needed to penetrate the top 200 mm of the pavement) as another variable in addition to the DN_{50} of Model 3. This
model (Model 4) is given below:

$$R_L = \frac{DSN_{200}}{10^{((3,82806-DN_{50})/(1,38572))}} \quad \text{.....6.6}$$

with R_L in mm per million E80s

DN_{50} in mm per blow

DSN_{200} = Total number of blows in the top 200 mm of the pavement.

Model 4 is also illustrated in Figure 6.28, which shows a linear relationship between DN_{50} and the log of the ratio between DSN_{200} and R_L. Figure 6.29 shows the accuracy of Model 4, relative to the HVS determined rate of deformation (R_L). It appears that Model 4 over-predicts at relatively low rates of deformation (R_L < 5 mm per million repetitions), and under-predict at relatively higher rates. This was also the case for Model 3. In Figure 6.30 the random scatter of the residuals of Model 4 is illustrated, indicating no specific trend. With the available data, Model 4 appears to be the best model for these pavements, at this stage, and is only applicable to pavements with lightly cemented bases with the following DCP conditions:

$$200 \leq DSN_{800} \leq 750$$
$$B \geq 0 \text{ and}$$
$$A \leq 3000.$$

Use of Model 4 outside these limits may lead to inaccurate structural capacities, because this model was empirically developed for pavements within the limits indicated above.

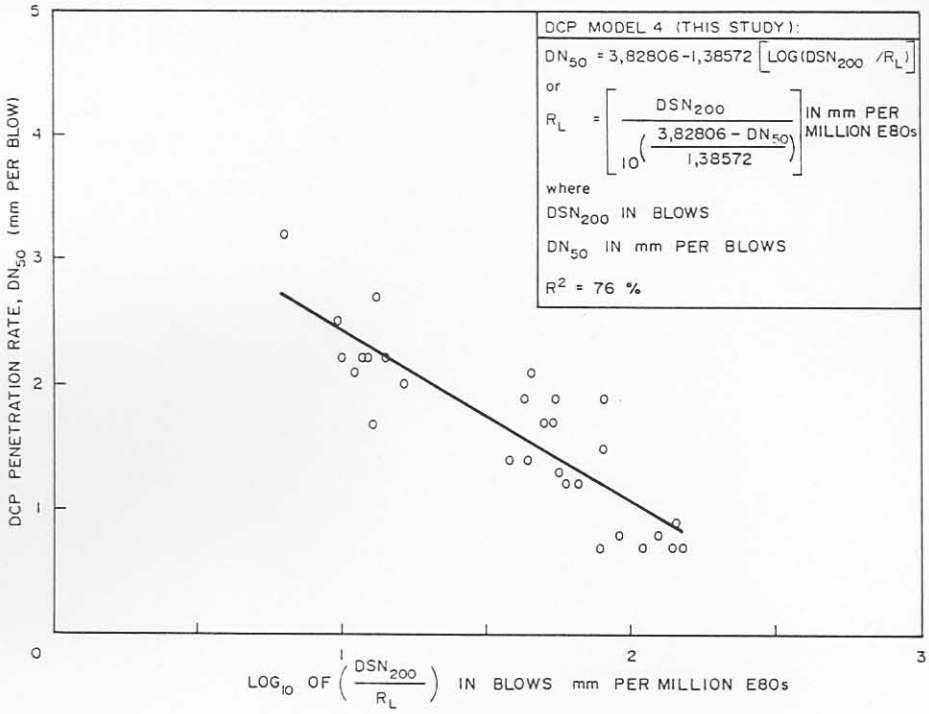

FIGURE 6.28

RELATIONSHIP BETWEEN DCP PENETRATION RATE DN_{50}, DSN_{200} AND THE RATE OF DEFORMATION, R_L

940-4-5915/8 BD

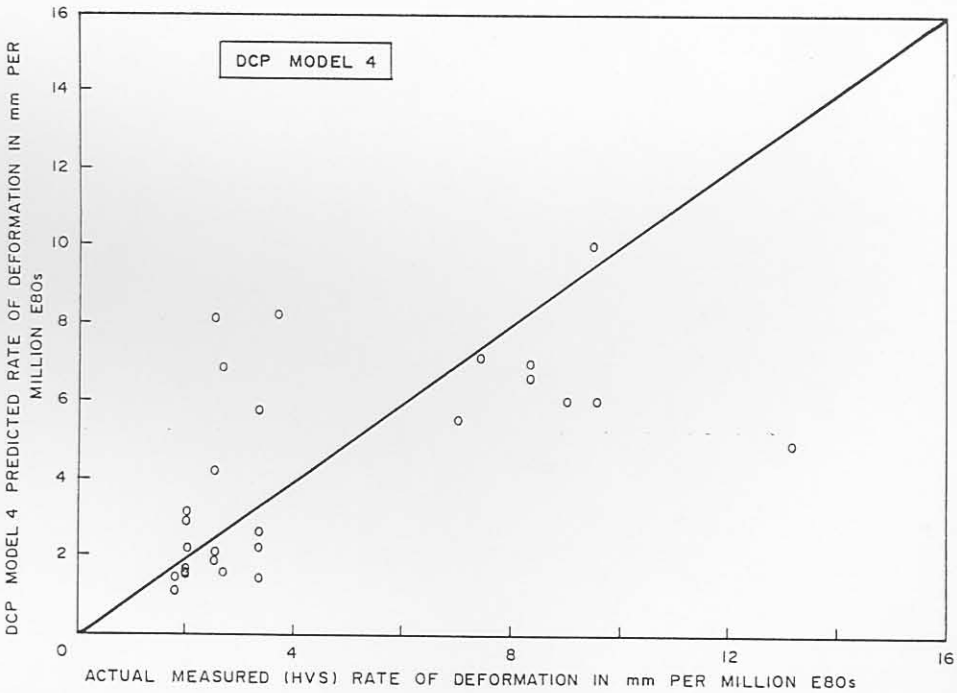

FIGURE 6.29

DCP MODEL 4 PREDICTION OF RATE OF DEFORMATION VERSUS ACTUAL MEASURED (HVS) RATE OF DEFORMATION

940-4-5915/6 BD

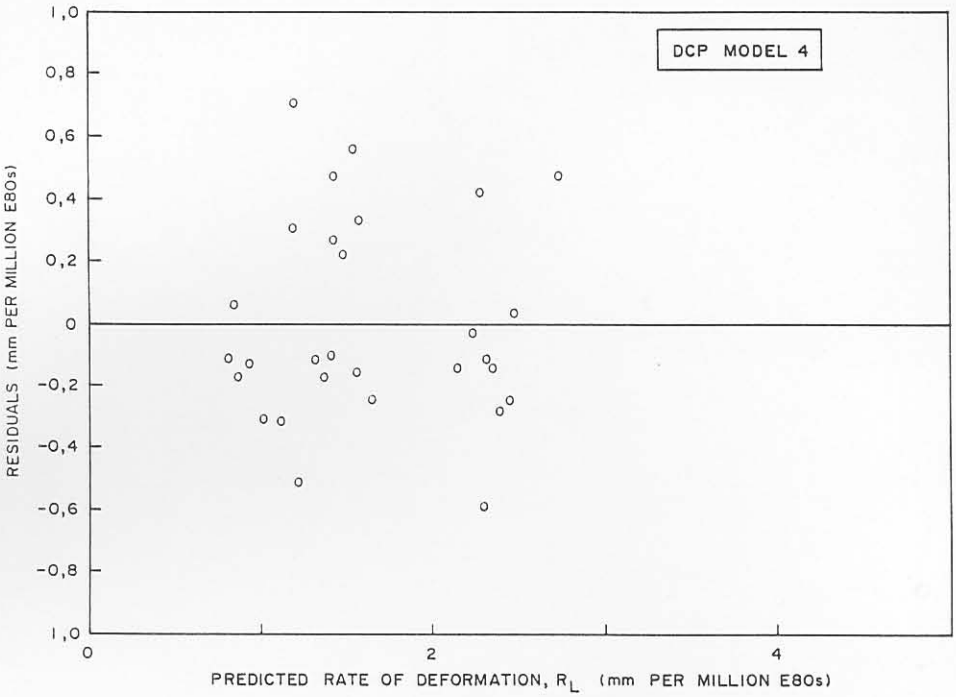

FIGURE 6.30

RANDOM SCATTER OF THE RESIDUALS OF DCP MODEL 4

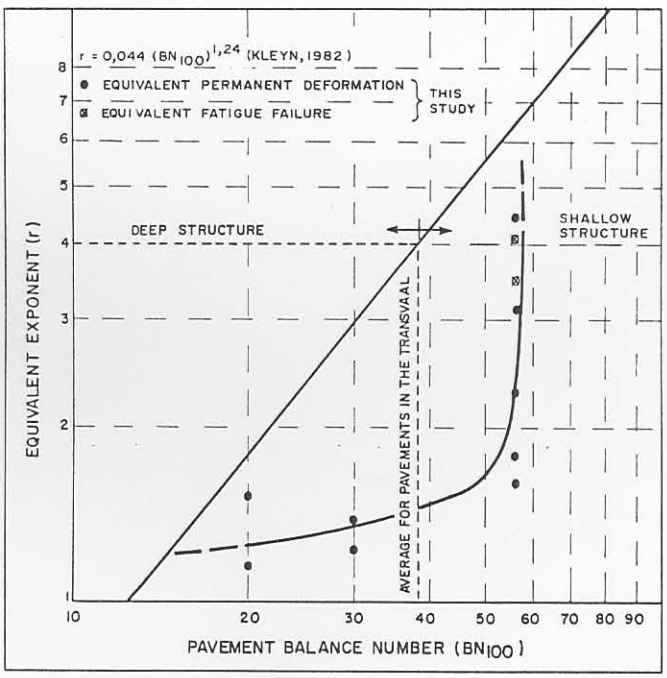

FIGURE 6.31

RELATIONSHIPS BETWEEN BN_{100} AND THE LOAD EQUIVALENT EXPONENT (r) FOR STRENGTH-BALANCED PAVEMENTS AND THE PAVEMENTS IN THIS STUDY

Various other models (Models 5, 6, 7 and 8, in Table 6.9) were evaluated using different DCP parameters, but with less success. Although it is accepted that many models other than those indicated in Table 6.9 are possible, it is my opinion that with the present available data, these models give an indication of some of the possibilities which may be investigated further on other types of pavements.

Research, however, should be continued in order to improve on these models in the future.

6.5 RELATIVE DAMAGE COEFFICIENTS

Kleyn (1984) published the first DCP-derived relative damage coefficients, in association with HVS research. In Chapter 4 (Paragraphs 4.2.4.4 and 4.3.4.4), discussions on the coefficients (r) determined for the two types of pavements discussed here, are given. The relationship proposed by Kleyn (1984) is illustrated in Figure 6.31, together with the results found in this study. Kleyn (1984) indicated that there appears to be a linear relationship between the log of the coefficient (r) and the pavement balance number, BN_{100}. The results of this study, however, indicate that this relationship is not linear, and that BN_{100} is not a good predictor of the relative damage coefficient, r, especially for the shallower pavements ($BN_{100} > 50$).

Further research, however, is necessary to define these relationships more accurately.

6.6 CONCLUSIONS AND RECOMMENDATIONS

6.6.1 Conclusions

The use of the Dynamic Cone Penetrometer (DCP) as a tool for predicting the behaviour of lightly cementitious base and subbase layers was studied. The concept of pavement strength - balance paths is introduced and appears to assist in describing pavement behaviour on a more quantitative basis than was done in the past. This is done by studying the changes caused by traffic loading in the two unique DCP parameters A and B. In general, parameter B, the balance number, appears to be more sensitive to change (owing to traffic) than parameter

A, the deviation from standard balance. Both parameters, however, are used to define the balance paths, introduced in this chapter.

The results from two basic types of pavements, deep and shallow, are discussed in detail and important differences are highlighted by the DCP. The main difference between these two pavements is reflected by the B parameter. For the deep pavement B showed an initial average of 19, and for the shallow pavement an average of 41. Both pavements were classified as averagely balanced, according to the classification system described in Chapter 3.

The DCP quantified the observed behaviour of these pavements adequately, in that higher penetration rates where measured where compression (crushing) failure occurred in the top of the base of the deep pavement, and compaction (densification) in the lower poorly cemented layers of the shallow pavement. As a result of traffic loading and prevailing moisture conditions, the balance paths of these pavements indicated that both pavements becomes deeper (decrease in B), but not necessarily better balanced. This was also found for pavement sections tested under excessively high single wheel load tests.

The structural capacity of these pavements was also evaluated and it was found that this capacity was overestimated by a factor of 2 to 29 by the original model (Model 1) developed by Kleyn (1984) and by a factor of 1 to 950 using Model 2 (Jordaan, 1988). Both these models are based on the structure number, DSN_{800}. The main reason for this overestimation is that most of the deformation originated in the upper layers of the pavements, tested in this study, and that DSN_{800}, which is a measure of all the layers in the pavement down to a depth of 800 mm, is not sensitive enough for this condition.

Alternative models were developed and evaluated, and it was found that the **rate of deformation** on the pavements studied here is adequately predicted by the number of blows needed to penetrate the upper 200 mm of the pavement, DSN_{200}, and the average penetration rate of the top 50 mm of the pavement, DN_{50}. These DCP parameters were selected because most of the deformation occurred in the upper 200 mm of these pavements.

Model 4 is only applicable for pavements with lightly cemented bases with the following DCP conditions:

$$200 \leq DSN_{800} \leq 750$$
$$B \geq 0 \text{ and}$$
$$A \leq 3000.$$

Use of Model 4 outside these limits may lead to inaccurate structural capacities, because it was empirically developed for pavements within the above limits.

6.6.2 Recommendations

It is recommended that the concept of strength - balance paths should be applied to other pavement types for further verification and refinement, as more data becomes available. It is also recommended that the effect of changes in the moisture content only on these paths be better studied as well as the natural variations in both the degree of balance, A and the balance number, B.

Further refinement of the models for the prediction of remaining structural capacity is necessary as more data becomes available. More experience with HVS will improve the data base of DCP/traffic loading, and may help to define the underlying fundamental relationship for these predictions properly. It is my opinion that a fundamental relationship exists between basic DCP parameters and the remaining structural capacity (shear strength, bearing capacity) for most normal pavements. Research should be guided to improve the understanding of and to quantify this relationship more accurately.

6.7 REFERENCES

Division of Roads and Transport Technology (DRTT), (1985). Guidelines for Road Construction Materials. Technical Recommendations for Highways, TRH14: 1985, CSIR, Pretoria, 1985.

Marais, G P, Maree, J H and Kleyn, E G (1982). The Impact of HVS testing on Transvaal Pavement Design. Paper delivered at the Annual Transportation Convention during 9-13 August 1982 (ATC 1982), Session H, S.313, Volume 3, CSIR, Pretoria, 1982.

Galpin, J S (1981). SWISK 25. Regression Package REGPAC (Version 3). Special Report, National Research Institute for Mathematical Science, CSIR, 1981.

Kleyn, E G (1984). Aspects of Pavement Evaluation and Design as determined with the Dynamic Cone Penetrometer (DCP). M Eng. thesis (In Afrikaans), Faculty of Engineering, University of Pretoria, Pretoria, 1984.

Jordaan, G J (1988). Analysis and Development of some Pavement Rehabilitation Design Methods. Ph.D Dissertation, Faculty of Engineering, Department of Civil Engineering, University of Pretoria, Pretoria, 1988.

Kennedy, C K and Lister, N W (1978). Prediction of Pavement Performance and the Design of Overlays. TRRL Laboratory Report 833, TRRL, Crowthorne, 1978.

CHAPTER 7

RESILIENT RESPONSE OF PAVEMENTS WITH CEMENTITIOUS LAYERS

CONTENTS PAGE

7.1 INTRODUCTION

In Chapters 4, 5 and 6, the discussions concerned the behaviour and evaluations related to permanent changes in both the deep (Road 1932, Rooiwal) and the shallow (Road 2212, Bultfontein) pavement. This included permanent (plastic) deformation, compression failure (crushing) and fatigue cracking. In this study the term "deflection" is used to describe resilient response, while "deformation" is used to describe permanent or plastic yield or rutting of the pavement layers.

In this chapter the resilient responses of these two types of pavements are summarised. The resilient response of pavements is a well-known indicator of pavement behaviour, similar to the behaviour indicators such as permanent deformation and cracking. These responses include road surface deflection (RSD) and multi-depth deflection (MDD). Radii of curvature (RC) were calculated for the surface deflection basin and are discussed. Effective elastic moduli for the different layers, back-calculated from the Multi - Depth Deflectometer (MDD) (De Beer et al, 1988), at various stages of trafficking, are summarised. Finally, an analysis of the tensile and vertical compressive strains using a quasi-elastic approach, is given.

The emphasis in this chapter is on the behaviour of these resilient indicators as a direct result of Heavy Vehicle Simulator (HVS) traffic loading. The results of this study are also compared to the current failure criteria for both cementitious layers and subgrade layers in South Africa.

Recommendations based on the results of this study are given to improve the current fatigue failure criteria for cementitious layers and the concept of effective fatigue life of these layers is introduced.

7.2 ROAD SURFACE DEFLECTION

7.2.1 Deep pavement (Road 1932, Rooiwal)

In full-scale HVS testing in South Africa, it is normal practice to

measure the road surface deflection with the Road Surface Deflectometer (RSD), similar to the Benkelman beam (Basson, 1985). The depth deflection profile is measured with the MDD (De Beer et al, 1988).

The standard deflection is measured with the legal load limit using a 40 kN dual wheel load, with tyre pressure at 520 kPa. These measurements were made at the start of the test as well as at various stages of trafficking. In Figure 7.1 (a) the average standard (40 kN) surface deflections at various stages of trafficking on four of the test sections on the deep pavement are illustrated. Note that the sections were trafficked at different wheel loads, ie 40, 70 and 100 kN, but the indicated deflection results are only the standard 40 kN load results. The figure indicates that the initial deflection varies between 0,2 mm and 0,3 mm, with a non-linear increase with trafficking. Initially the deflection slope is steeper than later and indicates possible fatigue failure in the cemented base layer. (This fatigue behaviour will be discussed later in Paragraph 7.6). The final deflection on the sections where the trafficking load was 40 kN (HVS Section 274A4 and 275A4) varied between 0,75 mm and 0,9 mm. On the sections with the higher trafficking loads (Sections 289A4, 70 kN, and 294A4, 100 kN), the final standard deflection varied between 1,3 mm and 1,5 mm. As found with the increase in permanent deformation on these sections discussed in Chapter 4, the increase in deflection is caused by the specific failure mechanism found for the deep pavement, viz fatigue and crushing (compression) failure in the upper section of the cemented base layer. Both the initial and final deflections on this pavement are comparable to deflections found on a similar pavement during full-scale testing in Australia (Kadar, 1988).

As a direct result of the crushing in the base, the contribution of the relative deflection from this layer to the total surface deflection increases. The lower layers also contribute to higher total surface deflection, because the weakening (crushing) of the base effectively reduces the protection of the lower layers, resulting in higher deflections, stresses and strains from these layers. During this process, the effective elastic moduli in most of the layers also reduce (see Paragraph 7.5).

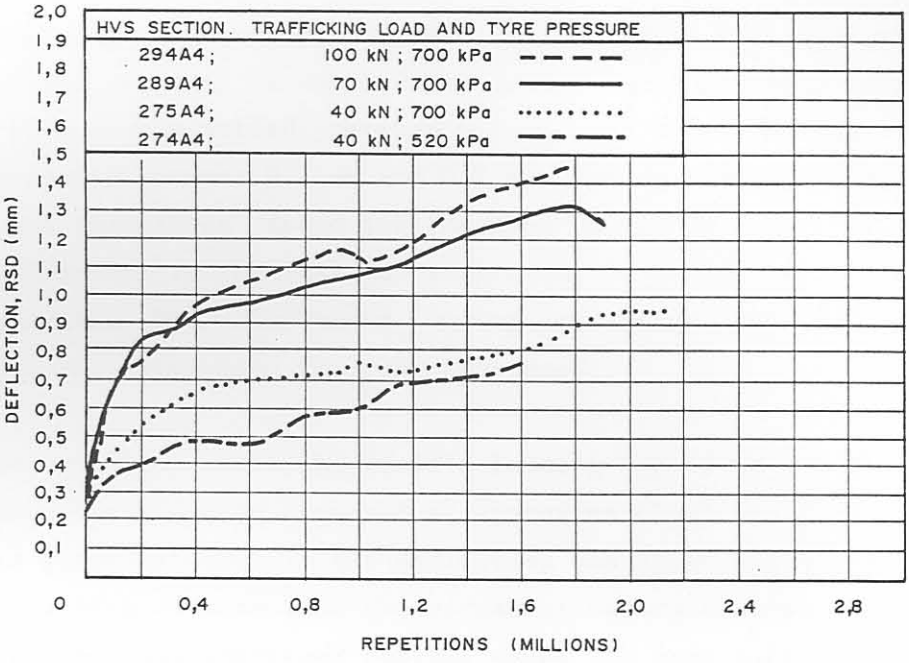

(a) DEFLECTION

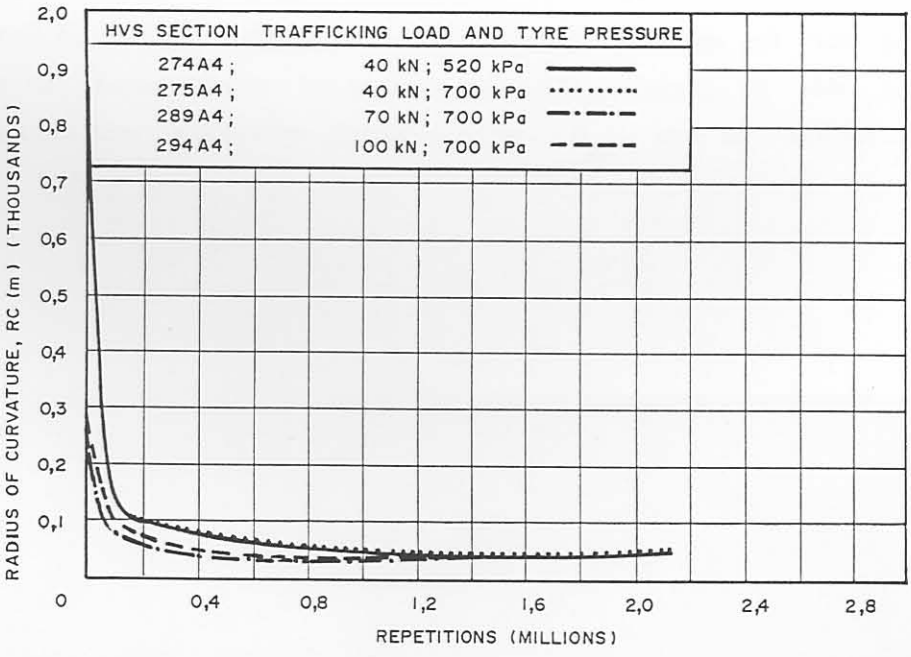

(b) RADIUS OF CURVATURE

FIGURE 7.1

SUMMARY OF THE AVERAGE STANDARD 40 kN SURFACE DEFLECTION AND RADIUS OF CURVATURE FOR THE FOUR TEST SECTIONS ON THE DEEP PAVEMENT (ROAD 1932, ROOIWAL)

In Figure 7.1 (b), the radii of curvature (RC), at various stages of trafficking on these four sections are illustrated. The figure indicates a rapid decrease in RC with trafficking from initial radii of 300 m to 850 m to a constant level of approximately 50 m, after 400 000 repetitions. The rapid decrease is indicative of structural failure in the upper layers, ie crushing of the upper section (approximately 50 - 75 mm) of the base, in this case.

These figures clearly indicate the damaging effect of the higher trafficking wheel loads in terms of both maximum deflection and curvature. The surface deflection and radius of curvature results for the individual test sections on the deep pavement, are illustrated in Appendix F, Figures F.1 and F.2.

7.2.2 Shallow pavement (Road 2212, Bultfontein)

In Figure 7.2 (a), the average standard surface deflections at various stages of trafficking on three of the HVS sections on the shallow pavement are illustrated. The deflections also increase with trafficking, similar to that found on the deep pavement. The initial deflection levels varied between 0,2 mm and 0,25 mm, while the final levels varied between 0,7 mm and 0,9 mm. These final deflection levels are lower than those found for the deep pavement, probably because of the differences in the failure mechanism. A relatively rapid increase in deflection was also noted during the first 100 000 to 200 000 repetitions, afterwhich the rate decreased.

On Section 306A4, where the traffic loading was 40 kN, another increase in standard deflection occurred at approximately 1 million repetitions. At this stage of the test the deflection was approximately 0,45 mm. It is interesting to note that the permanent deformation on the surface of this section also increased rapidly after the same amount of trafficking (see also Figure 4.8(a) in Chapter 4). Based on this result, as well as the MDD-deflections (see Paragraph 7.3), it is concluded that the cemented base layer effectively failed in fatigue at this point. The number of repetitions to introduce this change in the pavement is defined as the **effective fatigue life**, N_{ef}, and is associated with a

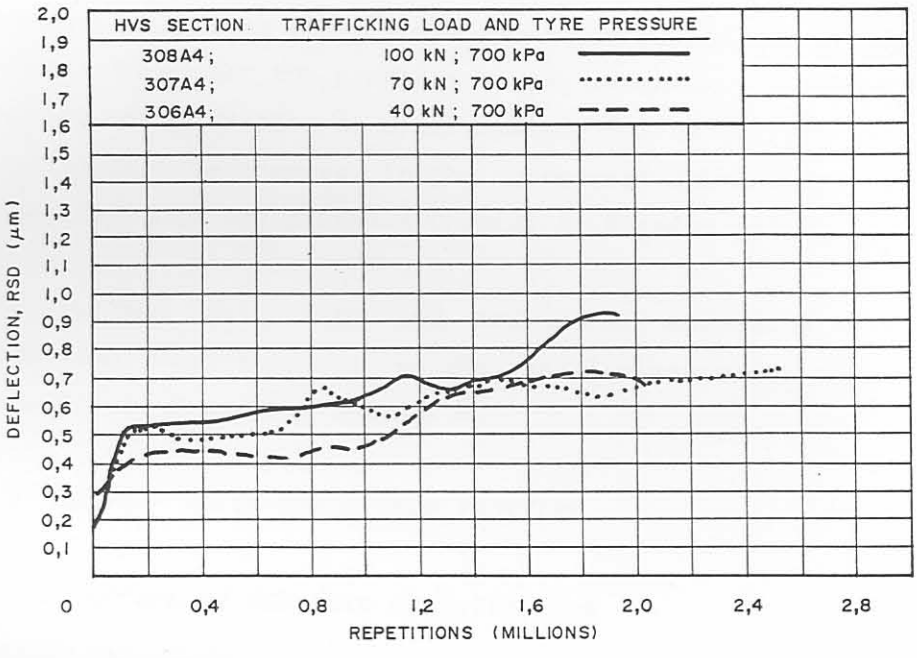

(a) DEFLECTION

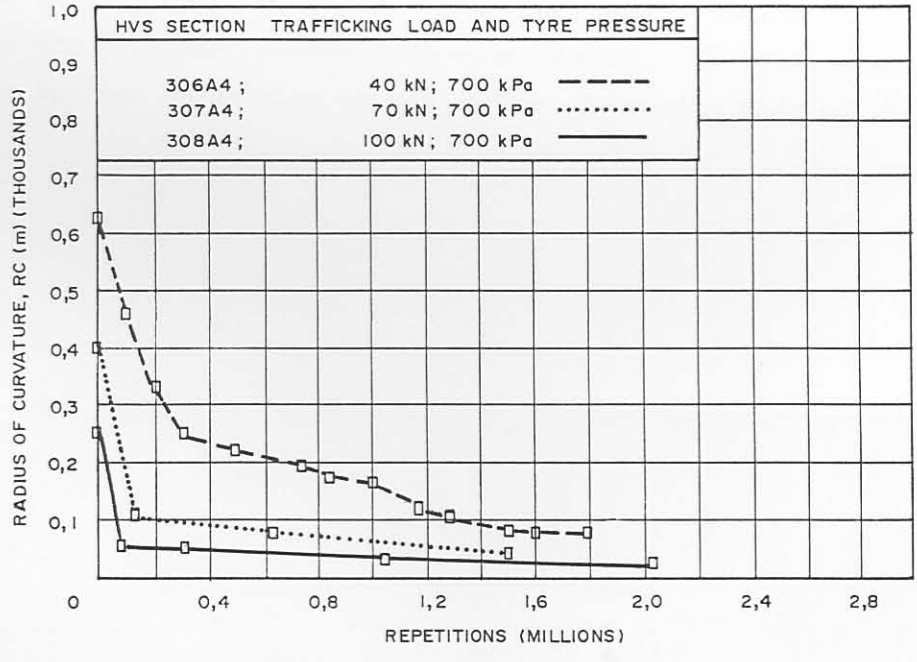

(b) RADIUS OF CURVATURE

FIGURE 7.2

SUMMARY OF THE AVERAGE STANDARD 40 kN SURFACE DEFLECTION AND RADIUS OF CURVATURE FOR THE THREE TEST SECTIONS ON THE SHALLOW PAVEMENT (ROAD 2212, BULTFONTEIN)

permanent deformation of approximately 2 mm, and a standard surface deflection between 0,5 mm and 0,75 mm. This is discussed in more detail in Paragraph 7.5.3.

In Figure 7.2 (b), the average standard (40 kN) RC values for the shallow pavement are illustrated. The figure indicates that the RC also decreases with trafficking but not as rapidly as the deep pavement. The RC changed from an original range of 600 m to 900 m, to a constant level of approximately 100 m. This is twice that found for the deep pavement and indicates that the structural failure is not associated with the base layer only, but is deeper in the pavement. In this case the subbase layer was found to be relatively weak and in an uncemented state from the start of the HVS testing (See Chapter 4, Paragraph 4.3). After the effective fatigue failure the base punched into the lower layers (see also Figure 4.15 for this mechanism) without the base layer being crushed to the same extent as that of the deep pavement. Hence the relatively higher final standard RC.

The figure also indicates the relatively higher damaging effect of the higher trafficking wheel loads in terms of surface deflection, similar to that found for the previous deeper pavement. Furthermore, the change in rate of deflection at approximately 0,5 mm is also indicated, and is similar to the changes in the permanent deformation development, as illustrated in the previous Chapter 4, Figures 4.8 and 4.9.

The surface deflection and radius of curvature results for the individual test sections on the shallow pavement, are illustrated in Appendix F, Figures F.3 and F.4.

7.3 MULTI - DEPTH DEFLECTION PROFILES

7.3.1 Effect of MDD hole on deflection

The multi - depth deflection profiles were measured with the MDDs. As for the permanent deformation measurements, it is important to compare the surface deflection on top of the MDDs with that of the rest of the

test section (between the MDDs) in order to evaluate the effect of the MDD hole on the response of the pavement during the test. This is to ensure that only representative deflection profiles are used in further analysis (in this case back-calculation of effective elastic moduli). If local failures occur at the MDD hole as a result of the disturbance of the hole in the pavement, incorrect and often over conservative deflections, and moduli, stresses and strain values result. In Figures 7.3 and 7.4 the surface deflection on the test section (omitting deflection measurements at the top of the MDDs) are compared to the deflections on the MDDs. In general, good agreement between the results exists, except for those on Sections 289A4 and 294A4, where the deflection on the MDDs were approximately 0,1 mm higher towards the end of the test. This larger deflection is most probably related to the higher trafficking wheel loads (70 and 100 kN) on these sections. Inspection during and after the HVS testing revealed slightly advanced crushing at the MDD top caps. A difference of 0,1 mm was not considered as too high. However, it is expected that the back-calculated moduli of the base layer are under estimated in these cases. Differences in these deflection levels larger than 0,1 mm are normally considered unacceptable for moduli back-calculation purposes.

7.3.2 Depth - deflection behaviour

7.3.2.1 Deep pavement

In Figure 7.5, typical depth - deflection profiles measured on the deep pavement, at various stages of HVS trafficking are illustrated. Three MDDs were installed on each HVS test section at measuring positions 4, 8 and 12. The depths of the MDD modules were located as previously indicated for permanent deformation measurements in Chapter 4 (Figure 4.3). Figure 7.5 (and Figures F.5 to F.10, in Appendix F), indicates a general decrease in deflection with depth. There was also an increase in deflection in all the layers with an increase in trafficking. The largest increase in relative deflection occurred in the base layer as a direct result of the crushing failure in the upper 50 mm to 75 mm of the base. This is well illustrated at measuring point 12 (MDD12). In Figure 7.6, the same deflection results as in Figure 7.5 are given, but in a different format, and clearly illustrate the contribution of the individual layers to the total deflection at the surface. The major

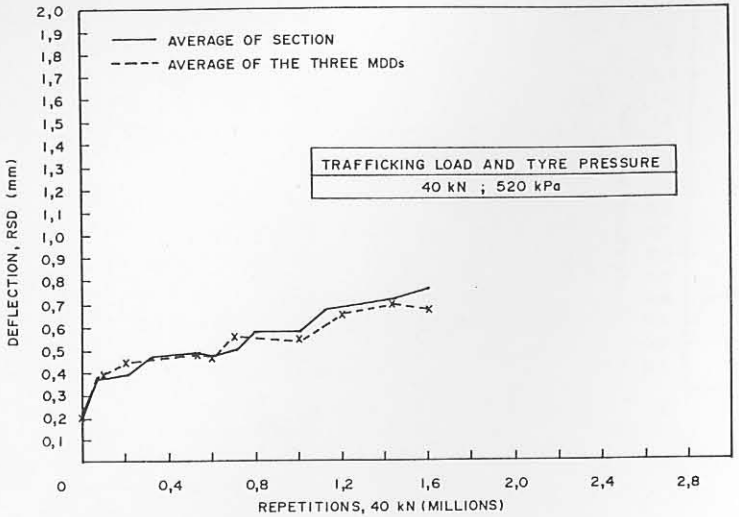

(a) SECTION 274A4

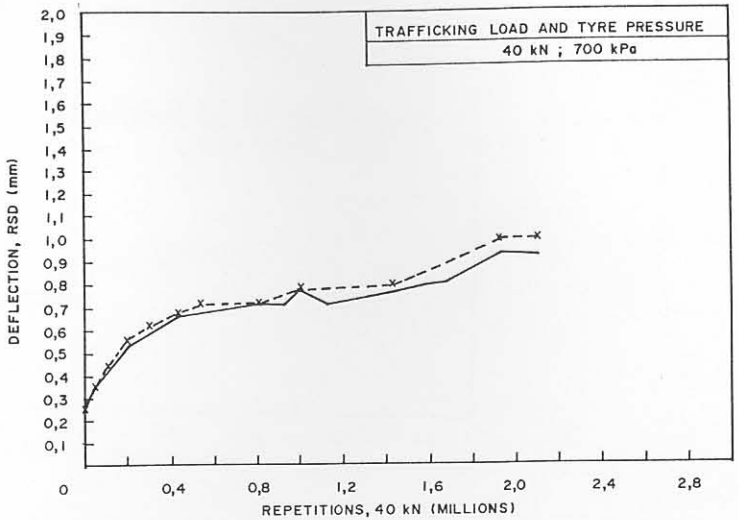

(b) SECTION 275A4

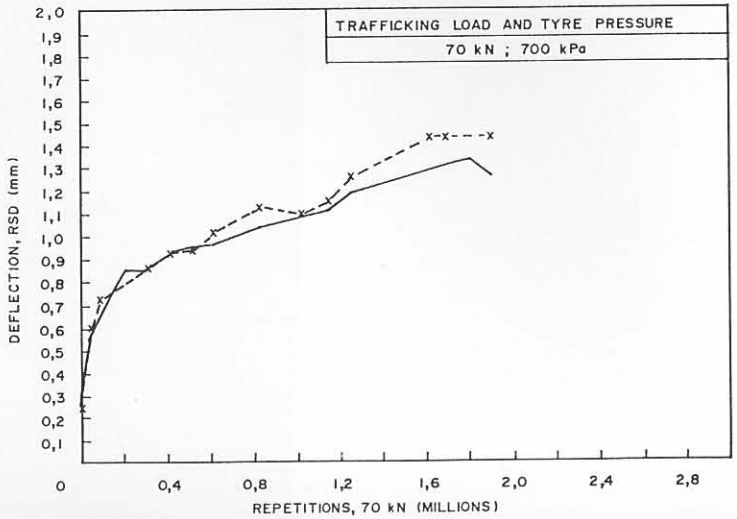

(c) SECTION 289A4

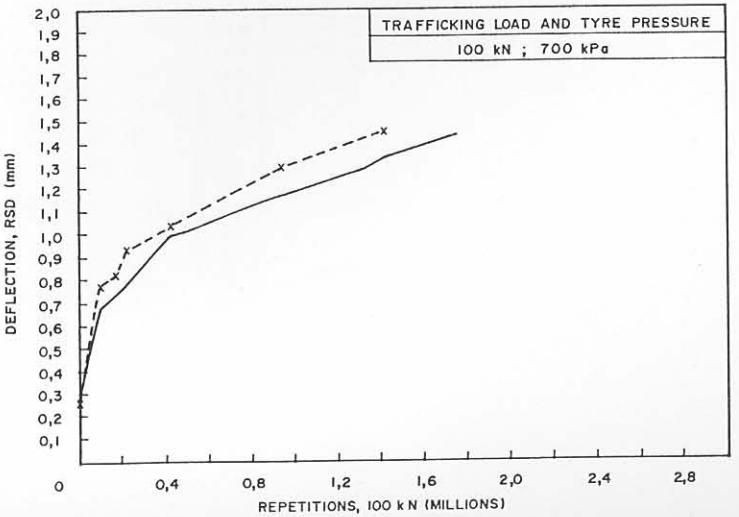

(d) SECTION 294A4

FIGURE 7.3

COMPARISON BETWEEN AVERAGE STANDARD 40 kN SURFACE DEFLECTION ON THE SECTION AND THOSE ON THE MDDs FOR THE FOUR TEST SECTIONS ON THE DEEP PAVEMENT (ROAD 1932, ROOIWAL)

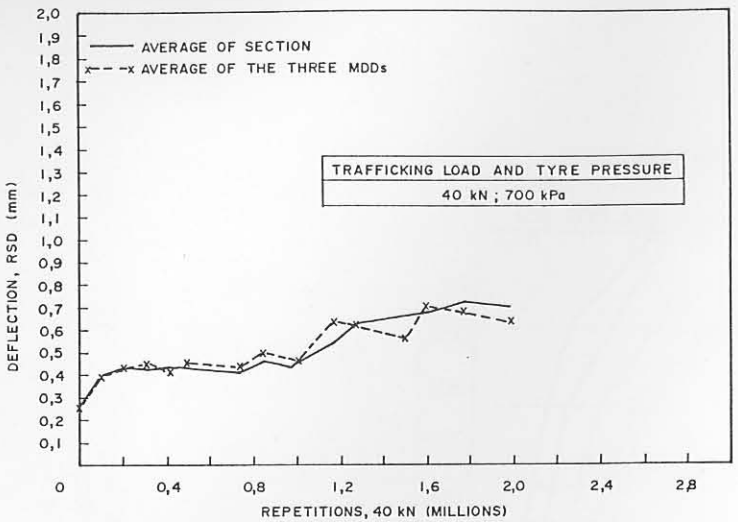

(a) SECTION 306A4

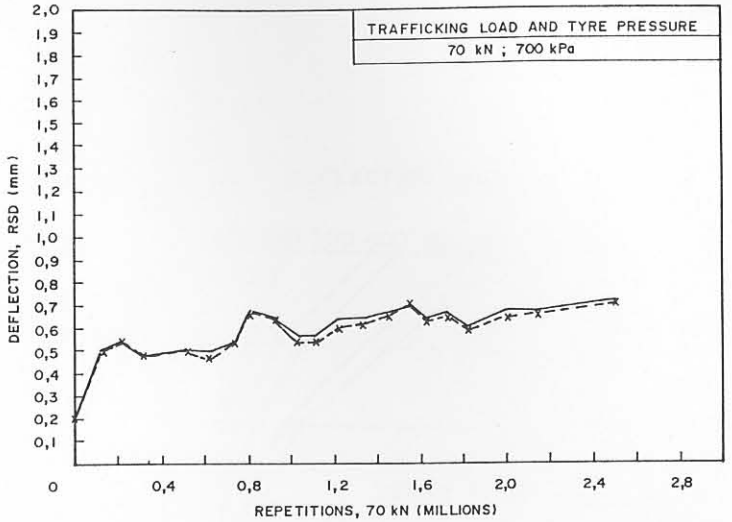

(b) SECTION 307A4

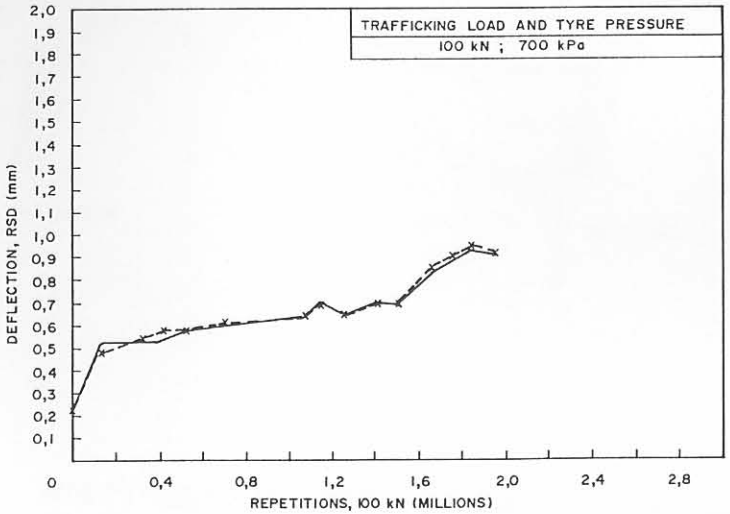

(c) SECTION 308A4

FIGURE 7.4

COMPARISON BETWEEN AVERAGE STANDARD 40 kN SURFACE DEFLECTION ON THE SECTION AND THOSE ON THE MDDs FOR THE THREE TEST SECTIONS ON THE SHALLOW PAVEMENT (ROAD 2212, BULTFONTEIN)

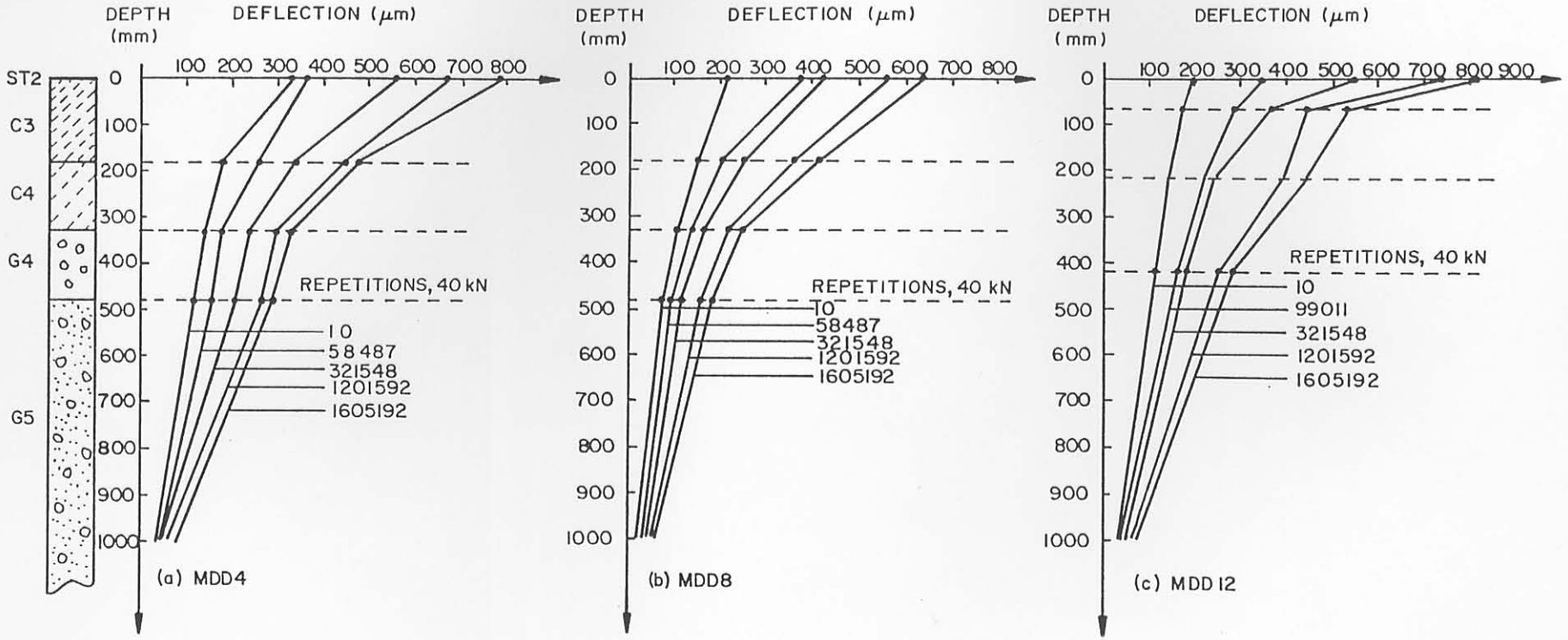

FIGURE 7.5

MULTI-DEPTH DEFLECTIONS AT MEASURING POSITIONS 4, 8 AND 12 AT VARIOUS STAGES OF TRAFFICKING ON HVS SECTION 274A4 OF THE DEEP PAVEMENT (ROAD 1932, ROOIWAL)

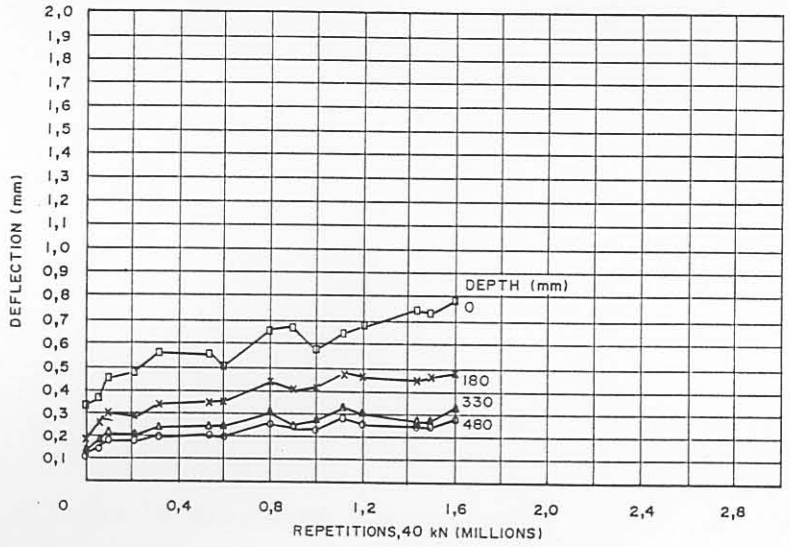

(a) MDD 4

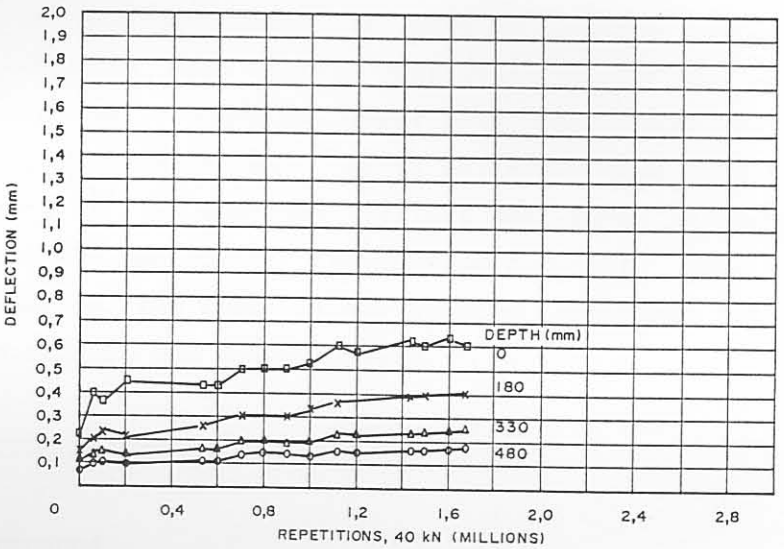

(b) MDD 8

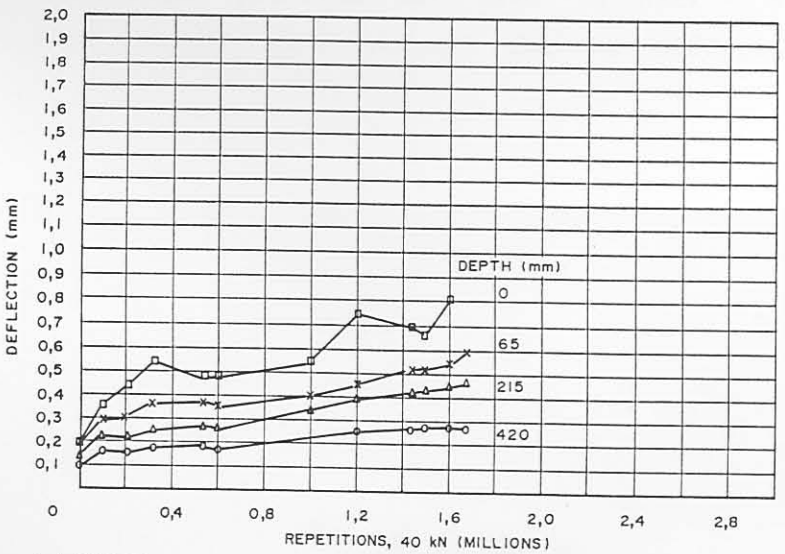

(c) MDD 12

FIGURE 7.6

AVERAGE STANDARD MDD DEFLECTION AT VARIOUS STAGES OF TRAFFICKING ON SECTION 274A4 (ROAD 1932, ROOIWAL)

portion of the total surface defection originated within the base and subgrade layers, probably exacerbated by the crushing failure in the cemented base layer.

7.3.2.2 Shallow pavement

In Figure 7.7, typical depth-deflection results from the shallow pavement are illustrated. As is the case of the deep pavement, the deflection decreases with depth, and increases as a result of traffic loading. In this case most of the deflection originates from the subgrade (480 mm downwards) and the relatively weaker subbase (110 mm to 310 mm). Figures 7.8 (a) and (c) indicate the relatively high increase in deflection (approximately 0,1 to 0,2 mm) of all the layers, at approximately 1 million repetitions (E80s), and is similar to that found with the surface deflection (see Figure 7.2). This indicates that the load bearing capacity of the base layer (0 mm to 110 mm) decreased at this point because of fatigue failure, thus transferring larger deflections to the lower layers.

In Appendix F, Figures F.11 to F.14, the increase in deflection is evident in all the layers, from the beginning of the test period. This is indicative of fatigue failure of the base from the the start of the HVS testing, under wheel loads greater than 40 kN.

Throughout the testing (except for MDD4 on Section 307A4, Figure J.12 (a), in Appendix J), the relative deflection in the base layer is small (0 mm to 0,1 mm), which is lower than that observed in the deep pavement (0,1 mm to 0,25 mm). It is believed that this is related to the difference in the dominant failure mechanism, ie crushing in the deep pavement and fatigue in the shallow pavement. Some crushing did, however, occur in the base of the shallow pavement, but to a lesser extent than that in the deep pavement.

7.4 EFFECTIVE ELASTIC MODULI

7.4.1 Background

The depth - deflection profiles were used to back - calculate the effective elastic moduli (E - values) for the different layers at

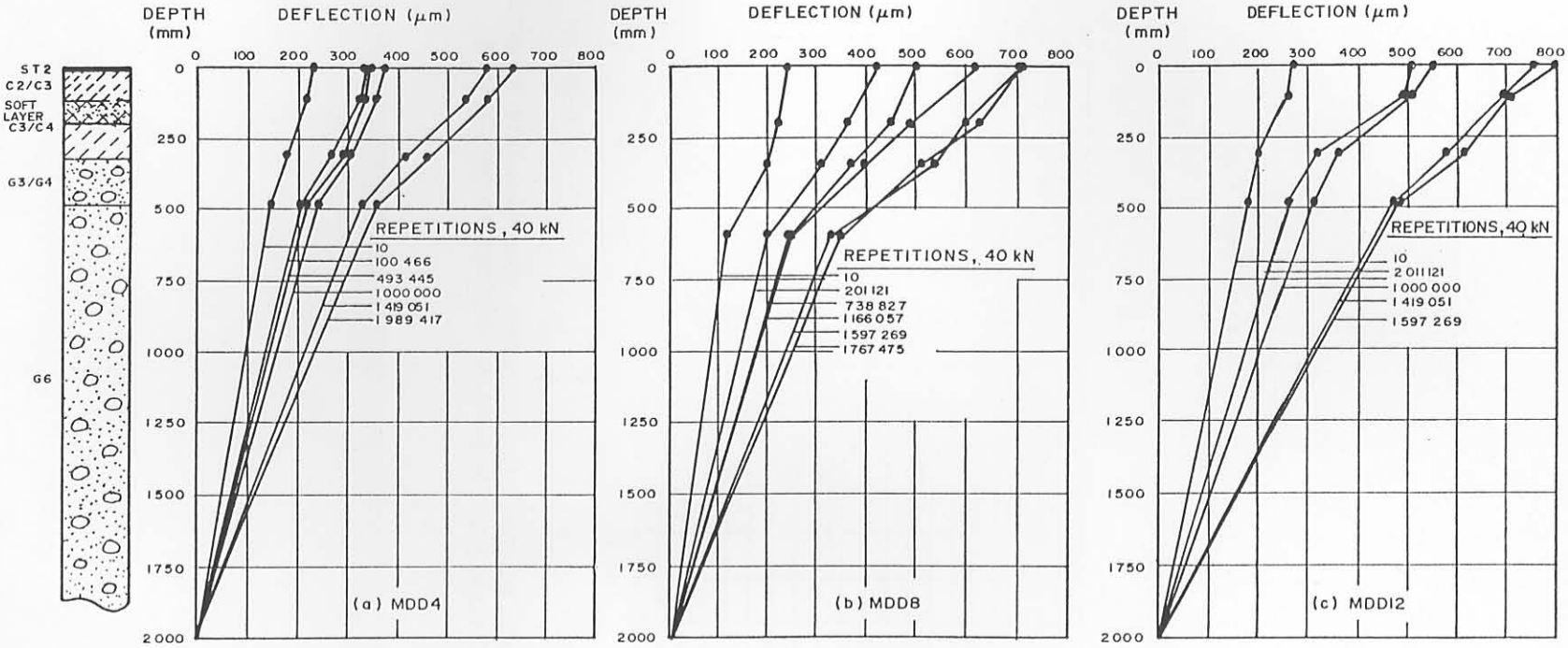

FIGURE 7.7

MULTI-DEPTH DEFLECTIONS AT MEASURING POSITIONS 4, 8 AND 12 AT VARIOUS STAGES OF TRAFFICKING ON HVS SECTION 306A4 OF THE SHALLOW PAVEMENT (ROAD 2212, BULTFONTEIN)

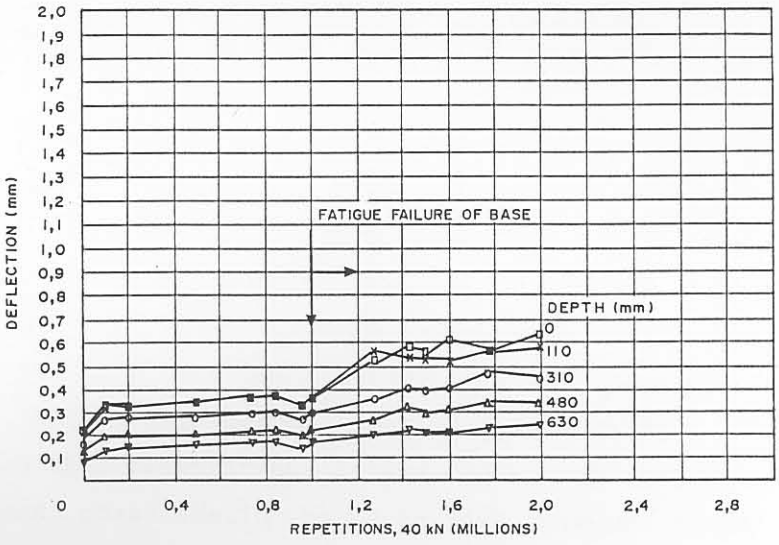

(a) MDD 4

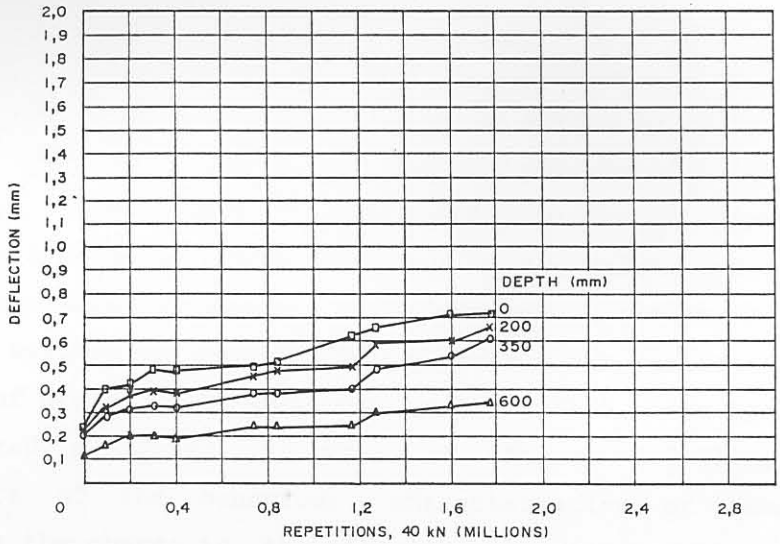

(b) MDD 8

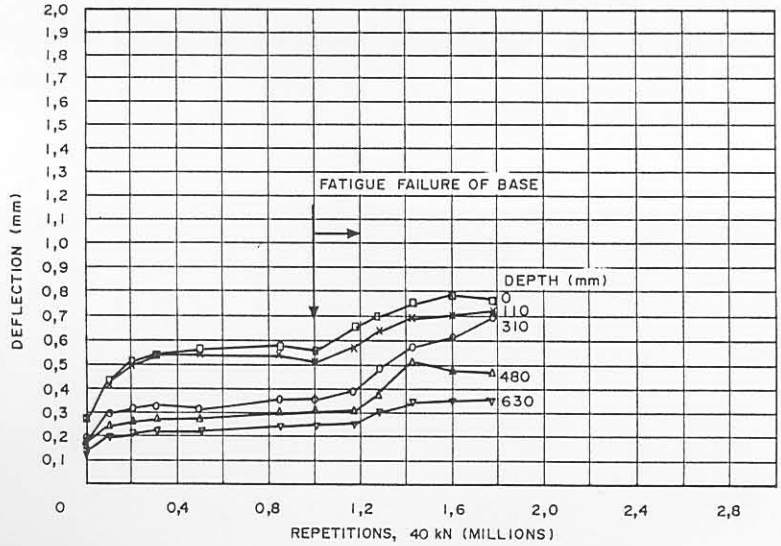

(c) MDD 12

FIGURE 7.8

AVERAGE STANDARD MDD DEFLECTION AT VARIOUS STAGES OF TRAFFICKING ON SECTION 306A4 (ROAD 2212, BULTFONTEIN)

various stages of trafficking. In this dissertation the subgrade was assumed to be of infinite depth (elastic half space), and the dual wheel loads spaced at 220 mm. The wheel spacing was smaller than that normally used, viz 350 mm, because more realistic effective moduli values were obtained for the base layers with this reduced spacing. The 220 mm spacing was fixed as twice the radius of the loaded area under standard loading conditions (40 kN, 520 kPa). It was found that unrealistically low moduli resulted for the base layers if an unloaded area between the two loads exists (350 mm spacing). It was therefore decided to reduce the spacing from 350 mm to 220 mm so that the contact areas could meet.

The results show that the moduli of all the layers decrease with trafficking, with the upper layers affected more than the lower layers. It is believed that this information on the change in moduli with trafficking will enhance the understanding of basic pavement behaviour. Over the years it has been established that the moduli, and therefore the stresses and strains in the various pavement layers, are not constant, but change because of traffic loading. It has long been recognised that cementitious layers crack and that the analysis during the cracked phase should be done with reduced moduli (Otte, 1978). Brown et al (1987) recently also indicated that data on the deterioration of the moduli of cementitious layers with time (traffic) is in short supply.

As indicated above, concepts of the reduction in moduli during the cracked phase were introduced into South Africa as early as 1978 (Otte, 1978). Freeme et al (1984) proposed the concept of "effective stiffness or moduli". For example, if a bound (bituminous or cementitious) layer cracks in fatigue or breaks down into an equivalent granular type layer, the layer ceases to behave as a homogeneous continuum in the manner normally assumed for theoretical analysis. For cementitious layers the concept of pre-cracked and post-cracked states were introduced, as is illustrated in Figures 7.9 and 7.10. Figure 7.9 illustrates several indicators of the behaviour characteristics of cemented layers, including the change in the effective elastic moduli. In Figure 7.10 (a), the conceptual reduction in the moduli of the various qualities of cementitious layers is illustrated, and in Figure 7.10 (b), a schematic presentation of the equivalent behaviour of a cemented material is illustrated.

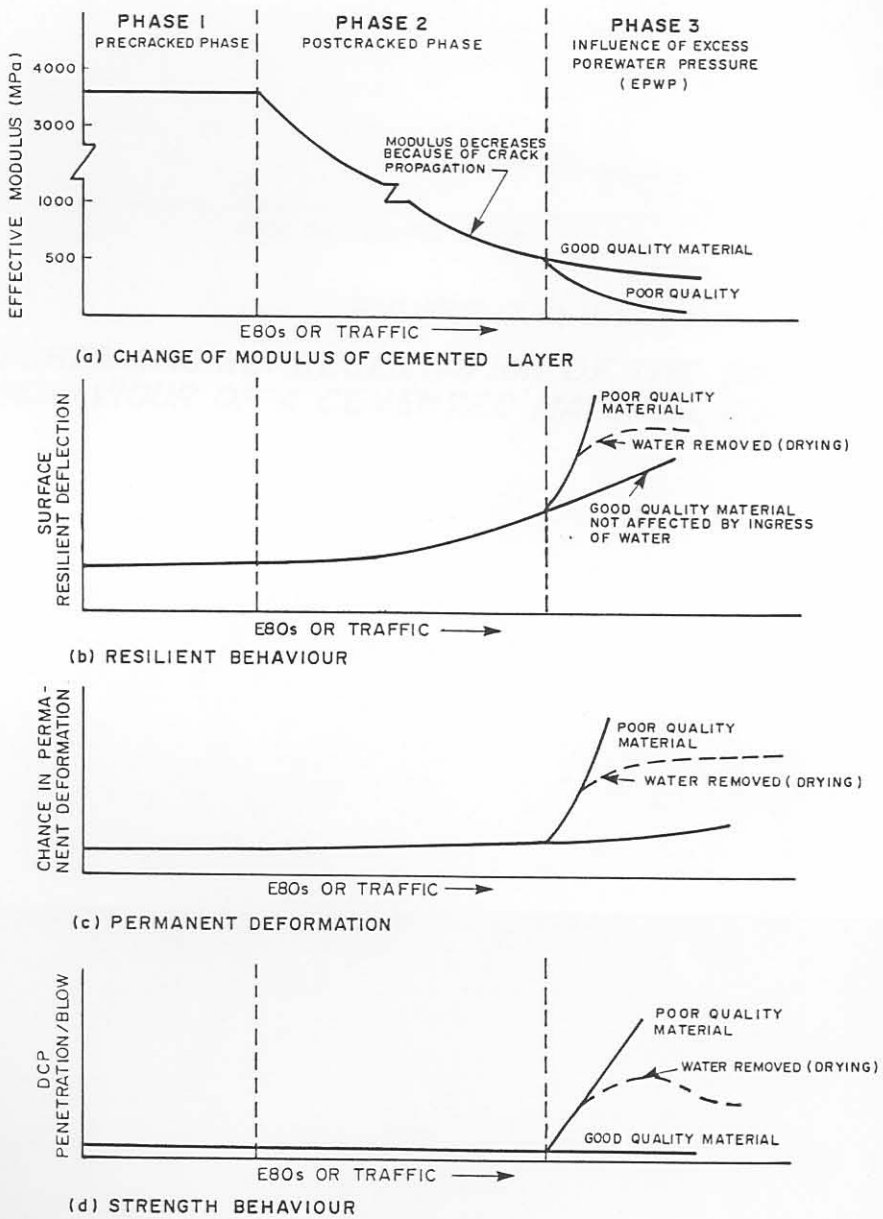

FIGURE 7.9

INDICATORS OF THE BEHAVIOUR OF CEMENTED (C2 QUALITY) LAYERS (AFTER FREEME, 1984)

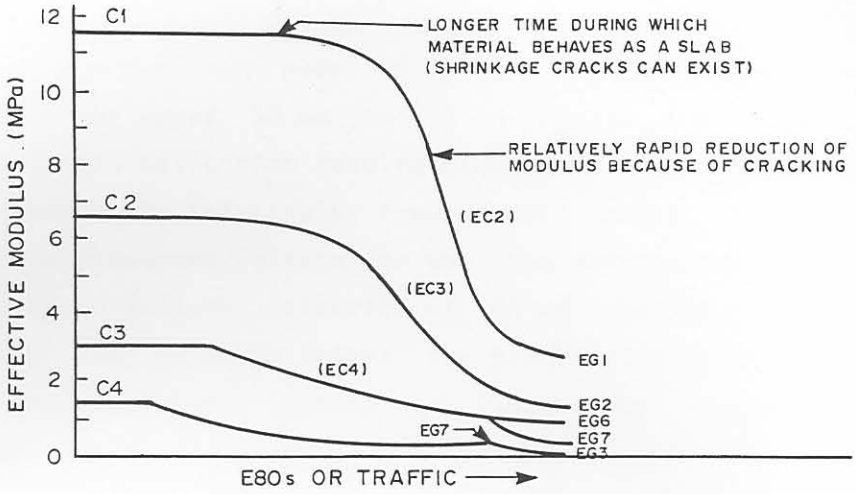

FIGURE 7.10 (a)

SHEMATIC DIAGRAM OF RELATIVE BEHAVIOUR OF CEMENTED LAYERS OF DIFFERENT QUALITY (FREEME, 1984)

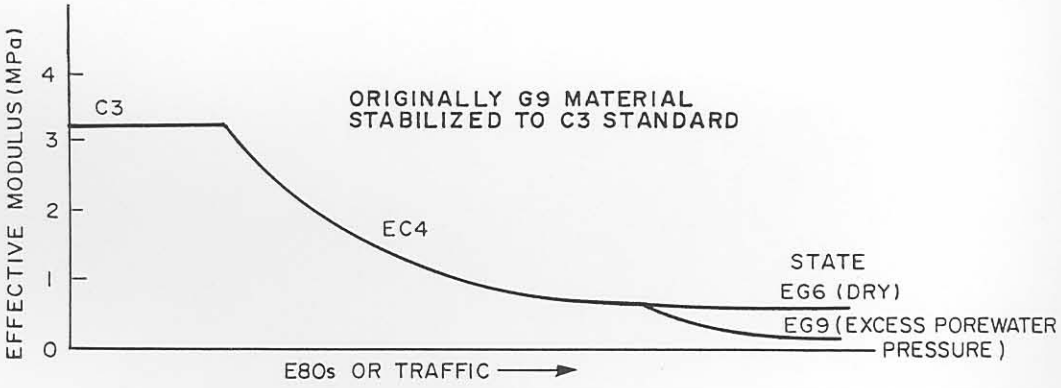

FIGURE 7.10 (b)

SCHEMATIC REPRESENTATION OF THE EQUIVALENT BEHAVIOUR OF A CEMENTED MATERIAL (FREEME, 1984)

A description of the various states of cemented layers is also given elsewhere (De Beer, 1985).

With the relatively large amount of data available from this study, it was possible to quantify the reduction in moduli of the cementitious base layers for both the deep and shallow pavements tested.

7.4.2 Deep pavement

In Figure 7.11 (a), the change in the moduli of the base (0 mm to 180 mm) for the deep pavement is illustrated, together with a reasonable (R^2 = 63 per cent) hyperbolic regression function describing the reduction. The figure indicates a rapid breakdown in the moduli from an initial range of 850 MPa to 1100 MPa, to a constant range of approximately 200 MPa to 300 MPa. Laboratory determined moduli on intact specimens of the base material varied between 1300 MPa and 1995 MPa. In Figure 7.11 (b), upper and lower limits for the found range of moduli are also given. From these figures it is evident that the cementitious base converts rapidly to an equivalent granular state. In this case, as described in Chapter 4, the dominant mode of failure on this deep pavement was crushing in the upper 50 mm to 75 mm of the base. This was also reflected in the deflection results discussed in Paragraphs 7.2 and 7.3. Notwithstanding the relatively lower moduli during the crushed state, the absolute permanent deformation on this pavement was relatively low and based on a failure criterion of 20 mm rutting. These pavements could carry two to three times the traffic originally anticipated, provided that moisture ingress is limited by regular sealing and maintenance.

In an earlier study it was indicted that the the reduction in effective moduli of cementitious subbase layers in bituminous base pavement structures is not as rapid as those of the base layers discussed here (De Beer, 1985). This is due to the fact that the bituminous base layer absorbs most of the severe stresses and not the deeper cemented subbase layers.

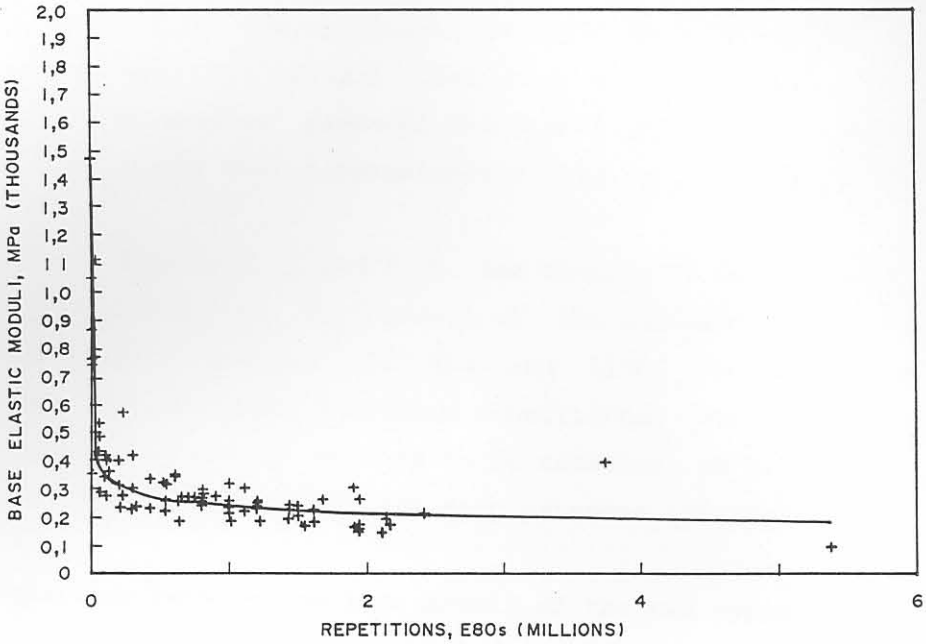

(a) AVERAGE REGRESSION

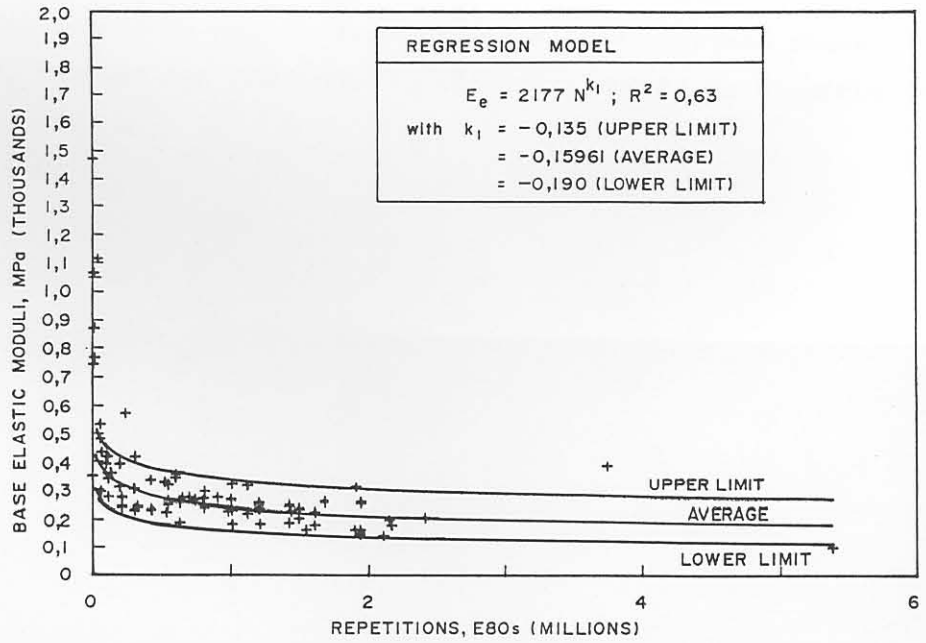

(a) AVERAGE REGRESSION WITH UPPER AND LOWER LIMITS

FIGURE 7.11

RELATIONSHIPS BETWEEN THE MDD BACK-CALCULATED EFFECTIVE ELASTIC MODULI OF THE BASE AND NUMBER OF EQUIVALENT 80 kN AXLES, ON THE DEEP PAVEMENT (ROAD 1932, ROOIWAL)

The moduli of the lower layers also decreased with an increase in trafficking. In Appendix F, Figures F.15 and F.16, the reduction in moduli of the subbase, selected and subgrade layers, are illustrated. For the selected layer the moduli were relatively high, and variable, without a distinct decrease notable. The reason for this is not clear, but it is possible that interference between the cemented subbase and the top of selected layer as a result of debonding may have contributed to this effect. The final moduli of the lower layers appears to be approximately 50 MPa.

7.4.3 Shallow pavement

In Figure 7.12 (a) and (b), the decrease in moduli of the base layer (0 mm to 110 mm) of the shallow pavement is illustrated. The figure illustrates greater variability compared to that of the deep pavement, but the average breakdown may also be described by an hyperbolic function (R^2 = 34 per cent). The moduli reduced from an initial range of 2250 MPa to 3400 MPa to a final range of approximately 500 MPa. This is larger than for the deep pavement, possibly because of the different failure mechanisms. The initial laboratory determined modulus for the base layer of the shallow pavement was also higher (approximately 5580 MPa) than that of the deep (approximately 1300 to 1995 MPa) pavement.

In Appendix F, Figures F.17 and F.18, the changes in moduli of the lower layers, are illustrated. The moduli of the subbase layer initially varied considerably between 430 MPa and 1150 MPa and reduced to approximately 100 MPa after 4 million repetitions. For the selected and subgrade layers the moduli appears to be constant at 100 MPa, and are also higher than that found for the deep pavement (50 MPa).

7.4.4 Comparison between the base moduli of the two types of pavement

In Figure 7.13(a) and (b), the change in moduli of the two pavements, are illustrated. The figures indicate the "intact state" together with the distressed state. From the results of this study it appears that distinction should be made between the type of distressed state of these pavements, because the reduction in effective moduli is directly related

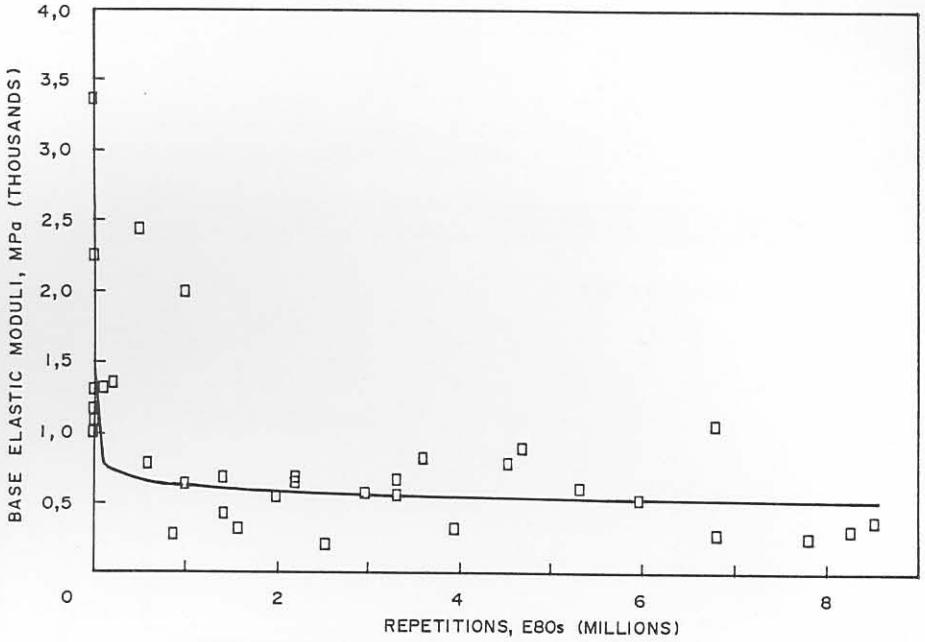

(a) AVERAGE REGRESSION

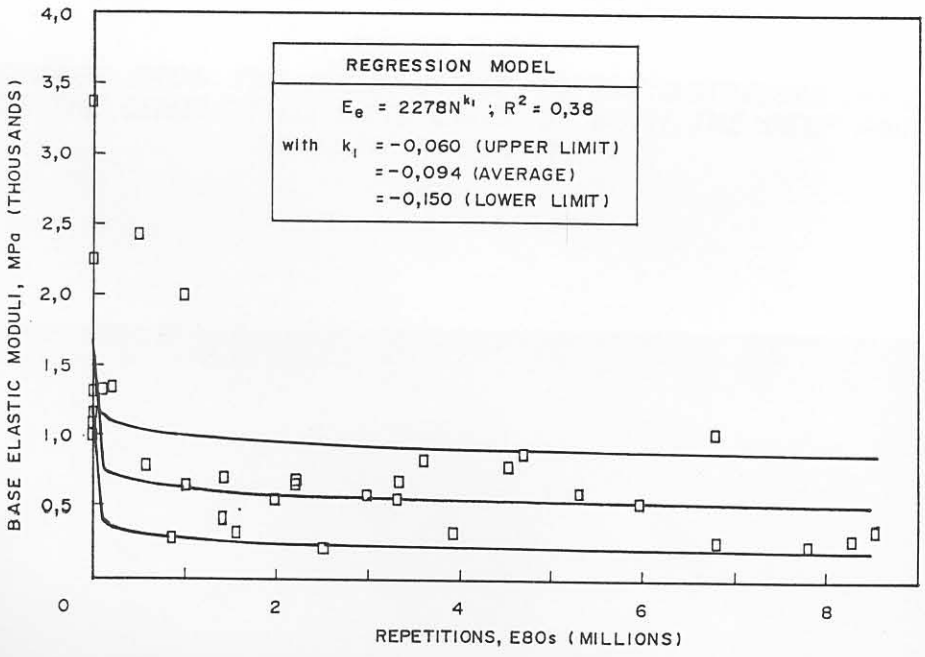

(b) AVERAGE REGRESSION WITH UPPER AND LOWER LIMITS

FIGURE 7.12

RELATIONSHIPS BETWEEN MDD-CALCULATED EFFECTIVE ELASTIC MODULI OF THE BASE AND NUMBER OF EQUIVALENT 80 kN AXLES, ON THE SHALLOW PAVEMENT (ROAD 2212, BULTFONTEIN)

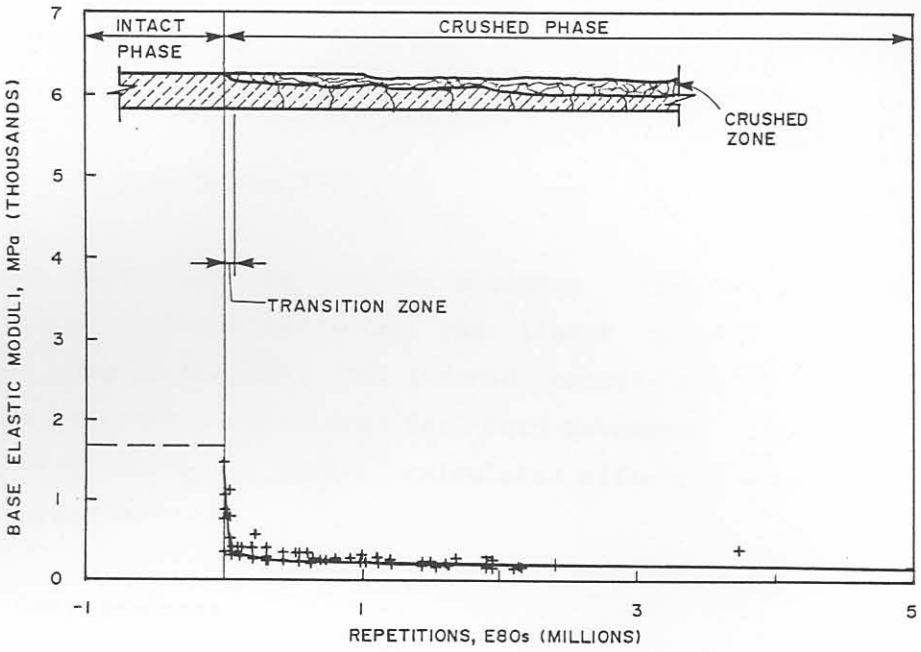

(a) DEEP PAVEMENT (ROAD 1932, ROOIWAL)

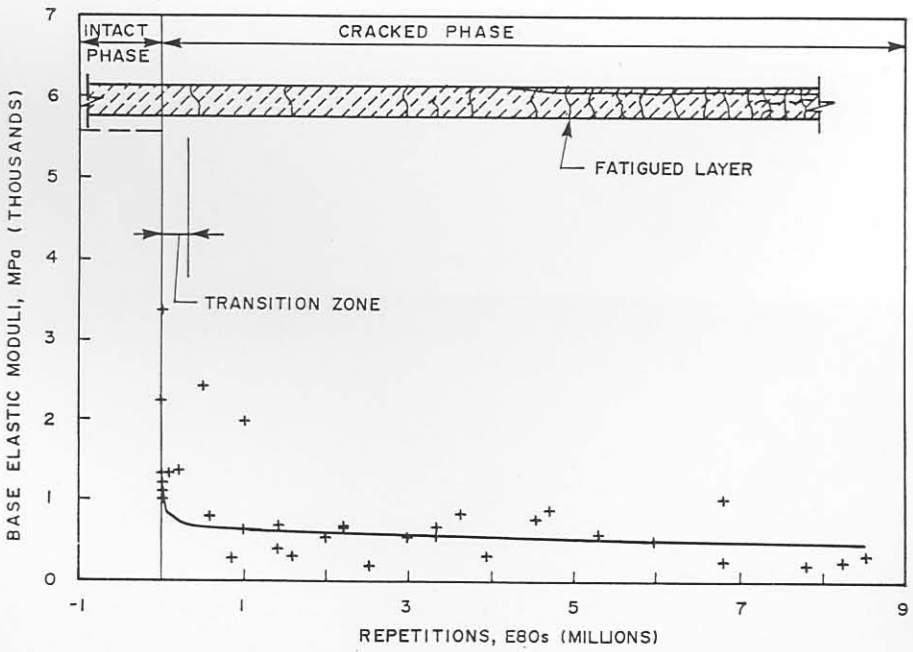

(b) SHALLOW PAVEMENT (ROAD 2212, BULTFONTEIN)

FIGURE 7.13

CHANGE FROM THE INTACT PHASE TO THE DISTRESSED PHASE OF THE CEMENTITOUS BASE LAYER OF BOTH THE DEEP AND SHALLOW PAVEMENTS

to either crushing or fatigue failure. Conceptually the distressed state was assumed to be the post - cracked state (see Figure 7.9 (a) and Figure 7.10). For the **deep pavement** the distress in the cementitious base is manifested as **crushing**, whilst for the **shallow pavement** the distress is **fatigue**. It is therefore advisable to differentiate between these two modes of failure. For the deep pavement the two major states in its life are **intact** and **crushed**, while for the shallower pavement these states are **intact** and **cracked** (see Figures 7.13 (a) and (b)).

For both pavement types there is a transition zone between the intact and distressed states. Closer inspection of these zones indicates that the average reduction in moduli occurs within the first 30 000 repetitions (E80s) for the deep pavement, and within 100 000 repetitions (E80s) for the shallower pavement. These zones are illustrated in Figure 7.14.

In Figure 7.15 the relationships of the average change in effective elastic moduli in the distressed states of the base layers of the deep and shallow pavements are compared. This figure may be a useful design guideline for these two pavements in mechanistic design.

7.5 TENSILE STRAIN ANALYSIS

With the moduli of the various pavement layers known, stresses and strains were calculated using the linear elastic multi - layered computer program ELSYM5A. The induced tensile strain at the bottom of the base layers was calculated for both pavements at various stages of trafficking (using the back - calculated effective elastic moduli) and is discussed below.

7.5.1 Deep pavement

In Figure 7.16 (a), the change in strain ratio (ϵ_s/ϵ_b) with increase in trafficking on the deep pavement is illustrated.

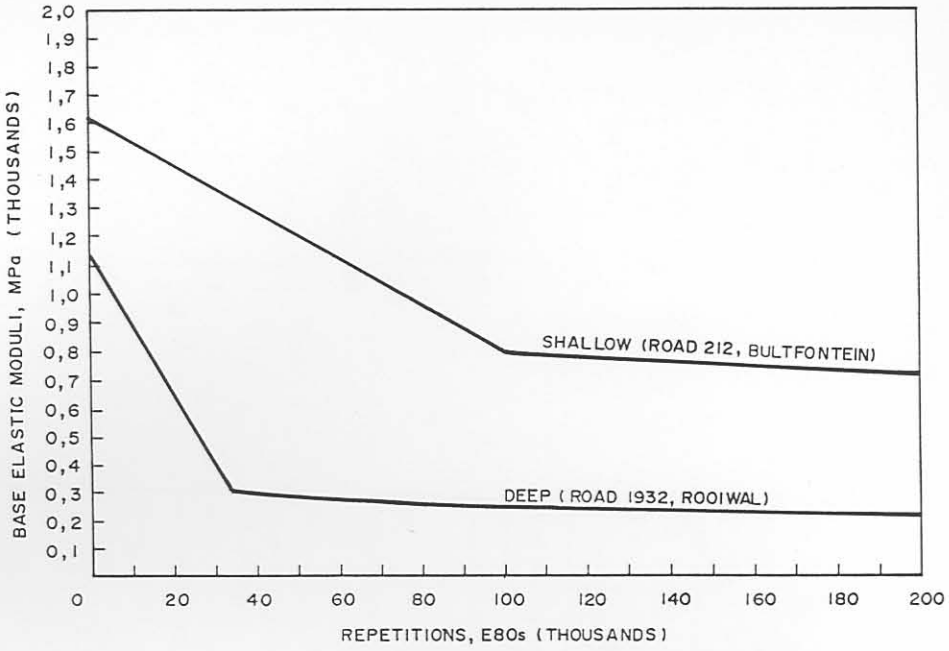

FIGURE 7.14

REDUCTION IN BASE MODULI IN THE TRANSITION ZONES FOR THE DEEP AND SHALLOW PAVEMENTS

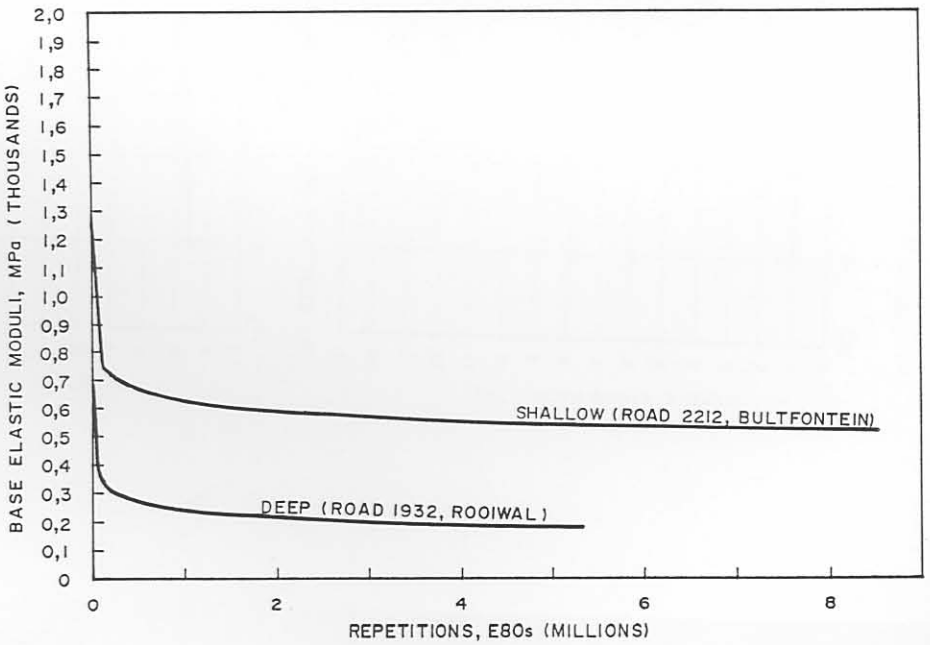

FIGURE 7.15

RELATIONSHIPS OF THE AVERAGE CHANGE IN THE EFFECTIVE ELASTIC MODULI OF THE BASE LAYERS OF THE RELATIVELY DEEP AND SHALLOW PAVEMENTS EVALUATED IN THIS STUDY

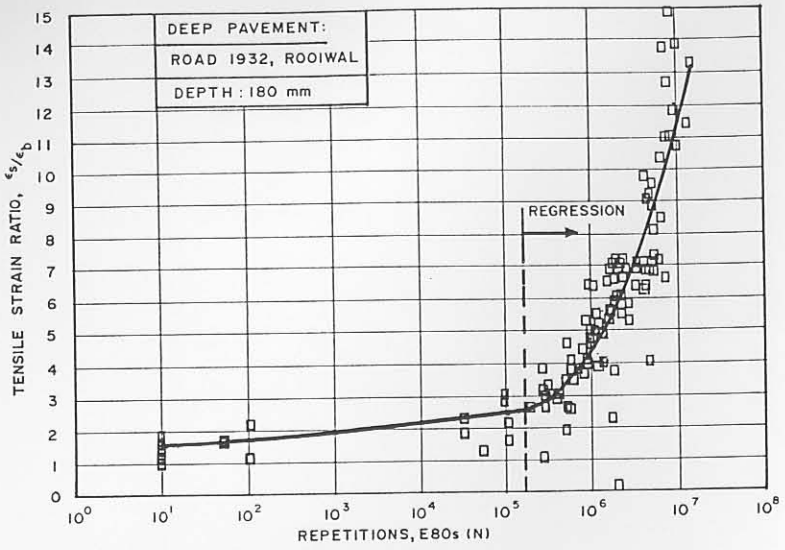

(a) STRAIN vs E80s (DEEP PAVEMENT, 1932)

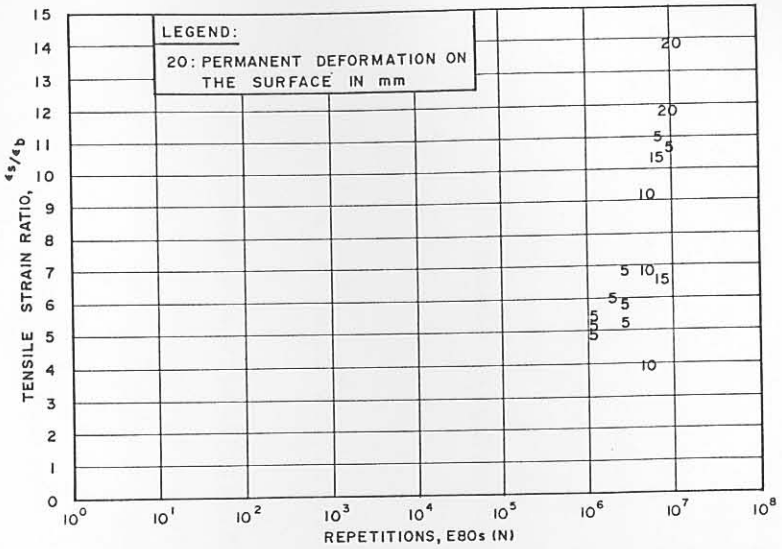

(b) STRAIN vs PERMANENT DEFORMATION (DEEP PAVEMENT, 1932)

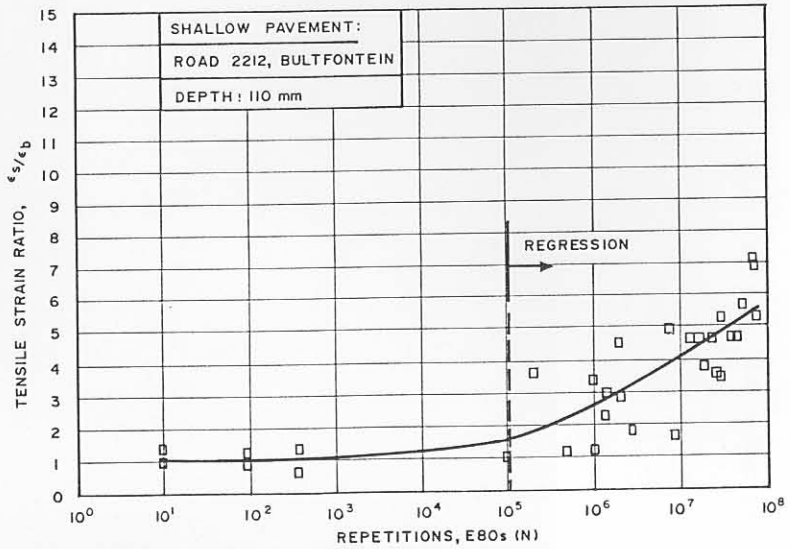

(c) STRAIN vs E80s (SHALLOW PAVEMENT, 2212)

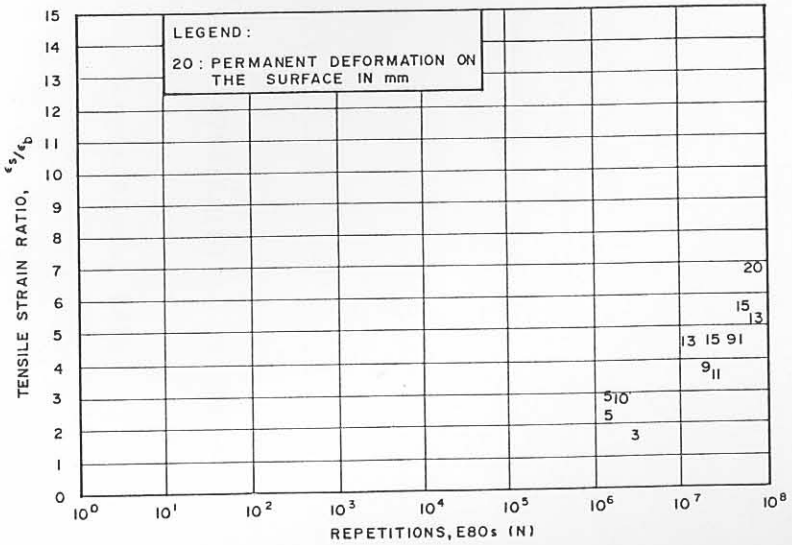

(d) STRAIN vs PERMANENT DEFORMATION (SHALLOW PAVEMENT, 2212)

FIGURE 7.16

SUMMARY OF THE CHANGE IN MAXIMUM TENSILE STRAIN (ϵ_s) AT THE BOTTOM OF THE BASE LAYER AT VARIOUS STAGES OF HVS TRAFFICKING, TOGETHER WITH THE ASSOCIATED PERMANENT DEFORMATION (RUT) ON THE SURFACE OF BOTH THE DEEP AND SHALLOW PAVEMENT

The strain ratio is defined as follow:

Let ϵ_i = the maximum calculated induced tensile strain
d = a factor to allow for the effect of shrinkage cracking in cemented layers (1,15 in this case)
ϵ_s = modified induced maximum tensile strain
= d x ϵ_i
Further if ϵ_b = tensile strain at break, then
ϵ_s/ϵ_b = the strain ratio

Detail of this argument is given elsewhere (Otte, 1978, Freeme et al, 1984, De Beer, 1985).

The ϵ_b for the cemented layers of the deep pavement was assumed to be 125 $\mu\epsilon$, because it was impossible to obtain intact beam specimens from the test sections before testing (Freeme et al, 1984). The figure indicates that the tensile strain ratio (ϵ_s/ϵ_b) increases with trafficking, ie ϵ_s increases. This increase, as with the decrease in modulus, is directly related to the breakdown of the base layer, and is also related to the subsequent permanent deformation associated with the pavement. The associated deformation levels are illustrated in Figure 7.16 (b). A regression analysis was performed on the strain/repetitions data from approximately 160 000 repetitions, and a relatively good (R^2 = 75 per cent) parabolic regression function was obtained. The relationship is given below:

$$(\epsilon_s/\epsilon_b) = 10^x \quad \text{.....7.1}$$

where $x = 2{,}640222(\text{Lg}(N))^2 - 27{,}4764(\text{Lg}(N)) + 74{,}08693$
(ϵ_s/ϵ_b) = induced strain ratio
N = number of equivalent repetitions, E80s

7.5.2 Shallow pavement

Similar behaviour in the strain ratio versus repetitions were obtained for the shallow pavement, but in this case it was possible to measure the breaking strain from intact field specimens. The measured breaking

strain was 152 $\mu\epsilon$, with a standard deviation of 53 $\mu\epsilon$. The change in strain ratio with trafficking on the shallow pavement is illustrated in Figure 7.16 (c). The subsequent permanent deformation is illustrated in Figure 7.16 (d). Although the strain ratio on the shallower pavement appears to be lower than that for the deep pavement, similar permanent deformation resulted. The strain ratio, however, is dependent on the ϵ_b, and, therefore variations in ϵ_b could result in variations in the strain ratio, without the permanent deformation being notably effected.

The regression (also parabolic, R^2 = 74 per cent) was performed on the data from approximately 100 000 repetitions, and is given below:

$$(\epsilon_s/\epsilon_b) = 10^x \quad \ldots\ldots\ldots\ldots\ldots\ldots\ldots\ldots\ldots\ldots\ldots\ldots\ldots\ldots 7.2$$

where $x = 0{,}208100(Lg(N))^2 - 1{,}24812(Lg(N)) + 2{,}56910$

(ϵ_s/ϵ_b) = induced strain ratio

N = number of equivalent repetitions, E80s

7.5.3 Fatigue life determination

The current method for calculating the fatigue life of cementitious layers in the South African mechanistic design method was proposed by Otte (1978). The calculation is based on the tensile strain ratio and is given below:

$$N_f = 10^{9{,}1(1 - \epsilon_s/\epsilon_b)} \quad \ldots\ldots\ldots\ldots\ldots\ldots\ldots\ldots\ldots\ldots 7.3$$

where N_f = fatigue life during the pre - cracked (intact) state.

and ϵ_s/ϵ_b = initial induced strain ratio

The above relation was obtained from a literature study based on a variety of laboratory tests, and was unverified for actual field conditions for lightly-cementitious layers until this study. Over the past few years experience with normal roads as well as with the HVS testing programme indicated that the above relation underestimates the fatigue life of lightly-cementitious layers. Therefore, in this study, research was also aimed to verify this relation for normal field conditions. Data were accumulated on the fatigue life of both the deep

and shallow pavements, and it was found that the effective fatigue in the cementitious base layers occurs at a deflection level between 0,5 mm to 0,75 mm, and an associated permanent deformation level of approximately 2 mm. Load tests at the start of the HVS testing on a number of sections were done at various loads, viz 40 kN, 70 kN and 100 kN, from which moduli where back-calculated and initial strain ratios determined. The same loading was then used to traffic the test sections and the effective fatigue life determined, using the above limiting conditions. The test sections and results used for this analysis are summarised in Table 7.1.

Table 7.1 Summary of the effective fatigue life information

HVS Section	Test load (kN)	Initial strain ϵ_i ($\mu\epsilon$)	Number of repetitions to real fatigue*
260A4	40	170	$1,0 \times 10^6$
274A4	40	175	$1,0 \times 10^6$
275A4	40	142	$1,25 \times 10^6$
289A4	40	128	$1,0 \times 10^6$
294A4	40	121	$1,0 \times 10^6$
275A4	40	175	$1,0 \times 10^6$
289A4	70	251	$0,2 \times 10^6$
294A4	100	243	$0,1 \times 10^6$
306A4	40	159	$1,1 \times 10^6$
307A4	40	147	$1,1 \times 10^6$
308A4	40	138	$1,1 \times 10^6$
308A4	100	446	30 000
337A4	150	434	5 000
338A4	150	382	5 000

* Number of repetitions to achieve a permanent deformation of 2 mm on the surface of the pavement, and a total standard surface deflection level of approximately 0,5 to 0,75 mm.

In Figure 7.17 the relationship between the strain ratio and number of repetitions to reach the defined fatigue failure condition is illustrated. The current fatigue relationship proposed by Otte (1978) is also shown. The figure shows that much higher strain ratios must be mobilised to reach effective fatigue failure than those of Otte. The relationship (R^2 = 94 per cent) between strain ratio and effective fatigue life, N_{ef}, is given below:

$$N_{ef} = 10^{7,19(1 - \epsilon_s/8\epsilon_b)} \quad \ldots\ldots\ldots\ldots\ldots\ldots\ldots\ldots 7.4$$

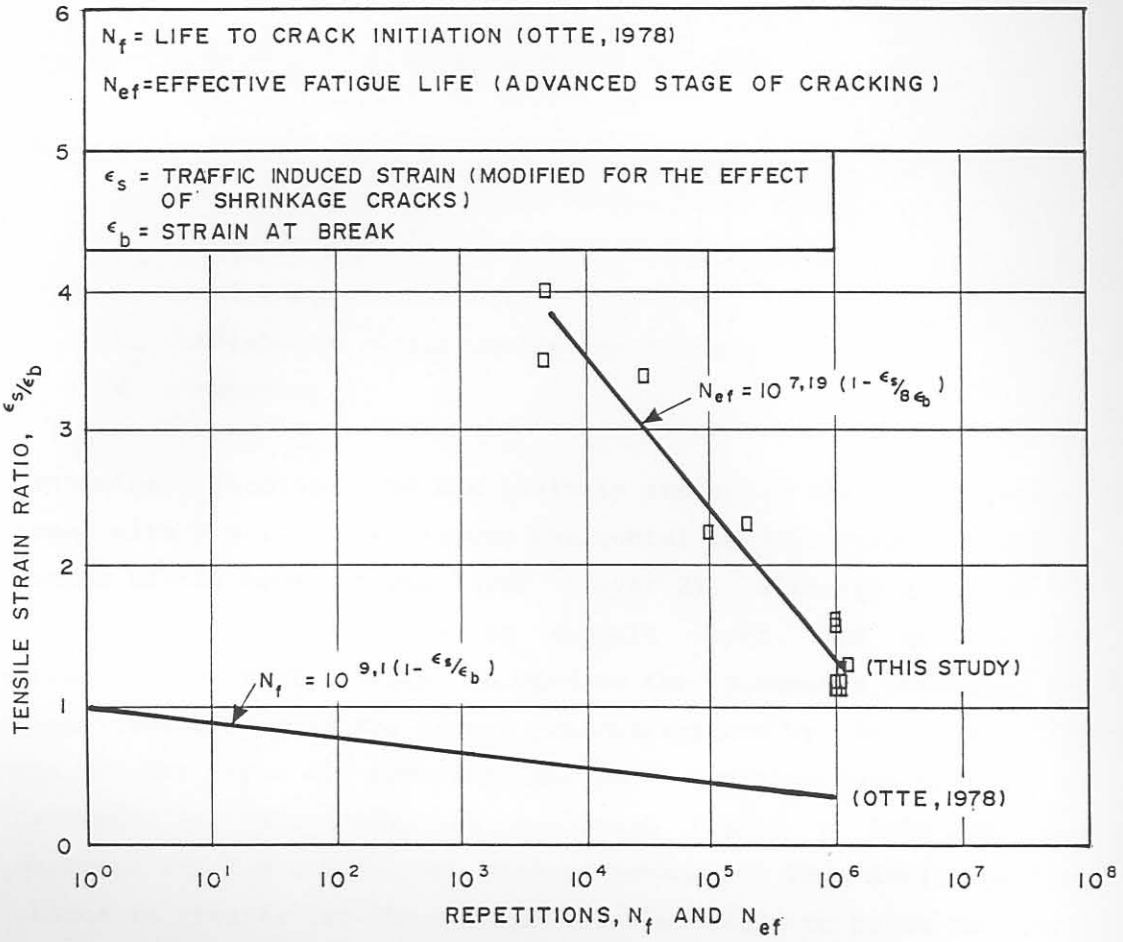

FIGURE 7.17

COMPARISON OF THE RELATIONSHIPS BETWEEN MAXIMUM TENSILE STRAIN RATIO (ϵ_s/ϵ_b) AND NUMBER OF STRAIN REPETITIONS TO INITIATE AND EFFECTIVE FATIGUE CRACKING IN CEMENTED LAYERS

This relationship (Equation 7.4) is proposed for pavements with lightly cementitious layers instead of the Otte relationship (Equation 7.3), as the latter grossly underestimates the actual (effective) fatigue life by factors of more than one million!. This was also observed by Jordaan (1988) on a similar pavement structure, but with a 35 mm asphalt surfacing on the cemented base. Based on the results of this HVS test, Jordaan suggested increasing the laboratory determined strain at break by a factor of 4,7 in order to determine the life to visible cracking on the surface of this pavement. This case is a further indication that the existing fatigue relationship (Equation 7.3) needs amendment if used on lightly cementitious base pavements.

7.5.4 Maximum tensile strain

As an aid to establish the position of the maximum horizontal tensile strain in cementitious layers, Jordaan (1988) suggested using the following relationship:

$$(E_3/E_2)^2(h_1(E_1/E_3)^{1/3} + h_2(E_2/E_3)^{1/3}) < K \quad (mm) \quad \ldots\ldots\ldots\ldots 7.5$$

where E_1 = elastic modulus of the first layer (MPa)
E_2 = elastic modulus of the second layer (MPa)
E_3 = elastic modulus of the third layer (MPa)
h_1 = thickness of the first layer (mm)
h_2 = thickness of the second layer (mm)
K = constant

Preliminary findings from his analysis indicated that if Equation 7.5 is true, with $K \approx 128$, the maximum horizontal tensile strain occurs at the bottom of the cementitious layer (layer 2). Although Equation 7.5 was derived for layer 1, as an asphalt layer, and the second the cementitious layer, it may be used on the pavements evaluated in this dissertation because the layers are represented by their elastic moduli and not the type of material, per se. Applying Equation 7.5 to the pavements in this study, it was found that $K \approx 1500$ for the deep pavement and $K \approx 250$ for the shallow pavement. This indicates that the chance is greater for the maximum tensile strain to be at the bottom of the cementitious layer (smaller K) in the shallow pavement, than the deep pavement (larger K). The HVS test results indicated that the

cementitious base layers of the deep pavement failed in compression, whilst that of the shallow pavement failed in fatigue, which confirms this conclusion.

The value of K ≈ 128 for the maximum strain to occur at the bottom of the cementitious layer suggested by Jordaan (1988) was based on a limited number of results. However, more research is needed to establish a general value for K, or different K values for different pavement compositions.

Future research, however, should also be guided towards the development of a general fatigue relationship (similar to Equation 7.4). This should be done for pavements with lightly-cementitious as well as bitumin-emulsion-treated bases if varying thickness of asphalt surfacings are to be included because the research discussed in this dissertation is related to pavements with relatively thin asphalt surfacings only.

7.6 VERTICAL COMPRESSIVE ELASTIC STRAIN

Similar to cracking, another primary indicator of pavement behaviour is permanent deformation. Since the early 1960s the vertical elastic strain, ϵ_v (based on the linear elastic theory) has been used to develop limiting strain criteria for subgrade soils in order to control permanent deformation in these layers and eventual serviceability of pavements (Dorman, 1962; Dorman et al, 1964; Finn et al, 1966; Edwards et al, 1974; ; Paterson et al, 1978, Visser, 1981). Although ϵ_v is an elastic parameter, it appears that it may be used readily as a predictor of permanent deformation and as a limiting criterion (Wang et al, 1980).

As in the case of tensile strain, one of the aims of this study was to verify the current deformation criteria used in the South African mechanistic design method, for the pavements evaluated in this study. The attempts to achieve this end follow in the next paragraph.

7.6.1 Vertical compressive strain profiles

Figures 7.18 (a) and (b) illustrate examples of the typical initial vertical strain profiles on the centre line through the deep and shallow pavements. The associated deflection profiles (measured with

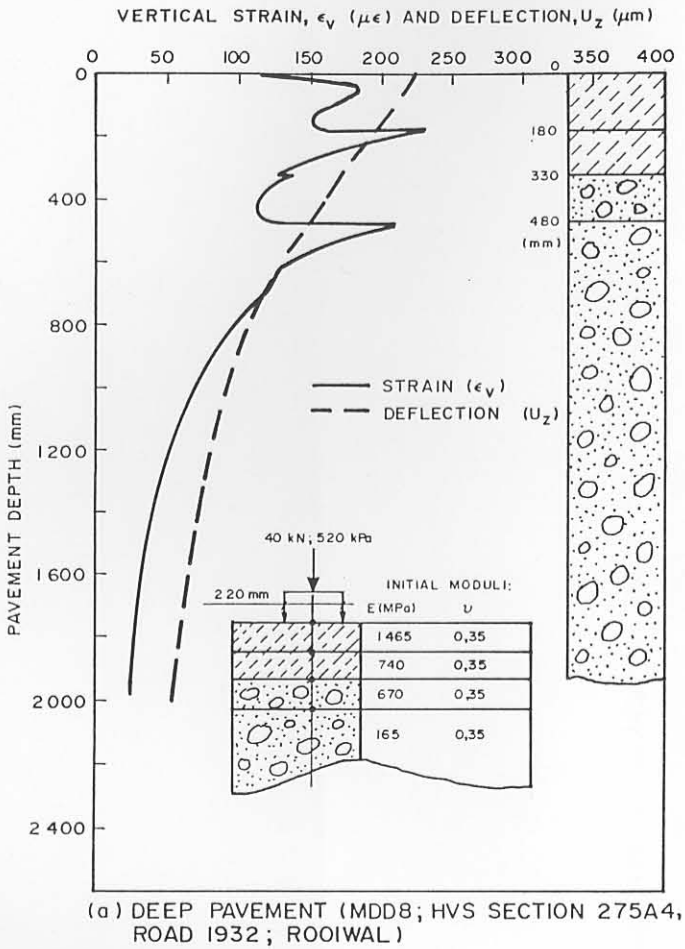

(a) DEEP PAVEMENT (MDD8; HVS SECTION 275A4, ROAD 1932; ROOIWAL)

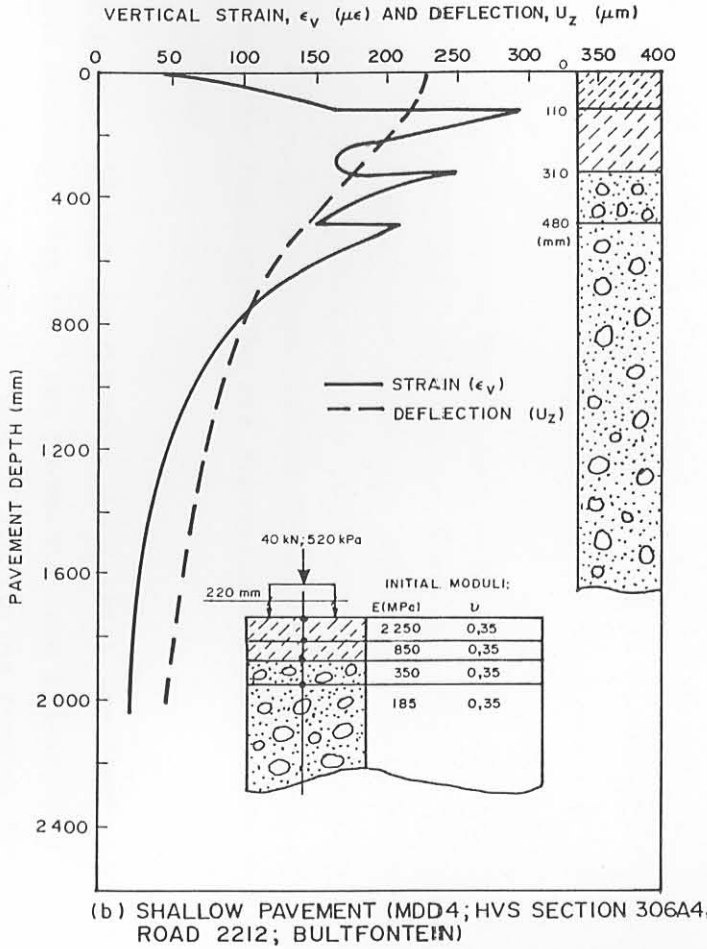

(b) SHALLOW PAVEMENT (MDD4; HVS SECTION 306A4, ROAD 2212; BULTFONTEIN)

FIGURE 7.18

EXAMPLES OF THE INITIAL (N=10) VERTICAL STRAIN (ϵ_v) AND DEFLECTION (U_z) PROFILES FOR THE DEEP AND SHALLOW PAVEMENTS ANALIZED IN THIS STUDY

the MDD and back-calculated effective elastic moduli) are also shown on the figures, since the surface deflection is the integration of the vertical strain with depth. The area under the strain curves gives the central deflection. The effect of the different layers, including the dominant effect of the subgrade on the central deflection, is therefore evident for both pavements.

Not only is the area (deflection) important, but also the shape of the strain curve with depth. Inspection of the strain curve of the deep pavement in Figure 7.18 (a) indicates that peak strains occurred at three depths, viz 65 mm (within the base); 181 mm (top of the subbase) and 481 mm (top of the subgrade). For the shallow pavement, the peak strains also occurred at three but different depths, at 111 mm (top of the subbase); 311 mm (top of the selected layer) and 481 mm (top of the subgrade).

According to the observed and measured failure mechanisms for these two types of pavements, viz crushing in the base of the deep pavement, and fatigue failure of the base for the shallower pavement, it appears that these peak strains may assist in explaining these behaviours. For the deep pavement (Figure 7.18 (a)) crushing of the base layer occurred within the upper 50 mm to 75 mm, in the region where a peak vertical strain occurred. For the shallow pavement (Figure 7.18 (b)) fatigue failure of the base layer occurred, which may be explained by the peak vertical strain on top of the subbase directly underneath the base. Deterioration in the base reduces the effective protection of the lower layers as is indicated by the increased vertical strain in the top of the subbase.

In Figures 7.19 (a) and (b) both the initial and final (end of HVS test) strain profiles for the two pavements are illustrated. The figures indicate that the general shape of the curves remains constant and that the peak strains increase as a result of traffic loading, because of reduced effective moduli for most layers. These final peak strains are at the same depths as those of the initial strains, and tend to explain the observed failure mechanisms for these two types of pavement.

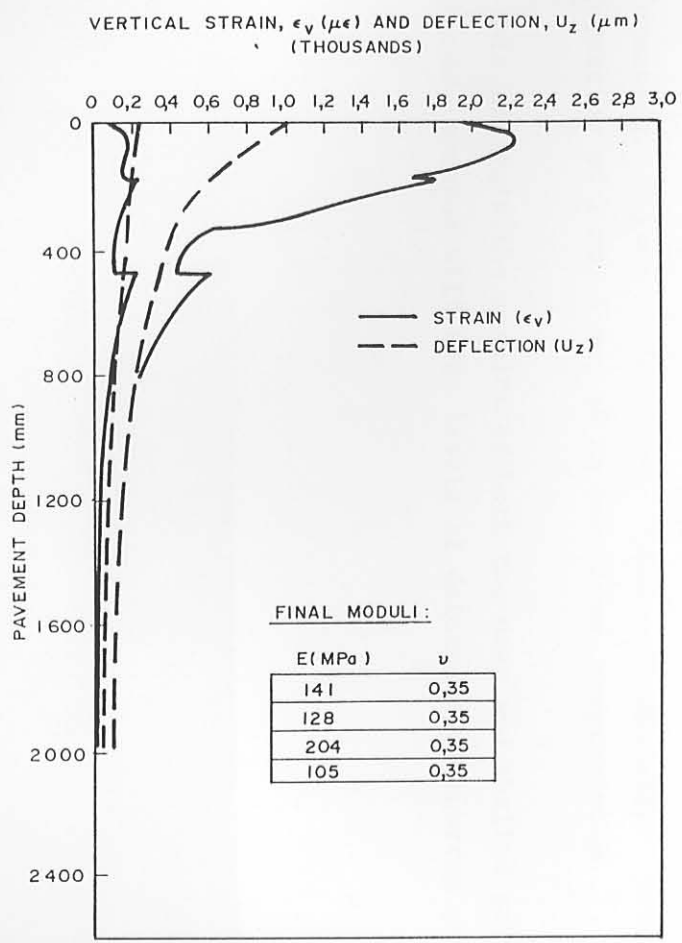

(a) DEEP PAVEMENT (MDD8; HVS SECTION 275A4; ROAD 1932, ROOIWAL)

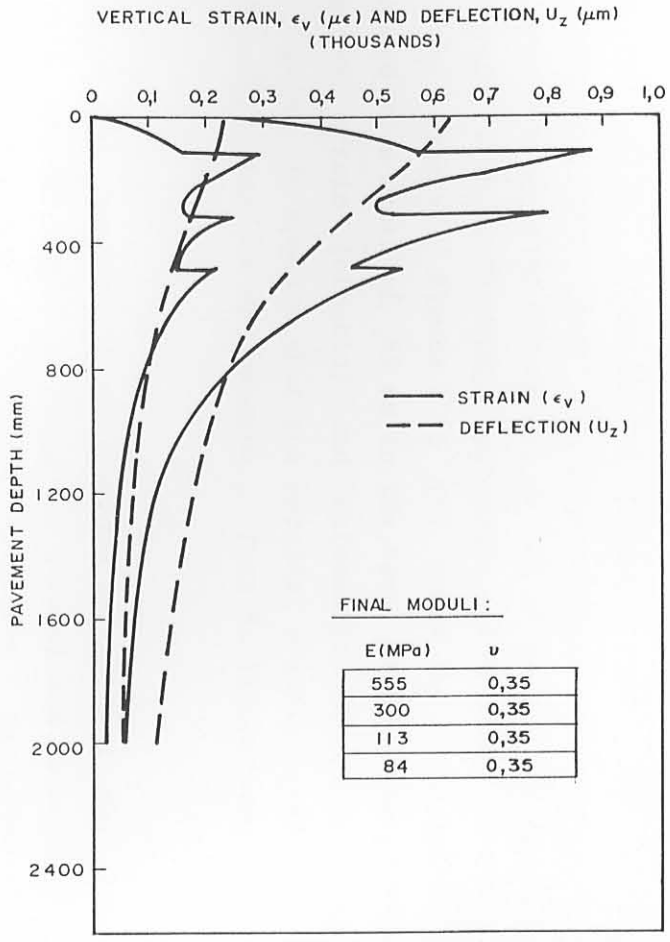

(b) SHALLOW PAVEMENT (MDD4; HVS SECTION 306A4; ROAD 2212, BULTFONTEIN)

FIGURE 7.19

INITIAL AND FINAL VERTICAL STRAIN AND DEFLECTION PROFILES OF THE DEEP AND SHALLOW PAVEMENTS ANALIZED IN THIS STUDY

7.6.2 Vertical strain behaviour

Based on the above, the changes in peak vertical strains at various depths for the deep pavement with trafficking were investigated further. As with the tensile strain behaviour discussed in Paragraph 7.5, the vertical strains also increase with trafficking. Figure 7.20 illustrates the increase at various depths with trafficking. According to these results there appears to be a linear relationship, on a log-log plot between vertical strain and traffic. The increase in strain is again a manifestation of the change in the pavement system owing to traffic loading, and as with tensile strain, it confirms that these pavements are subjected to variable (increasing) strain repetitions throughout their life, even under constant loading conditions.

7.6.3 Vertical strain and permanent deformation

In Figure 7.21 (a) a comparison of the strain/traffic relationship at two depths is illustrated. The figure clearly shows that the strain at 65 mm is greater than the strain at 481 mm depth. During this increase in strain with trafficking, permanent deformation is also associated with the change. Figure 7.21 (b) shows the associated deformation measured at a depth of 65 mm in the base of the deep pavement. Since both the strain (elastic) and deformation (plastic) increase with trafficking, it appears that the vertical elastic strain is adequate for evaluating permanent deformation. This is illustrated in Figure 7.21 (c).

Based on this result, it was decided to evaluate the current failure criteria for the subgrade, using the strains and deformations at various depths in both deep and shallow pavements. In order to verify the current subgrade failure criteria used in South Africa (Freeme et al, 1984), the initial induced vertical elastic strains were plotted against the number of repetitions to produce various levels of permanent deformation. Figure 7.22 shows these relationships for levels of deformation of 1 mm, 5 mm, 10 mm and 15 mm, respectively.

In this analysis the results of both the deep and shallow pavement were combined, because different levels of deformation occurred at different

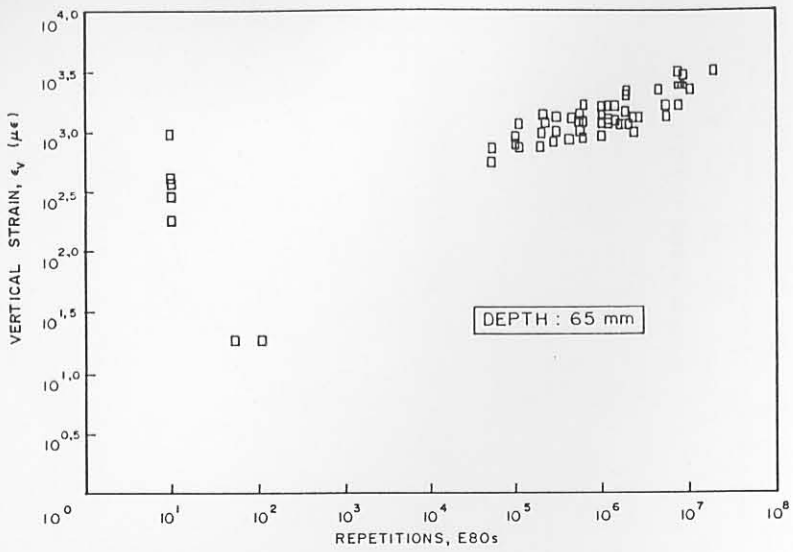

(a) DEPTH : 65 mm (IN BASE)

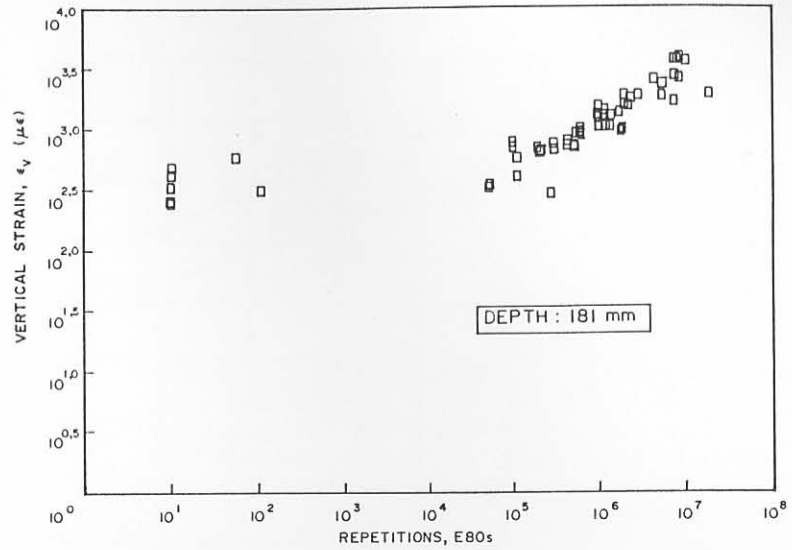

(b) DEPTH : 181 mm (TOP OF SUBBASE)

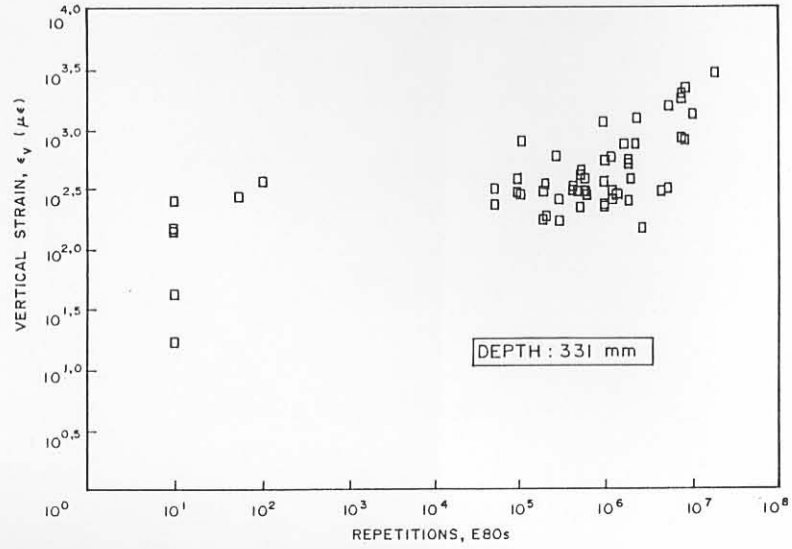

(c) DEPTH : 331 mm (TOP OF SELECTED LAYER)

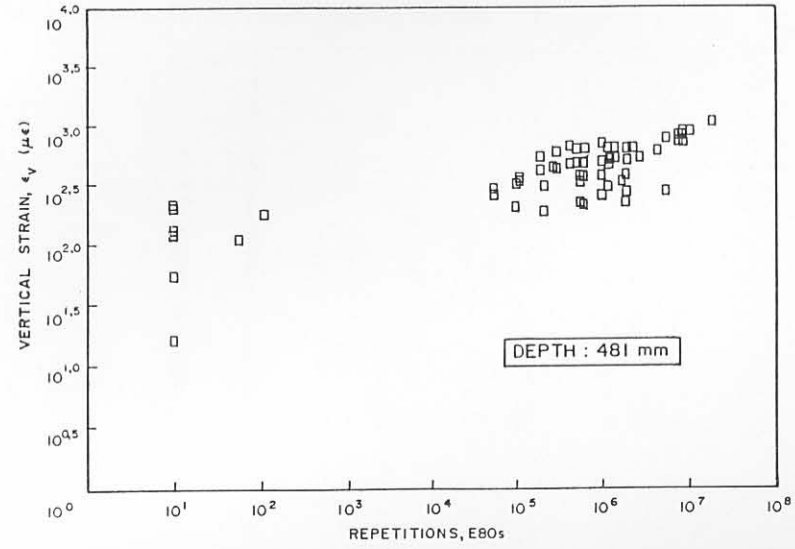

(d) DEPTH : 481 mm (TOP OF SUBGRADE)

FIGURE 7.20

SUMMARY OF THE CHANGE IN VERTICAL COMPRESSIVE STRAIN (ϵ_v) AT VARIOUS STAGES OF HVS TRAFFICKING ON THE VARIOUS TEST SECTIONS ON THE DEEP PAVEMENT (ROAD 1932, ROOIWAL)

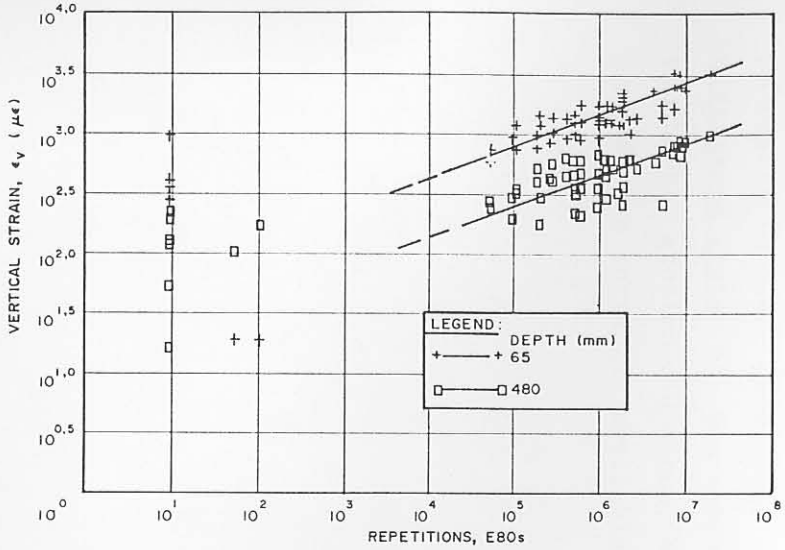

(a) COMPARISON BETWEEN STRAINS AT DIFFERENT DEPTHS (65 mm AND 480 mm)

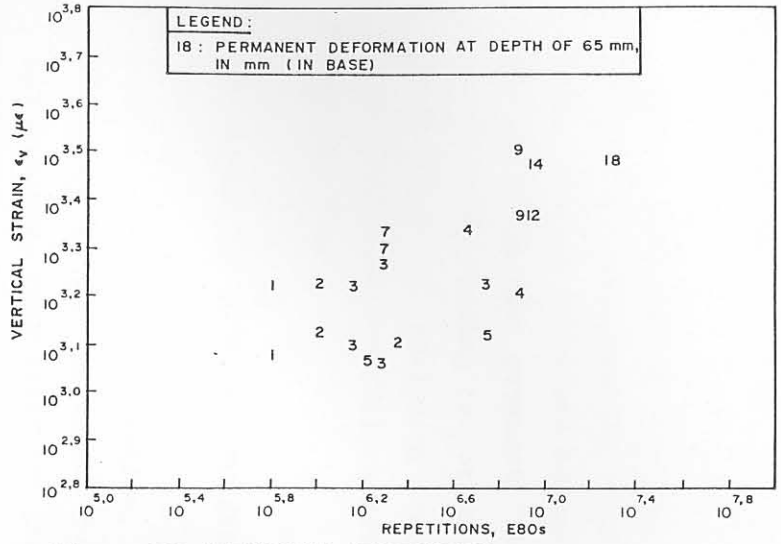

(b) ϵ_v AND PERMANENT DEFORMATION

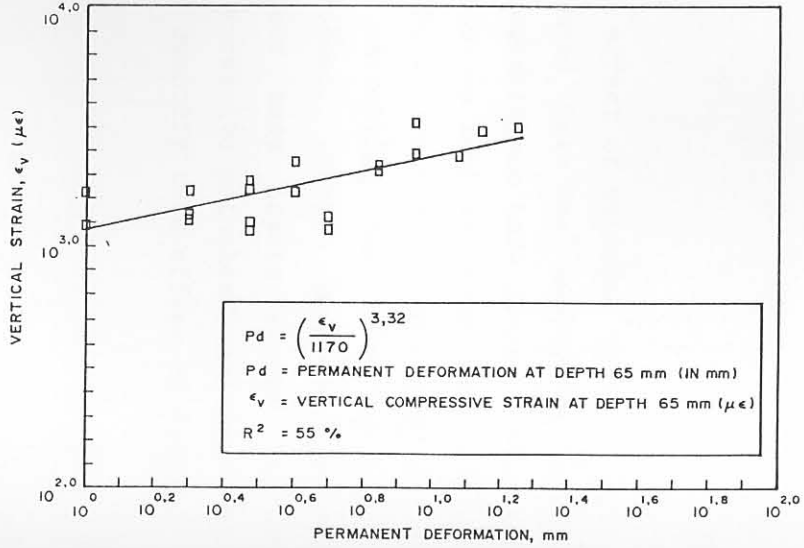

(c) RELATIONSHIP BETWEEN VERTICAL COMPRESSIVE STRAIN AND PERMANENT DEFORMATION AT A DEPTH OF 65 mm

FIGURE 7.21

SUMMARY OF THE CHANGE IN VERTICAL COMPRESSIVE STRAIN (ϵ_v) WITH DEPTH, REPETITIONS AND ASSOCIATED PERMANENT DEFORMATION ON THE DEEP PAVEMENT (ROAD 1932, ROOIWAL)

depths in these pavements and provided an adequate data base. According to Figure 7.22, the slope of the relationships appears to be independent of the magnitude of deformation and its depth of measurement. Although the accuracy of regressions was not very high, especially for the upper levels of deformation, the general trend of the relationships appears to be the same.

In Figure 7.23 the relationships for different levels of deformation is given, and also compared to failure criteria suggested by Paterson et al (1978) and Shell (Claessen et al, 1977).

In general, there is a high correlation between the results of this study and other criteria. The current criteria may therefore be used with greater confidence on the pavement types investigated in this study, particularly those of Paterson et al (1978) for a deformation of 18 mm.

A further interesting fact is that, according to the results of this study, the relationships indicated here appear to be independent of depth, and may therefore be used to evaluate strains and deformations at any depth in the pavement. More research, however, is necessary to extent this finding to other pavement types, and also to study the possibility of including variable strain (increasing strain with trafficking) in the failure criteria, rather than constant strain, as is normally done.

7.7 EFFECT OF MOISTURE INGRESS

As with permanent deformation, the effect of moisture into the base and sub-layers of the pavements evaluated here was negligible during the intact state, especially for the cementitious base layers. This finding is different from that for cementitious subbase layers in bitumin-base pavements, where erodibility of these layers was identified as one of the most important parameters controlling the behaviour of these pavements in wet conditions (De Beer, 1985). However, during the distressed state of the cementitous base layers (either fatigue or crushing), erosion did occur, and excessive potholes resulted. Limited methods are currently available to quantify this effect of erosion

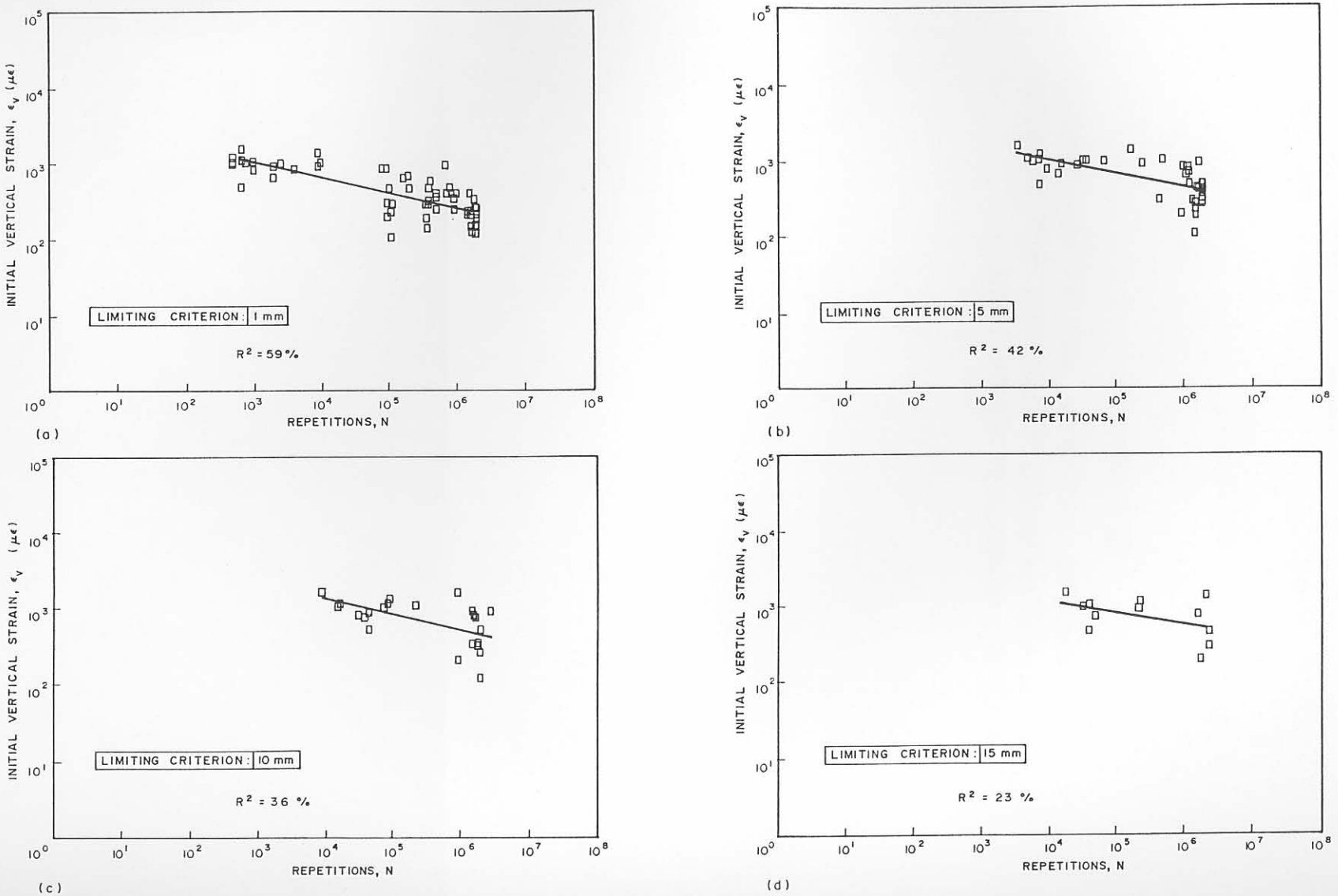

FIGURE 7.22

SUMMARY OF THE INITIAL MAXIMUM VERTICAL COMPRESSIVE STRAIN AT DIFFERENT LIMITING LEVELS OF PERMANENT DEFORMATION FOR BOTH THE SHALLOW AND DEEP PAVEMENT TESTED IN THIS STUDY

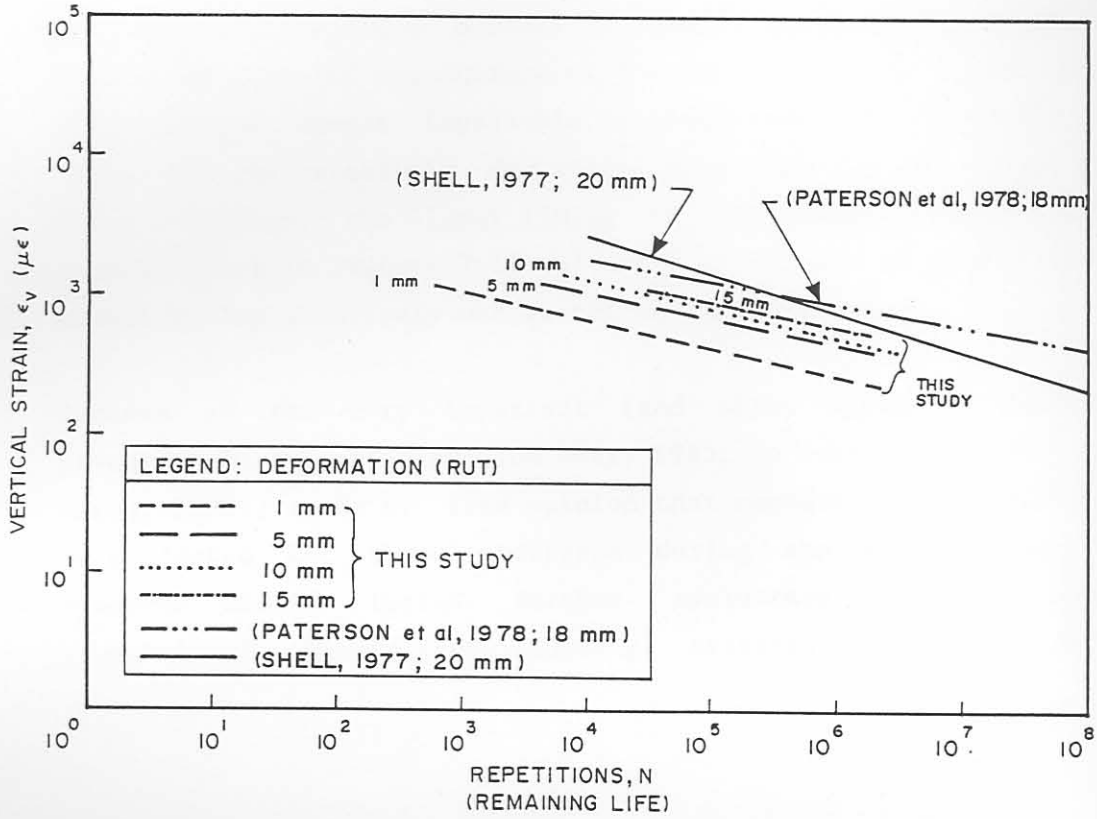

FIGURE 7.23

COMPARISON OF THE VERTICAL COMPRESSIVE STRAIN RESULTS FOR DIFFERENT DEFORMATION LEVELS TOGETHER WITH OTHER PUBLISHED CRITERIA

in the laboratory, and the related aspects thereof. As a result of these earlier findings on erodibility of cementitious subbase layers (De Beer, 1985), and the HVS results discussed in this dissertation, an erodibility test was developed by the author. Detail of this, together with a detailed laboratory evaluation on a series of different materials/stabiliser systems, are discussed elsewhere (De Beer, 1989).

With this new method erodibility tests on the cementitious base material for both the deep and shallow pavements investigated here indicate that during the intact state the in situ material is non-erodible and very durable, although it is highly carbonated, according to the carbonation tests (Netterberg et al, 1984).

Where the resilient response of these pavements is concerned, it was found that the deflections on the surface increased during the intact and relatively dry states because of the crushing and fatigue of the base layer. With moisture ingress very rapid moisture accelerated distress (MAD) followed, resulting in pumping, loss of the surfacing and subsequent potholes (see Photo Plates D.6(c), D.9(d) and (c),and D.12(b) in Appendix D). During these states it was very difficult to monitor the resilient responses because of damage to the MDDs as well as the distressed state of the surface of the test sections. Therefore it was difficult and almost impossible to differentiate accurately between moduli in the relatively dry state from that in the relatively wet state. However, the lower limits of the moduli versus repetitions relationships in Figures 7.11 (b) and 7.12 (b) are an indication of the moduli during relatively wet states of these pavements.

Because of the very important (and often dramatic) behaviour of pavements in the wet state (De Beer, 1985; De Beer et al, 1987; Van Der Merwe, 1988), it is my firm opinion that cementitious materials should be evaluated for these conditions during the design phase. Future research should include further evaluation of the erodibility (durability) aspects and limiting criteria for these materials.

7.8 SUMMARY AND CONCLUSIONS

In this chapter the resilient responses of the two pavements evaluated are discussed. These responses include the measurement of surface and depth deflection and the calculation of radii of curvature. The pavements were modelled using the linear elastic theory, and the effective elastic moduli of the different layers were back-calculated from multi-depth deflection results. The moduli were determined initially and at various stages of trafficking, and were used to determine stresses and strains in the pavement layers.

Both maximum tensile strain and vertical compressive strain analyses were used to describe the behaviour of these pavements, together with associated permanent deformation. Both the current fatigue and subgrade limiting strain criteria were also evaluated and verified.

The following conclusions resulted from this study:

(a) The resilient response behaviour of both the deep and shallow pavements investigated here is mechanistically adequately described using the surface and depth deflection results as input to linear elastic modelling.

(b) The damaging effect of traffic loading is well illustrated by surface deflection, depth deflection profiles and calculated radii of curvature. Both crushing and fatigue failure of the cementitious base layers result in drastic changes in these indicators.

(c) Local failures around the MDD hole adversely influence the back - calculated effective elastic moduli. Deflections on the MDD and regular monitoring of the pavement at the MDD position should be done to detect faulty deflection measurements before moduli back - calculation.

(d) Inspection of the depth deflection (MDD) at various stages of trafficking assists satisfactorily in determining which layers contributed largely to the majority of the total surface deflection. In this way the effect of the subgrade on total surface deflection is also well illustrated.

(e) Weakening of the cementitious base layer as a result of traffic loading not only increases the total surface deflection, but also reduces the effective protection of the lower layers, and hence increases the contribution of the lower layers to the total surface deflection.

(f) The average reduction in the effective elastic modulus of the cementitious base of the **deep pavement** is described by a hyperbolic function when the layer changes from the **intact state** to the **crushed state.**

(g) The average reduction in the effective elastic modulus of the cementitious base of the **shallow pavement** is also described by a hyperbolic function when the layer changes from the **intact state** to the **cracked state.**

(h) The average effective elastic modulus after approximately one million E80s of the base of the deep pavement is 200 MPa to 300 MPa, while that of the shallow pavement is approximately 500 MPa.

(i) The effective elastic moduli of the lower layers of both pavements also decrease with an increase in trafficking.

(j) The maximum tensile strain at the underside of the base of both pavements increased as a result of traffic loading and is associated with total permanent deformation on the surface of up to 20 mm.

(k) The concept of **effective fatigue life** for lightly-cementitious layers is introduced (Equation 7.4), and appears to describe the real fatigue life of these layers better than the current practise done by an unverified relation (Equation 7.3). The effective fatigue life of lightly cementitious base layers corresponds to a permanent deformation of approximately 2 mm and a total standard surface deflection between 0,5 mm and 0,75 mm for thin-surfaced (single and double seals) pavements.

(l) Initial and final vertical compressive strain profiles from the pavements evaluated assist in explaining the difference in measured behaviour of these pavements. For the deep pavement, maximum compressive strains occurred at a depth of approximately 65 mm in the base where crushing failure was noted, while for the shallow pavement, maximum strains occurred in the top of the subbase where large permanent deformations occurred because of the fatigue failure and "punch in" of the base layer into the subbase.

(m) Empirically, the vertical (elastic) compressive strain appears to be a valid indicator of permanent (plastic) deformation behaviour at any depth in the pavements evaluated here.

(n) The current limiting subgrade strain criterion used in the South African mechanistic design method appears to be accurate, and may also be used to evaluate permanent deformations at any depth in the pavements evaluated in this study.

7.9 REFERENCES

Basson, J E B (1985). The measurement of deflection and curvature of a road surface when loaded by a standard axle. Unpublished internal Technical Note TP/100/85, New Test Methods, NITRR, July 1985.

Brown, S F, Tam, W S and Brunton, J M (1987). Structural evaluation and overlay design: Analysis and Implementation. Proceedings of the Sixth International Conference on the Structural Design of Asphalt Pavements, University of Michigan, Ann Arbor, July 1987.

Claessen, A I M, Edwards, J M, Sommer, P and Ugé (1977). Asphalt Pavement Design: The Shell Method. Fourth International Conference on the Structural Design of Asphalt Pavements, University of Michigan, Ann Arbor, August 1977.

De Beer, M (1985). Behaviour of Cementitious Subbase Layers in Bitumen Base Road Structures. M(Eng), Faculty of Engineering, University of Pretoria, Pretoria, 1985.

De Beer M and Horak E (1987). The effect of poor drainage on pavement structures studied under accelerated testing. Proceedings of the Annual Transportation Convention (ATC 1987), Pretoria, August 1987, Vol. 5B, Paper 5B/1, 26 pp, 1987.

De Beer, M (1989). Aspects of erodibility of lightly cementitious materials. Research Report DVPT 39, DRTT, CSIR, Pretoria, April 1989.

De Beer M, Horak E and Visser A T (1988). The Multi - Depth Deflectometer (MDD) System for determining the Effective Elastic Moduli of Pavement Layers. Unpublished paper accepted for publication in a ASTM Special Technical Publication (STP) of the First International Symposium on Nondestructive Testing of Pavements and Backcalculation of Moduli, Baltimore, USA, 1988.

Dorman, G M (1962). The extension to practise of a fundamental procedure for the design of flexible pavements. Proceedings of the International Conference on the Structural Design of Asphalt Pavements, University of Michigan, Ann Arbor, August, 1962.

Dorman, G M and Metcalf, C T (1964). Design curves for Flexible Pavements based on Layered Theory. Highway Research Record, No. 71, 1964.

Edwards, J M and Valkering, C P (1974). Structural Design of Asphalt Pavements for Road Vehicles - the Influence of High Temperatures. Highways and Road Construction, February 1974.

Freeme, et al (1984). Symposium on: Recent findings of Heavy Vehicle Simulator Testing. Proceedings of the Annual Transportation Convention (ATC 1984), Pretoria, August 1984.

Finn et al (1977). Development of Pavement Structural Subsystems. Final Report, Project 1-10B, NCHRP, February 1977.

Jordaan, G J (1988). Analysis and development of some pavement rehabilitation design methods. Ph.D Dissertation, Department of Civil Engineering, Faculty of Engineering, University of Pretoria, Pretoria, 1988.

Kadar, P (1988). Findings and results of three years accelerated testing of typical heavy duty pavements - an overview. Proceedings of the 14th ARRB Conference, Volume 14, Part 8, 28 August - 2 September 1988, Canberra, Australia, 1988.

Netterberg, F and Paige - Green, P (1984). Carbonation of lime and cement stabilised layers in road construction. Technical Report R5/3/84, NITRR, CSIR, Pretoria, 1984.

Otte, E (1978). A Structural Design Procedure for Cement-Treated Layers in Pavements. DSc Dissertation, Faculty of Engineering, University of Pretoria, Pretoria, 1978.

Paterson, W D O and Maree, J H (1978). An interim mechanistic procedure for the structural design of asphalt pavements. Technical Report RP/5/78, NITRR, 1978.

Van Der Merwe, C J (1988). The Need for Effective Drainage. Technical note I/FP/26/88 (Unpublished), Division for Roads and Transport Technology, DRTT, CSIR, Pretoria, 1988.

Visser, A T (1981). An evaluation of unpaved road performance and maintenance. Ph.D Dissertation, Faculty of the Graduate School, University of Texas, Austin, May 1981.

Wang, M C and Gramling, W L (1980). Distress behaviour of flexible pavements that contain stabilized base courses. Transportation Research Record No. 755, Washington, 1980.

CHAPTER 8

CONCLUSIONS AND RECOMMENDATIONS

CONTENTS

8.1 CONCLUSIONS AND RECOMMENDATIONS

The conclusions and recommendations relevant to a particular chapter have been listed and discussed at the end of each chapter. This chapter contains only the overall conclusions and recommendations for future research, resulting from this study.

8.1.1 Conclusions

(a) Since the implementation of the Heavy Vehicle Simulator (HVS) test programmes in South Africa during the late 1970s, the understanding of basic pavement behaviour has been and is advancing very rapidly. Amongst others, the definition of the actual in situ pavement system has been identified as one of the most important factors influencing actual pavement behaviour. The difference in quality between cementitious materials produced in the field during the construction process, and those prepared in the laboratory is significant, and a method was urgently needed to identify and quantify these differences. An in situ pavement classification system, based on the results of the Dynamic Cone Penetrometer (DCP) has been developed, and assists largely in the proper definition of the in situ pavement system, ie actual layer thickness and quality.

(b) The dominant failure mechanism in deep pavements with lightly cementitious layers is compression (crushing) failure in the upper 50 mm to 75 mm of the base. The rate of deformation is largely controlled by the initial material state, trafficking wheel load, tyre contact pressure, effective moisture content especially in the top of the base and the degree of balance of the pavement. During wet conditions loss of the surfacing and excessive potholing occurs in the base, while the lower layers may be still in a relatively sound condition.

(c) The dominant failure mechanism in shallow pavements with cementitious layers is fatigue failure of the base, with subsequent deformation ("punch in") into the relatively weaker lower layers. The rate of deformation is largely controlled by the trafficking

wheel load, the state and moisture content of the lower layers and degree of balance of the pavement. On the shallow pavements, wheel load is initially more critical than tyre contact pressure, but later during reduced rate in deformation, the effect of tyre contact pressure increases and also produces compression failure in the top of the base, similar to that found for the deep pavements.

(d) The relative damage coefficient, based on the rate of deformation of these pavements with cementitious layers, is relatively low, and varies between 1,2 and 1,5 for deep, and 1,6 and 1,8 for shallow, and up to 4,5 for very shallow pavements. For equivalent fatigue failure (based on equivalent induced maximum tensile strain at the bottom of the base) these values increased to 2,8 for the deep, and 3,9 for the shallow pavements evaluated in this study.

(e) Compression (crushing) failure of lightly cementitious layers occurs with compressive axial strains in excess of approximately one per cent. Compression failure is noted by a marked reduction in the effective cohesion (cementation), initially introduced in the material to improve its strength (bearing capacity).

(f) The rate of compression failure is largely controlled by the initial material strength in the upper 50 mm to 75 mm of the base layer and the tyre contact pressure. The implications of this type of failure should be considered during the design phase, for which tentative guidelines are also given.

(g) The DCP aided in the description of the behaviour of the pavements in this study, and enabled better understanding of the actual pavement behaviour and failure mechanisms. The concept of pavement strength - balance paths assist largely in describing the behaviour more quantitatively than was perhaps done in the past. According to this concept both pavements evaluated became "deeper" as a direct result of trafficking.

(h) An alternative DCP model for the prediction of structural capacity for pavements with lightly cementitious layers was developed, as it was found that a current model, which was developed in the early 1980s mainly for light pavements with unbound gravel bases, largely overestimates the capacity for the pavements evaluated in this study. The alternative model predicts the linear rate of deformation based on two DCP parameters calculated from the DCP data.

(i) As with the permanent behavioural changes in the pavement, such as permanent deformation, crushing and cracking, the resilient response and behaviour are very useful in the furthering the understanding of mechanistic pavement behaviour. Both surface and depth deflections were used as input to the successful modelling of both the deep and shallow pavements, based on the linear elastic theory.

(j) The concept of effective fatigue life of lightly cementitious layers is introduced, as it was found that the current prediction model totally under predicts the actual (effective) fatigue life of these layers.

(k) The change in effective elastic moduli of the cementitious base layers of both pavements was quantified and it was found that those of the deep pavement decreased hyperbolically to a range of 200 MPa to 300 MPa, mainly as a result of crushing failure, and that of the shallow pavement to approximately 500 MPa, mainly as a result of fatigue failure.

(l) The effective elastic moduli of all the lower layers in both pavements also reduced as a result of traffic loading, but at variable rates and magnitudes.

(m) Both maximum tensile strain and vertical compressive strain in both pavements increased as a result of trafficking, and are associated with changes in permanent deformation of up to 20 mm.

(n) It was found that the vertical compressive strain contribute largely in explaining the actual failure mechanisms experienced for both pavements evaluated.

(o) The current limiting compressive strain criteria for subgrades were verified for the pavements evaluated and appear to be accurate. They also predict the associated permanent deformation accurately at virtually any depth within the pavement.

8.2 Recommendations for future research

(a) The DCP classification system proposed in Chapter 3 should be applied to pavement types other than those evaluated in this study, to verify its wider application.

(b) The following concepts identified during this study should also be verified for a wider range of pavement types, including, for example, pavements with bitumin emulsion treated bases :

- Traffic associated strength - balance paths
- Compression failure in the upper part of the base
- Effective fatigue life
- Vertical strain/permanent deformation quasi - elastic analysis

(c) Current finite element theory and available software should be investigated and models calibrated in order to predict pavement behaviour using in situ determined stress dependent characteristics such as the effective elastic moduli, Poisson's ratio, etc., of these lighlty cementitious materials. Research done by Duncan et al. (1968), Wilson (1965)) and Maree (1982) should also be consulted in this respect.

(d) It is strongly recommended to continue with the HVS testing on pavements with lightly cementitious layers in order to evaluate already proposed rehabilitation strategies, based on the findings of this study. Construction work on three experimental sections on the relatively shallow pavement on road 2212, near Bultfontein in the Transvaal, is currently underway, and includes pavement

sections where the in situ cementitious base layer was pre - cracked, using large vibratory rollers. Three basic rehabilitation options have been selected and include a 150 mm G1/2 base, 35 mm asphaltic surfacing and a conventional double seal on the cracked pavement.

In Appendix D, Photo Plates D.25 to D.28 illustrate aspects of the preparation of these experimental sections near Bultfontein (Road 2212).

(e) Evaluation of the erodibility of lightly stabilised materials should be extended to include stabilisers such as fly-ash, bitumin emulsions, granulated slag, reverseals, etc. The effects on erodibility of the following also needs attention:

- Carbonation (both detrimental and advantageous) of lime and cement treated pavement materials
- accelerated curing on long term durability

(f) Calibration of the Erosion test with other durability tests such as the mechanical wet-dry brushing test, etc.

(g) The current proposed tentative erodibility criteria (De Beer, 1989) should be incorporated in the current specifications for cementitious materials, and further research should be guided to obtain a broader experience base with the Erosion Test in order to improve on the proposed criteria, if necessary.

8.2 REFERENCES

De Beer, M (1989). Aspects of Erodibility of Lightly Cementitious Materials. Research Report DVPT 39, DRTT, CSIR, Pretoria, April 1989.

Duncan, J M and Monismith, C L (1968). Finite Element Analysis of Pavements. Highway Research Record No. 228.

Maree, H J (1982). Aspects of the Design and Behaviour of Pavements incorporating Granular Bases. DSc Dissertation (In Afrikaans), Faculty of Engineering, University of Pretoria, Pretoria, 1982.

Suddath, L P and Thompson, M R (1975). Load-Deflection Behaviour of Lime-Stabilised Layers. Army Construction Engineering Research Laboratory, Champaign, Illinois, January 1975.

Wilson, E L (1965). A digital computer programme for the finite element analysis of solids with non-linear material properties. Department of Civil Engineering, University of California, Berkeley, 1965.

APPENDIX A

SUPPLEMENTARY INFORMATION (TABLES AND FIGURES) TO ASSIST DISCUSSION IN CHAPTER 4

CONTENTS PAGE

CONTENTS CONTINUE:

A.I INTRODUCTION

In this Appendix supplementary information, mostly in the form of tables and figures are given to assist the discussion on permanent deformation behaviour of pavements with lightly cementitios layers, in Chapter 4.

No detailed discussions are given here, as it is already given in Chapter 4. However, a discussion on an anomali found in the permanent deformation on one of the HVS test sections (Section 289A4) is given here, because it is considered important from an pavement evaluation point of view. This anomali is discussed in the following Paragraph A.2, after the tables and figures relating to Chapter 4.

TABLE A.1 DESIGN DATA FOR THE BASE AND SUBBASE OF THE DEEP PAVEMENT, ROAD 1932 (ROOIWAL)

Characteristic	Base (Quarry No. 20)*	Subbase (Quarry No. 5)*
Lab. density at 100% mod. AASHTO (kg/m^3) (design stage)**	2280	2083
Lab. density at 100% mod. AASHTO (kg/m^3) (during construction)**	2190	2160
In situ density (kg/m^3)	2083	2072
% of mod. AASHTO	95,1	96,0
Lab. optimum moisture content, % (design stage)	10,3	9,0
Lab. optimum moisture content, % (during construction)	7,9	7,4
In situ optimum moisture content, %	8,9	6,1
TRB-classification	A2-6(0)	A2-4(0)
Grading modulus (GM)	1,98	2,0
Design stabiliser content, % (PBFC) (m/m)	3,0	3,0
In situ stabiliser content, % (EDTA)	3,6	3,7
Plasticity index, PI (After stabilisation), %	3,6	7,9
Linear shrinkage, %	1,6	3,5

* See TPA report S4/79 (Pienaar, 1979).

** The densities are for the unstabilised material only.

TABLE A.2 DESIGN UNCONFINED COMPRESSIVE STRENGTH (UCS) RESULTS OF THE DEEP PAVEMENT, ROAD 1932 (ROOIWAL).

Characteristic	Base (Quarry No. 20)*	Subbase (Quarry No. 5)*
Soaked-UCS after 7 days at 100 % mod. AASHTO, kPa (design stage)	2000	2350
Soaked-UCS after 7 days at indicated % mod. AASHTO, kPa (contruction stage)	1400 (95,1%)	2250 (96,0%)
In situ soaked-UCS after 7 days at indicated % mod. AASHTO, kPa (contruction stage)	780 (95,1%)	1000 (96,0%)
Soaked-UCS after 28 days at indicated % mod. AASHTO, kPa (contruction stage)	1800 (95,1%)	2950 (96,0%)
In situ soaked-UCS after 28 days at indicated % mod. AASHTO, kPa (construction stage)	1210 (95,1%)	1500 (96,0%)

* See Table A.1

TABLE A.3 SUMMARY OF HVS TEST PROGRAMMES FOR THE VARIOUS TESTS DONE ON ROAD 1932 AT ROOIWAL

HVS-SECTION	TRAFFICKING WHEEL-LOAD (kN)	TYRE PRESSURE (kPa)	RANGE OF ACTUAL REPETITIONS	E80s*	TOTAL E80s	TEST CONDITIONS
250A4	40	690	0 - 596 874	596 874		IN SITU MOISTURE AND TEMPERATURE
	70	690	596 874 - 805 318	1 955 205		"
	100	690	805 318 - 817 674	482 625	3 034 704	"
250A4A	70	690	817 674 - 1 386 674	5 337 220		"
	100	690	1 386 674 - 1 617 674	9 022 860		"
	40	690	1 617 674 - 2 131 618	513 944		"
	70	690	2 131 618 - 2 468 974	3 164 399	18 038 423	"
250A4B	70	690	0 - 569 000	5 337 220		WATER AT 450 mm AFTER 217 000
	100	690	569 000 - 800 000	9 022 860		REPETITIONS
	40	690	800 000 - 1 313 944	513 944		WATER AT 20 mm AFTER 800 000
	70	690	1 313 944 - 1 651 300	3 164 399	18 038 423	REPETITIONS TO END OF TEST
251A4	70	690	0 - 502 182	4 710 467		WATER AT 450 mm AFTER 217 000 REPETITIONS
	100	690	502 182 - 843 579	13 334 966	18 045 433	WATER CONTINUED
260A4	40	520	0 - 1 947 403	1 947 403	1 947 403	WATER AT 20 mm TO 450 mm FROM 10^6 REPETITIONS (MP 9 TO 15)
274A4	40	520	0 - 1 676 275	1 676 275	1 676 275	"
275A4	40	700	0 - 2 105 910	2 105 910	2 105 910	"
289A4	70	700	0 - 1 894 826	17 773 346	17 773 346	"
294A4	100	700	0 - 1 756 646	68 614 592	68 614 592	"
337A4	150(S)	1445	0 - 48 000	-		IN SITU MOISTURE AND TEMPERATURE
338A4	150(S)	960	0 - 200 000	-		"
345A4	40	420	?	TOTAL:	149 274 510	"

* For comparison purposes, d=4 in $(p/40)^d$, where d = relative damage coefficient and p = wheel load

(S) = Single wheel load tests (Aircraft wheel, Boeing 747)

TABLE A.4 PERCENTAGE PERMANENT DEFORMATION MEASURED AT THE END OF THE HVS TESTS ON THE VARIOUS TEST SECTIONS OF THE DEEP PAVEMENT. IN (%)

HVS-SECTION	DEPTHS (mm)	RELATIVELY DRY STATE	RELATIVELY WET STATE
260A4	0-180	64	70
	180-330	10	19
	330-480	10	3
	480- ∞	15	8
250A4	0-180	53	-
	180-330	6	-
	330-480	18	-
	480- ∞	24	-
274A4	0-180	86	-
	180-330	9	-
	330-480	2	-
	480- ∞	3	-
275A4	0-180	86	-
	180-330	2	-
	330-480	8	-
	480- ∞	4	-
289A4	0-180	-	73
	180-330	-	15
	330-480	-	7
	480- ∞	-	5
260A4	0-180	54	72
	180-480	30	19
	480- ∞	16	9
AVERAGE (STD. DEV)	0-180	67 (17)	75 (7)
	180-330	9 (4)	11 (7)
	330-480	10 (7)	7 (3)
	480- ∞	14 (9)	7 (2)

- No result

TABLE A.5 IN SITU DRY DENSITIES (kg/m^3) AND OVEN DRY MOISTURE CONTENTS (%) OF THE VARIOUS HVS TEST SECTIONS ON THE DEEP PAVEMENT, ROAD 1932 (ROOIWAL).

HVS-SECTION	DEPTH (mm)	A*	B	C	D
250A4A	0-100	1797(12,4)	1928(11,7)	1926(13,6)	1791(15,6)
	250-350	1730(12,3)	1692(13,4)	1829(14,2)	1780(15,8)
	360-460	1871(8,0)	1898(9,2)	1951(10,9)	1864(11,9)
	550-650	1845(6,5)	1974(6,4)	1983(7,1)	1918(7,0)
250A4B	0-100	1860(12,6)	1915(12,9)	1965(14,3)	1761(15,9)
	250-350	1898(9,8)	1903(11,1)	2011(10,4)	1877(13,4)
	360-460	1939(7,8)	1838(7,6)	1895(7,7)	1810(9,9)
	550-650	1939(6,0)	1918(6,4)	1901(6,3)	1872(7,1)
260A4	0-100	1768(13,1)	1766(13,4)	1743(13,8)	1768(13,8)
(MP 2)	260-360	1936(9,9)	1960(9,7)	1960(9,20	1985(9,0)
	360-460	1983(6,9)	2034(5,6)	193296,0)	1999(6,10
	520-620	1751(10,3)	1720(11,10	1946(8,4)	2014(7,7)
260A4	0-100	1830(13,1)	1821(14,2)	1833(15,2)	1830(14,6)
(MP 13)	300-400	1830(10,6)	1932(9,9)	1793(10,1)	1884(10,90
	400-500	2021(6,50	2006(6,3)	1972(7,4)	1952(7,5)
	500-600	1904(9,3)	1941(9,4)	2021(8,10)	2038(8,9)
251A4	0-100	1787(12,6)	1941(11,5)	2046(11,5)	1774(14,3)
	180-280	1714(12,1)	1768(13,2)	1833(14,0)	1833(14,0)
	300-400	1885(11,0)	1882(11,0)	1920(12,0)	1892(13,0)
	400-500	1921(5,0)	1998(5,6)	1991(6,6)	--
	0-100	1816(12,0)	1948(11,5)	1902(12,0)	1826(12,4)
	180-280	1782(11,3)	1750(12,2)	1809(12,0)	1752(13,0)
	300-400	1889(9,5)	1888(10,2)	1881(10,5)	1881(10,6)
275A4	0-100	1846(12,5)	1895(13,9)	1820(13,6)	1811(13,3)
(MP2)	180-280	1929(14,5)	1896(15,1)	1843(16,9)	1833(17,6)
	380-480	1932(9,7)	2007(9,0)	1940(8,4)	2009(8,4)
	520-620	1629(12,1)	--	1847(13,0)	1665(15,4)
275A4					
(MP 12)	0-100	1837(12,4)	1884(13,4)	1989(13,7)	1830(14,4)
	180-280	1893(12,9)	1839(13,6)	1889(13,3)	1797(16,1)
	400-500	1930(7,8)	1996(7,1)	1986(8,3)	1977(9,7)
	500-600	1683(9,3)	1722(9,4)	1778(9,4)	1771(10,7)

TABLE A.5 (CONTINUED) IN SITU DRY DENSITIES (kg/m^3) AND OVEN DRY MOISTURE CONTENTS (%) OF THE VARIOUS HVS TEST SECTIONS ON THE DEEP PAVEMENT, ROAD 1932 (ROOIWAL).

HVS-SECTION	DEPTH (mm)	A*	B	C	D
289A4	0-100	1989(12,0)	1953(15,0)	1962(14,1)	1995(8,3)
(MP 3)	180-280	1837(13,9)	1913(13,7)	1828(14,3)	1821(14,9)
	300-400	1866(12,0)	1985(11,3)	1759(10,6)	1895(10,3)
	500-600	2028(9,0)	2067(8,3)	2151(7,3)	2130(6,7)
289A4					
(MP 12)	0-100	1982(13,9)	1992(13,6)	1976(14,2)	1992(11,0)
	180-280	1873(13,4)	2033(14,0)	1959(14,5)	1870(14,6)
	300-400	1944(10,9)	2000(9,8)	1975(9,4)	1960(7,7)
	500-600	1868(9,4)	2061(6,1)	1827(11,3)	1808(10,3)
294A4					
(MP 2)	0-50	1862(13,5)	1888(13,8)	1861(13,6)	1849(13,7)
	50-100	1833(13,5)	1902(13,8)	1905(13,6)	1865(13,7)
	180-280	1866(13,3)	1895(12,6)	1736(12,1)	1849(12,1)
	320-420	1848(10,9)	1969(11,3)	1899(12,4)	1842(12,1)
	520-620	1955(8,5)	1920(8,7)	2023(9,3)	1979(8,6)
294A4					
(MP 12)	0-50	1918(13,9)	1854(14,9)	1790(13,0)	1918(14,0)
	50-100	1881(13,9)	1879(14,9)	1881(13,0)	1935(14,0)
	180-280	1830(14,3)	1968(13,9)	1837(15,3)	1716(16,2)
	320-420	1895(11,4)	1878(11,8)	1836(13,2)	1837(13,8)
	520-620	1829(8,5	1840(11,5)	1852(9,6)	2005(8,9)

* Measuring position in test pit (see Figure 4.6, in Chapter 4).

TABLE A.6 DESIGN DATA FOR THE SHALLOW PAVEMENT, ROAD 2212 (BULTFONTEIN).

Characteristic	Subbase (Quarry No. 1556)*	Base (Quarry No. 1556)*
Lab. density at 100% mod. AASHTO (kg/m^3) (design stage)**	2100	2210
Lab. density at 100% mod. AASHTO (kg/m^3) (during construction)**	-	2150
In situ density (kg/m^3)	-	2069
% of mod. AASHTO	-	96,3
Lab. optimum moisture content, % (design stage)	9,0	7,4
Lab. optimum moisture content, % (during construction)	-	7,7
In situ optimum moisture content, %	-	7,2
TRB-classification	A2-4(0)	A1-A(0)
Grading modulus (GM)	1,73	2,34
Design stabiliser content, % (PBFC) (m/m)	2,0	3,0
In situ stabiliser content, % (EDTA)	-	2,62
Plasticity index, PI (After stabilisation), %	NP	SP
Linear shrinkage, %	4,0	2,0

* See TPA report S2/81 (Marais, 1981).
** The densities are for the unstabilised material only.

TABLE A.7 DESIGN UNCONFINED COMPRESSIVE STRENGTH (UCS) RESULTS OF THE BASE AND SUBBASE OF THE SHALLOW PAVEMENT, ROAD 2212 (BULTFONTEIN).

Characteristic	Subbase (Quarry No. 1556)*	Base (Quarry No. 1556)*
Soaked-UCS after 7 days at 97 % mod. AASHTO, kPa (design stage)	2400	1800
Soaked-UCS after 7 days at indicated % mod. AASHTO, kPa (contruction stage)	-	1164 (96,3%)

* See previous Table A.6

TABLE A.8 SUMMARY OF HVS TEST PROGRAMMES FOR THE VARIOUS TESTS DONE ON ROAD 2212 AT BULTFONTEIN

HVS-SECTION	TRAFFICKING WHEEL-LOAD (kN)	TYRE PRESSURE (kPa)	RANGE OF ACTUAL REPETITIONS	E80s*	TEST CONDITIONS
306A4	40	700	0 - 2 450 000	2 450 000	WATER AT 20 mm TO 450 mm FROM 10^6 REPETITIONS (MP 9 TO 15)
307A4	70	700	0 - 2 450 000	22 978 320	"
308A4	100	700	0 - 2 640 000	103 125 000	"
309A4	150(S)	1445	46 000	-	"
			TOTAL:	128 553 000	

* For comparison purposes, d=4 in $(p/40)^d$, where d = relative damage coefficient and p = wheel load

(S) = Single wheel load tests (Aircraft wheel, Boeing 747)

TABLE A.9 IN SITU DRY DENSITIES (kg/m^3) AND OVEN DRY MOISTURE CONTENTS (%) OF THE VARIOUS HVS TEST SECTIONS ON THE SHALLOW PAVEMENT, ROAD 2212 (BULTFONTEIN).

HVS-SECTION	DEPTH (mm)	A*	B	C	D
306A4	0-100	1906(11,7)	2093 (9,6)	2023(10,5)	1933 (9,7)
(MP 13)	120-220	1896(10,2)	1982 (9,7)	2036(10,2)	1890(10,8)
	220-320	1724(10,1)	1883(10,0)	1796(10,7)	1818(11,4)
	320-420	2087 (3,6)	2083 (6,6)	2102 (6,5)	1986 (5,5)
	420-520	1929 (4,6)	1965 (3,5)	1927 (7,9)	1975 (6,5)
	520-620	1770 (7,5)	1770(11,1)	1867(12,2)	1795(11,3)
306A4	0-100	1865(10,7)	2034(10,3)	1980(11,0)	1903(10,6)
(MP 5)	120-220	- (10,5)	- (10,4)	- (10,4)	- (10,0)
	220-320	1926(10,0)	1942 (9,7)	2010 (9,4)	1825(10,0)
	320-420	2121 (5,5)	2032 (7,8)	2101 (5,5)	2032 (5,4)
	420-520	1759 (6,0)	1949 (3,5)	1969 (2,9)	-
	600-700	1797 (6,5)	1728 (5,8)	1785 (8,6)	1726 (9,7)
	700-800	1838 (6,3)	1680 (7,9)	1673(11,0)	1756(10,0)
307A4	0-60	1844(10,4)	1950 (9,0)	2036 (8,6)	2000 (6,7)
(MP 4)	60-110	1786 (9,7)	1879 (9,1)	1875 (7,6)	1851 (8,1)
	110-180	1837(11,4)	1954(11,4)	1897 (7,6)	1886 (9,0)
	180-450	2016 (8,3)	2066 (8,0)	2035 (8,8)	2030 (8,9)
	450-530	-	1872 (3,8)	1950 (4,4)	1945 (4,0)
	530-800	1847 (6,5)	1965 (4,7)	1996 (5,1)	1967 (3,8)
307A4	0-60	1853 (8,9)	1991 (8,8)	1990 (9,7)	2016 (7,1)
(MP 10)	60-110	1778(10,2)	1864 (9,8)	1920(10,3)	1897 (8,3)
	110-180	1795(11,5)	1957(10,7)	1904(12,8)	1899 (9,0)
	180-450	1930 (8,7)	2108 (8,2)	2026 (9,3)	2071 (8,1)
	450-530	1899 (5,0)	1895 (5,9)	1891 (6,4)	1873 (6,0)
	530-800	1782 (7,1)	2011 (3,9)	1912 (5,2)	1960 (6,6)
308A4	0-100	1806(11,7)	1928(10,6)	1939(10,8)	1866(12,4)
(MP 2,5)	180-280	1883(10,8)	2022 (9,8)	1936 (9,6)	1862(10,3)
	220-320	1887 (9,9)	1954 (9,8)	1841 (9,9)	1980 (9,7)
	350-500	1913 (7,7)	2072 (4,8)	2095 (4,6)	2103 (4,7)
	500-600	1893 (7,0)	1977 (2,3)	1990 (2,6)	1968 (6,3)
	650-800	1829 (9,0)	1822 (8,7)	1841 (8,7)	1835 (8,5)
308A4	0-100	1832(10,4)	2016(10,9)	1945(12,6)	1958(10,0)
(MP 12)	180-280	1896 (8,8)	1899 (9,6)	1942 (9,7)	1905 (9,8)
	210-310	1942 (8,4)	1961 (9,8)	1871(10,0)	1908(10,4)
	360-510	1814 (8,7)	2044 (5,2)	2112 (5,2)	2150 (4,9)
	460-560	1876 (5,0)	1946 (3,4)	2013 (3,8)	1983 (6,3)
	600-800	1820 (8,4)	1848 (8,7)	1865 (8,0)	1858 (8,8)

* Measuring position in test pit, see previous Figure 4.6 in Chapter 4.

TABLE A.10 IN SITU DRY DENSITIES (kg/m^3) AND OVEN DRY MOISTURE CONTENTS (%) OF THE TWO HVS TEST SECTIONS 309A4 (SHALLOW) AND 337A4 (DEEP).

HVS-SECTION	DEPTH (mm)	A*	B	C	D
309A4 (MP 4)	0-100	1811 (9,5)	1889(10,9)	1731(10,5)	-
	200-300	1836 (9,7)	1942 (9,7)	1907 (9,2)	1865 (9,6)
	310-410	1803(10,3)	2198 (5,3)	2181 (4,5)	2055 (4,4)
	500-600	1889 (2,0)	1967 (3,4)	1965 (4,3)	1896 (4,0)
	675-875	1809(10,2)	1884(11,6)	1901(10,6)	1951 (9,6)
309A4 (MP 13)	0-100	1732(11,4)	1870(10,7)	1843 (9,9)	1867(10,2)
	180-280	1904 (9,7)	1893(11,5)	1854(10,0)	1944 (9,8)
	220-320	1811 (8,8)	2133 (4,9)	2170 (3,9)	2084 (4,3)
	520-620	1840 (7,6)	1920 (2,2)	2012 (2,9)	1843 (5,3)
	650-850	1779 (9,4)	1880 (7,9)	1963 (6,4)	1910 (7,2)
337A4 (MP 8)	0-150	1699(14,0)	1851(15,1)	1903(14,5)	1834(14,2)
	180-280	1842(15,0)	1877(15,1)	1816(14,5)	1748(15,0)
	280-330	1926(13,6)	1923(15,3)	1905(11,5)	1868(10,1)
	420-620	1964 (9,5)	1957(10,0)	1927 (9,6)	1890(10,0)

* Measuring position in test pit, see previous Figure 4.6, in Chapter 4.

A.2 Anomaly in some of the permanent deformation results of the deeper pavement and discussion

If the permanent deformation development on Sections 275A4 (40 kN), 289A4 (70 kN) and 294A4 (100 kN) is compared (Figures A.2 (b), A.3 (a) and 4.5 (b)), it is seen that the rate of permanent deformation (before the introduction of excessive water or rain and potholing) on Section 289A4, which was the 70 kN test, was higher than those measured on the 100 kN test on Section 294A4. The previous Table 4.2 in Chapter 4, indicates that the rate of deformation during the relatively "dry" state on the 70 kN test (Section 289A4) is approximately 1,34 times higher than the rate in the "dry" state on the 100 kN test (Section 294A4).

The final dry densities of the upper 100 mm of the base layer in the trafficked area (positions B and C) on Section 289A4, compared to those of Sections 275A4 and 294A4, also indicates a relative densification on Section 289A4 (see previous Table A.5).

Initially, these three test were planned to study only one variable, ie the effect of wheel load, and therefore relative damage, on this pavement. These three test sections were originally selected on the basis of "similar" initial surface deflections and "similar" DCP characteristics in terms of balance, ie "deep" pavements. The irregularity in the permanent deformation result on Section 289A4, prompted closer investigation into the underlying reasons for this anomaly, as it is normally assumed that the rate of deformation (damage) on the "same" pavement is directly proportional to the wheel load on that pavement.

In Table A.11, the initial road surface deflection (RSD) and radius of curvature (RC) on these three sections are summarised.

TABLE A.11 INITIAL SURFACE DEFLECTION (40 kN) AND RADIUS OF CURVATURE (RC) OF THE THREE HVS TEST SECTIONS

SECTION	HVS-TEST LOAD* (kN)	RSD (μm)	RC (m)	STD. DEV.		COEFA. OF VARIATION	
				RSD (μm)	RC (m)	RSD (%)	RC (%)
275A4	40	263(24)	327(10)	33	133	13	41
289A4	70	276(64)	338(24)	60	185	22	55
294A4	100	244(62)	301(24)	47	151	19	50

* This is the trafficking dual wheel load on the test section. The surface deflections were measured under a 40 kN dual wheel load with the Road Surface Deflectometer. The radius of curvature was calculated from the surface deflection measurements, and is similar to the Dehlen radius of curvature (Horak, 1987).

() Number of measurements

The table indicates that the coefficient of variation in the deflection (RSD) results is markedly lower than those of the radius of curvature (RC). This is probably so because the RSD is a direct measurement, while the RC is calculated from the deflection basin of the RSD measurement, using approximately eight data points (4 data points each side of the maximum deflection value). This relatively low number of data points allows small variations in the data to influence the calculation of the RC. However, the RC is normally a good indicator of the structural state of the pavement system and may give a better explanation of its behaviour under accelerated trafficking.

The table also indicates that small differences exist between the RSD values of the three sections, but at the time of HVS testing, these differences were ignored, and the deflections on these three section were considered similar.

Greater differences, however, exist between the RC values, but because these RC values were indirectly obtained, the differences were ignored in the selection of these sections and it was considered that the RC values were also similar.

Closer investigation into the underlying reasons for the rather unexpected results of the HVS test showed that the majority of the deformation occurred in the base only.

The DCP was then used to evaluate the bases of the three test sections more critically. It was found that the relative strength of the upper 50 mm and the lower 170 mm of the bases differed significantly. The various DCP parameters measured on these sections are summarised in Table A.12.

TABLE A.12 DCP PARAMETERS MEASURED ON THE THREE SECTIONS.

SECTION	HVS LOAD REPS. (N)	DCP PARAMETERS* DN_{50} (mm/blow)	DN_{50-220} (mm/blow)	DNR	DSN_{200} (blows)
275A4	0	1,2	1,8	0,667	140
	10^6	1,3	2,0	0,650	144
	$2,1 \times 10^6$	2,7	2,3	1,173	90
289A4	0	1,9	1,1	1,727	200
	10^6	2,7	1,7	1,588	115
	$1,89 \times 10^6$	2,4	2,1	1,142	100
294A4	0	0,7	2,1	0,333	190
	10^6	1,2	2,6	0,461	115
	$1,7 \times 10^6$	2,0	2,9	0,689	100

* DN_{50} = Average rate of penetration of the DCP in the top 50 mm of the base layer.

DN_{50-220} = Average rate of penetration of the DCP from a depth of 50 mm to 220 mm in the base layer.

DNR = Ratio between DN_{50} and DN_{50-220}: DN_{50}/DN_{50-220}.

DSN_{220} = Total number of blows to penetrate to a depth of 220 mm in the pavement.

The table indicates the highest initial penetration rate of the upper 50 mm of the base (DN_{50}) and the lowest penetration rate of the layer between 50 mm and 220 mm (DN_{50-220}), was measured on Section 289A4. This result is more clearly indicated by the DNR parameter, which was the highest for Section 289A4

This means that the upper 50 mm of the base of this section is relatively "softer" than those on the other two sections, while the reverse is true for the lower 50 mm to 220 mm. It is concluded that this "softer" zone on a relatively "harder" bottom is directly responsible for the unexpected deformation, because for Section 294A4, the upper 50 mm appears to be relatively "harder" than the lower 50 mm to 220 mm.

The table also indicates another interesting result: the DNR on Sections 275A4 and 294A4 increased with increased HVS load repetitions, while for Section 289A4, the DNR decreased. In terms of pavement behaviour a decrease in DNR is an indication that densification occurred during trafficking (Section 289A4). This was also confirmed by the densities in the base measured with the nuclear apparatus, as was shown in the previous Paragraph 4.2.4.5, in Chapter 4. An increase in DNR, however, is indicative of a de-densification or crushing in the upper 50 mm of the base (Sections 275A4 and 294A4). This de-densification was also confirmed by the nuclear density measurements as well as the test pit investigations mentioned earlier.

The results of these three HVS test sections again demonstrates the complex nature of the behaviour of pavements and emphasises that surface deflection only does not predict the ultimate behaviour of these pavements accurately. However, intensive in situ measurements (DCP, depth-deflections, density etc) and observations during accelerated testing, better definitions and even quantification of different failure mechanisms is possible. It is my opinion that with this approach, relevant, accurate and valuable models for pavement behaviour can be established in future.

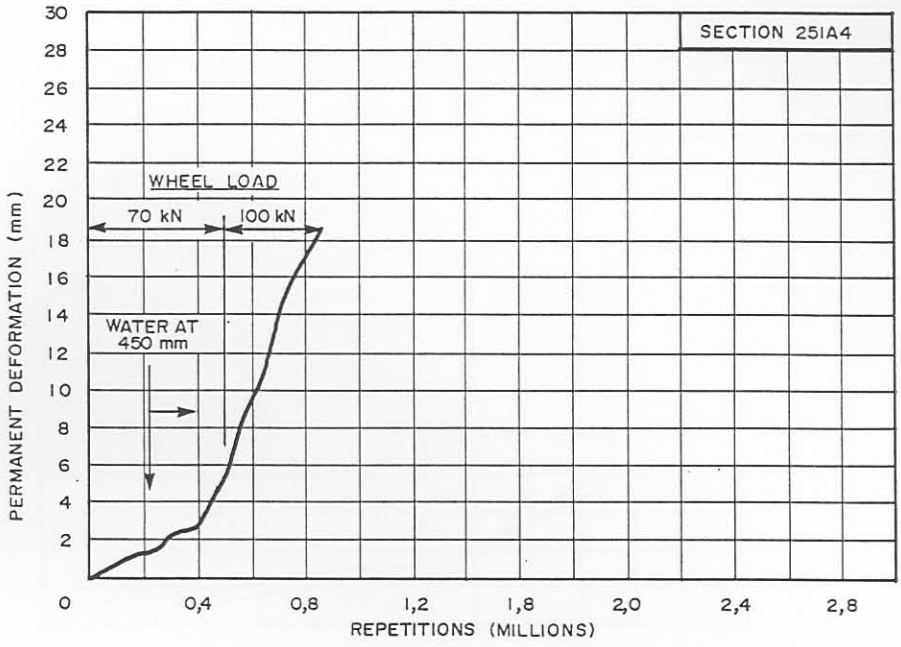

(a) HVS SECTION 251A4

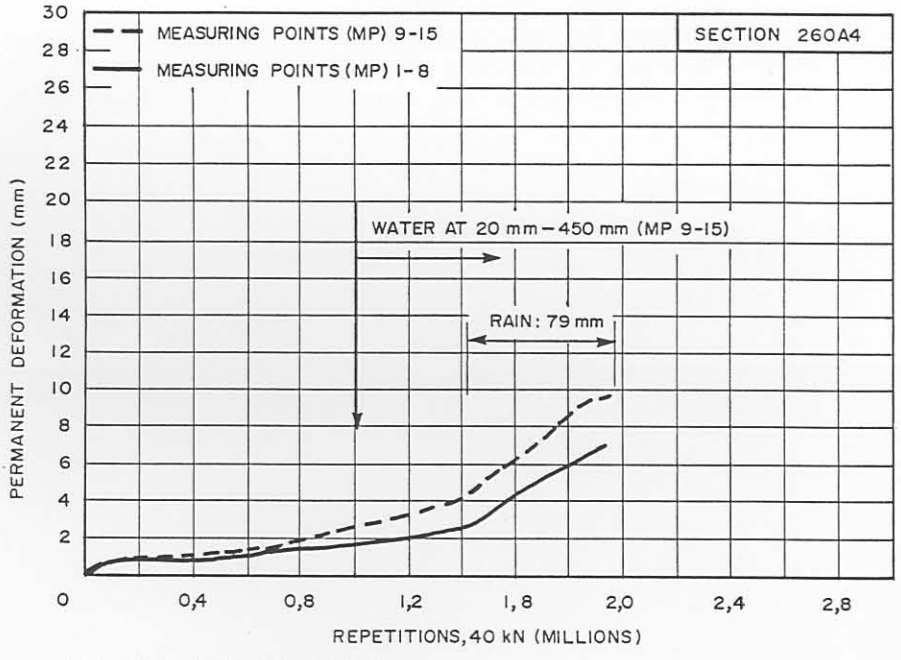

(b) HVS SECTION 260A4

FIGURE A.1

AVERAGE PAVEMENT DEFORMATION AS MEASURED IN HVS TESTS 251A4 AND 260A4 UNDER INDICATED DUAL WHEEL LOADS ON ROAD 1932 (ROOIWAL)

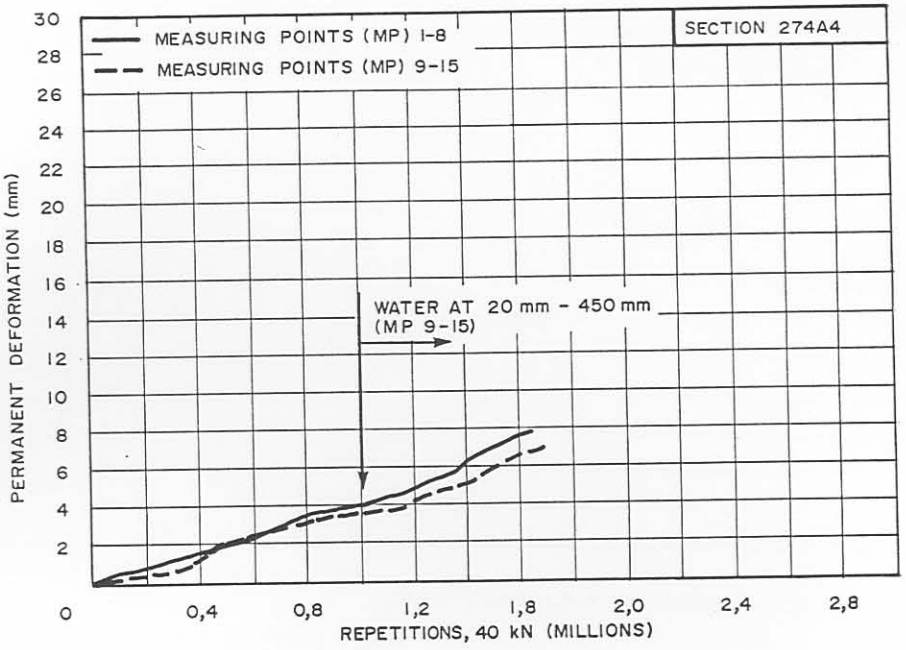

(a) HVS SECTION 274A4

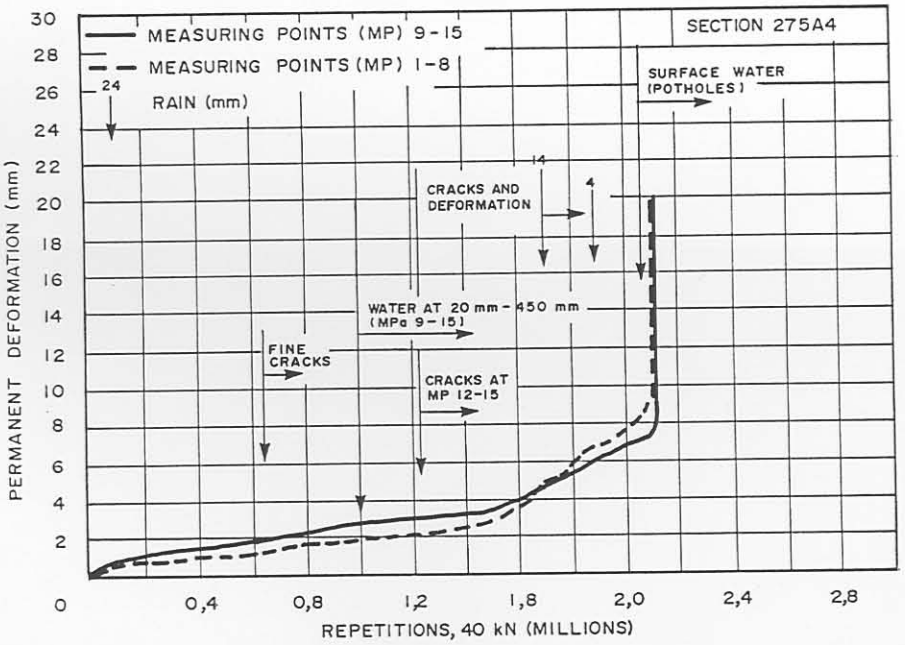

(b) HVS SECTION 275A4

FIGURE A.2

AVERAGE PERMANENT DEFORMATION AS MEASURED IN HVS TESTS 274A4 AND 275A4 AT VARIOUS STAGES OF TRAFFICKING AND MOISTURE CONDITIONS ON ROAD 1932 (ROOIWAL)

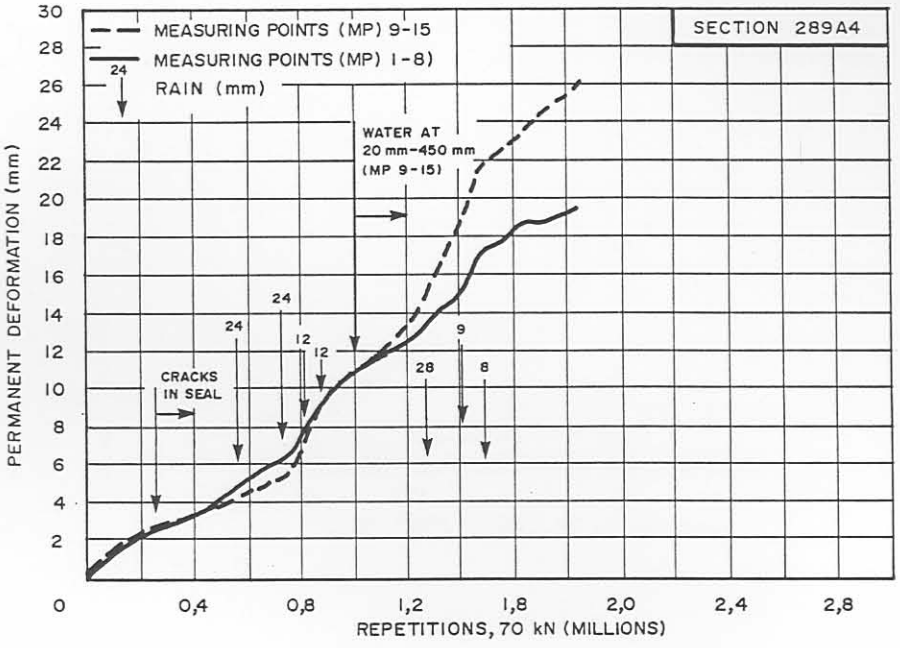

(a) HVS SECTION 289A4

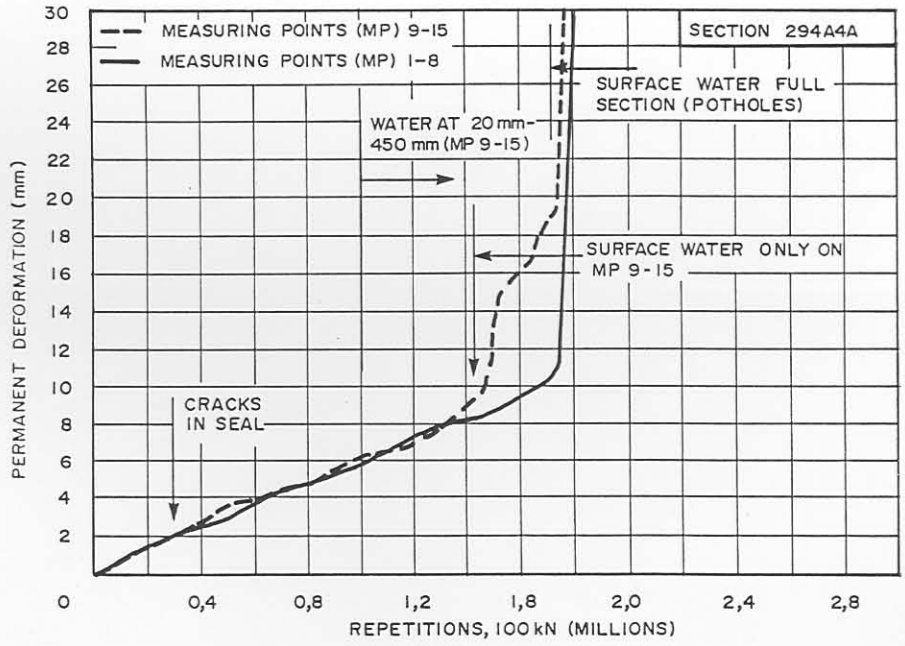

(b) HVS SECTION 294A

FIGURE A.3

AVERAGE PERMANENT DEFORMATION AS MEASURED IN HVS TESTS 289A4 AND 294A4 AT VARIOUS STAGES OF TRAFFICKING AND MOISTURE CONDITIONS UNDER THE INDICATED DUAL WHEEL LOADS ON ROAD 1932 (ROOIWAL)

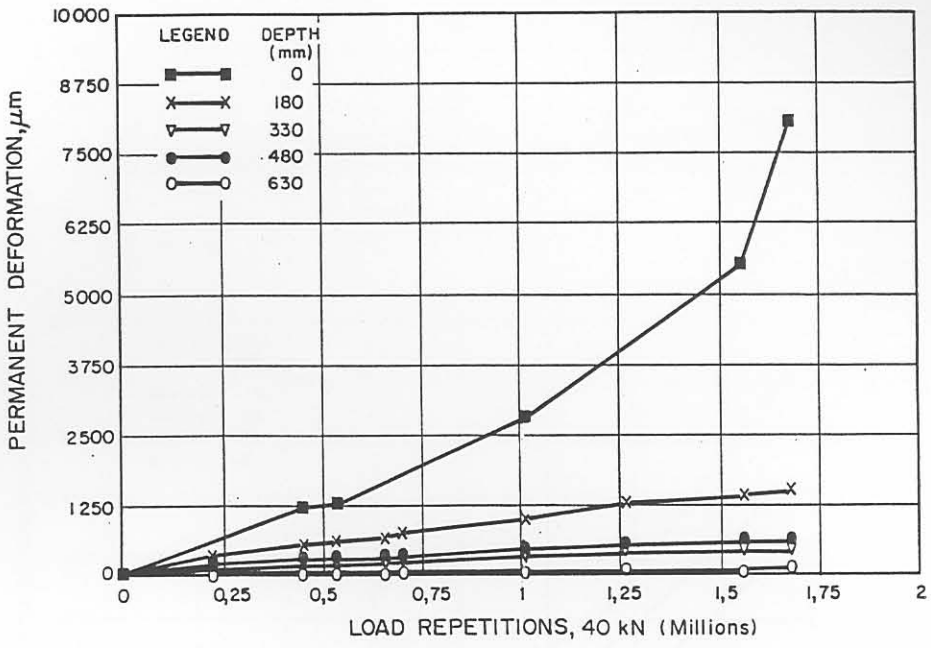

(a) MDD4

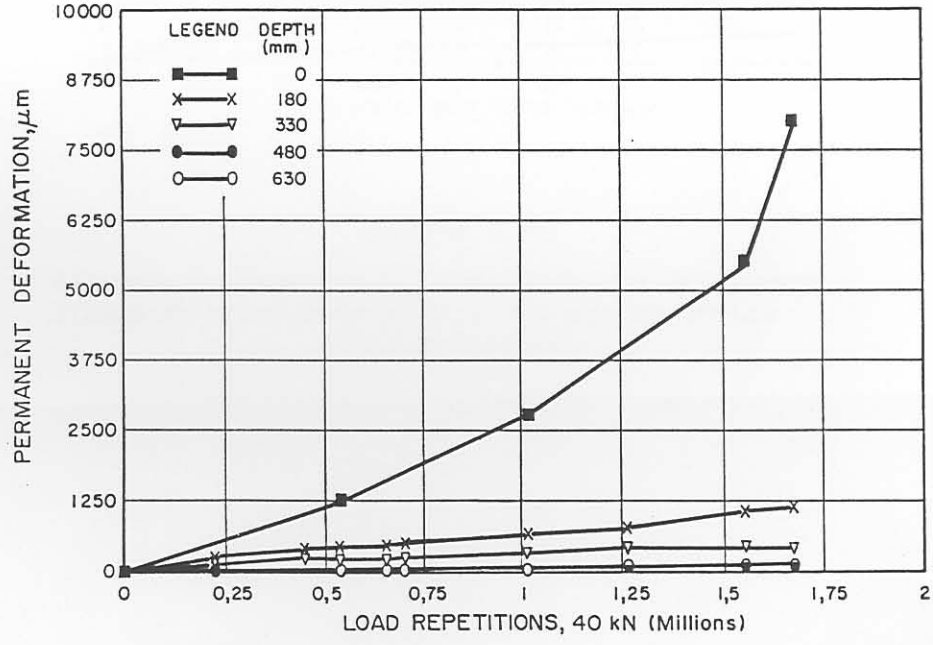

(b) MDD8

FIGURE A.4

PERMANENT DEFORMATION AT DIFFERENT DEPTHS AT VARIOUS STAGES OF TRAFFICKING ON HVS TEST SECTION 274A4 (ROAD 1932, ROOIWAL)

940-4-5900/12 BD

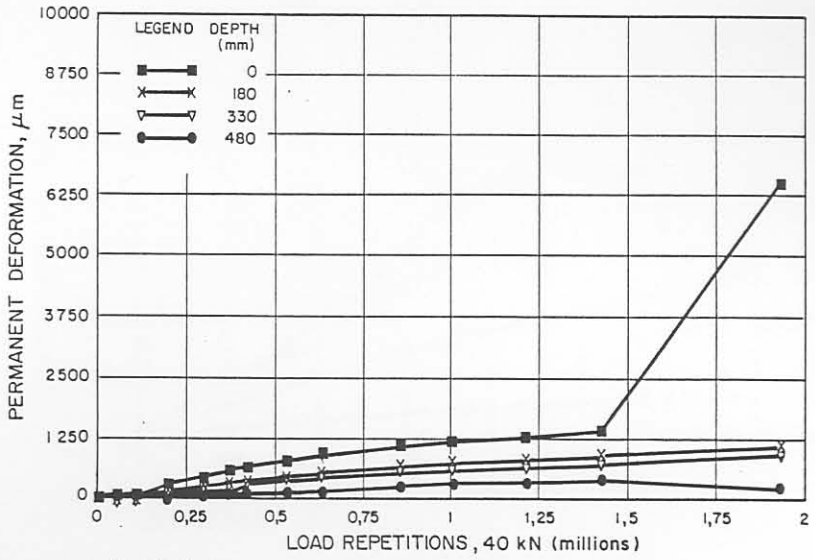

(a) MDD4

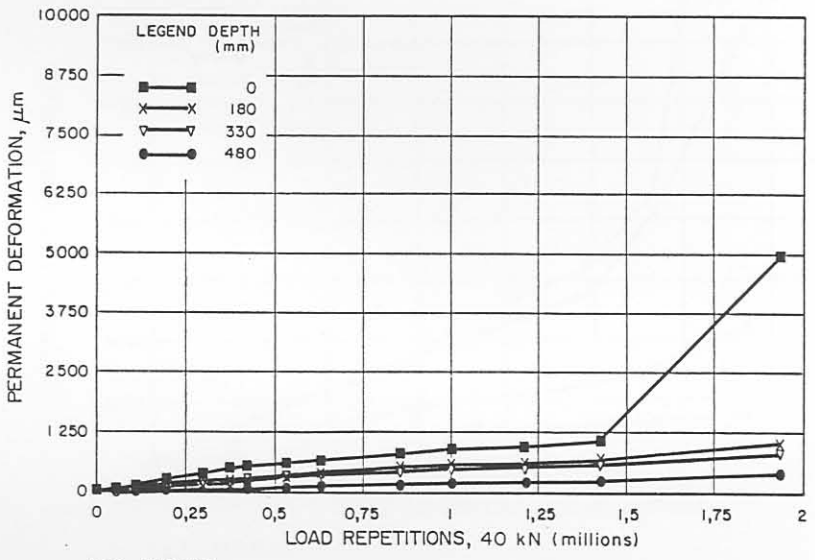

(b) MDD8

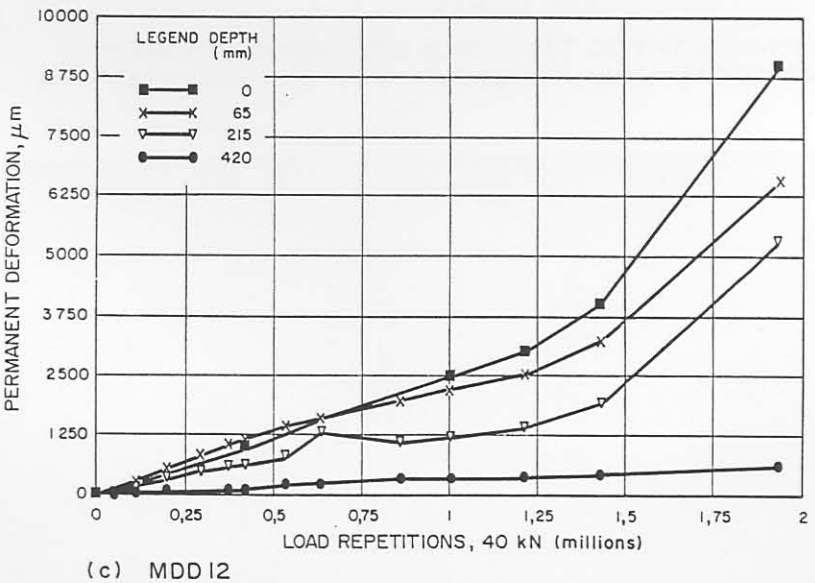

(c) MDD12

FIGURE A.5

PEMANENT DEFORMATION AT DIFFERENT DEPTHS AT VARIOUS STAGES OF TRAFFICKING ON HVS TEST SECTION 275A4 (ROAD 1932, ROOIWAL)

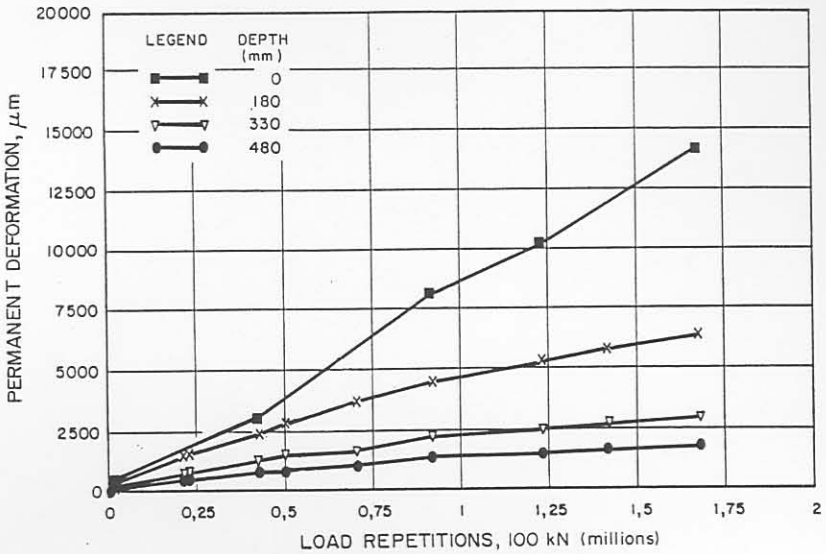

(a) MDD4

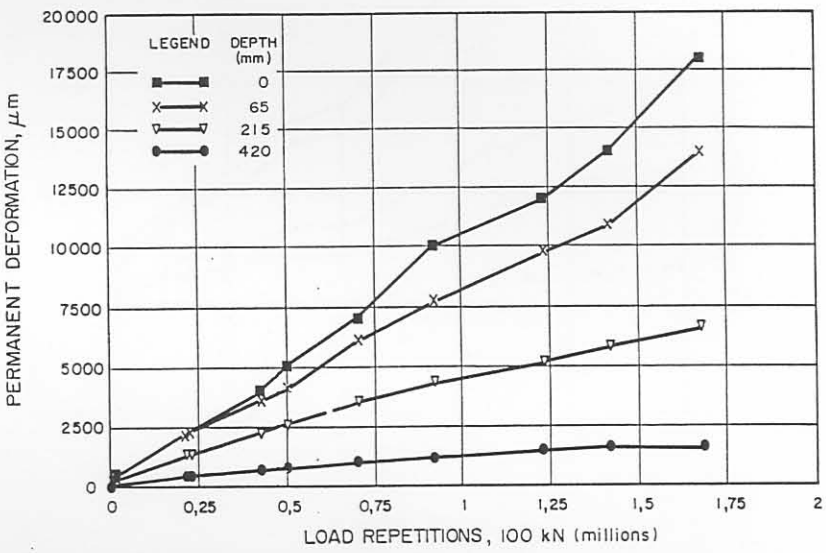

(b) MDD8

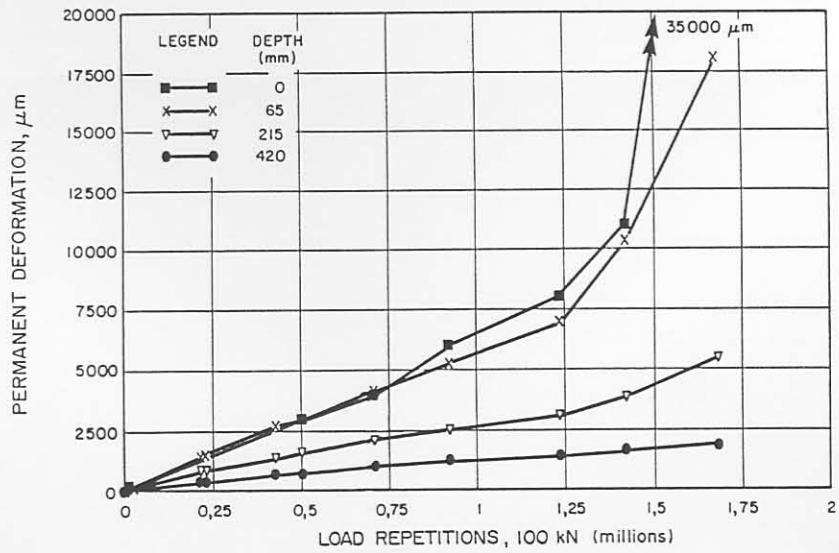

(c) MDD12

FIGURE A.6

PERMANENT DEFORMATION AT DIFFERENT DEPTHS AT VARIOUS STAGES OF TRAFFICKING ON HVS TEST SECTION 294A4 (ROAD 1932, ROOIWAL)

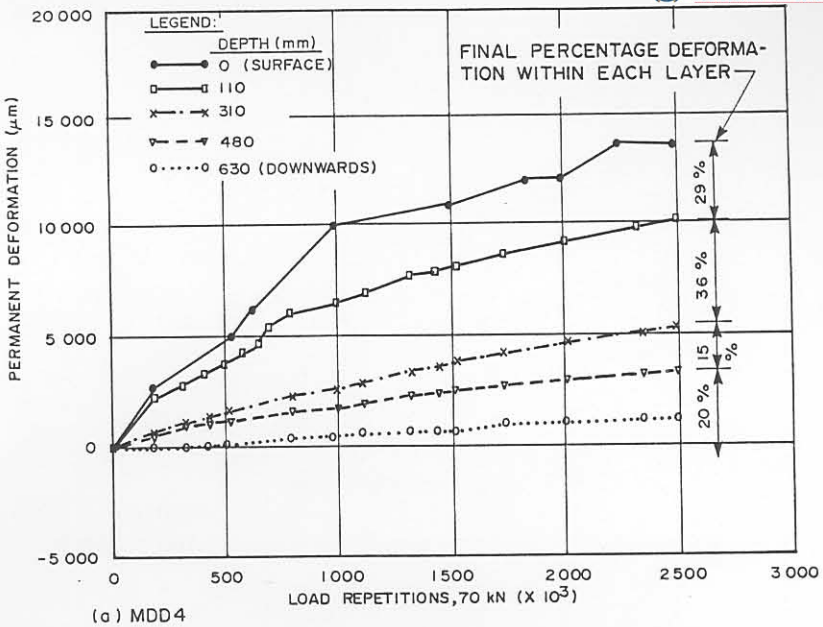

(a) MDD4

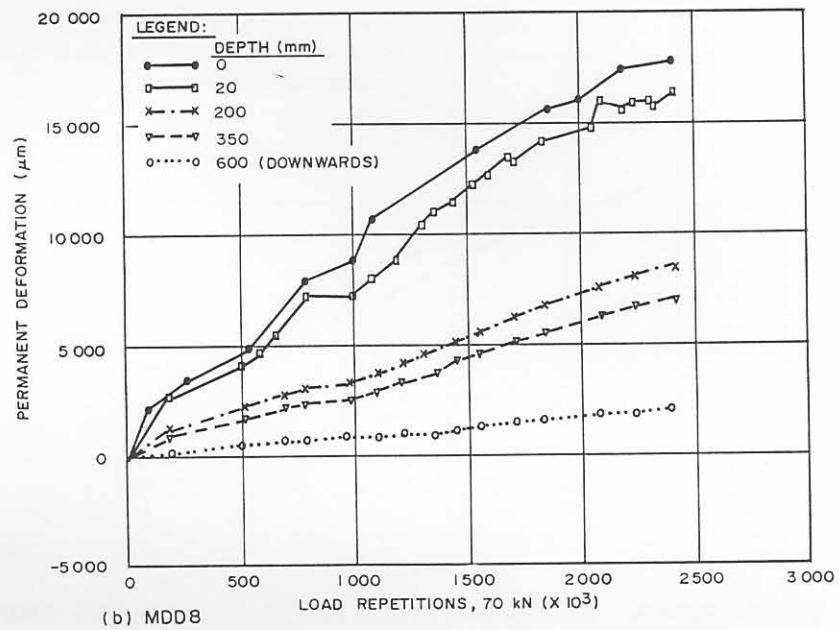

(b) MDD8

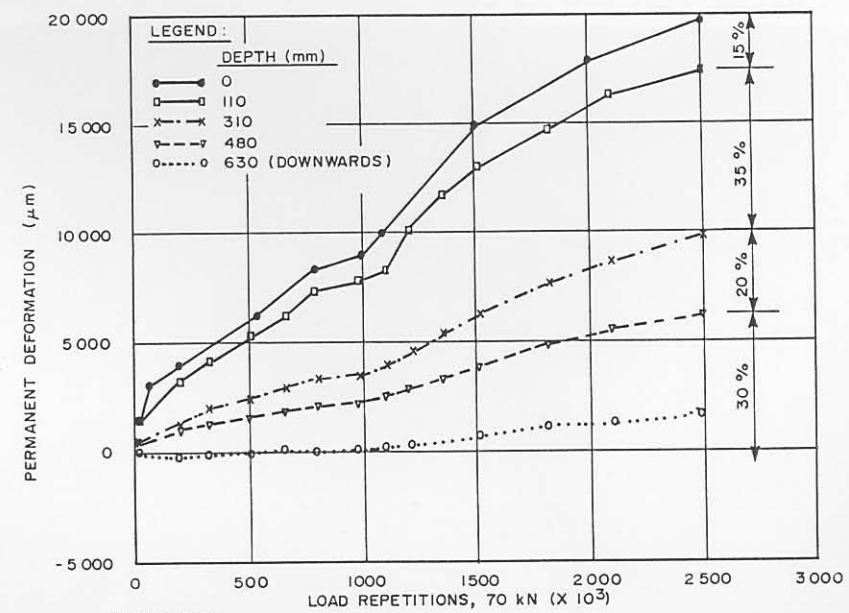

(c) MDD12

FIGURE A.7

PERMANENT DEFORMATION AT DIFFERENT DEPTHS AT VARIOUS STAGES OF TRAFFICKING OF A 70 kN DUAL WHEEL LOAD ON HVS TEST SECTION 307A4 (ROAD 2212, BULTFONTEIN)

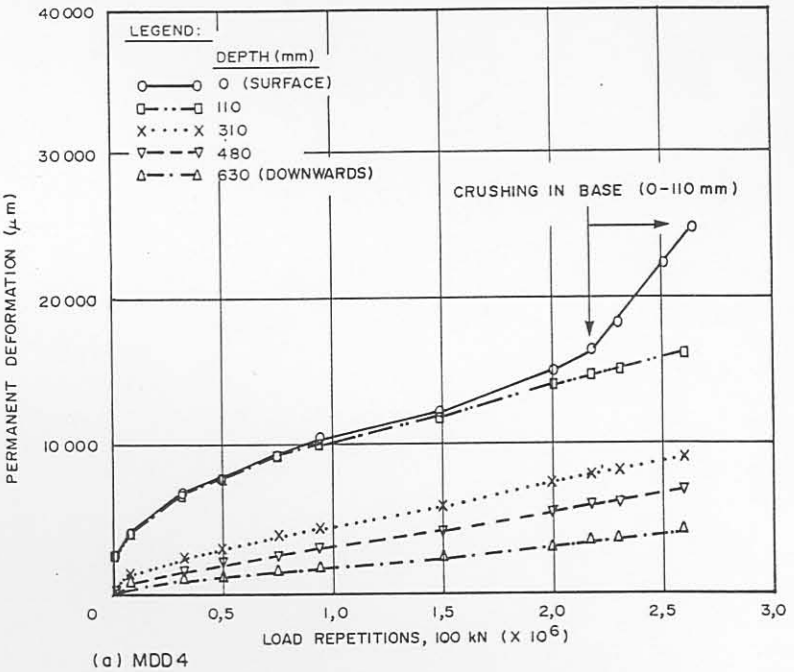

(a) MDD4

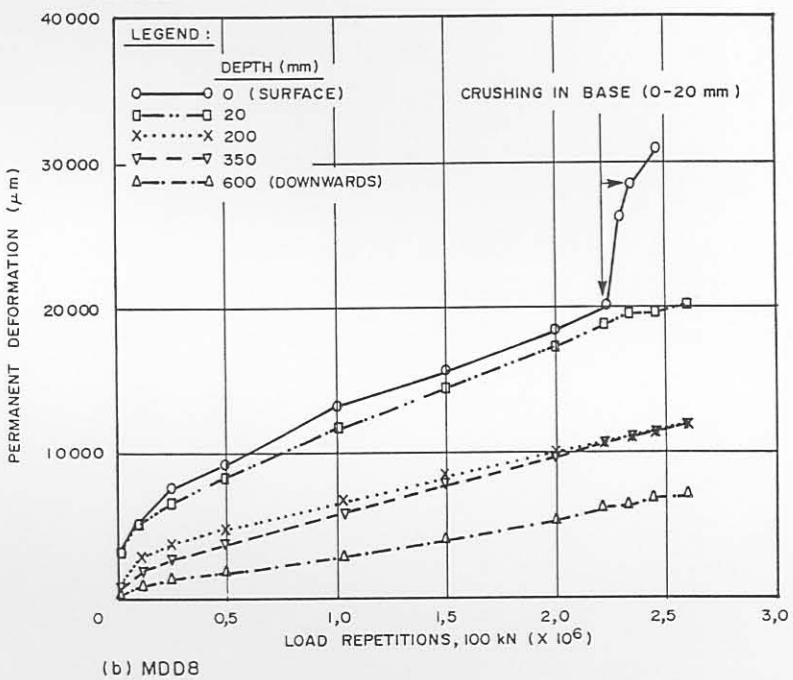

(b) MDD8

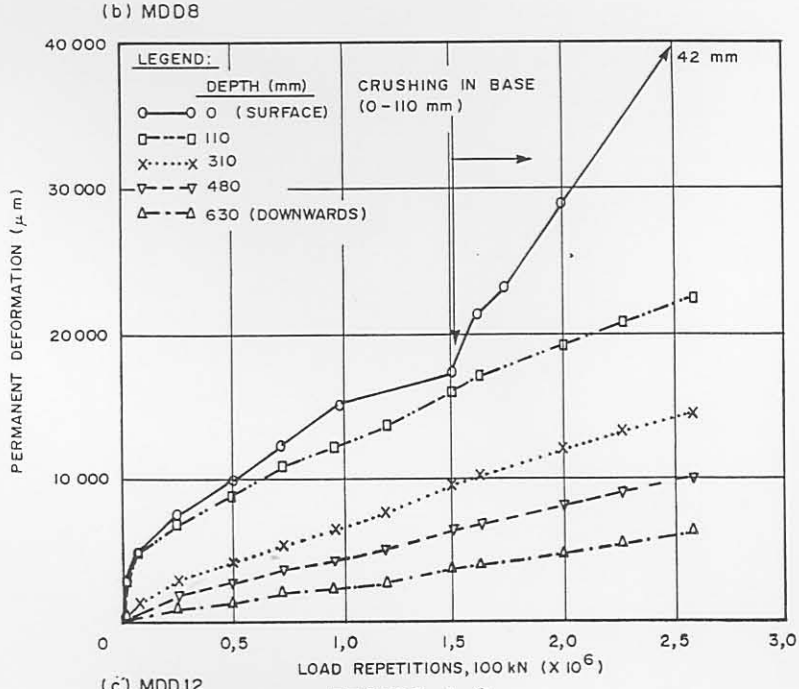

(c) MDD12

FIGURE A.8

PERMANENT DEFORMATION AT DIFFERENT DEPTHS AT VARIOUS STAGES OF TRAFFICKING OF A 100 kN DUAL WHEEL LOAD ON HVS TEST SECTION 308A4

APPENDIX B

SUPPLEMENTARY INFORMATION (TABLES AND FIGURES) TO ASSIST DISCUSSION IN CHAPTER 5

CONTENTS PAGE

B.1 INTRODUCTION

In this Appendix, supplementary information in the form of a table and several graphs without any discussion here, are given to assist the discussion on compression failure behaviour of pavements with lightly cementitious layers, in Chapter 5.

TABLE B.1 SUMMARY OF COMPRESSIVE FAILURE STRAINS OF NATURALLY AND CEMENTITIOUS MATERIALS AS MEASURED IN TRIAXIAL TESTS BY SEVERAL INVESTIGATORS

MATERIAL	TYPE OF STABILISER	CONTENT (%)	CONFINING PRESSURE (kPa)	AXIAL STRAIN (%)	AGE (Day)	CURING TEMP.DEG.	INVESTIGATOR
SANDY SOIL	NATURALLY CEMENTED	-	200	2,0	-	-	LIOYD (1987)
SANDY SOIL	CEMENT	5-10	-	0,6	-	-	ROBERTSON et al. (1987)
CLAYEY SOIL	LIME	5-10	-	1,0-2,1	-	-	ROBERTSON et al. (1987)
A-7-6(18)	LIME	5	0-35	0,7-1,6	1-6	49	THOMPSON (1966)
A-4(8)	LIME	3	0-35	0,7-1,2	1-6	49	THOMPSON (1966)
A-6(8)	LIME	5	0-35	0,5-1,0	1-6	49	THOMPSON (1966)
A-6(6)	LIME	3	0-35	1,0-1,5	1-6	49	THOMPSON (1966)
GRAVEL	CEMENT	7-9	-	0,3-0,7	-	-	ABBOUD (1973)
SAND	NAT. STRONGLY CEMENTED	-	35-414	1,0-1,5	-	-	ALFI (1978)
SL. PL. SAND*	NAT. MODERAT. CEMENTED	-	0-414	1,0-2,0	-	-	CLOUGH et al. (1981)
SL. PL. SAND	NAT. WEAKLY CEMENTED	-	0-414	1,0-9,0	-	-	CLOUGH et al. (1981)
SL. PL. SAND	CEMENT	4	35-414	0,5-2,5	14	22	CLOUGH et al. (1981)
SL. PL. SAND	CEMENT	2	103-414	1,0-5,0	14	22	CLOUGH et al. (1981)
SAND	CEMENT	5	100-500	0,8-1,5	180	22	DUPAS et al. (1979)
A-4(0)	NAT. UNCEMENTED	-	450	> 12	-	-	WISSA et al. (1965)
A-4(0)	LIME	5	35-480	1,6-3,2	4-20	22	WISSA et al. (1965)
LATERITIC SOIL	LIME	4	-	1,0-1,5	7-28	22	HAMMOND (1981)
A-1-b	NAT. UNCEMENTED	-	69	1,0	-	-	FERGUSON et al. (1968)
A-1-a	NAT. UNCEMENTED	-	550	7,0	-	-	FERGUSON et al. (1968)
A-1-b	CEMENT	1-3	69-550	0,5	7-28	22	FERGUSON et al. (1968)
A-1-a	CEMENT	1-3	69-550	0,5	7-28	22	FERGUSON et al. (1968)

* SLIGHTLY PLASTIC SAND

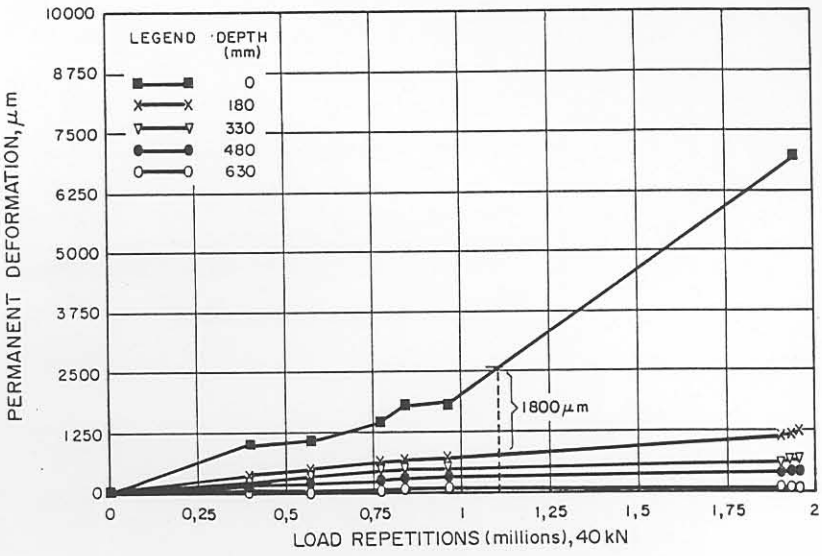

(a) MDD4

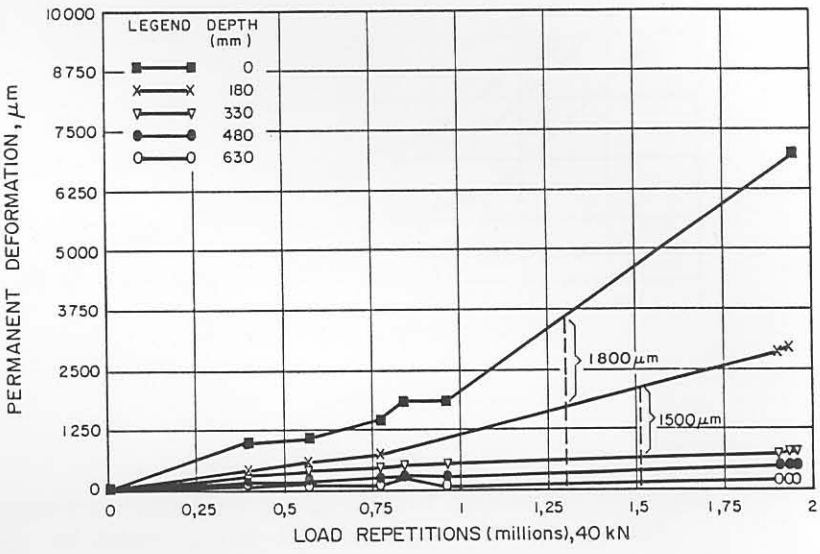

(b) MDD8

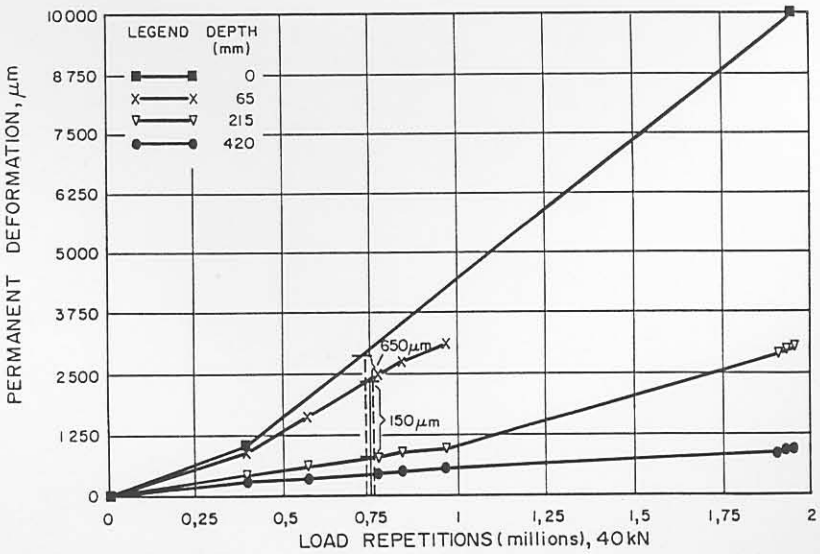

(c) MDD12

FIGURE B.1

PERMANENT DEFORMATION AT DIFFERENT DEPTHS AT VARIOUS STAGES OF TRAFFICKING ON HVS TEST SECTION 260A4 (ROAD 1932, ROOIWAL)

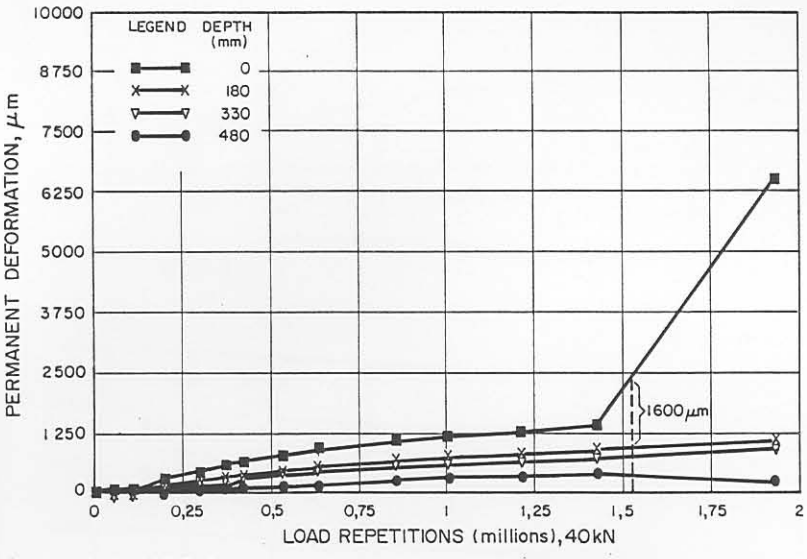

(a) MDD4

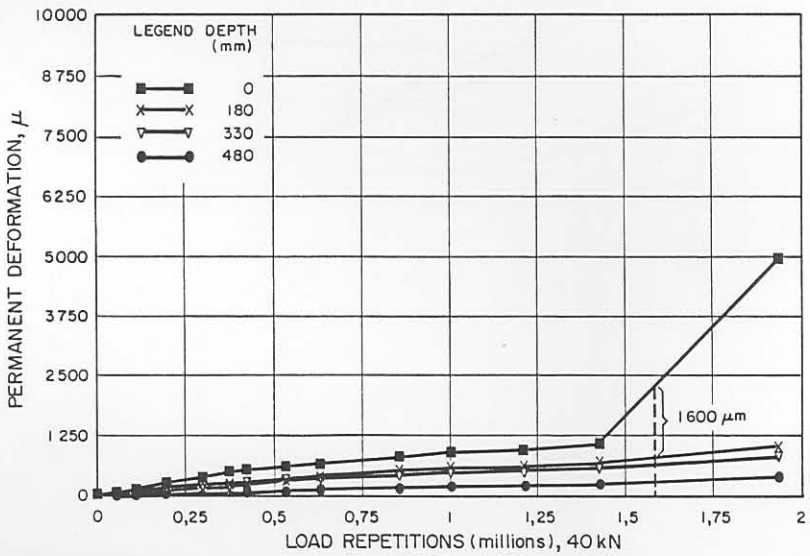

(b) MDD8

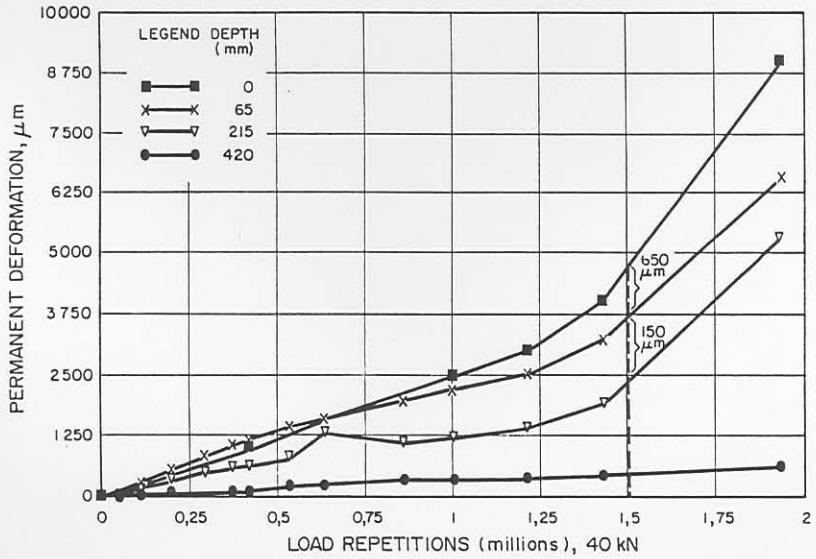

(c) MDD12

FIGURE B.2

PERMANENT DEFORMATION AT DIFFERENT DEPTHS AT VARIOUS STAGES OF TRAFFICKING ON HVS TEST SECTION 275A4 (ROAD 1932, ROODWAL)

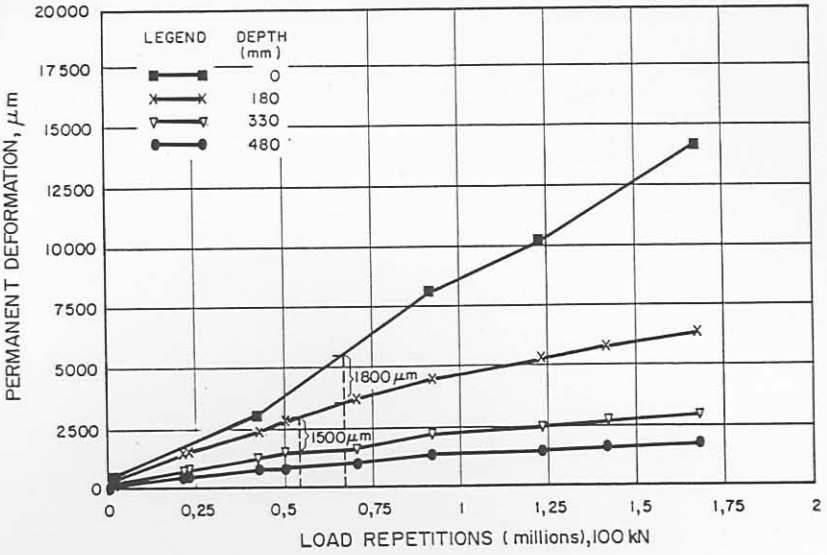

(a) MDD4

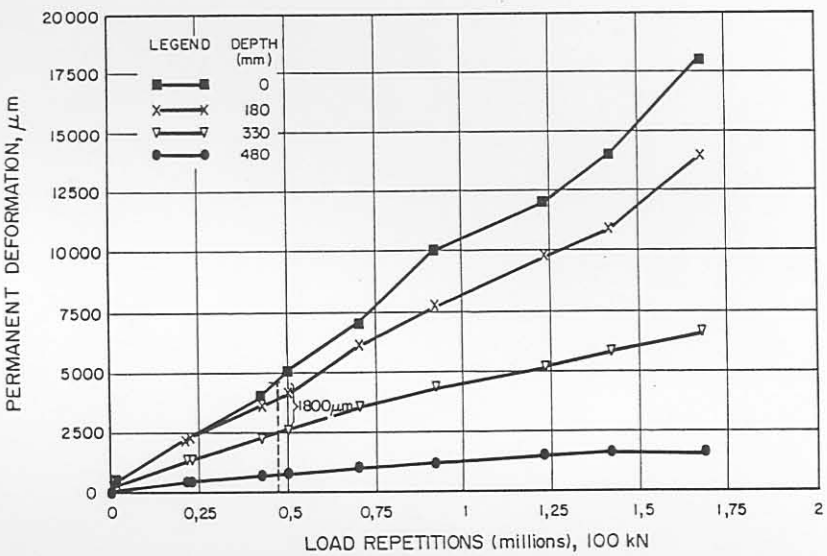

(b) MDD8

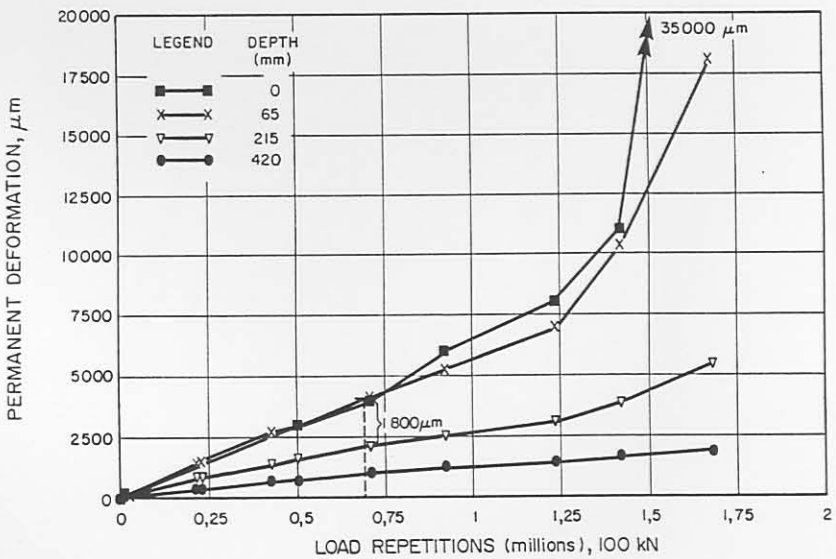

(c) MDD12

FIGURE B.3

PERMANENT DEFORMATION AT DIFFERENT DEPTHS AT VARIOUS STAGES OF TRAFFICKING ON HVS TEST SECTION 294A4 (ROAD 1932, ROOIWAL)

APPENDIX C

ASPECTS OF THE COMPUTER PROGRAMS TO PLOT DCP DATA

PREFACE

The Dynamic cone penetrometer (DCP) was developed for direct evaluation of the in situ strength properties of road pavement layers. Evaluation of the measurements obtained through the use of this instrument is facilitated by a representation in graphic form.

The programs DCPBP or DCPBL, AVEBP or AVEBL and DCPF1 and DCPF2 was developed on the basis of a computer program obtained from Transvaal Roads Department (TRD),(E G Kleyn). It calculates penetration rate (mm/blow), CBR and UCS values for user defined layers. It determines which standard pavement balance curve is closest to the data curve and on the bases of a curve fitting procedure. Further the layers are redefined and new penetration rates and CBR and UCS values are calculated for the redefined layers. (De Beer, et al, 1988 and Chapter 1 of this dissertation)) Two plots are produced, the first shows pavement characteristics, average equivalent strength, a DCP curve (field data), a Balance curve and a Layer Strength Diagram. The second plot shows the deviation from the standard pavement balance curve with depth, a Layer Strength Diagram for redefined layers and penetration rates and CBR and UCS values for the redefined layers.

The programs DCPF1 and DCPF2 are used to plot the sections of the plots that does not change for different data. DCPBP is used for data entry and to process data for single points. AVEBP uses data files created by DCPBP and can produce plots of the average of up to 50 points.

The manual is organised as follows:

- Paragraph C.1 Tells you how to install and run the DCP software.
- Paragraph C.2 Gives background information.
- Paragraph C.3 Discusses the running of DCPF1 and DCPF2.
- Paragraph C.4 Discusses the running of DCPBP.
- Paragraph C.5 Discusses the running of AVEBP.
- Paragraph C.6 Discusses the running of DCPBL and AVEBL.

CONTENTS

LIST OF FIGURES

C.1 GETTING STARTED

Before running a DCP program , make sure you have the following hardware and software:

C.1.1 HARDWARE REQUIREMENTS

- An IBM Personal Computer, or compatible. The DCP programs will run on a single disk drive PC, though ideally the PC should have two floppy disk drives, or one floppy disk and one hard disk.
- A monochrome or colour monitor.
- At least 256 Kbytes of memory.
- A parallel or serial printer, if hard copy is required. For printing speed, a parallel printer is recommended.
- A Math Co-processor (INTEL 8087 chip).
- A plotter that interfaces with HP-GL language
  or
- A laser printer with HP-GL capabilities and driver

C.1.2 SOFTWARE REQUIREMENTS

- PC-DOS or MS-DOS, version 2.1 or later.
- An ASCII text file editor, for example MS-DOS/PC-DOS EDIT; EDLIN, or SIDEKICK.

We would recommend that you make a BACK UP COPY of the DCP diskette, using the DOS command DISKCOPY or COPY. Store this backup in a safe place in case something happens to the original diskette.

C.1.3 INSTALLING THE DCP SOFTWARE

The following procedure will create a copy of the DCP programs, either on floppy disk or hard disk. If you are loading DCP from a floppy disk, the installation procedure described below will make a "boot" disk.

A. Dual Floppy Disk computers

Steps (a) to (e) will format a new floppy disk, with your DOS system files and copy the DCP programs onto the disk.

a. Place your DOS diskette in drive A and switch on the PC.

b. When the DOS prompt displays, put a new floppy disk in drive B:

c. Type **FORMAT B:/S** and press <RETURN>.

d. When the disk in drive B: has been formatted, take out your DOS disk from drive A:, and replace it with the original DCP disk.

e. Type **COPY A:*.* B:** and press <RETURN>.

Finally, ensure that your new DCP disk has a CONFIG.SYS file to set up the computers files and buffers. DOS allows by default 3 buffers and 8 files to be open at the same time. It is best to increase this to improve the operating speed of your PC. The CONFIG.SYS file is created by typing:

COPY CON B:CONFIG.SYS	and press <RETURN>
FILES=15	press <RETURN>
BUFFERS=15	press <RETURN>
<CONTROL>Z	press <RETURN>

B. Hard Disk computers

Switch on the computer and boot up on drive C: and ensure that you are in the root directory. Put the original DCP disk in Drive A: and type:

C>MD DCP	press <RETURN> to create a new directory
CD DCP	<RETURN> to change to the new DCP directory.
COPY A:*.* C:	<RETURN> to copy the DCP files.

The comments on the CONFIG.SYS file on the previous page are also relevant if you are running from a hard disk. However, this file, if it does exist, must lie in the hard disk root directory. You would use the following command to create the file if it does not already exist:

C>COPY CON C:\CONFIG.SYS <RETURN>

If the CONFIG.SYS file does exist, it can be changed using your DOS edit program (EDIT, EDLIN or SIDEKICK).

C.1.4 RUNNING THE DCP PROGRAMS

If you have a dual floppy system, and you have installed the DCP programs as described above, place your copy of the DCP disk in drive A and a formatted disk (for data files) in drive B and switch your PC on. Type DCPF1, DCPF2, DCPBP OR AVEBP at the DOS prompt, depending on which program is to be run.

If DCP has been installed on a hard disk, you can go to the DCP directory:
C>CD DCP
and run the required DCP program by typing the name of the program at the DOS prompt.

C.1.5 SETTING UP THE PLOTTER

C.1.5.1 Serial interface between PC and Plotter

If the connection interface between the PC and the Plotter is serial the following procedure must be set up.
Ascertain the baud rate, parity, data bits and the stop bits on the plotter. Using the DOS MODE command type the following before running the program for the first time.

MODE COMn:baud rate,parity,data bits,stop bits,P *
MODE LPT2:=COMn

Where baud rate is 110,150,etc
parity is either E,0,N
data bits is either 7 or 8
stop bits is either 1 or 2
n is either 1 or 2 depending on the serial port number

* refer to the DOS manual for details.

C.1.5.2 Parallel interface between PC and Plotter

If the plotter is connected to a parallel port check whether it is connected to the first or second parallel port. If it is connected to the first parallel port type the following:

MODE LPT2:=LPT1

C.1.5.3 Serial interface between PC and Printer

If the printer is serial ascertain the baud rate, parity, data bits and stop bits and which serial port it is connected to. Using the DOS MODE command set it up as follows:

MODE COMn:baud rate,parity,data bits,stop bit,P
MODE LPT1:=COMn

C.2 BACKGROUND INFORMATION

The DCP programs discussed here are based on original work done by Mr E G Kleyn of the Transvaal Roads Department (TRD). (See list of references at the back of this document). Later work, using some of these original work, as well as adding additional calculations and new concepts was undertaken by Mr M De Beer of the Division of Roads and Transport Technology, CSIR, Pretoria. The most important aspect of the latest work is the development of a DCP-classification system. This system is used to classify DCP data for relatively lightly cementitious and granular base thin surfaced flexible pavements. See De Beer et al., 1988 or Chapter 1 of this dissertation, for a description of the classification system.

These computer programs automatically classify the DCP data using the calculated relevant parameters, A and B, and also calculates:

- average penetration rates in mm/blow
- pavement structural number, DSN_{800}, in blows, which is the actual number of blows to penetrate 800 mm (approximately 31,5 inches) from the surface of the pavement.
- CBR values derived from the following formula :

  If average penetration rate (DN) $\geq$ 2 mm/blow :

  then $CBR = 405,3 \times DN^{(-1,259)}$

  and if DN $\leq$ 2 mm/blow :

  then $CBR = (66,66 \times DN^2) - (330 \times DN) + 563,33$

- UCS values derived from the following formula :

  $UCS = 15 \times CBR^{0,88}$

- Structural capacity in million E80s derived from the following formula :

$$\text{Million Standard Axles (MISA)} = Cm \times (DSN_{800})^{3,5} \times 10^{-9}$$

where Cm = moisture condition = 6,5 for wet
= 14,0 for moist
= 30,0 for optimum (omc)
= 64,0 for dry conditions

These Cm values are automatically taken into account when selecting the general moisture condition during data input phase, see Section C.4.1.

- Balance Number at 100 mm depth, BN_{100}, which is the DSN percentage at a depth of 100 mm of the pavement.

- Standard Pavement Balance Curve (SPBC) B-value for the data, which is the B-value describing the best fit standard pavement balance curve for the data, as is indicated in the second graph on Figures C.3 and C.6.

- Graphical output of penetration rates (See third graph on Figures C.3 and C.6.

- A Normalised curve, which is a summary of the deviation in terms of area versus depth of the DCP-data from the best fit Standard Pavement Balance Curve (SPBC). Maximum and minimum peaks on this curve are indicative of layer interfaces and give the depths where layers of different penetration rates are encountered. Basically the peaks are indicative of the interface between a relatively softer layer (high penetration rate) and a relatively harder layer (low penetration rate) or vice versa. These peaks are then used to redefine the depth and thickness of the different layers on the basis of relative strength in terms of penetration rate. See first graph on Figures C.4, C.8 or C.9.

- Lastly, a layer strength diagram of the redefined layers is given. See Figures C.4, C.8 and C.9.

C.3. DRAWING DCP FORMS

The programs DCPF1 and DCPF2 can be used to produce plots as shown in Figures C.1 and C.2.
These plots can be produced once and photocopied as this constant part of the DCP plots takes quite long to do. Photocopies of the plots can then be used when DCPBP or AVEBP is run. If a plot which is completely drawn by the plotter is required DCPF1 or DCPF2 can be run followed by DCPBP or AVEBP without removing the paper.

C.3.1 RUNNING DCPF1 AND DCPF2

To run the programs type: DCPF1
or DCPF2

The program displays only one prompting message:

PLACE PAPER ON THE PLOTTER
PRESS RETURN WHEN READY TO PLOT

When RETURN is pressed the program will draw the form on the plotter.

C.3.2 OUTPUT

Examples of the forms are shown in Figures C.1 and C.2.

C.4. RUNNING DCPBP

To run the program type: DCPBP

C.4.1 INPUT

A list of the prompting messages generated by the program is given below with explanations of the input required where necessary.

```
DO YOU WANT THE OUTPUT
1....ON THE SCREEN
2....ON THE PRINTER
ENTER 1 OR 2
```

If a 1 is entered the results of the calculations will be displayed on the screen.

If a 2 is entered a file named DCPBOUT will be created and the results of the calculations will be written to this file. This file can then, after the run is completed, be copied to a printer. If the output in the file is to be preserved the file must be renamed before a subsequent run is done as the contents of DCPBOUT will then be overwritten with new output.

```
DO YOU WANT TO:
1....ENTER MANUALLY RECORDED DATA
2....USE AN EXISTING COMPLETE DATA FILE
ENTER THE APPROPRIATE NUMBER
```

If a 2 is entered:

```
ENTER THE NAME OF THE FILE FROM WHICH DATA MUST BE READ
```

If a 1 is entered:

ENTER THE NAME OF THE FILE WHERE THE DATA MUST BE STORED
E.G. B:ABC123.DAT (MAX. DRIVE SPECIFICATION + 6 CHARACTERS + EXTENSION)

The drive specification is optional. If the program is run from drive A on a dual floppy system the data files can be stored on drive B, B: must then be specified when a file name is entered. If omitted the data file will be created on the default drive. If the drive specification is omitted (when a hard disk system is used it is not necessary) the file name can be eight characters long. The first character of the file name **must be a letter** and the last four characters must be .DAT. The name must not contain a character '/' or a '\' or a '.' before the .DAT.

Information about the DCP investigation can now be entered.

ENTER THE NAME OF THE REGION WHERE THE INVESTIGATION WAS DONE
MAXIMUM 34 CHARACTERS

ENTER THE ROAD NUMBER
MAXIMUM 34 CHARACTERS

ENTER THE Km DISTANCE

ENTER THE DATE IN THE FORMAT YY/MM/DD E.G. 84/01/26

```
-----------------------------------------
! SHL !   !   !   ! M !   !   !   ! SHR!
-----------------------------------------
   1    2   3   4   5   6   7   8    9
```

ACCORDING TO THE ABOVE CODE, ENTER POSITION OF DCP TEST ACROSS THE ROAD PROFILE
ENTER A NUMBER BETWEEN 1 AND 9

```
-------------------------------
!  SEVERE   ! WARNING ! SOUND !
!(TERMINAL)!         !       !
-------------------------------
     1           2        3
```

ACCORDING TO THE ABOVE CODE, WHAT IS THE CONDITION OF THE ROAD?
ENTER 1, 2 OR 3

WHICH OF THE FOLLOWING DISTRESS CONDITIONS APPLY TO THE ROAD?
ENTER an upper case Y OR N FOR EACH CONDITION

RUTTING ? (ENTER Y OR N)

DEFORMATION (OTHER THAN RUTTING) ? (ENTER Y OR N)

PUMPING ? (ENTER Y OR N)

CROCODILE CRACKS ? (ENTER Y OR N)

LONGITUDINAL CRACKS ? (ENTER Y OR N)

OTHER CRACKS ? (ENTER Y OR N)

```
-----------------------------------
!  DRY   ! OPTIMUM !  WET   ! SOAKED !
-----------------------------------
    1          2        3         4
```

WHAT IS THE GENERAL MOISTURE CONDITION
UNDER WHICH THE PAVEMENT MUST FUNCTION?
ENTER 1, 2, 3 OR 4

FUNCTIONAL CLASSIFICATION (TPA)

CODE	DESCRIPTION	TRAFFIC(E80S)
1	VERY LIGHT TRAFFIC	<0,1x10**6
2	LIGHT TRAFFIC	0,1-0,2x10**6
3	MEDIUM TRAFFIC	0,2-1,0x10**6
4	HEAVY TRAFFIC	1-3x10**6
5	VERY HEAVY TRAFFIC	3-10x10**6

ENTER 1, 2, 3, 4 OR 5

ENTER THE ROAD CATEGORY A, B OR C

Category A:
E.g. Inter urban freeways and major inter urban roads with a very high level of service. 95th and 5th percentile values used where applicable.
Category B:
E.g. Inter urban collectors, major rural roads and major industrial roads with a high level of service. 90th and 10th percentile values are applicable.
Category C:
E.g. Lightly trafficked rural roads with a moderate level of service. 80th and 20th percentile values are applicable.

DEFAULT IS 5 PAVEMENT LAYERS OF 150mm EACH
IF YOU WANT TO SPECIFY LAYERS (MAXIMUM 10)
ENTER THE NUMBER OF LAYERS YOU WANT TO SPECIFY
TO USE THE DEFAULT PRESS RETURN

If a number between 1 and 10 is entered the user will be prompted to enter the beginning and end of the specified number of layers. **The last layer must not end before the end of the data**. It is preferable to end the last layer at 800 mm.

All the information entered so far will then be displayed in the following format:

```
     ROAD INFORMATION ENTERED
1....REGION                        :
2....ROAD NUMBER                   :
3....DISTANCE                      :
4....DATE                          :
5....POSITION                      :
6....ROAD CONDITION                :
7....RUTTING                       :
8....DEFORMATION (NOT RUTTING)     :
9....PUMPING                       :
10...CROCODILE CRACKS              :
11...LONGITUDINAL CRACKS           :
12...OTHER CRACKS                  :
13...MOISTURE CONDITION            :
14...FUNCTIONAL CLASSIFICATION     :
15...ROAD CATEGORY                 :
16...NUMBER OF LAYERS              :
17...LAYERS:
DATA FILE NAME:

DO YOU WANT TO CHANGE ANY OF THE ABOVE INFORMATION?
TO CHANGE AN ITEM ENTER THE NUMBER NEXT TO IT
FOR NO CHANGE PRESS RETURN
```

If a number is entered, the prompt for the item next to the number will be displayed. The user must then enter the correct information for the item. The display of the information entered will be repeated showing the changed information. When only RETURN is pressed after the display the program will continue.

ENTER THE NUMBER OF DCP POINTS FOR WHICH DATA WILL BE ENTERED
MAXIMUM 300
(PLEASE CHECK DATA, THERE MUST NOT BE MORE THAN ONE DEPTH OF 800 OR MORE)

It is important that **there must not be more than one depth value of 800 or higher**. If more values beyond 800 were recorded it must not be entered.

THE NUMBER OF BLOWS FOR EACH DCP POINT WILL BE INCREMENTED BY 5
IF YOU WANT A DIFFERENT INCREMENT, ENTER THE NEW INCREMENTAL NUMBER
E.G.10
TO USE THE DEFAULT OF 5 PRESS RETURN

The next prompt will then be displayed for the number of points specified. The number of blows will be incremented automatically and displayed each time. Only the depth reading at each point need be entered.

ENTER THE DEPTH (mm) FOR POINT 1
NUMBER OF BLOWS: 0 DEPTH (mm): _

The depths in a set of data must start at 0. If a number larger than 0 is entered for the first depth, the program will deduct this number from all the depths entered to meet this requirement.

When data for all the points are entered the data will be displayed under the following headings:

DCP DATA

POINT NUMBER	NUMBER OF BLOWS	DEPTH

DO YOU WANT TO CHANGE ANY OF THE DCP DATA?
TO CHANGE SINGLE POINTS ENTER 1
TO CHANGE A NUMBER OF CONSECUTIVE POINTS ENTER THE NUMBER OF POINTS TO BE CHANGED
FOR NO CHANGE PRESS RETURN

If a 1 is entered:

ENTER THE NUMBER OF THE POINT YOU WANT TO CHANGE
If a number larger than 1 is entered:

ENTER THE NUMBERS OF THE FIRST AND LAST POINTS TO BE CHANGED
WITH A SPACE BETWEEN THE TWO NUMBERS

Prompts will then be displayed to change the depth of the points specified.

If the last depth entered is less than 800 the following prompts will be displayed:

THE LAST DEPTH IS ___
DO YOU WANT TO:
1...USE THIS DEPTH TO CALCULATE STRUCTURE NUMBER
2...USE THE SLANT OF THE LAST LINE TO ADD POINTS TO A DEPTH OF 800
3...MANUALLY ENTER POINTS TO A DEPTH OF 800
ENTER 1 2 OR 3

The last line referred to is the last line on the DCP curve, see Figure 2.
If the slant calculated is 0, i.e. when the depths of the last points are the same, an error message will be displayed:

THE LAST DEPTHS ARE THE SAME THEREFORE SLANT CAN NOT BE CALCULATED
DELETE LAST FEW DEPTHS FROM THE DATA FILE OR ADD POINTS MANUALLY
REMEMBER TO CHANGE THE NUMBER OF POINTS (LINE 3 OF THE DATA FILE)
IF YOU DELETE POINTS
ENTER:
1...TO END PROGRAM AND EDIT FILE WITH ASCII FILE EDITOR
2...TO ADD POINTS MANUALLY THROUGH THE PROGRAM

If option 1 is selected to delete points from the data file it can be edited using an ASCII text file editor. If option 2 is selected the prompt displayed will be:

LAST NUMBER OF BLOWS IS ___ LAST DEPTH IS ___
HOW MANY MORE POINTS DO YOU WANT TO ADD?
MAXIMUM ___ CAN BE ADDED

When a number is added prompts to enter this number of points will be displayed.

If there is very little difference between the last few points in the data, the calculated number of points to be added may exceed the limit of 300. If this happens the following message will be displayed:

THE NUMBER OF POINTS TO BE ADDED IS TOO LARGE
ADDITIONAL POINTS WILL HAVE TO BE ADDED MANUALLY

This message will be followed by the prompt for the number of points to be added as above.

When the data entry is completed or when an existing file is used the program will display:

CALCULATING BALANCE CURVE

DO YOU WANT TO PLOT THE DCP CURVE, BALANCE CURVE
AND LAYER STRENGTH DIAGRAM
ENTER Y OR N

If a Y is entered a plot as shown in Figure 3 will be produced after display of the following message:

PLEASE PLACE PAPER ON THE PLOTTER
PRESS RETURN WHEN READY TO PLOT

The DCP curve and Balance curve will be drawn. Before the Layer Strength Diagram is drawn the following prompt will be displayed:

DO YOU WANT TO PLOT:
1...SINGLE POINTS
2...POINTS IN GROUPS OF FIVE
3...LAYERS
4...MEAN PENETRATION/LAYER AND PERCENTILE VALUES
ENTER 1 2 3 OR 4

If a 1 is entered the value for each data point (as measured) will be plotted on the layer strength diagram.

If a 2 is entered average values for groups of five data points will be plotted.

If a 3 or 4 is entered:

DO YOU WANT TO REDEFINE THE LAYERS?
(THE LAST LAYER MUST NOT END BEFORE THE END OF THE DATA)
ENTER Y OR N

If a Y is entered:

ENTER THE NUMBER OF LAYERS
MAXIMUM 10

ENTER THE BEGINNING AND END OF LAYER 1 WITH A SPACE BETWEEN THE TWO NUMBERS E.G. 0 125

This prompt will be repeated for the number of layers specified.

The layer strength diagram will then be drawn and the plot completed.

DO YOU WANT TO PLOT THE NORMALISED CURVE AND
LAYER STRENGTH DIAGRAM AND AVERAGE EQUIVALENT
STRENGTH FOR REDEFINED LAYERS?
ENTER Y OR N

If a Y is entered a plot as shown in Figure 4 will be produced after display of the following messages:

PLEASE PREPARE THE PLOTTER
PRESS RETURN WHEN READY TO PLOT

DO YOU WANT TO PLOT:
1...LAYERS
2...MEAN PENETRATION/LAYER AND PERCENTILE VALUES
ENTER 1 OR 2

The second plot will then be drawn.

DO YOU WANT TO DO ANOTHER CALCULATION
ENTER Y OR N

If a Y is entered the program will run again from the beginning.
If a N is entered the program will end.

C.4.2 **OUTPUT**

The program will write a curve fitting table with DCP category classification, an average equivalent strength table for the user defined layers, a table of DCP penetration rate with CBR and UCS values, an average equivalent strength table for redefined layers and a summary of + and - areas (Normalised curve) to a file named DCPBOUT. This file can be copied to a printer to obtain a printed output. If the output file is to be preserved it must be renamed before the next run of DCPBP as DCPBOUT will be overwritten. An example of the printed output of DCPBP is shown in Figure C.5.

The program can produce two plots. An example of the first plot is shown in Figure C.3. The second plot is shown in Figure C.4.

C.5. RUNNING AVEBP

To run the program type: AVEBP

C.5.1 INPUT

The prompting messages displayed by AVEBP is given below with explanations of the input required where necessary.

ENTER THE NUMBER OF SETS OF DATA YOU WANT TO USE
MAXIMUM 50

ENTER THE NAME OF DATA FILE 1

This prompt will be repeated for the number of files specified above. If a file is not found an error message will be displayed giving the name of the file and the IBM Professional FORTRAN error number:

FILE _____ NOT FOUND ___

ENTER THE NUMBER OF LAYERS (MAXIMUM 10)

ENTER THE BEGINNING AND END OF LAYER 1 WITH A SPACE BETWEEN THE NUMBERS
E.G. 0 125

This prompt will be repeated for the number of layers specified.

DO YOU WANT TO PLOT THE DCP CURVE, BALANCE CURVE
AND LAYER STRENGTH DIAGRAM
ENTER Y OR N

If a Y is entered:

PLEASE PREPARE THE PLOTTER
PRESS ANY KEY WHEN READY TO PLOT

A number of options can be selected to determine what the plots will show:

DO YOU WANT TO PLOT:
1...ALL LAYER STRENGTH DIAGRAMS, AND AVERAGE VALUES ON OTHER DIAGRAMS
2...AVERAGE VALUES ON ALL DIAGRAMS
3...AVERAGE AND PERCENTILE VALUES ACCORDING TO ROAD CATEGORIES ON ALL DIAGRAMS
4...AVERAGE AND 95, 90, 80, 20, 10 AND 5 TH PERCENTILE VALUES ON BALANCE AND NORMALISED CURVES
5...ONLY AVERAGE NORMALISED CURVE AND REDEFINED LAYER STRENGTH DIAGRAM
ENTER 1 2 3 OR 4

If option 1 is selected:
The Layer Strength Diagram on plot one will show the layer strength diagrams for all the data sets as well as an average layer strength diagram, all drawn on the same diagram. The rest of the diagrams will show only average values.

If option 2 is selected:
All diagrams on both plots will show only average values.

If option 3 is selected:
Plot one will show an average DCP curve as well as a Balance Curve and Layer Strength Diagram showing the average values and the 95th and 5th percentile or the 90th and 10th percentile or the 80th and 20th percentile, according to the road category specified for the last data file entered. The Normalised Curve and Layer Strength Diagram on plot two will show average and percentile values according to the road category.

If option 4 is selected:
The Balance Curve on plot one and the Normalised Curve on plot two will show the average values and the 95th, 90th, 80th, 20th, 10th and 5th percentile values. The other diagrams will show average values.

If option 5 is selected:
This option can be used when only plot two is required. It will show only average values on both diagrams.

DO YOU WANT TO PLOT ON LAYER STRENGTH DIAGRAM
1...EVERY MILLIMETRE
2...LAYERS
ENTER 1 OR 2

CALCULATING BALANCE TABLE

If the option to draw plot one is selected:

The diagrams on plot one will be drawn.

ENTER A FILE IDENTIFICATION (MAX 30 CHARACTERS)

The string entered here will be written on the plot to indicate which files were used.
The first plot will then be completed.

DO YOU WANT TO DRAW THE NORMALISED CURVE AND
LAYER STRENGTH DIAGRAM AND AVERAGE EQUIVALENT
STRENGTH FOR REDEFINED LAYERS
ENTER Y OR N

If a Y is entered:

PLEASE PREPARE THE PLOTTER
PRESS ANY KEY WHEN READY TO PLOT

The second plot will then be drawn.

DO YOU WANT TO:
1...DO ANOTHER RUN WITH THE SAME DATA FILES
2...DO ANOTHER RUN WITH NEW DATA FILES
3...END THE PROGRAM

If option 1 is selected another run can be done without the user having to enter all the file names again if they are not changed.

C.5.2 **OUTPUT**

The program will write information about the DCP investigation, a curve fitting table with category classification, an average equivalent strength table for the user defined layers, a table of DCP penetration rate with CBR and UCS values, an average equivalent strength table for redefined layers and a summary of + and - areas to a file named AVEBOUT. This file can be copied to a printer to obtain a printed output. If the output file is to be saved it must be renamed before the next run of AVEBP as it will be overwritten. An example of the printed output is shown in Figure C.10.

AVEBP can produce two plots. Examples of the first plot for different options are shown in Figures C.6 and C.7. Examples of the second plot for different options are shown in Figures C.8 and C.9.

C.6 RUNNING DCPBL AND AVEBL

The versions of the programs ending with a L is prepared to write the HP-GL commands to an output file which can then be used by a laser plotter interface program to produce the plots on a laser printer.
The programs were tested using the package 'LaserPlotter' of Insight Development Corporation.

The programs are run as described in the preceding paragraphs, except for the fact that it prompts the user for a output file name for each of the two plots.

C.7 REFERENCES

KLEYN, E G, MAREE, J H and SAVAGE, P F, 1982. "Application of a Portable Pavement Dynamic Cone Penetrometer to determine in situ Bearing Properties of Road Pavement Layers and Subgrades in South Africa." Proceedings of the Second European Symposium on Penetration Testing, 24-27 May 1982, Amsterdam, 1982.

KLEYN, E G and SAVAGE, P F, 1982. "The application of the Pavement DCP to determine the Bearing Properties and Performance of Road Pavements." International Symposium on Bearing Capacity of Roads and Airfields, 23-25 June 1982, Trondheim, Norway, 1982.

KLEYN, E G, VAN HEERDEN, M J J and ROSSOUW, A J, 1982. "An Investigation to determine the Structural Capacity and Rehabilitation Utilization of a Road Pavement using the Pavement Dynamic Cone Penetrometer." International Symposium on Bearing Capacity of Roads and Airfields, 23-25 June 1982, Trondheim, Norway, 1982.

KLEYN, E G, DE WET, L F and SAVAGE, P F, 1987. The Development of an Equation for the Strength- Balance of Road Pavement Structures. Transvaal Provincial Administration, Roads Branch, Report L7/87, PRETORIA, 1987.

KLEYN, E G, 1984. Aspects of Pavement Evaluation and Design as determined with the Dynamic Cone Penetrometer. M Eng thesis (in Afrikaans), Faculty of Engineering, University of Pretoria, Pretoria, 1984.

DE BEER M, KLEYN E G and SAVAGE P F, 1988. Towards a classification system for the strength-balance of thin surfaced flexible pavements. Eighth Quinquennial convention of SAICE in co-operation with the Annual Transportation Convention (ATC 1988), Session 3D, 4 - 8 July 1988, University of Pretoria, South Africa, 1988.

C.9 FIGURES

ATT. CSIR, SA

SUMMARY OF DCP INVESTIGATION

DATA FILE :
REGION :
ROAD NUMBER :
DISTANCE :
POSITION : L | | | M | | | R
CONDITION : FAILED | OVERSTRESSED | SOUND
RUT. | DEFORM. | PUMP. | CRACKS : CROCK. | LONG. | OTHER
DATE :

PAVEMENT CHARACTERISTICS

STRUCTURE NUMBER :
BALANCE NUMBER :
DIFFERENCE IN BN100 :
BALANCE CURVE IS WHERE B =
STRUCT. CAP. (E80 X 10^6) :
ROAD CATEGORY :
TRAFFIC :

AVERAGE EQUIVALENT STRENGTH

FROM - TO	AV. PENETRATION	SD	P	CBR	UCS

DCP CURVE

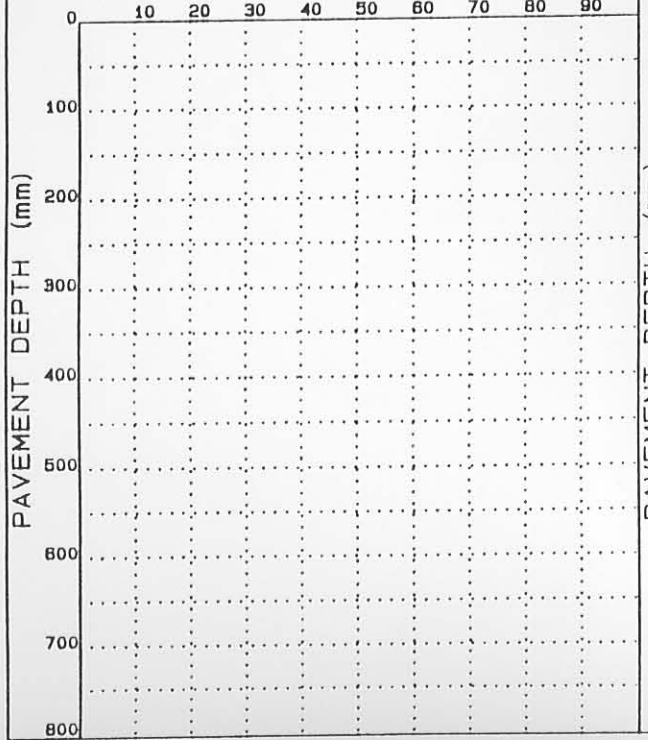

BALANCE CURVE

(-90 ≤ B ≤ +90)

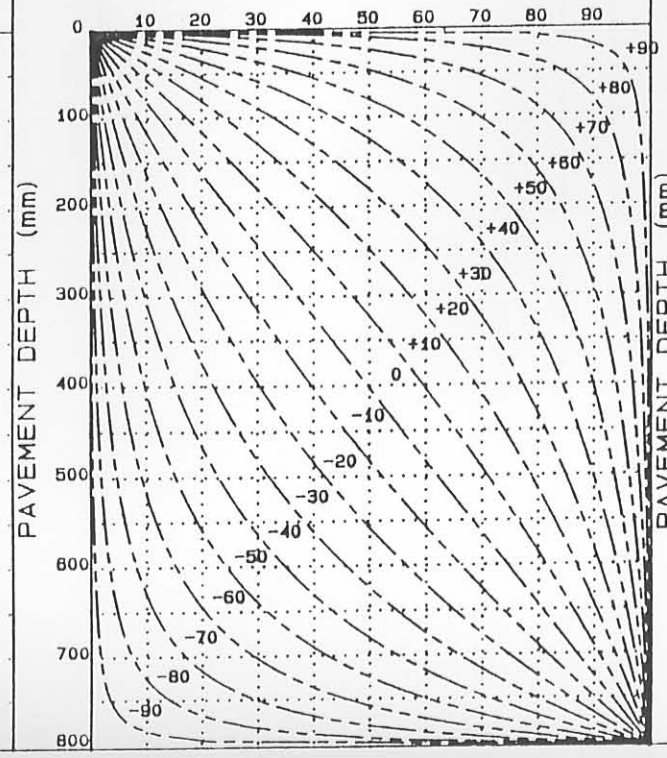

LAYER STRENGTH DIAGRAM

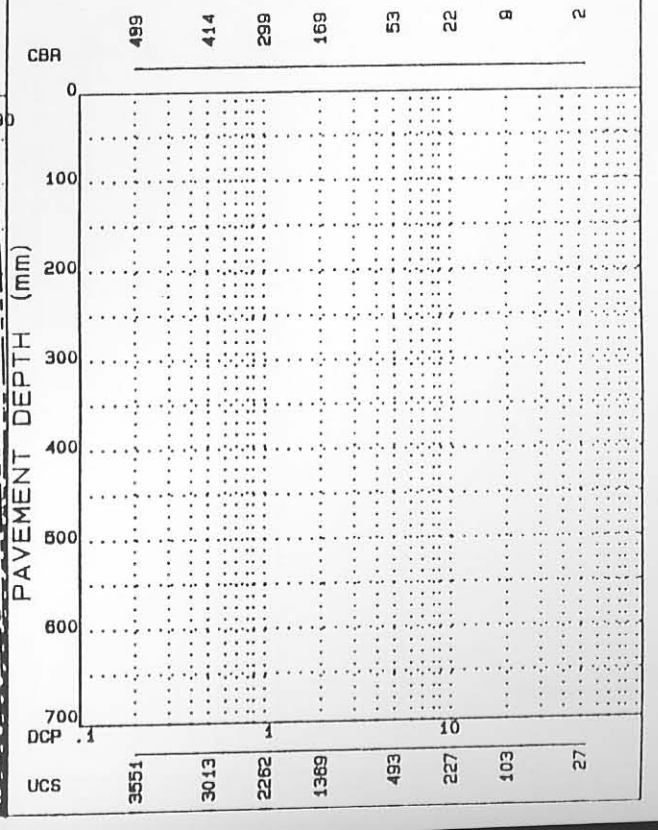

Figure C.1 Example of form produced by DCPFL

RTT, CSIR, SA

SUMMARY OF DCP INVESTIGATION

AVERAGE EQUIVALENT STRENGTH (REDEFINED)

EBOM - IO AV. PENETRATION SD P CBR% UCS (kPa)
(mm) (mm/blow)

DATA FILE:

NORMALIZED CURVE

DEVIATION (A_i) FROM STANDARD PAVEMENT BALANCE CURVE (SPBC), %.mm

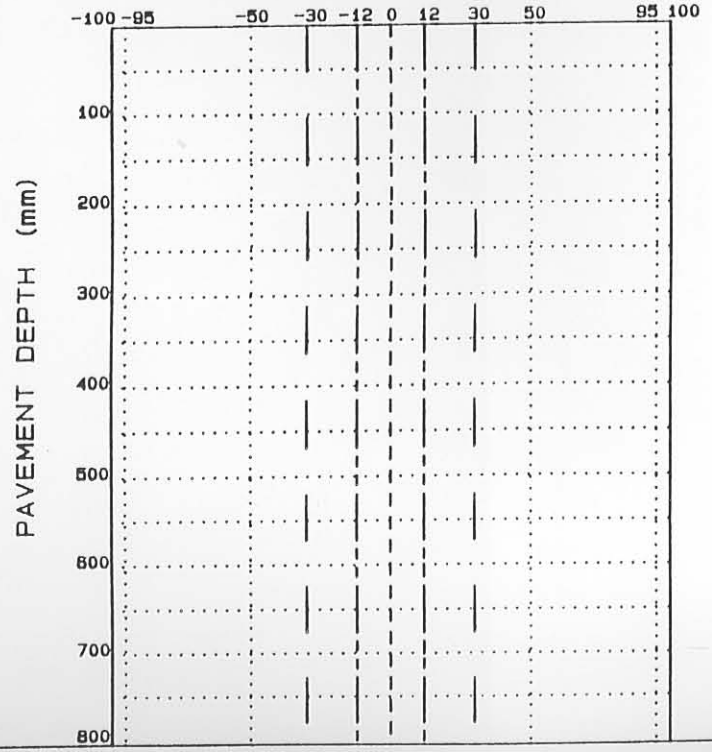

LAYER STRENGTH DIAGRAM (REDEFINED)

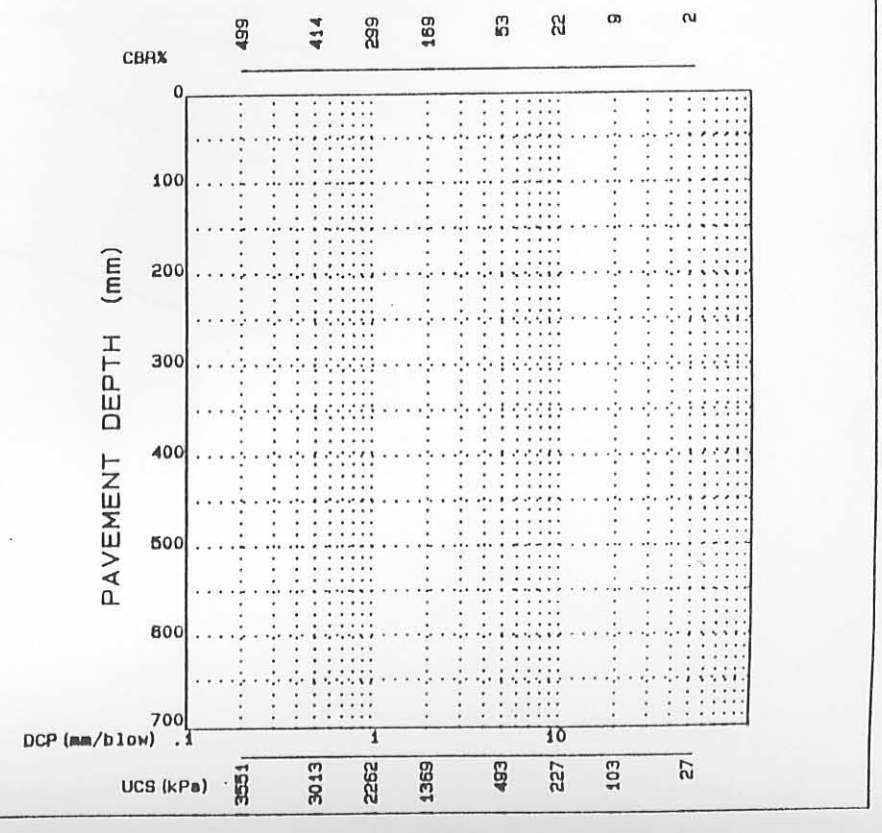

Figure C.2 Example of form produced by DCPF2

ATT, CSIR, SA

SUMMARY OF DCP INVESTIGATION

DATA FILE : R3.DAT
REGION : RODIWAL (N=10)
ROAD NUMBER : P1932
DISTANCE : 2.9
POSITION : L | M | R
CONDITION : FAILED | OVERSTRESSED | SOUND
BST. | DEFORM. | PUMP. | CRACKS : BROCK | LONG. | OTHER
DATE : 85/06/06

PAVEMENT CHARACTERISTICS

	DATA	B/CURVE
STRUCTURE NUMBER :	382	
BALANCE NUMBER (BN 100) :	29	22
DIFFERENCE IN BN100 :	7	
BALANCE CURVE IS WHERE B =	17	A= 2515
STRUCT. CAP. (E80 X 10^6) :	>10	*
ROAD CATEGORY :	C	

TRAFFIC : LIGHT TRAFFIC
* Structural capacity not reliable

AVERAGE EQUIVALENT STRENGTH

FROM - TO	AV. PENETRATION	SD	80 P	CBR	UCS
0-180	1.2	0.6	1.7	267	2048
181-330	2.2	0.4	2.6	150	1233
331-480	2.4	0.8	3.1	134	1116
481-600	5.0	1.0	5.9	52	485
601-800	2.6	1.2	3.6	122	1028

CATEGORY V : AVERAGELY BALANCED DEEP STRUCTURE (ABD)

DCP CURVE

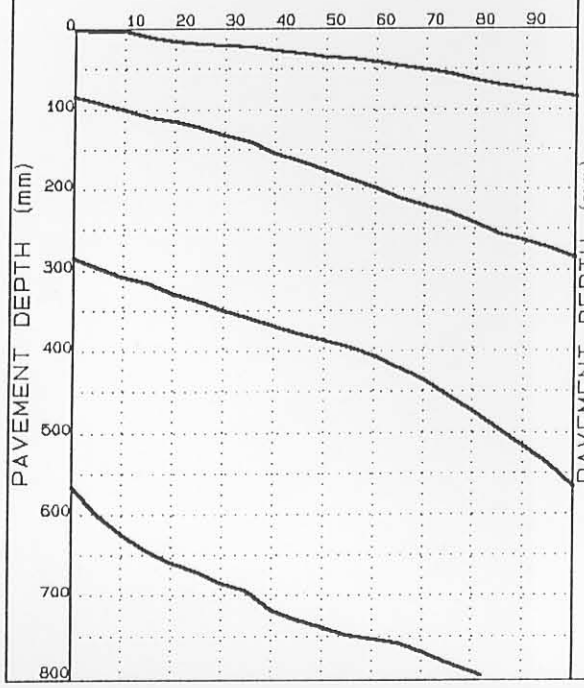

BALANCE CURVE

(DSN 800) (−90 ≤ B ≤ +90)
% OF PAVEMENT STRUCTURE NUMBER

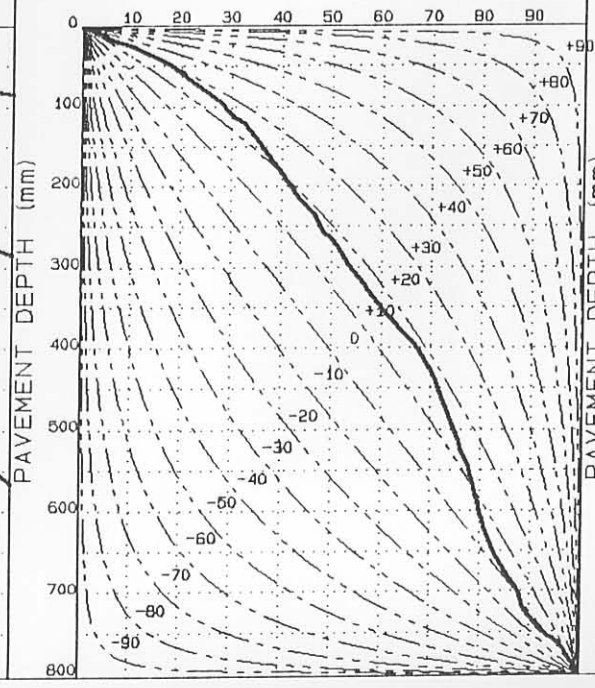

LAYER STRENGTH DIAGRAM

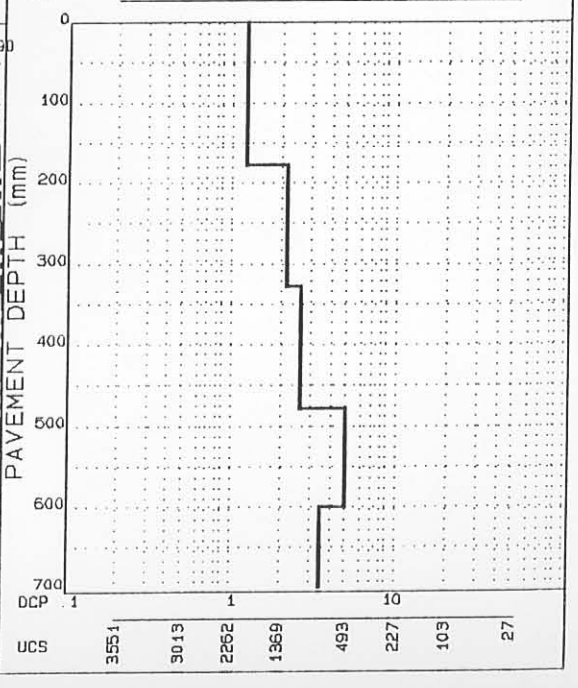

Figure C.3 Example of first plot produced by DCPBP

ATT. CSIR. SA

SUMMARY OF DCP INVESTIGATION

AVERAGE EQUIVALENT STRENGTH (REDEFINED)

FROM - TO (mm)	AV. PENETRATION (mm/blow)	SD	BOP	CBR%	UCS (kPa)
0- 88	0.9	0.4	1.2	330	2468
89-248	2.0	0.5	2.3	173	1398
249-264	2.2	1.1	3.2	150	1233
265-328	2.2	0.3	2.4	153	1254
329-400	2.0	0.3	2.3	171	1383
401-640	4.2	1.3	5.2	67	606
641-696	2.8	0.8	3.6	110	938
697-800	2.2	1.1	3.2	146	1204

DATA FILE: R3.DAT

NORMALIZED CURVE

DEVIATION (A_i) FROM STANDARD PAVEMENT BALANCE CURVE (SPBC), %.mm

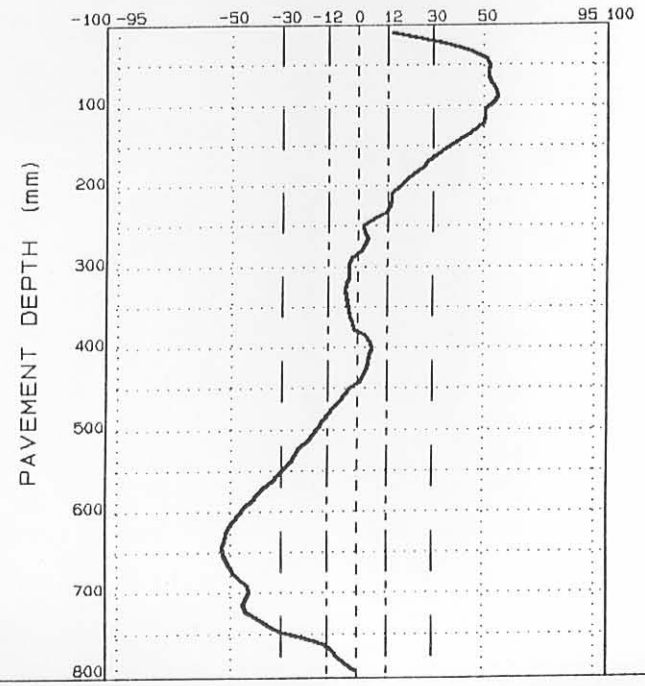

LAYER STRENGTH DIAGRAM (REDEFINED)

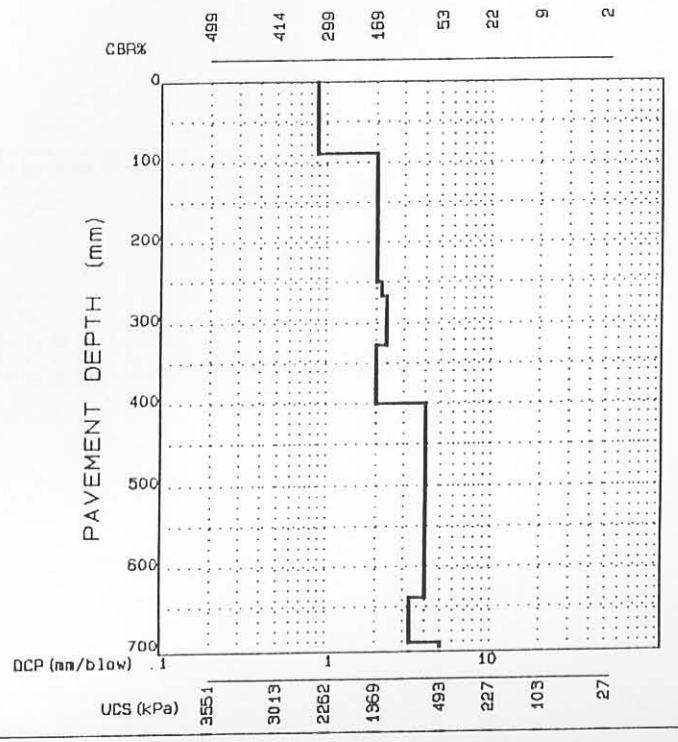

Figure C.4 Example of second plot produced by DCPBP

DCP INVESTIGATION

DATA FILE NAME : R3.DAT

REGION : ROOIWAL(N=10)
ROAD NUMBER : P1932
Km DISTANCE : 2.9
DATE : 85/06/06
STRUCTURE NUMBER (DSN 800) : 382
BALANCE NUMBER (BN 100) OF DATA : 29
BN 100 OF BALANCE CURVE : 22
STRUCTURAL CAPACITY(E80 x10**6) : 32.7 (TPA method (Kleyn)) *
ROAD CATEGORY : C
TRAFFIC : LIGHT TRAFFIC

BALANCE CURVE IS WHERE B = 17 A = 2515 , RK = 811

CATEGORY V: AVERAGELY BALANCED DEEP STRUCTURE (ABD)

KATEGORIE V: REDELIK GEBALANSEERDE DIEPSTRUKTUUR (RGD)

AVERAGE EQUIVALENT STRENGTH (Existing structure)

FROM - TO (mm)	AV.PENETRATION (mm/blow)	SD	80P	CBR%	UCS (kPa)
0 - 180	1.2	0.6	1.7	267	2048
181 - 330	2.2	0.4	2.6	150	1233
331 - 480	2.4	0.8	3.1	134	1116
481 - 600	5.0	1.0	5.9	52	485
601 - 800	2.6	1.2	3.6	122	1028

DCP PENETRATION RATE

	DEPTH(mm)	NO OF BLOWS	mm/BLOW	CBR%	UCS (kPa)
DCP (0 - 2)	2	5	0.4	441	3185
DCP (2 - 2)	2	10	0.0	563	3949
DCP (2 - 10)	10	15	1.6	205	1623
DCP (10 - 15)	15	20	1.0	299	2262
DCP (15 - 18)	18	25	0.6	389	2852
DCP (18 - 20)	20	30	0.4	441	3185
DCP (20 - 22)	22	35	0.4	441	3185
DCP (22 - 26)	26	40	0.8	341	2540
DCP (26 - 30)	30	45	0.8	341	2540
DCP (30 - 34)	34	50	0.8	341	2540
DCP (34 - 36)	36	55	0.4	441	3185
DCP (36 - 40)	40	60	0.8	341	2540
DCP (40 - 46)	46	65	1.2	263	2021
DCP (46 - 50)	50	70	0.8	341	2540
DCP (50 - 56)	56	75	1.2	263	2021
DCP (56 - 63)	63	80	1.4	231	1803
DCP (63 - 70)	70	85	1.4	231	1803

Figure C.5 Example of printout of DCPBP

DCP (70 - 74)	74	90	0.8	341	2540
DCP (74 - 80)	80	95	1.2	263	2021
DCP (80 - 85)	85	100	1.0	299	2262
DCP (85 - 92)	92	105	1.4	231	1803
DCP (92 - 100)	100	110	1.6	205	1623
DCP (100 - 110)	110	115	2.0	169	1369
DCP (110 - 115)	115	120	1.0	299	2262
DCP (115 - 122)	122	125	1.4	231	1803
DCP (122 - 132)	132	130	2.0	169	1369
DCP (132 - 141)	141	135	1.8	185	1483
DCP (141 - 154)	154	140	2.6	121	1020
DCP (154 - 165)	165	145	2.2	150	1233
DCP (165 - 176)	176	150	2.2	150	1233
DCP (176 - 187)	187	155	2.2	150	1233
DCP (187 - 198)	198	160	2.2	150	1233
DCP (198 - 210)	210	165	2.4	134	1116
DCP (210 - 220)	220	170	2.0	169	1369
DCP (220 - 228)	228	175	1.6	205	1623
DCP (228 - 241)	241	180	2.6	121	1020
DCP (241 - 256)	256	185	3.0	101	870
DCP (256 - 263)	263	190	1.4	231	1803
DCP (263 - 273)	273	195	2.0	169	1369
DCP (273 - 285)	285	200	2.4	134	1116
DCP (285 - 298)	298	205	2.6	121	1020
DCP (298 - 308)	308	210	2.0	169	1369
DCP (308 - 317)	317	215	1.8	185	1483
DCP (317 - 330)	330	220	2.6	121	1020
DCP (330 - 340)	340	225	2.0	169	1369
DCP (340 - 350)	350	230	2.0	169	1369
DCP (350 - 360)	360	235	2.0	169	1369
DCP (360 - 370)	370	240	2.0	169	1369
DCP (370 - 380)	380	245	2.0	169	1369
DCP (380 - 387)	387	250	1.4	231	1803
DCP (387 - 396)	396	255	1.8	185	1483
DCP (396 - 407)	407	260	2.2	150	1233
DCP (407 - 421)	421	265	2.8	110	938
DCP (421 - 436)	436	270	3.0	101	870
DCP (436 - 455)	455	275	3.8	75	670
DCP (455 - 474)	474	280	3.8	75	670
DCP (474 - 497)	497	285	4.6	59	542
DCP (497 - 518)	518	290	4.2	66	598
DCP (518 - 540)	540	295	4.4	62	566
DCP (540 - 567)	567	300	5.4	48	452
DCP (567 - 600)	600	305	6.6	37	359
DCP (600 - 625)	625	310	5.0	53	493
DCP (625 - 646)	646	315	4.2	66	598
DCP (646 - 660)	660	320	2.8	110	938
DCP (660 - 672)	672	325	2.4	134	1116
DCP (672 - 685)	685	330	2.6	121	1020
DCP (685 - 695)	695	335	2.0	169	1369
DCP (695 - 720)	720	340	5.0	53	493
DCP (720 - 730)	730	345	2.0	169	1369
DCP (730 - 740)	740	350	2.0	169	1369
DCP (740 - 750)	750	355	2.0	169	1369
DCP (750 - 755)	755	360	1.0	299	2262
DCP (755 - 760)	760	365	1.0	299	2262
DCP (760 - 770)	770	370	2.0	169	1369
DCP (770 - 783)	783	375	2.6	121	1020
DCP (783 - 795)	795	380	2.4	134	1116
DCP (795 - 800)	800	382	2.5	127	1065

AVERAGE EQUIVALENT STRENGTH (Redefined layers)

LAYER	DEPTH (mm) FROM - TO	THICKNESS (mm)	DN mm/blow	SD mm/blow	CBR%	UCS (kP
1	0 - 88	88	0.9	0.4	330	2468
2	89 - 248	160	2.0	0.5	173	1398
3	249 - 264	16	2.2	1.1	150	1233
4	265 - 328	64	2.2	0.3	153	1254
5	329 - 400	72	2.0	0.3	171	1383
6	401 - 640	240	4.2	1.3	67	606
7	641 - 696	56	2.8	0.8	110	938
8	697 - 800	104	2.2	1.1	146	1204

* TRH 14 and Kleyn M Ing

SUMMARY OF + AND - AREAS (CURVE FITTING TABLE - Existing structure)

DEPTH (mm) FROM - TO	CUMULATIVE AREA (% mm),Ak
0 280	1075.06
281 376	-41.66
377 440	30.46
441 792	-1368.32
ABSOLUTE AREA	2515.49

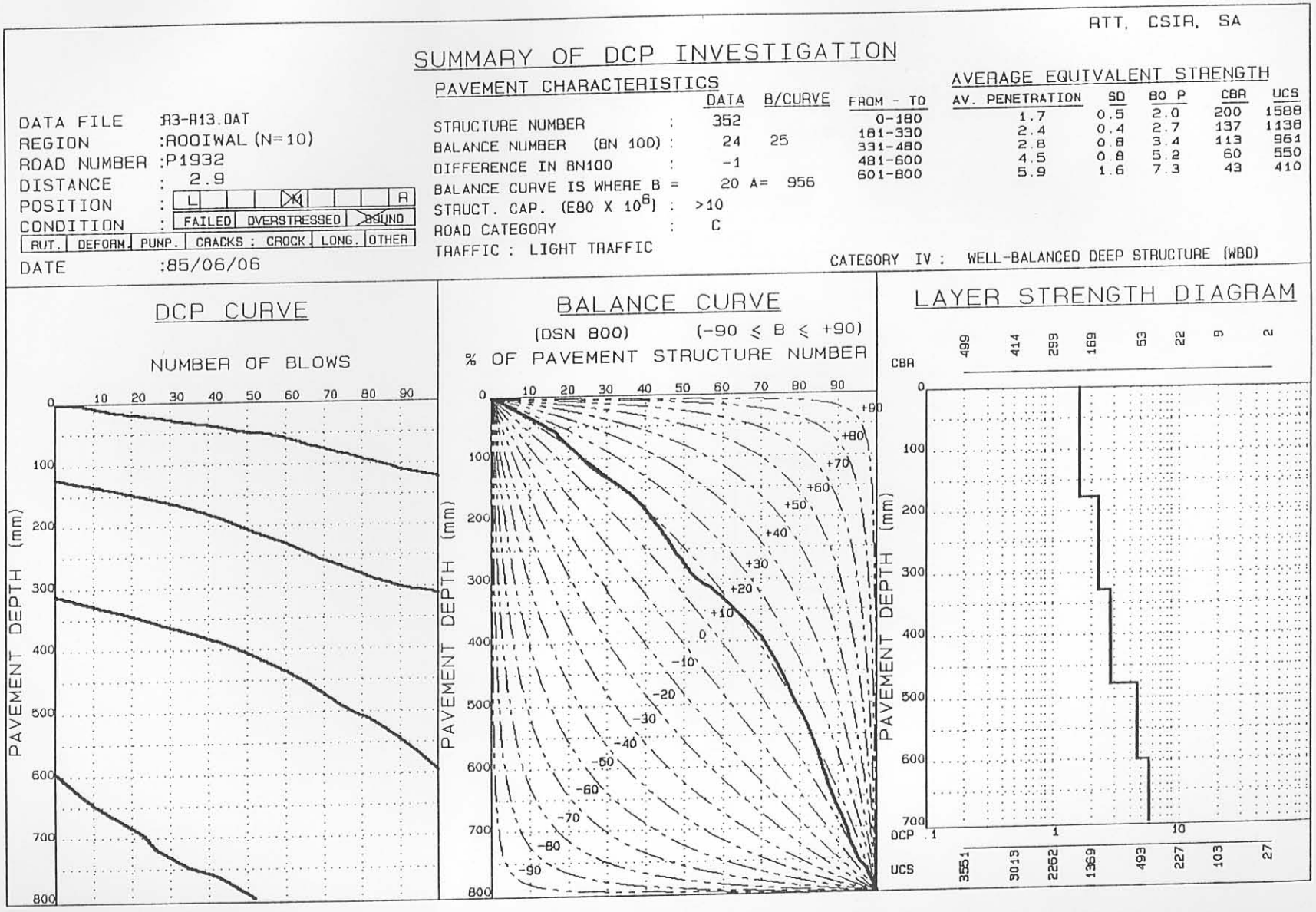

Figure C.6 Example of first plot produced by AVEBP

RTT, CSIR, SA

SUMMARY OF DCP INVESTIGATION

DATA FILE :R3-R13.DAT
REGION :ROOIWAL (N=10)
ROAD NUMBER :P1932
DISTANCE : 2.9
POSITION : L ⋈ R
CONDITION : FAILED | OVERSTRESSED | SOUND
RUT. | DEFORM. | PUMP. | CRACKS : CROCK. | LONG. | OTHER
DATE :85/06/06

PAVEMENT CHARACTERISTICS

	DATA	B/CURVE
STRUCTURE NUMBER :	352	
BALANCE NUMBER (BN 100) :	24	25
DIFFERENCE IN BN100 :	-1	
BALANCE CURVE IS WHERE B =	20 A=	956
STRUCT. CAP. (E80 X 10^6) :	>10	
ROAD CATEGORY :	C	
TRAFFIC : LIGHT TRAFFIC		

FROM - TO
0-180
181-330
331-480
481-600
601-800

AVERAGE EQUIVALENT STRENGTH

AV. PENETRATION	SD	80 P	CBR	UCS
1.7	0.5	2.0	200	1588
2.4	0.4	2.7	137	1138
2.8	0.8	3.4	113	961
4.5	0.8	5.2	60	550
5.9	1.6	7.3	43	410

CATEGORY IV : WELL-BALANCED DEEP STRUCTURE (WBD)

DCP CURVE

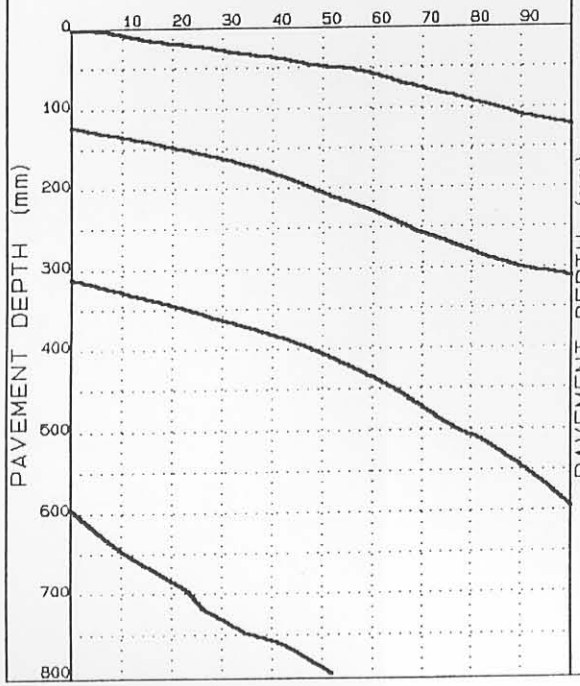

BALANCE CURVE

(DSN 800) (-90 ≤ B ≤ +90)
% OF PAVEMENT STRUCTURE NUMBER

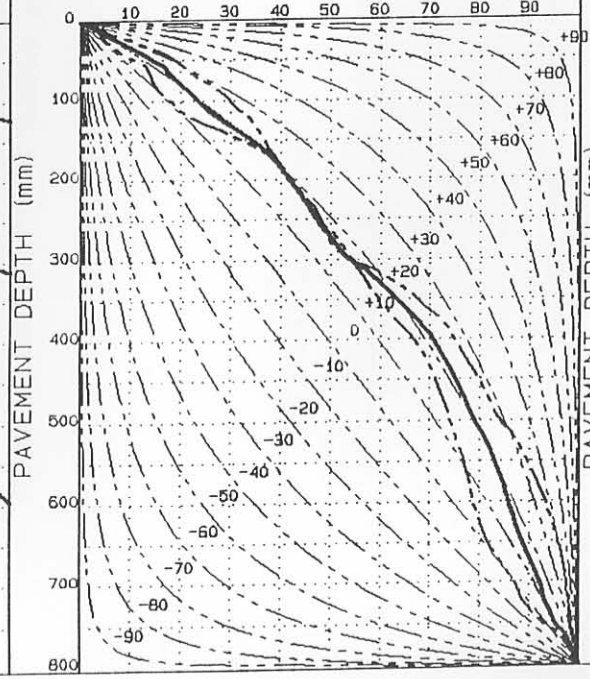

LAYER STRENGTH DIAGRAM

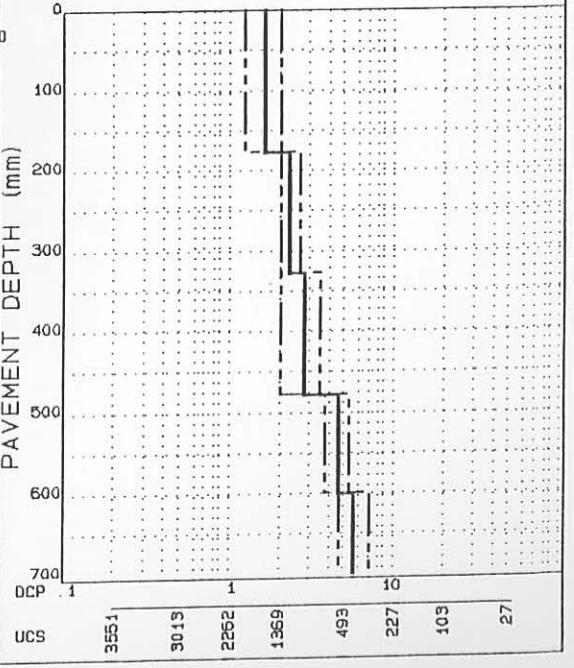

Figure C.7 Example of first plot produced by AVEBP

ATT, CSIR, SA

SUMMARY OF DCP INVESTIGATION

AVERAGE EQUIVALENT STRENGTH (REDEFINED)

FROM - TO (mm)	AV. PENETRATION (mm/blow)	SD	80P	CBR%	UCS (kPa)
0- 48	1.2	0.3	1.5	257	1980
49-112	2.0	0.5	2.4	170	1376
113-160	1.5	0.2	1.7	214	1685
161-280	2.5	0.4	2.8	130	1087
281-400	2.0	0.4	2.3	171	1383
401-496	3.5	0.5	4.0	83	732
497-512	3.3	0.3	3.5	91	794
513-648	4.9	0.6	5.5	54	501
649-688	5.0	0.7	5.6	53	493
689-800	6.6	1.9	8.1	37	359

DATA FILE: R3-R13.DAT

NORMALIZED CURVE

DEVIATION (A_i) FROM STANDARD PAVEMENT BALANCE CURVE (SPBC), %.mm

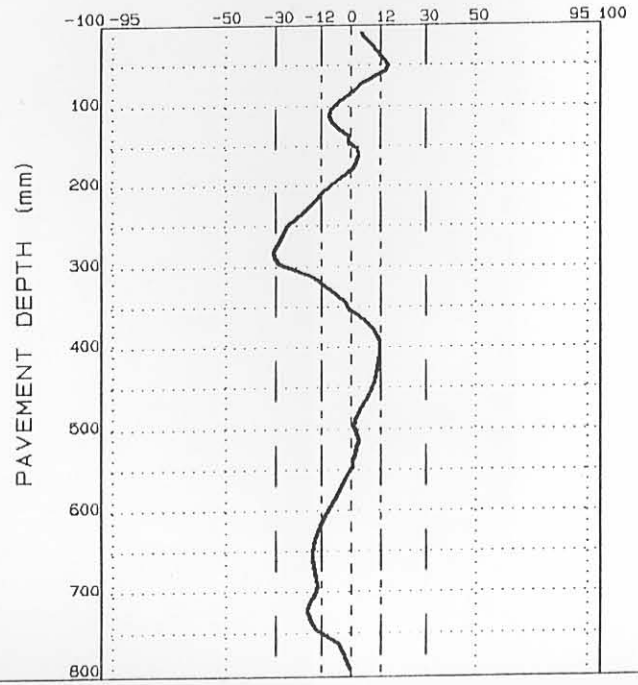

LAYER STRENGTH DIAGRAM (REDEFINED)

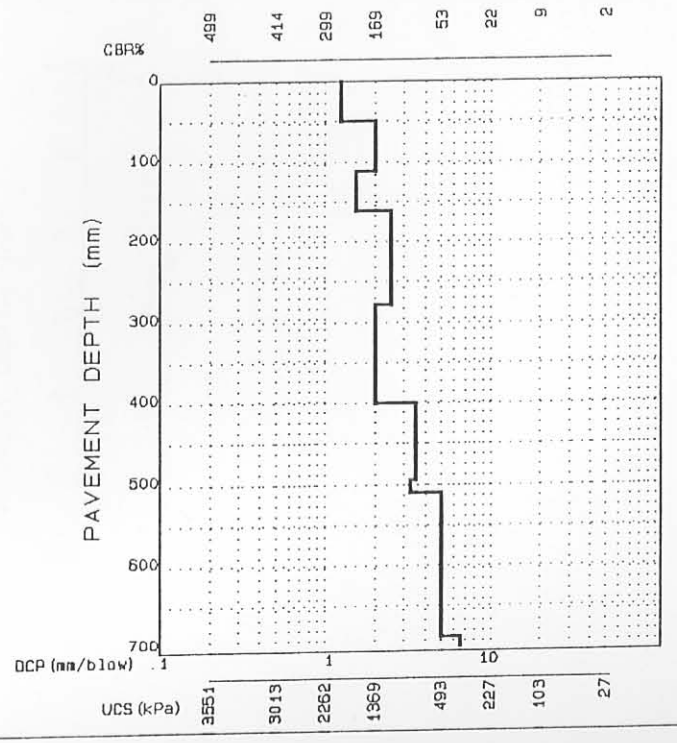

Figure C.8 Example of second plot produced by AVEBP

RTT, CSIR, SA

SUMMARY OF DCP INVESTIGATION

AVERAGE EQUIVALENT STRENGTH (REDEFINED)

FROM - TO (mm)	AV. PENETRATION (mm/blow)	SD	BDP	CBR%	UCS (kPa)
0- 48	1.2	0.3	1.5	257	1980
49-112	2.0	0.5	2.4	170	1376
113-160	1.5	0.2	1.7	214	1685
161-280	2.5	0.4	2.8	130	1087
281-400	2.0	0.4	2.3	171	1383
401-496	3.5	0.5	4.0	83	732
497-512	3.3	0.3	3.6	91	794
513-648	4.9	0.6	5.5	54	501
649-688	5.0	0.7	5.6	53	493
689-800	6.6	1.9	8.1	37	359

DATA FILE: R3-R13.DAT

NORMALIZED CURVE

DEVIATION (A_i) FROM STANDARD PAVEMENT BALANCE CURVE (SPBC), %.mm

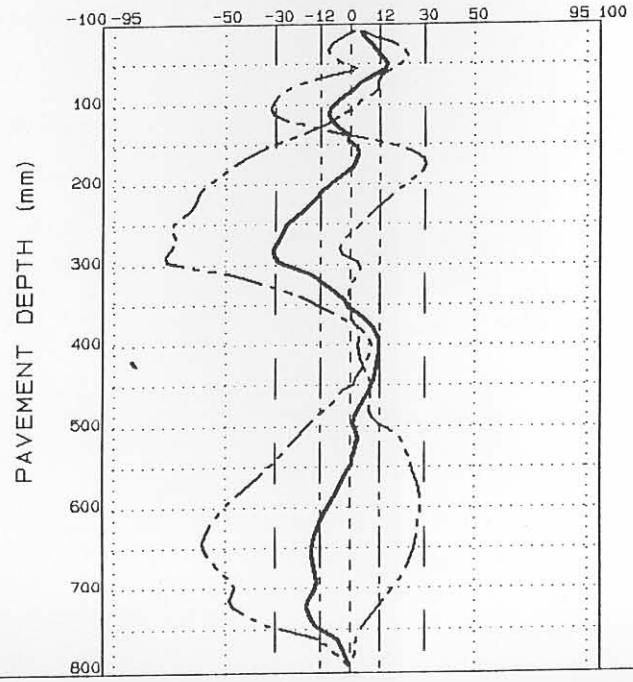

LAYER STRENGTH DIAGRAM (REDEFINED)

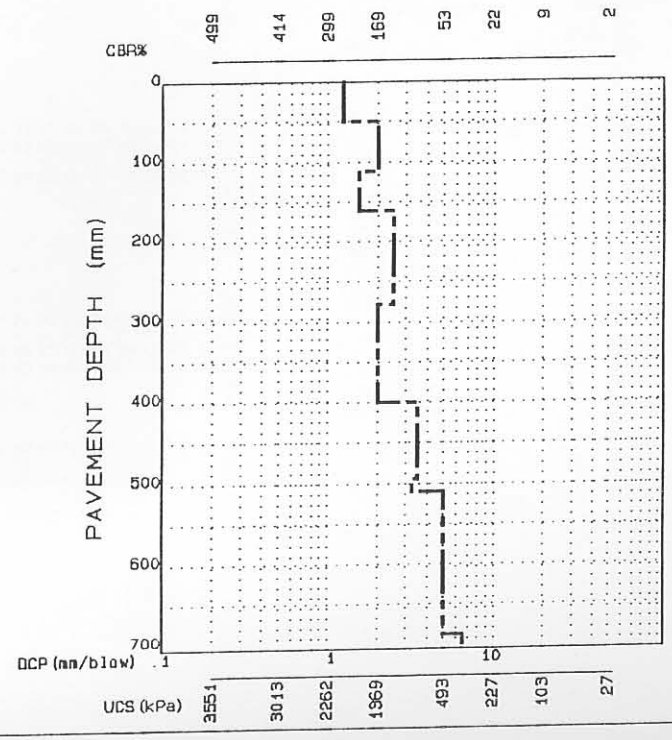

Figure C.9 Example of second plot produced by AVEBP

DCP INVESTIGATION

DATA FILES:
r3.dat r13.dat

REGION	: ROOIWAL(N=10)
ROAD NUMBER	: P1932
Km DISTANCE	: 2.9
DATE	: 85/06/06
STRUCTURE NUMBER (DSN 800)	: 351
BALANCE NUMBER (BN 100) OF DATA	: 24
BN 100 OF BALANCE CURVE	: 25
STRUCTURAL CAPACITY(E80 x10**6)	: 52 (TPA method (Kleyn))
ROAD CATEGORY	: C
TRAFFIC	: LIGHT TRAFFIC

BALANCE CURVE IS WHERE B = 20 A = 956 , RK = 276

CATEGORY IV: WELL-BALANCED DEEP STRUCTURE (WBD)

KATEGORIE IV: GOED GEBALANSEERDE DIEPSTRUKTUUR (GGD)

AVERAGE EQUIVALENT STRENGTH (EXISTING STRUCTURE)

FROM - TO (mm)	AV.PENETRATION (mm/blow)	SD	80P	CBR%	UCS (kPa)
0 - 180	1.7	0.5	2.0	200	1588
181 - 330	2.4	0.4	2.7	137	1138
331 - 480	2.8	0.8	3.4	113	961
481 - 600	4.5	0.8	5.2	60	550
601 - 800	5.9	1.6	7.3	43	410

AVERAGE DCP PENETRATION RATE

	DEPTH(mm)	NO OF BLOWS	mm/blow	CBR%	UCS (kPa)
DCP (1 - 10)	10	11.8	0.85	331	2474
DCP (11 - 20)	20	22.5	0.93	313	2355
DCP (21 - 30)	30	32.5	1.00	299	2262
DCP (31 - 40)	40	43.7	0.89	322	2415
DCP (41 - 50)	50	55.0	0.89	322	2415
DCP (51 - 60)	60	61.4	1.56	211	1665
DCP (61 - 70)	70	66.3	2.07	161	1312
DCP (71 - 80)	80	72.5	1.60	205	1623
DCP (81 - 90)	90	78.9	1.57	209	1651
DCP (91 - 100)	100	85.0	1.63	202	1602
DCP (101 - 110)	110	90.0	2.00	169	1369
DCP (111 - 120)	120	98.0	1.24	255	1967
DCP (121 - 130)	130	105.8	1.30	247	1912

Figure C.10 Example of printout of AVEBP

DCP (131 - 140)	140	114.2	1.18	266	2041
DCP (141 - 150)	150	121.7	1.33	242	1878
DCP (151 - 160)	160	128.4	1.51	217	1706
DCP (161 - 170)	170	134.3	1.70	195	1553
DCP (171 - 180)	180	139.4	1.94	173	1398
DCP (181 - 190)	190	143.8	2.25	145	1197
DCP (191 - 200)	200	147.7	2.56	123	1035
DCP (201 - 210)	210	151.6	2.59	122	1028
DCP (211 - 220)	220	155.8	2.37	137	1138
DCP (221 - 230)	230	160.4	2.20	150	1233
DCP (231 - 240)	240	164.0	2.79	111	946
DCP (241 - 250)	250	167.3	2.98	102	878
DCP (251 - 260)	260	171.4	2.44	131	1094
DCP (261 - 270)	270	175.9	2.23	147	1211
DCP (271 - 280)	280	179.9	2.50	127	1065
DCP (281 - 290)	290	184.2	2.35	138	1146
DCP (291 - 300)	300	189.6	1.86	180	1447
DCP (301 - 310)	310	198.8	1.09	283	2156
DCP (311 - 320)	320	204.9	1.64	201	1595
DCP (321 - 330)	330	210.7	1.71	194	1546
DCP (331 - 340)	340	216.8	1.65	200	1588
DCP (341 - 350)	350	222.5	1.75	189	1511
DCP (351 - 360)	360	227.5	2.00	169	1369
DCP (361 - 370)	370	233.4	1.68	196	1560
DCP (371 - 380)	380	238.5	1.99	170	1376
DCP (381 - 390)	390	243.6	1.94	174	1405
DCP (391 - 400)	400	247.7	2.47	129	1079
DCP (401 - 410)	410	251.4	2.71	115	976
DCP (411 - 420)	420	254.8	2.90	106	908
DCP (421 - 430)	430	258.2	2.99	102	878
DCP (431 - 440)	440	261.4	3.13	96	832
DCP (441 - 450)	450	264.3	3.35	88	771
DCP (451 - 460)	460	266.9	3.90	73	654
DCP (461 - 470)	470	269.5	3.90	73	654
DCP (471 - 480)	480	271.9	4.12	68	614
DCP (481 - 490)	490	274.2	4.28	64	582
DCP (491 - 500)	500	277.1	3.44	85	748
DCP (501 - 510)	510	280.7	2.80	110	938
DCP (511 - 520)	520	283.7	3.35	88	771
DCP (521 - 530)	530	286.2	3.96	71	638
DCP (531 - 540)	540	288.7	4.07	69	622
DCP (541 - 550)	550	290.9	4.46	61	558
DCP (551 - 560)	560	293.1	4.60	59	542
DCP (561 - 570)	570	295.2	4.71	57	526
DCP (571 - 580)	580	297.1	5.28	49	460
DCP (581 - 590)	590	299.0	5.28	49	460
DCP (591 - 600)	600	300.7	5.89	43	410
DCP (601 - 610)	610	302.6	5.28	49	460
DCP (611 - 620)	620	304.5	5.28	49	460
DCP (621 - 630)	630	306.4	5.19	51	477
DCP (631 - 640)	640	308.5	4.94	54	501
DCP (641 - 650)	650	310.7	4.42	62	566
DCP (651 - 660)	660	313.2	4.00	70	630
DCP (661 - 670)	670	316.0	3.57	81	717
DCP (671 - 680)	680	318.7	3.75	76	677
DCP (681 - 690)	690	321.4	3.62	80	709
DCP (691 - 700)	700	323.6	4.68	57	526
DCP (701 - 710)	710	325.0	7.22	33	325
DCP (711 - 720)	720	326.3	7.22	33	325
DCP (721 - 730)	730	329.2	3.47	84	740
DCP (731 - 740)	740	332.1	3.47	84	740
DCP (741 - 750)	750	335.0	3.47	84	740
DCP (751 - 760)	760	340.8	1.74	191	1525
DCP (761 - 770)	770	344.0	3.07	98	847

DCP (771 - 780)	780	346.7	3.73	77	685
DCP (781 - 790)	790	349.4	3.72	77	685
DCP (791 - 800)	800	351.9	3.93	72	646

AVERAGE EQUIVALENT STRENGTH (EXISTING STRUCTURE - REDEFINED LAYERS)

LAYER	DEPTH (mm) FROM - TO	THICKNESS (mm)	DN mm/blow	SD mm/blow	80P	CBR%	UCS (kPa)
1	0 - 48	48	1.2	0.3	1.5	257	1980
2	49 - 112	64	2.0	0.5	2.4	170	1376
3	113 - 160	48	1.5	0.2	1.7	214	1685
4	161 - 280	120	2.5	0.4	2.8	130	1087
5	281 - 400	120	2.0	0.4	2.3	171	1383
6	401 - 496	96	3.5	0.5	4.0	83	732
7	497 - 512	16	3.3	0.3	3.5	91	794
8	513 - 648	136	4.9	0.6	5.5	54	501
9	649 - 688	40	5.0	0.7	5.6	53	493
10	689 - 800	112	6.6	1.9	8.1	37	359

WARNING ! MORE THAN TEN LAYERS FOUND

SUMMARY OF + AND - AREAS (CURVE FITTING TABLE - EXISTING STRUCTURE)

DEPTH (mm) FROM - TO	CUMULATIVE AREA (% mm),Ak
0 80	83.37
81 144	-38.32
145 176	9.09
177 352	-359.52
353 544	145.78
545 792	-320.29
ABSOLUTE AREA	956.38

APPENDIX D

PHOTOGRAPHIC RECORD OF HEAVY VEHICLE SIMULATOR (HVS) TESTS ON PAVEMENTS WITH LIGHTLY CEMENTITIOUS LAYERS

CONTENTS:

PLATE D.15 RELATIVELY SHALLOW PAVEMENT: ROAD 2212 - FATIGUE CRACKING AND DEFORMATION ON HVS TEST SECTION 307A4 (TRAFFICKING DUAL WHEEL LOAD: 70 kN; TYRE PRESSURE: 700 kPa)

PLATE D.16 RELATIVELY SHALLOW PAVEMENT: ROAD 2212 - FATIGUE CRACKING AND DEFORMATION ON HVS TEST SECTION 308A4 (TRAFFICKING DUAL WHEEL LOAD: 100 kN; TYRE PRESSURE: 700 kPa)

PLATE D.17 RELATIVELY SHALLOW PAVEMENT: ROAD 2212 - FATIGUE CRACKING AND DEFORMATION ON HVS TEST SECTION 309A4 (TRAFFICKING SINGLE WHEEL LOAD: 150 kN; TYRE PRESSURE: 1445 kPa)

PLATE D.18 RELATIVELY SHALLOW PAVEMENT: ROAD 2212 - FATIGUE CRACKING AND DEFORMATION ON HVS TEST SECTION 309A4 (TRAFFICKING SINGLE WHEEL LOAD: 150 kN; TYRE PRESSURE: 1445 kPa)

PLATE D.19 RELATIVELY SHALLOW PAVEMENT: ROAD 2212 - EXCESSIVE DEFORMATION DEVELOPMENT DURING THE FINAL STAGES OF TESTING (41 803 REPETITIONS) ON HVS TEST SECTION 309A4 (TRAFFICKING SINGLE WHEEL LOAD: 150 kN; TYRE PRESSURE: 1445 kPa)

PLATE D.20 RELATIVELY SHALLOW PAVEMENT: ROAD 2212 - EXCESSIVE FATIGUE AND CRUSHING FAILURE AT THE END OF THE TEST (41 803 REPETITIONS) ON HVS TEST SECTION 309A4, MEASURING POINT 4 (TRAFFICKING SINGLE WHEEL LOAD: 150 kN; TYRE PRESSURE: 1445 kPa)

PLATE D.21 RELATIVELY SHALLOW PAVEMENT: ROAD 2212 - EXCESSIVE FATIGUE AND CRUSHING FAILURE AT THE END OF THE TEST (41 803 REPETITIONS) ON HVS TEST SECTION 309A4, MEASURING POINT 5,5 (TRAFFICKING SINGLE WHEEL LOAD: 150 kN; TYRE PRESSURE: 1445 kPa)

PLATE D.22 RELATIVELY SHALLOW PAVEMENT: ROAD 2212 - CLOSE VIEW OF THE CRUSHING (COMPRESSION) FAILURE OF THE CEMENTED BASE LAYER AT THE END OF THE TEST (41 803 REPETITIONS) ON HVS TEST SECTION 309A4, (TRAFFICKING SINGLE WHEEL LOAD: 150 kN; TYRE PRESSURE: 1445 kPa)

PLATE D.23 RELATIVELY DEEP PAVEMENT: ROAD 1932 - EXCESSIVE CRUSHING FAILURE AT THE END OF THE TEST (48 000 REPETITIONS) ON HVS TEST SECTION 337A4 (TRAFFICKING SINGLE WHEEL LOAD: 150 kN; TYRE PRESSURE: 1445 kPa)

PLATE D.24 RELATIVELY DEEP PAVEMENT: ROAD 1932 - CRUSHING FAILURE AT THE END OF THE TEST (143 000 REPETITIONS) ON HVS TEST SECTION 338A4. DEFORMATION APPROXIMATELY 10 mm (TRAFFICKING SINGLE WHEEL LOAD: 150 kN; TYRE PRESSURE: 960 kPa)

PLATE D.25 RELATIVELY SHALLOW PAVEMENT: ROAD 2212 - PREPARATION OF THE 40 m REHABILITATION TEST SECTIONS, USING A HEAVY VIBRATORY ROLLER IN A "CRACK AND SEAT" OPERATION

PLATE D.26 RELATIVELY SHALLOW PAVEMENT: ROAD 2212 - PREPARATION OF THE REHABILITATION TEST SECTIONS, USING A HEAVY VIBRATORY ROLLER IN A "CRACK AND SEAT" OPERATION. NOTE THE CRACK DEVELOPMENT IN THE CEMENTED BASE LAYER.

PLATE D.27 RELATIVELY SHALLOW PAVEMENT: ROAD 2212 - REHABILITATION SECTIONS: ASPECTS OF THE 150 mm GRANULAR BASE LAYER ON TOP OF THE PRECRACKED CEMENTED LAYER

PLATE D.28 RELATIVELY SHALLOW PAVEMENT: ROAD 2212 - REHABILITATION SECTIONS: ASPECTS OF THE 35 mm ASPHALT PREMIX LAYER ON TOP OF THE PRECRACKED CEMENTED LAYER

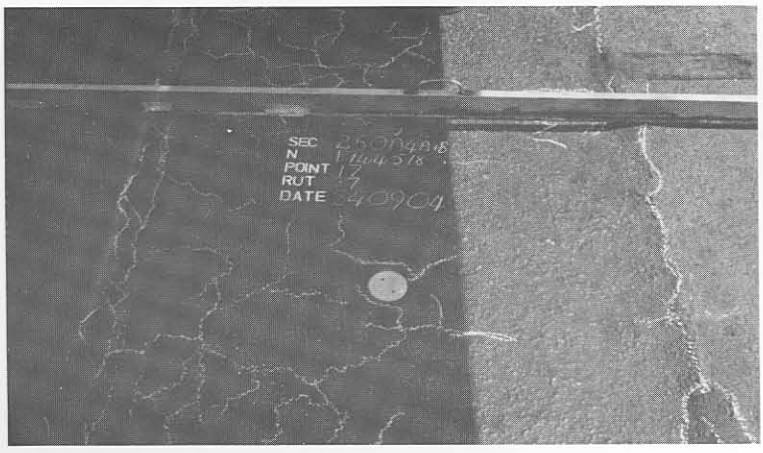

(a) Relatively fine cracks after $1{,}74 \times 10^6$ repetitions (E80s).

(b) Approximately 20 mm deformation after $2{,}4 \times 10^6$ repetitions (E80s).

PLATE D.1 RELATIVELY DEEP PAVEMENT: ROAD 1932 – CRACKING AND DEFORMATION OF HVS TEST SECTION 250A4A&B (VARIABLE LOADING: 40 TO 100 kN; TYRE PRESSURE: 690 kPa).

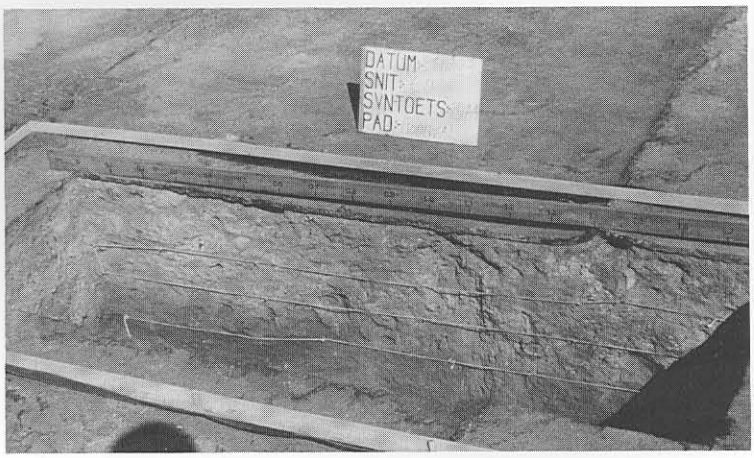

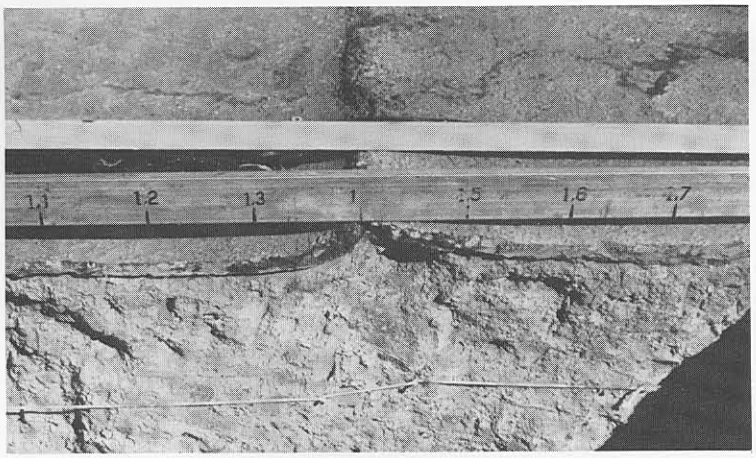

PLATE D.2 RELATIVELY DEEP PAVEMENT: ROAD 1932 – EXCESSIVE DEFORMATION ON HVS TEST SECTION 251A4A OWING TO COMPACTION OF THE BASE LAYER (VARIABLE LOADING: 70, 100 kN; TYRE PRESSURE: 690 kPa).

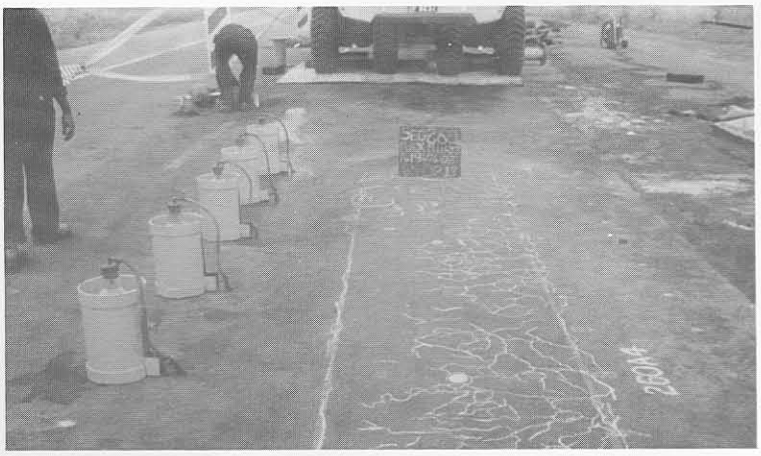

(a) Relatively fine crack pattern after 1,95 × 10^6 repetitions (E80s). Note the waterbottels for introduction of depth water (20 mm to 450 mm) on the side of the section at measuring positions 9 to 15.

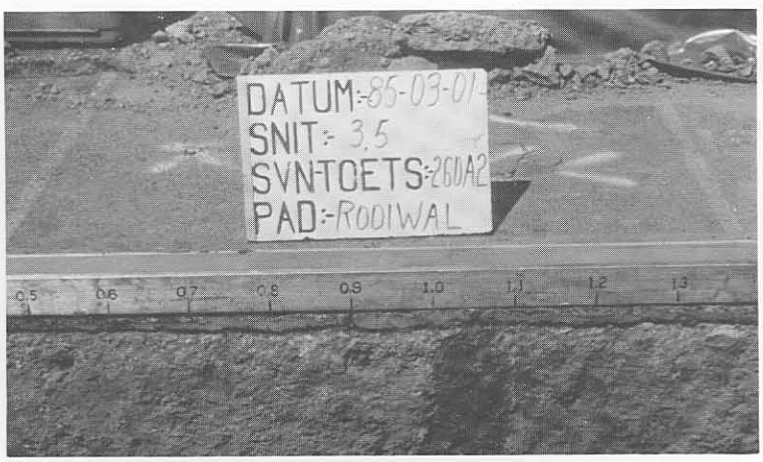

PLATE D.3 RELATIVELY DEEP PAVEMENT: ROAD 1932 – CRACKING AND DEFORMATION OF HVS TEST SECTION 260A4 (TRAFFICKING DUAL WHEEL LOAD: 40 kN; TYRE PRESSURE: 520 kPa).

(a) Condition before testing; some fine cracking evident from measuring points 9 to 15 at the start of the test.

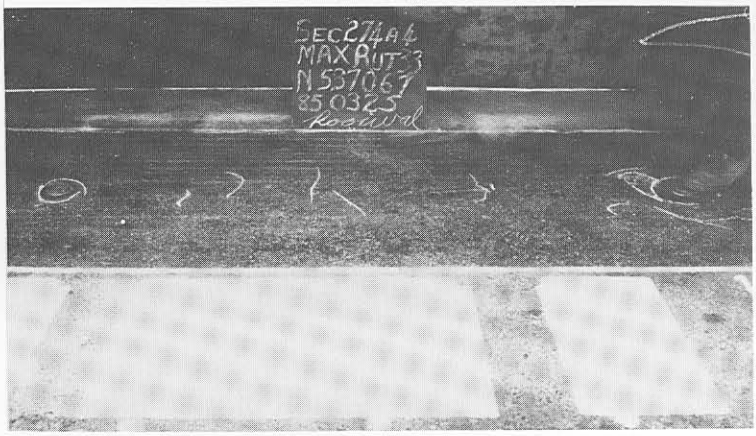

(b) Initiation of crack development after approximately 537 067 repetitions (E80s).

(c) Crack development after 1,20 × 10^6 repetitions (E80s).

(d) Cracking and pumping after 1,35 × 10^6 repetitions (E80s).

PLATE D.4 RELATIVELY DEEP PAVEMENT: ROAD 1932 – CRACKING AND PUMPING ON HVS TEST SECTION 274A4 (TRAFFICKING DUAL WHEEL LOAD: 40 kN; TYRE PRESSURE: 520 kPa).

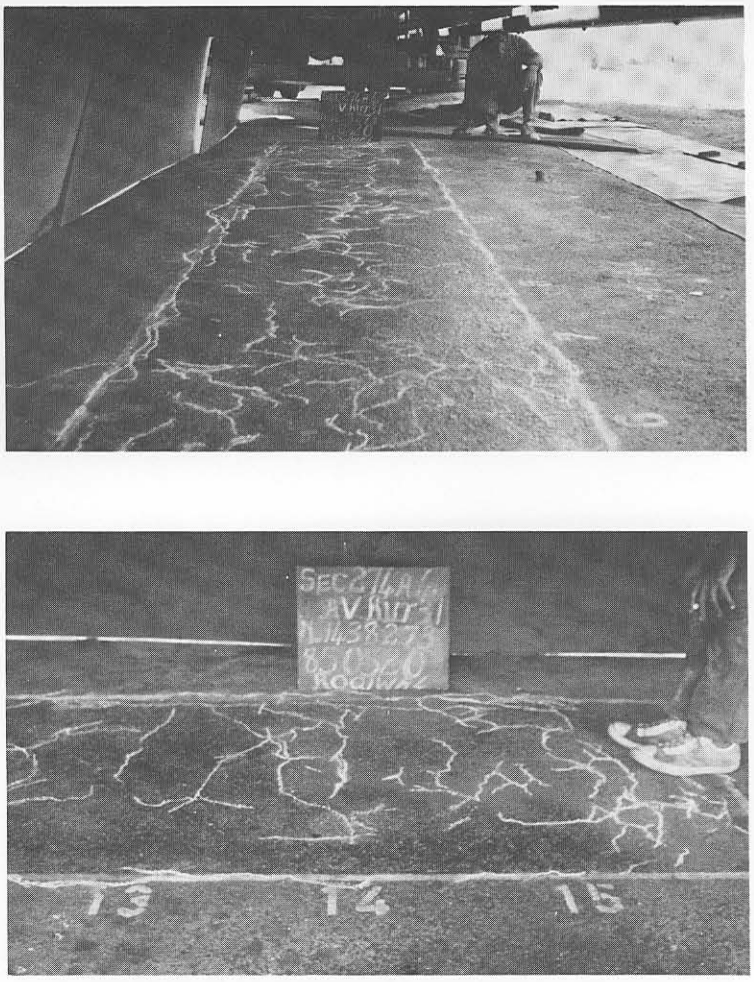

(a) Relatively fine crack pattern after $1{,}44 \times 10^6$ repetitions (E80s).

(b) Deformation less than 8 mm at end of test.

PLATE D.5 RELATIVELY DEEP PAVEMENT: ROAD 1932 – CRACKING AND DEFORMATION ON HVS TEST SECTION 274A4 (TRAFFICKING DUAL WHEEL LOAD: 40 kN; TYRE PRESSURE: 520 kPa).

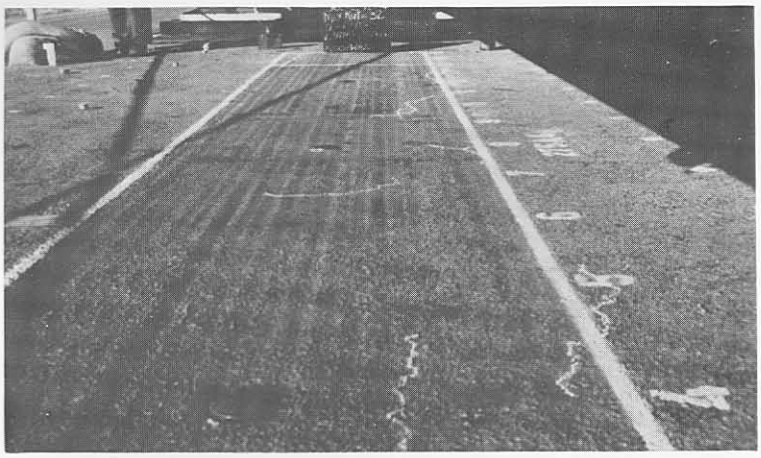

(a) Initial state of section with some cracking at start of test.

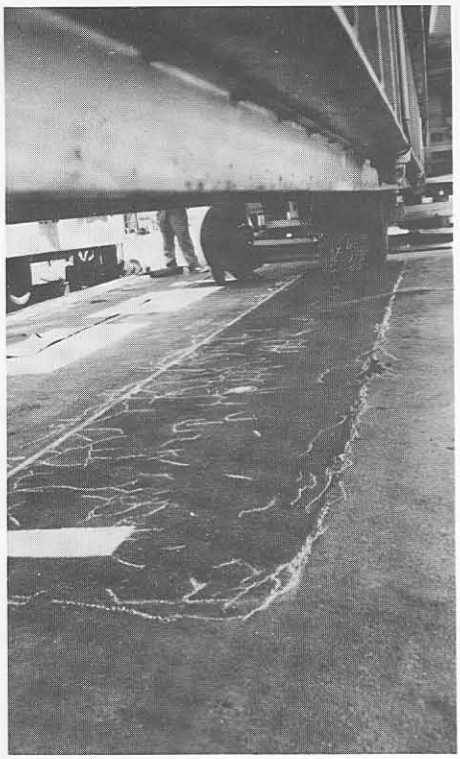

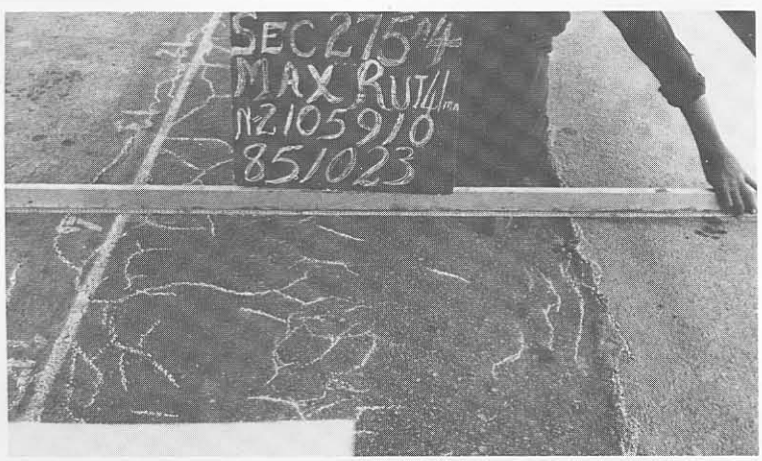

(b) Relatively fine cracking at end of test.

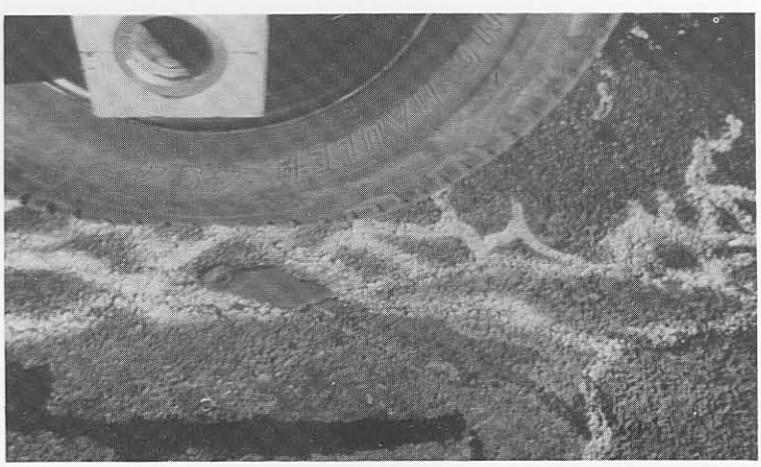

(c) Pumping of the crushed cemented base material.

PLATE D.6 RELATIVELY DEEP PAVEMENT: ROAD 1932 – CRACKING AND PUMPING ON HVS TEST SECTION 275A4 (TRAFFICKING DUAL WHEEL LOAD: 40 kN; TYRE PRESSURE: 700 kPa).

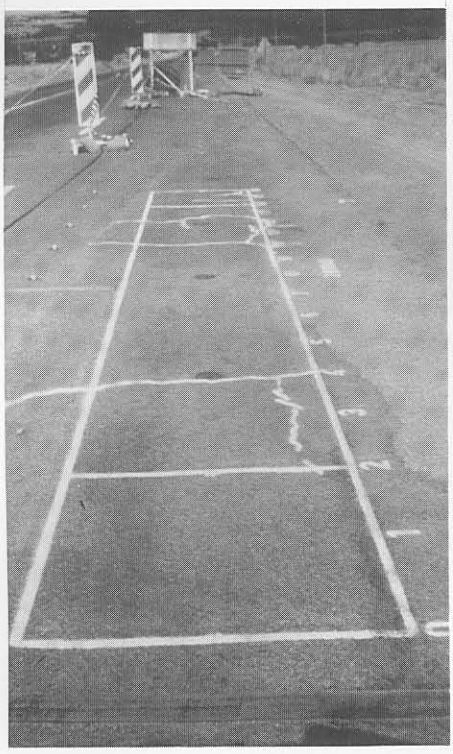

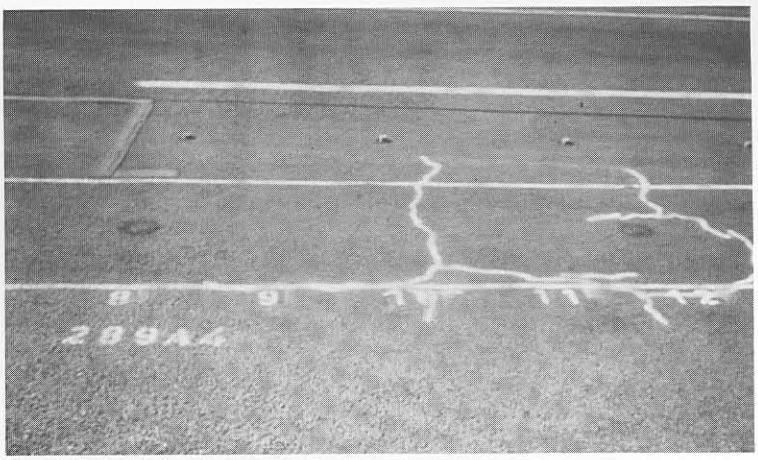

(a) Initial stabilisation cracking before HVS testing.

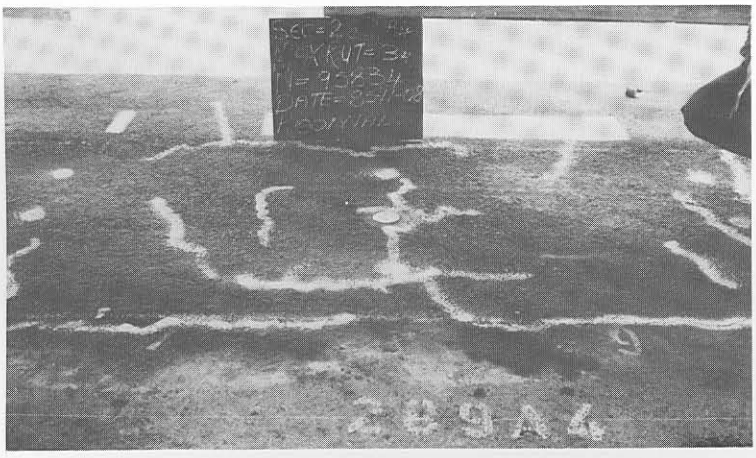

(b) Crack development after 95 834 70 kN repetitions.

(c) Final cracking and deformation (approximately 22 mm) on section.

PLATE D.7 RELATIVELY DEEP PAVEMENT: ROAD 1932 – CRACKING AND DEFORMATION ON HVS TEST SECTION 289A4 (TRAFFICKING DUAL WHEEL LOAD: 70 kN; TYRE PRESSURE: 700 kPa).

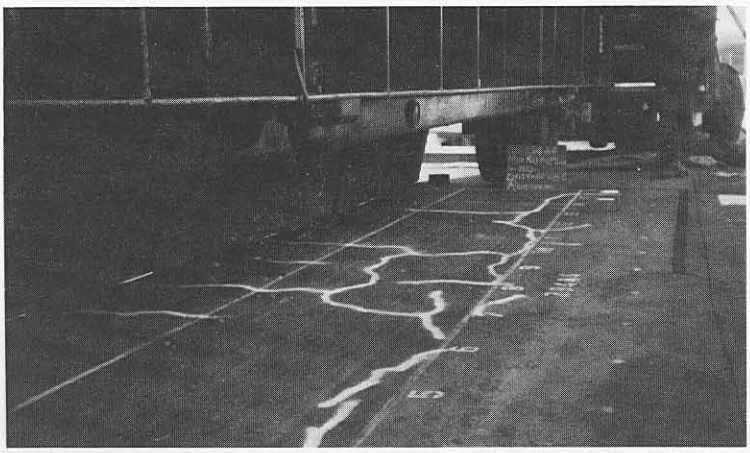

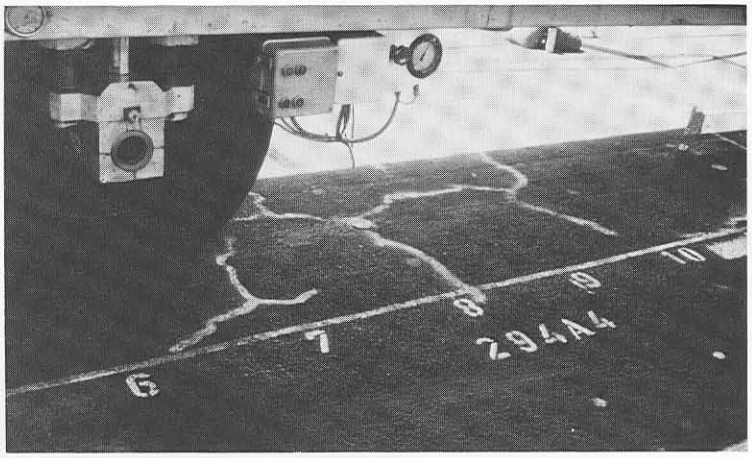

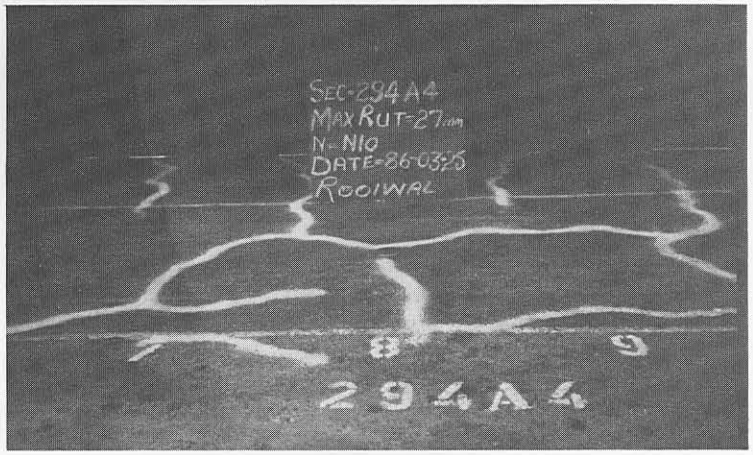

PLATE D.8 RELATIVELY DEEP PAVEMENT: ROAD 1932 – INITIAL STABILISATION CRACKING AT THE START OF THE TEST ON HVS TEST SECTION 294A4.

(a) Relatively fine cracking after $1{,}44 \times 10^6$ 100 kN repetitions.

(b) Artificial surface water introduction on section.

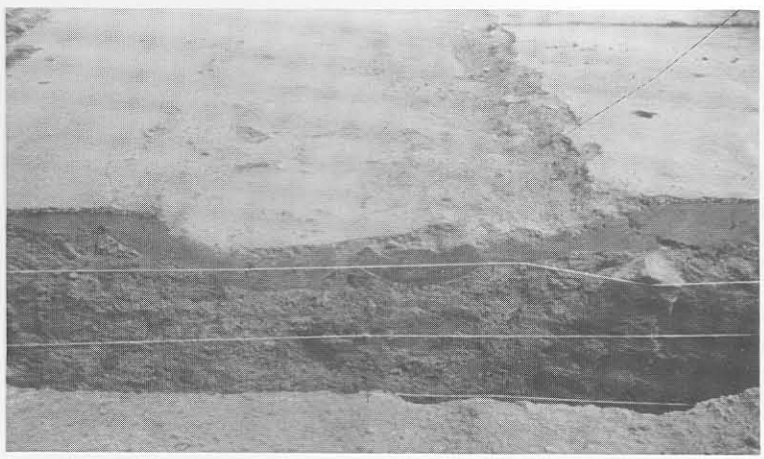

(c) Excessively high degree of potholing owing to the loss crushed cemented base material after introduction of surface water.

PLATE D.9 RELATIVELY DEEP PAVEMENT: ROAD 1932 – CRACKING AND HIGH DEGREE OF PUMPING ON HVS TEST SECTION 294A4 (TRAFFICKING DUAL WHEEL LOAD: 100 kN; TYRE PRESSURE: 700 kPa).

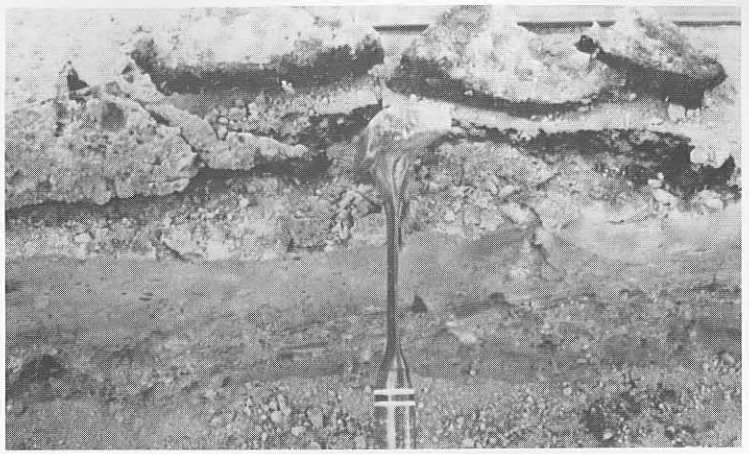

(a) Relatively loose surfacing owing to horisontal cracking in the cemented base.

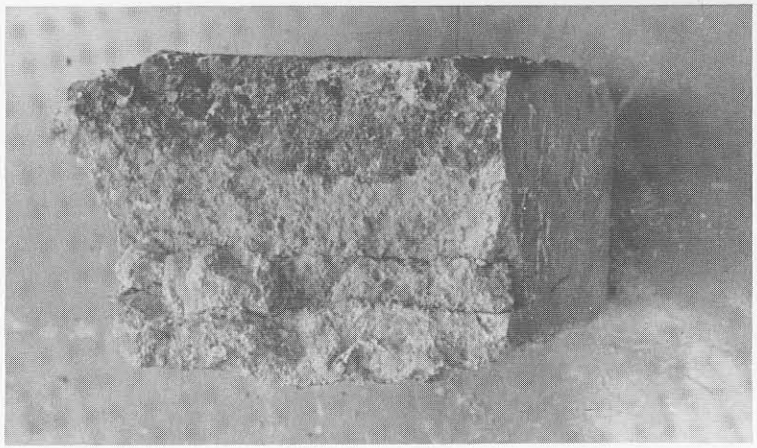

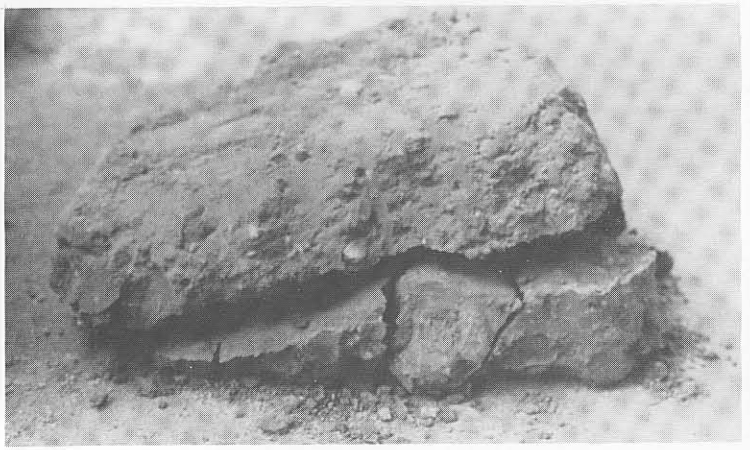

(b) Horisontal cracking in the cemented base, prior to HVS testing.

PLATE D.10 HORISONTAL CRACKING IN THE CEMENTED BASE OF THE RELATIVELY DEEP PAVEMENT, PRIOR TO HVS TESTING ON ROAD 1932 AT ROOIWAL.

(a) Progress of both horisontal cracking and crushing of the top 50 mm to 75 mm of the cemented base after HVS testing.

(b) Fatigue cracking in cemented base layer.

PLATE D.11 CRACKING IN THE CEMENTED BASE LAYER OWING TO HVS TRAFFICKING ON THE RELATIVELY DEEP PAVEMENT, ROAD 1932 AT ROOIWAL.

(a) Final crushed state (compression failure) in the top 50 mm to 75 mm of the cemented base layer, after testing in relatively dry conditions.

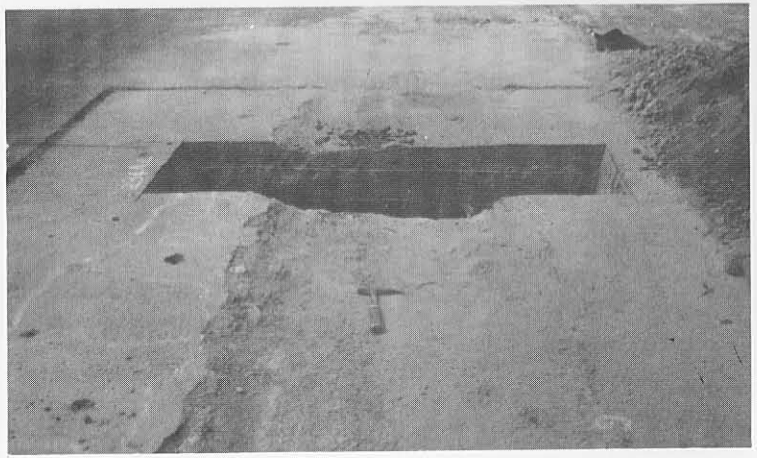

(b) Potholing (approximately 75 mm) and loss of crushed base material after testing in soaked conditions on Section 294A4.

(c) Relatively low deformation (approximately 10 mm) after testing in the relatively dry conditions on Section 294A4.

PLATE D.12 CRUSHING IN THE CEMENTED BASE LAYER OWING TO HVS TRAFFICKING ON THE RELATIVELY DEEP PAVEMENT, ROAD 1932 AT ROOIWAL.

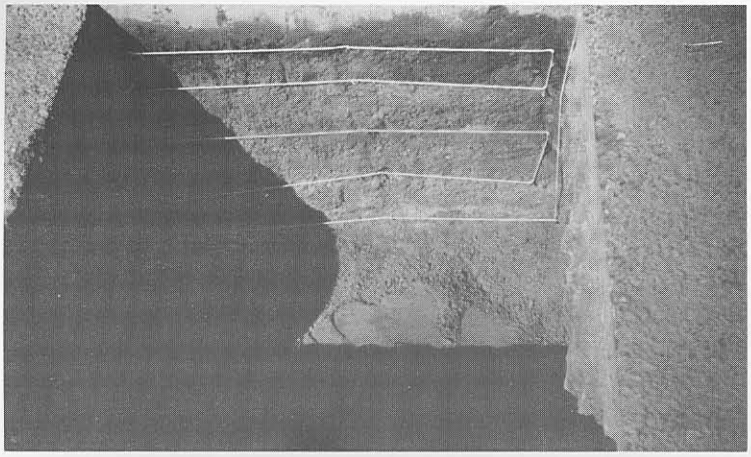

← Relatively weak interlayer, between well cemented base and subbase layer

(b) Stabilisation crack.

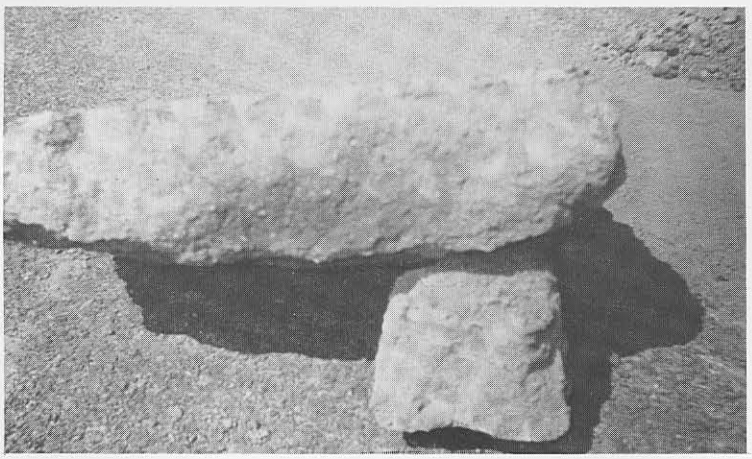

(c) Chunks of well cemented Ferricrete and Granophyre (3 % PBFC).

PLATE D.13 DETAIL OF RELATIVELY SHALLOW PAVEMENT STRUCTURE ON ROAD 2212 AT BULTFONTEIN (TVL).

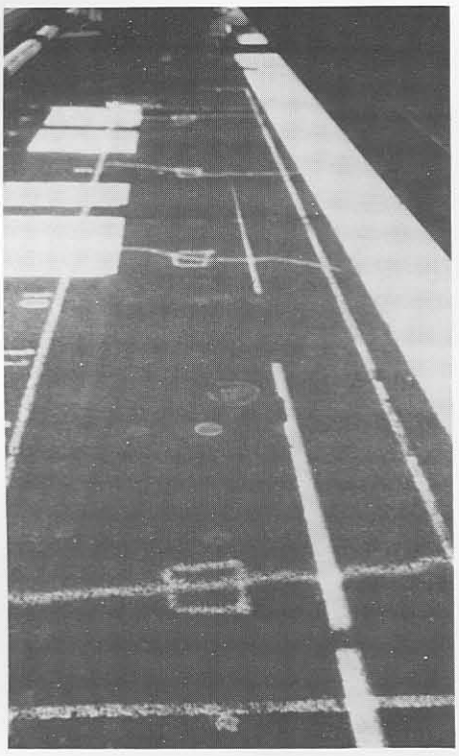

(a) Initial stabilisation cracking at the start of the test.

(b) Fatigue cracking (100 mm × 100 mm blocks) after approximately $1{,}0 \times 10^6$ repetitions (E80s).

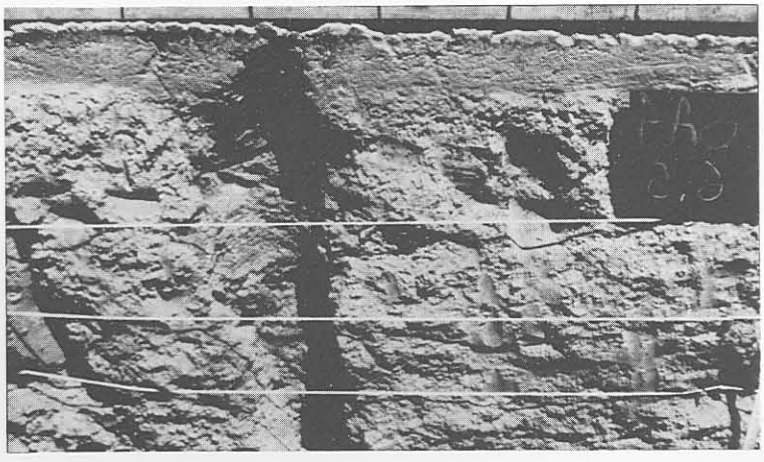

(c) Crushing and deformation (approximately 12 mm) of the cemented base at the end of the test.

PLATE D.14 RELATIVELY SHALLOW PAVEMENT: ROAD 2212 – FATIGUE CRACKING, DEFORMATION AND CRUSHING ON HVS TEST SECTION 306A4 (TRAFFICKING DUAL WHEEL LOAD: 40 kN; TYRE PRESSURE: 700 kPa).

(a) Fatigue cracking after approximately 731 783 70 kN repetitions.

(b) Fatigue cracking after approximately $1{,}46 \times 10^6$ 70 kN repetitions.

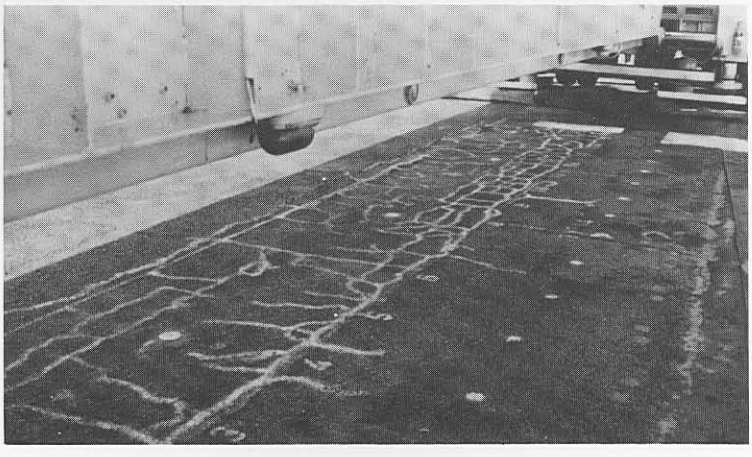

(c) Fatigue cracking after approximately $2{,}45 \times 10^6$ 70 kN repetitions.

PLATE D.15 RELATIVELY SHALLOW PAVEMENT: ROAD 2212 – FATIGUE CRACKING AND DEFORMATION ON HVS TEST SECTION 307A4 (TRAFFICKING DUAL WHEEL LOAD: 70 kN; TYRE PRESSURE: 700 kPa).

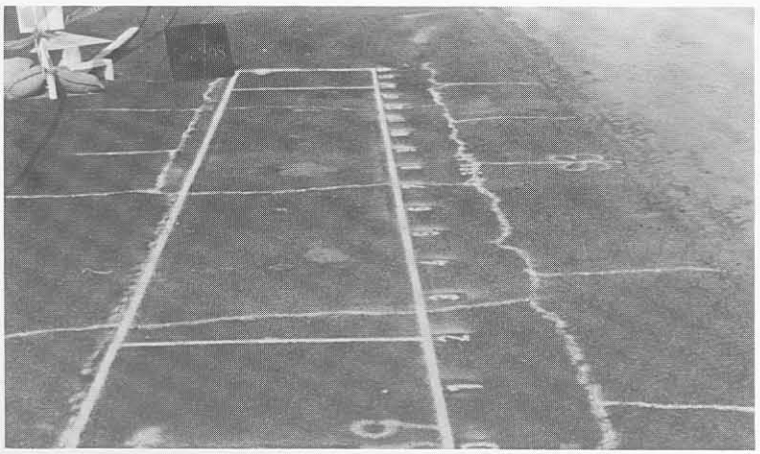

(a) Initial stabilisation cracks at start of test.

(b) Final fatigue cracking and crushing after approximately 2,64 × 10^6 100 kN repetitions.

(c) Final deformation (approximately 24 mm) at measuring point 13,5 after approximately 2,64 × 10^6 100 kN repetitions.

PLATE D.16 RELATIVELY SHALLOW PAVEMENT: ROAD 2212 – FATIGUE CRACKING AND DEFORMATION ON HVS TEST SECTION 308A4 (TRAFFICKING DUAL WHEEL LOAD: 100 kN; TYRE PRESSURE: 700 kPa).

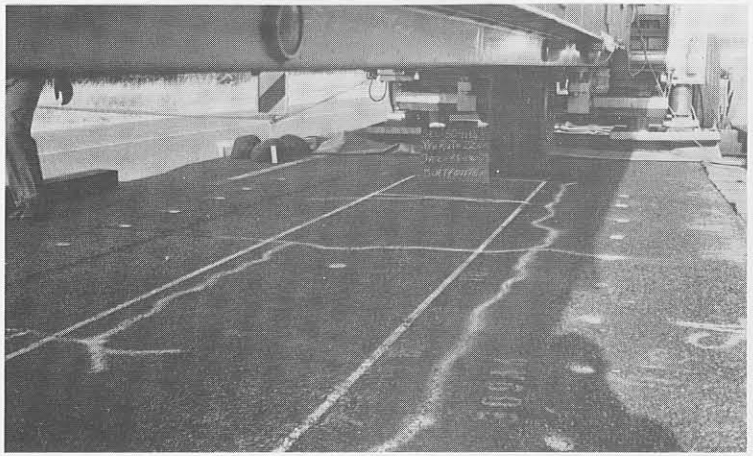

(a) Initial stabilisation cracking at start of test.

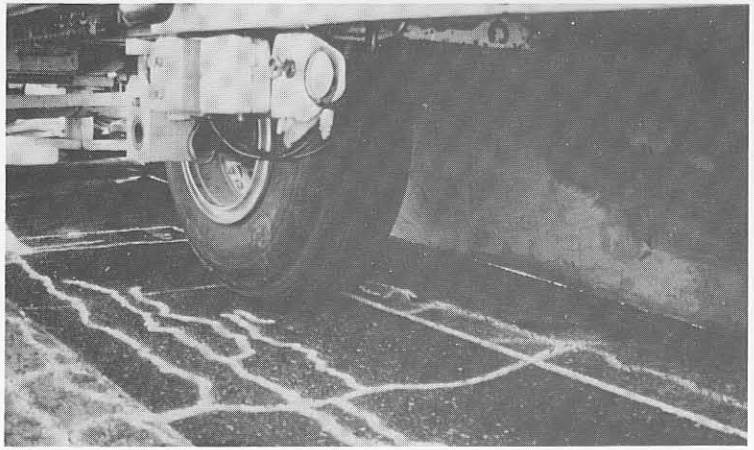

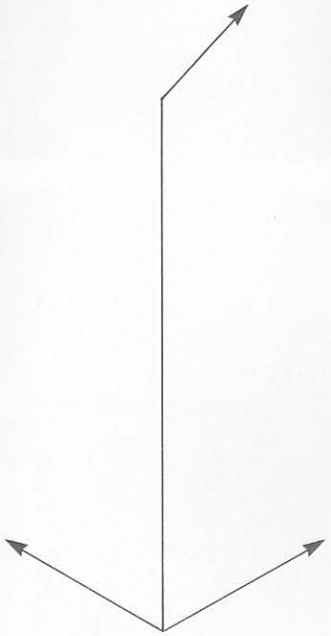

(b) Fatigue cracking and deformation (approximately 40 mm) after 11 331 repetitions of a 150 kN, 1445 kPa single aircraft wheel load.

PLATE D.17 RELATIVELY SHALLOW PAVEMENT: ROAD 2212 – FATIGUE CRACKING AND DEFORMATION ON HVS TEST SECTION 309A4 (TRAFFICKING SINGLE WHEEL LOAD: 150 kN; TYRE PRESSURE: 1445 kPa).

(a) Fatigue cracking and deformation (maximum 40 mm) after 11 331 repetitions.

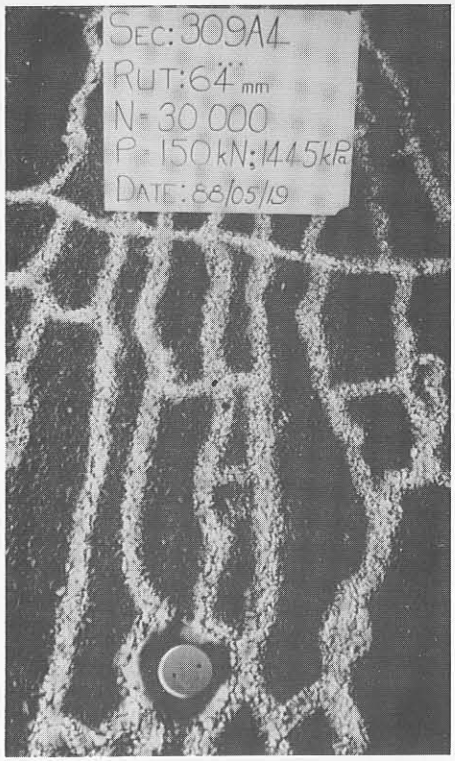

(b) Further fatigue cracking and deformation (maximum 64 mm) after 30 000 repetitions.

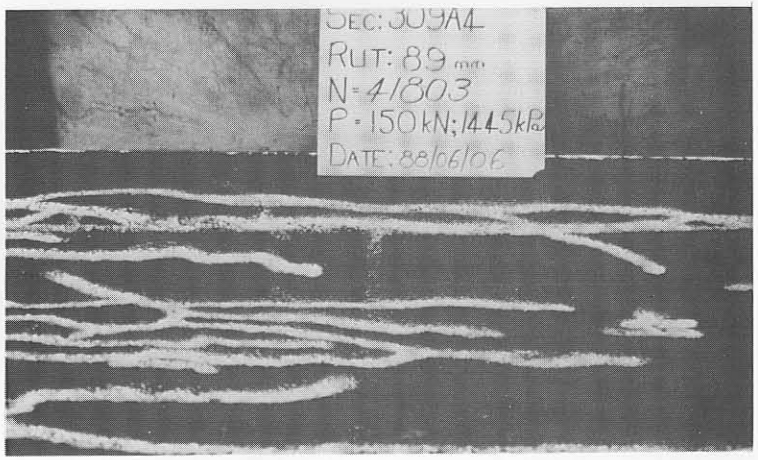

(c) Further fatigue cracking and deformation (maximum 89 mm) after 41 803 repetitions..

PLATE D.18 RELATIVELY SHALLOW PAVEMENT: ROAD 2212 – FATIGUE CRACKING AND DEFORMATION ON HVS TEST SECTION 309A4 (TRAFFICKING SINGLE WHEEL LOAD: 150 kN; TYRE PRESSURE: 1445 kPa).

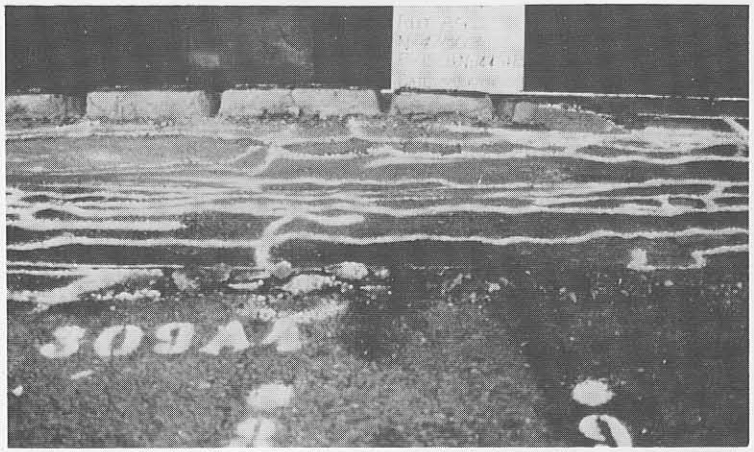

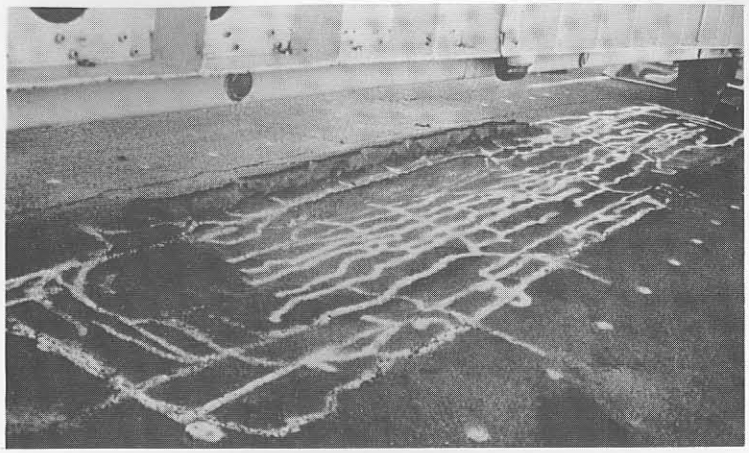

Upheaving of cemented base material outside the tested area, owing to the "punching" of the base material into the weak interlayer, and subsequent horisontal movement of the base material towards the outside of the section

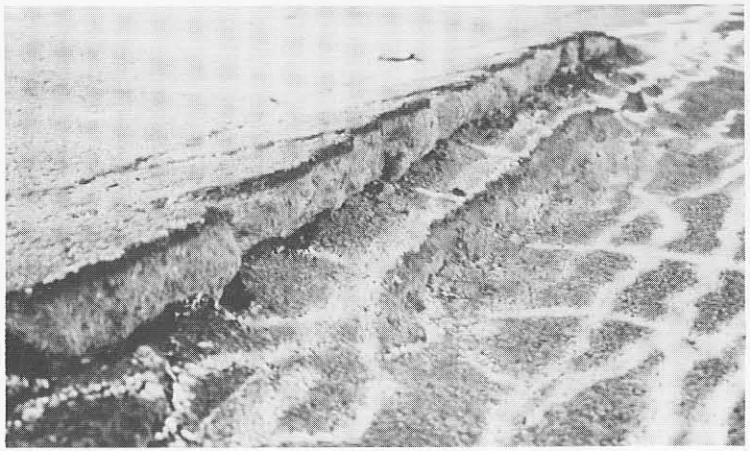

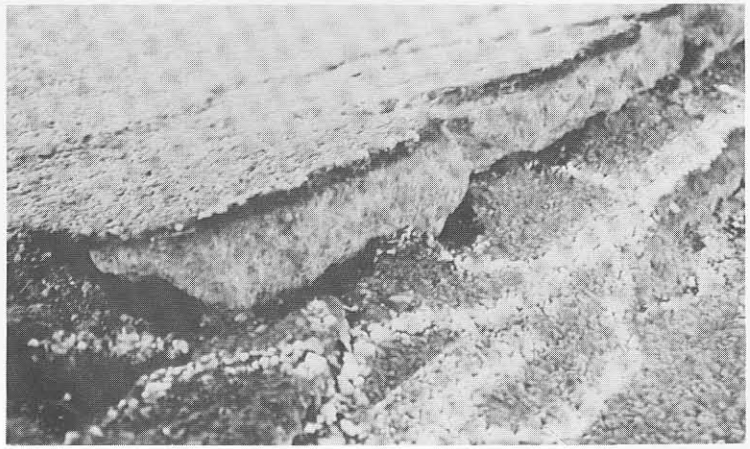

PLATE D.19 RELATIVELY SHALLOW PAVEMENT: ROAD 2212 – EXCESSIVE DEFORMATION DEVELOPMENT DURING THE FINAL STAGES OF TESTING (41 803 REPETITIONS) ON HVS TEST SECTION 309A4 (TRAFFICKING SINGLE WHEEL LOAD: 150 kN; TYRE PRESSURE: 1445 kPa).

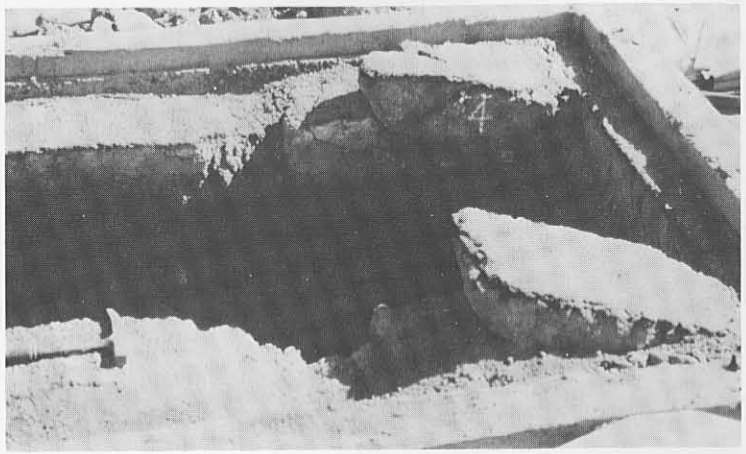

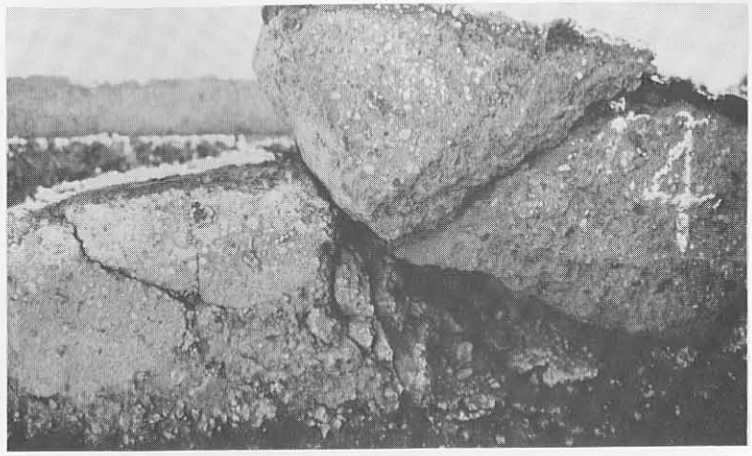

PLATE D.20 RELATIVELY SHALLOW PAVEMENT: ROAD 2212 – EXCESSIVE FATIGUE AND CRUSHING FAILURE AT THE END OF THE TEST (41 803 REPETITIONS) ON HVS TEST SECTION 309A4, MEASURING POINT 4 (TRAFFICKING SINGLE WHEEL LOAD: 150 kN; TYRE PRESSURE: 1445 kPa).

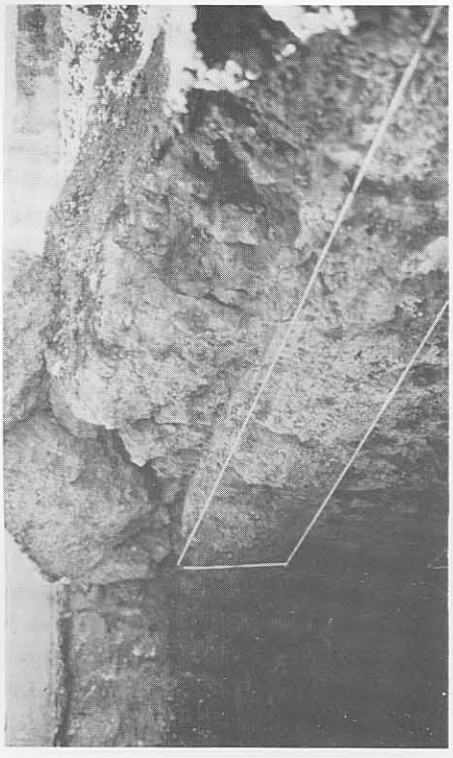

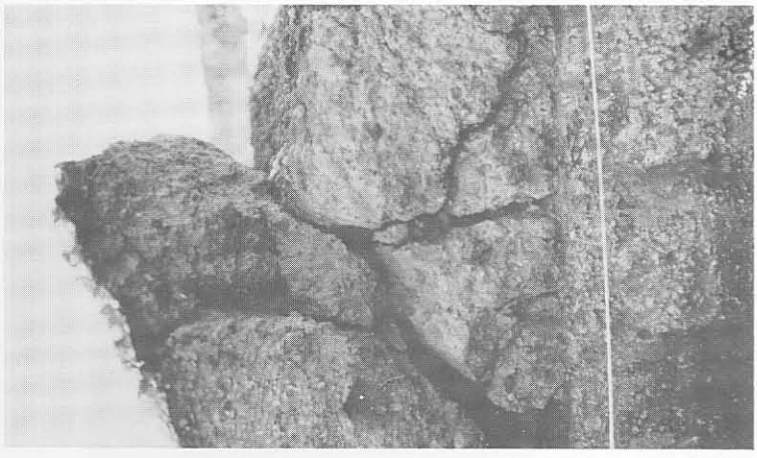

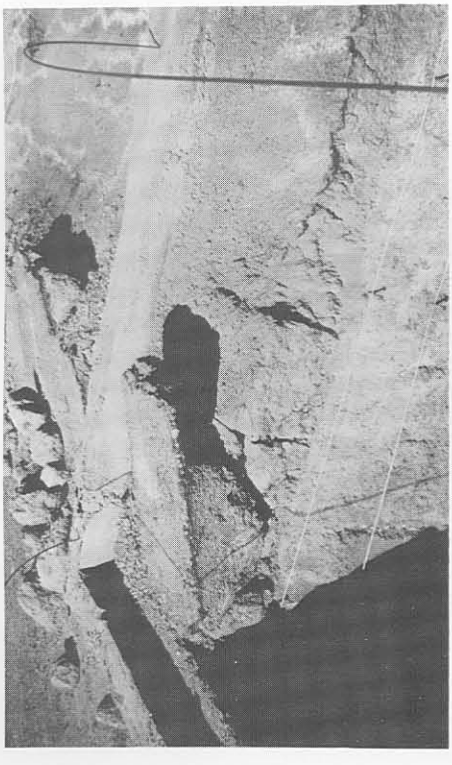

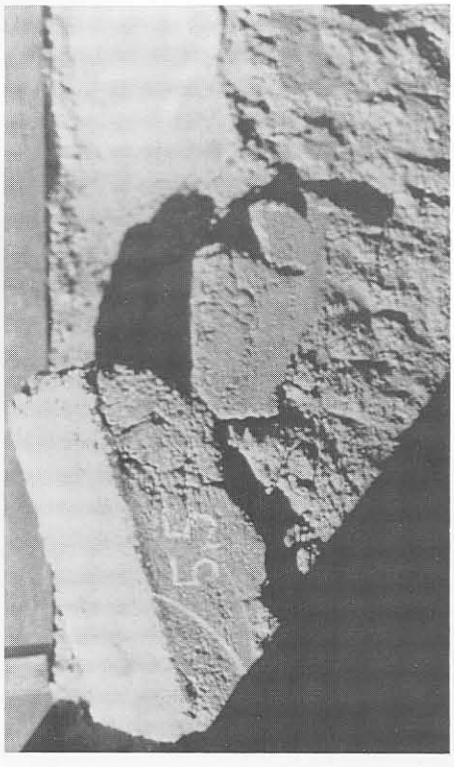

PLATE D.21 RELATIVELY SHALLOW PAVEMENT: ROAD 2212 – EXCESSIVE FATIGUE AND CRUSHING FAILURE AT THE END OF THE TEST (41 803 REPETITIONS) ON HVS TEST SECTION 309A4, MEASURING POINT 5 (TRAFFICKING SINGLE WHEEL LOAD: 150 kN; TYRE PRESSURE: 1445 kPa).

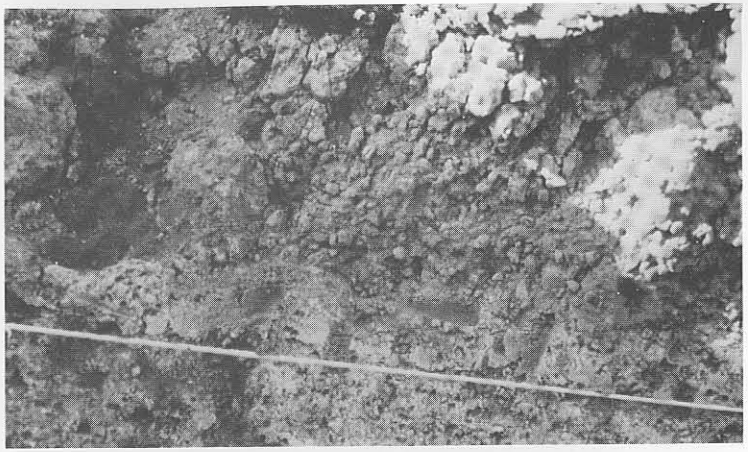

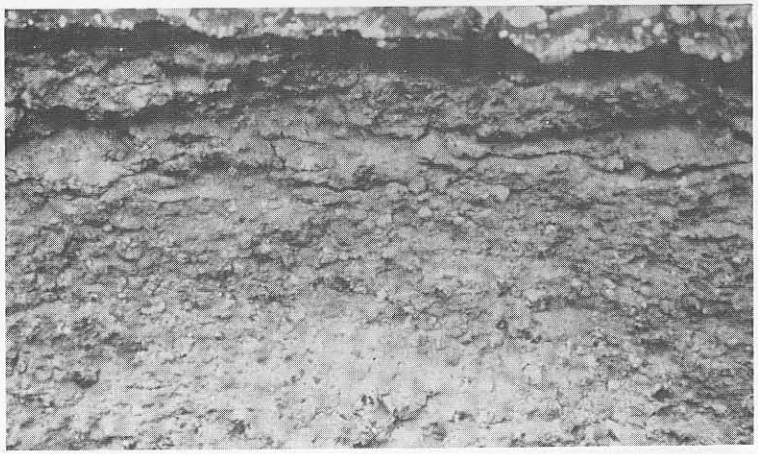

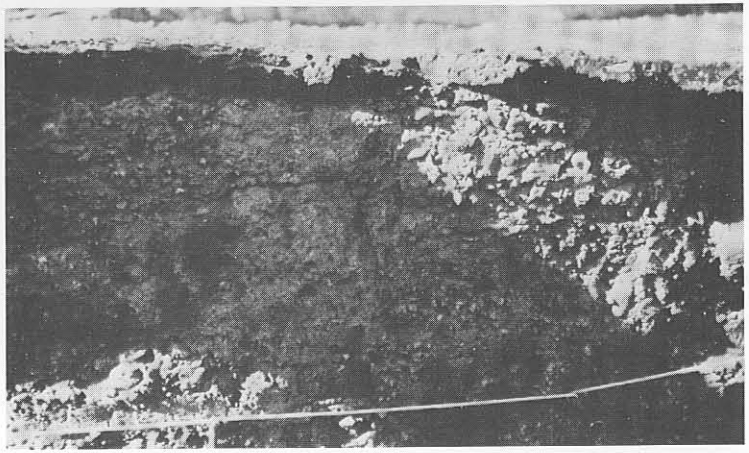

PLATE D.22 RELATIVELY SHALLOW PAVEMENT: ROAD 2212 – CLOSE VIEW OF THE CRUSHING (COMPRESSION) FAILURE OF THE CEMENTED BASE LAYER AT THE END OF THE TEST (41 803 REPETITIONS) ON HVS TEST SECTION 309A4 (TRAFFICKING SINGLE WHEEL LOAD: 150 kN; TYRE PRESSURE: 1445 kPa).

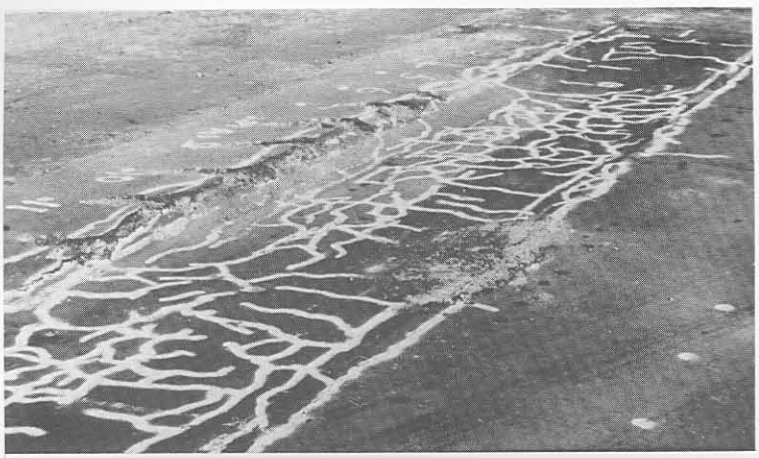

PLATE D.23 RELATIVELY DEEP PAVEMENT: ROAD 1932 – EXCESSIVE CRUSHING FAILURE AT THE END OF THE TEST (48 000 REPETITIONS) ON HVS TEST SECTION 337A4 (TRAFFICKING SINGLE WHEEL LOAD: 150 kN; TYRE PRESSURE: 1445 kPa).

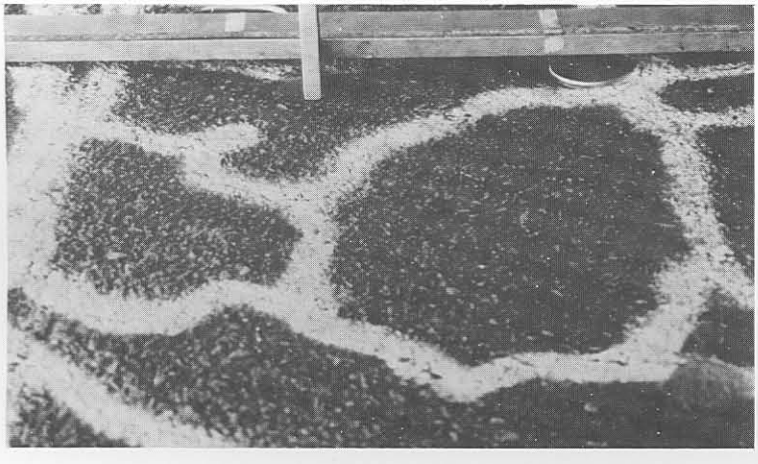

PLATE D.24 RELATIVELY DEEP PAVEMENT: ROAD 1932 – CRUSHING FAILURE AT THE END OF THE TEST (143 000 REPETITIONS) ON HVS TEST SECTION 338A4. DEFORMATION APPROXIMATELY 10 mm (TRAFFICKING SINGLE WHEEL LOAD: 150 kN; TYRE PRESSURE: 960 kPa).

(a) Layout of the rehabilitation section on which the "crack and seat" method had been applied.

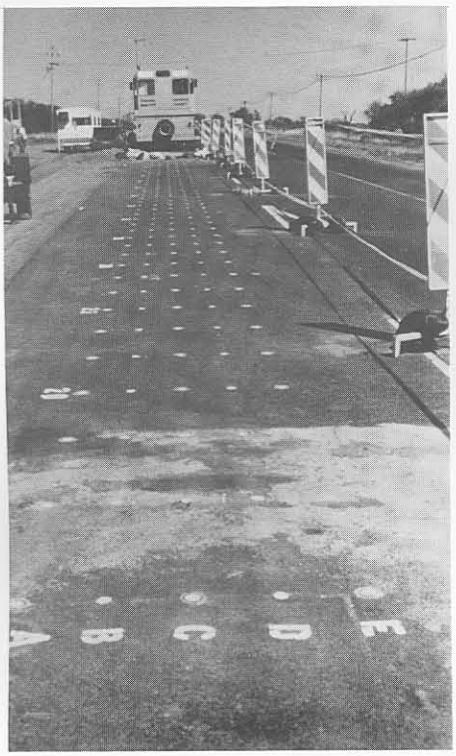

(b) Measurement of surface deflection prior to "crack and seat" operation.

(c) Rubbermatress (3 mm) used as protection of the surface seal on the experimental section during the "crack and seat" operation.

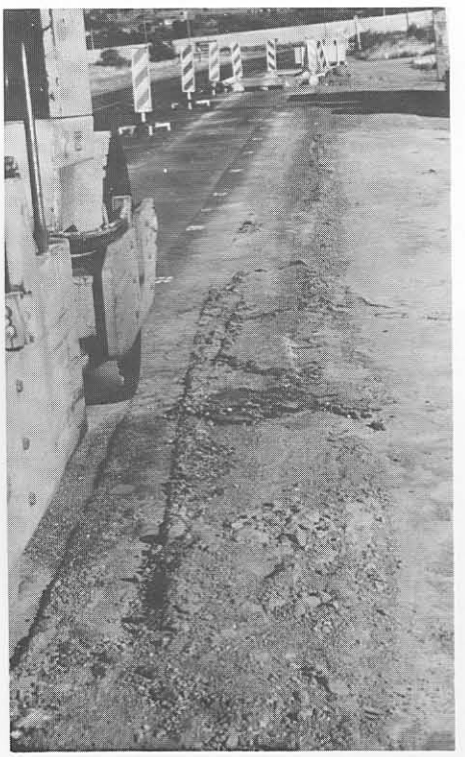

(d) Vibratory roller in operation during the "crack and seat" method.

PLATE D.25 RELATIVELY SHALLOW PAVEMENT: ROAD 2212 – PREPARATION OF THE 40 m REHABILITATION TEST SECTIONS, USING A HEAVY VIBRATORY ROLLER IN A "CRACK AND SEAT" OPERATION.

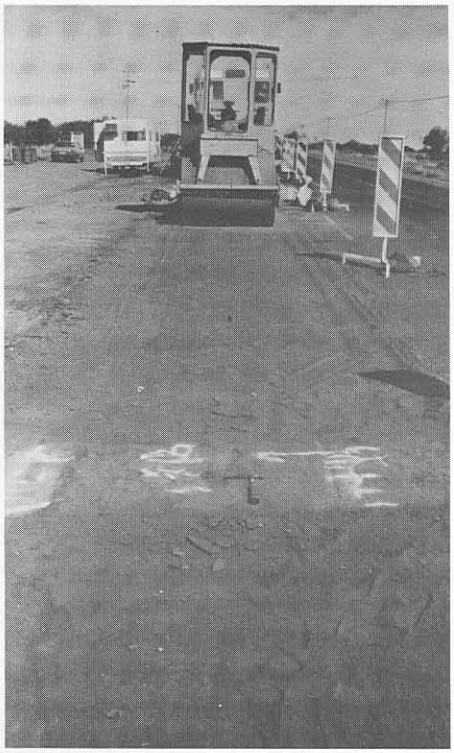

PLATE D.26 RELATIVELY SHALLOW PAVEMENT: ROAD 2212 – PREPARATION OF THE REHABILITATION TEST SECTIONS, USING A HEAVY VIBRATORY ROLLER IN A "CRACK AND SEAT" OPERATION. NOTE THE CRACK DEVELOPMENT IN THE CEMENTED BASE LAYER.

(a) Granular base material on the precracked cemented subbase.

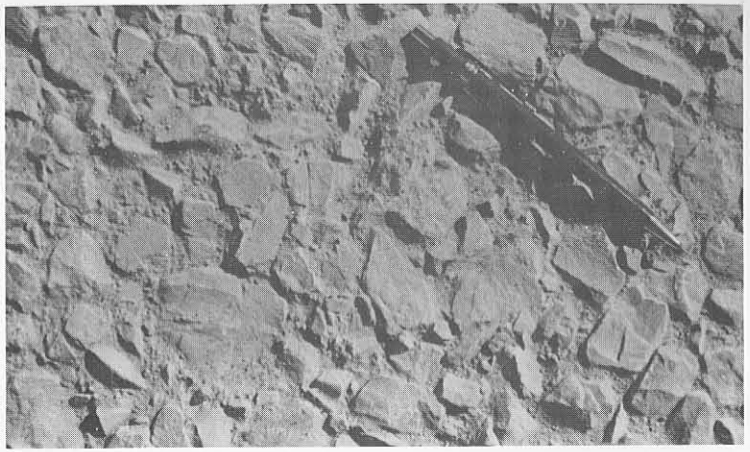

(b) Mosiac pattern of the 150 mm G1 – granular base prior to application of the prime coat.

(c) Base layer after the application of the prime coat.

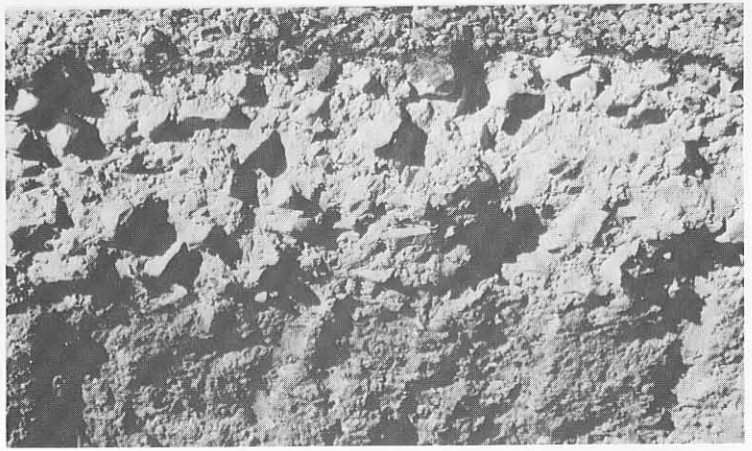

(d) Test pit indicating the 150 mm G1 – base layer on top of the precracked cemented layer.

PLATE D.27 RELATIVELY SHALLOW PAVEMENT: ROAD 2212 – REHABILITATION SECTIONS: ASPECTS OF THE 150 mm G1 – GRANULAR BASE LAYER ON TOP OF THE PRECRACKED CEMENTED LAYER.

(a) Brooming of surface of the cemented base layer after the "crack and seat" operation, before the application of the prime coat.

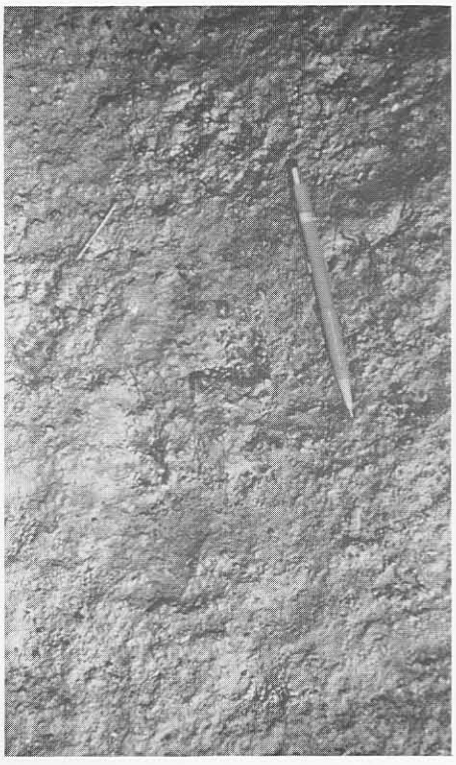

(b) Surface of the precracked cemented base after application of the prime coat.

(c) Final surface of the 35 mm asphalt premix section (40 m in length).

PLATE D.28 RELATIVELY SHALLOW PAVEMENT: ROAD 2212 – REHABILITATION SECTIONS: ASPECTS OF THE 35 mm ASPHALT PREMIX LAYER ON TOP OF THE PRECRACKED CEMENTED LAYER.

APPENDIX E

DETAILED COMPUTER OUTPUT SUMMARY OF THE DYNAMIC CONE PENETROMETER (DCP) INVESTIGATIONS ON THE HVS TEST SECTIONS EVALUATED IN THIS STUDY

NOTE: These figures are self explainatory and the detail identification is given on the top of each figure

RTT, CSIR, SA

SUMMARY OF DCP INVESTIGATION

DATA FILE :DEEP PAVEMENT: ROAD 1932
REGION :ROOIWAL (N=10)
ROAD NUMBER :P1932
DISTANCE : 2.9
POSITION : L | X | | M | | | R
CONDITION : ~~FAILED~~ | OVERSTRESSED | SOUND
RUT. | DEFORM. | PUMP. | CRACKS : CROCK | LONG. | OTHER
DATE :860325

PAVEMENT CHARACTERISTICS

	DATA	B/CURVE
STRUCTURE NUMBER :	397	
BALANCE NUMBER (BN 100) :	27	24
DIFFERENCE IN BN100 :	3	
BALANCE CURVE IS WHERE B =	19	A= 1398
STRUCT. CAP. (E80 X 10^6) :	>10	
ROAD CATEGORY :	C	
TRAFFIC : LIGHT TRAFFIC		

AVERAGE EQUIVALENT STRENGTH

FROM - TO	AV. PENETRATION	SD	80 P	CBR	UCS
0- 50	1.3	0.2	1.4	251	1940
51-180	1.7	0.3	1.9	198	1574
181-330	3.2	0.7	3.8	93	809
331-480	3.1	0.4	3.5	96	832
481-800	4.2	1.2	5.2	66	598

CATEGORY V : AVERAGELY BALANCED DEEP STRUCTURE (ABD)

DCP CURVE

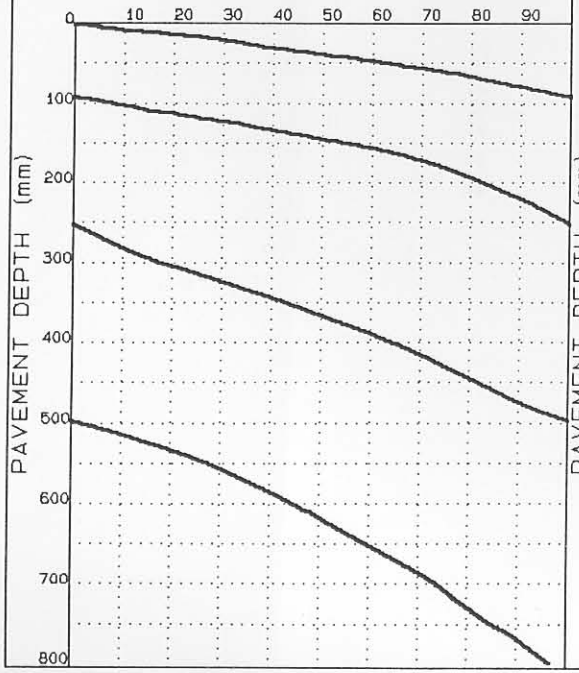

BALANCE CURVE

(DSN 800) (-90 ≤ B ≤ +90)
% OF PAVEMENT STRUCTURE NUMBER

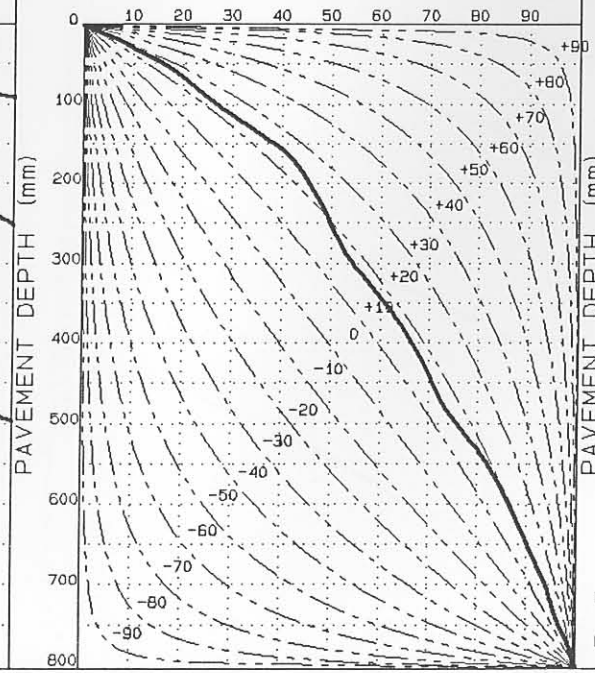

LAYER STRENGTH DIAGRAM

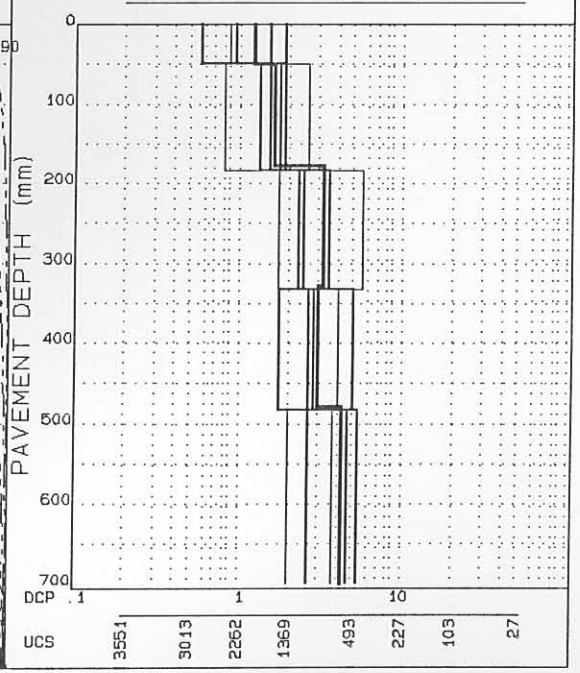

FIGURE E.1

RTT, CSIR, SA

SUMMARY OF DCP INVESTIGATION

DATA FILE :DEEP PAVEMENT: ROAD 1932
REGION :ROOIWAL (N=10)
ROAD NUMBER :P1932
DISTANCE : 2.9
POSITION : L | M | R
CONDITION : FAILED | OVERSTRESSED | SOUND
RUT. | DEFORM. | PUMP. | CRACKS : CROCK. | LONG. | OTHER
DATE :860325

PAVEMENT CHARACTERISTICS

	DATA	B/CURVE
STRUCTURE NUMBER :	397	
BALANCE NUMBER (BN 100) :	27	24
DIFFERENCE IN BN100 :	3	
BALANCE CURVE IS WHERE B =	19	A= 1398
STRUCT. CAP. (E80 X 10^6) :	>10	
ROAD CATEGORY :	C	
TRAFFIC : LIGHT TRAFFIC		

AVERAGE EQUIVALENT STRENGTH

FROM - TO	AV. PENETRATION	SD	80 P	CBR	UCS
0- 50	1.3	0.2	1.4	251	1940
51-180	1.7	0.3	1.9	198	1574
181-330	3.2	0.7	3.8	93	809
331-480	3.1	0.4	3.5	96	832
481-800	4.2	1.2	5.2	66	598

CATEGORY V : AVERAGELY BALANCED DEEP STRUCTURE (ABD)

DCP CURVE

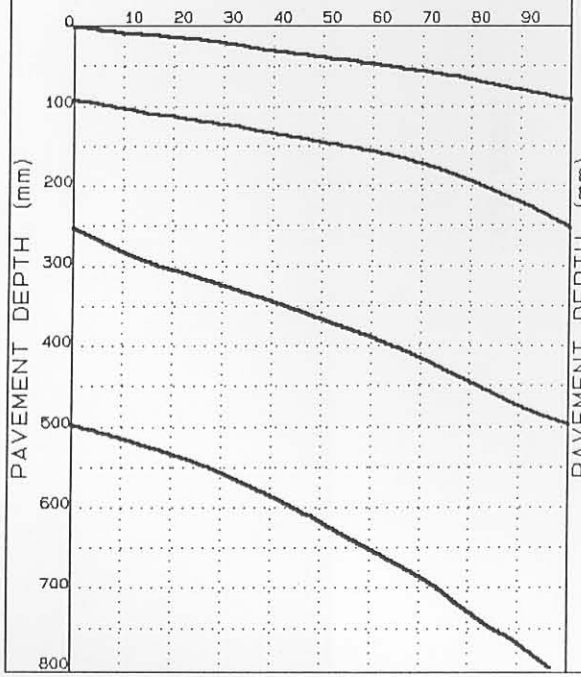

BALANCE CURVE

(DSN 800) (-90 ≤ B ≤ +90)
% OF PAVEMENT STRUCTURE NUMBER

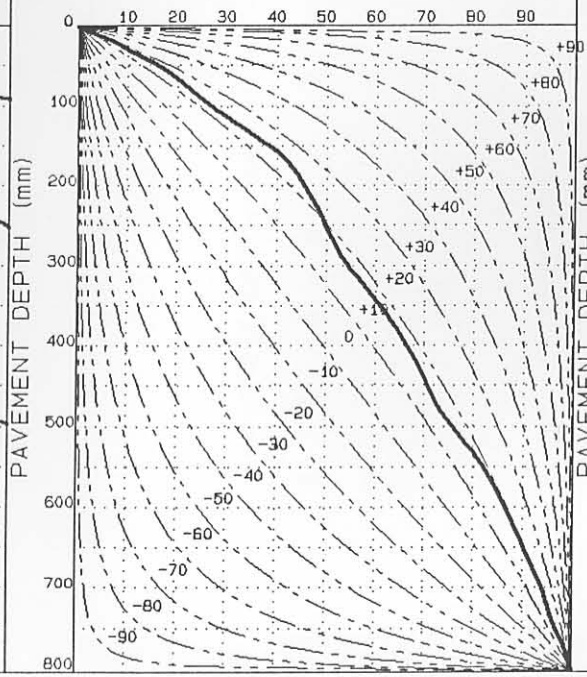

LAYER STRENGTH DIAGRAM

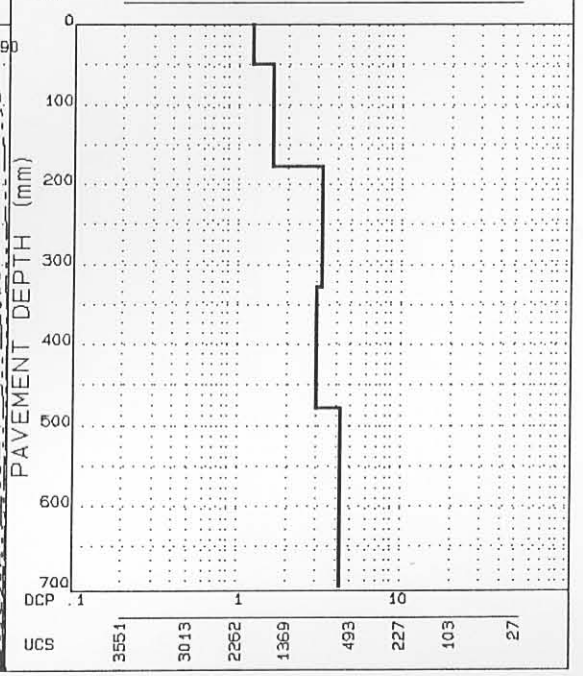

FIGURE E.2

ATT, CSIR, SA

SUMMARY OF DCP INVESTIGATION

AVERAGE EQUIVALENT STRENGTH (REDEFINED)

FROM - TO (mm)	AV. PENETRATION (mm/blow)	SD	BOP	CBR%	UCS (kPa)
0- 56	1.3	0.2	1.4	251	1940
57- 88	1.7	0.2	1.9	194	1546
89-152	1.6	0.1	1.7	211	1665
153-296	3.2	0.9	3.9	95	825
297-344	2.3	0.1	2.5	138	1146
345-472	3.2	0.3	3.5	92	802
473-616	3.1	0.6	3.6	97	840
617-640	4.1	0.1	4.1	69	622
641-688	4.0	0.3	4.3	70	630
689-800	5.6	0.6	6.1	46	435

DATA FILE: DEEP PAVEMENT: ROAD 1932 (ROOI

NORMALIZED CURVE

DEVIATION (A_i) FROM STANDARD PAVEMENT BALANCE CURVE (SPBC), %.mm

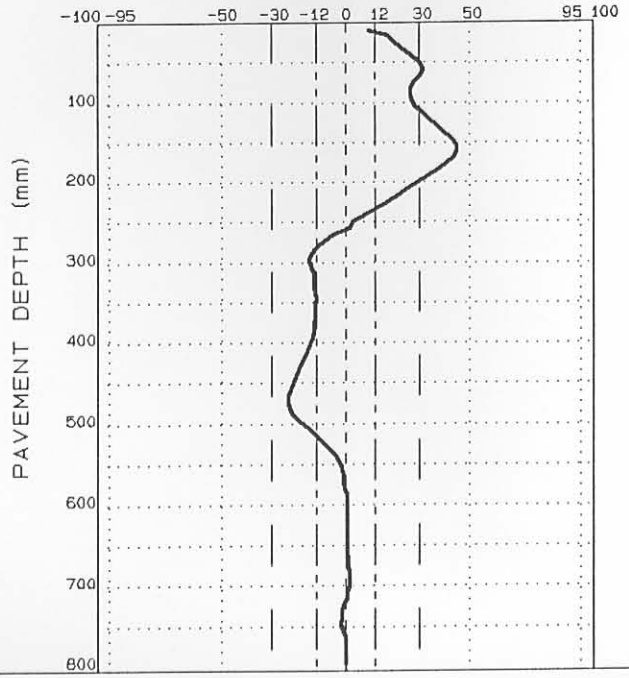

LAYER STRENGTH DIAGRAM (REDEFINED)

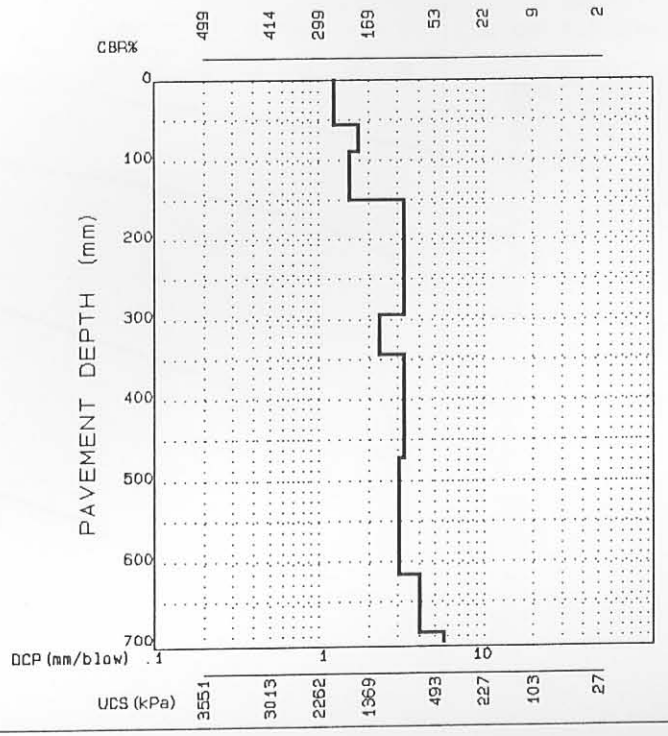

FIGURE E.3

RTT, CSIR, SA

SUMMARY OF DCP INVESTIGATION

DATA FILE :DEEP PAVEMENT: ROAD 1932
REGION :ROOIWAL (N=10)
ROAD NUMBER :P1932
DISTANCE : 2.9
POSITION : L [X] M R
CONDITION : FAILED | OVERSTRESSED | SOUND
RUT. | DEFORM. | PUMP. | CRACKS : CROCK. | LONG. | OTHER
DATE :860325

PAVEMENT CHARACTERISTICS

	DATA	B/CURVE
STRUCTURE NUMBER :	397	
BALANCE NUMBER (BN 100) :	27	24
DIFFERENCE IN BN100 :	3	
BALANCE CURVE IS WHERE B =	19	A= 1398
STRUCT. CAP. (E80 X 10^6) :	>10	
ROAD CATEGORY :	C	
TRAFFIC : LIGHT TRAFFIC		

AVERAGE EQUIVALENT STRENGTH

FROM - TO	AV. PENETRATION	SD	80 P	CBR	UCS
0- 50	1.3	0.2	1.4	251	1940
51-180	1.7	0.3	1.9	198	1574
181-330	3.2	0.7	3.8	93	809
331-480	3.1	0.4	3.5	96	832
481-800	4.2	1.2	5.2	66	598

CATEGORY V : AVERAGELY BALANCED DEEP STRUCTURE (ABD)

DCP CURVE

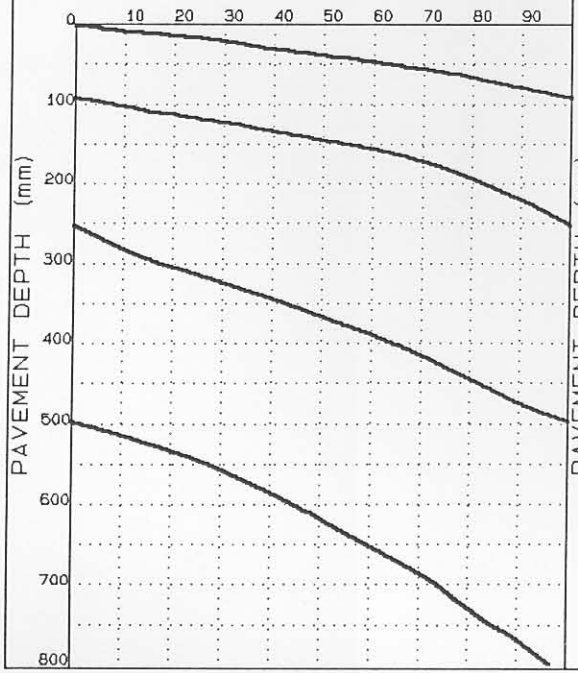

BALANCE CURVE

(DSN 800) (−90 ≤ B ≤ +90)
% OF PAVEMENT STRUCTURE NUMBER

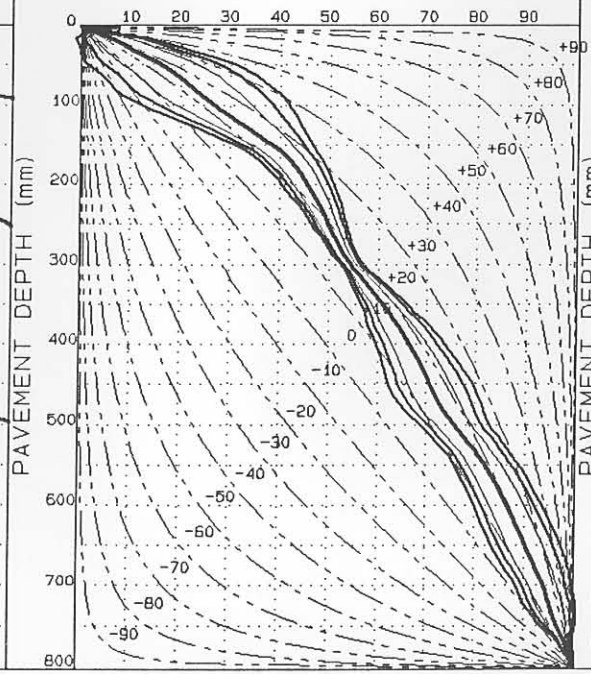

LAYER STRENGTH DIAGRAM

MEAN — 20/80 TH PERCENTILE

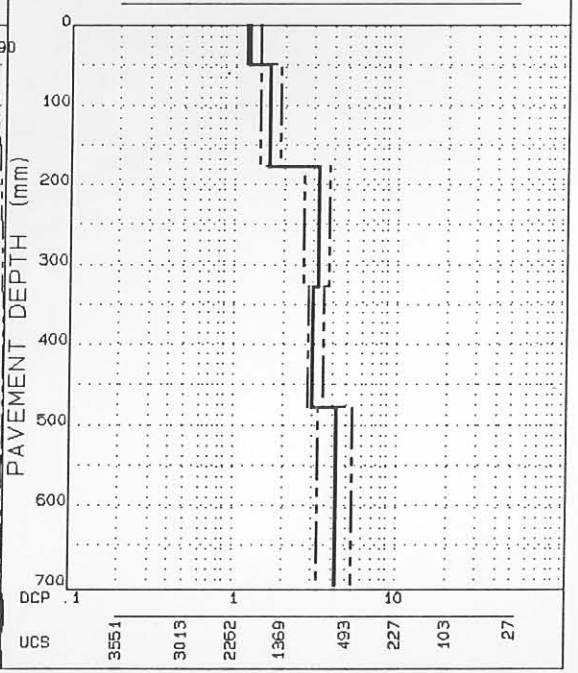

FIGURE E.4

RTT, CSIR, SA

SUMMARY OF DCP INVESTIGATION

AVERAGE EQUIVALENT STRENGTH (REDEFINED)

FROM - TO (mm)	AV. PENETRATION (mm/blow)	SD	BOP	CBR%	UCS (kPa)
0- 56	1.3	0.2	1.4	251	1940
57- 88	1.7	0.2	1.9	194	1546
89-152	1.6	0.1	1.7	211	1665
153-296	3.2	0.9	3.9	95	825
297-344	2.3	0.1	2.5	138	1146
345-472	3.2	0.3	3.5	92	802
473-616	3.1	0.6	3.6	97	840
617-640	4.1	0.1	4.1	69	622
641-688	4.0	0.3	4.3	70	630
689-800	5.6	0.6	6.1	46	435

DATA FILE: DEEP PAVEMENT: ROAD 1932

NORMALIZED CURVE

DEVIATION (A_i) FROM STANDARD PAVEMENT BALANCE CURVE (SPBC), %.mm

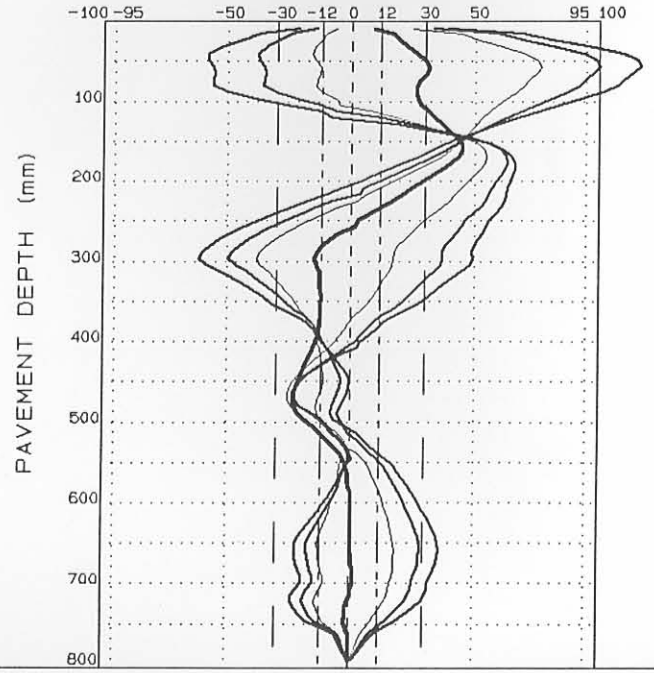

LAYER STRENGTH DIAGRAM (REDEFINED)

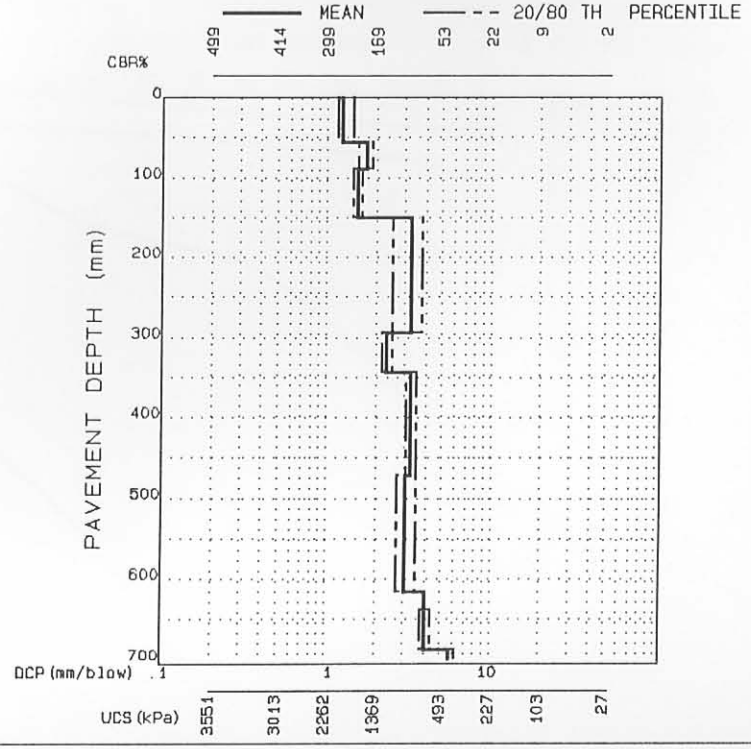

FIGURE E.5

RTT, CSIR, SA

SUMMARY OF DCP INVESTIGATION

DATA FILE :SHALLOW PAVEMENT: ROAD 2212
REGION :BULTFONTEIN
ROAD NUMBER :P2212
DISTANCE : 12.6
POSITION : L | M | R
CONDITION : FAILED | OVERSTRESSED | SOUND
RUT. | DEFORM. | PUMP. | CRACKS : CROCK | LONG. | OTHER
DATE :860324

PAVEMENT CHARACTERISTICS

	DATA	B/CURVE	FROM - TO
STRUCTURE NUMBER :	352		0- 80
BALANCE NUMBER (BN 100) :	56	46	81-160
DIFFERENCE IN BN100 :	10		161-210
BALANCE CURVE IS WHERE B =	41	A= 2089	211-375
STRUCT. CAP. (E80 X 10^6) :	>10		376-800
ROAD CATEGORY :	C		

TRAFFIC : LIGHT TRAFFIC

AVERAGE EQUIVALENT STRENGTH

AV. PENETRATION	SD	80 P	CBR	UCS
0.8	0.3	1.1	331	2474
3.5	0.7	4.0	85	748
2.3	0.4	2.6	145	1197
5.9	1.0	6.7	43	410
7.7	2.0	9.4	30	299

CATEGORY II : AVERAGELY BALANCED SHALLOW STRUCTURE (ABS)

DCP CURVE

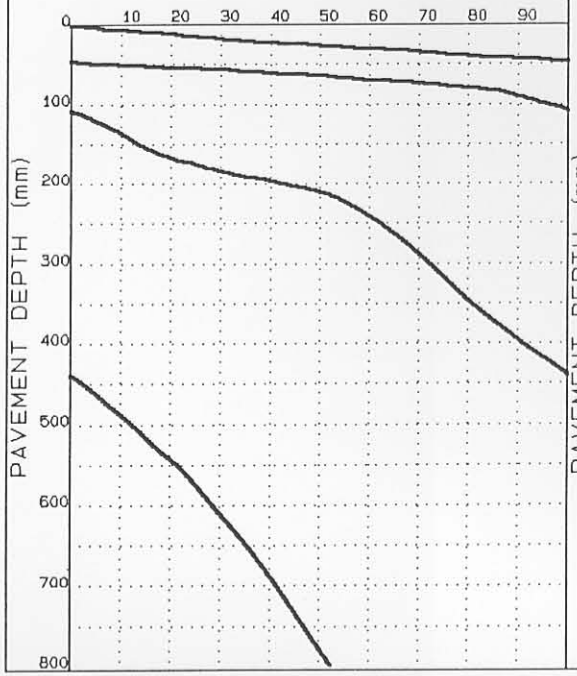

BALANCE CURVE

(DSN 800) (−90 ≤ B ≤ +90)

% OF PAVEMENT STRUCTURE NUMBER

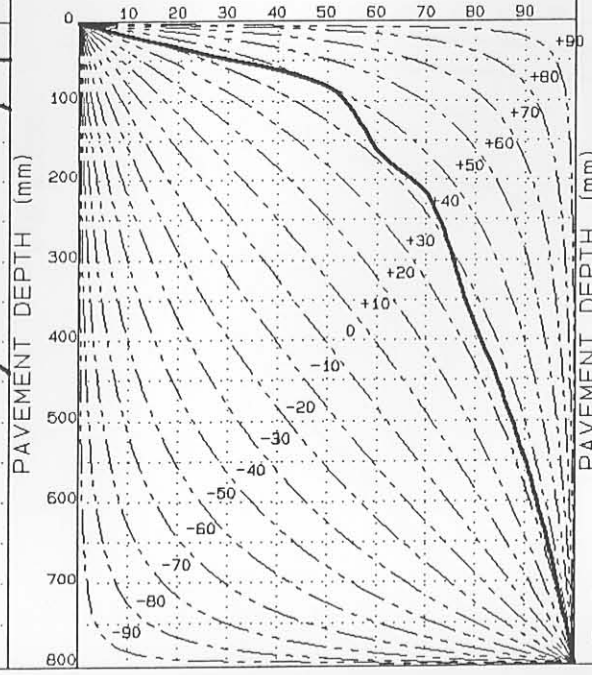

LAYER STRENGTH DIAGRAM

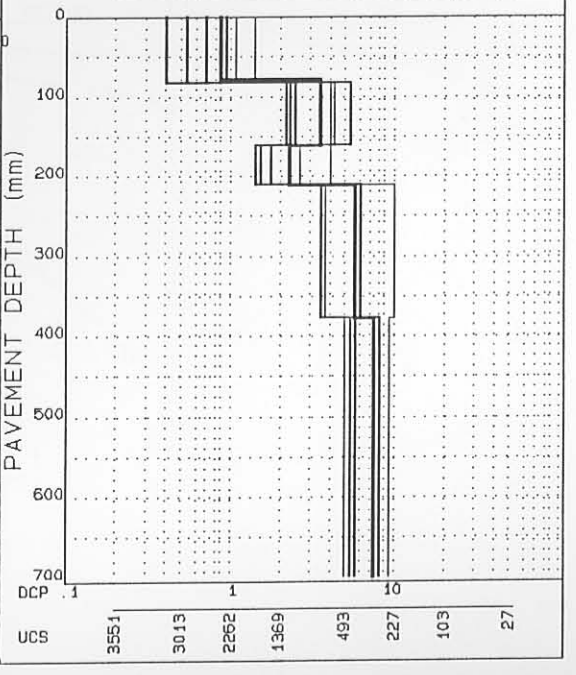

FIGURE E.6

RTT, CSIR, SA

SUMMARY OF DCP INVESTIGATION

DATA FILE :SHALLOW PAVEMENT: ROAD 2212
REGION :BULTFONTEIN
ROAD NUMBER :P2212
DISTANCE : 12.6
POSITION : L | | | M | X | | R
CONDITION : ~~FAILED~~ | OVERSTRESSED | SOUND
RUT. | DEFORM. | PUMP. | CRACKS : CROCK | LONG. | OTHER
DATE :860324

PAVEMENT CHARACTERISTICS

	DATA	B/CURVE
STRUCTURE NUMBER :	352	
BALANCE NUMBER (BN 100) :	56	46
DIFFERENCE IN BN100 :	10	
BALANCE CURVE IS WHERE B =	41	A= 2089
STRUCT. CAP. (E80 X 10^6) :	>10	
ROAD CATEGORY :	C	
TRAFFIC : LIGHT TRAFFIC		

AVERAGE EQUIVALENT STRENGTH

FROM - TO	AV. PENETRATION	SD	80 P	CBR	UCS
0- 80	0.8	0.3	1.1	331	2474
81-160	3.5	0.7	4.0	85	748
161-210	2.3	0.4	2.6	145	1197
211-375	5.9	1.0	6.7	43	410
376-800	7.7	2.0	9.4	30	299

CATEGORY II : AVERAGELY BALANCED SHALLOW STRUCTURE (ABS)

DCP CURVE

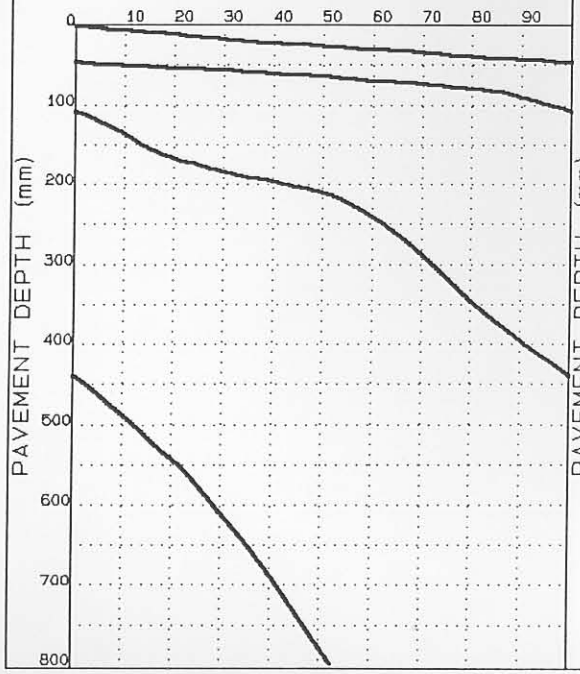

BALANCE CURVE

(DSN 800) (−90 ≤ B ≤ +90)
% OF PAVEMENT STRUCTURE NUMBER

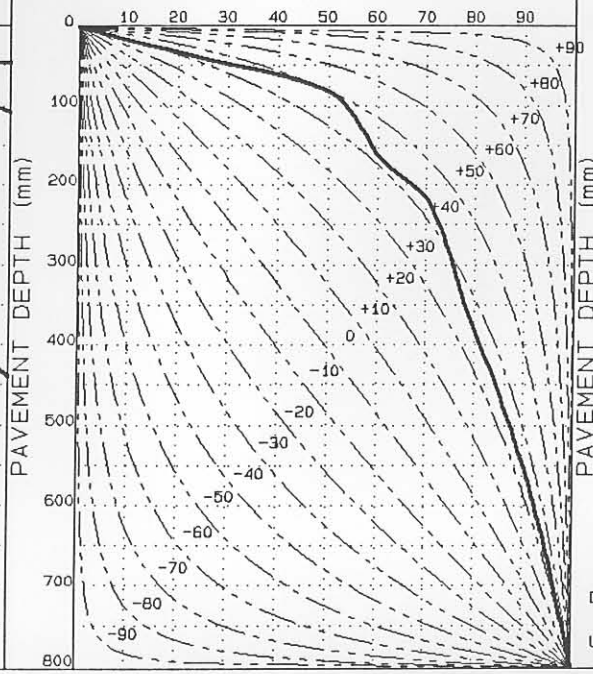

LAYER STRENGTH DIAGRAM

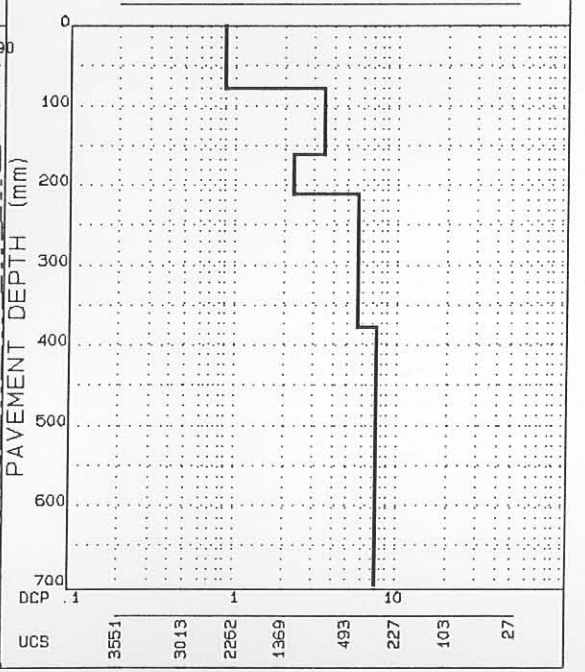

FIGURE E.7

ATT. CSIR. SA

SUMMARY OF DCP INVESTIGATION

AVERAGE EQUIVALENT STRENGTH (REDEFINED)

FROM - TO (mm)	AV. PENETRATION (mm/blow)	SD	BOP	CBR%	UCS (kPa)
0- 8	0.7	0.2	0.9	356	2638
9- 72	0.8	0.2	1.0	345	2566
73-168	3.3	0.8	4.0	91	794
169-208	2.1	0.3	2.3	158	1290
209-400	5.8	1.0	6.6	44	419
401-800	7.9	2.0	9.5	30	299

DATA FILE: SHALLOW PAVEMENT: ROAD 2212

NORMALIZED CURVE

DEVIATION (A_i) FROM STANDARD PAVEMENT BALANCE CURVE (SPBC), %.mm

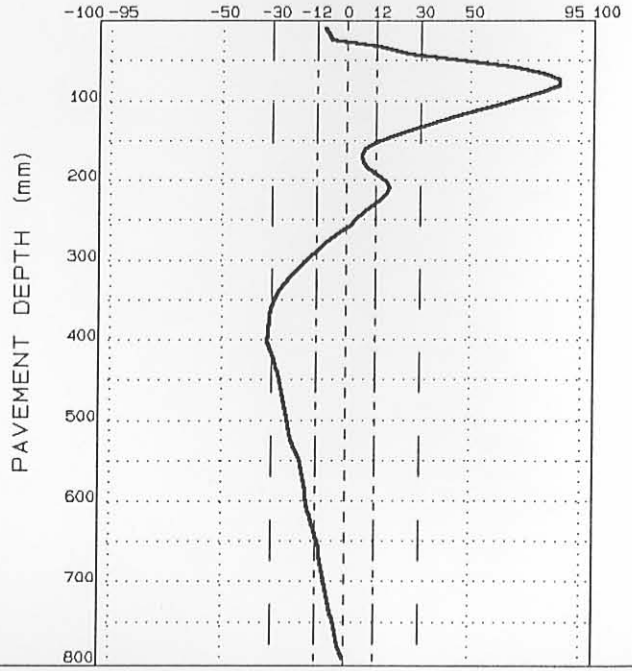

LAYER STRENGTH DIAGRAM (REDEFINED)

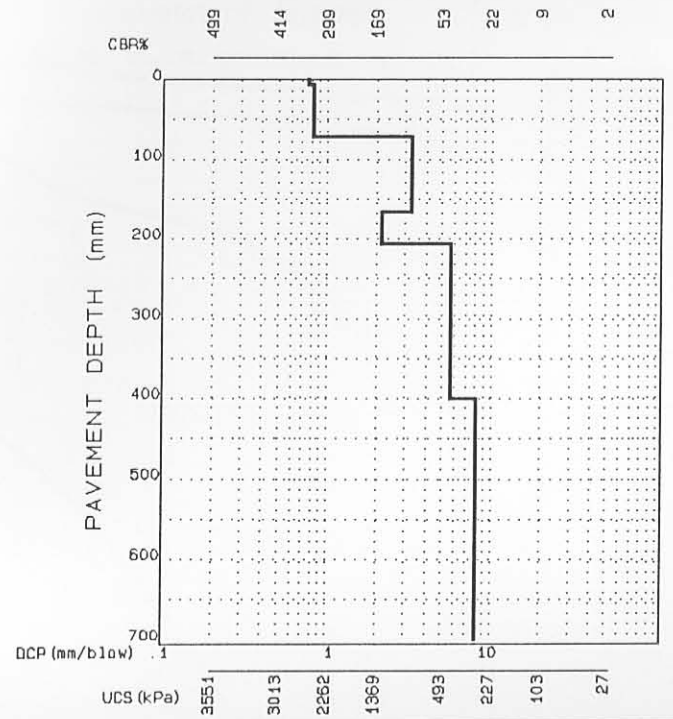

FIGURE E.8

RTT, CSIR, SA

SUMMARY OF DCP INVESTIGATION

DATA FILE :SHALLOW PAVEMENT: ROAD 2212
REGION :BULTFONTEIN
ROAD NUMBER :P2212
DISTANCE : 12.6
POSITION : L | M | R
CONDITION : FAILED | OVERSTRESSED | SOUND
RUT. | DEFORM. | PUMP. | CRACKS : CROCK | LONG. | OTHER
DATE :860324

PAVEMENT CHARACTERISTICS

	DATA	B/CURVE
STRUCTURE NUMBER :	352	
BALANCE NUMBER (BN 100) :	56	46
DIFFERENCE IN BN100 :	10	
BALANCE CURVE IS WHERE B =	41	A= 2089
STRUCT. CAP. (E80 X 10^6) :	>10	
ROAD CATEGORY :	C	

TRAFFIC : LIGHT TRAFFIC

AVERAGE EQUIVALENT STRENGTH

FROM - TO	AV. PENETRATION	SD	80 P	CBR	UCS
0- 80	0.8	0.3	1.1	331	2474
81-160	3.5	0.7	4.0	85	748
161-210	2.3	0.4	2.6	145	1197
211-375	5.9	1.0	6.7	43	410
376-800	7.7	2.0	9.4	30	299

CATEGORY II : AVERAGELY BALANCED SHALLOW STRUCTURE (ABS)

DCP CURVE

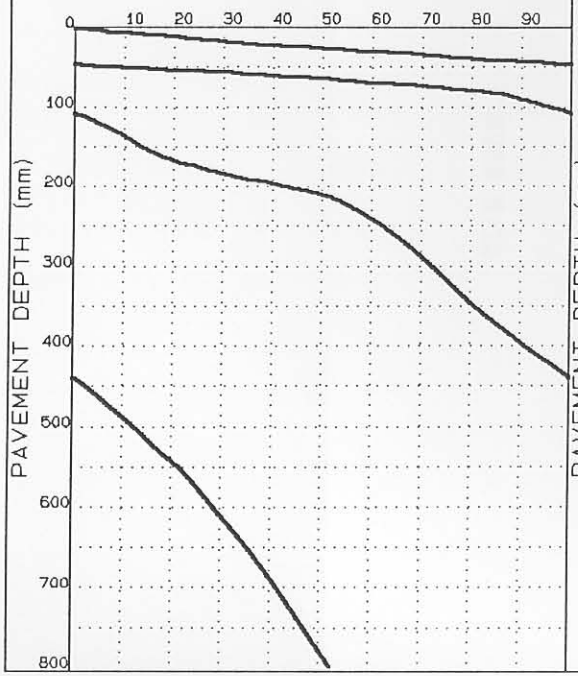

BALANCE CURVE

(DSN 800) (−90 ≤ B ≤ +90)

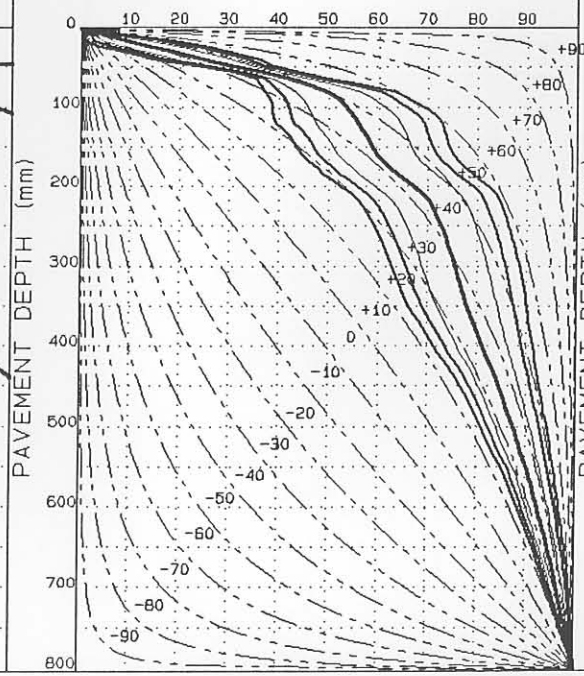

LAYER STRENGTH DIAGRAM

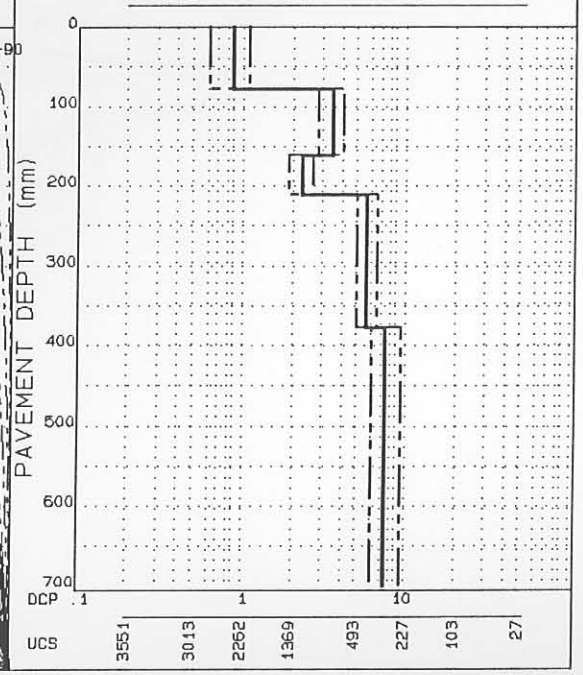

FIGURE E.9

RTT, CSIR, SA

SUMMARY OF DCP INVESTIGATION

AVERAGE EQUIVALENT STRENGTH (REDEFINED)

FROM - TO (mm)	AV. PENETRATION (mm/blow)	SD	80P	CBR%	UCS (kPa)
0- 8	0.7	0.2	0.9	356	2638
9- 72	0.8	0.2	1.0	345	2566
73-168	3.3	0.8	4.0	91	794
169-208	2.1	0.3	2.3	158	1290
209-400	5.8	1.0	6.6	44	419
401-800	7.9	2.0	9.5	30	299

DATA FILE: SHALLOW PAVEMENT: ROAD 2212

NORMALIZED CURVE

DEVIATION (A_i) FROM STANDARD PAVEMENT BALANCE CURVE (SPBC), %.mm

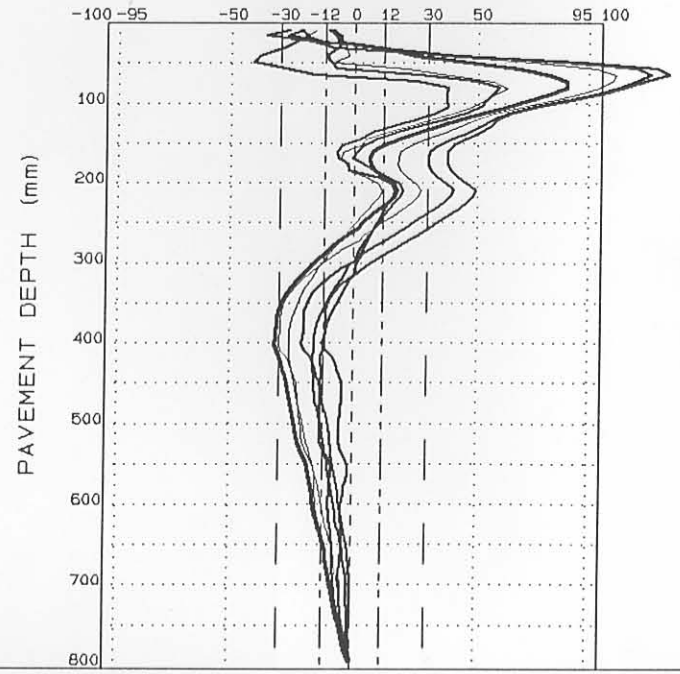

LAYER STRENGTH DIAGRAM (REDEFINED)

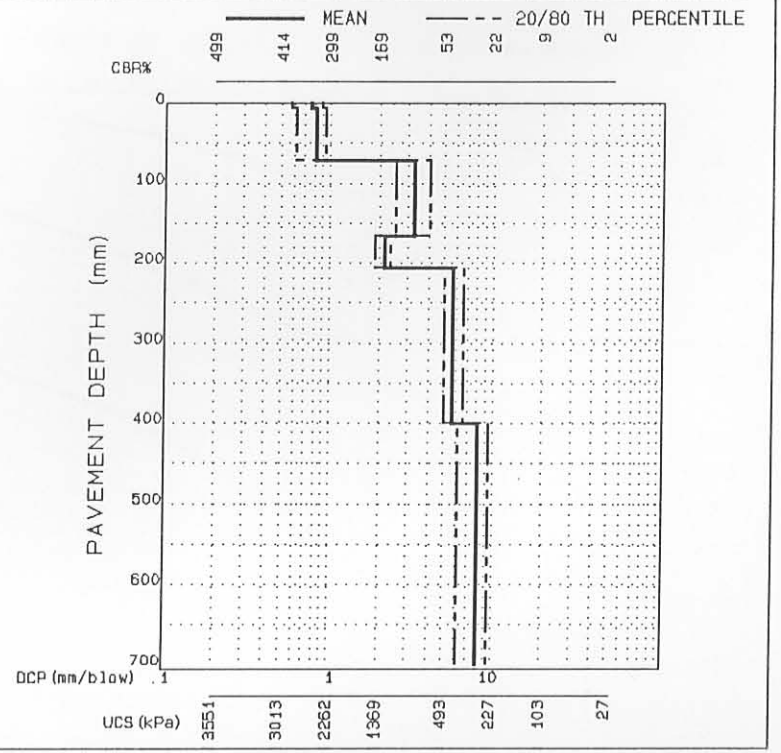

FIGURE E.10

RTT, CSIR, SA

SUMMARY OF DCP INVESTIGATION

DATA FILE :275A4, 3CL, 13CL; N=10
REGION :ROOIWAL (N=10)
ROAD NUMBER :P1932
DISTANCE : 2.9
POSITION : L | M | R
CONDITION : FAILED | OVERSTRESSED | SOUND
RUT. | DEFORM. | PUMP. | CRACKS : CROCK | LONG. | OTHER
DATE :85/06/06

PAVEMENT CHARACTERISTICS

	DATA	B/CURVE
STRUCTURE NUMBER :	352	
BALANCE NUMBER (BN 100) :	24	25
DIFFERENCE IN BN100 :	-1	
BALANCE CURVE IS WHERE B =	20	A= 956
STRUCT. CAP. (E80 X 10^6) :	>10	
ROAD CATEGORY :	C	
TRAFFIC : LIGHT TRAFFIC		

AVERAGE EQUIVALENT STRENGTH

FROM - TO	AV. PENETRATION	SD	80 P	CBR	UCS
0- 50	1.2	0.3	1.5	261	2007
51-180	1.8	0.4	2.2	183	1469
181-330	2.4	0.4	2.7	137	1138
331-480	2.8	0.8	3.4	113	961
481-800	5.4	1.5	6.7	48	452

CATEGORY IV : WELL-BALANCED DEEP STRUCTURE (WBD)

DCP CURVE

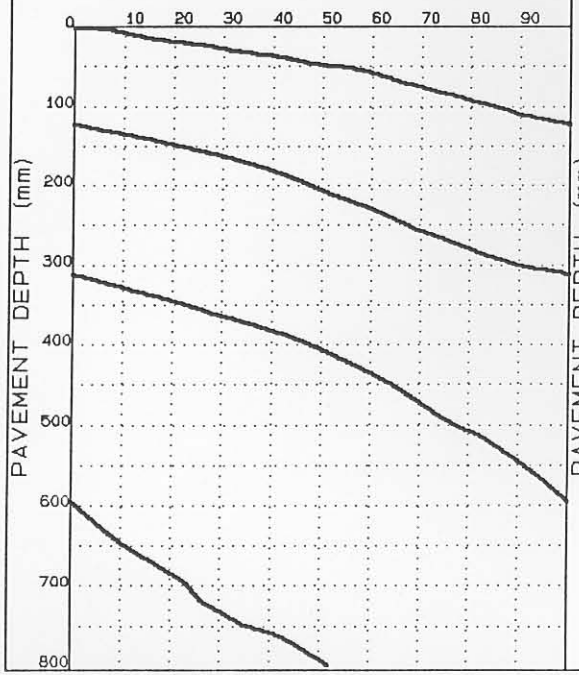

BALANCE CURVE

(DSN 800) (-90 ≤ B ≤ +90)
% OF PAVEMENT STRUCTURE NUMBER

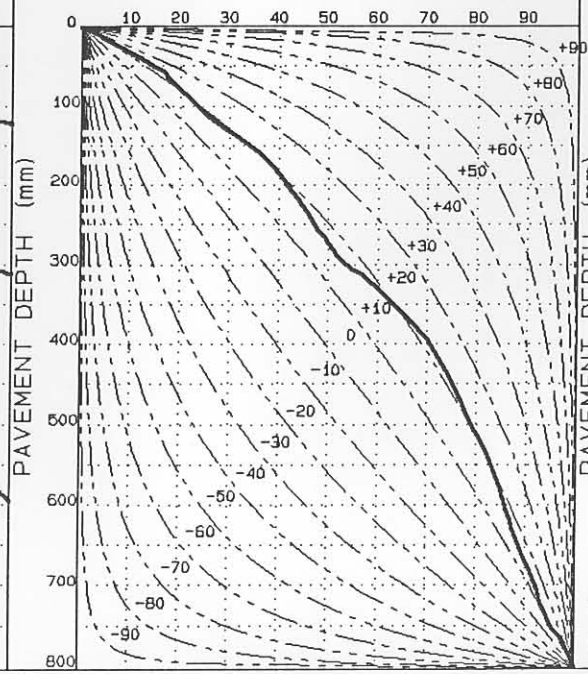

LAYER STRENGTH DIAGRAM

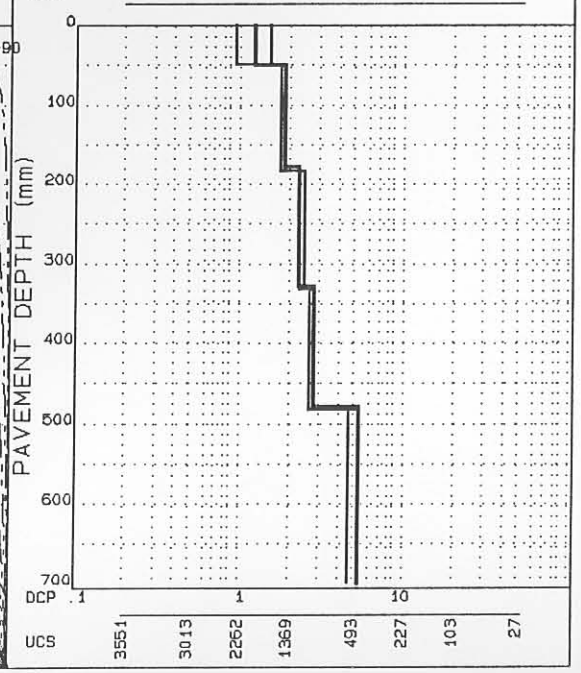

FIGURE E.11

RTT, CSIR, SA

SUMMARY OF DCP INVESTIGATION

AVERAGE EQUIVALENT STRENGTH (REDEFINED)

FROM - TO (mm)	AV. PENETRATION (mm/blow)	SD	BOP	CBR%	UCS (kPa)
0- 48	1.2	0.3	1.5	257	1980
49-112	2.0	0.5	2.4	170	1376
113-160	1.5	0.2	1.7	214	1685
161-280	2.5	0.4	2.8	130	1087
281-400	2.0	0.4	2.3	171	1383
401-496	3.5	0.5	4.0	83	732
497-512	3.3	0.3	3.5	91	794
513-648	4.9	0.6	5.5	54	501
649-688	5.0	0.7	5.6	53	493
689-800	6.6	1.9	8.1	37	359

DATA FILE: 275A4, 3CL, 13CL; N=10

NORMALIZED CURVE

DEVIATION (A_i) FROM STANDARD PAVEMENT BALANCE CURVE (SPBC), %.mm

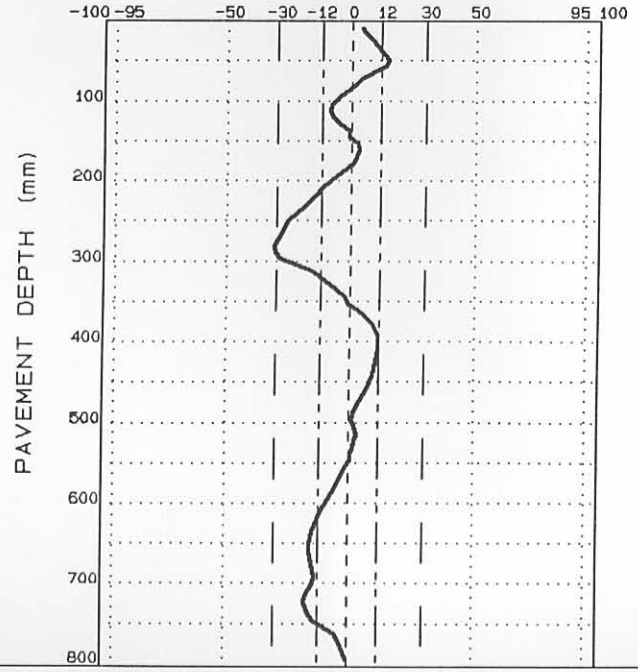

LAYER STRENGTH DIAGRAM (REDEFINED)

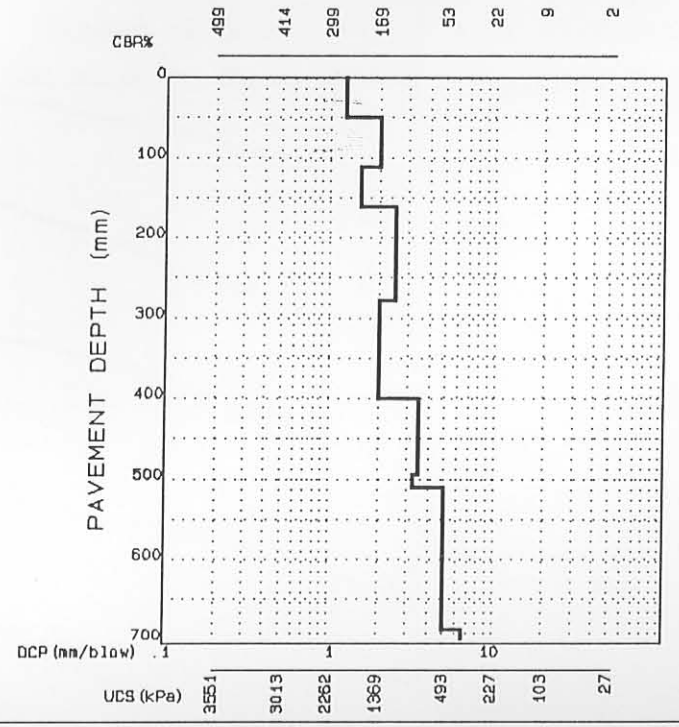

FIGURE E.12

RTT, CSIR, SA

SUMMARY OF DCP INVESTIGATION

DATA FILE :275A4, 5CL, 10CL; N= 1000000
REGION :ROOIWAL (N=1005069)
ROAD NUMBER :P1932
DISTANCE : 2.9
POSITION : L | M | R
CONDITION : FAILED | OVERSTRESSED | SOUND
RUT. | DEFORM. | PUMP. | CRACKS : CROCK. | LONG. | OTHER
DATE :85/05/05

PAVEMENT CHARACTERISTICS

	DATA	B/CURVE
STRUCTURE NUMBER :	456	
BALANCE NUMBER (BN 100) :	16	17
DIFFERENCE IN BN100 :	-1	
BALANCE CURVE IS WHERE B =	9	A= 1109
STRUCT. CAP. (E80 X 10^6) :	>10	
ROAD CATEGORY :	C	
TRAFFIC : LIGHT TRAFFIC		

AVERAGE EQUIVALENT STRENGTH

FROM - TO	AV. PENETRATION	SD	80 P	CBR	UCS
0- 50	1.3	0.3	1.5	242	1878
51-180	1.8	0.5	2.2	182	1462
181-330	2.4	1.0	3.2	137	1138
331-480	2.5	0.6	3.0	128	1072
481-800	2.8	0.8	3.5	110	938

CATEGORY IV : WELL-BALANCED DEEP STRUCTURE (WBD)

DCP CURVE

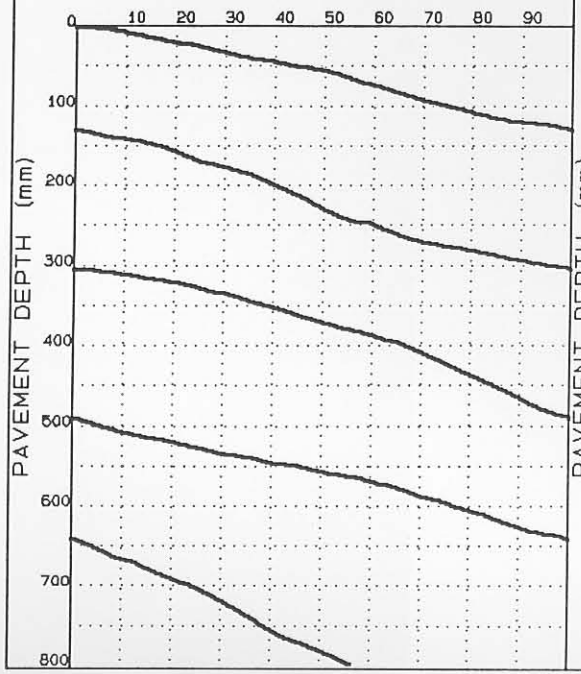

BALANCE CURVE

(DSN 800) (-90 ≤ B ≤ +90)
% OF PAVEMENT STRUCTURE NUMBER

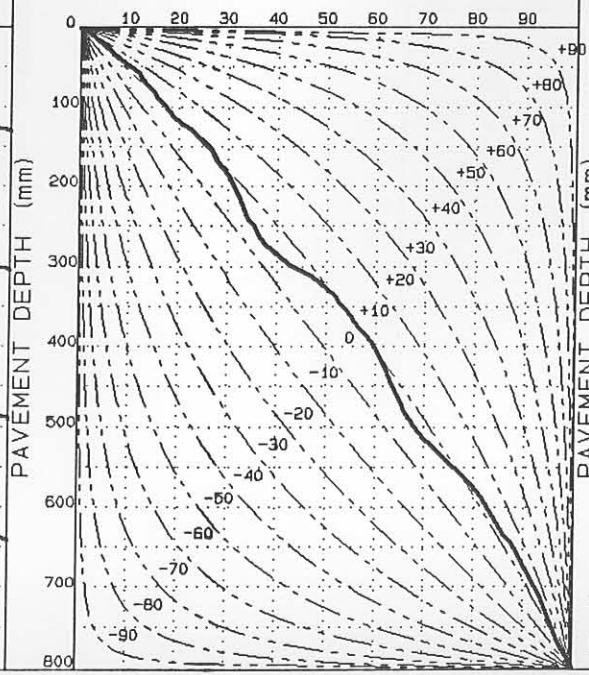

LAYER STRENGTH DIAGRAM

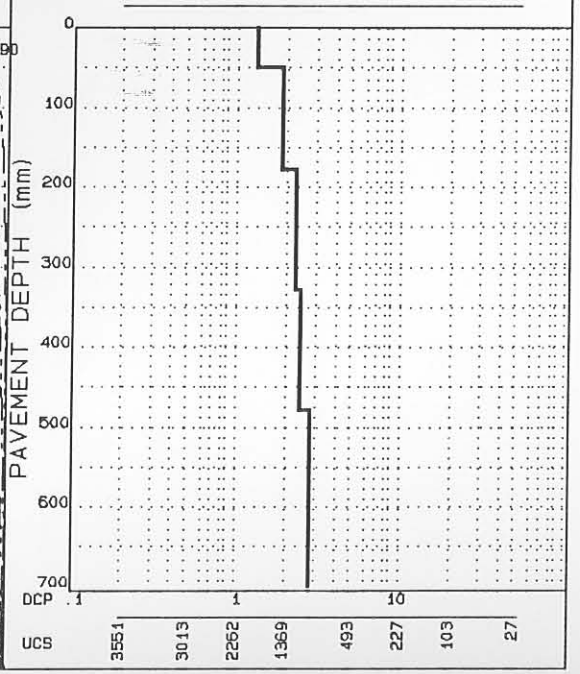

FIGURE E.13

ATT, CSIR, SA

SUMMARY OF DCP INVESTIGATION

AVERAGE EQUIVALENT STRENGTH (REDEFINED)

FROM - TO (mm)	AV. PENETRATION (mm/blow)	SD	BOP	CBR%	UCS (kPa)
0- 56	1.3	0.3	1.5	245	1899
57-112	1.8	0.3	2.1	181	1454
113-144	1.4	0.2	1.5	237	1844
145-264	2.9	0.6	3.4	104	893
265-352	1.4	0.4	1.8	227	1775
353-368	1.9	0.1	2.0	176	1419
369-384	1.7	0.2	1.8	193	1539
385-480	2.9	0.4	3.2	106	908
481-592	2.0	0.4	2.3	170	1376
593-800	3.2	0.6	3.7	92	802

DATA FILE: 275A4, 5CL, 10CL; N=1000000

NORMALIZED CURVE

DEVIATION (A_i) FROM STANDARD PAVEMENT BALANCE CURVE (SPBC), %.mm

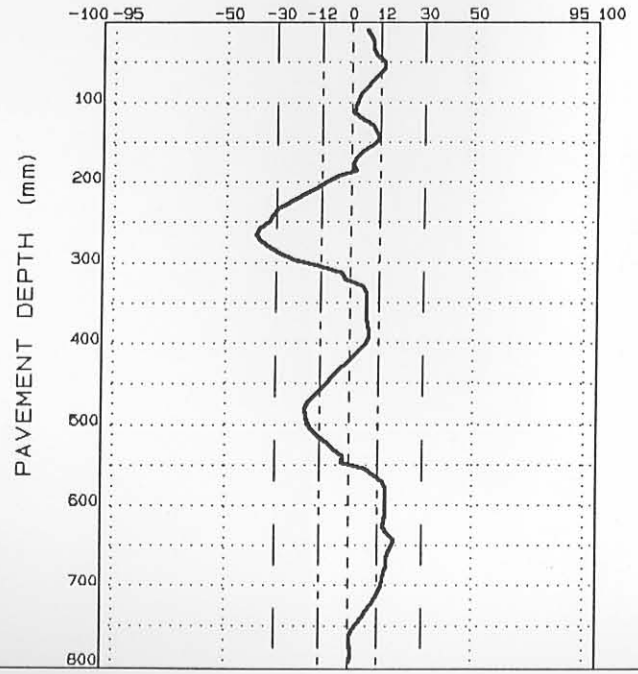

LAYER STRENGTH DIAGRAM (REDEFINED)

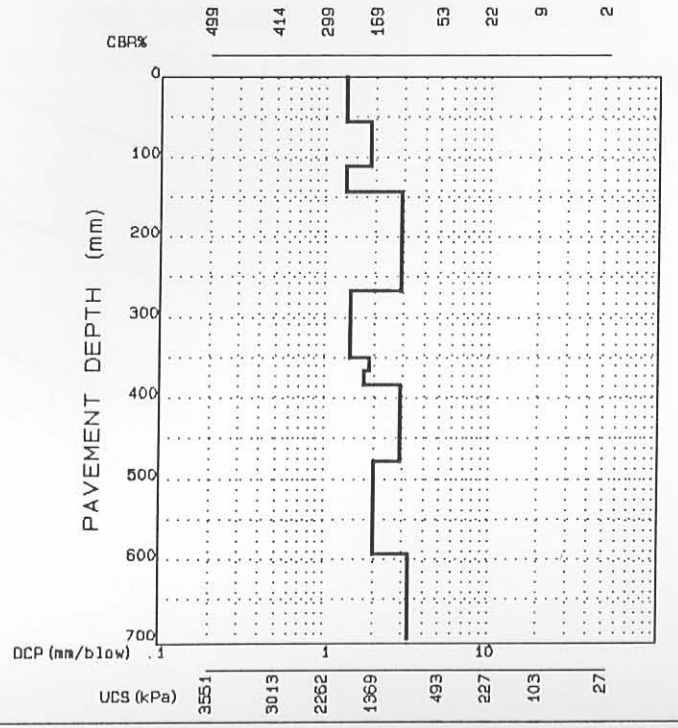

FIGURE E.14

RTT, CSIR, SA

SUMMARY OF DCP INVESTIGATION

DATA FILE :275A4, 1, 3, 5, 6, 7 (IN); N=2105910
REGION :ROOIWAL (N=2105910)
ROAD NUMBER :P1932
DISTANCE : 2.9
POSITION : X | M | R
CONDITION : FAILED | OVERSTRESSED | SOUND
RUT. | DEFORM. | PUMP. | CRACKS : CROCK | LONG. | OTHER
DATE :85/10/24

PAVEMENT CHARACTERISTICS

	DATA	B/CURVE
STRUCTURE NUMBER :	390	
BALANCE NUMBER (BN 100) :	13	18
DIFFERENCE IN BN100 :	-5	
BALANCE CURVE IS WHERE B =	11	A= 1413
STRUCT. CAP. (E80 X 10^6) :	>10	
ROAD CATEGORY :	C	
TRAFFIC : LIGHT TRAFFIC		

AVERAGE EQUIVALENT STRENGTH

FROM - TO	AV. PENETRATION	SD	80 P	CBR	UCS
0- 50	2.2	0.5	2.6	148	1218
51-180	1.8	0.4	2.2	184	1476
181-330	2.1	0.5	2.5	162	1319
331-480	2.3	0.3	2.5	144	1189
481-800	3.5	1.1	4.4	83	732

CATEGORY V : AVERAGELY BALANCED DEEP STRUCTURE (ABD)

DCP CURVE

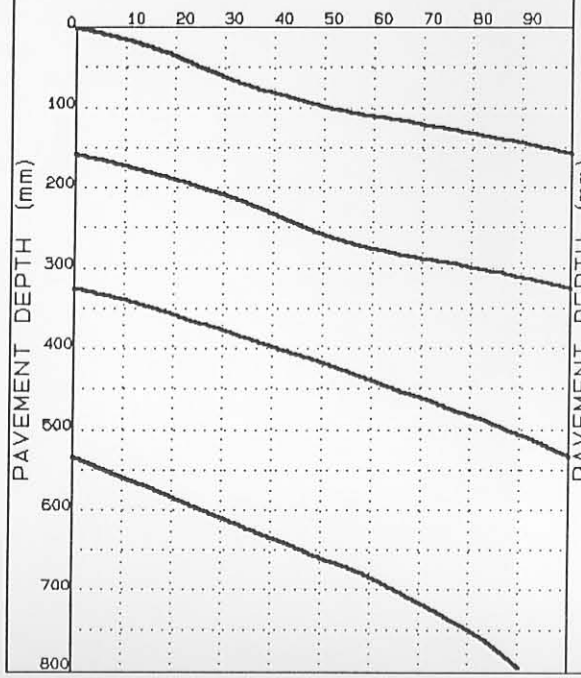

BALANCE CURVE

(DSN 800) (-90 ≤ B ≤ +90)

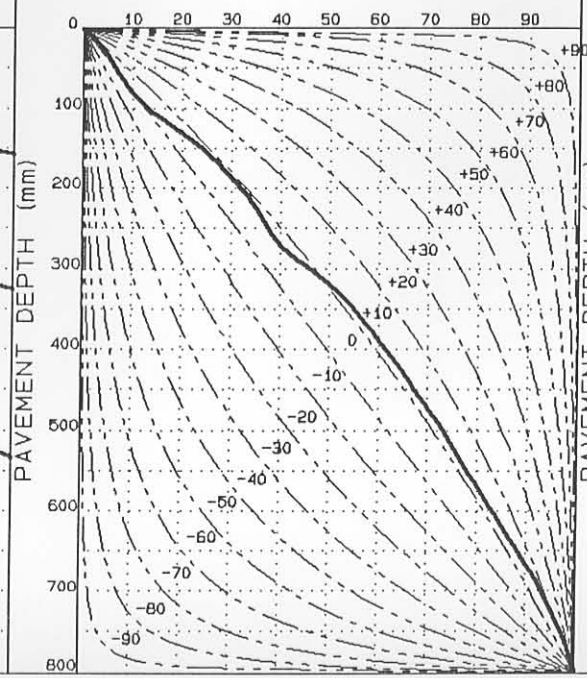

LAYER STRENGTH DIAGRAM

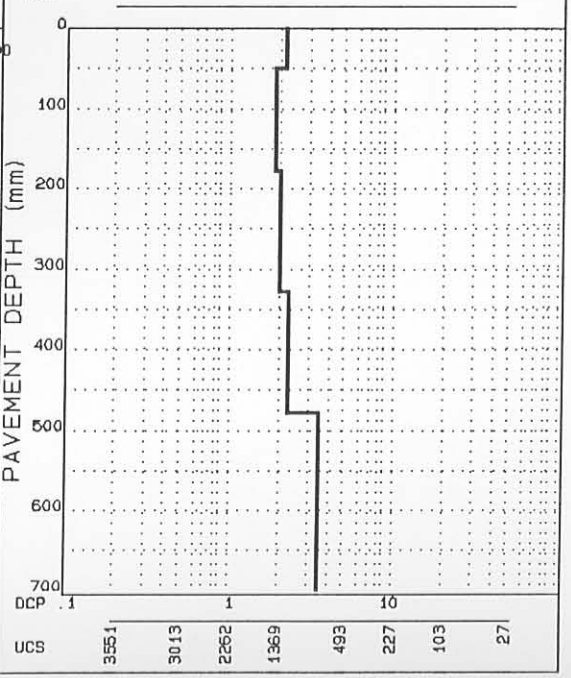

FIGURE E.15

ATT, CSIR, SA

SUMMARY OF DCP INVESTIGATION

AVERAGE EQUIVALENT STRENGTH (REDEFINED)

FROM - TO (mm)	AV. PENETRATION (mm/blow)	SD	BOP	CBR%	UCS (kPa)
0- 96	2.3	0.4	2.6	145	1197
97-184	1.6	0.3	1.8	210	1658
185-264	2.5	0.3	2.7	128	1072
265-424	1.9	0.4	2.2	176	1419
425-448	2.4	0.1	2.4	135	1124
449-488	2.5	0.2	2.7	128	1072
489-552	2.9	0.3	3.2	105	901
553-680	2.9	0.1	3.0	108	923
681-800	4.6	1.0	5.4	59	542

DATA FILE: 275A4, 1, 3, 5, 6, 7 (IN); N=2105910

NORMALIZED CURVE

DEVIATION (A_i) FROM STANDARD PAVEMENT BALANCE CURVE (SPBC), %.mm

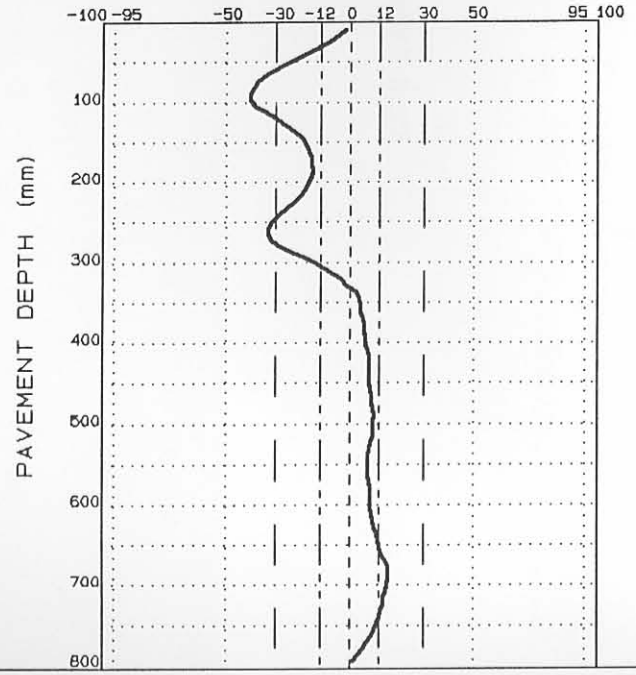

LAYER STRENGTH DIAGRAM (REDEFINED)

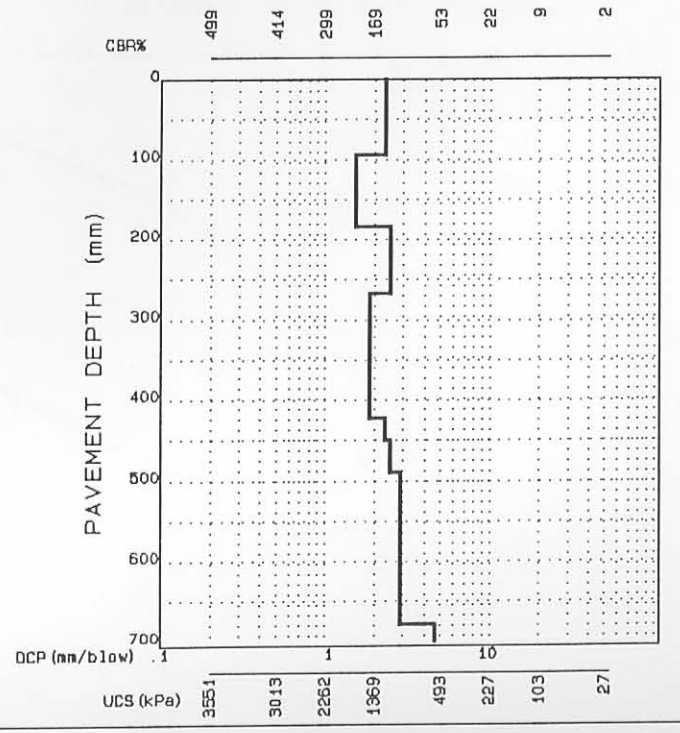

FIGURE E.16

ATT. CSIR, SA

SUMMARY OF DCP INVESTIGATION

DATA FILE :275A4, 8, 9, 10, 12, 13, 15 (IN); WET
REGION :ROOIWAL (N=2105910)
ROAD NUMBER :P1932
DISTANCE : 2.9
POSITION : [X] | | | | M | | | | R
CONDITION : FAILED | OVERSTRESSED | SOUND
RUT. | DEFORM. | PUMP. | CRACKS : CROCK | LONG. | OTHER
DATE :85/10/24

PAVEMENT CHARACTERISTICS

	DATA	B/CURVE
STRUCTURE NUMBER :	246	
BALANCE NUMBER (BN 100) :	14	15
DIFFERENCE IN BN100 :	-1	
BALANCE CURVE IS WHERE B =	5	A= 956
STRUCT. CAP. (E80 X 10^6) :	>10	
ROAD CATEGORY :	C	
TRAFFIC : LIGHT TRAFFIC		

AVERAGE EQUIVALENT STRENGTH

FROM - TO	AV. PENETRATION	SD	80 P	CBR	UCS
0- 50	3.2	0.3	3.5	94	817
51-180	2.9	0.4	3.3	104	893
181-330	3.5	0.6	4.0	83	732
331-480	3.5	0.5	3.9	82	724
481-800	4.1	1.0	5.0	67	606

CATEGORY IV : WELL-BALANCED DEEP STRUCTURE (WBD)

DCP CURVE

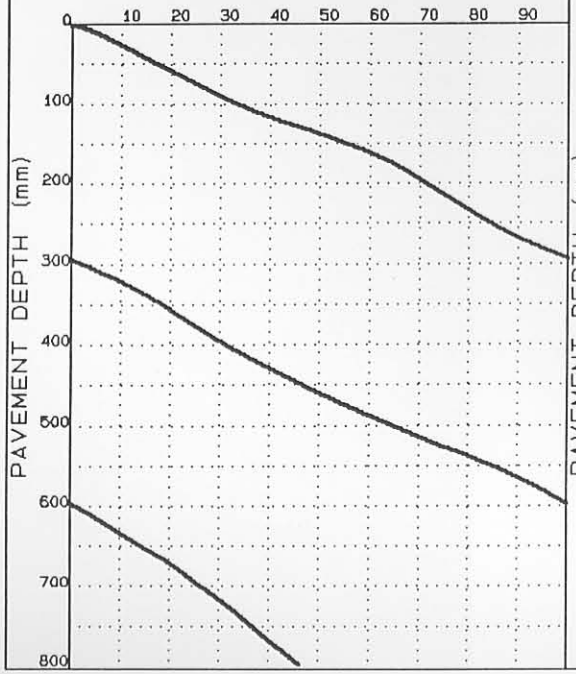

BALANCE CURVE

(DSN 800) (-90 ≤ B ≤ +90)
% OF PAVEMENT STRUCTURE NUMBER

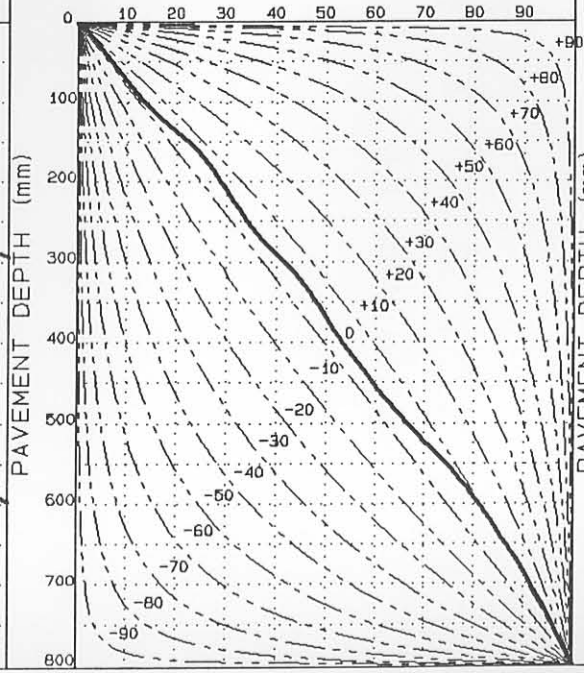

LAYER STRENGTH DIAGRAM

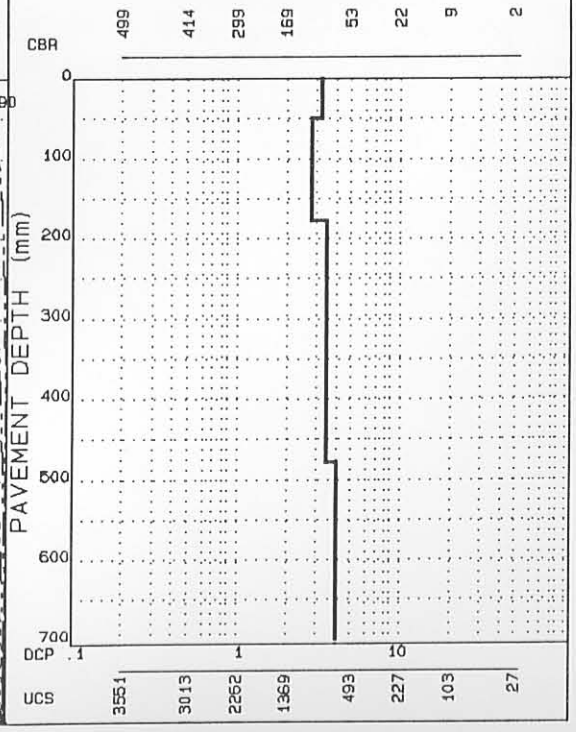

FIGURE E.17

RTT, CSIR, SA

SUMMARY OF DCP INVESTIGATION

AVERAGE EQUIVALENT STRENGTH (REDEFINED)

FROM - TO (mm)	AV. PENETRATION (mm/blow)	SD	BOP	CBR%	UCS (kPa)
0- 8	2.5	0.2	2.7	128	1072
9- 96	3.3	0.2	3.4	89	779
97-160	2.5	0.2	2.7	124	1043
161-256	3.9	0.3	4.1	74	662
257-320	2.9	0.3	3.2	105	901
321-408	3.9	0.3	4.1	74	662
409-608	3.1	0.4	3.4	96	832
609-800	4.8	0.6	5.3	56	518

DATA FILE: 275A4, 8, 9, 10, 12, 15 (IN) ; WET N=2

NORMALIZED CURVE

DEVIATION (A_i) FROM STANDARD PAVEMENT BALANCE CURVE (SPBC), %.mm

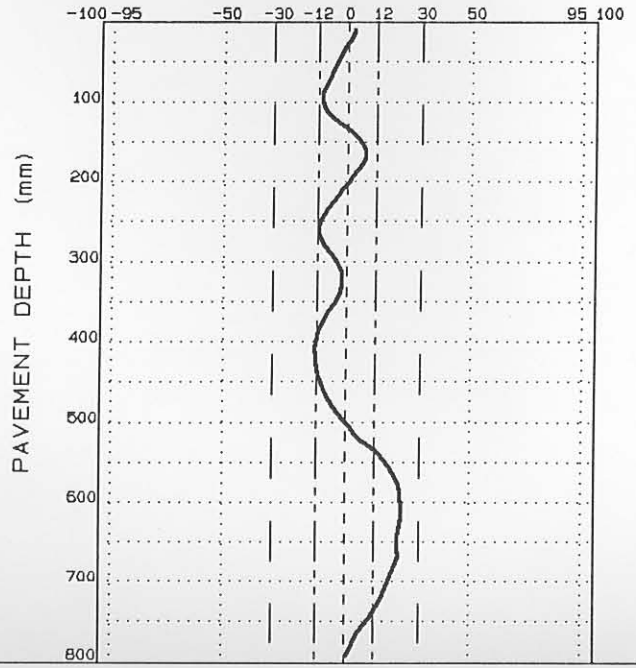

LAYER STRENGTH DIAGRAM (REDEFINED)

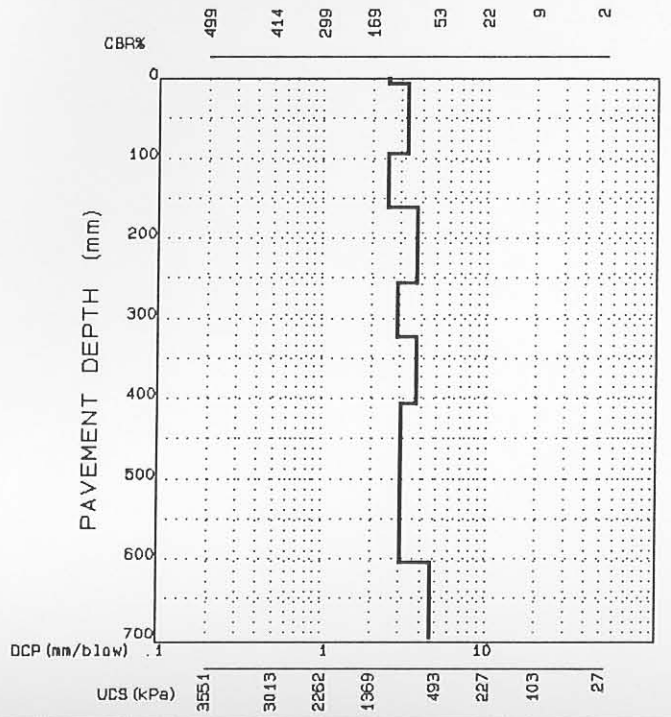

FIGURE E.18

RTT, CSIR, SA

SUMMARY OF DCP INVESTIGATION

DATA FILE :289A4, 2CL, 130C; N=10
REGION :ROOIWAL (N=10)
ROAD NUMBER :P1932
DISTANCE : 2.9
POSITION : L X M R
CONDITION : FAILED OVERSTRESSED SOUND
RUT. DEFORM. PUMP. CRACKS : CROCK LONG. OTHER
DATE :29/10/85

PAVEMENT CHARACTERISTICS

	DATA	B/CURVE
STRUCTURE NUMBER :	437	
BALANCE NUMBER (BN 100) :	20	23
DIFFERENCE IN BN100 :	-3	
BALANCE CURVE IS WHERE B =	18	A= 2285
STRUCT. CAP. (E80 X 10^6) :	>10	
ROAD CATEGORY :	C	
TRAFFIC : LIGHT TRAFFIC		

AVERAGE EQUIVALENT STRENGTH

FROM - TO	AV. PENETRATION	SD	80 P	CBR	UCS
0- 50	1.9	0.4	2.2	178	1433
51-180	1.1	0.3	1.4	287	2182
181-330	2.6	0.4	3.0	121	1020
331-480	3.8	0.8	4.5	74	662
481-800	3.5	1.8	5.0	84	740

CATEGORY V : AVERAGELY BALANCED DEEP STRUCTURE (ABD)

DCP CURVE

NUMBER OF BLOWS

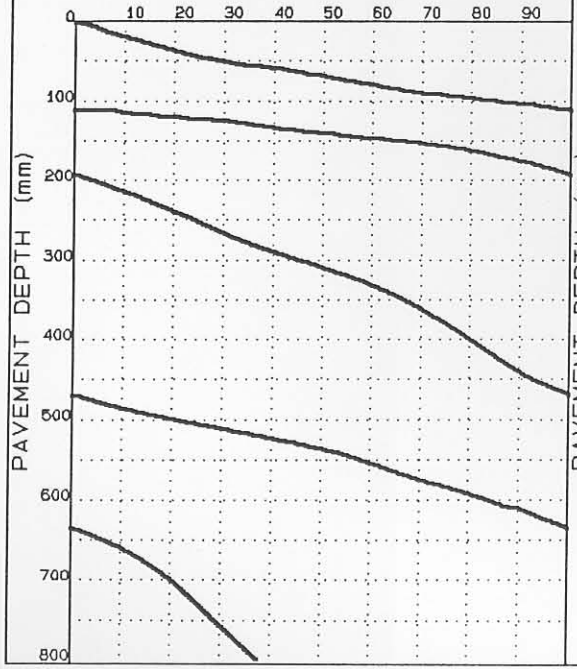

BALANCE CURVE

(DSN 800) (-90 ≤ B ≤ +90)
% OF PAVEMENT STRUCTURE NUMBER

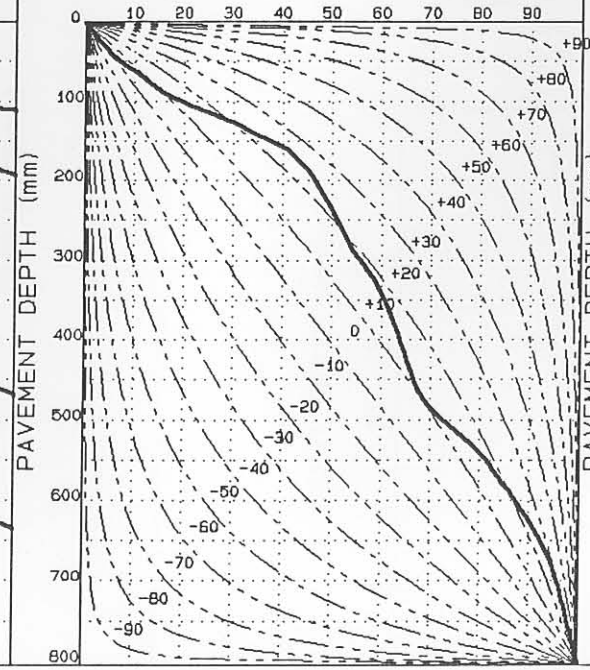

LAYER STRENGTH DIAGRAM

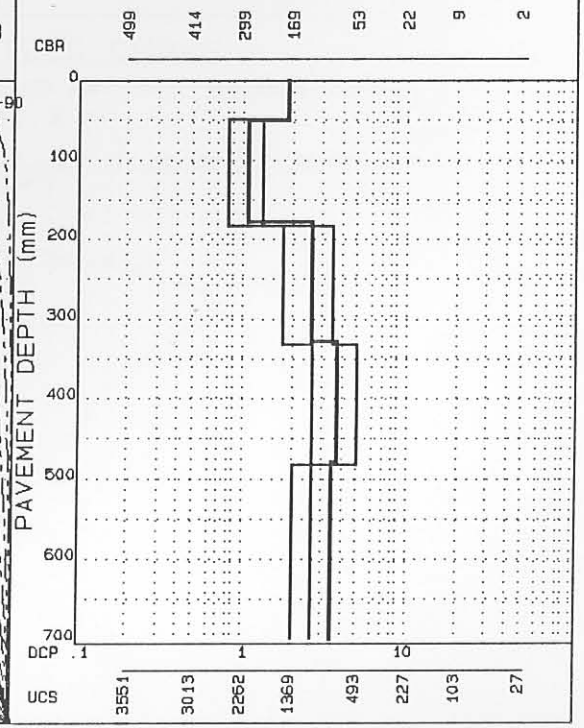

FIGURE E.19

RTT, CSIR, SA

SUMMARY OF DCP INVESTIGATION

AVERAGE EQUIVALENT STRENGTH (REDEFINED)

FROM - TO (mm)	AV. PENETRAIION (mm/blow)	SD	BOP	CBR%	UCS (kPa)
0- 48	1.9	0.4	2.3	176	1419
49-168	1.0	0.3	1.3	294	2229
169-464	3.2	0.9	4.0	93	809
465-656	2.0	0.6	2.5	168	1362
657-800	5.3	1.0	6.1	49	460

DATA FILE: 289A4, 2CL, 130C, N=10

NORMALIZED CURVE

DEVIATION (A_i) FROM STANDARD PAVEMENT BALANCE CURVE (SPBC), %.mm

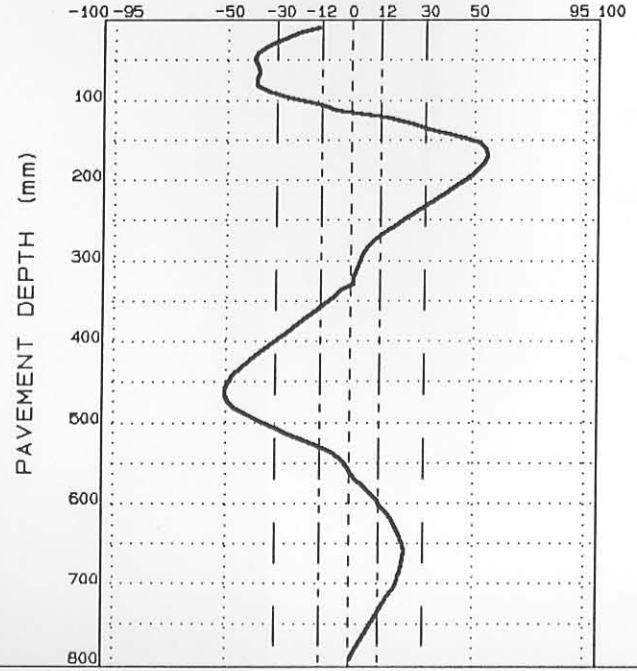

LAYER STRENGTH DIAGRAM (REDEFINED)

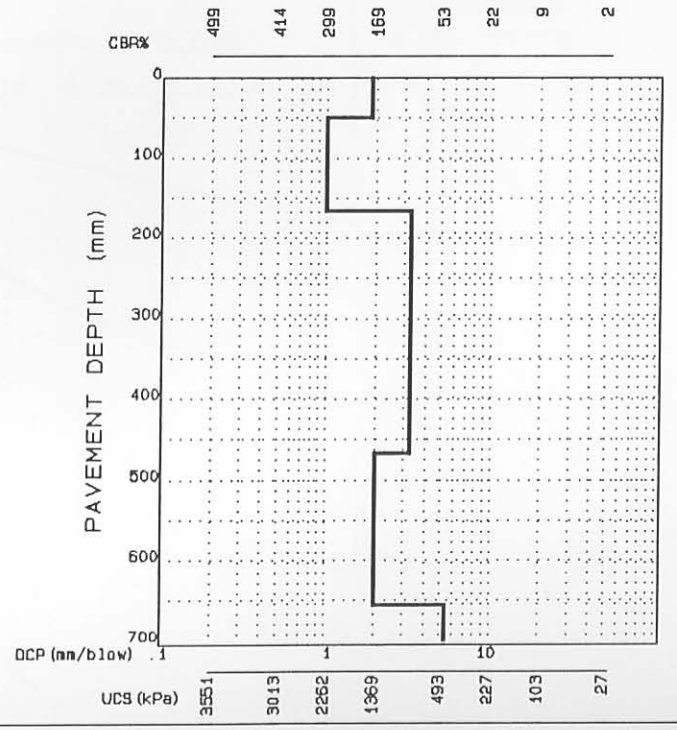

FIGURE E.20

ATT. CSIR, SA

SUMMARY OF DCP INVESTIGATION

DATA FILE :289A4, 5CL, 11CL, N=1022611
REGION :ROOIWAL (N=10022811)
ROAD NUMBER :P1932
DISTANCE : 2.9
POSITION : [X] | M | R
CONDITION : FAILED | OVERSTRESSED | SOUND
RUT. | DEFORM. | PUMP. | CRACKS : CROCK. | LONG. | OTHER
DATE :860113

PAVEMENT CHARACTERISTICS

	DATA	B/CURVE
STRUCTURE NUMBER :	347	
BALANCE NUMBER (BN 100) :	15	17
DIFFERENCE IN BN100 :	-2	
BALANCE CURVE IS WHERE B =	8	A= 1772
STRUCT. CAP. (E80 X 10^6) :	>10	
ROAD CATEGORY :	C	

TRAFFIC : LIGHT TRAFFIC

AVERAGE EQUIVALENT STRENGTH

FROM - TO	AV. PENETRATION	SD	BO P	CBR	UCS
0- 50	2.7	0.5	3.1	116	983
51-180	1.7	0.4	2.0	195	1553
181-330	2.9	0.7	3.4	105	908
331-480	3.0	0.7	3.6	101	870
481-800	3.7	1.7	5.1	78	693

CATEGORY V : AVERAGELY BALANCED DEEP STRUCTURE (ABD)

DCP CURVE

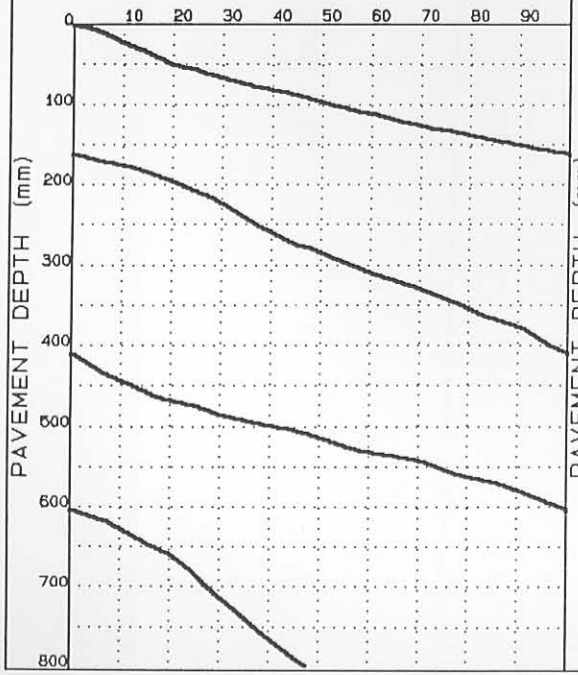

BALANCE CURVE

(DSN 800) (-90 ≤ B ≤ +90)
% OF PAVEMENT STRUCTURE NUMBER

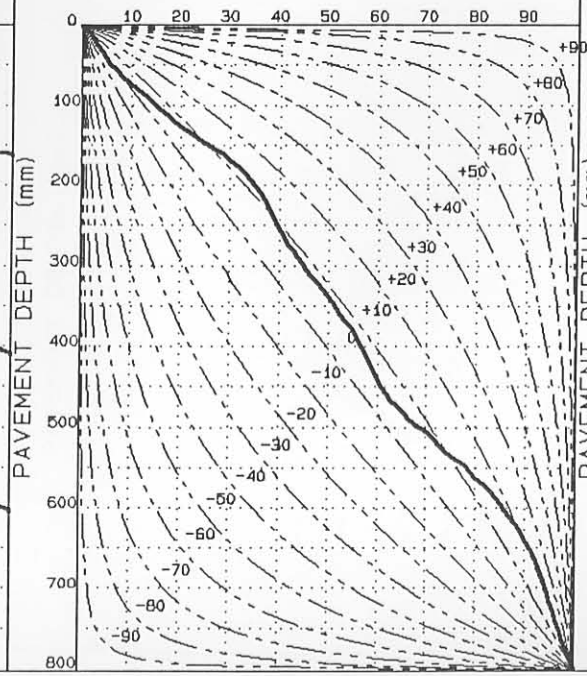

LAYER STRENGTH DIAGRAM

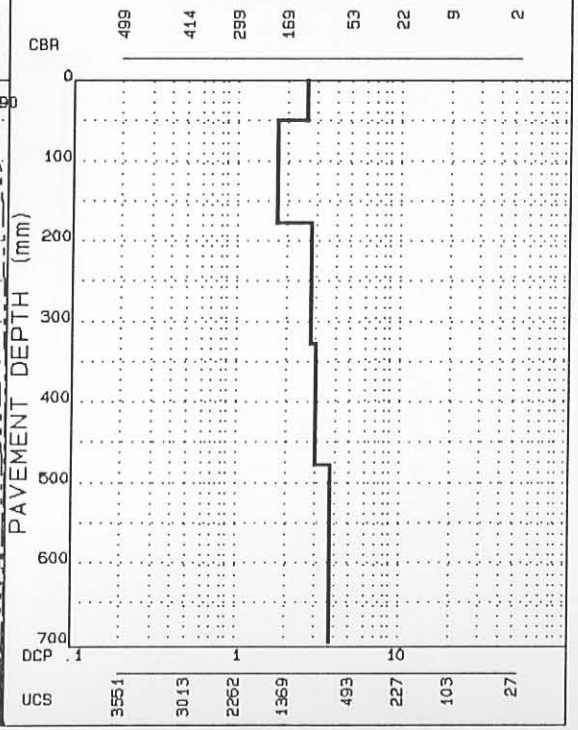

FIGURE E.21

RTT, CSIR, SA

SUMMARY OF DCP INVESTIGATION

AVERAGE EQUIVALENT STRENGTH (REDEFINED)

FROM - TO (mm)	AV. PENETRATION (mm/blow)	SD	BOP	CBR%	UCS (kPa)
0- 8	1.9	0.5	2.3	178	1433
9- 64	2.6	0.5	3.0	122	1028
65-184	1.7	0.4	2.0	195	1553
185-304	3.1	0.6	3.6	98	847
305-328	2.1	0.2	2.3	156	1276
329-456	3.1	0.7	3.7	96	832
457-616	2.0	0.5	2.4	167	1355
617-800	4.9	1.1	5.8	54	501

DATA FILE: 289A4, 5CL, 11CL; N=1022611

NORMALIZED CURVE

DEVIATION (A_i) FROM STANDARD PAVEMENT BALANCE CURVE (SPBC), %.mm

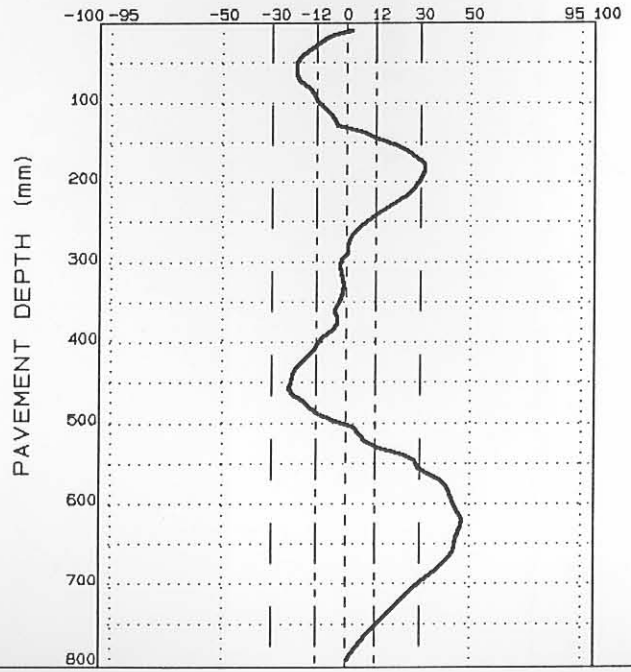

LAYER STRENGTH DIAGRAM (REDEFINED)

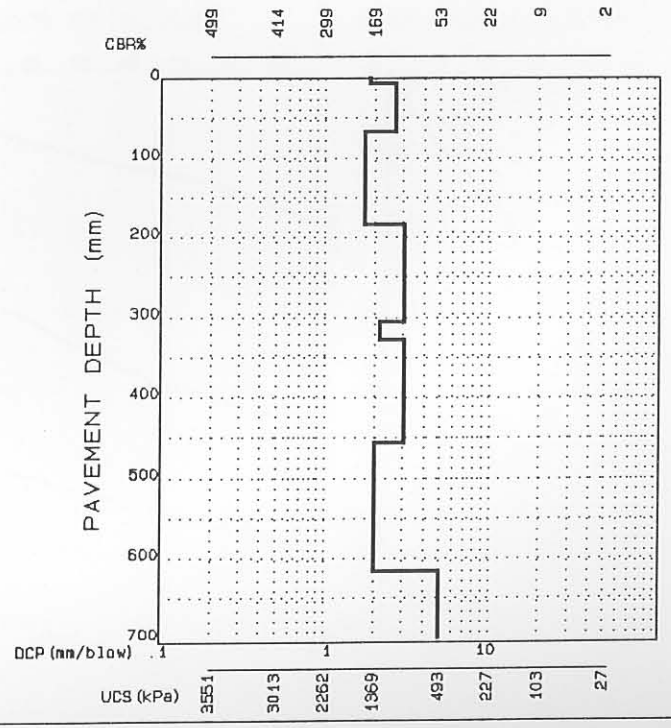

FIGURE E.22

RTT, CSIR, SA

SUMMARY OF DCP INVESTIGATION

DATA FILE :289A4, 1B, 2, 4, 6; N=1894826
REGION :ROOIWAL (N=1000 000)
ROAD NUMBER :P1932
DISTANCE : 2.9
POSITION : [X] | | | M | | | R
CONDITION : FAILED | OVERSTRESSED | SOUND
RUT. | DEFORM. | PUMP. | CRACKS : CROCK | LONG. | OTHER
DATE :86/04/25

PAVEMENT CHARACTERISTICS

	DATA	B/CURVE
STRUCTURE NUMBER :	415	
BALANCE NUMBER (BN 100) :	12	11
DIFFERENCE IN BN100 :	1	
BALANCE CURVE IS WHERE B =	-3 A= 1226	
STRUCT. CAP. (E80 X 10^6) :	>10	
ROAD CATEGORY :	C	

TRAFFIC : LIGHT TRAFFIC

AVERAGE EQUIVALENT STRENGTH

FROM - TO	AV. PENETRATION	SD	80 P	CBR	UCS
0- 50	2.6	0.3	2.9	119	1005
51-180	2.2	0.5	2.7	147	1211
181-330	3.3	0.5	3.7	90	786
331-480	2.4	0.7	2.9	135	1124
481-800	2.9	0.8	3.6	107	916

CATEGORY VII : WELL-BALANCED INVERTED STRUCTURE (WBI)

DCP CURVE

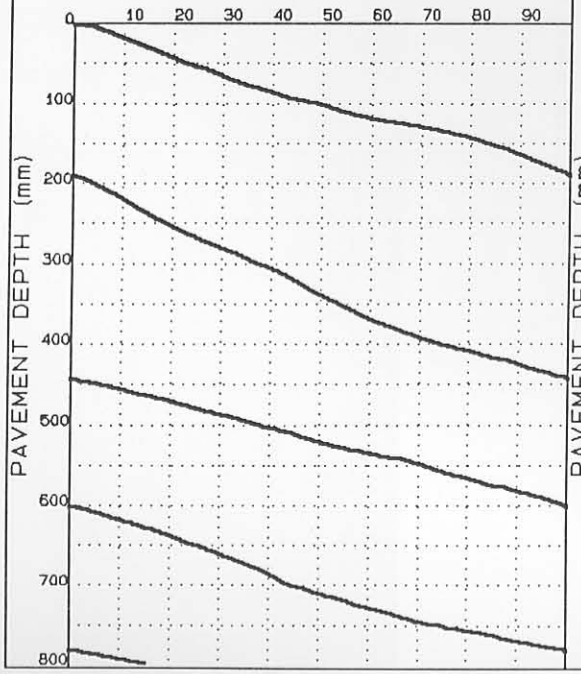

BALANCE CURVE

(DSN 800) (-90 ≤ B ≤ +90)
% OF PAVEMENT STRUCTURE NUMBER

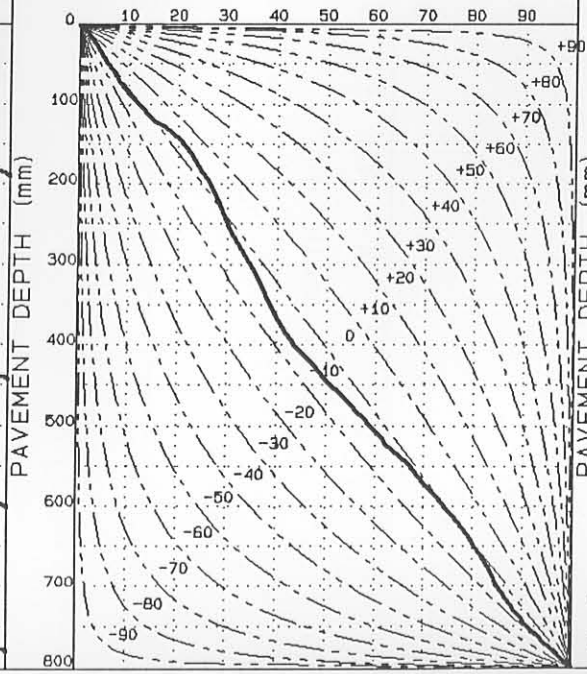

LAYER STRENGTH DIAGRAM

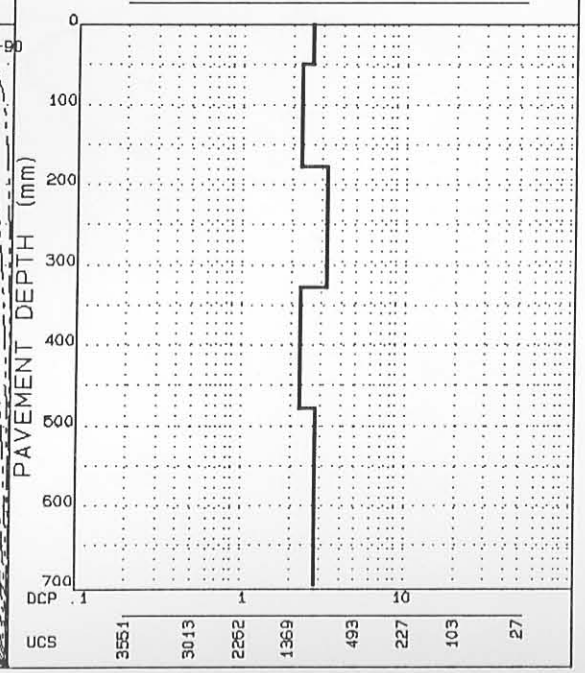

FIGURE E.23

RTT, CSIR, SA

SUMMARY OF DCP INVESTIGATION

AVERAGE EQUIVALENT STRENGTH (REDEFINED)

FROM - TO (mm)	AV. PENETRATION (mm/blow)	SD	BOP	CBR%	UCS (kPa)
0- 8	1.9	0.5	2.3	178	1433
9- 64	2.6	0.5	3.0	122	1028
65-184	1.7	0.4	2.0	195	1553
185-304	3.1	0.6	3.6	98	847
305-328	2.1	0.2	2.3	156	1276
329-456	3.1	0.7	3.7	96	832
457-616	2.0	0.6	2.4	157	1355
617-800	4.9	1.1	5.8	54	501

DATA FILE: 289A4, 5CL, 11CL; N=1022611

NORMALIZED CURVE

DEVIATION (A_i) FROM STANDARD PAVEMENT BALANCE CURVE (SPBC), %.mm

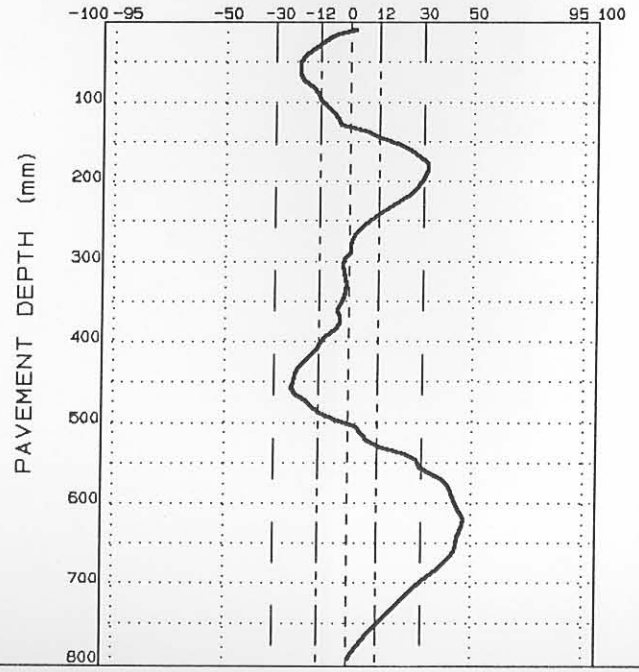

LAYER STRENGTH DIAGRAM (REDEFINED)

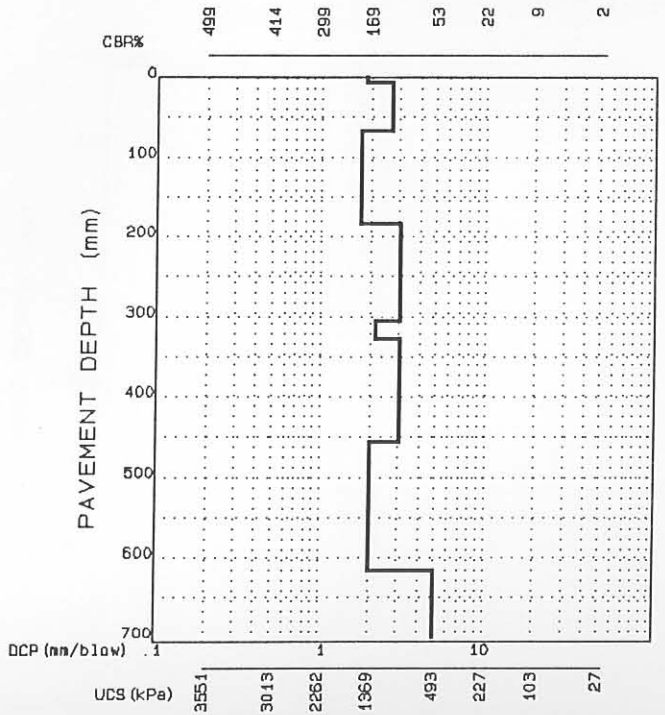

FIGURE E.22

ATT, CSIR, SA

SUMMARY OF DCP INVESTIGATION

AVERAGE EQUIVALENT STRENGTH (REDEFINED)

FROM - TO (mm)	AV. PENETRATION (mm/blow)	SD	BOP	CBR%	UCS (kPa)
0- 8	2.4	0.6	2.9	136	1131
9- 72	2.7	0.3	2.9	117	991
73-160	2.0	0.4	2.4	168	1362
161-392	3.2	0.5	3.6	95	825
393-584	1.9	0.3	2.2	174	1405
585-736	3.1	0.6	3.6	98	847
737-800	3.9	0.3	4.1	74	662

DATA FILE: 289A4, 1B, 2, 4, 6; N=1894826

NORMALIZED CURVE

DEVIATION (A_i) FROM STANDARD PAVEMENT BALANCE CURVE (SPBC), %.mm

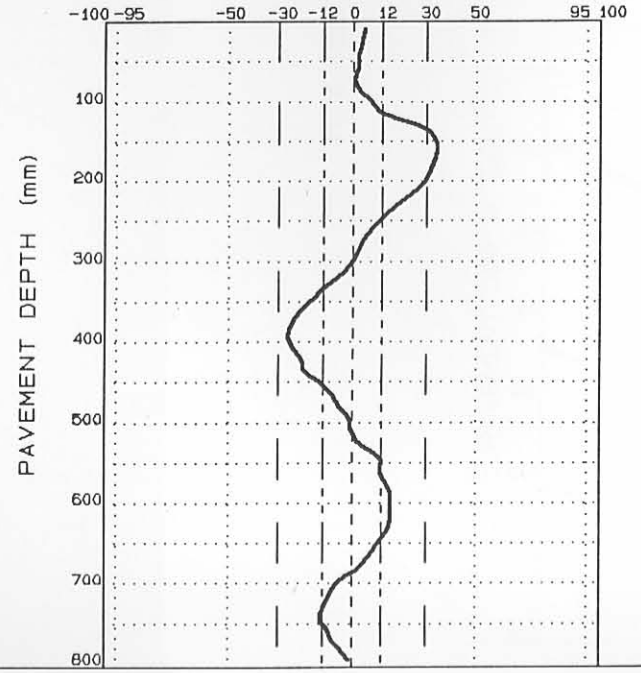

LAYER STRENGTH DIAGRAM (REDEFINED)

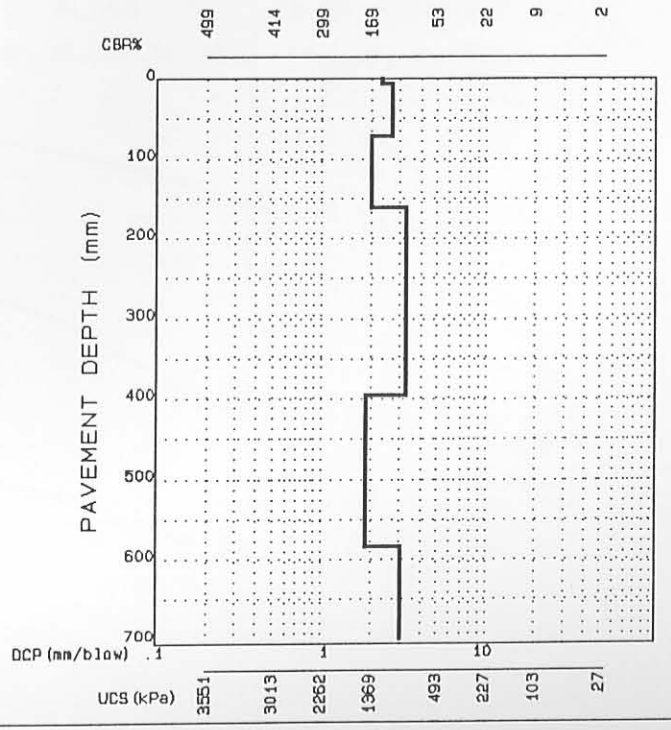

FIGURE E.24

RTT, CSIR, SA

SUMMARY OF DCP INVESTIGATION

DATA FILE :289A4, 8, 11; N=1894826
REGION :ROOIWAL (N=1 894 826)
ROAD NUMBER :P1932
DISTANCE : 2.9
POSITION : [L] [ ] [ ] [ ] [M] [ ] [ ] [ ] [R]
CONDITION : [FAILED] [OVERSTRESSED] [SOUND]
[RUT.] [DEFORM.] [PUMP.] [CRACKS : CROCK.] [LONG.] [OTHER]
DATE :86/06/13

PAVEMENT CHARACTERISTICS

	DATA	B/CURVE
STRUCTURE NUMBER :	384	
BALANCE NUMBER (BN 100) :	12	13
DIFFERENCE IN BN100 :	-1	
BALANCE CURVE IS WHERE B =	1	A= 1224
STRUCT. CAP. (E80 X 10^6) :	>10	
ROAD CATEGORY :	C	

TRAFFIC : LIGHT TRAFFIC

AVERAGE EQUIVALENT STRENGTH

FROM - TO	AV. PENETRATION	SD	80 P	CBR	UCS
0- 50	2.2	0.3	2.5	146	1204
51-180	2.0	0.6	2.5	165	1341
181-330	2.5	0.4	2.8	126	1057
331-480	2.9	0.6	3.5	104	893
481-800	2.4	0.9	3.2	131	1094

CATEGORY IV : WELL-BALANCED DEEP STRUCTURE (WBD)

DCP CURVE

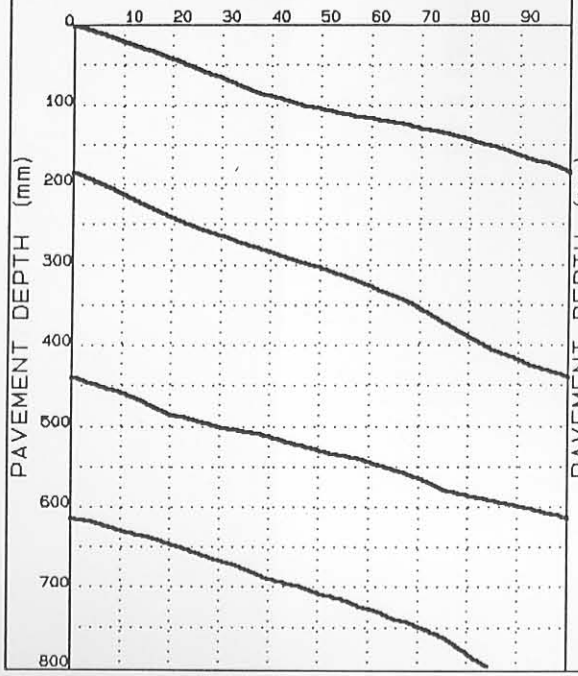

BALANCE CURVE

(DSN 800) (-90 ≤ B ≤ +90)

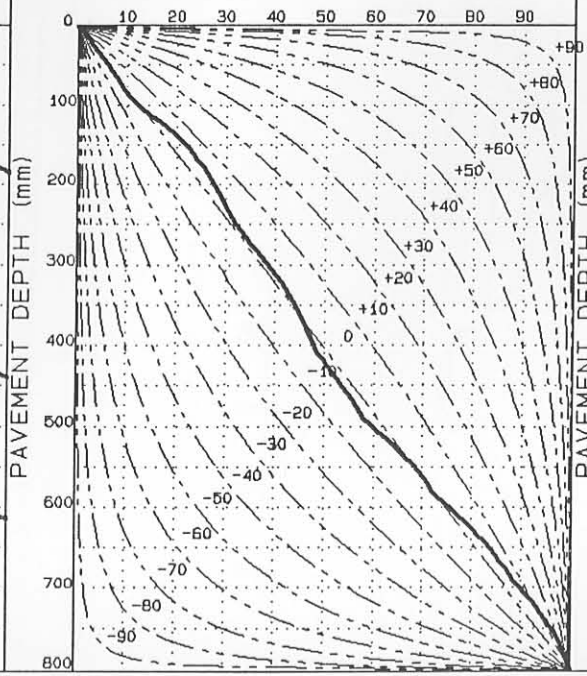

LAYER STRENGTH DIAGRAM

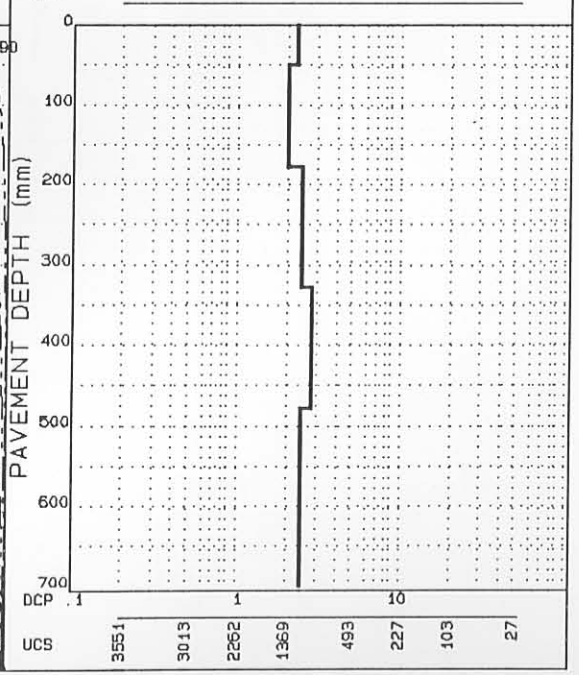

FIGURE E.25

ATT, CSIR, SA

SUMMARY OF DCP INVESTIGATION

AVERAGE EQUIVALENT STRENGTH (REDEFINED)

FROM - TO (mm)	AV. PENETRATION (mm/blow)	SD	BOP	CBR%	UCS (kPa)
0- 8	1.9	0.0	1.9	176	1419
9- 80	2.5	0.3	2.8	128	1072
81-152	1.7	0.5	2.0	199	1581
153-272	2.6	0.4	2.9	122	1028
273-304	2.1	0.3	2.3	161	1312
305-424	3.1	0.5	3.6	97	840
425-456	2.0	0.2	2.2	158	1362
457-480	2.8	0.3	3.0	112	953
481-720	2.0	0.5	2.4	166	1348
721-800	3.7	0.9	4.4	78	693

DATA FILE: 289A4, 8, 11; N=1894826

NORMALIZED CURVE

DEVIATION (A_i) FROM STANDARD PAVEMENT BALANCE CURVE (SPBC), %.mm

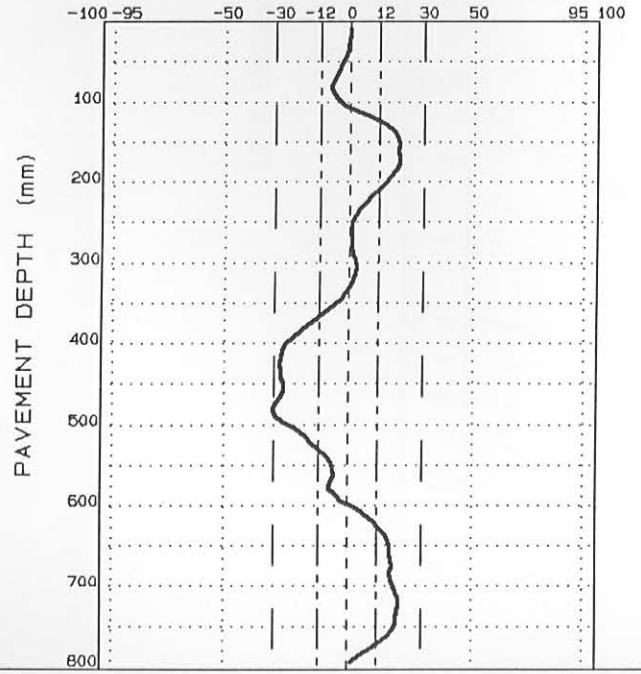

LAYER STRENGTH DIAGRAM (REDEFINED)

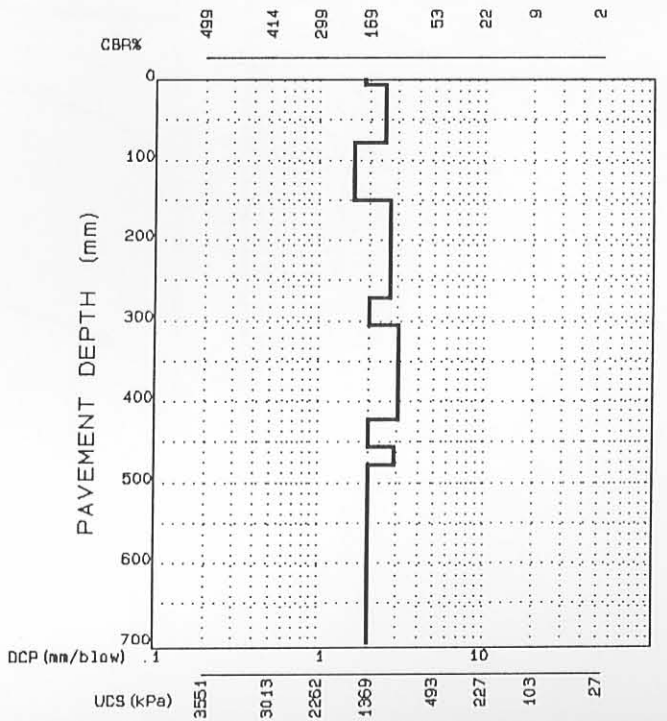

FIGURE E.26

RTT, CSIR, SA

SUMMARY OF DCP INVESTIGATION

DATA FILE :294A4, 3N10, 11; N=10
REGION :ROOIWAL (N=10) [B13]
ROAD NUMBER :P1932
DISTANCE : 2.9
POSITION : L | X | | M | | | | R
CONDITION : FAILED | OVERSTRESSED | SOUND
RUT. | DEFORM. | PUMP. | CRACKS : CROCK | LONG. | OTHER
DATE :860325

PAVEMENT CHARACTERISTICS

	DATA	B/CURVE
STRUCTURE NUMBER :	400	
BALANCE NUMBER (BN 100) :	38	23
DIFFERENCE IN BN100 :	15	
BALANCE CURVE IS WHERE B =	18	A= 3134
STRUCT. CAP. (E80 X 10^6) :	>10	
ROAD CATEGORY :	C	

TRAFFIC : LIGHT TRAFFIC

AVERAGE EQUIVALENT STRENGTH

FROM - TO	AV. PENETRATION	SD	80 P	CBR	UCS
0- 50	0.7	0.3	0.9	361	2671
51-180	2.1	0.6	2.6	158	1290
181-330	4.7	1.6	6.0	58	534
331-480	2.8	0.4	3.1	108	923
481-800	3.7	0.9	4.4	78	693

CATEGORY VI : POORLY BALANCED DEEP STRUCTURE (PBD)

DCP CURVE

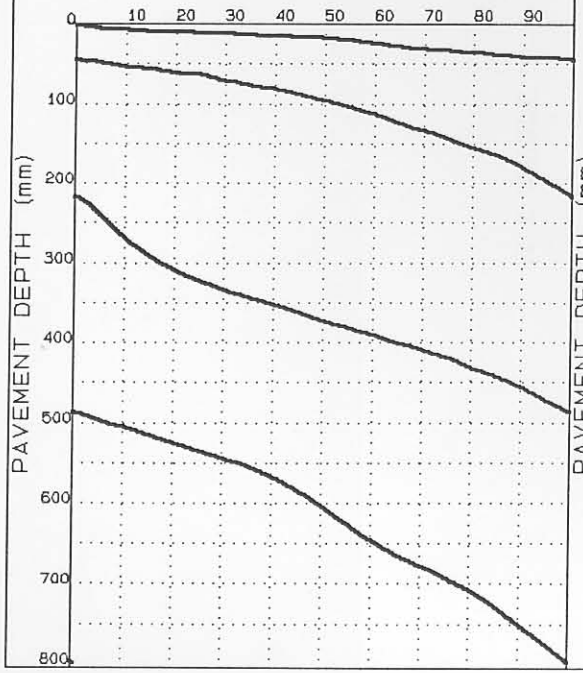

BALANCE CURVE

(DSN 800) (-90 ≤ B ≤ +90)
% OF PAVEMENT STRUCTURE NUMBER

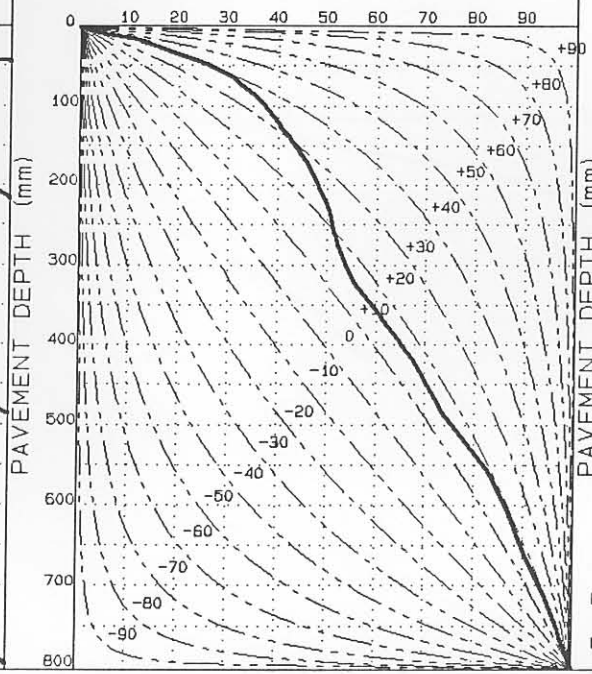

LAYER STRENGTH DIAGRAM

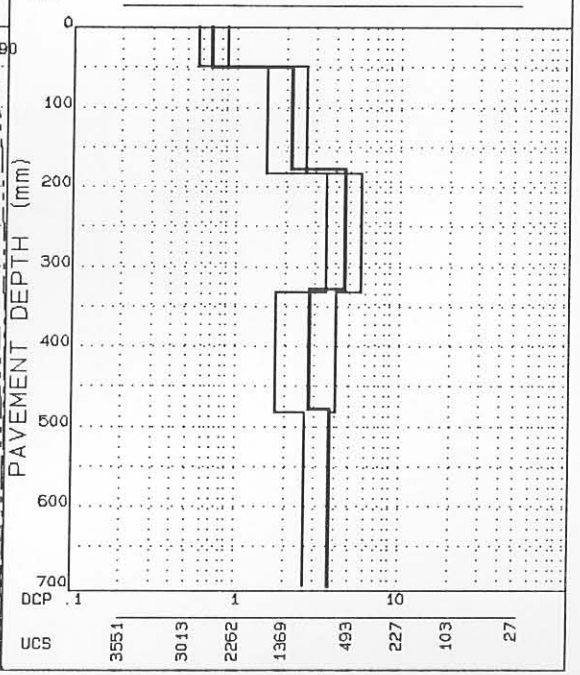

FIGURE E.27

RTT, CSIR, SA

SUMMARY OF DCP INVESTIGATION

DATA FILE :294A4, 5-5, 10-8; N=1 000 000
REGION :ROOIWAL (N=1000 000)
ROAD NUMBER :P1932
DISTANCE : 2.9
POSITION : X | M | R
CONDITION : FAILED | OVERSTRESSED | SOUND
RUT. | DEFORM. | PUMP. | CRACKS : CROCK | LONG. | OTHER
DATE :86/06/03

PAVEMENT CHARACTERISTICS

	DATA	B/CURVE
STRUCTURE NUMBER :	312	
BALANCE NUMBER (BN 100) :	26	17
DIFFERENCE IN BN100 :	9	
BALANCE CURVE IS WHERE B =	9	A= 2790
STRUCT. CAP. (E80 X 10^6) :	>10	
ROAD CATEGORY :	C	
TRAFFIC : LIGHT TRAFFIC		

AVERAGE EQUIVALENT STRENGTH

FROM - TO	AV. PENETRATION	SD	80 P	CBR	UCS
0- 50	1.2	0.2	1.4	266	2041
51-180	2.6	1.0	3.4	123	1035
181-330	4.5	0.9	5.3	60	550
331-480	3.3	0.4	3.6	91	794
481-800	3.2	0.9	3.9	94	817

CATEGORY V : AVERAGELY BALANCED DEEP STRUCTURE (ABD)

DCP CURVE

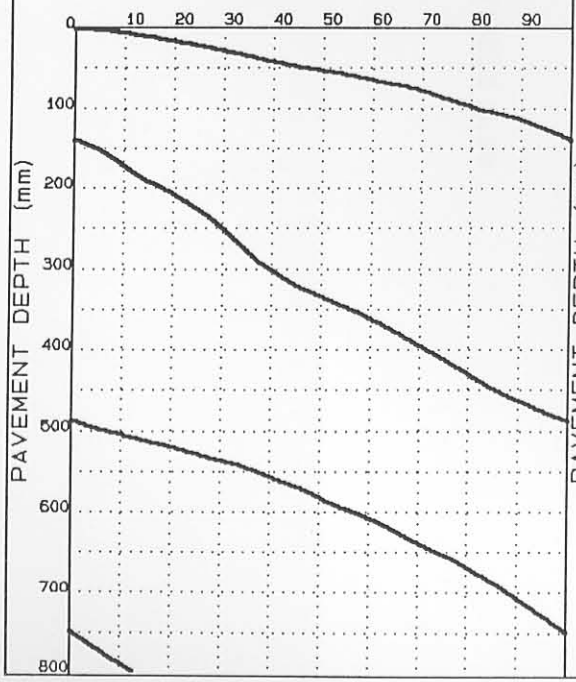

BALANCE CURVE

(DSN 800) (−90 ≤ B ≤ +90)

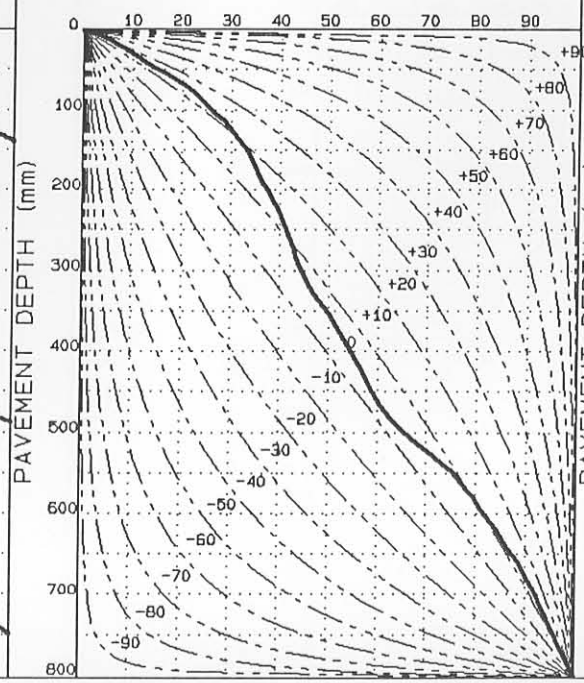

LAYER STRENGTH DIAGRAM

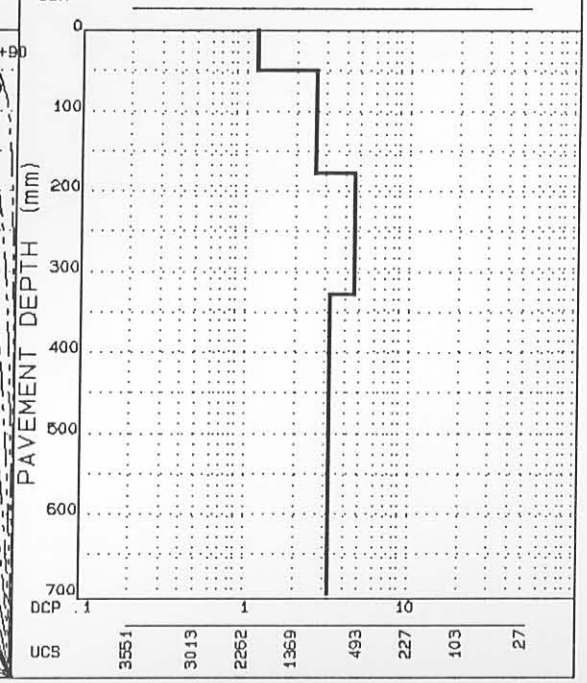

FIGURE E.28

RTT, CSIR, SA

SUMMARY OF DCP INVESTIGATION

AVERAGE EQUIVALENT STRENGTH (REDEFINED)

FROM - TO (mm)	AV. PENETRATION (mm/blow)	SD	BOP	CBR%	UCS (kPa)
0-112	1.5	0.5	1.9	218	1713
113-456	3.8	1.0	4.6	74	662
457-656	2.5	0.6	3.0	128	1072
657-800	4.1	0.3	4.3	69	622

DATA FILE: 294A4, 5-5, 10-8; N=1 000 000

NORMALIZED CURVE

DEVIATION (A_i) FROM STANDARD PAVEMENT BALANCE CURVE (SPBC), %.mm

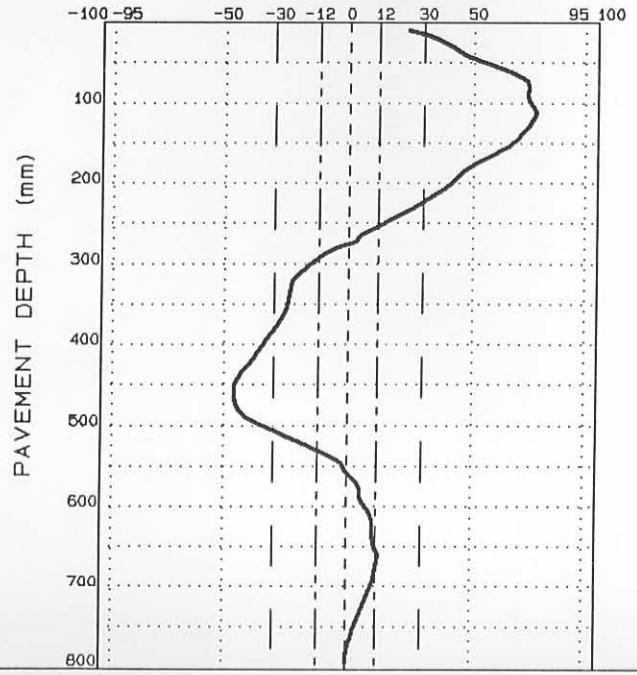

LAYER STRENGTH DIAGRAM (REDEFINED)

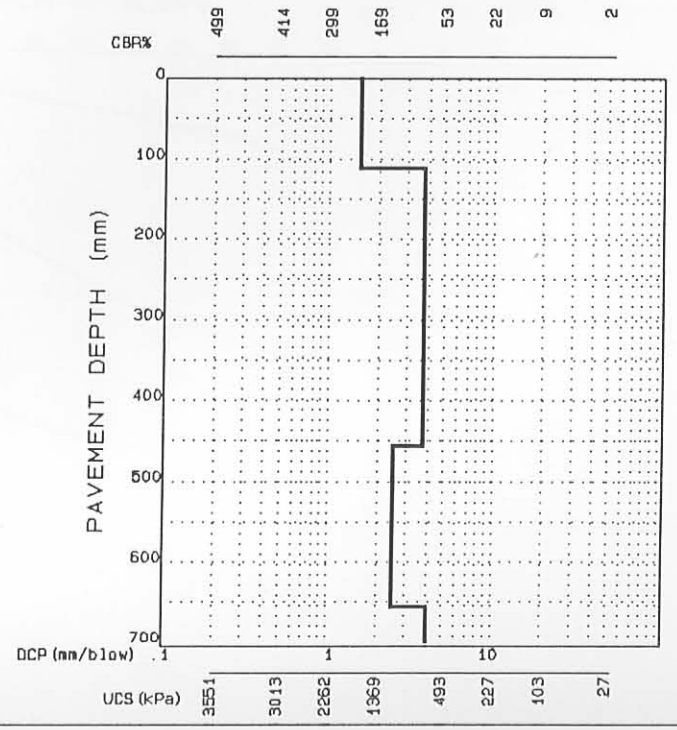

FIGURE E.29

RTT, CSIR, SA

SUMMARY OF DCP INVESTIGATION

DATA FILE :294A4, 2, 5, 7; N=1 798 642
REGION :ROOIWAL
ROAD NUMBER :1932
DISTANCE : 2.9
POSITION : [X] | | | M | | | R
CONDITION : | FAILED | OVERSTRESSED | SOUND |
| RUT. | DEFORM. | PUMP. | CRACKS : CROCK | LONG. | OTHER |
DATE :86/08/19

PAVEMENT CHARACTERISTICS

	DATA	B/CURVE
STRUCTURE NUMBER :	485	
BALANCE NUMBER (BN 100) :	17	11
DIFFERENCE IN BN100 :	6	
BALANCE CURVE IS WHERE B =	-3 A= 2077	
STRUCT. CAP. (E80 X 10^6) :	>10	
ROAD CATEGORY :	C	
TRAFFIC : LIGHT TRAFFIC		

AVERAGE EQUIVALENT STRENGTH

FROM - TO	AV. PENETRATION	SD	80 P	CBR	UCS
0- 50	1.8	0.6	2.3	187	1497
51-180	2.5	0.5	2.9	129	1079
181-330	3.1	0.4	3.5	96	832
331-480	2.1	0.4	2.5	157	1283
481-800	2.3	1.0	3.2	139	1153

CATEGORY VIII : AVERAGELY BALANCED INVERTED STRUCTURE (ABI)

DCP CURVE

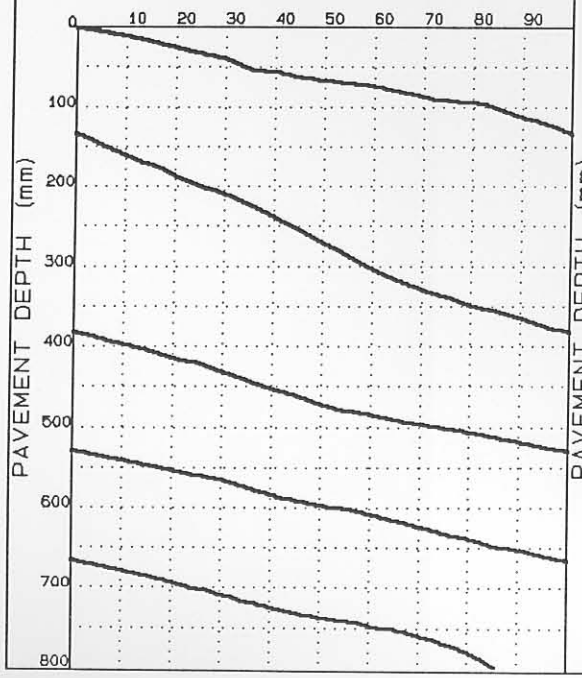

BALANCE CURVE

(DSN 800) (-90 ≤ B ≤ +90)
% OF PAVEMENT STRUCTURE NUMBER

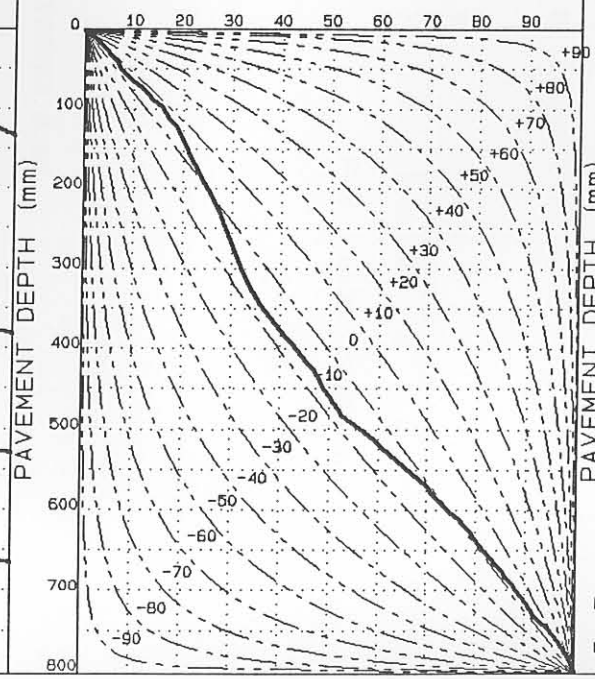

LAYER STRENGTH DIAGRAM

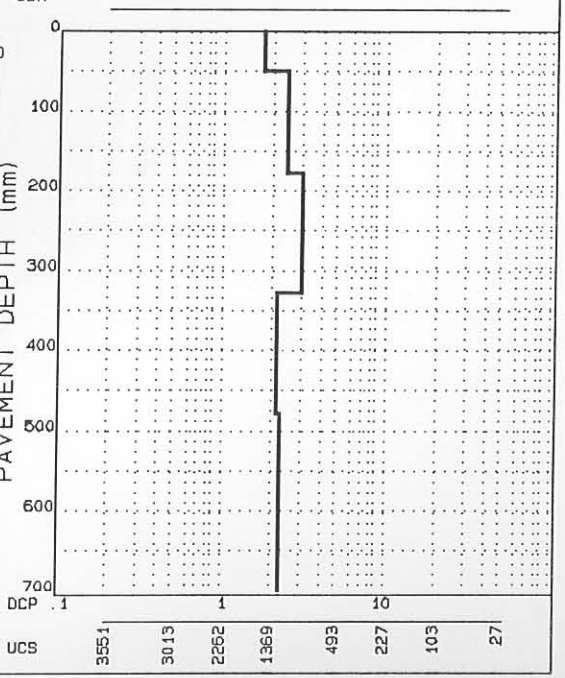

FIGURE E.30

ATT, CSIR, SA

SUMMARY OF DCP INVESTIGATION

AVERAGE EQUIVALENT STRENGTH (REDEFINED)

FROM - TO (mm)	AV. PENETRATION (mm/blow)	SD	BOP	CBR%	UCS (kPa)
0- 96	1.9	0.5	2.4	175	1412
97-352	2.9	0.5	3.3	105	901
353-424	1.9	0.4	2.2	178	1433
425-472	2.4	0.4	2.7	134	1116
473-616	1.5	0.3	1.7	222	1741
617-640	2.0	0.3	2.2	170	1376
641-656	2.0	0.2	2.2	172	1391
657-728	2.9	0.6	3.3	108	923
729-752	3.0	0.2	3.1	103	885
753-800	4.0	0.6	4.5	70	630

DATA FILE: 294A4, 2, 5, 7; N=1 798 642

NORMALIZED CURVE

DEVIATION (A_i) FROM STANDARD PAVEMENT BALANCE CURVE (SPBC), %.mm

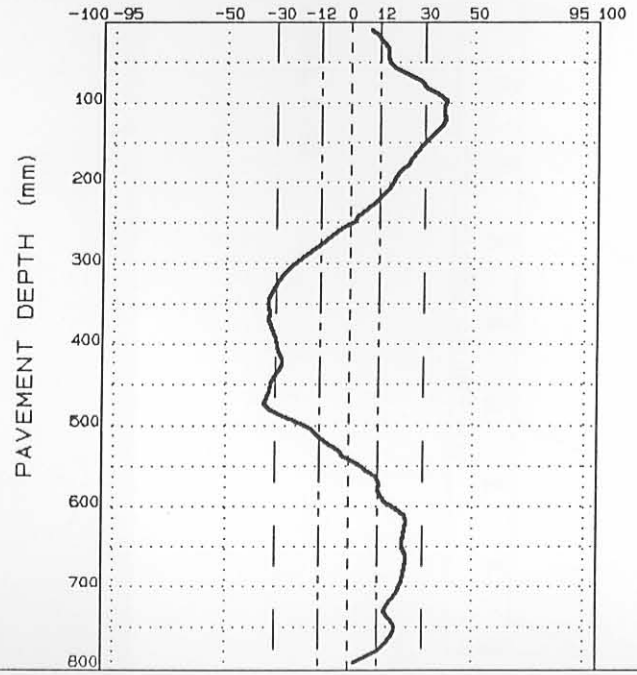

LAYER STRENGTH DIAGRAM (REDEFINED)

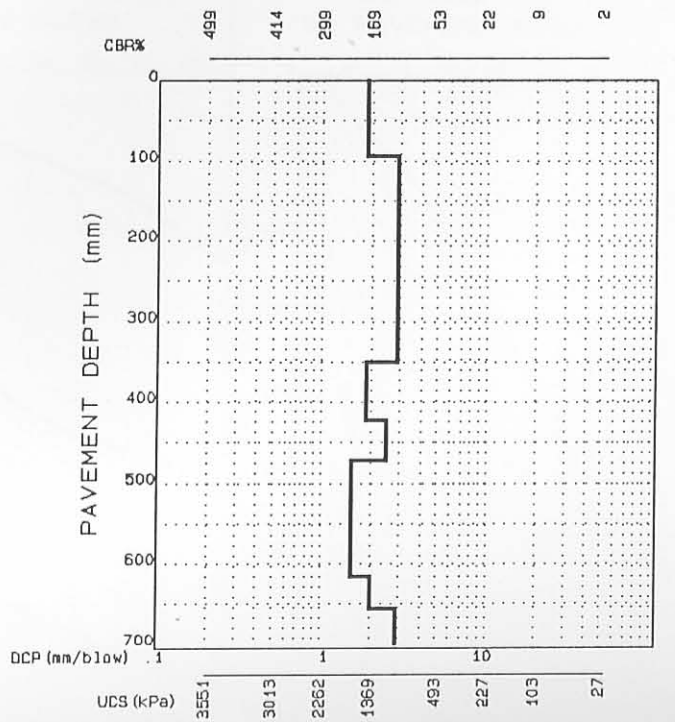

FIGURE E.31

RTT, CSIR, SA

SUMMARY OF DCP INVESTIGATION

DATA FILE :294A4, 9, 11, 13, 15; N=1 798 642
REGION :ROOIWAL
ROAD NUMBER :1932
DISTANCE : 2.9
POSITION : [X] | | | M | | | R
CONDITION : FAILED | OVERSTRESSED | SOUND
[XX] | DEFORM. | PUMP. | CRACKS : CROCK | LONG. | OTHER
DATE :86/08/19

PAVEMENT CHARACTERISTICS

	DATA	B/CURVE
STRUCTURE NUMBER :	314	
BALANCE NUMBER (BN 100) :	18	13
DIFFERENCE IN BN100 :	5	
BALANCE CURVE IS WHERE B =	1	A= 1637
STRUCT. CAP. (E80 X 10^6) :	>10	
ROAD CATEGORY :	C	
TRAFFIC : LIGHT TRAFFIC		

AVERAGE EQUIVALENT STRENGTH

FROM - TO	AV. PENETRATION	SD	80 P	CBR	UCS
0- 50	2.2	0.8	2.9	154	1262
51-180	3.3	1.4	4.5	89	779
181-330	4.2	0.8	4.9	65	590
331-480	3.1	0.6	3.7	95	825
481-800	3.5	0.9	4.3	82	724

CATEGORY V : AVERAGELY BALANCED DEEP STRUCTURE (ABD)

DCP CURVE

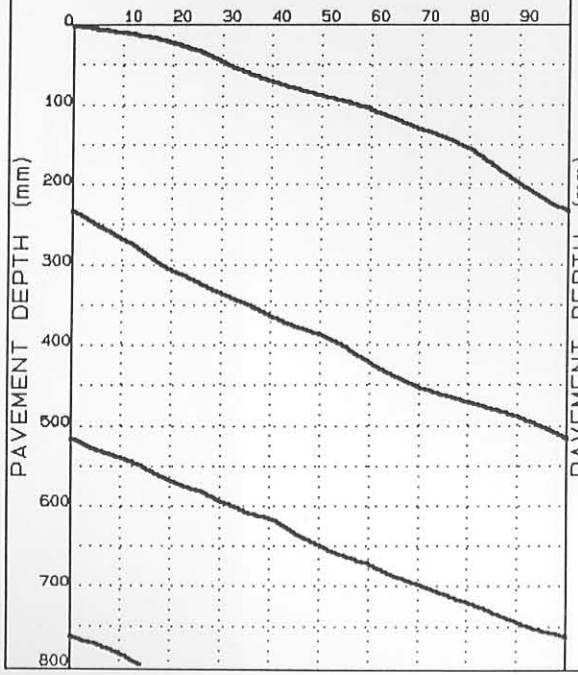

BALANCE CURVE

(DSN 800) (−90 ≤ B ≤ +90)
% OF PAVEMENT STRUCTURE NUMBER

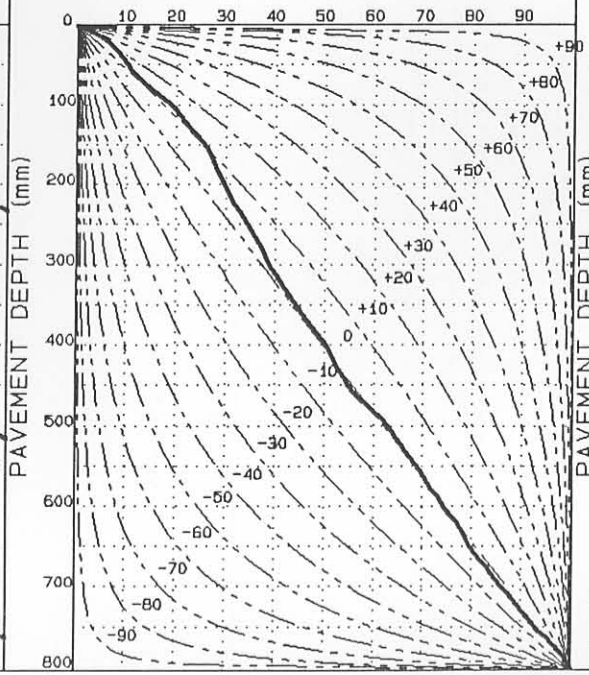

LAYER STRENGTH DIAGRAM

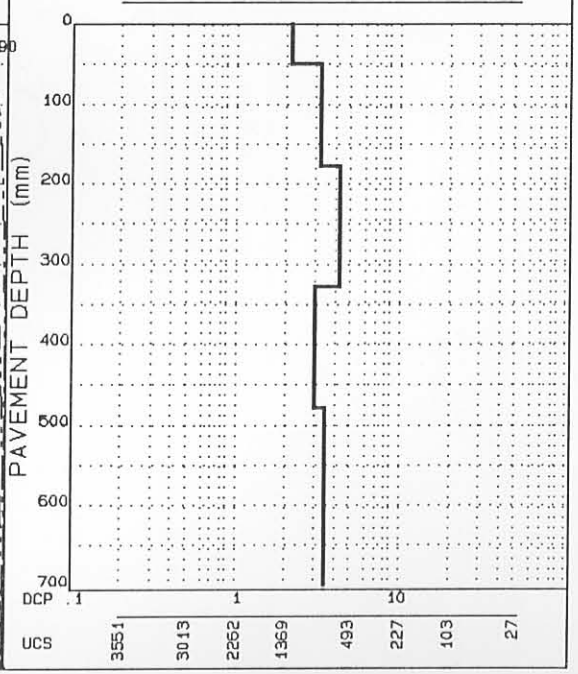

FIGURE E.32

ATT, CSIR, SA

SUMMARY OF DCP INVESTIGATION

AVERAGE EQUIVALENT STRENGTH (REDEFINED)

FROM - TO (mm)	AV. PENETRATION (mm/blow)	SD	BOP	CBR%	UCS (kPa)
0- 32	1.6	0.5	2.0	204	1616
33- 48	3.1	0.2	3.3	97	840
49-136	2.5	0.4	2.8	126	1057
137-368	4.2	1.0	5.0	67	606
369-384	2.7	0.2	2.9	114	968
385-448	3.7	0.5	4.1	78	693
449-496	2.4	0.2	2.6	133	1109
497-528	3.4	0.4	3.8	86	755
529-544	3.1	0.2	3.3	95	825
545-800	3.6	0.9	4.4	79	701

DATA FILE: 294A4, 9, 11, 13, 15; N=1 798 642

NORMALIZED CURVE

DEVIATION (A_i) FROM STANDARD PAVEMENT BALANCE CURVE (SPBC), %.mm

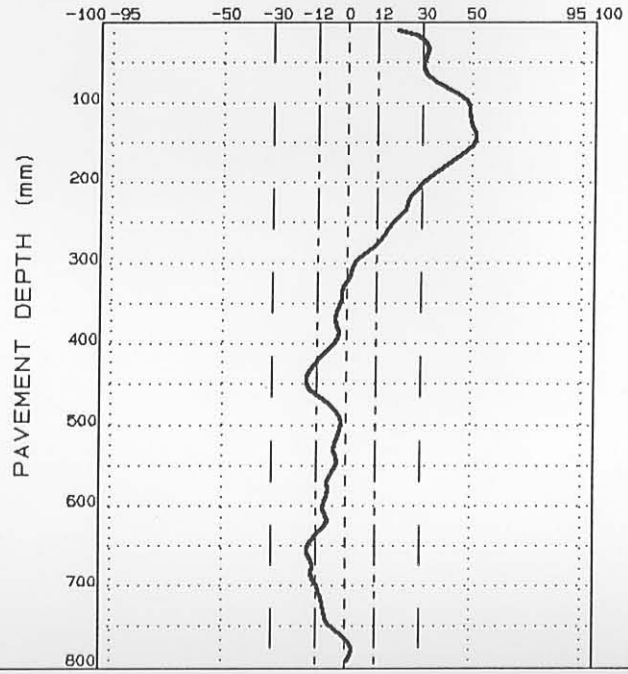

LAYER STRENGTH DIAGRAM (REDEFINED)

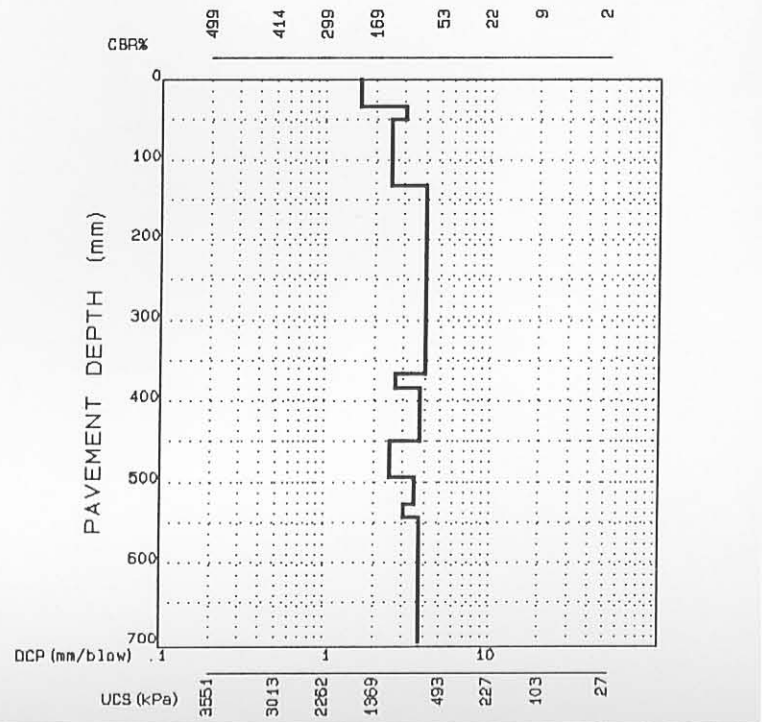

FIGURE E.33

RTT, CSIR, SA

SUMMARY OF DCP INVESTIGATION

DATA FILE :337A4, 1, 16; N=10
REGION :ROOIWAL
ROAD NUMBER :1932
DISTANCE : 2.0
POSITION : L [X] M R
CONDITION : FAILED | OVERSTRESSED | SOUND
RUT. | DEFORM. | PUMP. | CRACKS : CROCK | LONG. | OTHER
DATE :88/05/24

PAVEMENT CHARACTERISTICS

	DATA	B/CURVE
STRUCTURE NUMBER :	223	
BALANCE NUMBER (BN 100) :	38	42
DIFFERENCE IN BN100 :	-4	
BALANCE CURVE IS WHERE B =	38 A= 1108	
STRUCT. CAP. (E80 X 10^6) :	4.97	
ROAD CATEGORY :	A	
TRAFFIC : LIGHT TRAFFIC		

AVERAGE EQUIVALENT STRENGTH

FROM - TO	AV. PENETRATION	SD	95 P	CBR	UCS
0-112	1.5	0.5	2.3	217	1706
113-272	2.9	0.9	4.4	107	916
273-344	3.6	1.0	5.2	79	701
345-464	7.9	1.2	9.8	30	299
465-800	17.4	7.2	29.3	11	123

CATEGORY IV : WELL-BALANCED DEEP STRUCTURE (WBD)

DCP CURVE

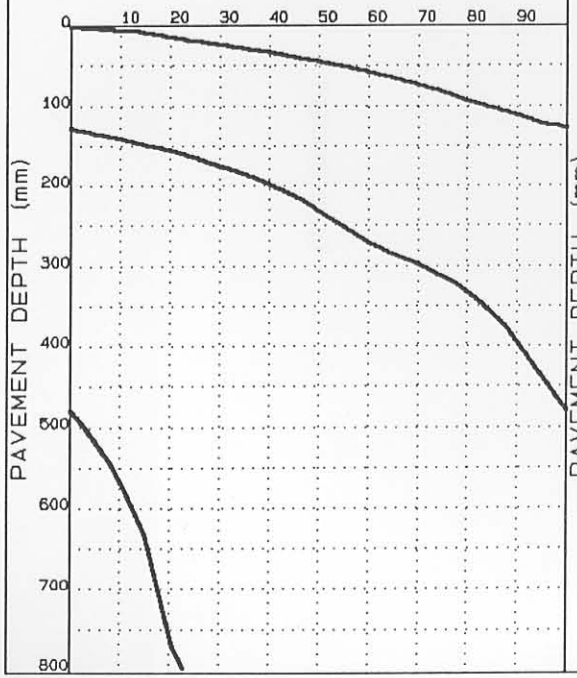

BALANCE CURVE

(DSN 800) (-90 ≤ B ≤ +90)

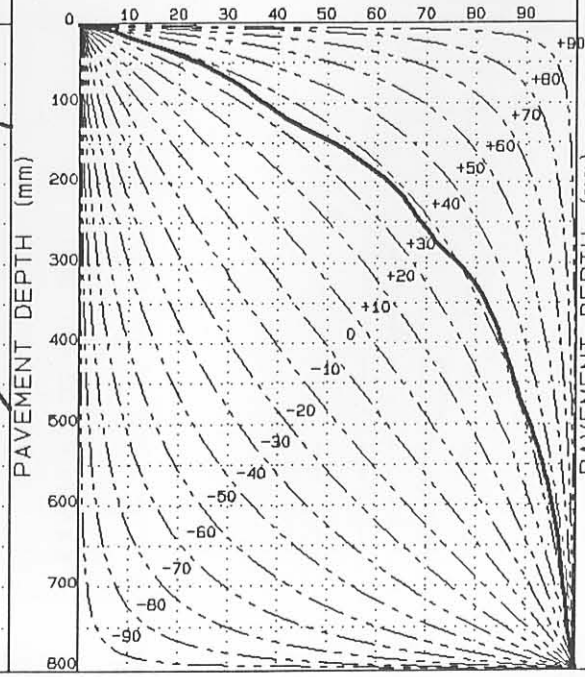

LAYER STRENGTH DIAGRAM

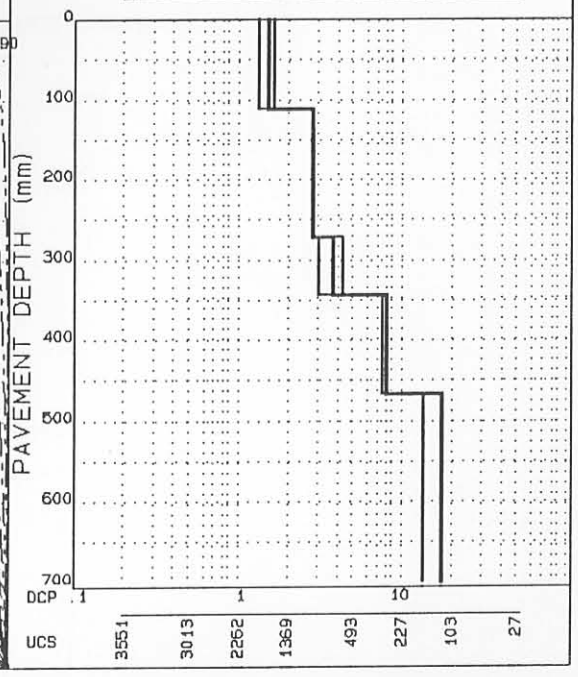

FIGURE E.34

ATT, CSIR, SA

SUMMARY OF DCP INVESTIGATION

AVERAGE EQUIVALENT STRENGTH (REDEFINED)

FROM - TO (mm)	AV. PENETRATION (mm/blow)	SD	95P	CBR%	UCS (kPa)
0- 8	0.8	0.2		344	2560
9-112	1.6	0.4		210	1658
113-208	2.2	0.4		154	1262
209-272	3.9	0.3		72	646
273-344	3.6	1.0		79	701
345-464	7.9	1.2		30	299
465-536	8.1	0.6		29	290
537-768	20.4	6.1		9	103
769-800	16.9	3.4		11	123

DATA FILE: 337A4, 1, 16; N=10

NORMALIZED CURVE

DEVIATION (A_i) FROM STANDARD PAVEMENT BALANCE CURVE (SPBC), %.mm

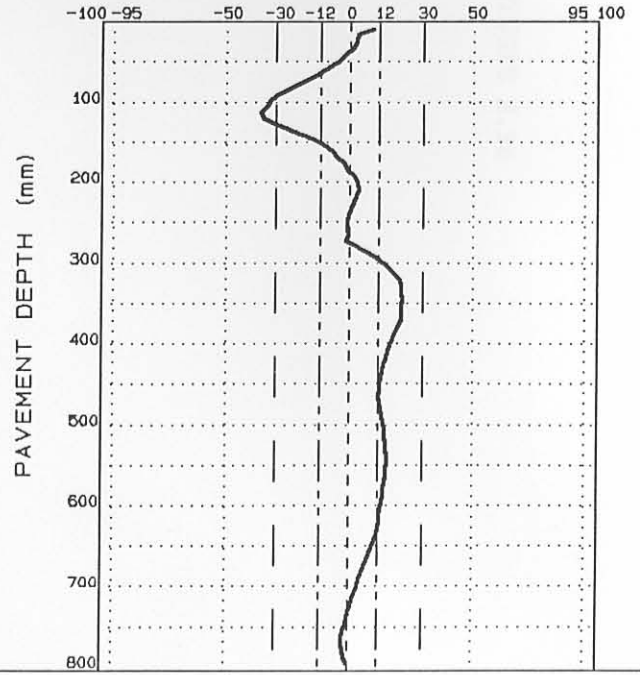

LAYER STRENGTH DIAGRAM (REDEFINED)

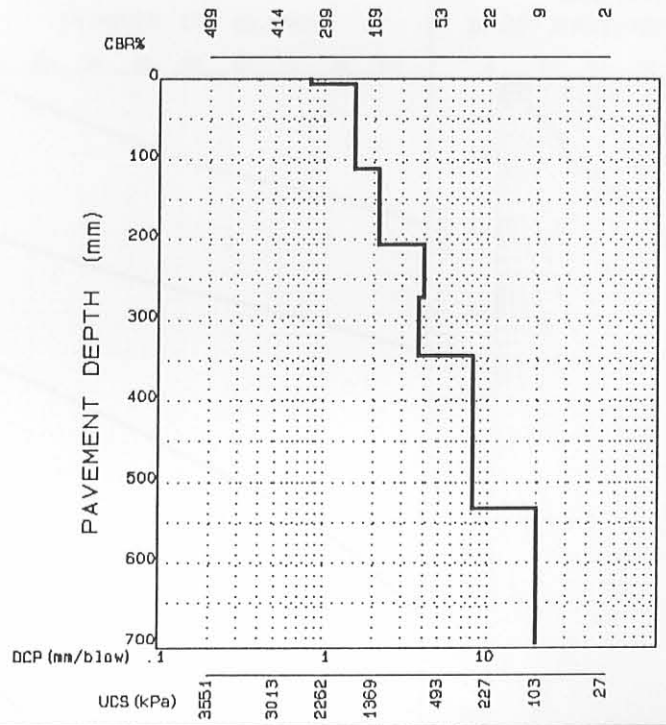

FIGURE E.35

RTT, CSIR, SA

SUMMARY OF DCP INVESTIGATION

DATA FILE :337A4, FINAL; N=48 000
REGION :Rooiwal TVL
ROAD NUMBER :
DISTANCE : 3.0
POSITION : L [X] M R
CONDITION : FAILED [X] OVERSTRESSED SOUND
[X] DEF. [X] DEFORM. PUMP. CRACKS : BROCK [X] LONG. OTHER
DATE :88/09/09

PAVEMENT CHARACTERISTICS

	DATA	B/CURVE
STRUCTURE NUMBER :	320	
BALANCE NUMBER (BN 100) :	15	25
DIFFERENCE IN BN100 :	-10	
BALANCE CURVE IS WHERE B =	20	A= 3463
STRUCT. CAP. (E80 X 10^6) :	>10	
ROAD CATEGORY :	B	
TRAFFIC : LIGHT TRAFFIC		

AVERAGE EQUIVALENT STRENGTH

FROM - TO	AV. PENETRATION	SD	90 P	CBR	UCS
0-112	2.4	0.4	2.9	132	1102
113-272	1.8	0.1	1.9	189	1511
273-344	1.8	0.2	2.0	188	1504
345-464	2.9	0.5	3.5	107	916
465-800	10.1	4.1	15.4	22	227

CATEGORY VI : POORLY BALANCED DEEP STRUCTURE (PBD)

DCP CURVE

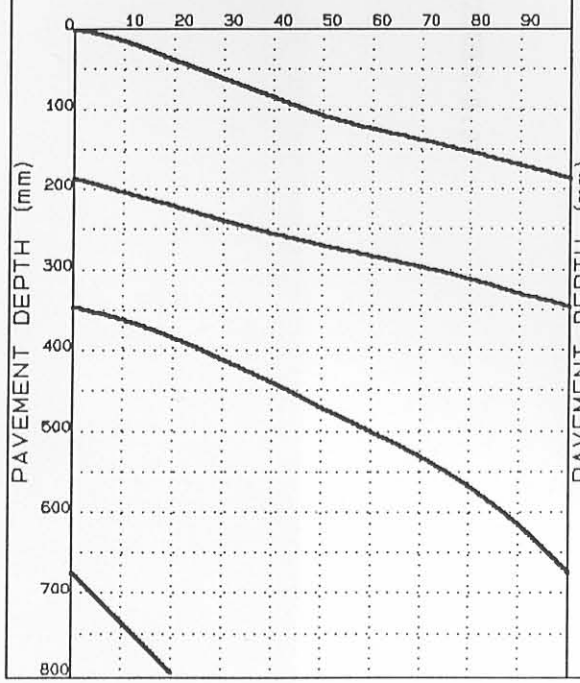

BALANCE CURVE

(DSN 800) (-90 ≤ B ≤ +90)
% OF PAVEMENT STRUCTURE NUMBER

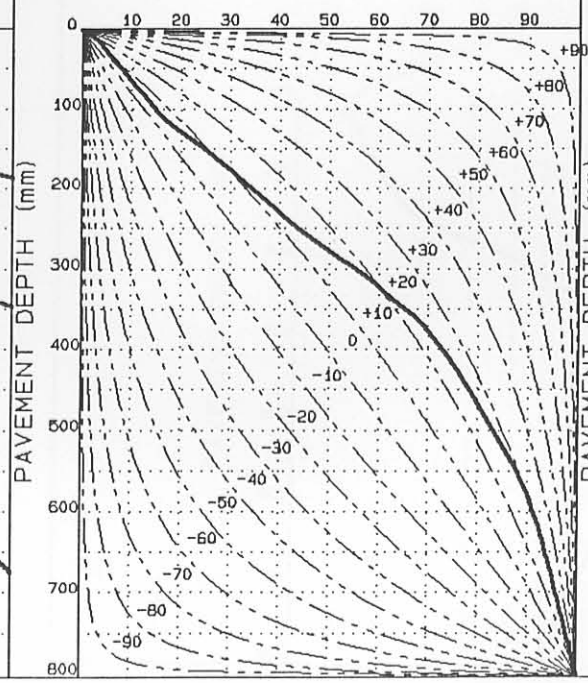

LAYER STRENGTH DIAGRAM

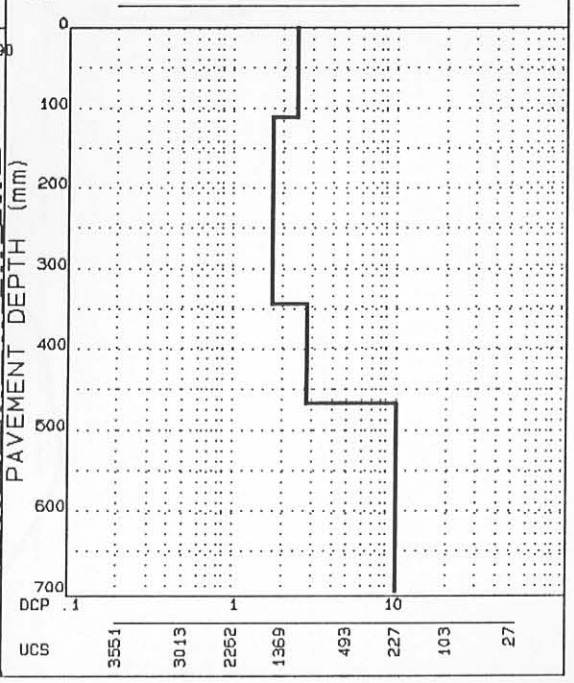

FIGURE E.36

RTT, CSIR, SA

SUMMARY OF DCP INVESTIGATION

AVERAGE EQUIVALENT STRENGTH (REDEFINED)

FROM - TO (mm)	AV. PENETRATION (mm/blow)	SD	90P	CBR%	UCS (kPa)
0-112	2.4	0.4		132	1102
113-536	2.5	1.0		128	1072
537-800	11.7	3.0		18	190

DATA FILE: 337A4, FINAL; N=48 000

NORMALIZED CURVE

DEVIATION (A_i) FROM STANDARD PAVEMENT BALANCE CURVE (SPBC), %.mm

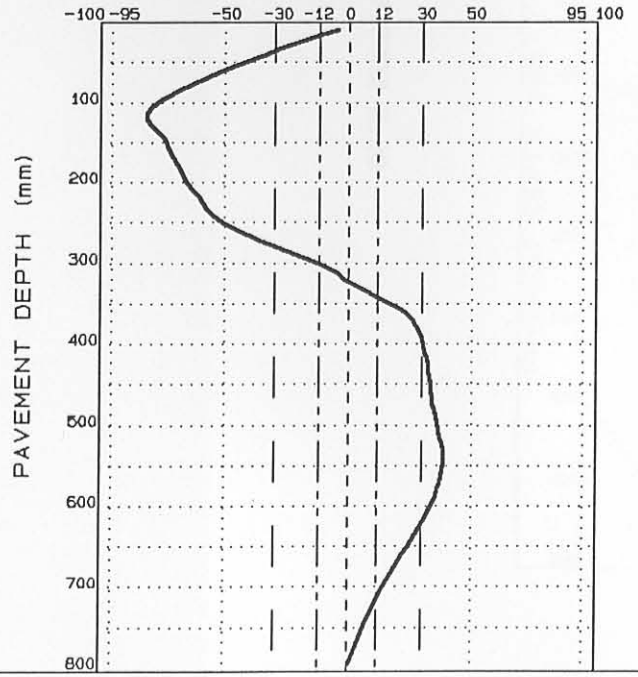

LAYER STRENGTH DIAGRAM (REDEFINED)

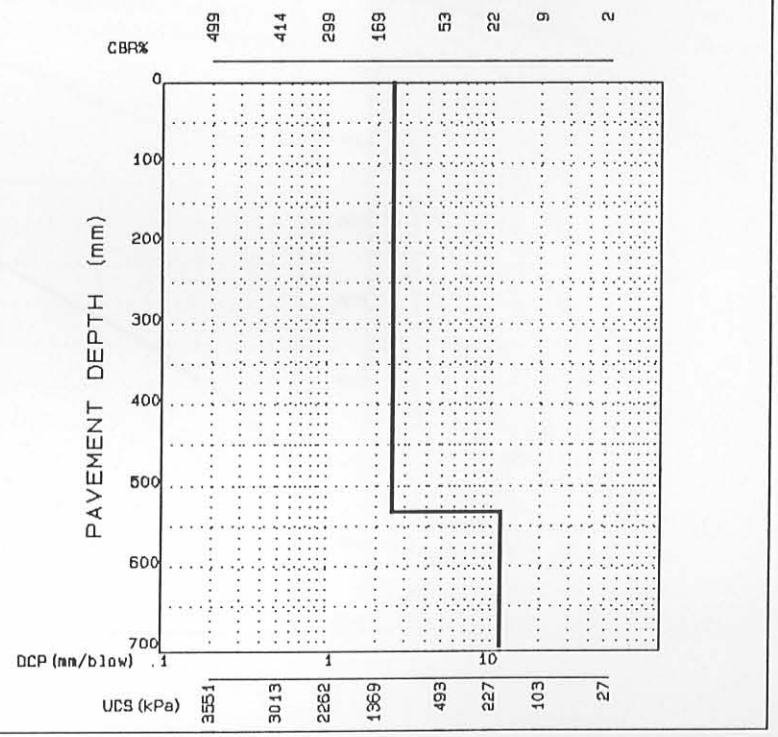

FIGURE E.37

RTT, CSIR, SA

SUMMARY OF DCP INVESTIGATION

DATA FILE :306A4, 9B, 17B; N=10
REGION :BULTFONTEIN
ROAD NUMBER :P2212
DISTANCE : 12.6
POSITION : L | | | M | X | | R
CONDITION : FAILED | OVERSTRESSED | SOUND
RUT. | DEFORM. | PUMP. | CRACKS : CROCK. | LONG. | OTHER
DATE :86/03/06

PAVEMENT CHARACTERISTICS

		DATA	B/CURVE
STRUCTURE NUMBER	:	424	
BALANCE NUMBER (BN 100)	:	57	47
DIFFERENCE IN BN100	:	10	
BALANCE CURVE IS WHERE B =		42	A= 1711
STRUCT. CAP. (E80 X 10^6)	:	>10	
ROAD CATEGORY	:	C	

TRAFFIC : LIGHT TRAFFIC

AVERAGE EQUIVALENT STRENGTH

FROM - TO	AV. PENETRATION	SD	80 P	CBR	UCS
0- 90	0.7	0.4	1.0	356	2638
91-170	2.5	0.4	2.8	130	1087
171-210	1.5	0.5	1.8	223	1748
211-350	5.1	1.4	6.3	51	477
351-500	3.6	0.4	4.0	79	701
501-800	8.7	3.0	11.2	26	263

CATEGORY II : AVERAGELY BALANCED SHALLOW STRUCTURE (ABS)

DCP CURVE

NUMBER OF BLOWS

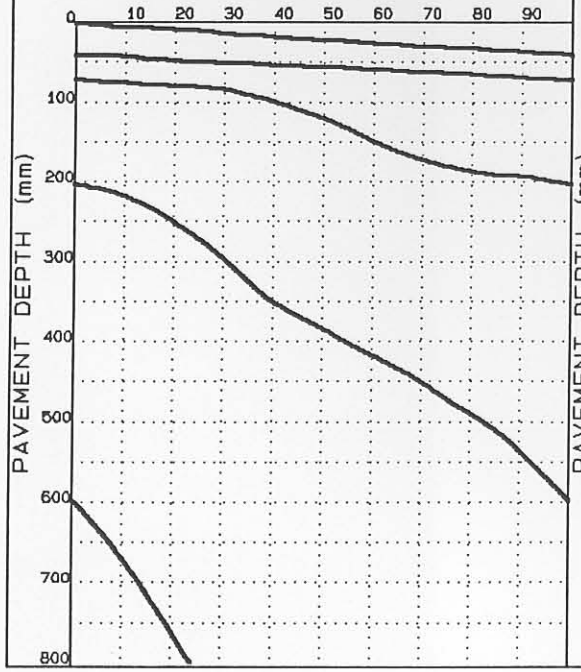

BALANCE CURVE

(DSN 800) (-90 ≤ B ≤ +90)
% OF PAVEMENT STRUCTURE NUMBER

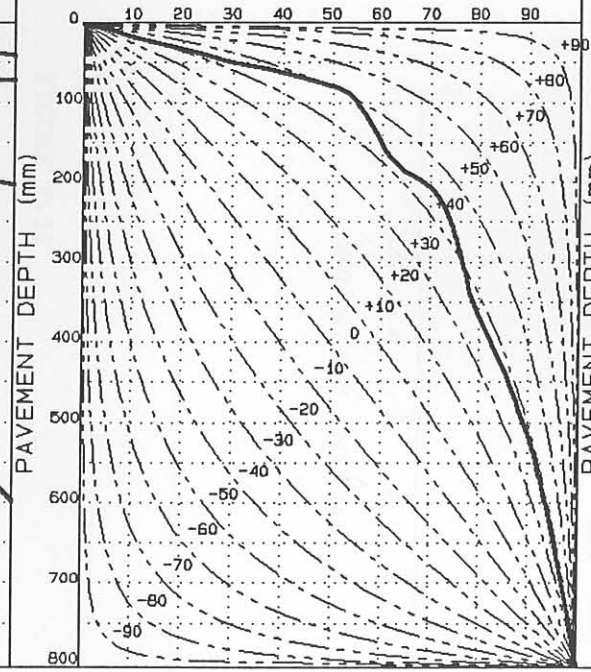

LAYER STRENGTH DIAGRAM

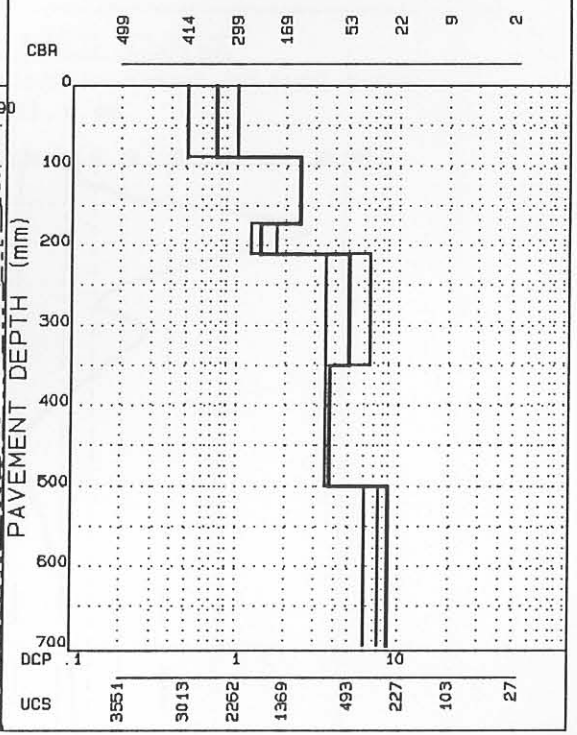

FIGURE E.38

ATT, CSIR, SA

SUMMARY OF DCP INVESTIGATION

AVERAGE EQUIVALENT STRENGTH (REDEFINED)

FROM - TO (mm)	AV. PENETRATION (mm/blow)	SD	BOP	CBR%	UCS (kPa)
0- 16	0.6	0.2	0.8	378	2781
17- 80	0.7	0.3	0.9	372	2742
81-176	2.3	0.5	2.8	141	1167
177-208	1.3	0.4	1.7	241	1871
209-352	5.1	1.4	6.2	52	485
353-800	7.0	3.4	9.9	34	334

DATA FILE: 306A4, 9B, 17B; N=10

NORMALIZED CURVE

DEVIATION (A_i) FROM STANDARD PAVEMENT BALANCE CURVE (SPBC), %.mm

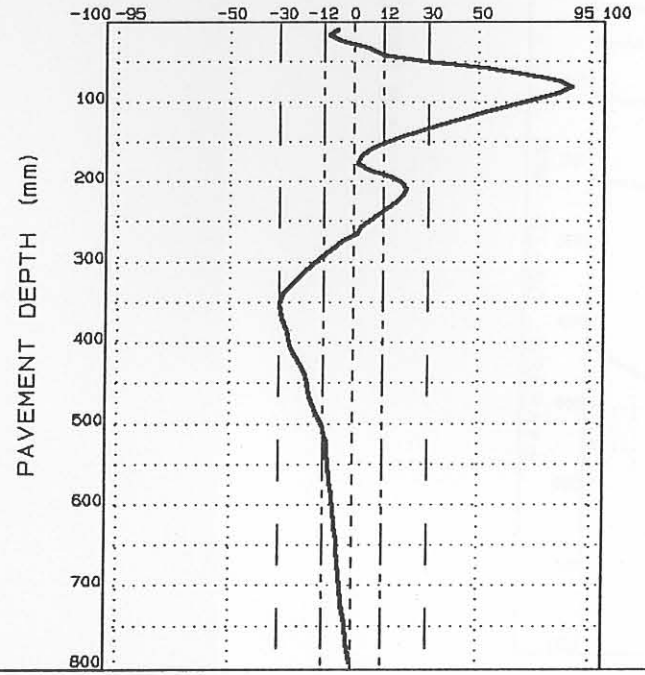

LAYER STRENGTH DIAGRAM (REDEFINED)

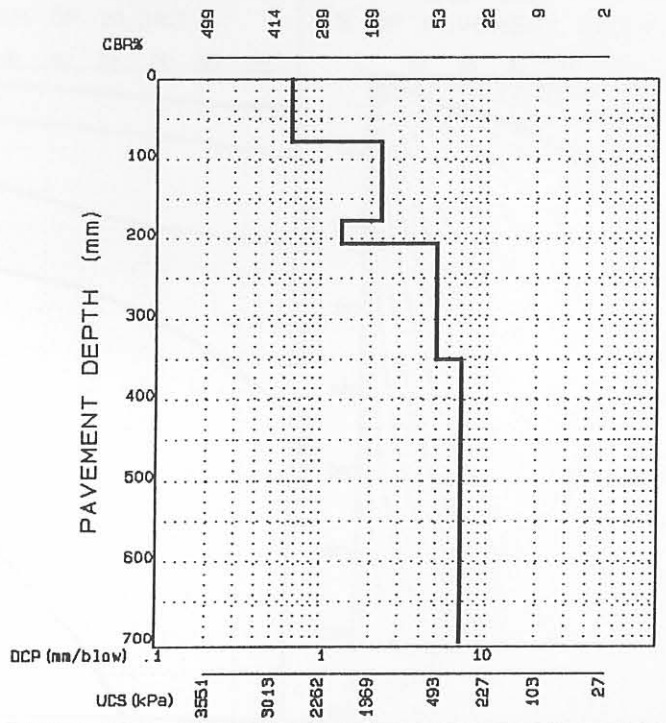

FIGURE E.39

RTT, CSIR, SA

SUMMARY OF DCP INVESTIGATION

DATA FILE :306A4, 5CL, 11CL; N=1 000 000
REGION :BULTFONTEIN
ROAD NUMBER :2212
DISTANCE : 12.6
POSITION : L | M | R
CONDITION : FAILED | OVERSTRESSED | SOUND
RUT. | DEFORM. | PUMP. | CRACKS : CROCK | LONG. | OTHER
DATE :86/10/15

PAVEMENT CHARACTERISTICS

	DATA	B/CURVE
STRUCTURE NUMBER :	468	
BALANCE NUMBER (BN 100) :	41	43
DIFFERENCE IN BN100 :	-2	
BALANCE CURVE IS WHERE B =	39	A= 1057
STRUCT. CAP. (E80 X 10^6) :	>10	
ROAD CATEGORY :	C	
TRAFFIC : LIGHT TRAFFIC		

AVERAGE EQUIVALENT STRENGTH

FROM - TO	AV. PENETRATION	SD	80 P	CBR	UCS
0- 90	0.7	0.3	0.9	367	2710
91-170	1.4	0.3	1.7	235	1830
171-210	1.3	0.4	1.7	245	1899
211-350	2.3	1.1	3.2	142	1175
351-500	4.1	0.5	4.5	68	614
501-800	7.1	2.0	8.7	34	334

CATEGORY IV : WELL-BALANCED DEEP STRUCTURE (WBD)

DCP CURVE

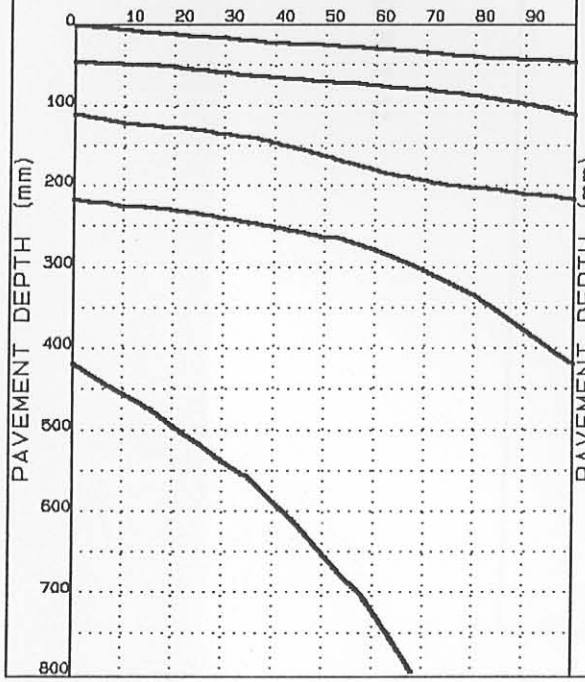

BALANCE CURVE

(DSN 800) (-90 ≤ B ≤ +90)

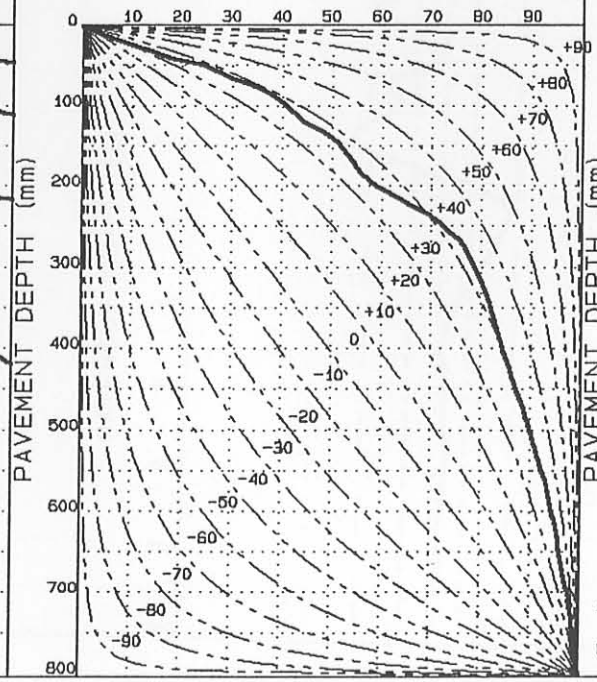

LAYER STRENGTH DIAGRAM

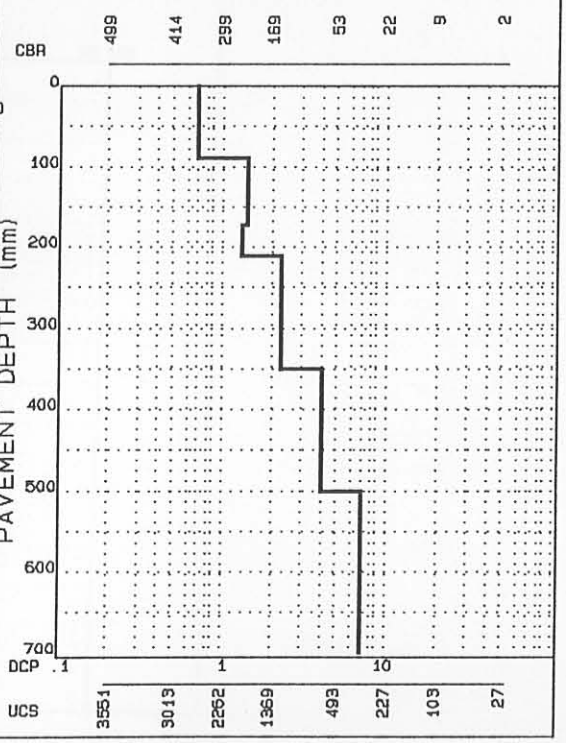

FIGURE E.40

ATT. CSIR, SA

SUMMARY OF DCP INVESTIGATION

AVERAGE EQUIVALENT STRENGTH (REDEFINED)

FROM - TO (mm)	AV. PENETRATION (mm/blow)	SD	80P	CBR%	UCS (kPa)
0- 32	0.6	0.1	0.7	392	2871
33- 72	0.6	0.2	0.8	384	2820
73-112	1.2	0.3	1.4	267	2048
113-136	1.1	0.3	1.4	277	2115
137-184	1.7	0.2	1.9	199	1581
185-264	1.1	0.3	1.4	275	2102
265-440	3.6	0.8	4.3	80	709
441-472	3.5	0.2	3.6	84	740
473-496	4.5	0.3	4.8	61	558
497-800	7.0	2.0	8.7	34	334

DATA FILE: 306A4, 5CL, 11CL; N=1 000 000

NORMALIZED CURVE

DEVIATION (A_i) FROM STANDARD PAVEMENT BALANCE CURVE (SPBC), %.mm

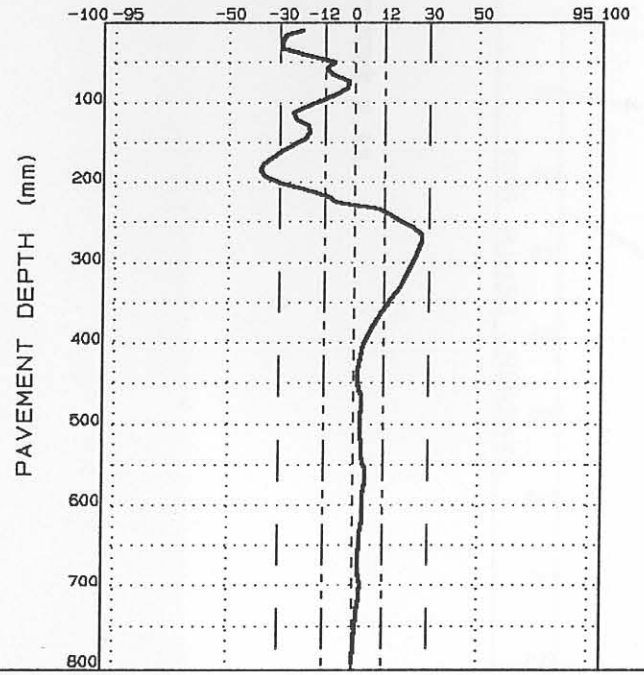

LAYER STRENGTH DIAGRAM (REDEFINED)

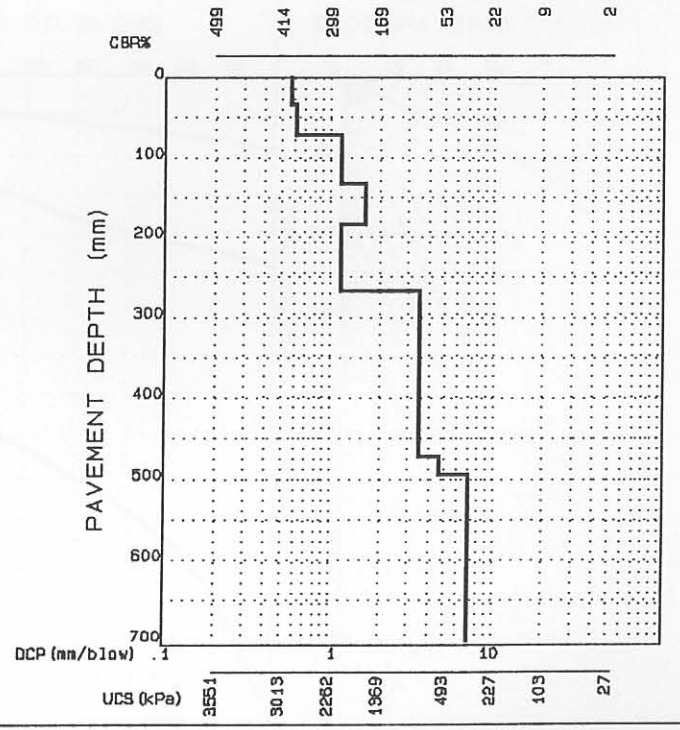

FIGURE E.41

ATT, CSIR, SA

SUMMARY OF DCP INVESTIGATION

DATA FILE :306A4, 2-5, 13-5; N=1 400 000
REGION :BULTFONTEIN
ROAD NUMBER :2212
DISTANCE : 12.6
POSITION : L | X | M | R
CONDITION : FAILED | OVERSTRESSED | SOUND
RUT. | DEFORM. | PUMP. | CRACKS : CROCK | LONG. | OTHER
DATE :86/10/10

PAVEMENT CHARACTERISTICS

	DATA	B/CURVE
STRUCTURE NUMBER :	300	
BALANCE NUMBER (BN 100) :	35	37
DIFFERENCE IN BN100 :	-2	
BALANCE CURVE IS WHERE B =	33	A= 1235
STRUCT. CAP. (E80 X 10^6) :	>10	
ROAD CATEGORY :	C	
TRAFFIC : LIGHT TRAFFIC		

AVERAGE EQUIVALENT STRENGTH

FROM - TO	AV. PENETRATION	SD	80 P	CBR	UCS
0- 90	1.2	0.3	1.4	271	2075
90-170	1.8	0.7	2.4	188	1504
171-210	2.3	0.5	2.7	142	1175
211-350	4.6	2.4	6.6	59	542
351-500	4.9	0.7	5.6	54	501
501-800	10.8	5.3	15.2	20	209

CATEGORY IV : WELL-BALANCED DEEP STRUCTURE (WBD)

DCP CURVE

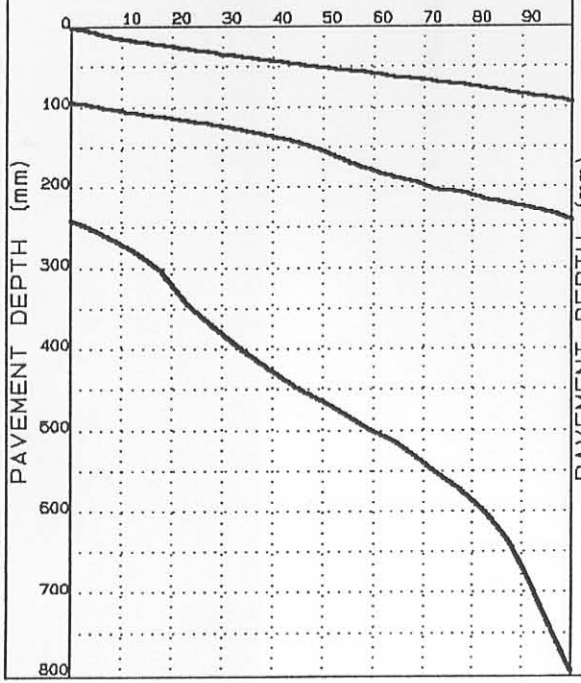

BALANCE CURVE

(DSN 800) (-90 ≤ B ≤ +90)
% OF PAVEMENT STRUCTURE NUMBER

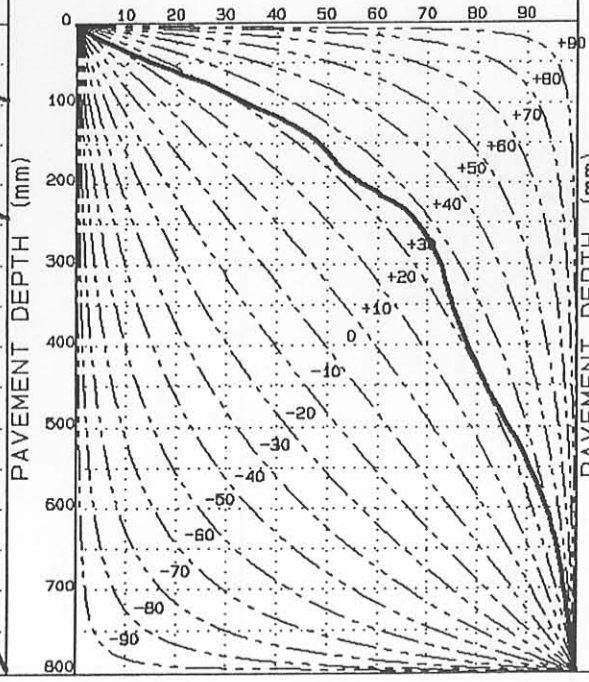

LAYER STRENGTH DIAGRAM

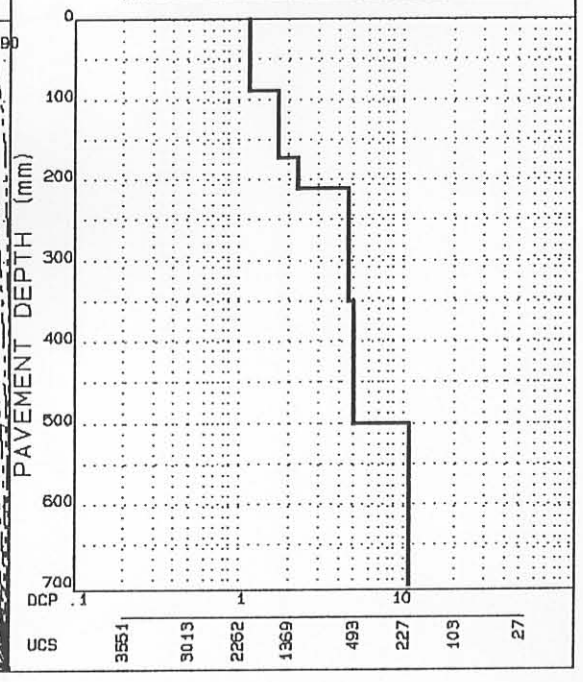

FIGURE E.42

RTT, CSIR, SA

SUMMARY OF DCP INVESTIGATION

AVERAGE EQUIVALENT STRENGTH (REDEFINED)

FROM - TO (mm)	AV. PENETRATION (mm/blow)	SD	BOP	CBR%	UCS (kPa)
0- 32	1.4	0.3	1.7	226	1768
33-136	1.1	0.2	1.3	281	2142
137-176	2.5	0.5	2.9	125	1050
177-240	2.0	0.5	2.4	172	1391
241-424	5.5	1.6	6.8	47	444
425-600	4.6	0.8	5.2	59	542
601-792	13.7	3.8	15.9	15	152
793-800	15.7	1.0	16.6	12	133

DATA FILE: 306A4, 2-5, 13-5; N=1 400 000

NORMALIZED CURVE

DEVIATION (A_i) FROM STANDARD PAVEMENT BALANCE CURVE (SPBC), %.mm

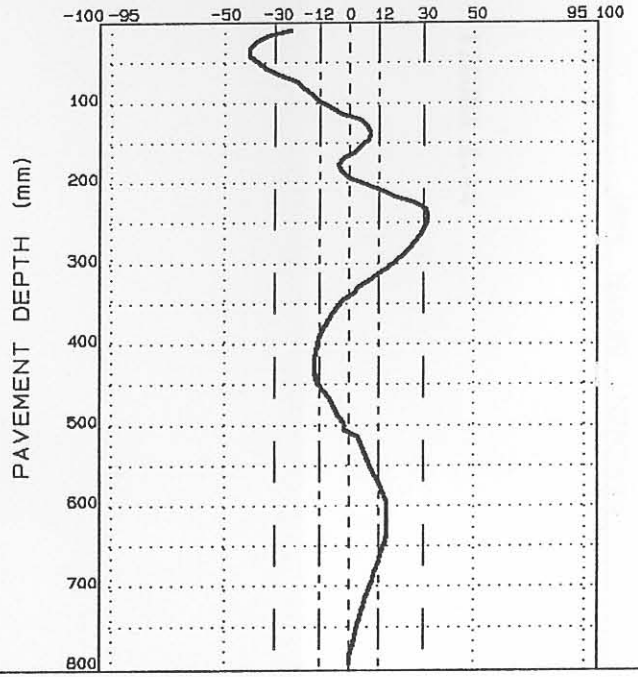

LAYER STRENGTH DIAGRAM (REDEFINED)

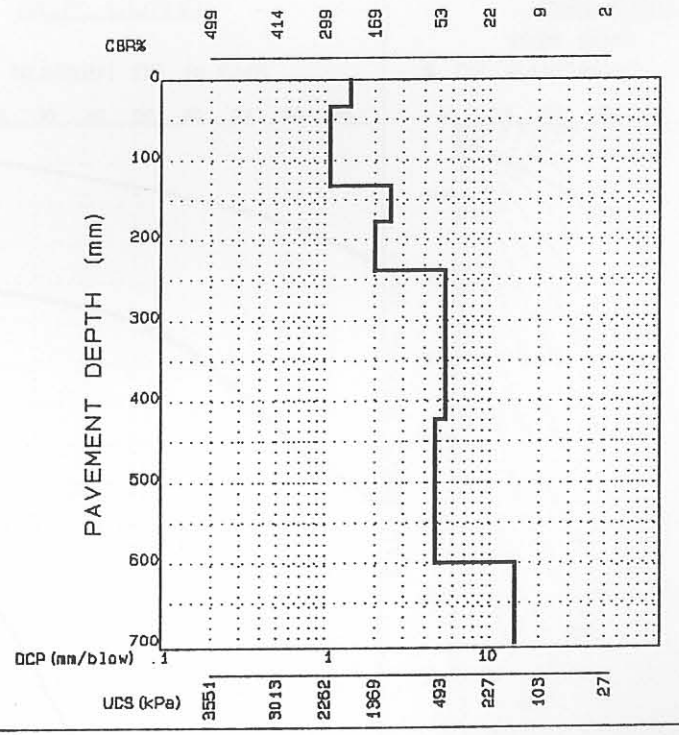

FIGURE E.43

RTT, CSIR, SA

SUMMARY OF DCP INVESTIGATION

DATA FILE :306A4, 2, 4, 6, 7, 7AD; N=2 450 000
REGION :BULTFONTEIN
ROAD NUMBER :2212
DISTANCE : 12.6
POSITION : [X] | | | M | | | R
CONDITION : FAILED | OVERSTRESSED | SOUND
RUT. | DEFORM. | PUMP. | CRACKS : CROCK. | LONG. | OTHER
DATE :87/02/10

PAVEMENT CHARACTERISTICS

	DATA	B/CURVE
STRUCTURE NUMBER :	243	
BALANCE NUMBER (BN 100) :	27	32
DIFFERENCE IN BN100 :	-5	
BALANCE CURVE IS WHERE B =	28	A= 1629
STRUCT. CAP. (E80 X 10^6) :	>10	
ROAD CATEGORY :	C	

TRAFFIC : LIGHT TRAFFIC

AVERAGE EQUIVALENT STRENGTH

FROM - TO	AV. PENETRATION	SD	80 P	CBR	UCS
0- 90	2.0	0.7	2.6	171	1383
91-170	2.8	0.8	3.4	112	953
171-210	2.2	1.0	3.0	150	1233
211-350	4.2	1.7	5.7	66	598
351-500	6.1	0.8	6.7	42	402
501-800	10.3	3.0	12.8	21	218

CATEGORY V : AVERAGELY BALANCED DEEP STRUCTURE (ABD)

DCP CURVE

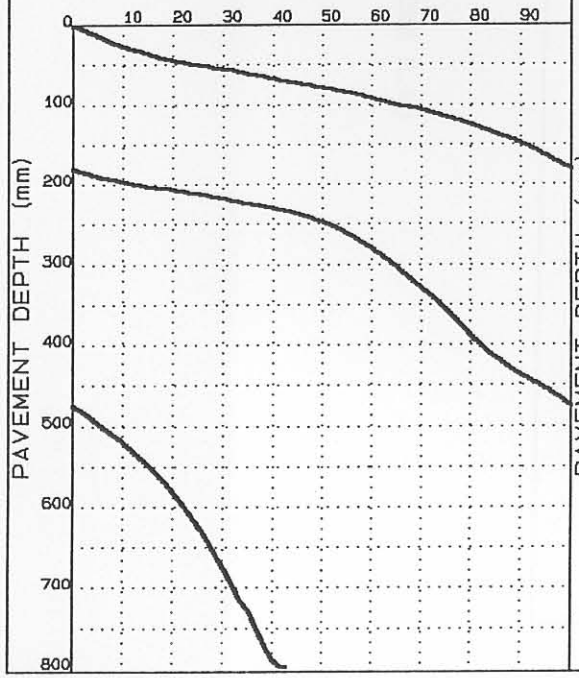

BALANCE CURVE

(DSN 800) (-90 ≤ B ≤ +90)
% OF PAVEMENT STRUCTURE NUMBER

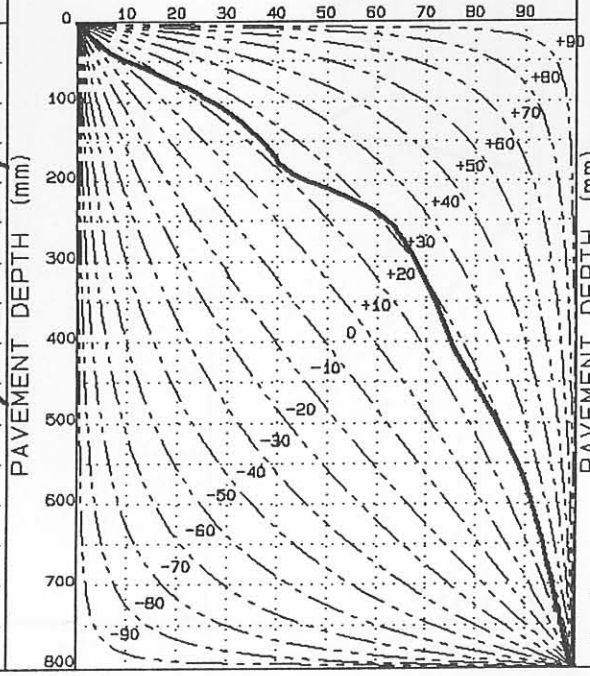

LAYER STRENGTH DIAGRAM

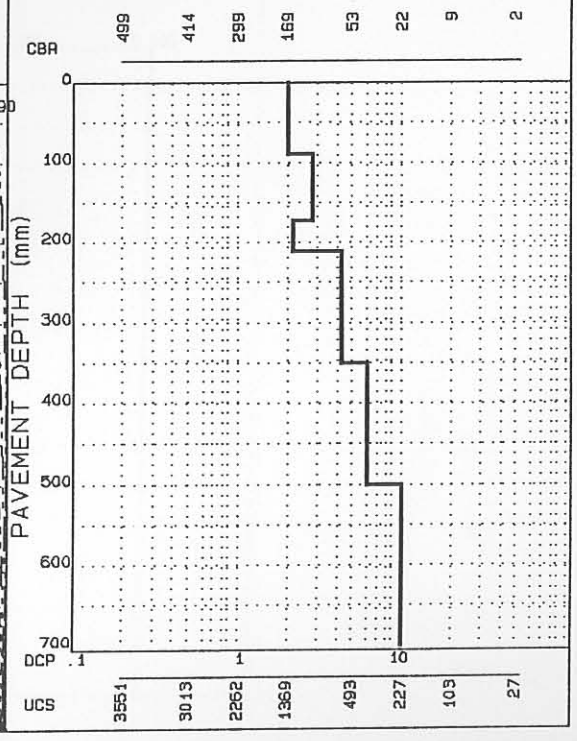

FIGURE E.44

ATT, CSIR, SA

SUMMARY OF DCP INVESTIGATION

AVERAGE EQUIVALENT STRENGTH (REDEFINED)

FROM - TO (mm)	AV. PENETRATION (mm/blow)	SD	BOP	CBR%	UCS (kPa)
0- 40	2.7	0.5	3.1	118	998
41-104	1.5	0.2	1.7	219	1720
105-176	3.1	0.7	3.6	99	855
177-256	1.9	0.7	2.4	178	1433
257-408	6.0	0.9	6.7	42	402
409-560	5.8	0.5	6.2	44	419
561-776	11.2	2.5	13.3	19	200
777-800	12.4	1.7	13.8	17	181

DATA FILE: 306A4, 2, 4, 6, 7, 7AD; N=2 450 000

NORMALIZED CURVE

DEVIATION (A_i) FROM STANDARD PAVEMENT BALANCE CURVE (SPBC), %.mm

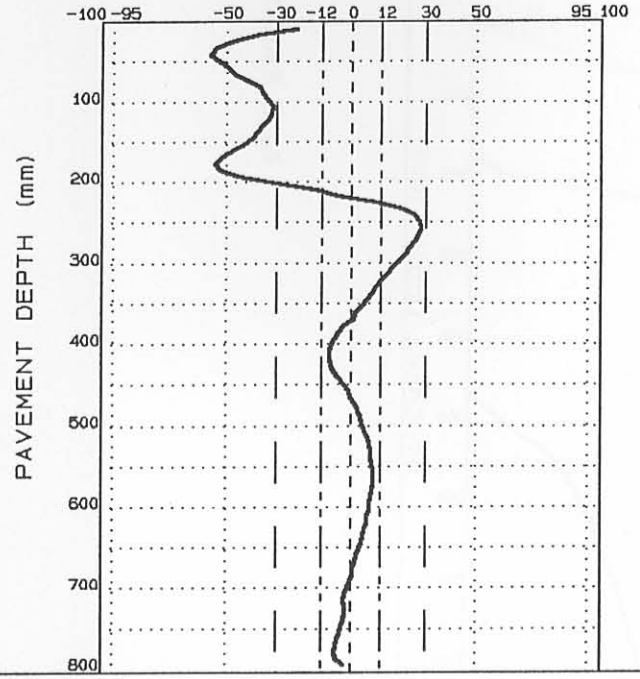

LAYER STRENGTH DIAGRAM (REDEFINED)

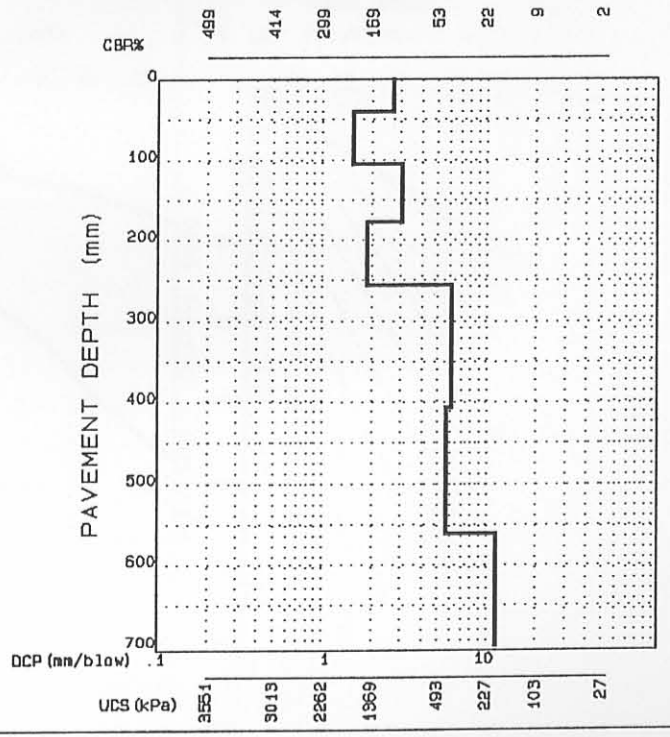

FIGURE E.45

RTT, CSIR, SA

SUMMARY OF DCP INVESTIGATION

DATA FILE :306A4, B, 11CL, 15, 15AN; N=2 450
REGION :BULTFONTEIN
ROAD NUMBER :2212
DISTANCE : 12.6
POSITION : [X] | | | M | | | | R
CONDITION : FAILED | OVERSTRESSED | SOUND
RUT. | DEFORM. | PUMP. | CRACKS : CROCK. | LONG. | OTHER
DATE :87/02/10

PAVEMENT CHARACTERISTICS

	DATA	B/CURVE
STRUCTURE NUMBER :	235	
BALANCE NUMBER (BN 100) :	25	37
DIFFERENCE IN BN100 :	-12	
BALANCE CURVE IS WHERE B =	33	A= 2717
STRUCT. CAP. (E80 X 10^6) :	>10	
ROAD CATEGORY :	C	
TRAFFIC : LIGHT TRAFFIC		

AVERAGE EQUIVALENT STRENGTH

FROM - TO	AV. PENETRATION	SD	80 P	CBR	UCS
0- 90	2.0	0.5	2.4	165	1341
91-170	1.9	0.4	2.3	173	1398
171-210	2.0	0.6	2.5	167	1355
211-350	3.9	1.9	5.6	72	646
351-500	5.7	1.1	6.6	45	427
501-800	14.8	5.7	19.6	13	143

CATEGORY V : AVERAGELY BALANCED DEEP STRUCTURE (ABD)

DCP CURVE

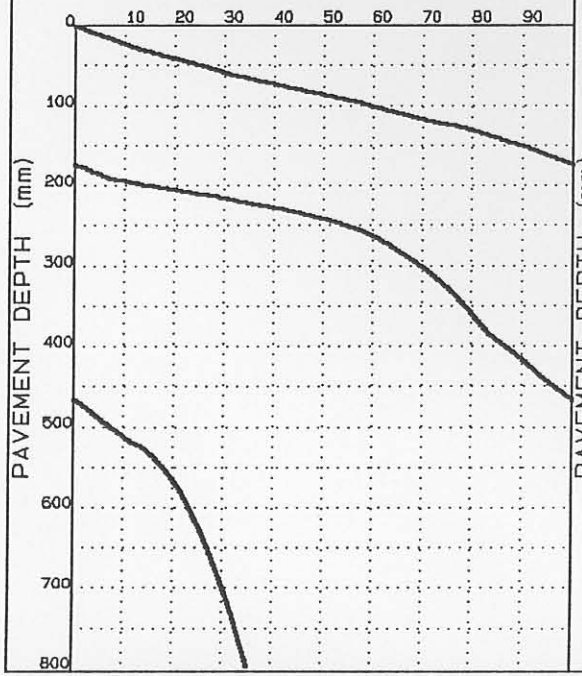

BALANCE CURVE

(DSN 800) (-90 ≤ B ≤ +90)

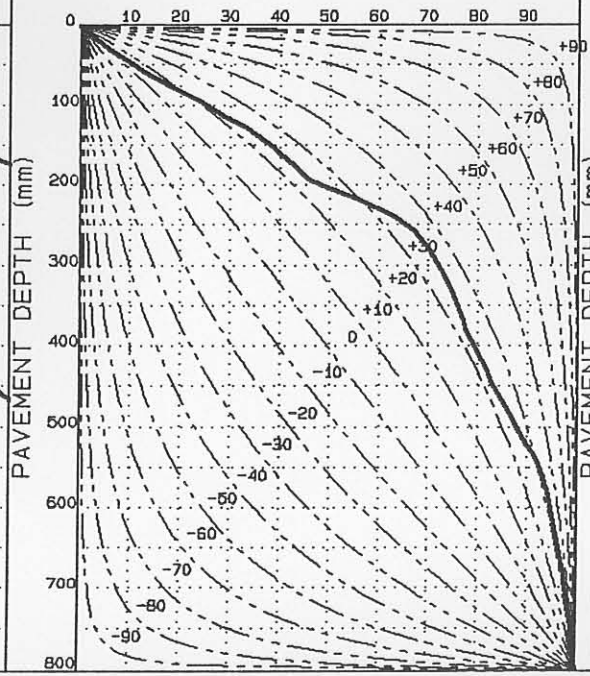

LAYER STRENGTH DIAGRAM

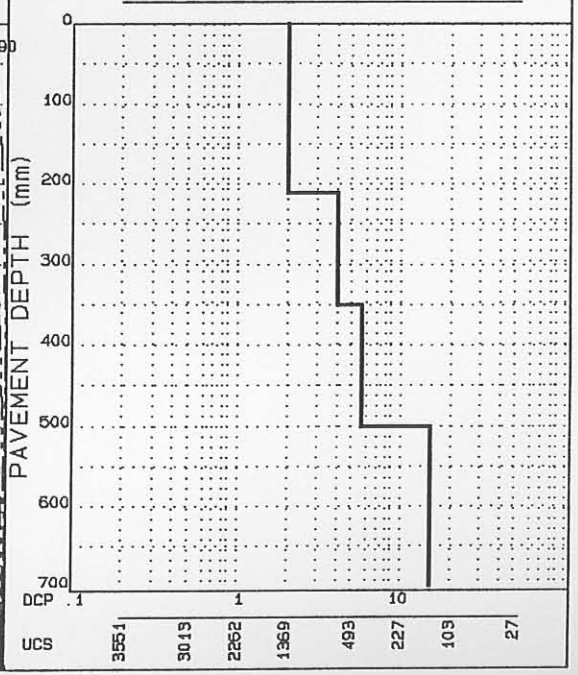

FIGURE E.46

ATT, CSIR, SA

SUMMARY OF DCP INVESTIGATION

AVERAGE EQUIVALENT STRENGTH (REDEFINED)

FROM - TO (mm)	AV. PENETRATION (mm/blow)	SD	BOP	CBR%	UCS (kPa)
0- 64	2.3	0.3	2.6	143	1182
65-144	1.7	0.3	1.9	199	1581
145-184	2.4	0.3	2.6	133	1109
185-264	1.8	0.6	2.3	184	1476
265-384	5.9	1.5	7.1	43	410
385-560	5.3	0.8	6.0	49	460
561-800	17.1	3.8	20.2	11	123

DATA FILE: 306A4, 8, 11CL, 15, 15AN; N=2 450

NORMALIZED CURVE

DEVIATION (A_i) FROM STANDARD PAVEMENT BALANCE CURVE (SPBC), %.mm

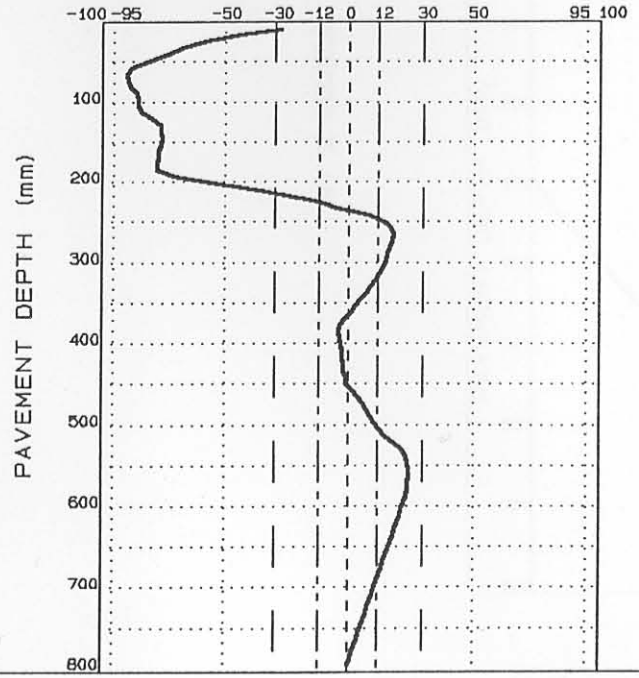

LAYER STRENGTH DIAGRAM (REDEFINED)

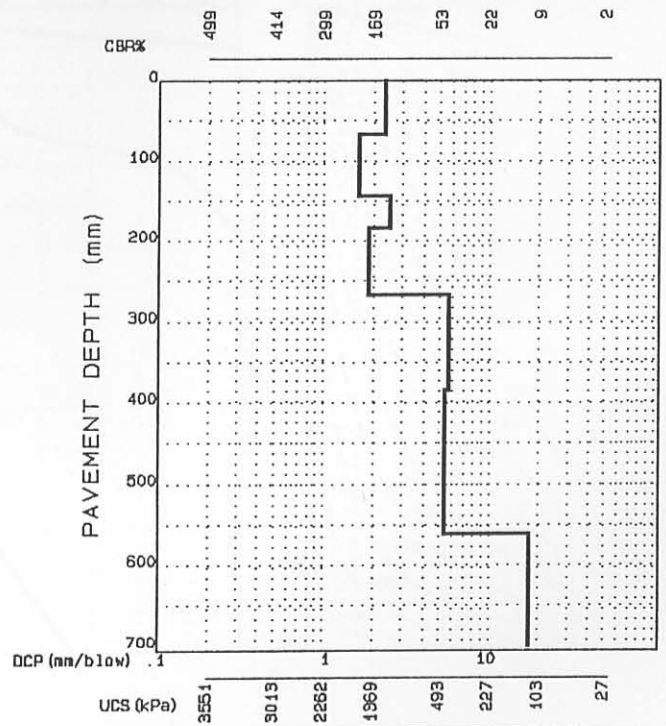

FIGURE E.47

ATT. CSIR, SA

SUMMARY OF DCP INVESTIGATION

DATA FILE :307A4, 57B, 65B; N=10
REGION :BULTFONTEIN
ROAD NUMBER :P2212
DISTANCE : 12.6
POSITION : L | M (X) | R
CONDITION : FAILED | OVERSTRESSED | SOUND
RUT. | DEFORM. | PUMP. | CRACKS : CROCK. | LONG. | OTHER
DATE :860306

PAVEMENT CHARACTERISTICS

	DATA	B/CURVE	FROM - TO
STRUCTURE NUMBER :	266		0- 64
BALANCE NUMBER (BN 100) :	54	47	65-152
DIFFERENCE IN BN100 :	7		153-192
BALANCE CURVE IS WHERE B =	42	A= 2986	193-408
STRUCT. CAP. (E80 X 10^6) :	>10		409-800
ROAD CATEGORY :	C		

TRAFFIC : LIGHT TRAFFIC

AVERAGE EQUIVALENT STRENGTH

AV. PENETRATION	SD	80 P	CBR	UCS
0.9	0.3	1.2	314	2362
4.3	1.6	5.6	64	582
2.2	0.6	2.7	153	1254
7.5	1.4	8.7	31	307
9.0	1.7	10.4	25	254

CATEGORY II : AVERAGELY BALANCED SHALLOW STRUCTURE (ABS)

DCP CURVE

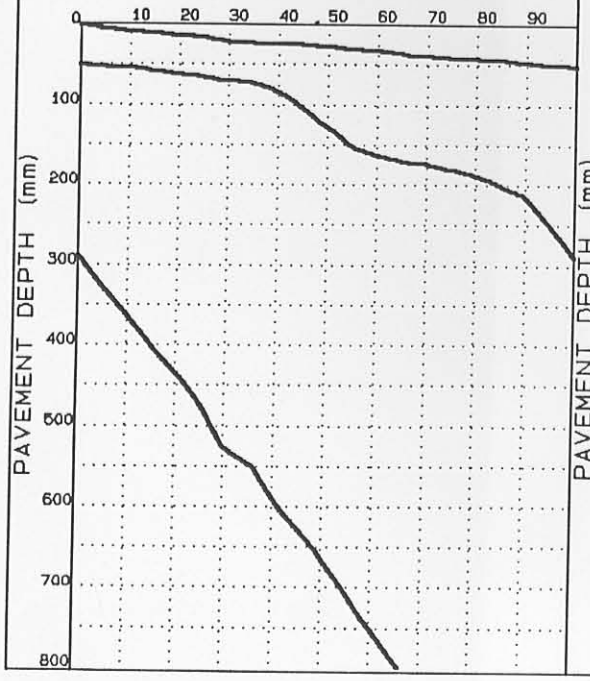

BALANCE CURVE

(DSN 800) (-90 ≤ B ≤ +90)
% OF PAVEMENT STRUCTURE NUMBER

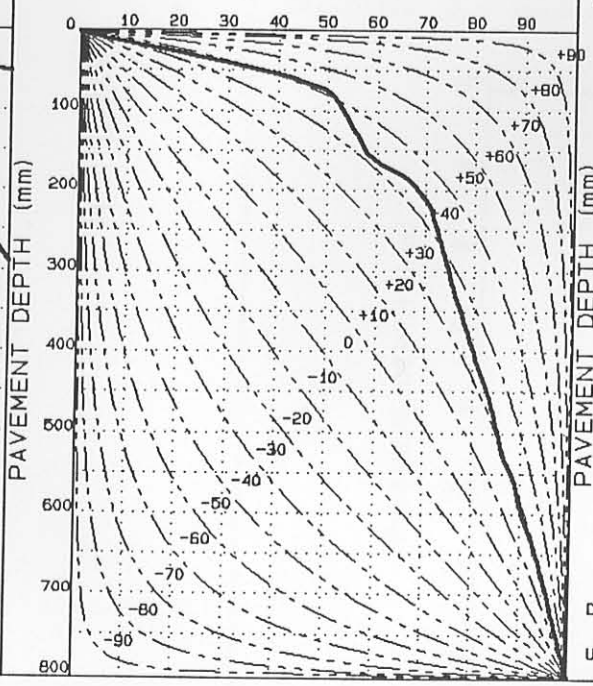

LAYER STRENGTH DIAGRAM

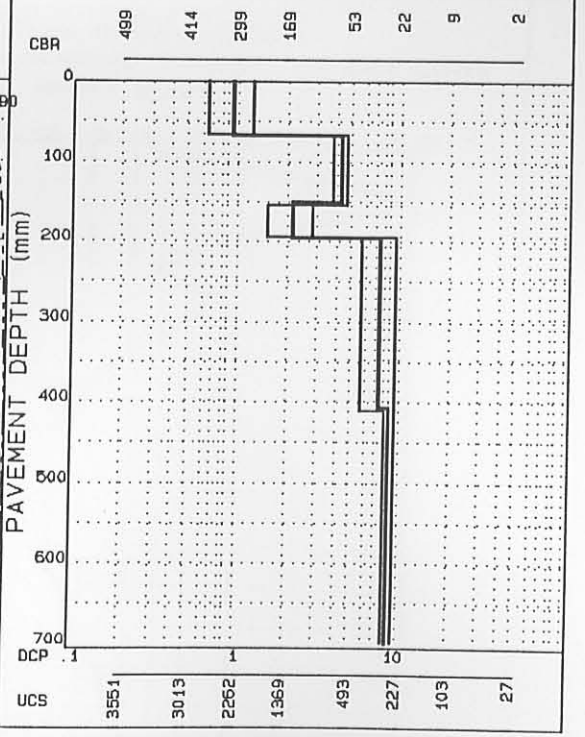

FIGURE E.48

RTT, CSIR, SA

SUMMARY OF DCP INVESTIGATION

AVERAGE EQUIVALENT STRENGTH (REDEFINED)

FROM - TO (mm)	AV. PENETRATION (mm/blow)	SD	SOP	CBR%	UCS (kPa)
0- 8	1.0	0.3	1.3	292	2216
9- 64	0.9	0.3	1.2	317	2382
65-152	4.3	1.6	5.6	64	582
153-192	2.2	0.6	2.7	153	1254
193-408	7.5	1.4	8.7	31	307
409-464	7.0	0.6	7.4	35	342
465-512	10.7	0.7	11.4	20	209
513-800	9.1	1.6	10.4	25	254

DATA FILE: 307A4, 57B, 65B; N=10

NORMALIZED CURVE

DEVIATION (A_i) FROM STANDARD PAVEMENT BALANCE CURVE (SPBC), %.mm

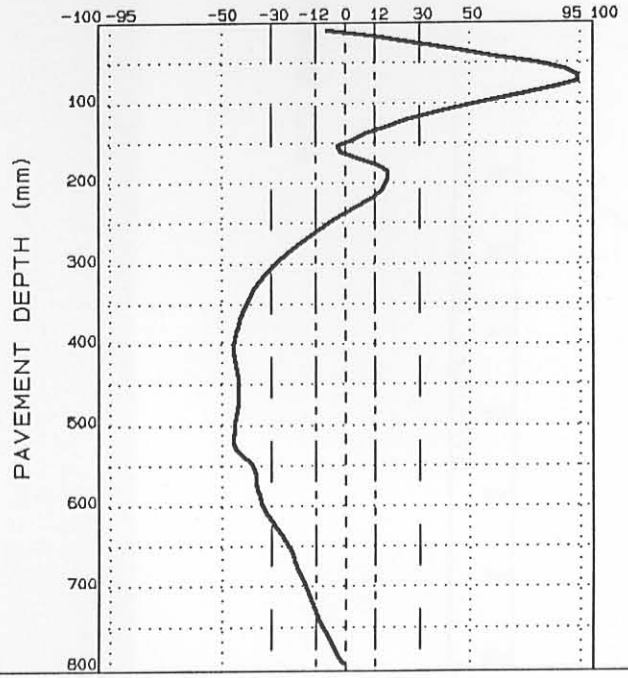

LAYER STRENGTH DIAGRAM (REDEFINED)

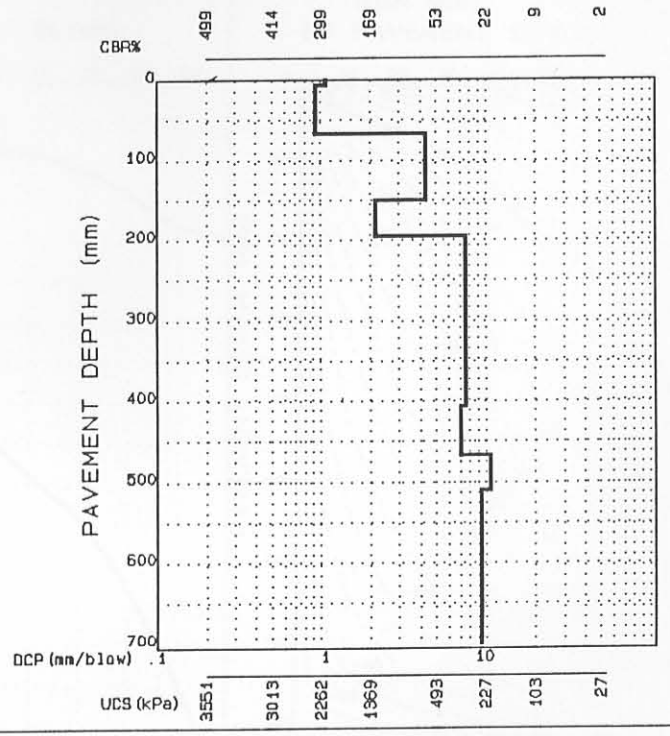

FIGURE E.49

ATT. CSIR. SA

SUMMARY OF DCP INVESTIGATION

DATA FILE :307A4, 13C, 5C; N=1 000 000
REGION :BULTFONTEIN
ROAD NUMBER :2212 (N=980 000)
DISTANCE : 12.6
POSITION : L | R
CONDITION : FAILED | OVERSTRESSED | SOUND
RUT. | DEFORM. | PUMP. | CRACKS : CROCK | LONG. | OTHER
DATE :86/06/06

PAVEMENT CHARACTERISTICS

	DATA	B/CURVE
STRUCTURE NUMBER :	194	
BALANCE NUMBER (BN 100) :	34	33
DIFFERENCE IN BN100 :	1	
BALANCE CURVE IS WHERE B =	29	A= 836
STRUCT. CAP. (E80 X 10^6) :	6.51	
ROAD CATEGORY :	C	

TRAFFIC : LIGHT TRAFFIC

AVERAGE EQUIVALENT STRENGTH

FROM - TO	AV. PENETRATION	SD	80 P	CBR	UCS
0- 64	1.7	0.5	2.1	195	1553
65-152	2.6	1.0	3.5	119	1005
153-192	3.5	1.2	4.6	83	732
193-408	5.7	2.2	7.6	45	427
409-800	10.0	3.1	12.6	22	227

CATEGORY IV : WELL-BALANCED DEEP STRUCTURE (WBD)

DCP CURVE

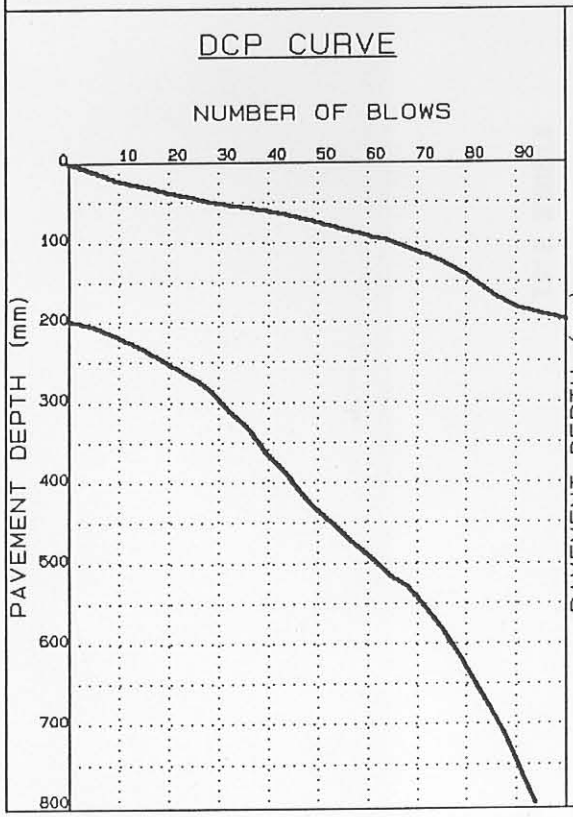

BALANCE CURVE

(DSN 800) (-90 ≤ B ≤ +90)

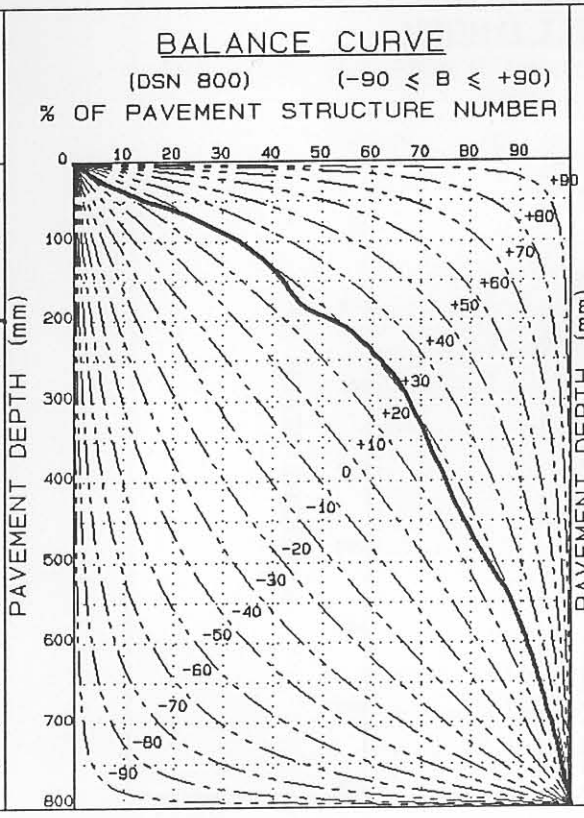

LAYER STRENGTH DIAGRAM

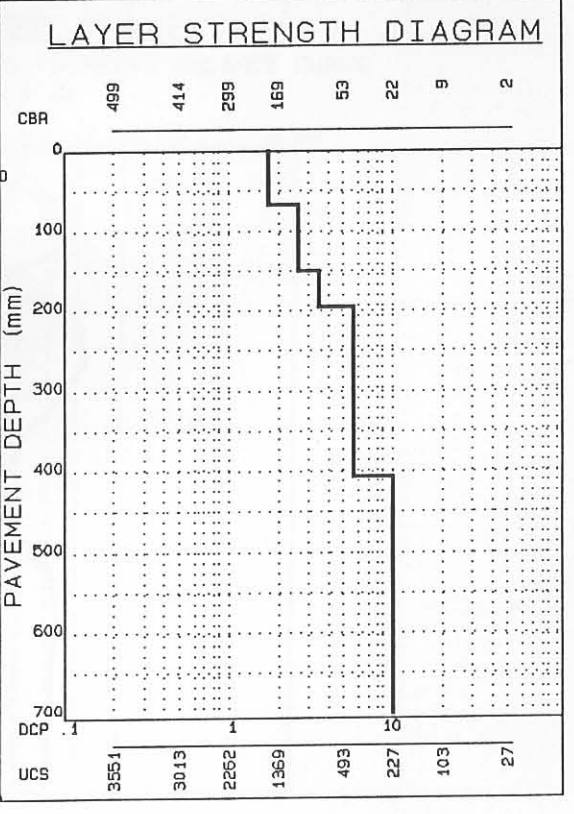

FIGURE E.50

RTT, CSIR, SA

SUMMARY OF DCP INVESTIGATION

AVERAGE EQUIVALENT STRENGTH (REDEFINED)

FROM - TO (mm)	AV. PENETRATION (mm/blow)	SD	BOP	CBR%	UCS (kPa)
0- 24	2.3	0.1	2.4	143	1182
25- 96	1.5	0.3	1.7	219	1720
97-176	3.5	0.9	4.2	83	732
177-264	2.9	0.8	3.6	106	908
265-424	7.1	1.2	8.1	34	334
425-576	6.8	1.4	8.0	36	351
577-672	11.0	0.5	11.4	19	200
673-704	11.0	0.0	11.0	19	200
705-800	14.1	0.9	14.9	14	152

DATA FILE: 307A4, 13C, 5C; N=1 000 000

NORMALIZED CURVE

DEVIATION (A_i) FROM STANDARD PAVEMENT BALANCE CURVE (SPBC), %.mm

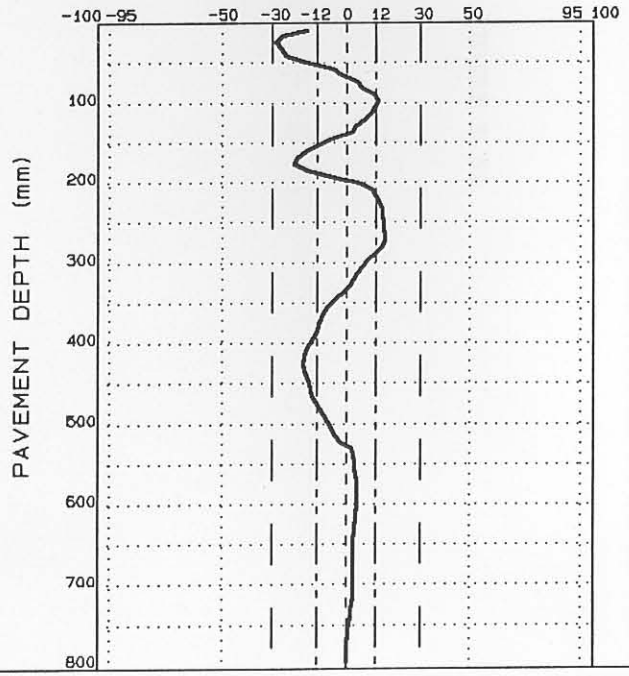

LAYER STRENGTH DIAGRAM (REDEFINED)

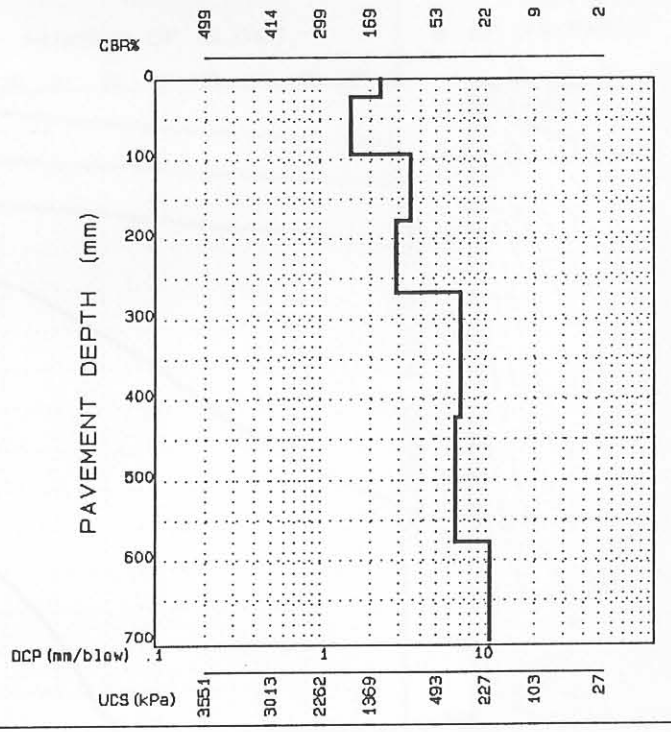

FIGURE E.51

RTT, CSIR, SA

SUMMARY OF DCP INVESTIGATION

DATA FILE :307A4, 20,60; N=2 450 000
REGION :BULTFONTEIN
ROAD NUMBER :2212
DISTANCE : 12.6
POSITION : L | X | | M | | | R
CONDITION : | FAILED | OVERSTRESSED | SOUND |
| RUT. | DEFORM. | PUMP. | CRACKS : BROCK. | LONG. | OTHER |
DATE :87/08/28

PAVEMENT CHARACTERISTICS

		DATA	B/CURVE
STRUCTURE NUMBER	:	442	
BALANCE NUMBER (BN 100)	:	34	41
DIFFERENCE IN BN100	:	-7	
BALANCE CURVE IS WHERE B =		37	A= 1984
STRUCT. CAP. (E80 X 10^6)	:	>10	
ROAD CATEGORY	:	C	
TRAFFIC : LIGHT TRAFFIC			

AVERAGE EQUIVALENT STRENGTH

FROM - TO	AV. PENETRATION	SD	80 P	CBR	UCS
0- 64	1.2	0.4	1.6	261	2007
65-152	0.7	0.2	0.9	361	2671
153-192	1.0	0.3	1.3	296	2242
193-408	3.5	1.2	4.5	83	732
409-800	6.6	3.2	9.3	37	359

CATEGORY V : AVERAGELY BALANCED DEEP STRUCTURE (ABD)

DCP CURVE

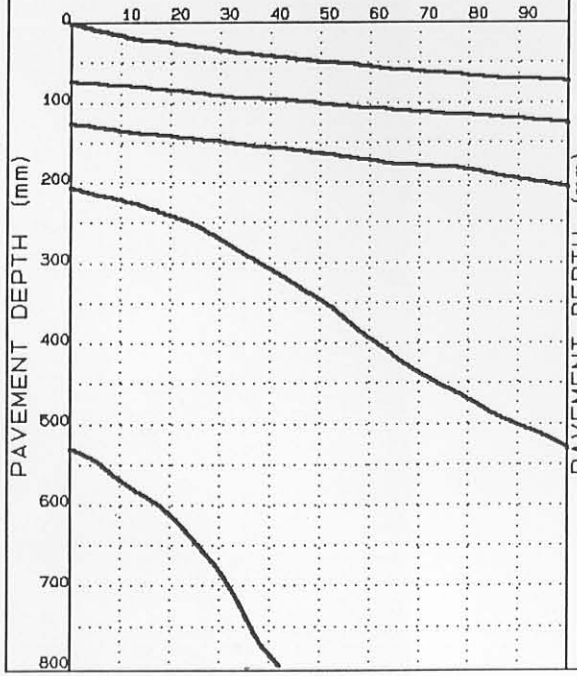

BALANCE CURVE

(DSN 800) (-90 ≤ B ≤ +90)

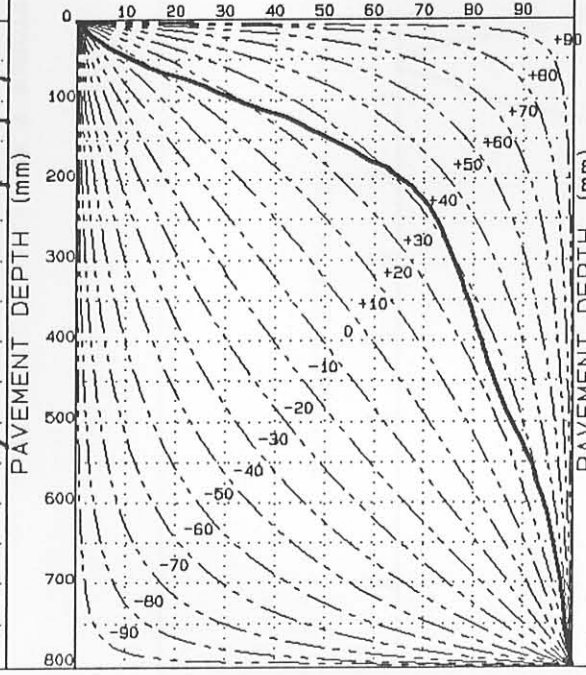

LAYER STRENGTH DIAGRAM

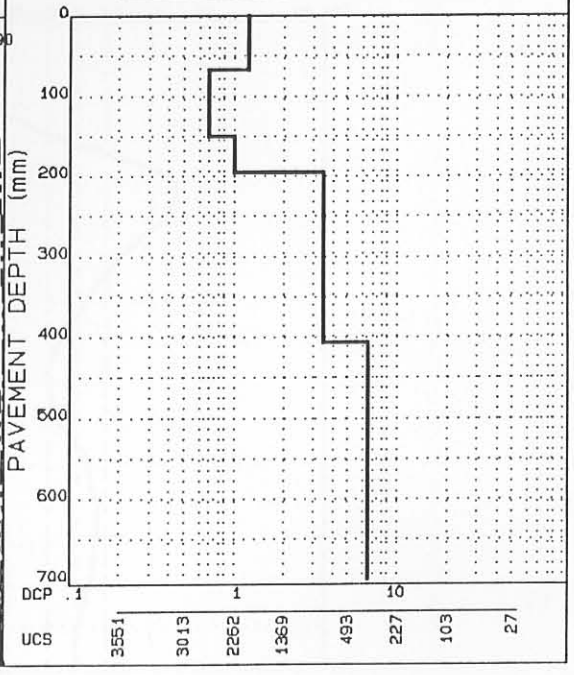

FIGURE E.52

ATT, CSIR, SA

SUMMARY OF DCP INVESTIGATION

AVERAGE EQUIVALENT STRENGTH (REDEFINED)

FROM - TO (mm)	AV. PENETRATION (mm/blow)	SD	BOP	CBR%	UCS (kPa)
0- 56	1.3	0.4	1.6	249	1926
57-216	0.9	0.4	1.2	322	2415
217-440	3.9	1.0	4.7	73	654
441-608	3.9	0.9	4.7	72	646
609-768	9.5	2.3	11.5	23	236
769-800	8.6	1.1	9.5	27	272

DATA FILE: 307A4, 2D, 6D; N=2 450 000

NORMALIZED CURVE

DEVIATION (A_i) FROM STANDARD PAVEMENT BALANCE CURVE (SPBC), %.mm

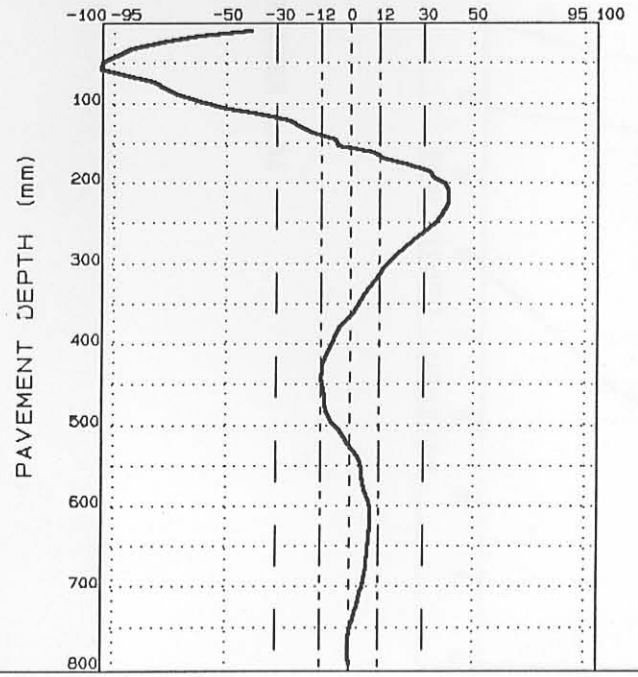

LAYER STRENGTH DIAGRAM (REDEFINED)

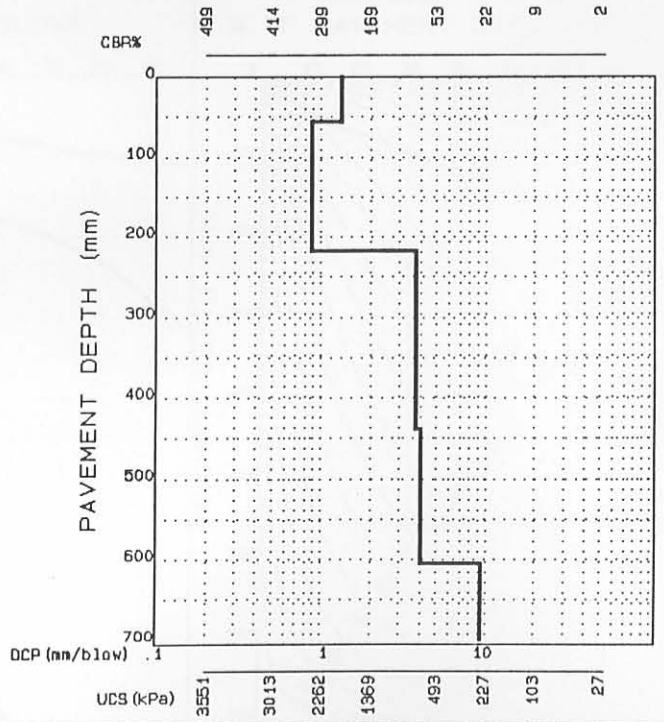

FIGURE E.53

ATT, CSIR, SA

SUMMARY OF DCP INVESTIGATION

DATA FILE :307A4, BN, 10N; N=2 450 000
REGION :BULTFONTEIN
ROAD NUMBER :2212-307
DISTANCE : 12.6
POSITION : L [X] M R
CONDITION : FAILED | OVERSTRESSED | SOUND
[X] SOIL | DEFORM | PUMP | CRACKS : BROCK | LONG | OTHER
DATE :87/08/28

PAVEMENT CHARACTERISTICS

	DATA	B/CURVE
STRUCTURE NUMBER :	263	
BALANCE NUMBER (BN 100) :	32	42
DIFFERENCE IN BN100 :	-10	
BALANCE CURVE IS WHERE B =	38 A= 1724	
STRUCT. CAP. (E80 X 10^6) :	8.85	
ROAD CATEGORY :	C	

TRAFFIC : LIGHT TRAFFIC

AVERAGE EQUIVALENT STRENGTH

FROM - TO	AV. PENETRATION	SD	80 P	CBR	UCS
0- 64	1.7	0.3	2.0	192	1532
65-152	1.0	0.2	1.2	303	2289
153-192	1.9	0.4	2.2	175	1419
193-408	4.7	1.0	5.6	58	534
409-800	11.4	5.6	16.0	18	190

CATEGORY V : AVERAGELY BALANCED DEEP STRUCTURE (ABD)

DCP CURVE

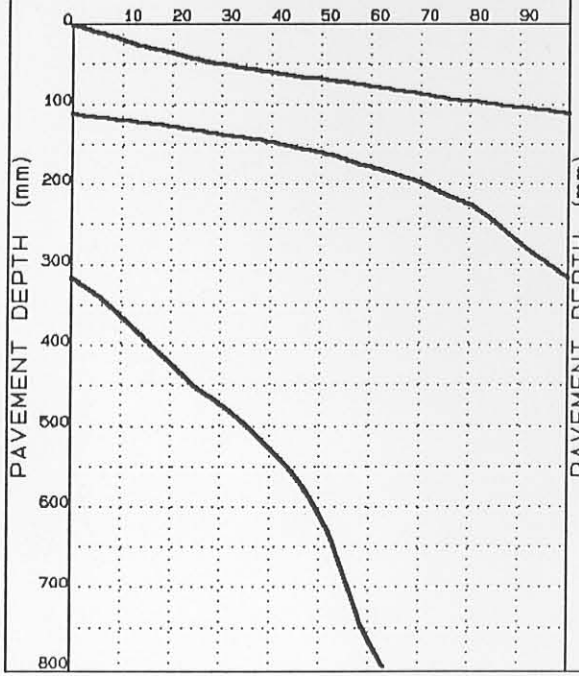

BALANCE CURVE

(DSN 800) (-90 ≤ B ≤ +90)
% OF PAVEMENT STRUCTURE NUMBER

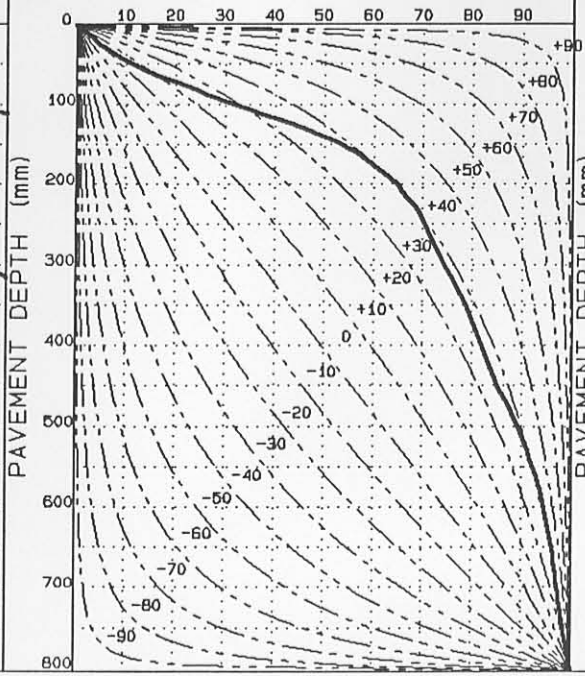

LAYER STRENGTH DIAGRAM

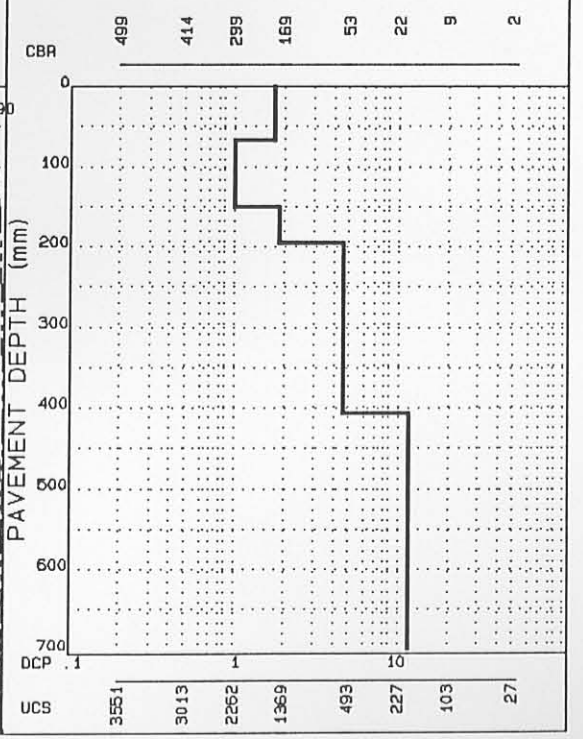

FIGURE E.54

RTT, CSIR, SA

SUMMARY OF DCP INVESTIGATION

AVERAGE EQUIVALENT STRENGTH (REDEFINED)

FROM - TO (mm)	AV. PENETRATION (mm/blow)	SD	BOP	CBR%	UCS (kPa)
0- 56	1.8	0.3	2.1	186	1490
57-192	1.3	0.5	1.7	250	1933
193-408	4.7	1.0	5.6	58	534
409-576	6.0	1.2	7.0	42	402
577-744	16.3	3.9	19.6	12	133
745-800	12.7	2.4	14.7	16	172

DATA FILE: 307A4, 8N, 10N; N=2 450 000

NORMALIZED CURVE

DEVIATION (A_i) FROM STANDARD PAVEMENT BALANCE CURVE (SPBC), %.mm

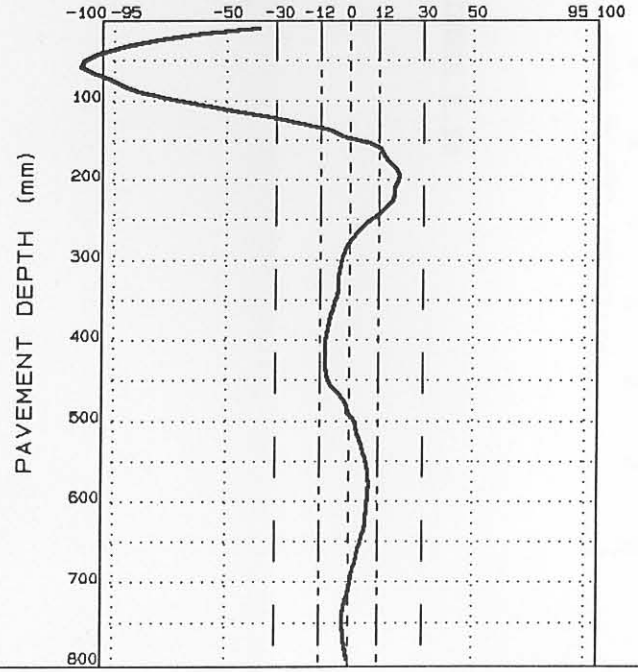

LAYER STRENGTH DIAGRAM (REDEFINED)

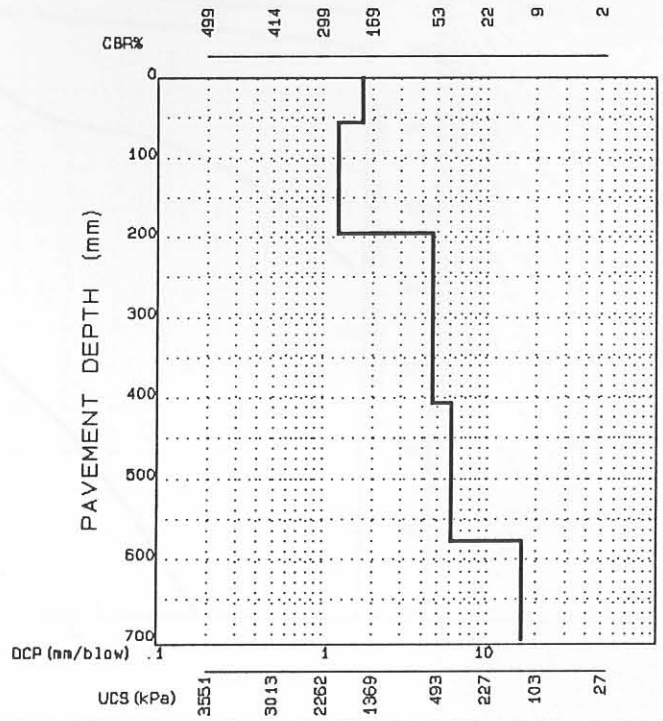

FIGURE E.55

RTT, CSIR, SA

SUMMARY OF DCP INVESTIGATION

DATA FILE :30BA4, B1B, B9B; N=10
REGION :BULTFONTEIN
ROAD NUMBER :P2212
DISTANCE : 12.6
POSITION : L | | | M | X | | R
CONDITION : | FAILED | OVERSTRESSED | SOUND |
| RUT. | DEFORM. | PUMP. | CRACKS : CROCK | LONG. | OTHER |
DATE :860324

PAVEMENT CHARACTERISTICS

	DATA	B/CURVE
STRUCTURE NUMBER :	367	
BALANCE NUMBER (BN 100) :	55	43
DIFFERENCE IN BN100 :	12	
BALANCE CURVE IS WHERE B =	39	A= 1709
STRUCT. CAP. (E80 X 10^6) :	>10	
ROAD CATEGORY :	C	
TRAFFIC : LIGHT TRAFFIC		

FROM - TO
0- 80
81-184
185-208
209-400
401-800

AVERAGE EQUIVALENT STRENGTH

AV. PENETRATION	SD	80 P	CBR	UCS
0.8	0.4	1.1	341	2540
3.4	1.0	4.3	86	755
1.4	0.4	1.7	233	1817
4.8	1.7	6.2	56	518
7.2	1.8	8.7	33	325

CATEGORY V : AVERAGELY BALANCED DEEP STRUCTURE (ABD)

DCP CURVE

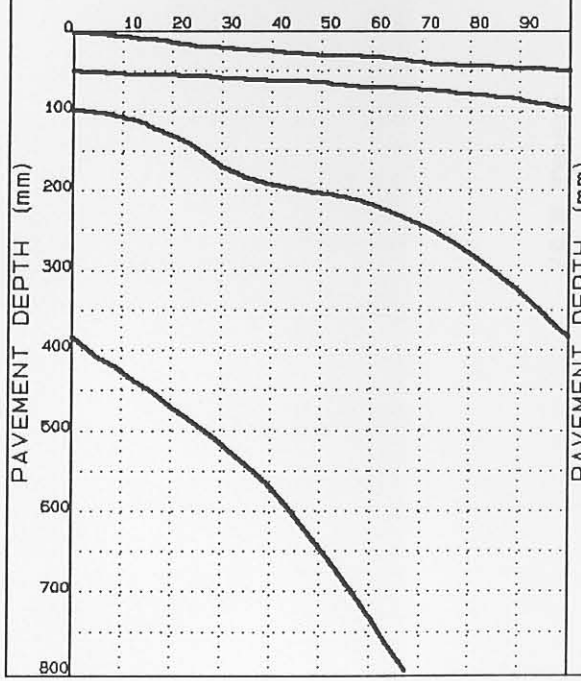

BALANCE CURVE

(DSN 800) (-90 ≤ B ≤ +90)
% OF PAVEMENT STRUCTURE NUMBER

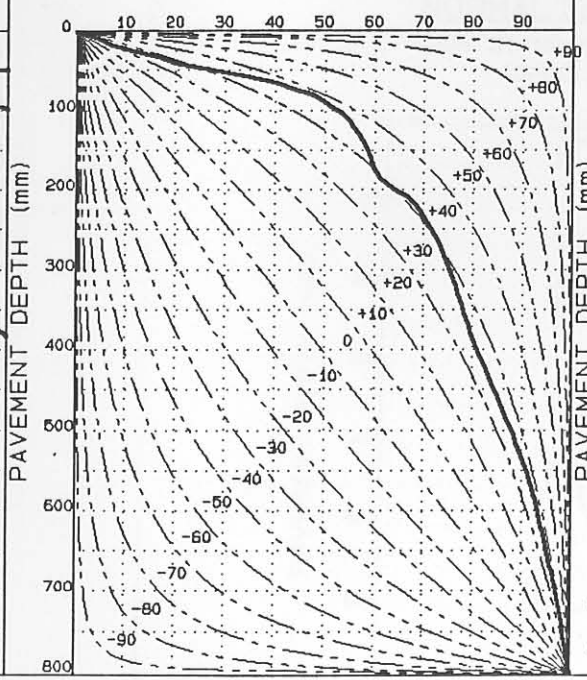

LAYER STRENGTH DIAGRAM

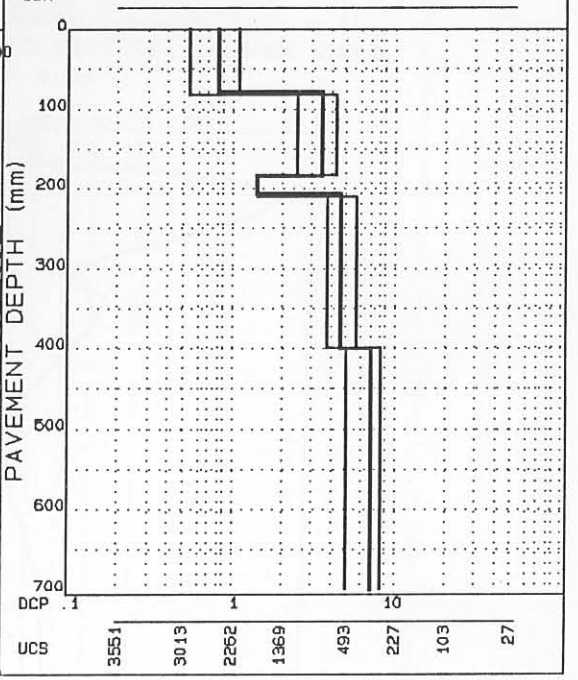

FIGURE E.56

ATT, CSIR, SA

SUMMARY OF DCP INVESTIGATION

AVERAGE EQUIVALENT STRENGTH (REDEFINED)

FROM - TO (mm)	AV. PENETRATION (mm/blow)	SD	BOP	CBR%	UCS (kPa)
0- 16	0.8	0.3	1.1	331	2474
17- 80	0.8	0.4	1.1	343	2553
81-184	3.4	1.0	4.3	86	755
185-216	1.5	0.4	1.8	219	1720
217-400	4.9	1.6	6.3	54	501
401-600	7.2	1.8	8.7	33	325

DATA FILE: 308A4, 81B, 89B; N=10

NORMALIZED CURVE

DEVIATION (A_i) FROM STANDARD PAVEMENT BALANCE CURVE (SPBC), %.mm

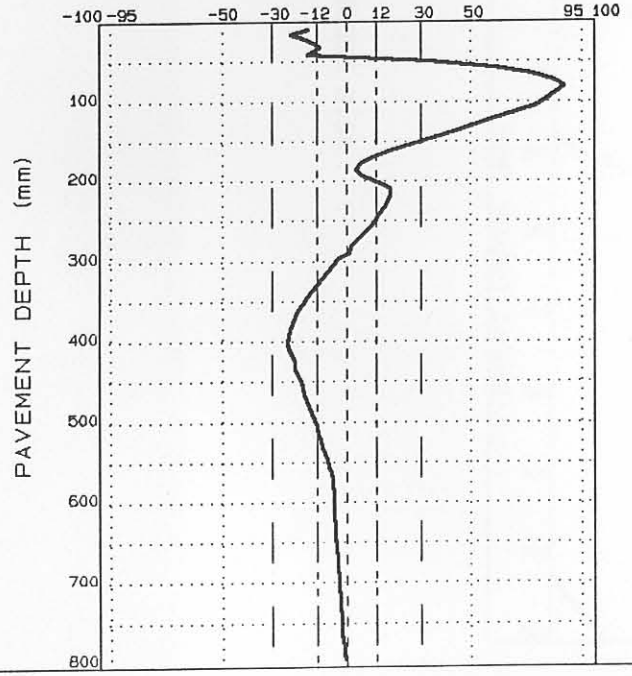

LAYER STRENGTH DIAGRAM (REDEFINED)

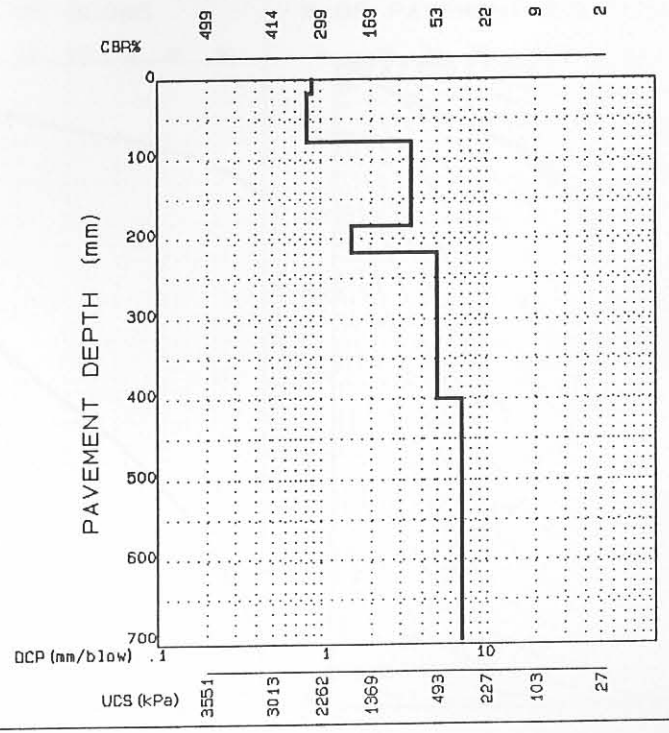

FIGURE E.57

RTT, CSIR, SA

SUMMARY OF DCP INVESTIGATION

DATA FILE :30BA4, 5CL, 11CL; N=1 000 000
REGION :BULTFONTEIN
ROAD NUMBER :2212
DISTANCE : 12.0
POSITION : L | X | | M | | | | R
CONDITION : | FAILED | OVERSTRESSED | SOUND |
| EXT. | DEFORM. | PUMP. | CRACKS : BROCK | LONG. | OTHER |
DATE :87/11/13

PAVEMENT CHARACTERISTICS

	DATA	B/CURVE
STRUCTURE NUMBER :	211	
BALANCE NUMBER (BN 100) :	35	31
DIFFERENCE IN BN100 :	4	
BALANCE CURVE IS WHERE B =	27 A= 1311	
STRUCT. CAP. (E80 X 10^6) :	4.09	
ROAD CATEGORY :	C	

TRAFFIC : LIGHT TRAFFIC

AVERAGE EQUIVALENT STRENGTH

FROM - TO	AV. PENETRATION	SD	80 P	CBR	UCS
0- 16	1.5	0.3	1.7	223	1748
17- 80	1.8	0.5	2.2	189	1511
81-184	3.1	1.4	4.3	97	840
185-208	3.6	0.3	3.8	80	709
209-400	6.3	2.3	8.2	40	385
401-800	8.2	2.4	10.2	28	281

CATEGORY IV : WELL-BALANCED DEEP STRUCTURE (WBD)

DCP CURVE

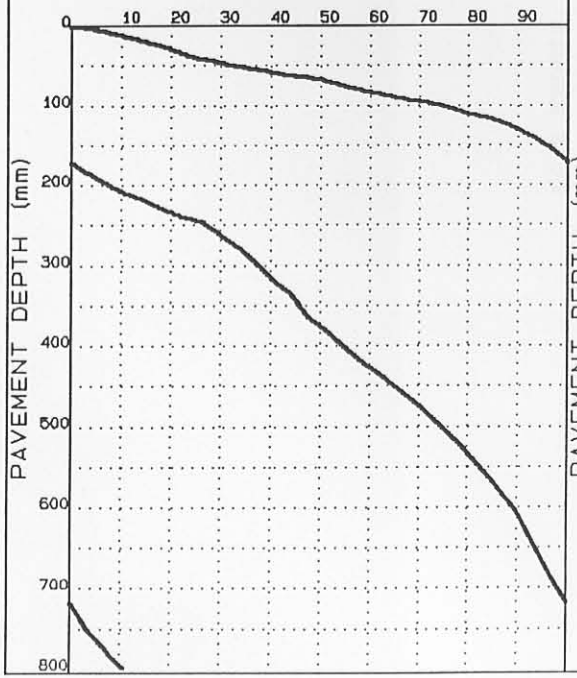

BALANCE CURVE

(DSN 800) (-90 ≤ B ≤ +90)
% OF PAVEMENT STRUCTURE NUMBER

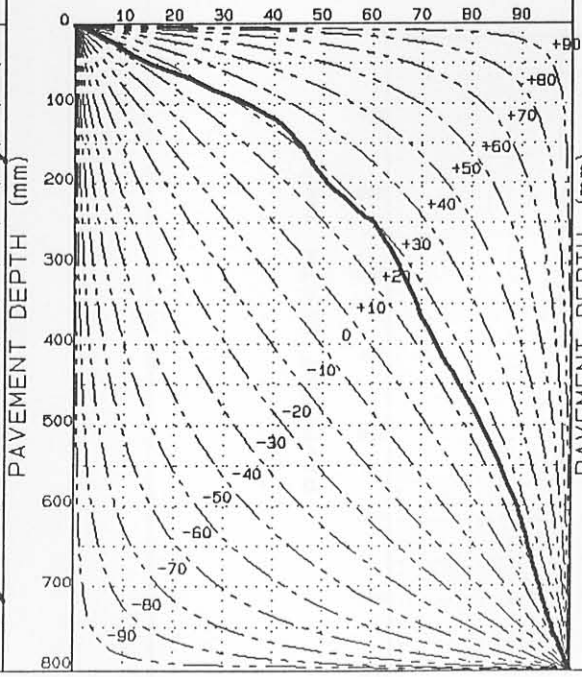

LAYER STRENGTH DIAGRAM

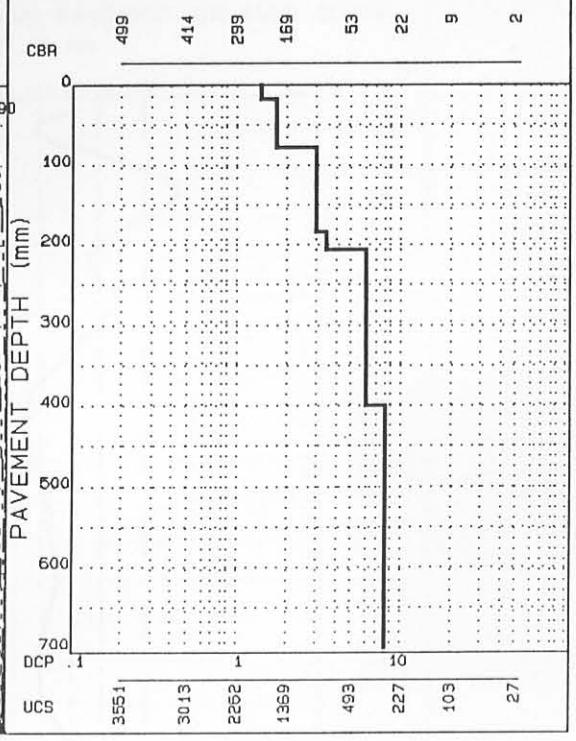

FIGURE E.58

RTT, CSIR, SA

SUMMARY OF DCP INVESTIGATION

AVERAGE EQUIVALENT STRENGTH (REDEFINED)

FROM - TO (mm)	AV. PENETRATION (mm/blow)	SD	BOP	CBR%	UCS (kPa)
0- 8	1.2	0.2	1.4	257	1980
9- 40	2.1	0.3	2.4	160	1305
41-120	1.6	0.4	1.8	211	1665
121-200	4.0	0.9	4.7	71	638
201-248	3.0	0.5	3.4	102	878
249-408	7.1	1.6	8.4	34	334
409-600	6.3	1.1	7.3	39	376
601-704	11.3	1.0	12.2	19	200
705-800	8.7	1.4	9.9	26	263

DATA FILE: 308A4, 5CL, 11CL; N=1 000 000

NORMALIZED CURVE

DEVIATION (A_i) FROM STANDARD PAVEMENT BALANCE CURVE (SPBC), %.mm

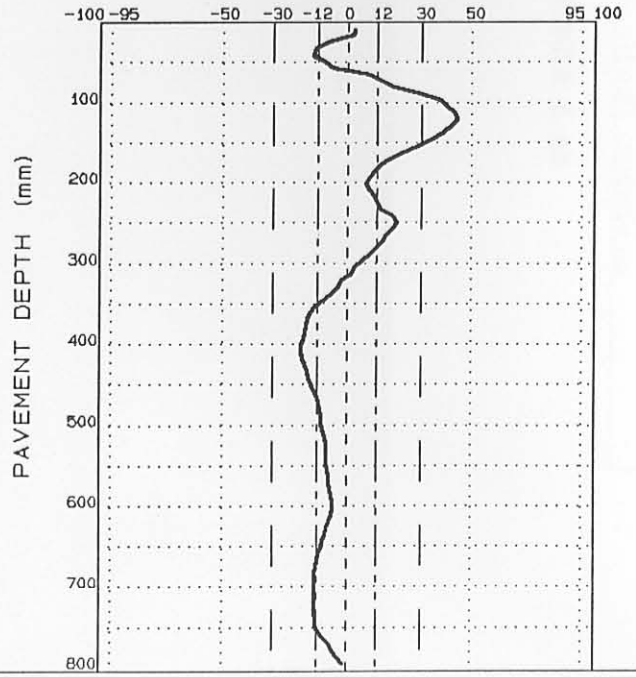

LAYER STRENGTH DIAGRAM (REDEFINED)

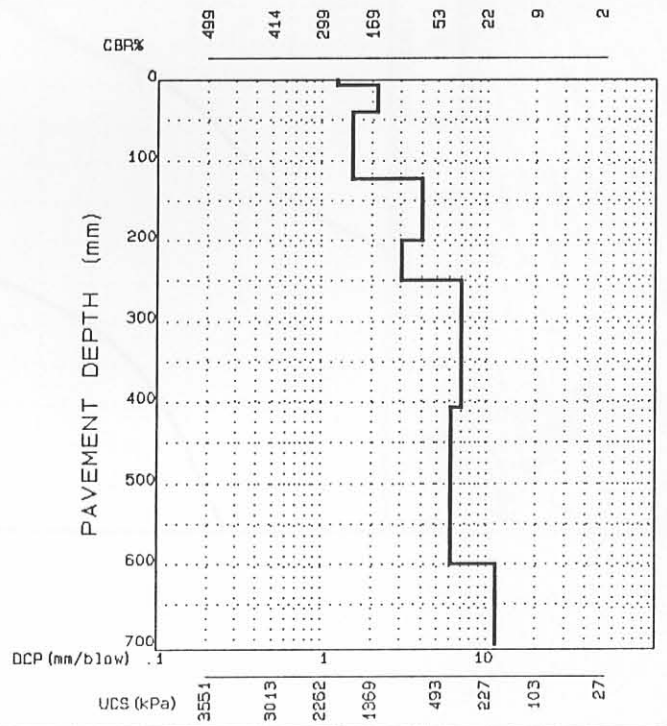

FIGURE E.59

DIVISION OF ROADS AND TRANSPORT TECHNOLOGY — ATT, CSIR, SA

SUMMARY OF DCP INVESTIGATION

DATA FILE :308A4, 8B, 8C; N=2 460 000
REGION :BULTFONTEIN TVL
ROAD NUMBER :P2212
DISTANCE : 12.0
POSITION : L [X] M R
CONDITION : FAILED | OVERSTRESSED | SOUND
[X] RUT. | DEFORM. | PUMP. | CRACKS : [X] BROCK | [X] LONG. | OTHER
DATE :88/09/14

PAVEMENT CHARACTERISTICS

	DATA	B/CURVE
STRUCTURE NUMBER :	267	
BALANCE NUMBER (BN 100) :	37	31
DIFFERENCE IN BN100 :	6	
BALANCE CURVE IS WHERE B =	27 A= 2304	
STRUCT. CAP. (E80 X 10^6) :	9.33	
ROAD CATEGORY :	B	

TRAFFIC : LIGHT TRAFFIC

CATEGORY V : AVERAGELY BALANCED DEEP STRUCTURE (ABD)

AVERAGE EQUIVALENT STRENGTH

FROM - TO	AV. PENETRATION	SD	90 P	CBR	UCS
0- 16	1.3	0.4	1.7	252	1946
17- 80	1.2	0.4	1.7	257	1980
81-184	3.2	0.6	3.9	94	817
185-208	3.2	0.2	3.5	94	817
209-400	5.3	1.5	7.2	49	460
401-800	7.6	4.3	13.1	31	307

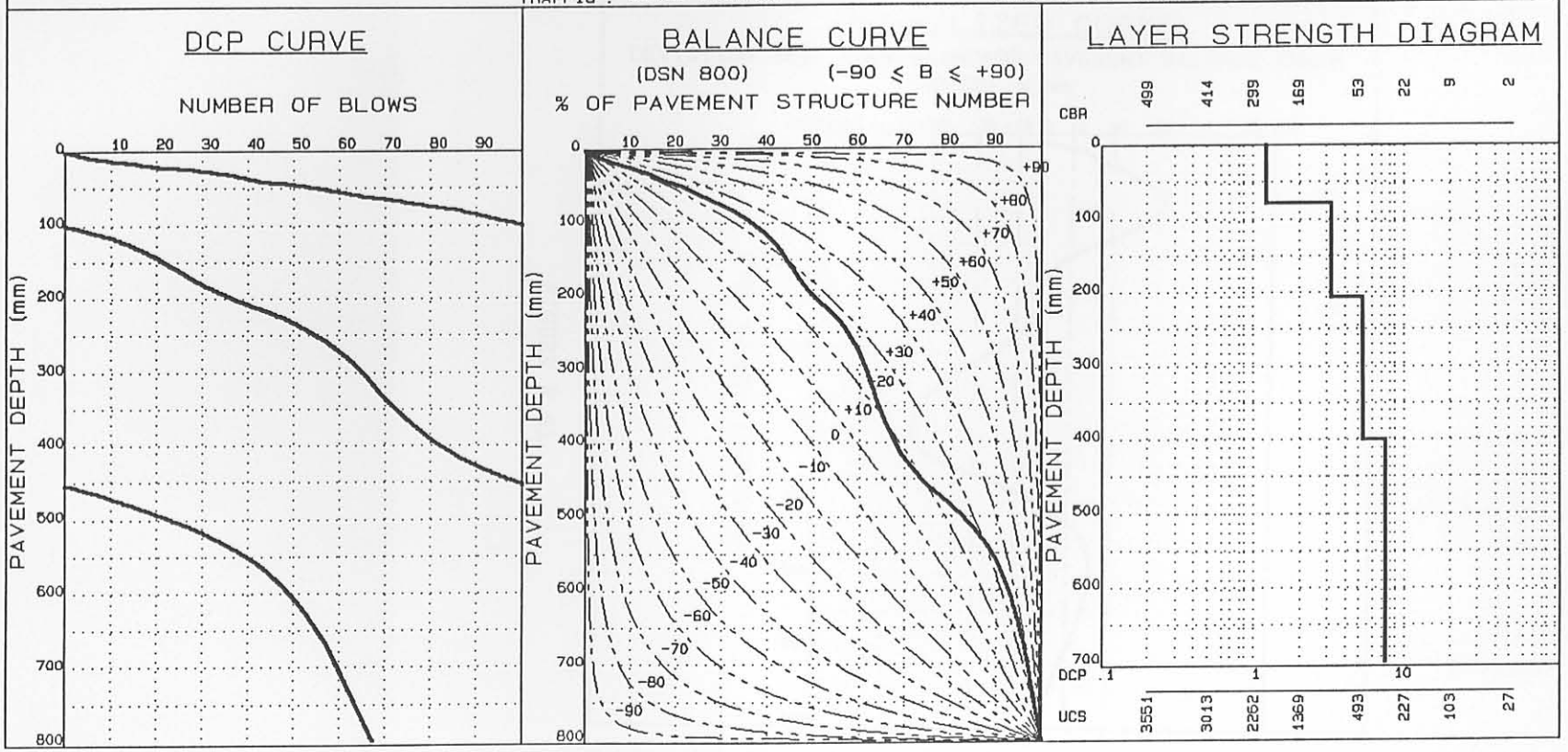

FIGURE E.60

DIVISION OF ROADS AND TANSPORT TECHNOLOGY

RTT, CSIR, SA

SUMMARY OF DCP INVESTIGATION

AVERAGE EQUIVALENT STRENGTH (REDEFINED)

FROM - TO (mm)	AV. PENETRATION (mm/blow)	SD	90P	CBR%	UCS (kPa)
0- 8	1.6	0.1		208	1644
9- 80	1.2	0.4		262	2014
81-200	3.2	0.6		94	817
201-224	2.7	0.2		113	961
225-400	5.5	1.4		47	444
401-564	3.4	1.1		86	755
565-800	11.1	2.6		19	200

DATA FILE: 308A4, 8B, 8C; N=2 460 000

NORMALIZED CURVE

DEVIATION (A_i) FROM STANDARD PAVEMENT BALANCE CURVE (SPBC), %.mm

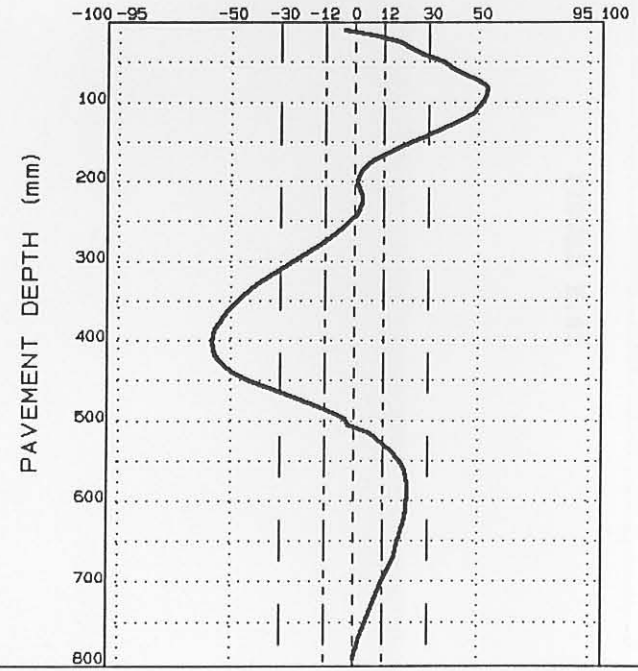

LAYER STRENGTH DIAGRAM (REDEFINED)

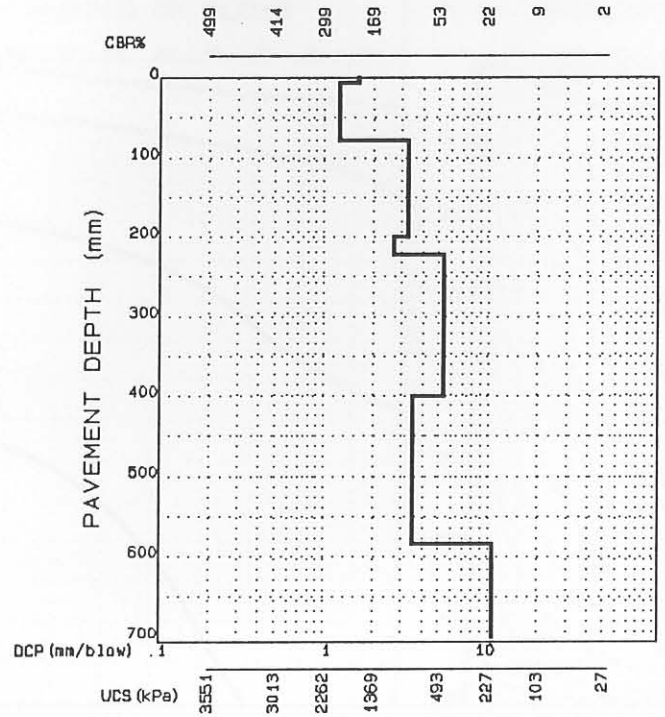

FIGURE E.61

DIVISION OF ROADS AND TRANSPORT TECHNOLOGY — ATT, CSIR, SA

SUMMARY OF DCP INVESTIGATION

DATA FILE :30BA4, 10C; N=2 460 000
REGION :BULTFONTEIN TVL
ROAD NUMBER :P2212
DISTANCE : 12.0
POSITION : L X M R
CONDITION : FAILED OVERSTRESSED SOUND
DEF. DEFORM. PUMP. CRACKS : CROCK. LONG. OTHER
DATE :88/09/14

PAVEMENT CHARACTERISTICS

	DATA	B/CURVE
STRUCTURE NUMBER :	369	
BALANCE NUMBER (BN 100) :	43	40
DIFFERENCE IN BN100 :	3	
BALANCE CURVE IS WHERE B =	36 A= 1218	
STRUCT. CAP. (E80 X 10^6) :	28.95	
ROAD CATEGORY :	B	

TRAFFIC : LIGHT TRAFFIC

AVERAGE EQUIVALENT STRENGTH

FROM - TO	AV. PENETRATION	SD	90 P	CBR	UCS
0- 16	0.7	0.2	1.0	372	2742
17- 80	0.7	0.2	0.9	373	2749
81-184	2.0	0.9	3.1	171	1383
185-208	1.4	0.2	1.7	228	1782
209-400	3.7	1.4	5.6	77	685
401-800	6.7	3.2	10.8	37	359

CATEGORY IV : WELL-BALANCED DEEP STRUCTURE (WBD)

DCP CURVE

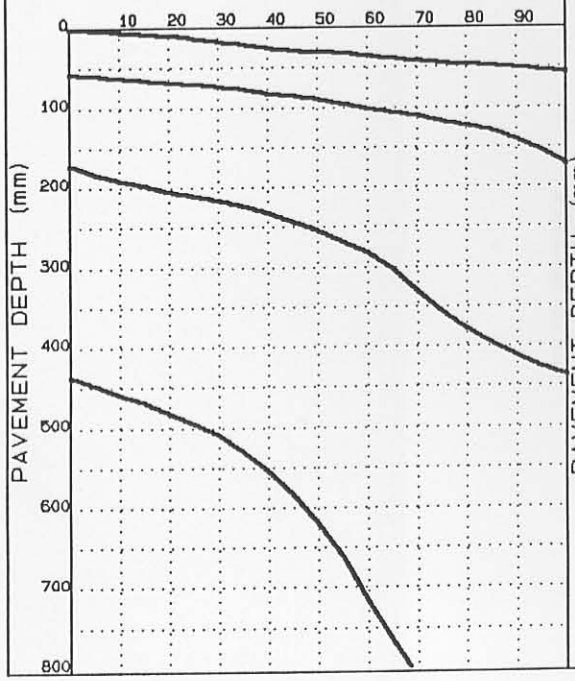

BALANCE CURVE

(DSN 800) (-90 ≤ B ≤ +90)

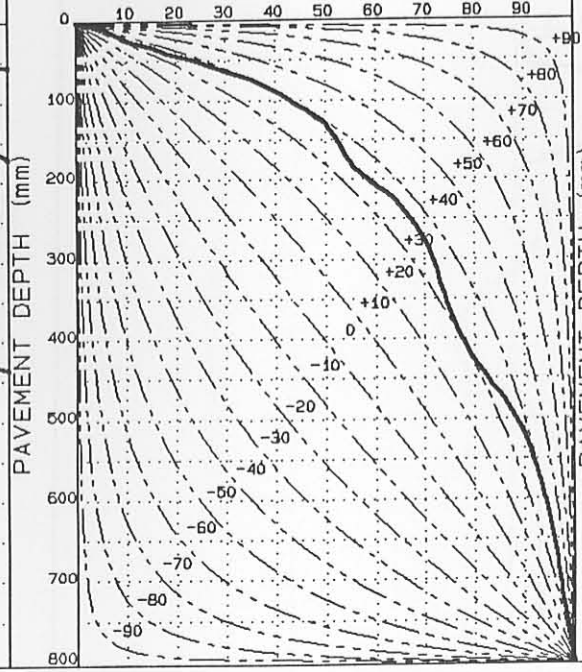

LAYER STRENGTH DIAGRAM

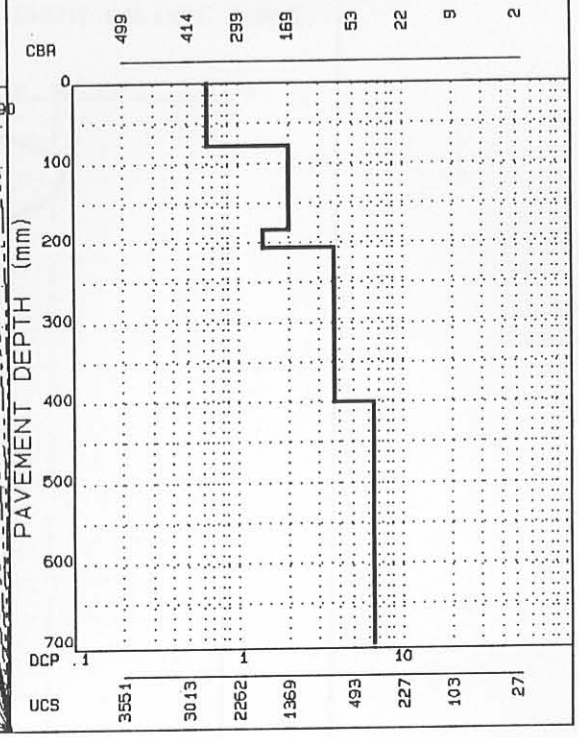

FIGURE E.62

DIVISION OF ROADS AND TANSPORT TECHNOLOGY

RTT, CSIR, SA

SUMMARY OF DCP INVESTIGATION

AVERAGE EQUIVALENT STRENGTH (REDEFINED)

FROM - TO (mm)	AV. PENETRATION (mm/blow)	SD	90P	CBR%	UCS (kPa)
0- 8	0.4	0.1		431	3121
9- 16	0.9	0.0		320	2402
17- 88	0.7	0.2		368	2716
89-184	2.1	0.9		161	1312
185-224	1.4	0.2		235	1830
225-384	4.0	1.3		70	630
385-576	3.5	1.2		85	748
577-768	9.2	1.6		24	245
769-800	9.2	0.0		24	245

DATA FILE: 308A4, 10C; N=2 460 000

NORMALIZED CURVE

DEVIATION (A_i) FROM STANDARD PAVEMENT BALANCE CURVE (SPBC), %.mm

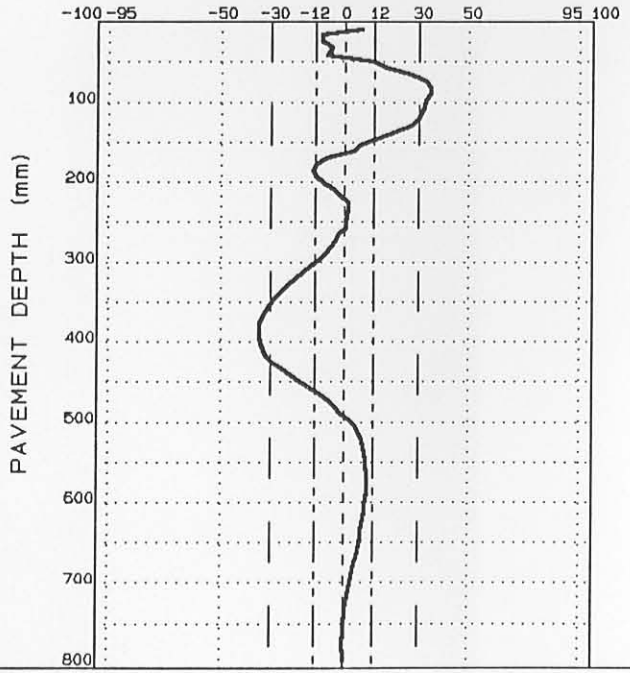

LAYER STRENGTH DIAGRAM (REDEFINED)

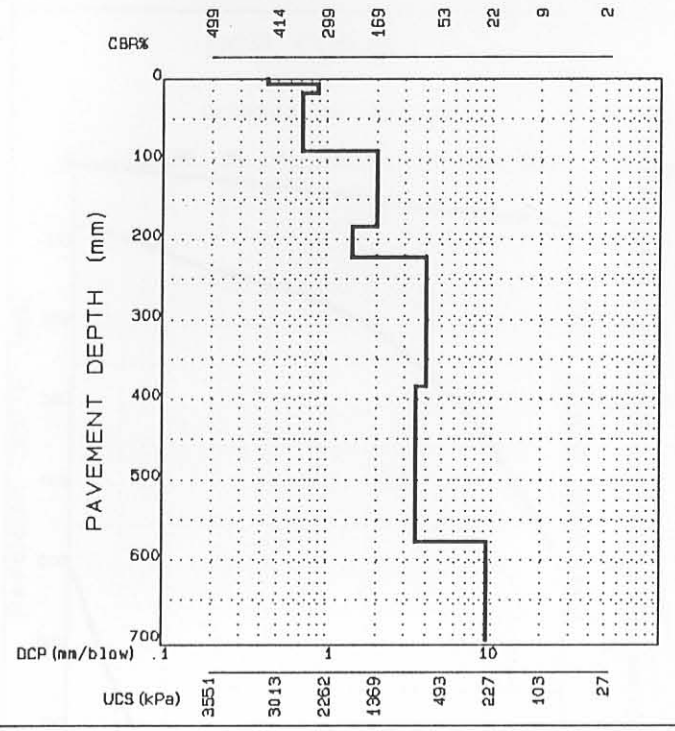

FIGURE E.63

RTT, CSIR, SA

SUMMARY OF DCP INVESTIGATION

DATA FILE :309A4, 105C, 105A, 113; N=10
REGION :BULTFONTEIN
ROAD NUMBER :P2212
DISTANCE : 12.6
POSITION : L | M | R
CONDITION : FAILED | OVERSTRESSED | SOUND
RUT. | DEFORM. | PUMP. | CRACKS : CROCK | LONG. | OTHER
DATE :860307

PAVEMENT CHARACTERISTICS

	DATA	B/CURVE
STRUCTURE NUMBER :	219	
BALANCE NUMBER (BN 100) :	52	52
DIFFERENCE IN BN100 :	0	
BALANCE CURVE IS WHERE B =	46 A=	946
STRUCT. CAP. (E80 X 10^6) :	9.95	
ROAD CATEGORY :	C	

TRAFFIC : LIGHT TRAFFIC

AVERAGE EQUIVALENT STRENGTH

FROM - TO	AV. PENETRATION	SD	80 P	CBR	UCS
0- 64	1.1	0.2	1.3	277	2115
65-120	2.1	0.4	2.4	159	1298
121-192	2.6	0.6	3.1	120	1013
193-456	9.6	2.2	11.4	23	236
457-800	20.4	3.9	23.7	9	103

CATEGORY I : WELL-BALANCED SHALLOW STRUCTURE (WBS)

DCP CURVE

NUMBER OF BLOWS

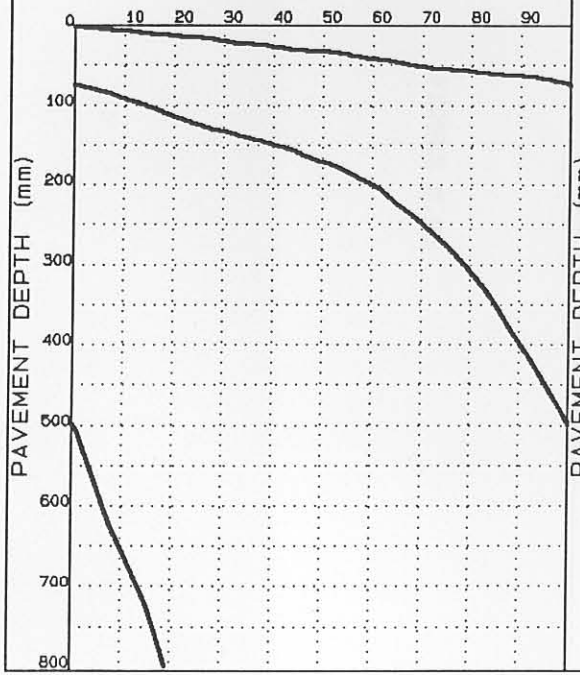

BALANCE CURVE

(DSN 800) (−90 ≤ B ≤ +90)
% OF PAVEMENT STRUCTURE NUMBER

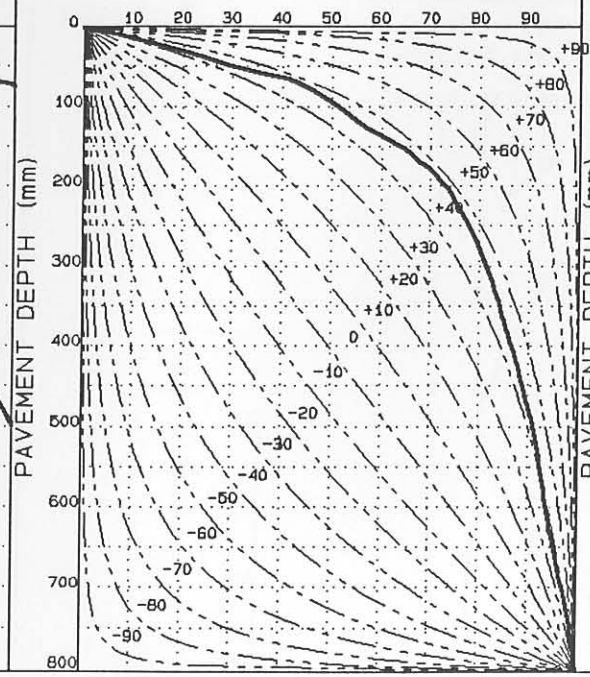

LAYER STRENGTH DIAGRAM

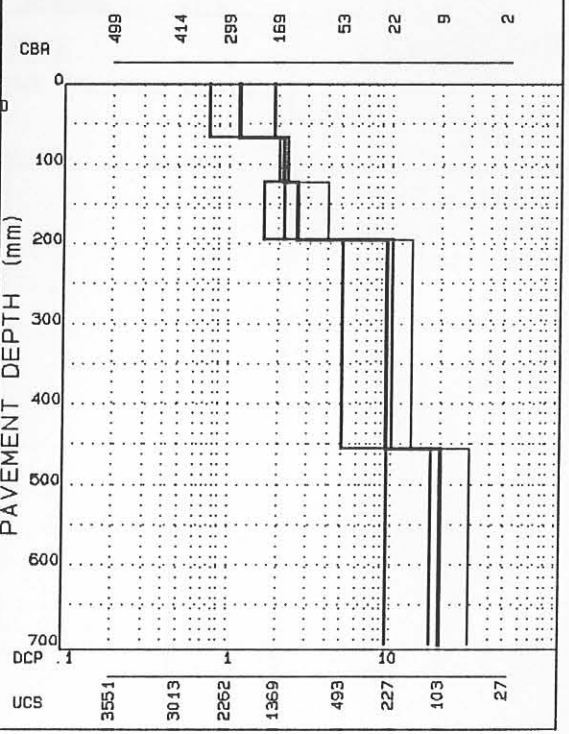

FIGURE E.64

RTT, CSIR, SA

SUMMARY OF DCP INVESTIGATION

AVERAGE EQUIVALENT STRENGTH (REDEFINED)

FROM - TO (mm)	AV. PENETRATION (mm/blow)	SD	BOP	CBR%	UCS (kPa)
0- 40	1.1	0.2	1.3	287	2182
41- 64	1.2	0.2	1.3	262	2014
65-120	2.1	0.4	2.4	159	1298
121-192	2.6	0.6	3.1	120	1013
193-400	9.1	2.1	10.8	25	254
401-416	9.9	0.8	10.6	22	227
417-456	12.0	1.0	12.8	17	181
457-504	12.2	0.5	12.6	17	181
505-608	22.7	2.5	24.8	7	83
609-800	21.3	1.9	22.8	8	93

DATA FILE: 309A4, 105C, 105A, 113; N=10

NORMALIZED CURVE

DEVIATION (A_i) FROM STANDARD PAVEMENT BALANCE CURVE (SPBC), %.mm

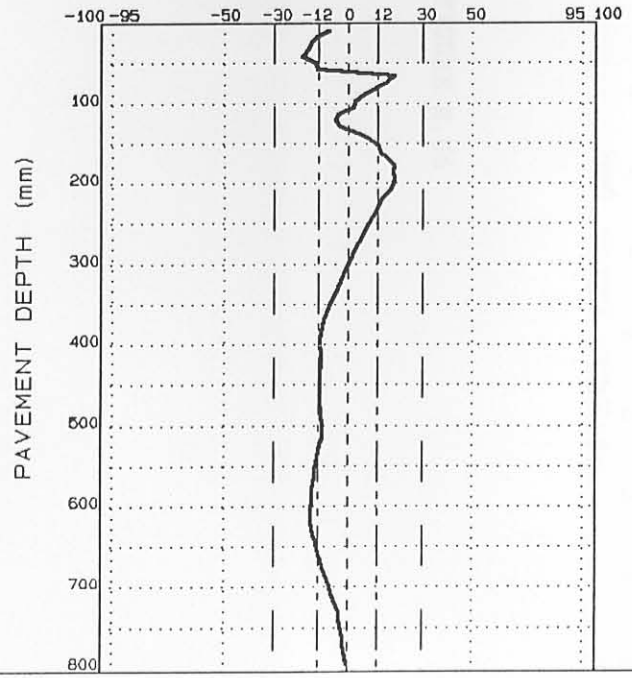

LAYER STRENGTH DIAGRAM (REDEFINED)

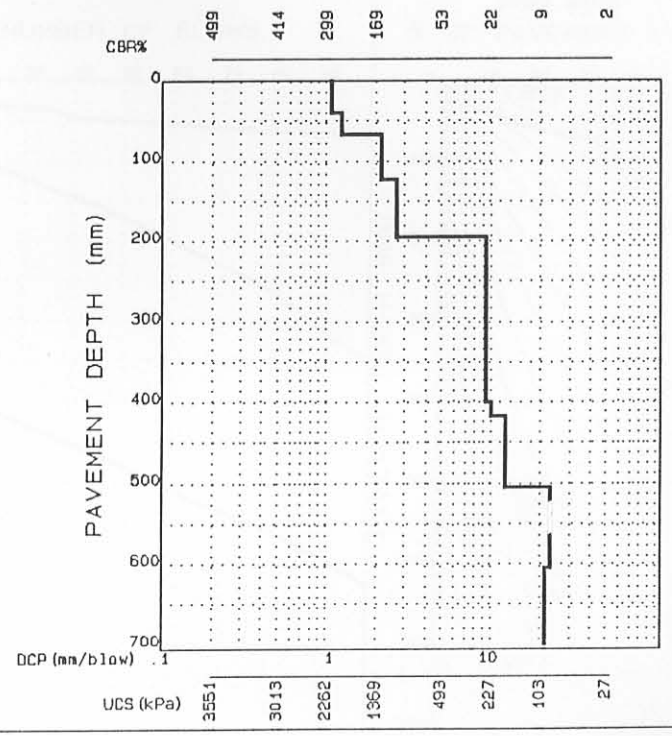

FIGURE E.65

RTT, CSIR, SA

SUMMARY OF DCP INVESTIGATION

DATA FILE :309A4,C; N=19 000
REGION :BULTFONTEIN
ROAD NUMBER :P2212
DISTANCE : 12.0
POSITION : L [X] M R
CONDITION : FAILED ~~OVERSTRESSED~~ SOUND
~~DEF.~~ DEFORM. PUMP. CRACKS : CROCK. ~~LONG.~~ OTHER
DATE :88/05/16

PAVEMENT CHARACTERISTICS

	DATA	B/CURVE
STRUCTURE NUMBER :	320	
BALANCE NUMBER (BN 100) :	38	29
DIFFERENCE IN BN100 :	9	
BALANCE CURVE IS WHERE B =	25	A= 2484
STRUCT. CAP. (E80 X 10^6) :	>10	
ROAD CATEGORY :	A	
TRAFFIC : LIGHT TRAFFIC		

AVERAGE EQUIVALENT STRENGTH

FROM - TO	AV. PENETRATION	SD	95 P	CBR	UCS
0- 40	1.5	0.7	2.6	224	1755
41- 64	0.7	0.6	1.7	360	2664
65-120	1.8	0.7	3.0	184	1476
121-192	2.6	0.3	3.2	119	1005
193-456	3.3	0.8	4.6	89	779
457-800	6.2	3.6	12.1	40	385

CATEGORY V : AVERAGELY BALANCED DEEP STRUCTURE (ABD)

DCP CURVE

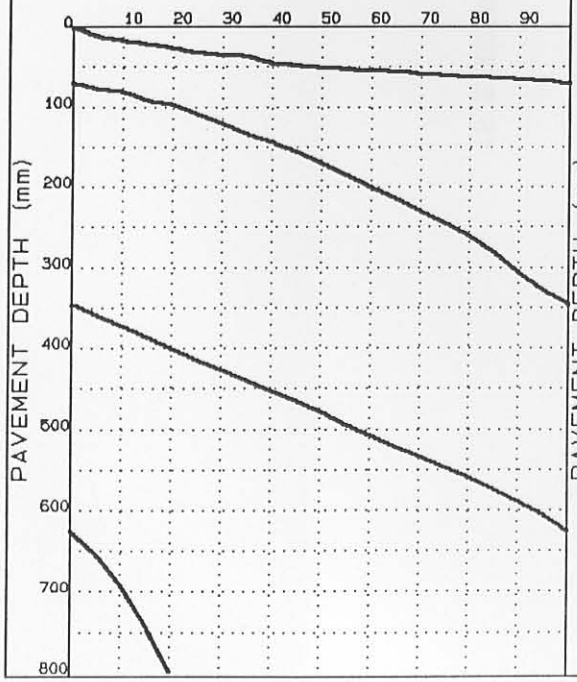

BALANCE CURVE

(DSN 800) (-90 ≤ B ≤ +90)
% OF PAVEMENT STRUCTURE NUMBER

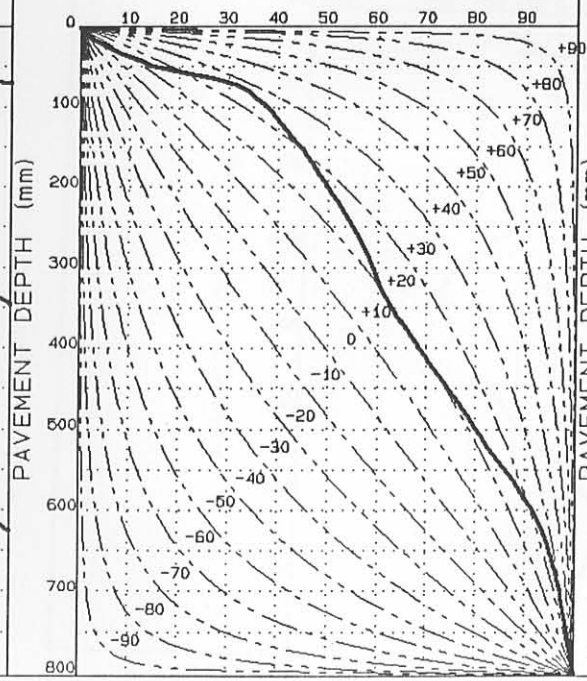

LAYER STRENGTH DIAGRAM

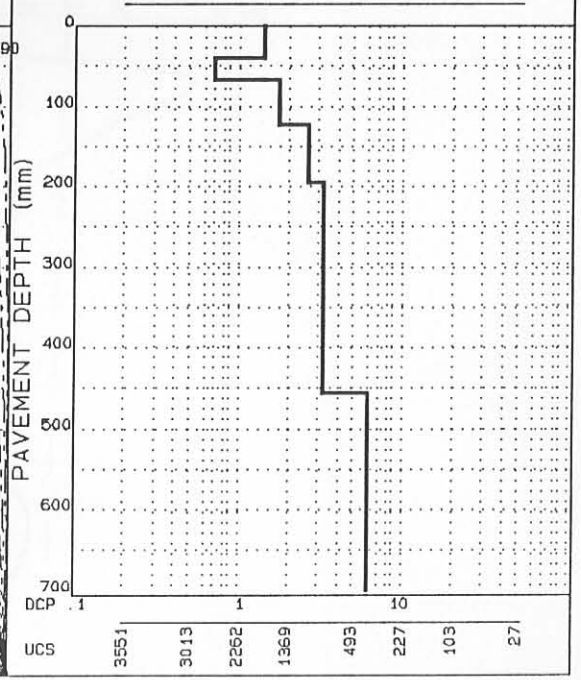

FIGURE E.66

RTT, CSIR, SA

SUMMARY OF DCP INVESTIGATION

AVERAGE EQUIVALENT STRENGTH (REDEFINED)

FROM - TO (mm)	AV. PENETRATION (mm/blow)	SD	95P	CBR%	UCS (kPa)
0- 24	1.7	0.8		198	1574
25- 72	0.9	0.6		326	2441
73-352	3.1	1.0		95	825
353-624	2.9	0.4		108	923
625-800	9.3	2.3		24	245

DATA FILE: 309A4, C; N=19 000

NORMALIZED CURVE

DEVIATION (A_i) FROM STANDARD PAVEMENT BALANCE CURVE (SPBC), %.mm

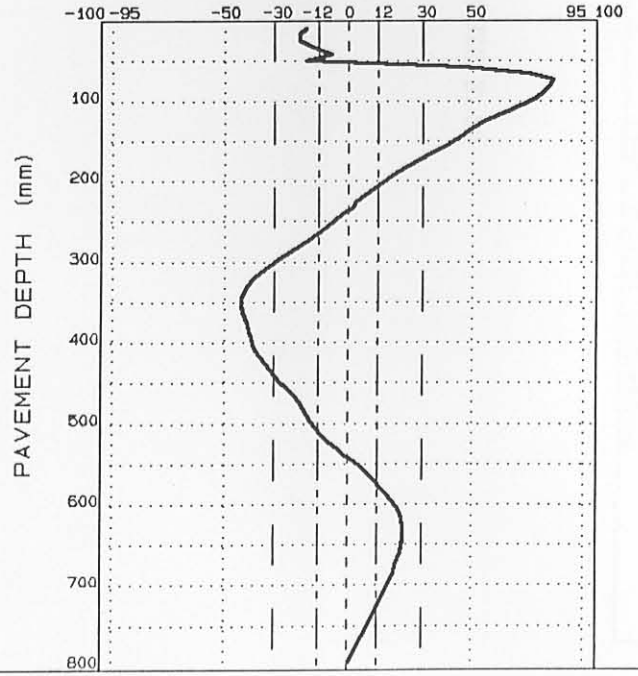

LAYER STRENGTH DIAGRAM (REDEFINED)

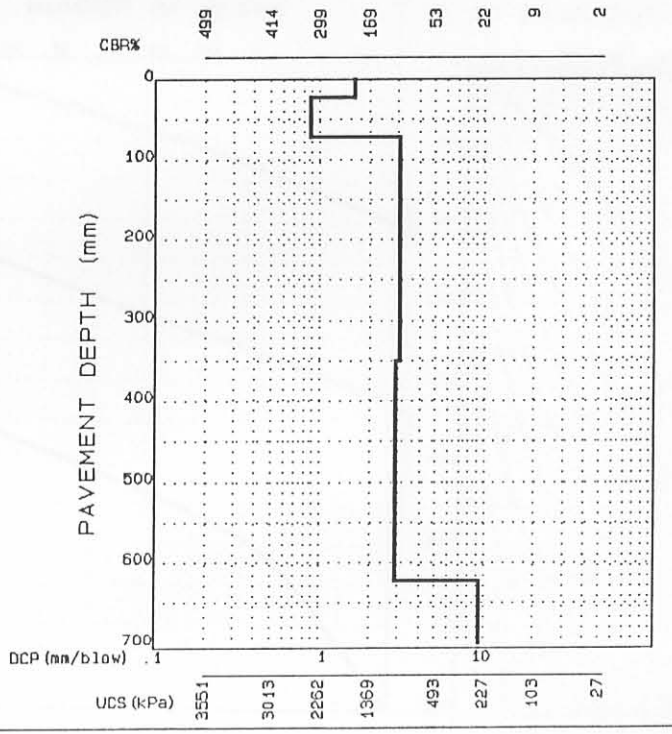

FIGURE E.67

RTT, CSIR, SA

SUMMARY OF DCP INVESTIGATION

DATA FILE :309A4, FINAL; N=46 000
REGION :BULTFONTEIN TVL
ROAD NUMBER :P2212
DISTANCE : 12.0
POSITION : L X M R
CONDITION : FAILED OVERSTRESSED SOUND
BOG. DEFORM. PUMP. CRACKS : BROCK LONG. OTHER
DATE :88/09/13

PAVEMENT CHARACTERISTICS

	DATA	B/CURVE
STRUCTURE NUMBER :	300	
BALANCE NUMBER (BN 100) :	19	19
DIFFERENCE IN BN100 :	0	
BALANCE CURVE IS WHERE B =	12	A= 2327
STRUCT. CAP. (E80 X 10^6) :	>10	
ROAD CATEGORY :	B	
TRAFFIC : LIGHT TRAFFIC		

FROM - TO
0- 40
41- 64
65-120
121-192
193-456
457-800

AVERAGE EQUIVALENT STRENGTH

AV. PENETRATION	SD	90 P	CBR	UCS
2.0	0.1	2.1	171	1383
1.9	0.1	2.0	178	1433
2.0	0.2	2.2	171	1383
2.5	0.1	2.6	130	1087
2.3	0.2	2.6	139	1153
5.6	2.6	8.9	46	435

CATEGORY V : AVERAGELY BALANCED DEEP STRUCTURE (ABD)

DCP CURVE

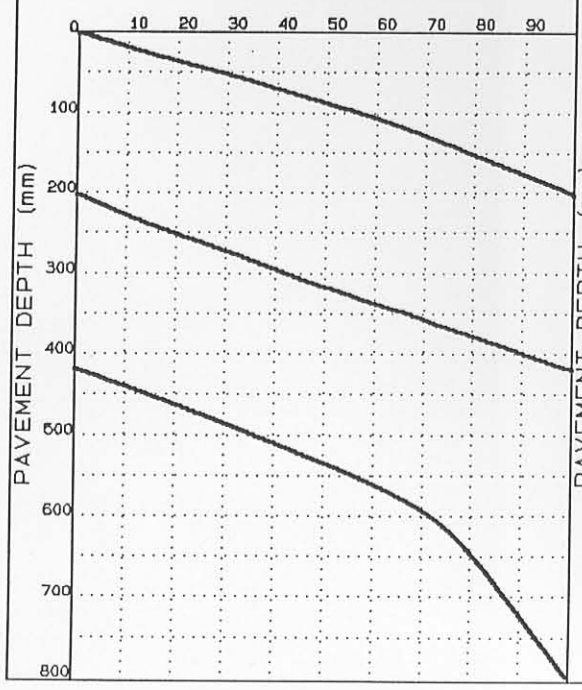

BALANCE CURVE

(DSN 800) (-90 ≤ B ≤ +90)
% OF PAVEMENT STRUCTURE NUMBER

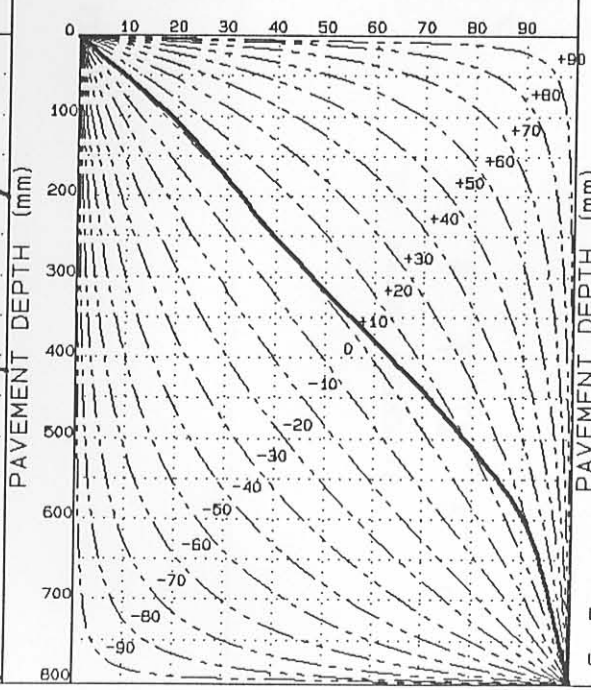

LAYER STRENGTH DIAGRAM

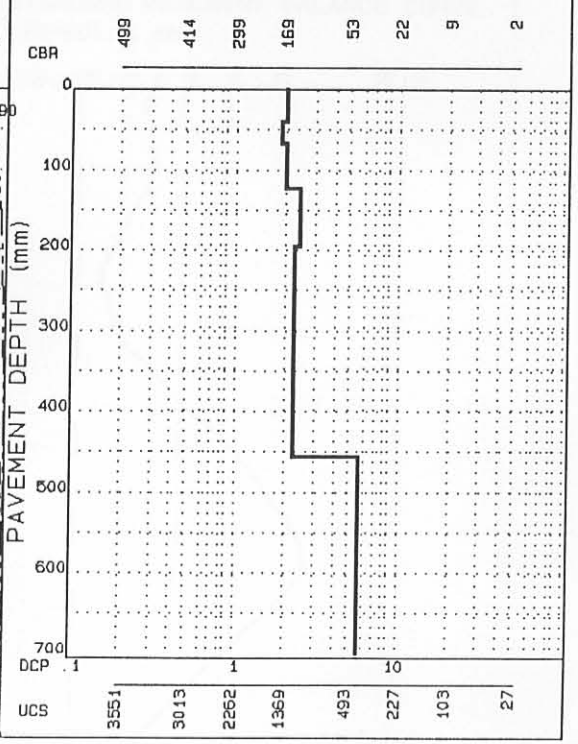

FIGURE E.68

ATT, CSIR, SA

SUMMARY OF DCP INVESTIGATION

AVERAGE EQUIVALENT STRENGTH (REDEFINED)

FROM - TO (mm)	AV. PENETRATION (mm/blow)	SD	90P	CBR%	UCS (kPa)
0- 24	2.0	0.1		165	1341
25-104	1.9	0.1		177	1426
105-240	2.5	0.2		127	1065
241-584	2.4	0.3		134	1116
585-800	7.4	1.4		32	316

DATA FILE: 309A4, FINAL; N=46 000

NORMALIZED CURVE

DEVIATION (A_i) FROM STANDARD PAVEMENT BALANCE CURVE (SPBC), %.mm

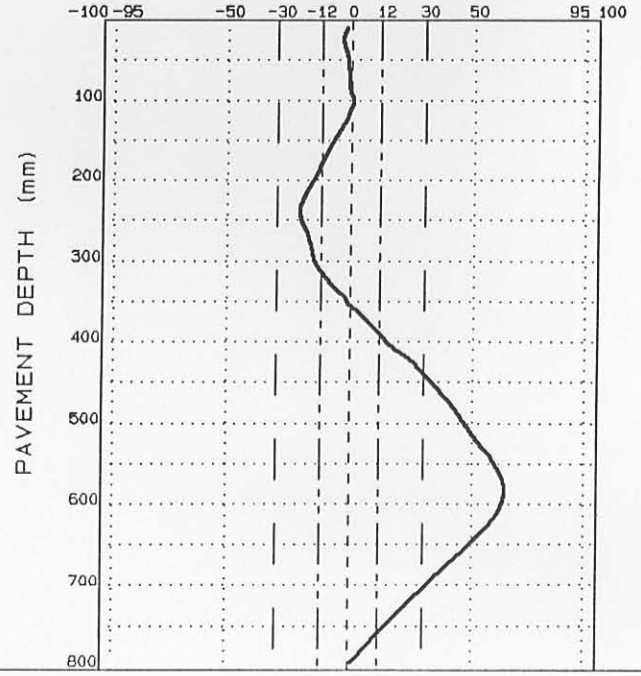

LAYER STRENGTH DIAGRAM (REDEFINED)

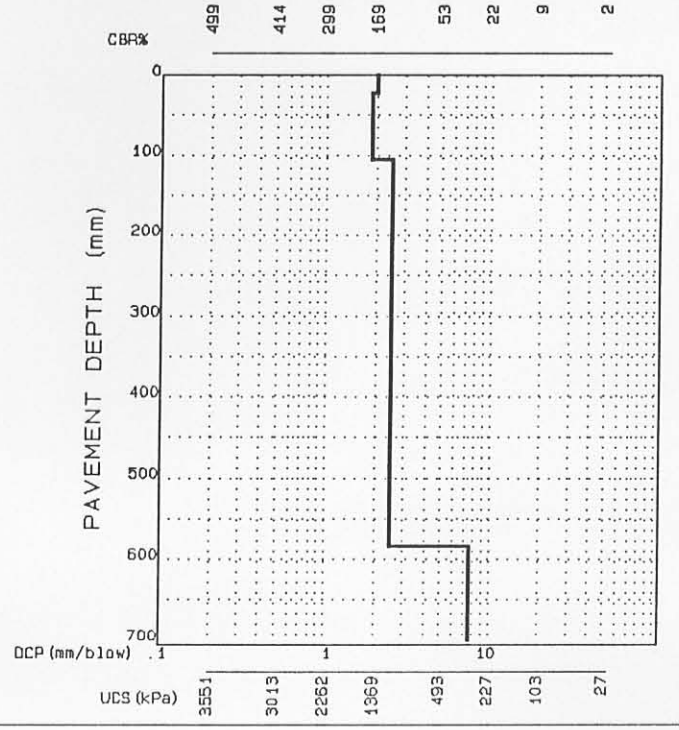

FIGURE E.69

APPENDIX F

SUPPLEMENTARY INFORMATION (FIGURES) TO ASSIST DISCUSSION IN CHAPTER 7

F.I INTRODUCTION

In this Appendix supplementary information, mostly in the form of figures are given to assist the discussion on the resilient response of of pavements with cementitios layers, in Chapter 7.

No detailed discussions are given here, as it is already given in Chapter 7, in which particular reference is made to the relevant figure.

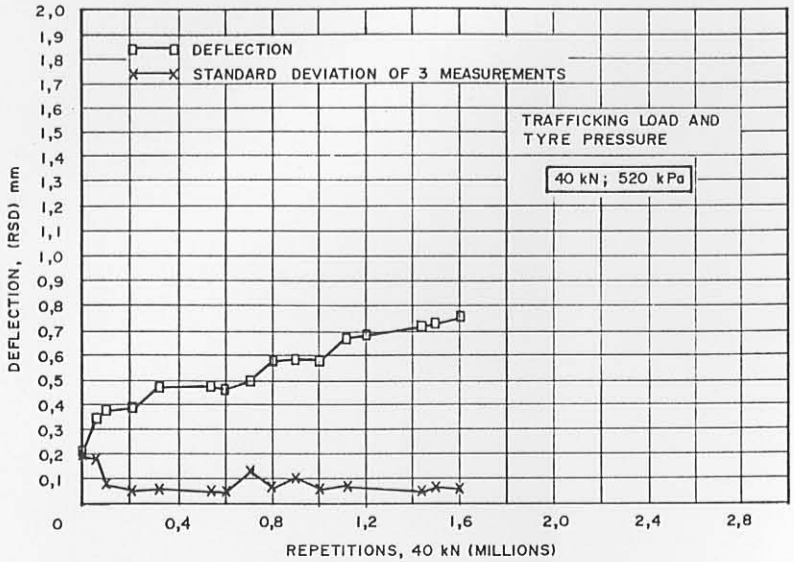

(a) SECTION 274A4

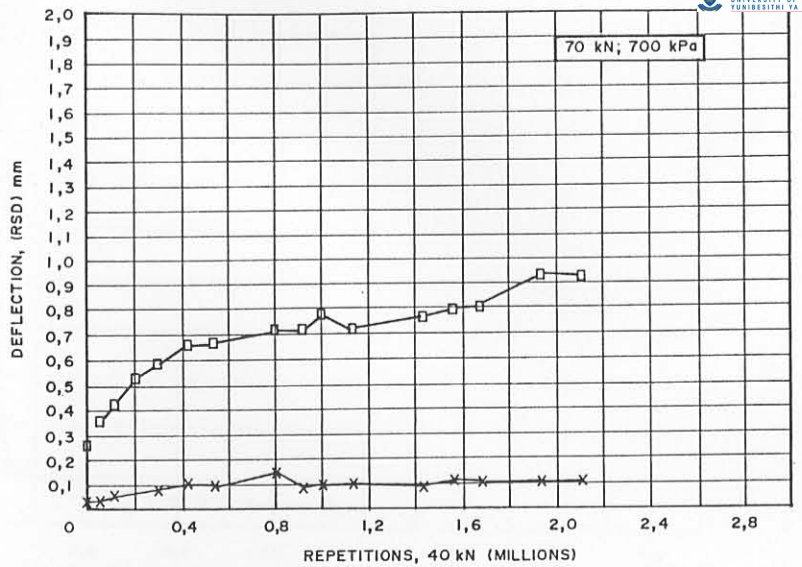

(b) SECTION 275A4

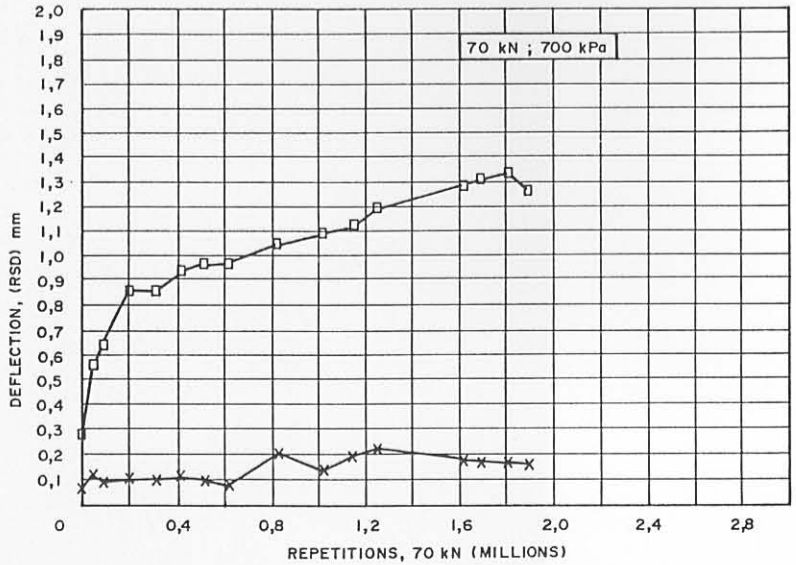

(c) SECTION 289A4

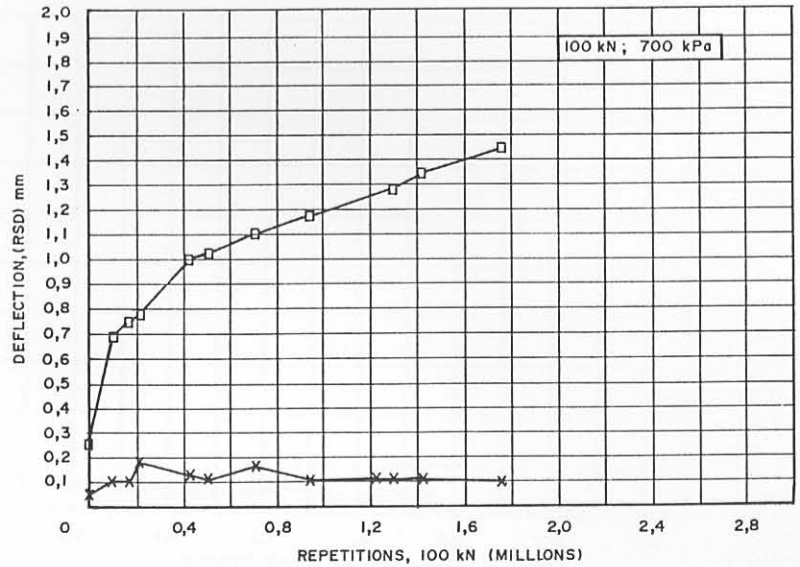

(b) SECTION 294A4

FIGURE F.1

AVERAGE STANDARD 40 kN SURFACE DEFLECTION (RSD) AT VARIOUS STAGES OF TRAFFICKING WITH THE INDICATED DUAL WHEEL LOAD ON FOUR DIFFERENT TEST SECTIONS ON THE DEEP PAVEMENT ON ROAD 1932 (ROOIWAL)

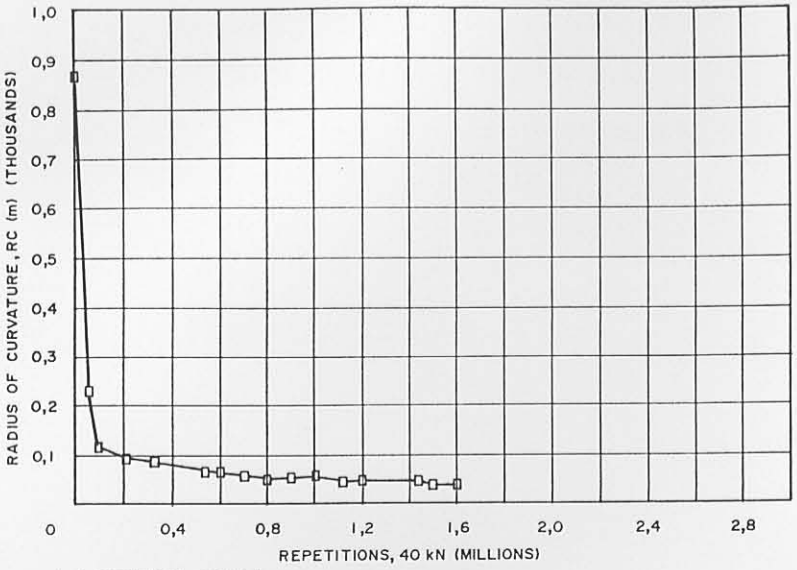

(a) SECTION 274A4

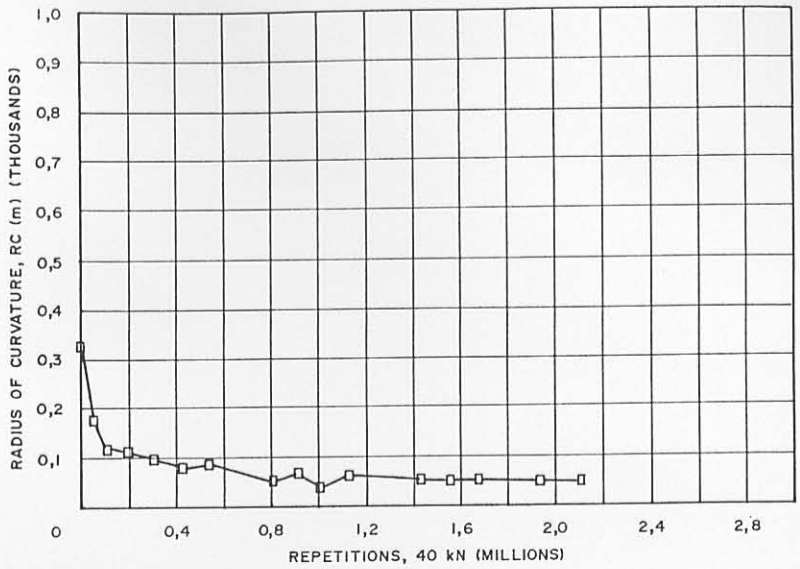

(b) SECTION 275A4

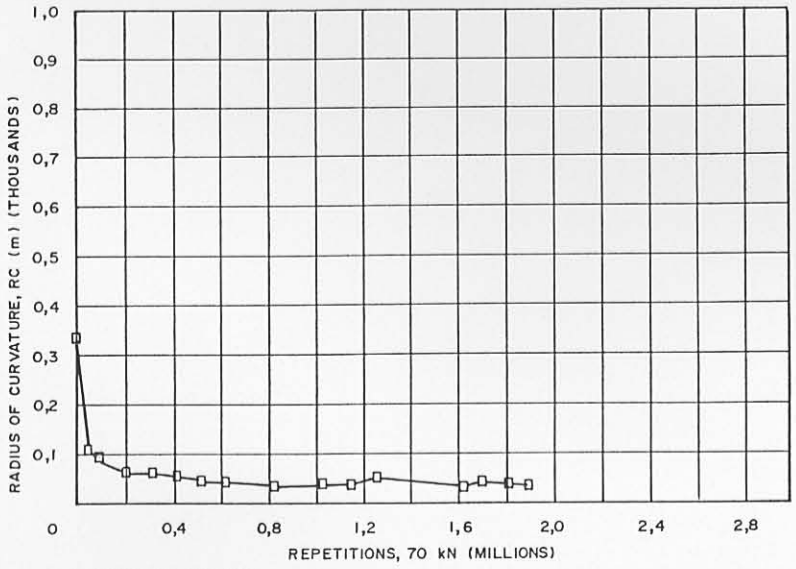

(c) SECTION 289A4

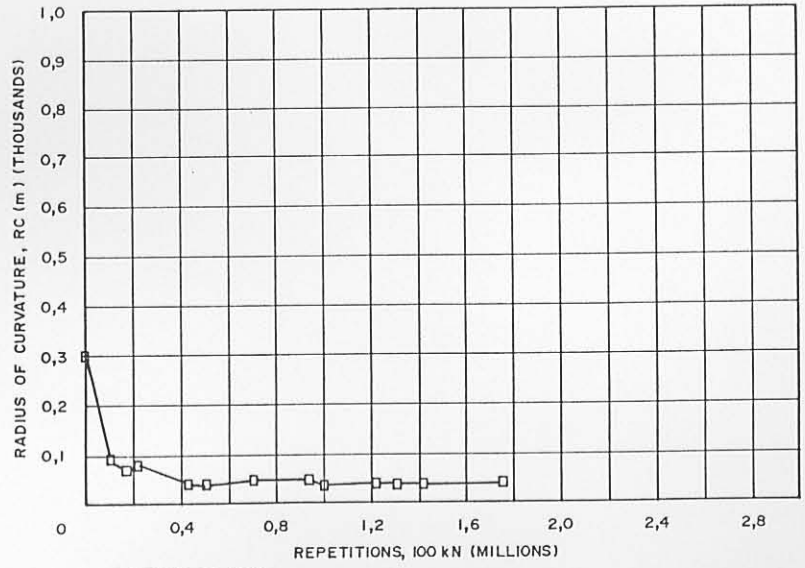

(d) SECTION 294A4

FIGURE F.2

AVERAGE RADIUS OF CURVATURE (RC) AT VARIOUS STAGES OF TRAFFICKING WITH THE INDICATED DUAL WHEEL LOAD ON FOUR DIFFERENT TEST SECTIONS ON THE DEEP PAVEMENT ON ROAD 1932 (ROOIWAL)

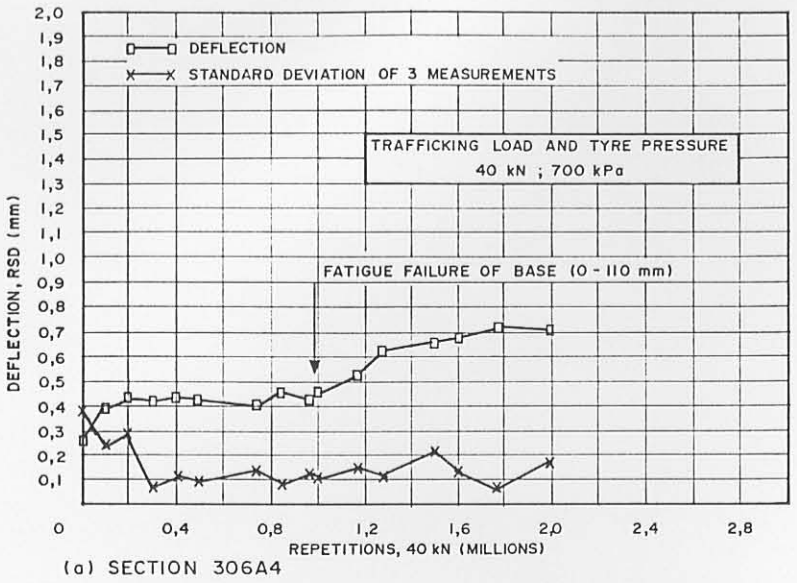

(a) SECTION 306A4

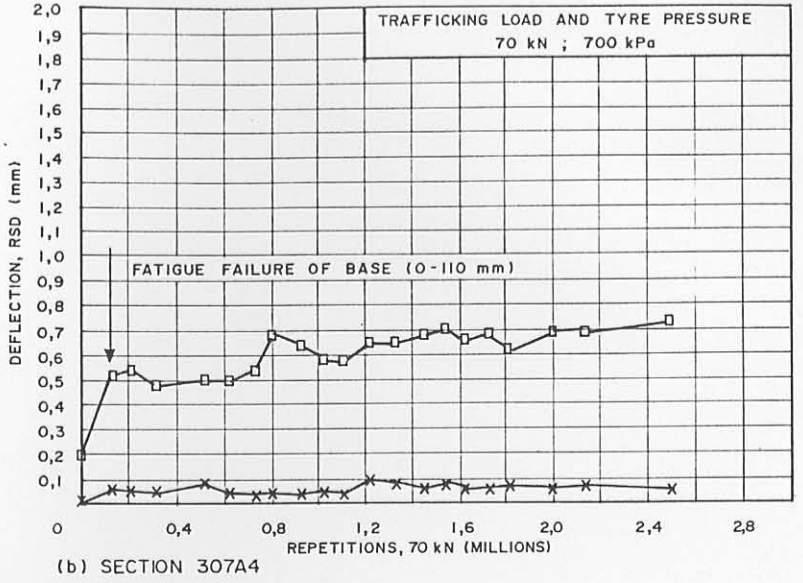

(b) SECTION 307A4

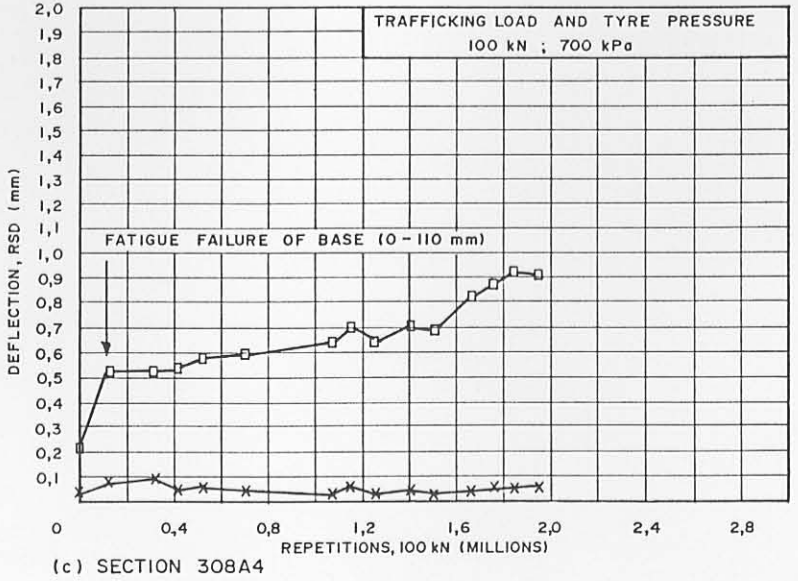

(c) SECTION 308A4

FIGURE F.3

AVERAGE STANDARD 40 kN SURFACE DEFLECTION (RSD) AT VARIOUS STAGES OF TRAFFICKING WITH THE INDICATED DUAL WHEEL LOAD ON THREE DIFFERENT TEST SECTIONS ON THE SHALLOW PAVEMENT (ROAD 2212, BULTFONTEIN)

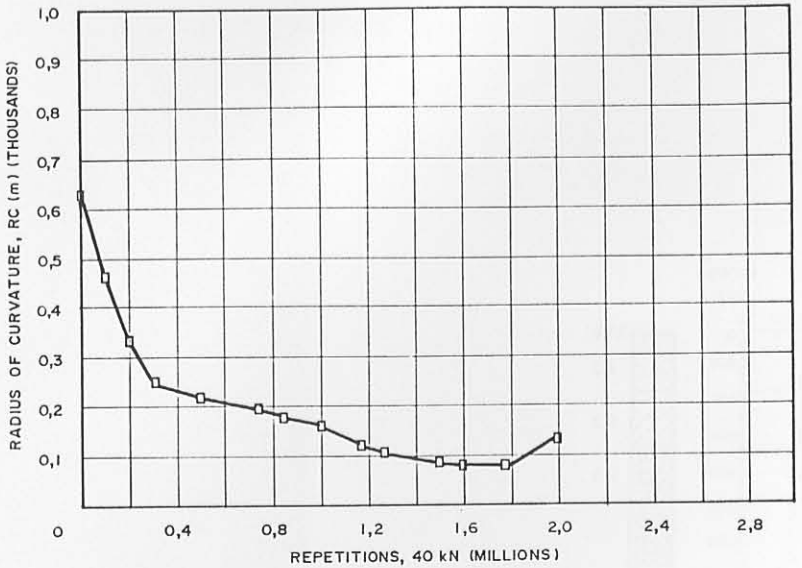

(a) SECTION 306A4

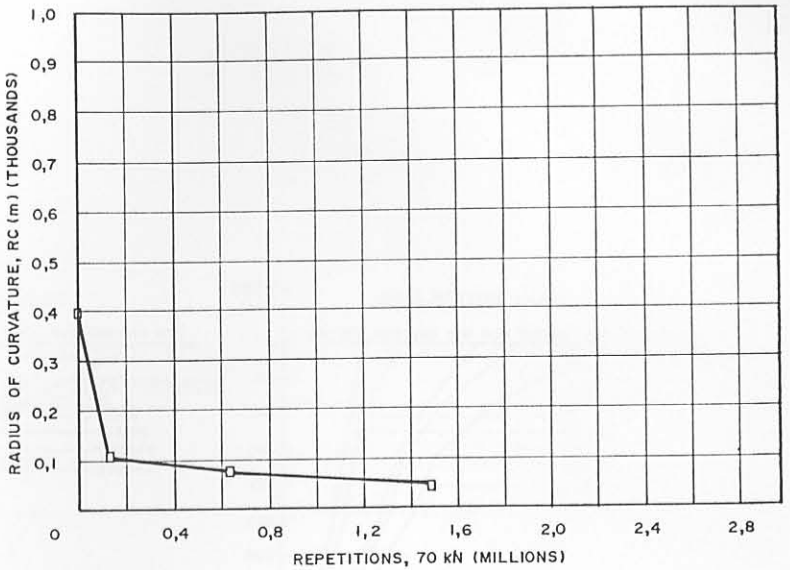

(b) SECTION 307A4

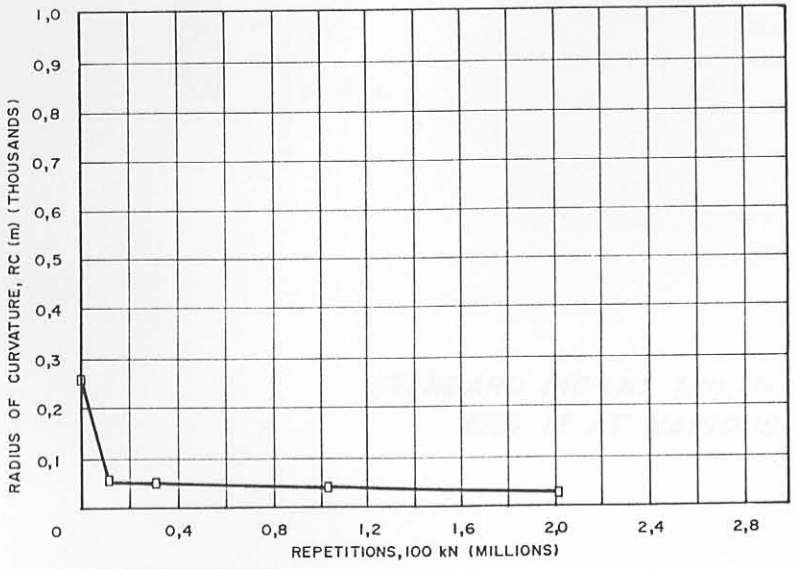

(c) SECTION 308A4

FIGURE F.4

AVERAGE RADIUS OF CURVATURE (RC) AT VARIOUS STAGES OF TRAFFICKING WITH THE INDICATED DUAL WHEEL LOAD ON THE THE THREE TEST SECTIONS ON THE SHALLOW PAVEMENT ON ROAD 2212 (BULTFONTEIN)

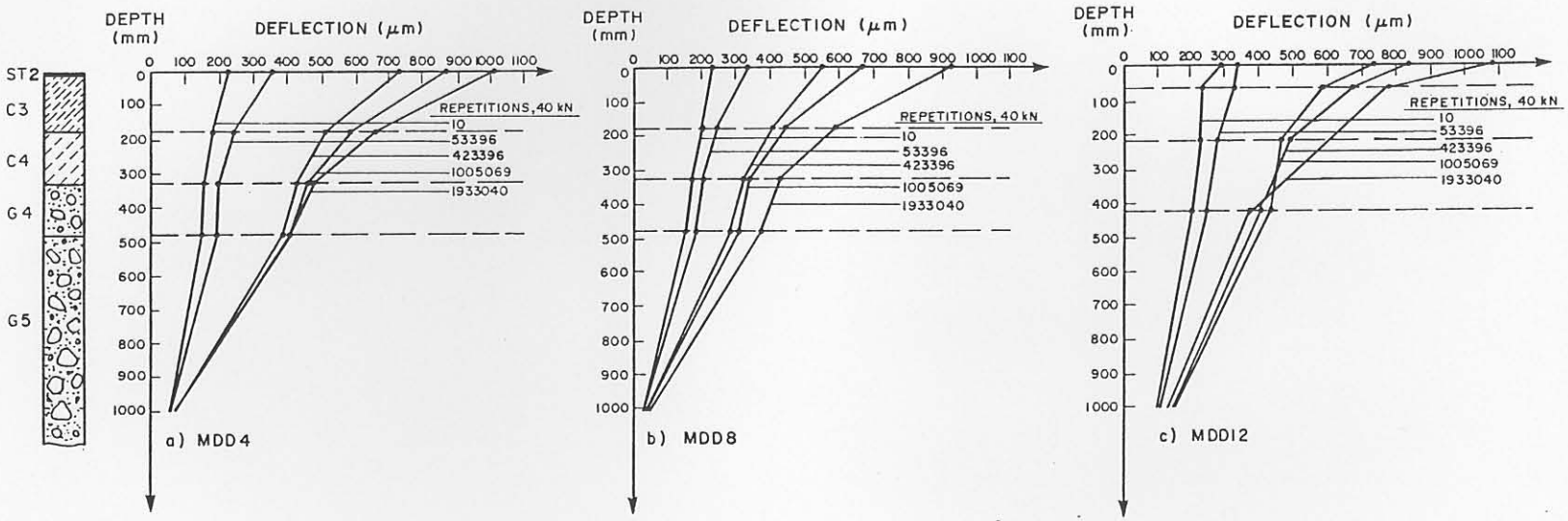

FIGURE F.5

STANDARD (40 kN) MULTI-DEPTH DEFLECTIONS AT MEASURING POSITIONS 4, 8 AND 12 AT VARIOUS STAGES OF TRAFFICKING ON HVS SECTION 275A4

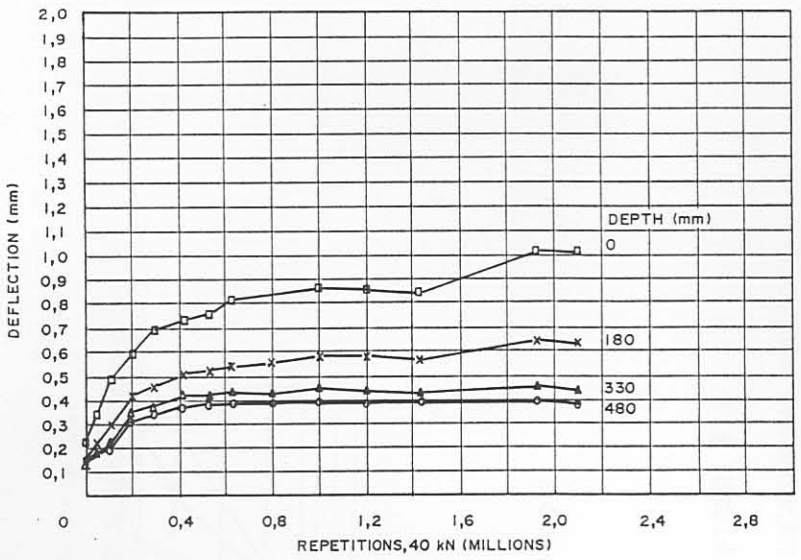

(a) MDD 4

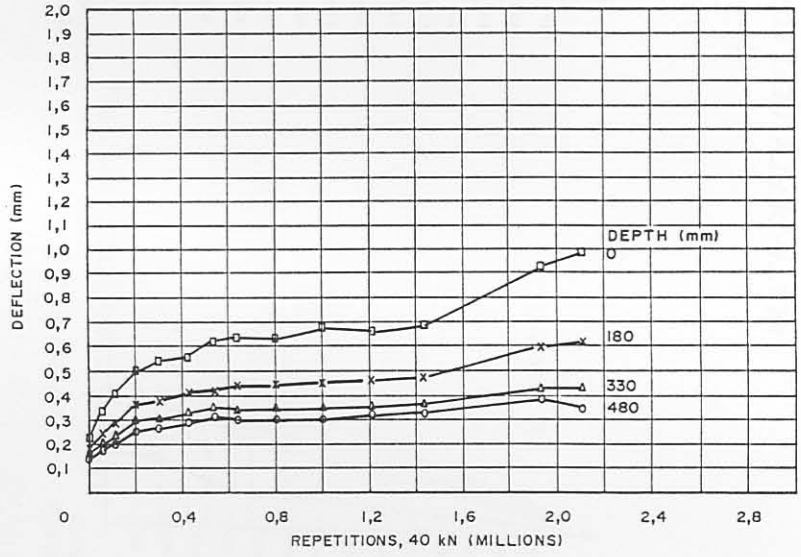

(b) MDD 8

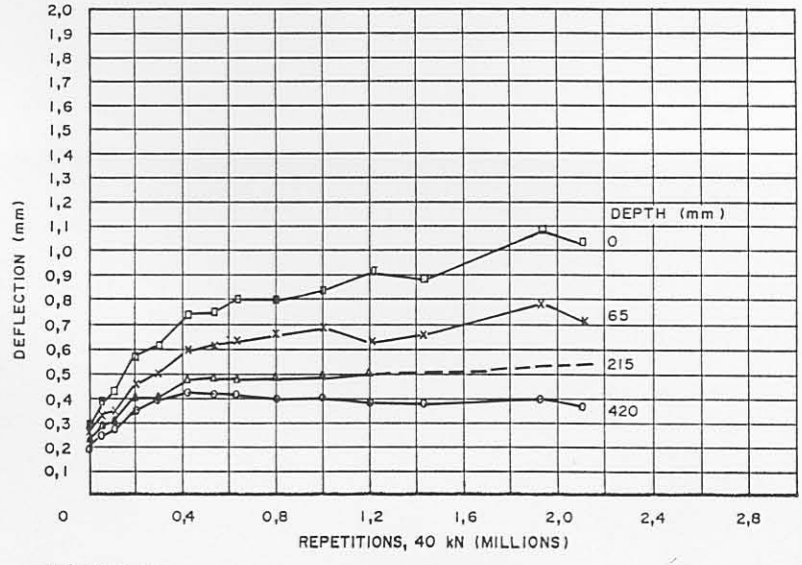

(c) MDD 12

FIGURE F.6

AVERAGE STANDARD MDD DEFLECTION AT VARIOUS STAGES OF TRAFFICKING ON SECTION 275A4 (ROAD 1932, ROOIWAL)

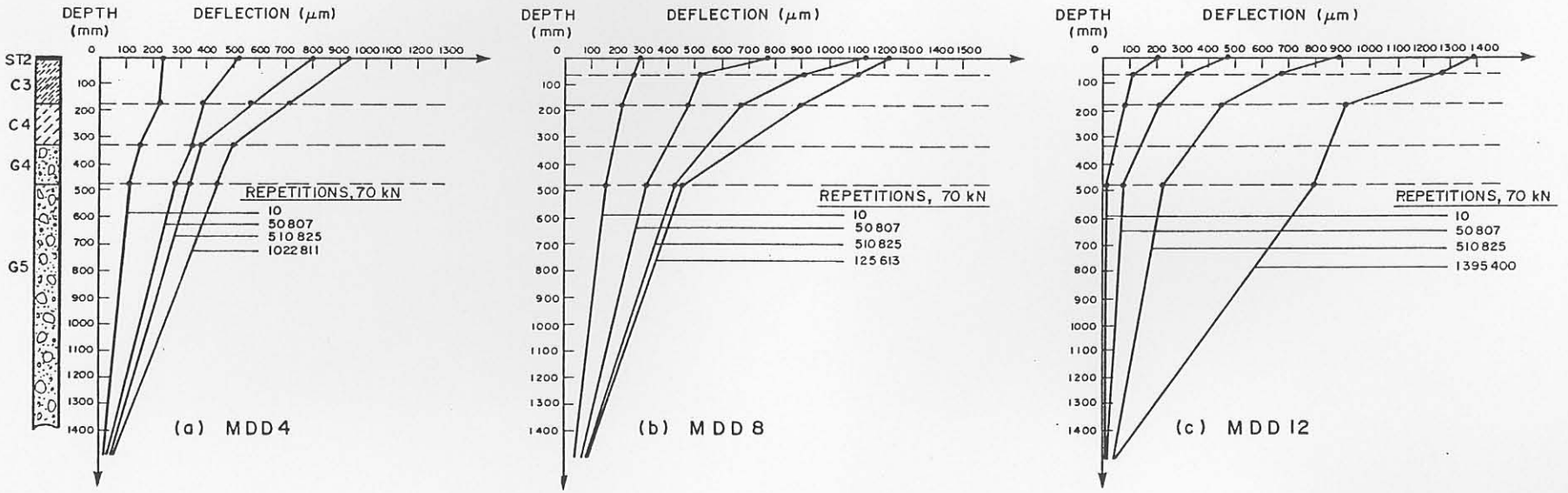

FIGURE F.7

MULTI-DEPTH DEFLECTIONS AT MEASURING POSITIONS 4, 8 AND 12 AT VARIOUS STAGES OF TRAFFICKING ON HVS SECTION 289A4

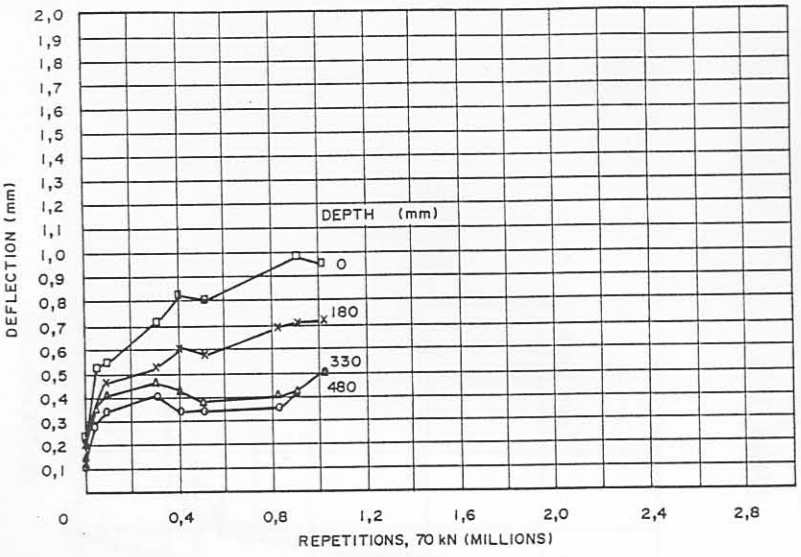

(a) MDD 4

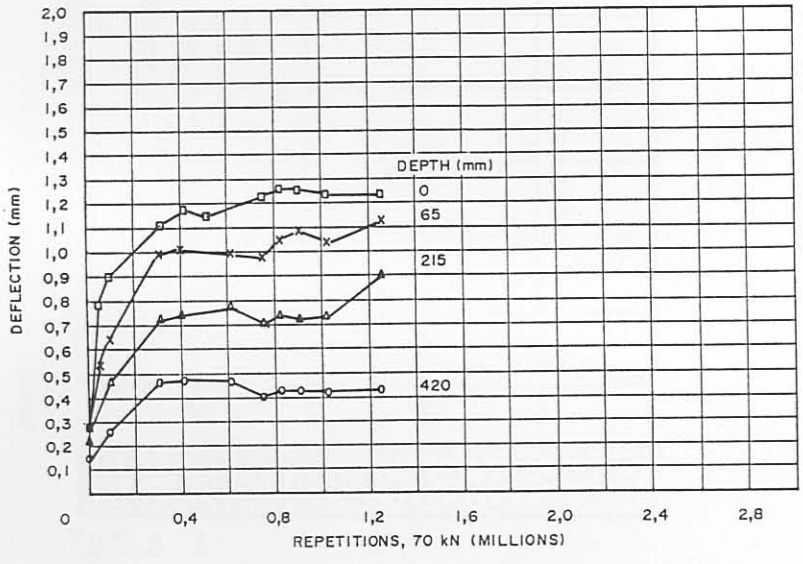

(b) MDD 8

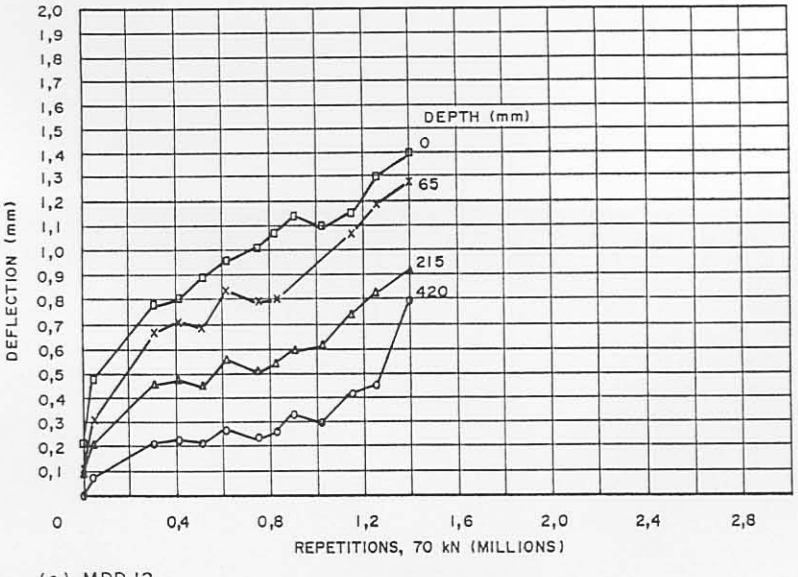

(c) MDD 12

FIGURE F.8

AVERAGE STANDARD MDD DEFLECTION AT VARIOUS STAGES OF TRAFFICKING ON SECTION 289A4 (ROAD 1932, ROOIWAL)

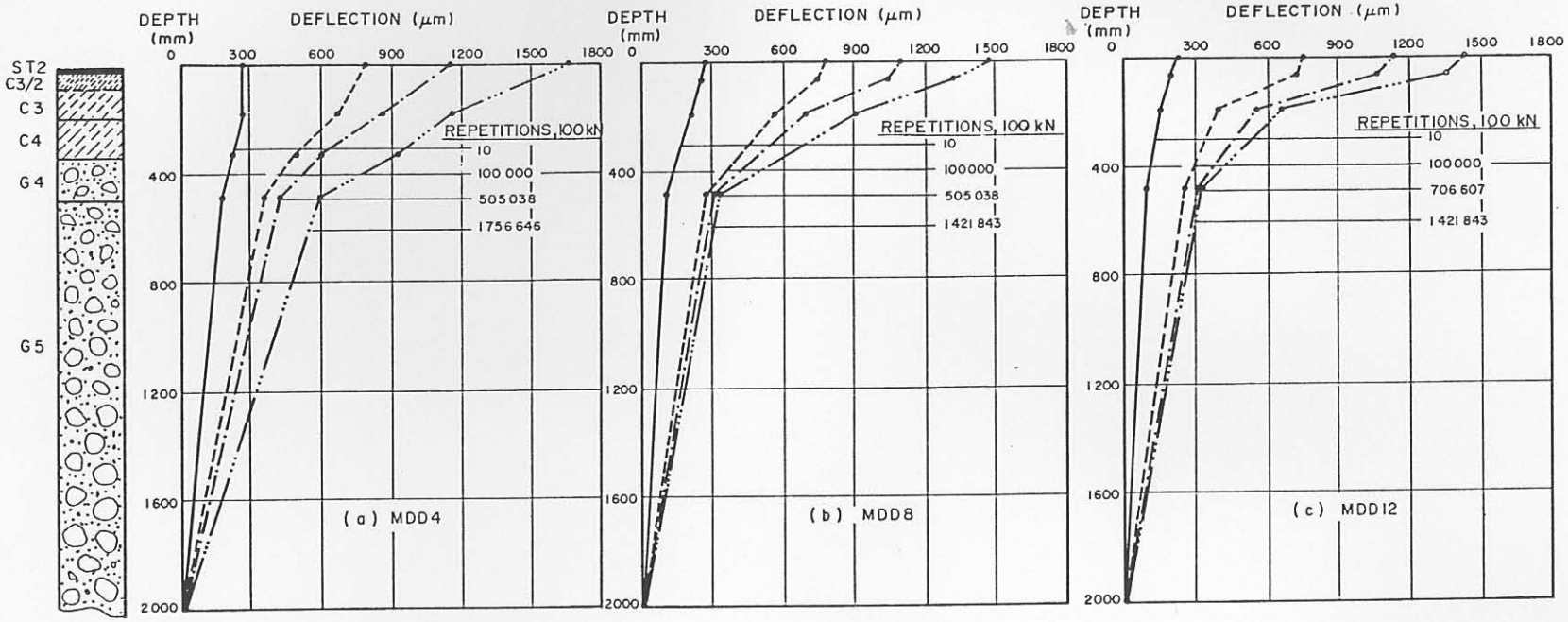

FIGURE F.9

MULTI-DEPTH DEFLECTIONS AT MEASURING POSITIONS 4, 8 AND 12 AT VARIOUS STAGES OF TRAFFICKING ON HVS SECTION 294A4

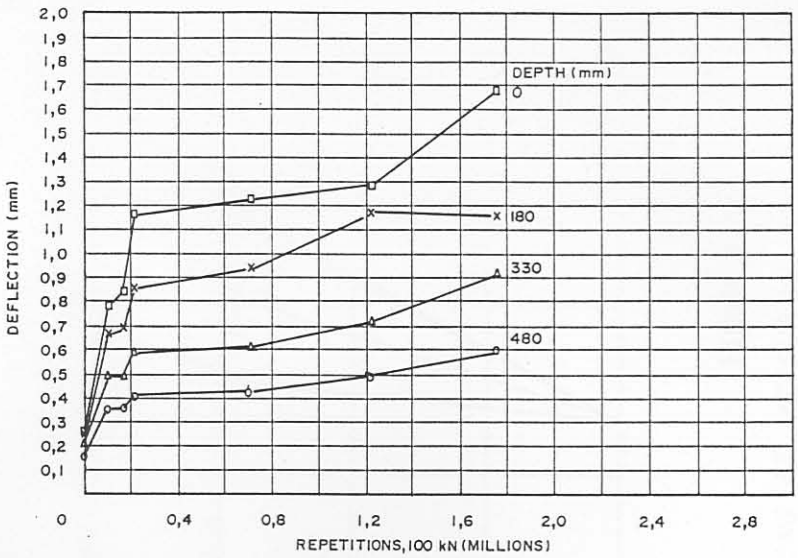

(a) MDD 4

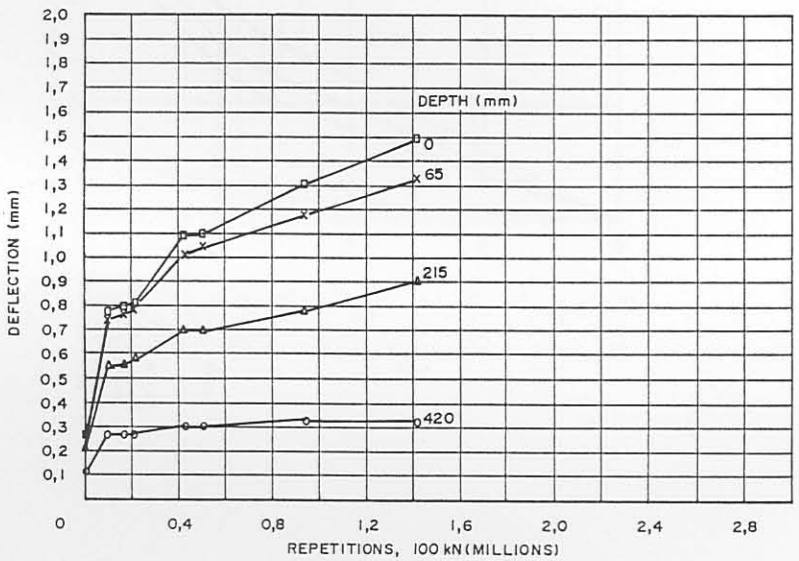

(b) MDD 8

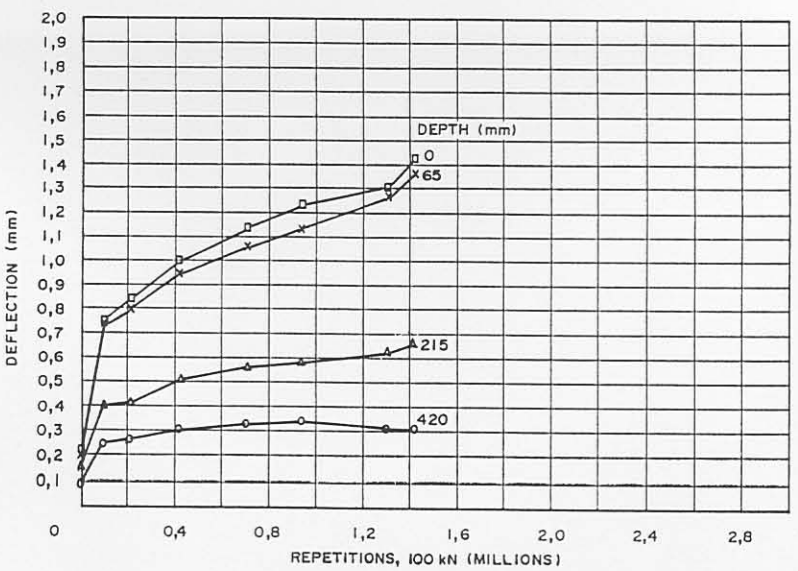

(c) MDD 12

FIGURE F.10

AVERAGE STANDARD MDD DEFLECTION AT VARIOUS STAGES OF TRAFFICKING ON SECTION 294A4 (ROAD 1932, ROOIWAL)

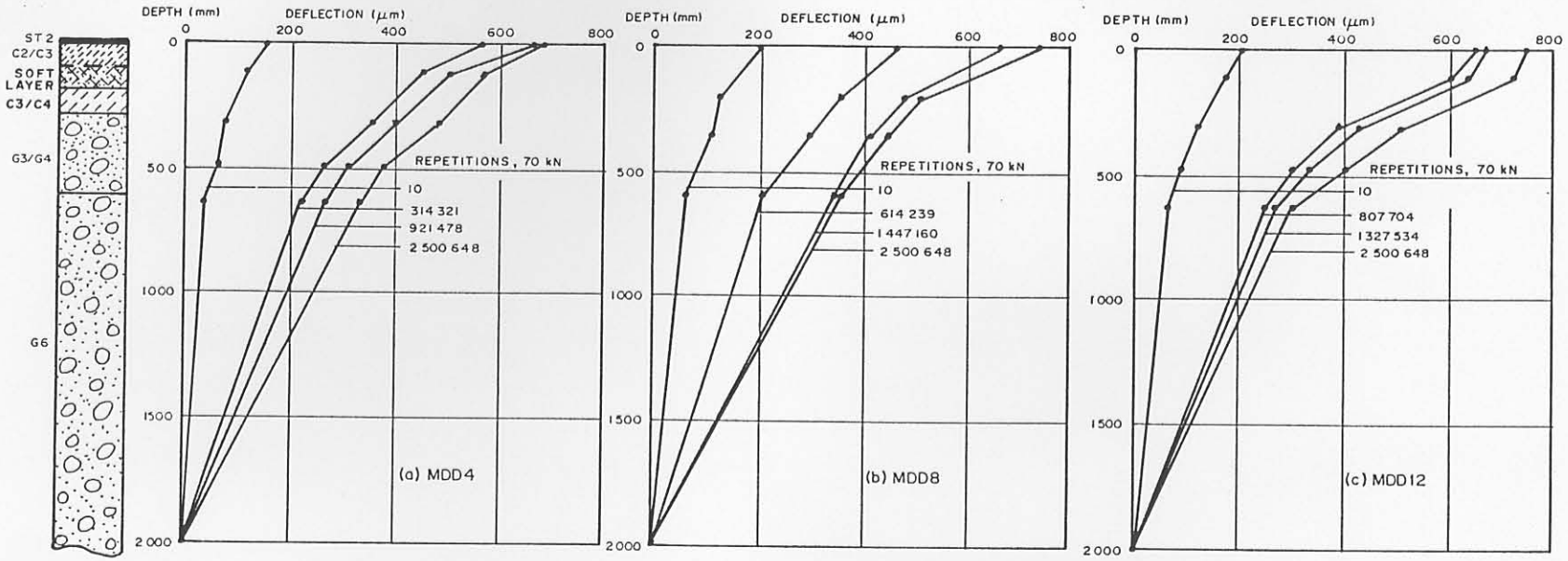

FIGURE F.11

MULTI-DEPTH DEFLECTIONS AT MEASURING POSITIONS 4, 8 AND 12 AT VARIOUS STAGES OF TRAFFICKING ON HVS SECTION 307A4

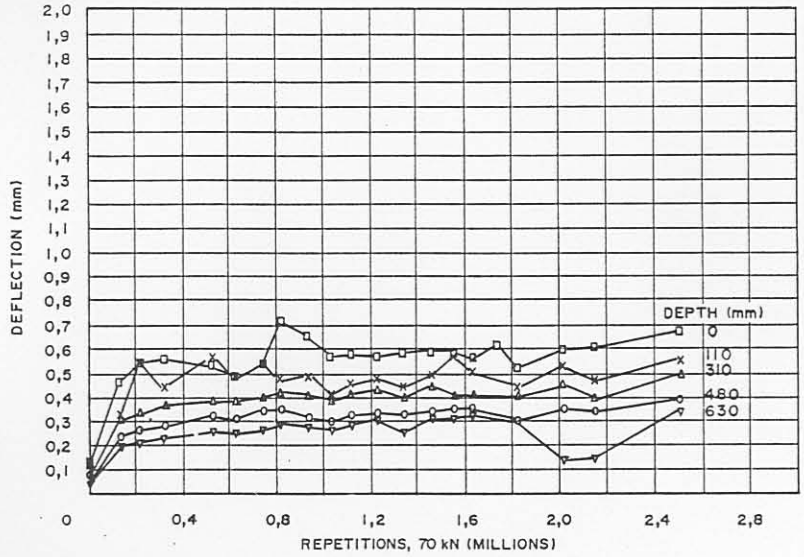

(a) MDD 4

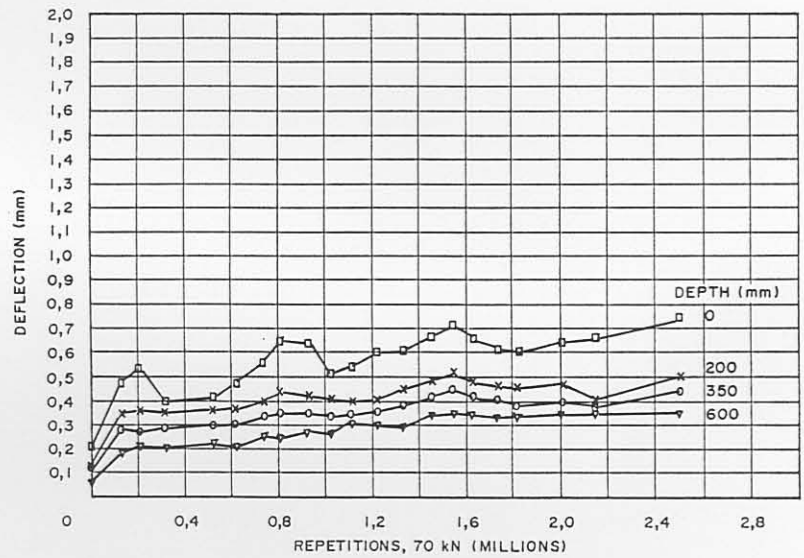

(b) MDD 8

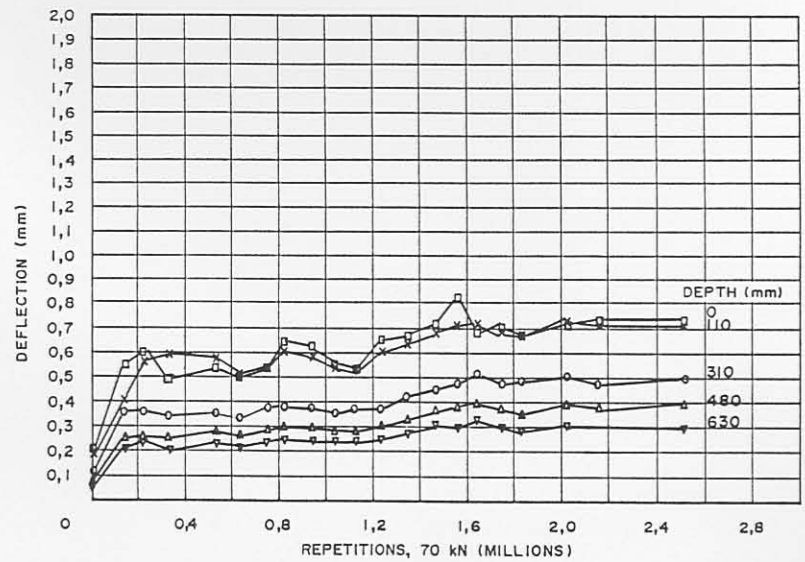

(c) MDD 12

FIGURE F.12

AVERAGE STANDARD MDD DEFLECTION AT VARIOUS STAGES OF TRAFFICKING ON SECTION 307A4 (ROAD 2212, BULTFONTEIN)

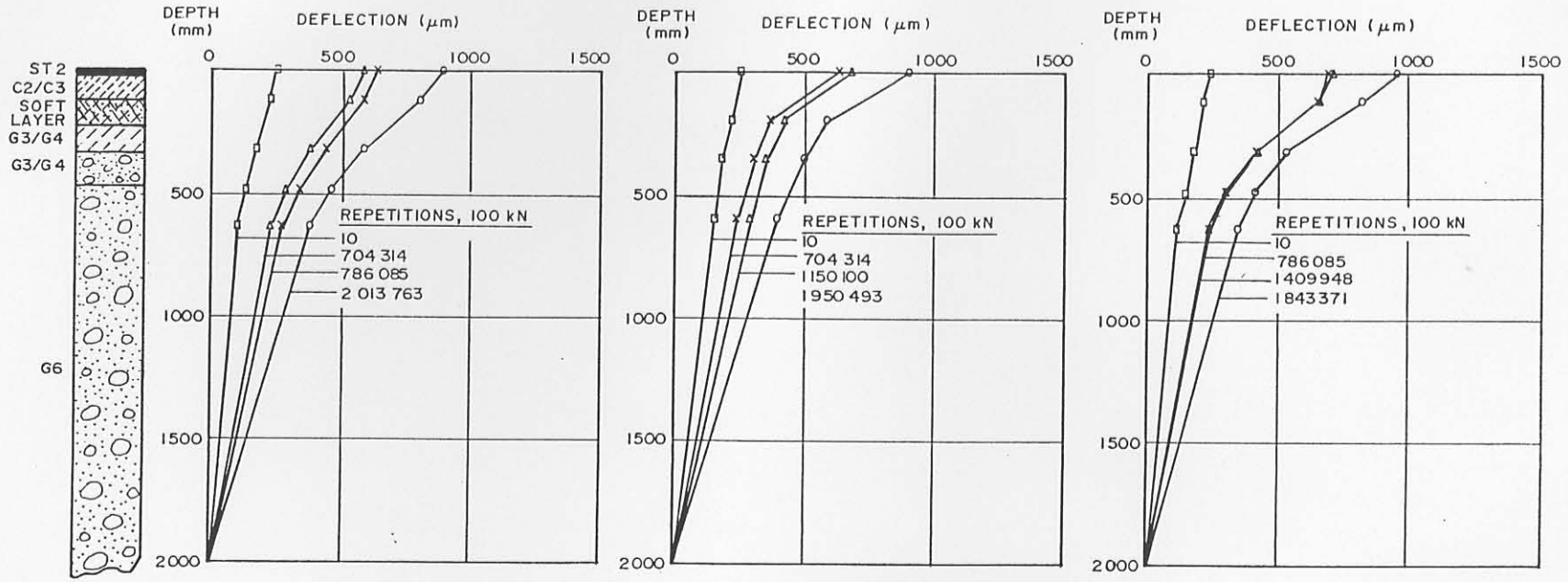

FIGURE F.13

STANDARD 40 kN MULTI-DEPTH DEFLECTIONS AT MEASURING POSITIONS 4, 8 AND 12 AT VARIOUS STAGES OF TRAFFICKING ON HVS SECTION 306A4

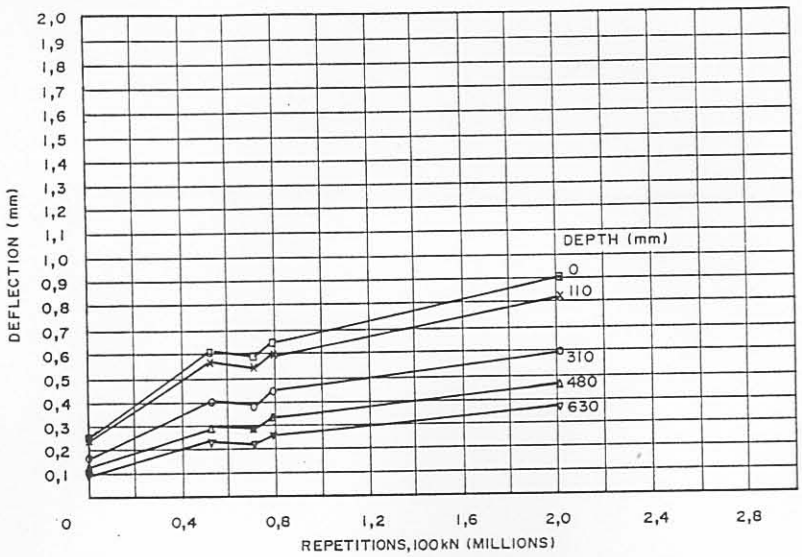

(a) MDD 4

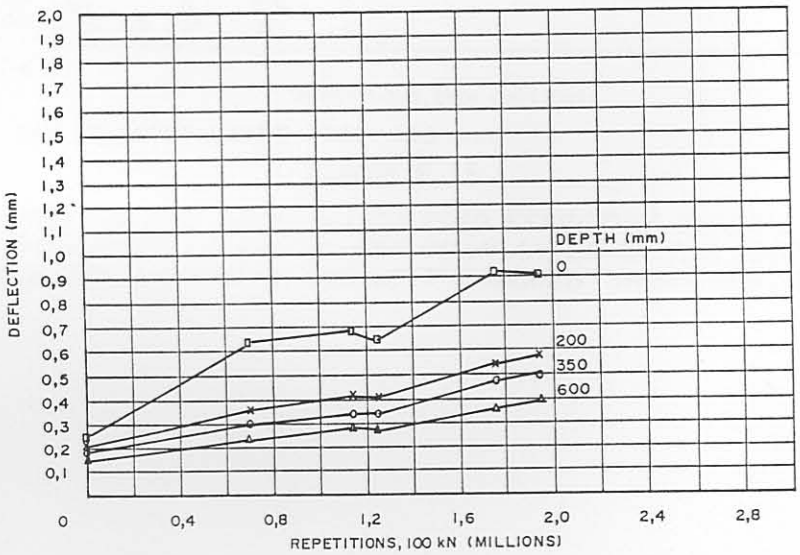

(b) MDD 8

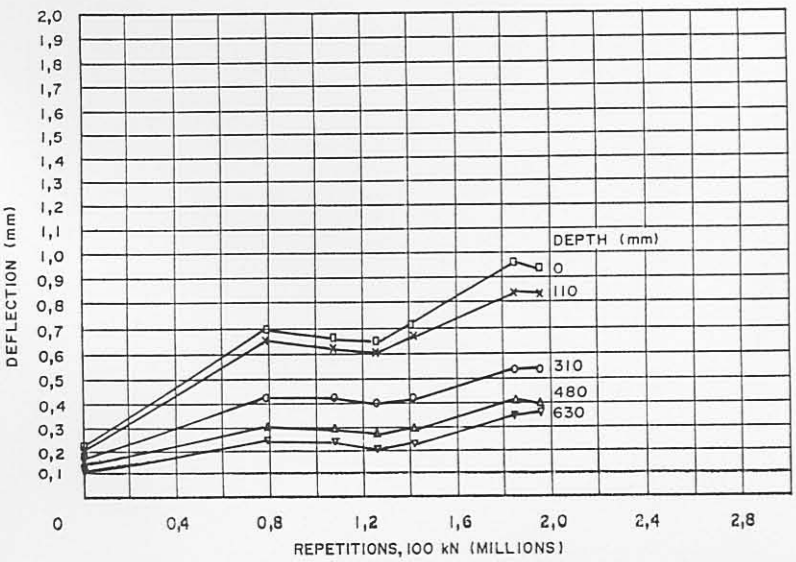

(c) MDD 12

FIGURE F.14

AVERAGE STANDARD MDD DEFLECTION AT VARIOUS STAGES OF TRAFFICKING ON SECTION 308A4 (ROAD 2212, BULTFONTEIN)

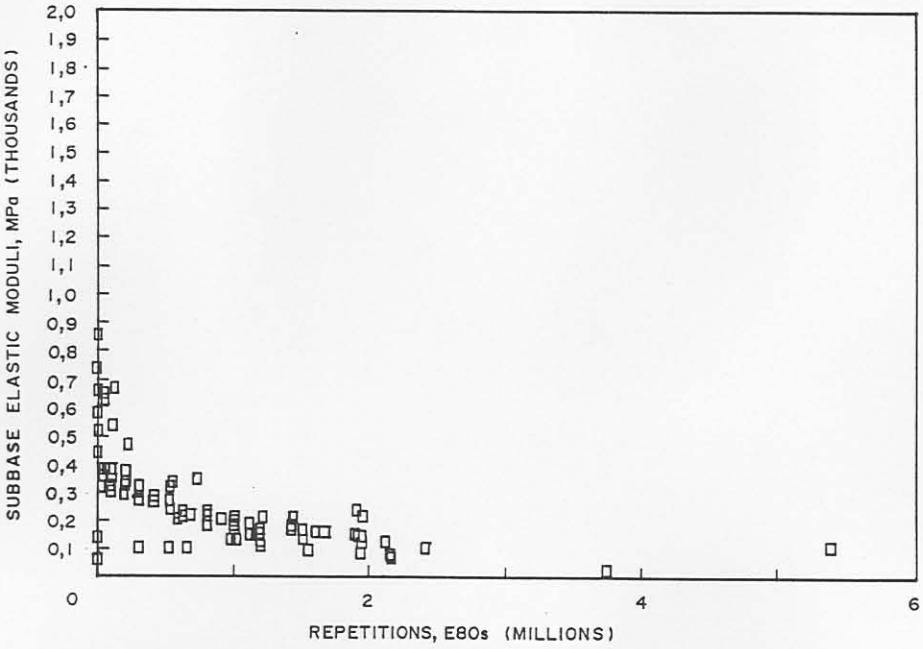

(a) SUBBASE (180 - 330 mm)

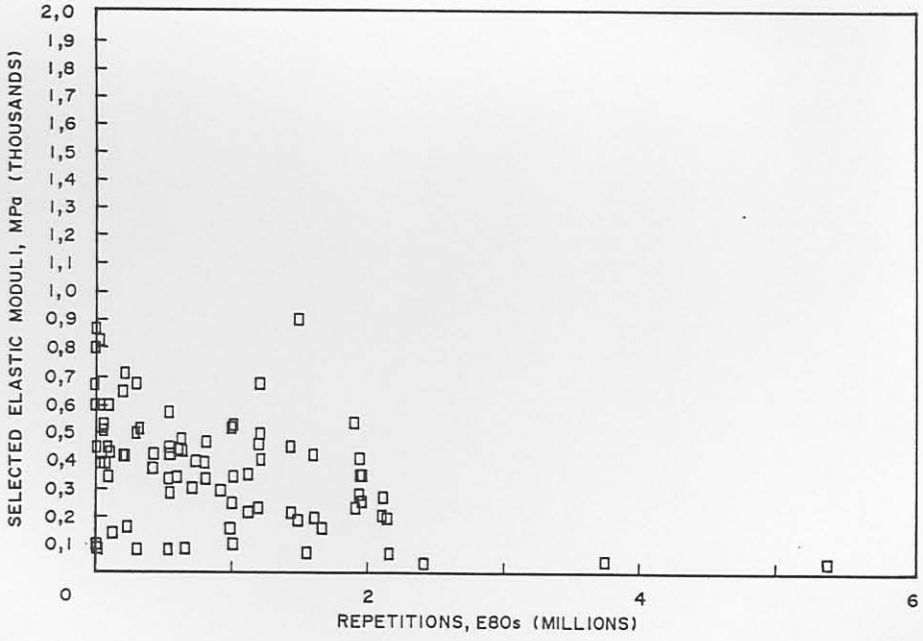

(b) SELECTED LAYER (330 - 480 mm)

FIGURE F.15

CHANGE IN MDD BACK-CALCULATED EFFECTIVE ELASTIC MODULI WITH NUMBER OF EQUIVALENT 80 kN AXLES OF THE SUBBASE AND SELECTED LAYERS IN THE DEEP PAVEMENT (ROAD 1932, ROOIWAL)

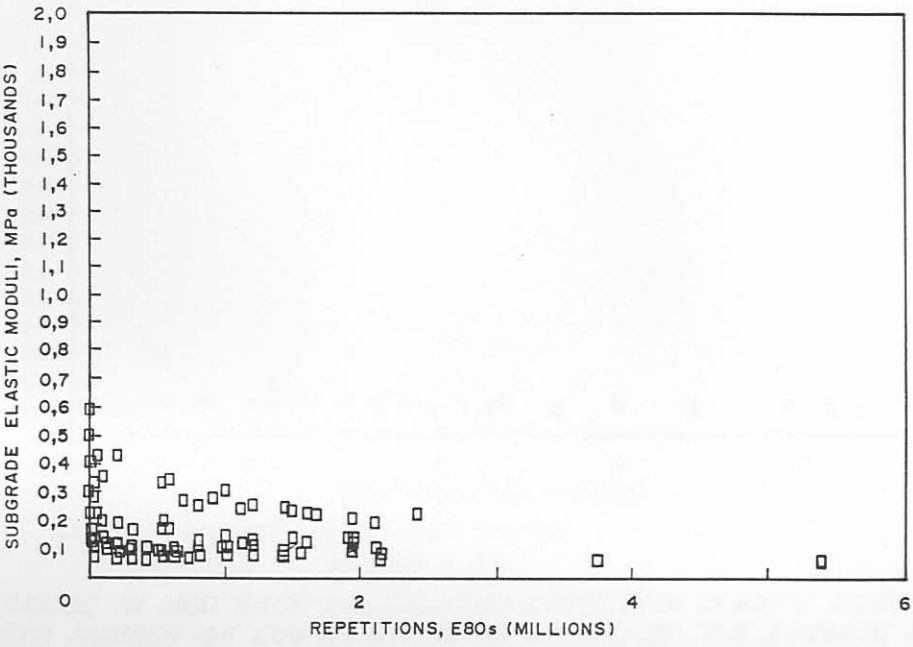

FIGURE F.16

CHANGE IN MDD BACK-CALCULATED EFFECTIVE ELASTIC MODULI WITH NUMBER OF EQUIVALENT 80 kN AXLES OF THE SUBGRADE (480 mm DOWNWARDS) OF THE DEEP PAVEMENT (ROAD 1932, ROOIWAL)

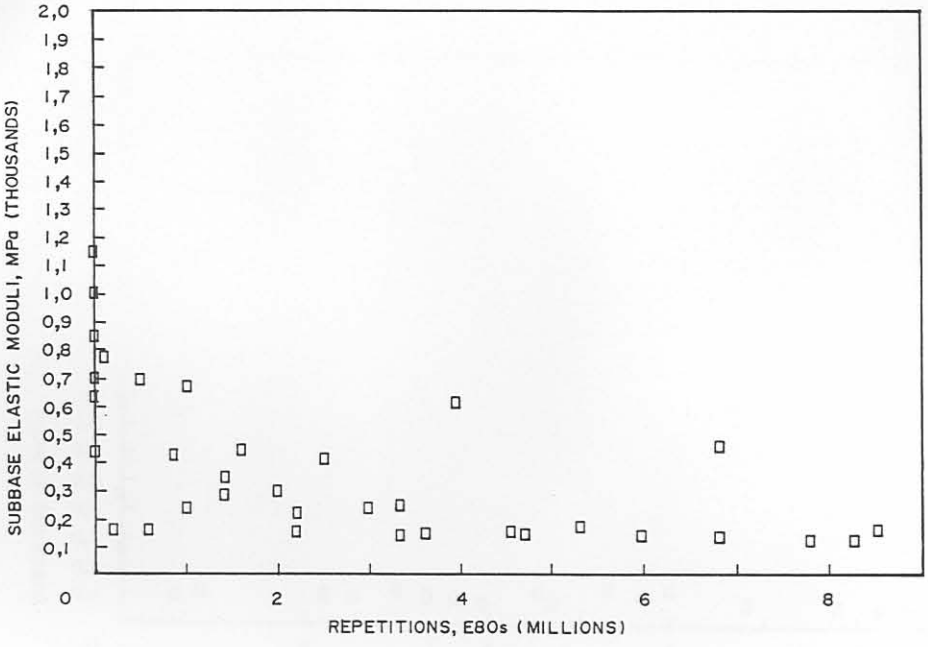

(a) SUBBASE (110 - 310 mm)

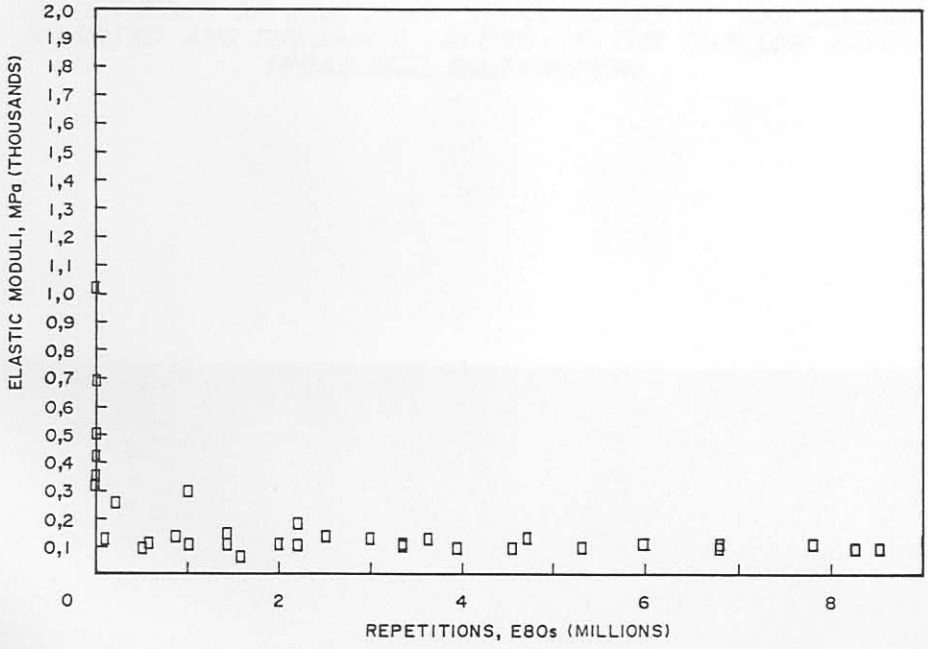

(b) FIRST SELECTED LAYER (310 - 480 mm)

FIGURE F.17

CHANGE IN MDD BACK-CALCULATED EFFECTIVE ELASTIC MODULI WITH NUMBER OF EQUIVALENT 80 kN AXLES, OF THE SUBBASE AND FIRST SELECTED LAYER IN THE SHALLOW PAVEMENT (ROAD 2212, BULTFONTEIN)

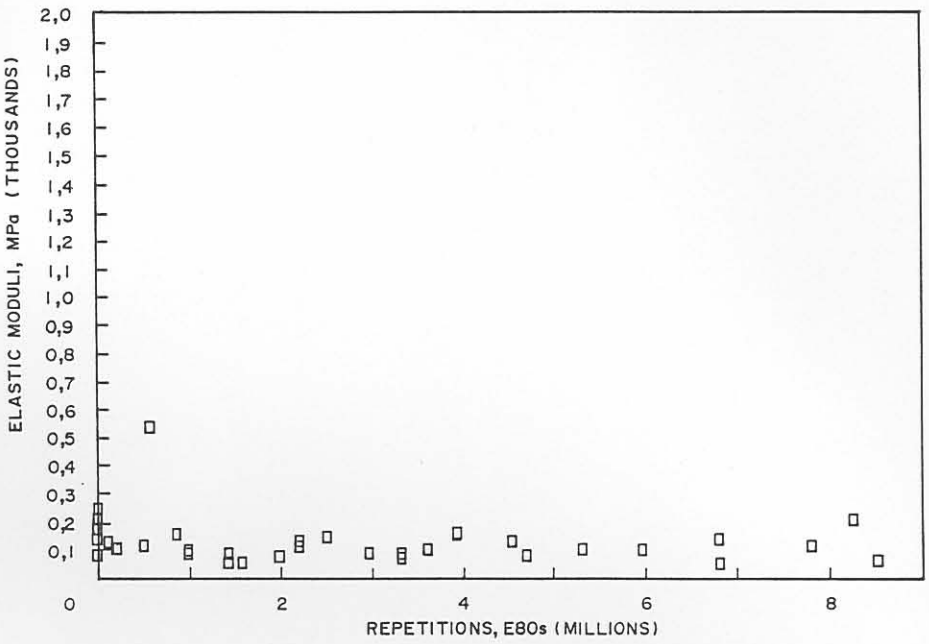

(a) SECOND SELECTED LAYER (480-630 mm)

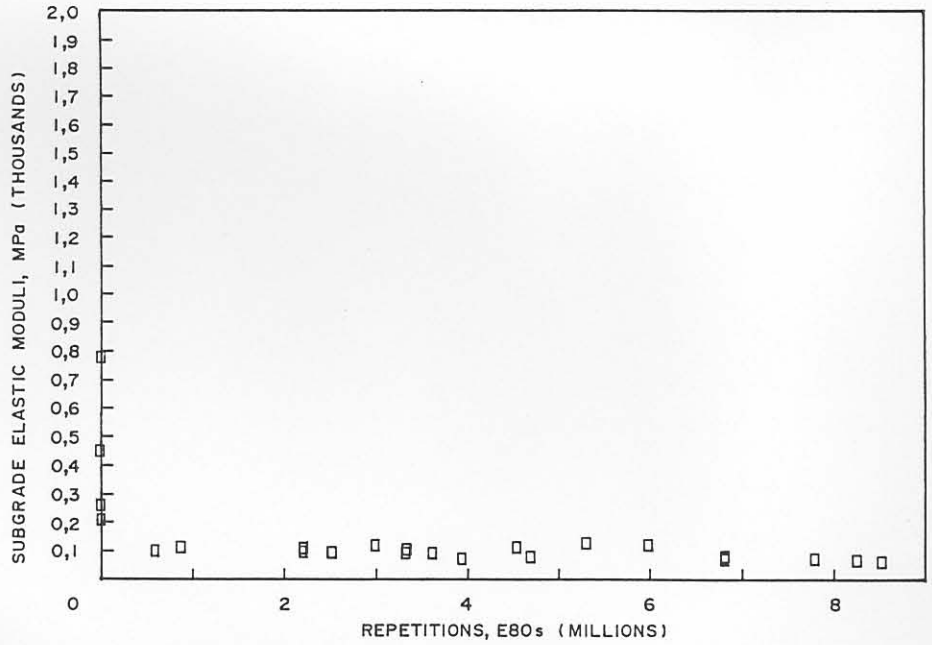

(b) SUBGRADE LAYER (630 mm DOWNWARDS)

FIGURE F.18

CHANGE IN MDD BACK-CALCULATED EFFECTIVE ELASTIC MODULI WITH NUMBER OF EQUIVALENT 80 kN AXLES OF THE SECOND SELECTED AND SUBGRADE LAYERS OF THE SHALLOW PAVEMENT (ROAD 2212, BULTFONTEIN)